

AD 722283

FOREIGN TECHNOLOGY DIVISION



THEORY OF JET ENGINES

By

A. L. Klyachkin



D D C  
RECEIVED  
MAY 4 1971  
REGISTERED  
E

Distribution of this document is unlimited. It may be released to the Clearinghouse, Department of Commerce, for sale to the general public.

Reproduced by  
NATIONAL TECHNICAL  
INFORMATION SERVICE  
Springfield, Va. 22151

679

**Best  
Available  
Copy**

# EDITED MACHINE TRANSLATION

THEORY OF JET ENGINES

By: A. L. Klyachkin

English pages: 657

SOURCE: Teoriya Vozdushno-reaktivnykh Dvigatelye.  
Izd-vo "Mashinostroyeniye", Moscow,  
1969, pp. 1-512.

This document is a Systran machine aided translation,  
post-edited for technical accuracy by: Robert D. Hill.

UR/0000-69-000-000

THIS TRANSLATION IS A RENDITION OF THE ORIGINAL FOREIGN TEXT WITHOUT ANY ANALYTICAL OR EDITORIAL COMMENT. STATEMENTS OR THEORIES ADVOCATED OR IMPLIED ARE THOSE OF THE SOURCE AND DO NOT NECESSARILY REFLECT THE POSITION OR OPINION OF THE FOREIGN TECHNOLOGY DIVISION.

PREPARED BY:

TRANSLATION DIVISION  
FOREIGN TECHNOLOGY DIVISION  
WP-afb, OHIO.

TABLE OF CONTENTS

U. S. Board on Geographic Names Transliteration System..... viii  
Acronyms and Abbreviations..... ix  
Preface..... xii  
Symbols..... xv

PART ONE

General Information on Jet Engines

Chapter 1. Principle of Operation, Design and Classification  
of Jet Engines..... 2  
    1.1. Concept of Reactive Force and Jet Engine..... 2  
    1.2. Classification of Reaction Engines..... 4  
    1.3. Layouts, Design and Principle of Operation of  
    Jet Engines..... 11  
Chapter 2. Brief Description of the History of Development  
of Reaction Engines..... 19  
    2.1. From Gunpowder Rockets to First Designs of  
    Reaction Engines..... 19  
    2.2. Development of Principles of the Theory of  
    Reaction Engines..... 24  
    2.3. Development of the First Reaction Engines and  
    Their Subsequent Development..... 27  
    2.4. Contemporary Level of Development of Aircraft  
    Reaction Engines..... 30  
Chapter 3. Thrust of the Jet Engine. Basic Parameters of  
the Jet Engines..... 47  
    3.1. Theorem of Thrust of Jet Engine..... 47  
    3.2. Reversing and Deviation in Thrust of Turbojet  
    Engines..... 53

3.3.	Basic Parameters of the TRD (VRD).....	57
------	--	----

PART TWO  
Thermodynamic Cycles and Working Processes  
of Jet Engines

Chapter 4.	Thermodynamic Cycles Airbreathing Jet Engine.....	62
4.1.	Ideal Cycles of Jet Engines $p = \text{const}$ .....	62
4.2.	Real Cycle of the Jet Engine.....	64
4.3.	Efficiency of the Process of Compression.....	69
4.4.	Efficiency of the Expansion Process.....	71
4.5.	Other Ideal Cycles of Airbreathing Jet Engines.....	72
Chapter 5.	Intake Systems of Jet Engine.....	78
5.1.	Purpose of Intake Devices and Their Requirements....	78
5.2.	Thermodynamic Processes in Air Intake (Diffusers)...	83
5.3.	Operation of a Standard Subsonic Diffuser at Supersonic Flight Speeds.....	86
5.4.	Supersonic Diffusers (Design Conditions).....	87
5.5.	Partial Load Conditions of the Operation of a Supersonic Diffuser.....	92
5.6.	Characteristics of Supersonic Diffusers.....	100
5.7.	Joint Operation of the Supersonic Diffuser and Compressor.....	107
5.8.	Adjustment of the Supersonic Diffuser of the TRD....	109
Chapter 6.	Combustion Chambers of the Jet Engine.....	114
6.1.	Assignment of Combustion Chambers.....	114
6.2.	Basic Requirements of Combustion Chambers. Basic Parameters of the Combustion Chamber.....	115
6.3.	Design and Principle of Operation Combustion Chambers. Types of Combustion Chambers.....	119
6.4.	Change in Pressure in the Combustion Chamber.....	127
6.5.	Factors Affecting the Completeness of Combustion and Stability of Combustion of the Fuel.....	136
6.6.	Determination of Relative Fuel Consumption in the Combustion Chamber.....	141
Chapter 7.	Exhaust Systems of Jet Engines.....	143
7.1.	Purpose of Exhaust Systems of Jet Engines and Basic Requirements of Them.....	143
7.2.	Process of the Outflow of Gas from the Jet Nozzle...	144

7.3.	Methods of Estimating Losses in the Jet Nozzle.....	146
7.4.	Control of Process of Work of Engine.....	150
7.5.	Adjustment of the Jet Nozzle at Supersonic Flight Speeds.....	152
7.6.	Gas-Dynamic and Design Diagrams of Jet Nozzles.....	159
7.7.	Concept on Base (Stern) Drag of the Exhaust System of the Engine.....	168
Chapter 8.	Mixing Chambers of the Jet Engine.....	172
8.1.	Principles of the Theory of the Mixing of Gas Flows in the Jet Engine.....	172
8.2.	Process of Mixing in the Cylindrical Chamber.....	181

PART THREE  
Turbojet Engines

Chapter 9.	Effect of Parameters of the Working Process on Specific Parameters and Efficiency of the Turbojet Engine.....	188
9.1.	Work of the Real Cycle of the TRD (Internal Work of the Turbojet Engine).....	188
9.2.	Specific Thrust of a Turbojet Engine.....	199
9.3.	Effect of Parameters of the Working Process on Efficiency of the Turbojet Engine.....	202
9.4.	Effect of Parameters of the Working Process on Specific Fuel Consumption.....	213
Chapter 10.	Thermodynamic Principles of the Control of Turbojet Engines.....	220
10.1.	Concept Operational Characteristics of Aircraft Engines.....	220
10.2.	Control Programs of the Engine.....	225
10.3.	Joint Work of Turbine and of Compressor in System TRD.....	231
Chapter 11.	Throttle Characteristics of Turbojet Engines.....	243
11.1.	Concept of Throttle Characteristics of Turbojet Engines.....	243
11.2.	Throttle Characteristic of the Turbojet Engine with Fixed Geometry.....	245
11.3.	Throttle Characteristics of the Turbojet Engine with Special Adjustment.....	260
11.4.	Region of Possible Regimes of Operation of the Turbojet Engine.....	268

11.5.	Unstable Operation of the Compressor (Surging).....	270
11.6.	Nomenclature of Basic Processes of Operation of the Turbojet Engine.....	276
11.7.	Effect of External Atmospheric Conditions on the Work of the Turbojet Engine.....	279
11.8.	Application of the Theory of Gas-Dynamic Similarity to the Turbojet Engine.....	282
Chapter 12.	High-Speed Characteristics of Turbojet Engines....	292
12.1.	High-Speed Characteristics of Single-Shaft Turbojet Engines Without Afterburners.....	292
12.2.	Peculiarities of High-Speed Characteristics of Double-Shaft TRD.....	311
Chapter 13.	Altitude Characteristics of Turbojet Engines.....	314
13.1.	Altitude Characteristics of Single-Shaft Turbojet Engines Without Afterburners.....	314

PART FOUR

Turbojet Engines with Afterburners. Ramjet Engines

Chapter 14.	Methods of Thrust Augmentation.....	323
14.1.	Concept of Thrust Augmentation.....	323
14.2.	Methods of Thrust Augmentation of Gas-Turbine Engines.....	323
14.3.	Comparison of Various Methods of Forcing.....	331
Chapter 15.	Turbojet Engines with Afterburners (TRDF).....	333
15.1.	Peculiarity of the Working Process of the Turbojet Engine with Afterburner.....	333
15.2.	Effect of Parameters of the Working Process on Specific Parameters of the TRDF.....	339
15.3.	Peculiarities of Altitude-High-Speed Characteristics of the Turbojet Engine with Afterburner.....	351
Chapter 16.	Ramjet Engines.....	356
16.1.	Designs and Types of Ramjet Engines.....	356
16.2.	Real Cycle of the Ramjet Engine.....	358
16.3.	Effect of Parameters of the Working Process and Parameters of Flight ( $T_3^*$ , $\sigma_\Sigma^*$ or $\eta_p \eta_c$ , $M_0$ on Specific Parameters of the Ramjet Engine.....	361
16.4.	Characteristics of Ramjet Engines.....	370

PART FIVE  
Ducted-Fan Engines

Chapter 17.	Basic Principles of the Operation and Classification of Aircraft Ducted-Fan Gas Turbines.....	379
17.1.	Concept on Ducted-Fan Aircraft Gas-Turbine Engines.....	379
17.2.	Principle of the Addition of Mass (Mass Transfer) in the Ducted-Fan Jet Engine.....	382
17.3.	Principle of Energy Exchange in the Ducted-Fan Jet Engine.....	387
17.4.	Principle of Operation of Ducted-Fan Engine. Classification of the Ducted-Fan Engine.....	390
17.5.	Thermodynamic Cycle of the Ducted-Fan Engine.....	399
17.6.	Basic Parameters of the Ducted-Fan Engine.....	410
Chapter 18.	Thermodynamic Properties of Nonboosted and Boosted Ducted-Fan Engines.....	415
18.1.	Effect of Bypass Parameter on Specific Parameters of Nonboosted Ducted-Fan Engines.....	415
18.2.	Effect in Parameters of Working Process on the Specific and Dimensionless Parameters of the Ducted-Fan Engine.....	427
18.3.	Heat Balance of Nonboosted Ducted-Fan TRD.....	430
18.4.	Thermodynamic Properties of Boosted Ducted-Fan Engines.....	432
18.5.	Ducted-Fan Engine with the Mixing of Flows.....	446
Chapter 19.	Operational Characteristics of the Ducted-Fan Engine.....	448
19.1.	Thermodynamic Bases of Control of the Ducted-Fan Engine.....	448
19.2.	Throttle Characteristics of Ducted-Fan Jet Engines.	468
19.3.	High-Speed Characteristics of Ducted-Fan Jet Engines.....	485
19.4.	Altitude Characteristics of Ducted-Fan Engines.....	497
19.5.	Peculiarities of Operational Characteristics of Ducted-Fan TRD at High Bypass Ratios.....	502
19.6.	Forcing of Ducted-Fan TRD on Takeoff.....	506

PART SIX  
Turboprop Engines

Chapter 20.	Design of Turboprop Engines and Their Classification. Basic Parameters of the Turboprop Engine.....	511
-------------	---	-----

20.1.	Design and Principle of Operation of the Turboprop Engine.....	511
20.2.	Basic Parameters of the Turboprop Engine.....	517
20.3.	Peculiarity of Expansion Process of Gas in Turboprop Engine.....	523
Chapter 21.	Effect of Parameters of the Working Process on Basic Parameters of the Turboprop Engine.....	526
21.1.	Optimum Distribution of Work of the Cycle of the Turboprop Engine Between the Propeller and Reaction.....	526
21.2.	Effect of Basic Parameters of the Working Process on Specific Parameters, Efficiency and Effective Fuel Consumption of the Turboprop Engine.....	534
21.3.	Use of Heat Recovery in the Turboprop Engine.....	538
Chapter 22.	Operational Characteristics of the Turboprop Engine.....	546
22.1.	Throttle Characteristics of the Turboprop Engine...	546
22.2.	High-Speed Characteristics of the Turboprop Engine.....	562
22.3.	Altitude Characteristics of the Turboprop Engine...	574

PART SEVEN  
Special Operational Characteristics  
of Aircraft Gas Turbines

Chapter 23.	Starting and Transitional Regimes of Gas Turbines.....	581
23.1.	Starting of the Gas Turbine.....	581
23.2.	Transient Conditions of the Gas Turbine.....	586
23.3.	Accelerating Capacity of the Gas Turbine.....	589
Chapter 24.	Effect of Conditions of Operation on Characteristics of Aircraft Gas Turbines.....	593
24.1.	Effect of Various Operational Factors on the Regime of Operation and Parameters of the Turbojet (Turboramjet) Engine.....	593
24.2.	Limitation of Thrust of the Turbojet Engine at Low Temperatures of the Surrounding Atmosphere.....	598
24.3.	Effect of Humidity of the Atmosphere on Parameters of the Aircraft Gas Turbine.....	600
24.4.	Effect of Thrust Reversing on the Operation of Turbojet Engines.....	602
24.5.	Service Life and Reliability of Aircraft Gas-Turbine Engines.....	605

24.6.	Tapping of Compressed Air (Gas) from Aircraft Gas Turbines.....	608
Chapter 25.	Characteristics of Aircraft Gas Turbines with Respect to the Level of Noise.....	620
25.1.	Noise Source of the Gas-Turbine Engine.....	621
25.2.	Estimation of the Level of Noise of an Outflowing Jet.....	623
25.3.	Methods of Lowering of Level of Noise.....	627
Chapter 26.	Technical-Economic Characteristics of Aircraft Gas Turbines.....	638
26.1.	Criteria of the Estimate of Technical-Economic Effectiveness of Aircraft Gas Turbines.....	638
26.2.	Specific Weight of Aircraft Gas Turbines.....	639
26.3.	Relative Drag of the Engine Nacelle.....	645
26.4.	Specific Weight of the Powerplant and Fuel System.....	647
26.5.	Cost of Transportation of a Ton-Kilometer of Load..	648
Appendix 1.	Nomogram for the Determination of Relative Fuel Consumption of a Jet Engine.....	653
Appendix 2.	Nomogram for the Determination of Specific Parameters of a Ducted-Fan Engine ( $M_0 = 0.8$ ; $H = 11$ km; $T_3^* = 1300^\circ\text{K}$ ).....	654
Appendix 3.	Nomogram for the Determination of Specific Parameters of the Ducted-Fan Engine ( $\gamma = 8$ ).....	654
Bibliography.....		655

U. S. BOARD ON GEOGRAPHIC NAMES TRANSLITERATION SYSTEM

Block	Italic	Transliteration	Block	Italic	Transliteration
А а	<i>А а</i>	A, a	Р р	<i>Р р</i>	R, r
Б б	<i>Б б</i>	B, b	С с	<i>С с</i>	S, s
В в	<i>В в</i>	V, v	Т т	<i>Т т</i>	T, t
Г г	<i>Г г</i>	G, g	У у	<i>У у</i>	U, u
Д д	<i>Д д</i>	D, d	Ф ф	<i>Ф ф</i>	F, f
Е е	<i>Е е</i>	Ye, ye; E, e*	Х х	<i>Х х</i>	Kh, kh
Ж ж	<i>Ж ж</i>	Zh, zh	Ц ц	<i>Ц ц</i>	Ts, ts
З з	<i>З з</i>	Z, z	Ч ч	<i>Ч ч</i>	Ch, ch
И и	<i>И и</i>	I, i	Ш ш	<i>Ш ш</i>	Sh, sh
Й й	<i>Й й</i>	Y, y	Щ щ	<i>Щ щ</i>	Shch, shch
К к	<i>К к</i>	K, k	Ъ ъ	<i>Ъ ъ</i>	"
Л л	<i>Л л</i>	L, l	Ы ы	<i>Ы ы</i>	Y, y
М м	<i>М м</i>	M, m	Ь ь	<i>Ь ь</i>	'
Н н	<i>Н н</i>	N, n	Э э	<i>Э э</i>	E, e
О о	<i>О о</i>	O, o	Ю ю	<i>Ю ю</i>	Yu, yu
П п	<i>П п</i>	P, p	Я я	<i>Я я</i>	Ya, ya

\* ye initially, after vowels, and after ъ, ь; e elsewhere.  
 When written as ѣ in Russian, transliterate as yѣ or ѣ.  
 The use of diacritical marks is preferred, but such marks  
 may be omitted when expediency dictates.

### ACRONYMS AND ABBREVIATIONS

VED	ВД	Jet engine
TRD	ТРД	Turbojet engine
RTD	РТД	Turbojet engine
TVD	ТВД	Turboprop engine
GTD	ГТД	Gas-turbine engine
MKGSS	МКГСС	Meter-kilogramforce-second
SI	СИ	International System of Units
PVRD	ПВД	Ramjet engine
PuVRD	ПуВД	Pulsejet engine
RPD	РПД	Rocket-ramjet engine
MRD	МРД	Jet engine with piston-driven engine
TRDF	ТРДФ	Turboramjet engine
TPD	ТПД	Turboramjet engine
DTRDF	ДТРДФ	Ducted-fan engine with afterburner
RDTT	РДТТ	Solid-propellant rocket engine
ZhRD	ЖРД	Liquid-propellant rocket engine
UPS	УПС	Boundary-layer control
VTOL	СВВП	Vertical takeoff and landing aircraft
DTRD	ДТРД	Ducted-fan turbojet engine
TVID	ТВлД	Turbofan engine
PTV	ПТВ	Turboramjet engine (see Translator's note on page 5)
ZOT	ЗОТ	Zone of reverse flows
s.a	с.а	Nozzle box assembly
RUD	РУД	Engine control level
TK	ТН	Turbocompressor

LRR	ЛРР	Line of operating regimes
VD	ВД	High pressure
LD	ЛД	Low pressure
FND	ФНД	Low-pressure compressor
KVD	КВД	High-pressure compressor
TND	ТНД	Low-pressure turbine
TVD	ТВД	High-pressure turbine
RDST	РДСТ	Blended-fuel rocket engine
ED	РД	Jet engine
SG	СГ	Supersonic combustion
DGTD	ДГТД	Ducted-fan gas-turbine engine
KTA	КТА	Command-fuel unit
ISA	ИСА	International Standard Atmosphere
VPP	ВПП	Runway
GSV	ГСВ	Compressed-air generator
RSA	РСА	Control of nozzle box assembly
RRS	РРС	Control of jet nozzle
R.S	Р.С	Jet stream
T	Т	Turbine
V	В	Second circuit
p.v.	п.в	Front fan
z.v.	з.в	Rear fan
n.a	н.а	Guide vane
SMS	СМС	Main-line aircraft
SMVL	СМВЛ	Aircraft of local airlines
m.d.	м.д	Sustainer engine
p.d.	п.д	Lift Engine

The book examines the design operating processes, principles of control and operational characteristics of jet engines of various types used in civil aviation (including turbojet, turboprop and turbofan). The classification of engines is given.

Special attention is given to the analysis of peculiarities of throttle and high-altitude and high-speed characteristics of gas-turbine aircraft engines, and also the study on the effect of various operating conditions on these characteristics.

The book is intended as a textbook for students of mechanical engineering institutes of the Department of Civil Aviation and Civilian Aviation Colleges of the Ministry of Higher and Secondary Special Education.

The book can be used also as a manual for engineers specializing in field of aircraft engine construction.

The article has 12 tables, 376 figures, and a bibliography of 34 names.

Reviewers Prof. A. N. Govorov and Candidate of Technical Sciences V. M. Akimov.

Editor Engineer K. Ya. Zaytseva.

## PREFACE

The book called to the attention of the readers is intended as a textbook for students of mechanical engineering departments of institutes of civil aviation of the Ministry of Civil Aviation and Departments of Civil Aviation [GA] (ГА) Colleges of the Ministry of Higher Secondary Education [MV i SSO] (ИВ и ССО) of the USSR. It is written in accordance with the approved program on the course of the theory of aircraft engines for colleges of Aeroflot.

In compiling the textbook there has been generalized the 20-year experience of reading by the author of lectures on the course of the theory of aircraft engines at the Riga Institute of Civil Air Fleet Engineers.

The book consists of seven parts (26 chapters).

*The first part* (consisting of three chapters) gives general information about jet engines used in civil aviation (design, principle of operation, classification of the VRD; a brief description of the development of the VRD).

*The second part* (consisting of five chapters) gives the theorem of thrust and examines thermodynamic cycles of the VRD and also processes in basic elements of the DVRD except for processes in the compressor and turbine, which, as is known, are studied in detail in a course on turbomachines.

*The third part* (consisting of five chapters) is devoted to research on the theory of turbojet engines. Initially the effect of parameters of the working process on specific parameters and efficiency of the TRD is examined. Then an account of thermodynamic bases of control is given, and operational characteristics of TRD (throttle and high-altitude and high-speed) are examined.

*In the fourth part* of the book (consisting of three chapters) the theory of forced TRD and ramjet VRD is stated.

*The fifth part* (consisting of three chapters) examines in detail the theory two-circuit TRD, including the effect of bypass parameters on specific parameters of the ducted-fan jet engine DTRD and also operational characteristics of the DTRD of various types and schemes.

*In the sixth part* (consisting of three chapters) thermodynamic peculiarities and operational characteristics of turboprop engines, including TVD with heat regeneration are examined.

Finally, *the seventh part* (consisting of four chapters) examines special characteristics of aircraft GTD including starting and transitional processes, characteristics on noise level, and also the technical-economic characteristics of the GTD.

The general theory of the VRD is presented according to method of useful operation of the cycle worked out by Academician B. S. Stechkin and his students.

In accordance with the curriculum the material of the book has the operational directivity, which is expressed in the detailed examination of operational characteristics of aircraft GTD, and in the explanation of physical regularities of processes accomplished in the engines.

Special sections and questions which deepen the program material are distinguished with a brevier.

In working on the book there has been widely used the experience of operation of Soviet gas-turbine engines accumulated in flight subunits of civil aviation and also clinical information data on foreign aircraft engines published in aviation periodicals.

In the book units of measurement in the MKGSS system are used, since at present courses of thermodynamics and turbomachines have not undergone appropriate reorganization, and the necessary reference materials in the International System of Units are absent.

The author expresses deep gratitude to the reviewers - Prof. A. N. Govorov (Kiev) and Candidate of Technical Sciences V. M. Akimov (Moscow) for the valuable remarks expressed by them upon examining the manuscript.

## SYMBOLS

- $p$ ;  $T$ ;  $\gamma$ ;  $\rho$  - pressure, temperature, specific weight, density of gas, respectively;
- $V$  - speed
- $M_0$  -  $M$  flight number;
- $H$  - altitude of flight;
- $R$  - reaction thrust; gas constant;
- $R_{y\Delta}$  - specific thrust;
- $C_{y\Delta}$  - specific fuel consumption;
- $C_e$  - effective fuel consumption;
- $R_{\text{лоб}}$  - frontal thrust;
- $\gamma_{\text{дб}}$  - specific weight of the engine;
- $\pi = e^{\frac{k}{k-1}}$  - degree of compression (expansion);
- $\delta$ ;  $\Delta$  - degree of preheating of the gas during the cycle;
- $G_B$  - mass flow rate of air;
- $G_{\Gamma}$  - mass flow rate of gas;
- $G_T$  - mass flow rate of fuel;
- $x$  - degree of energy exchange;
- $y$  - bypass ratio (coefficient of the distribution of air between ducts); coefficient of ejection;
- $x$ ,  $y$  - bypass parameters;
- $N_H$ ;  $N_T$  - power of the compressor and of turbine, respectively;
- $N_e$  - effective power;

$N_{yA}$  - specific power;  
 $n$  - number of revolutions; polytropic exponent;  
 $u$  - peripheral speed;  
 $\alpha$  - coefficient of air surplus;  
 $m_T$  - relative fuel consumption;  
 $\xi_{H.C}$  - coefficient of completeness of combustion;  
 $L_{ad}$  - adiabatic work;  
 $L_{пол}$  - polytropic work;  
 $L_f$  - work of friction;  
 $L_T; L_H; L_p; L_C$  - work of the turbine, compressor, expansion and compression, respectively;  
 $L_e$  - effective (useful) work of the cycle;  
 $q_{BH}$  - thermochemical energy of fuel referred to 1 kg of air;  
 $q_I$  - heat imparted to 1 kg of air (supplied heat);  
 $q_{II}$  - removed heat;  
 $\eta$  - efficiency;  
 $\eta_H; \eta_T; \eta_p; \eta_C$  - efficiency of compressor, turbine expansion and compression, respectively;  
 $\eta_B$  - efficiency of a propeller;  
 $\eta_e$  - effective efficiency;  
 $\eta_R$  - thrust efficiency;  
 $\eta_0$  - total efficiency;  
 $c$  - speed of gas;  
 $a$  - speed of sound;  
 $M$  - Mach number;  
 $D$  - diameter;  
 $l, x$  - length;  
 $f$  - area of cross section;  
 $c_p; c_v$  - specific heat of gas at constant pressure and at constant volume, respectively;  
 $k = c_p/c_v$  - specific heat ratio;  
 $\bar{d}$  - hub-tip ratio;  
 $\phi$  - coefficient of velocity; coefficient of consumption;  
 $i$  - enthalpy;  
 $\beta$  - air (gas) bleeding factor;  
 $\sigma^*$  - coefficient of the conservation of complete pressure;

$f(\lambda)$ ;  $q(\lambda)$ ;  $\mu(\lambda)$ ;  $z(\lambda)$ ;  $y(\lambda)$  - gas-dynamic functions.

### Superscripts and Subscripts

\* - parameters of braked flow;  
I, II - parameters of the first and second ducts, respectively;  
"''" - the same;  
 $\Phi$  - boost;  
 $\kappa$ ;  $\tau$  - compressor, turbine;  
пр - reduced;  
0 - during operation on the ground ( $V = 0$ );  
р; с - expansion compression;  
в - propeller;  
R - thrust;  
e - effective;  
р.с - reactive (exit) nozzle;  
к.с - combustion chamber;  
 $\Phi$ .к - afterburner;  
н.а - guide vane;  
с.а - nozzle box assembly;  
св.э - free energy;  
см - mixing;  
к.см - mixing chamber;  
р; 0 - calculated;  
ид - ideal;  
лоб - frontal;  
кр - critical;  
э - effective; ejector;  
д - diffuser;  
0 - available, initial;  
н - external;  
в - internal;  
ад - adiabatic;  
пол - polytropic;  
уд - specific;  
дв - engine;

ex - inlet;  
e.c - outlet (exhaust) nozzle;  
T.B - turbine of propeller;  
T.H - turbine of compressor.

Basic Flow Areas

H, 0 - area of undisturbed flow;  
1 - inlet into compressor;  
2 - outlet from compressor (inlet into combustion chamber);  
3 - outlet from combustion chamber;  
4 - outlet from turbine;  
4 $\phi$  - outlet from afterburner;  
5; 5 $\phi$  - outlet from jet nozzle;  
cm; e - outlet from mixing chamber (of the ejector).

P A R T O N E

GENERAL INFORMATION ON JET ENGINES

## C H A P T E R 1

### PRINCIPLE OF OPERATION, DESIGN AND CLASSIFICATION OF JET ENGINES

#### 1.1. Concept of Reactive Force and Jet Engine

From physics it is known that with the action of one body on another with a certain force the second body acts on first with an equal and opposite guided force. The indicated interaction of bodies is expressed by the law of equality of action and counter-action of Newton.

If we call the action of the first body on the second *active force*, then the action of the second body on the first will be called *reactive force*. Judgment about just which force is active and which is reactive is arbitrary.

Forces of interaction are applied to different bodies. When they are not balanced, each of these forces can become the cause of motion.

Let us give several examples of the action of active and reactive forces (Fig. 1.1).

During a shot from a gun gunpowder gases, expanding under the action of high pressure, eject with great force a projectile from the channel of the barrel; the force of return of gases appearing here is reactive force. Actually, during movement of the projectile in the channel of the barrel there is an interaction of two bodies -

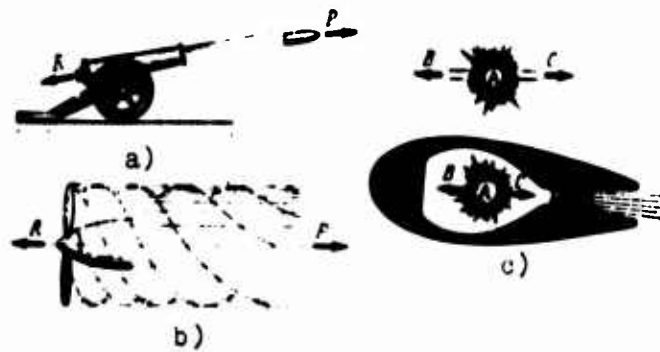


Fig. 1.1. Examples of the action active and reactive forces: a) recoil force of a gun; b) reactive thrust of a propeller; c) principle of action of a powder rocket.

the barrel of effluent gases. The end of the barrel "ejects" the gases with a definite force (active force). In turn, gases with the same force act on the end of the barrel; the force acting on the end of channel will be the reactive force or of coil force (see Fig. 1.1a).

On the basis of the flight of an aircraft equipped with an engine with a propeller, there is also the reactive principle. The propeller, in revolving, acts by its working surfaces on the air with force  $P$  and rejects with definite velocity a large mass of air. In turn, the jet of air acts with equal and opposite force  $R = P$  on the propeller and creates thrust, which moves the aircraft in a direction opposite to the movement of the jet (see Fig. 1.1b). Thus, the thrust of the propeller is the result of reactive action of rejected air masses on the propeller.

Finally, this principle is assumed as the basis of motion of the standard powder rocket. Powder gases, flowing out under the action of high pressure with an enormous velocity back, are repulsed from walls of the nozzle; the appearing reaction moves the rocket forward (see Fig. 1.1c).

In this case what we will call a reaction engine if in any engine the reactive principle is used.

A *reaction engine* is such a thermal engine whose thermal energy, which was liberated during combustion of the fuel, directly turns into kinetic energy of the gas flow, and the appearing reaction is used as a moving force or thrust. Such an engine is called engine of direct reaction, as opposed to engines of indirect reaction, which refers, for example, to piston propeller-driven unit; in this latter case the thermal energy turns preliminarily with the help of crank-connecting rod mechanism into mechanical energy of rotation of the propeller shaft (*engine* itself) and then the mechanical energy of rotation of the propeller turns into work of thrust as a result of the rejection of air masses (*propelling agent*).

A reaction engine does not have intermediate links for the conversion of energy (crank-connecting rod mechanism, reduction gear etc.); it also does not have a separate propelling agent creating a moving force (thrust), which are for example, wheels of an automobile, caterpillar tracks of a tractor, water propeller of a steamer, propeller of an aircraft, hydroplane and snowmobiles.

A reaction engine combines the function of an engine and that of the propelling agent, and in this sense it must be compared not simply with a piston engine but with propeller-driven engine, which is the combination of an engine with a propelling agent.

## 1.2. Classification of Reaction Engines

The classification of *thermal reaction engines* (Fig. 1.2, 1.3), first of all, is connected with the kind chemical fuel used and methods of its obtaining and use.

It is known that the heat energy expended for the creation of tractive work of a reactive engine is released as a result of the thermochemical reaction of combustion or oxidation. Realization of this reaction appears possible, as a rule, in the presence of two components of fuel: *combustible* and *oxidizer*.

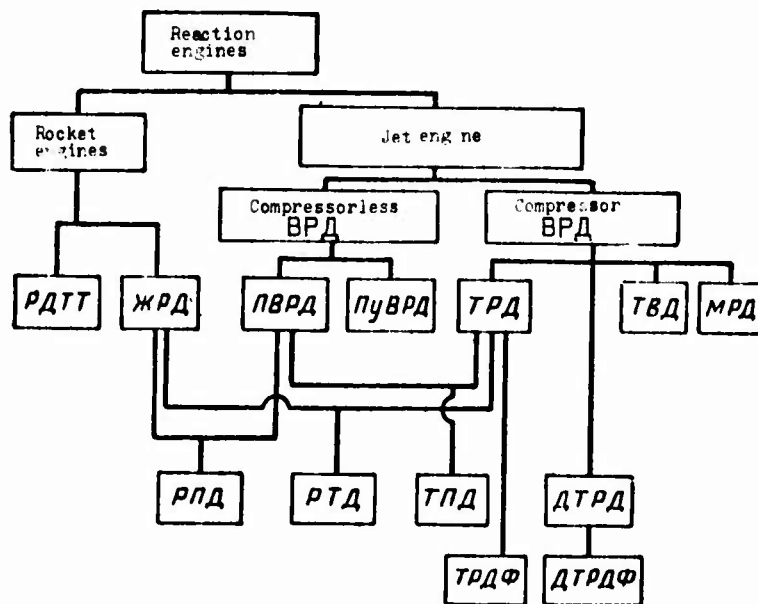


Fig. 1.2. Classification of reaction engines (according to the type of fuel used and principle of operation).

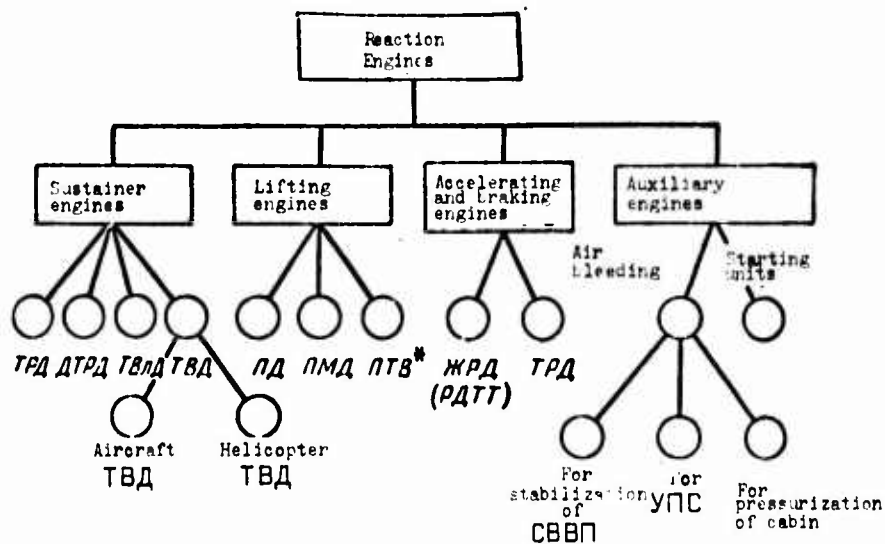


Fig. 1.3. Classification of reaction engines used in civil aviation (according to the purpose and duration of operation).

[Translator's Note: ПТВ - this acronym was not found and possibly should be ПТД (turboramjet engine)].

To ensure continuous operation of an engine in flight, on aircraft there must be a sufficient fuel reserve. The oxidizer can also earlier be stored in the form of various oxygen-containing solid and liquid substances. As an oxidizer it is convenient to use atmospheric air - up to very high altitudes (30-50 km) the atmosphere contains about 20% (in weight) oxygen.

Depending on the method of obtaining and using the oxidizer reaction engines are subdivided into two large classes: *rocket* (RD) and *jet engines* (VRD).

Rocket engines, in turn, are subdivided in accordance with the phase state of the fuel used on *solid-propellant rocket engines* (RDTP) and *liquid-propellant rocket engines* (ZhRD).

Used as solid fuel (containing both the combustible and oxidizer) is smokeless powder (charges of plasticized nitrocelluloses and nitroglycerine) and in recent years - a mixture of a polymer combustible (rubber with powder-like aluminum) and an active oxygen-containing substances (for example, ammonium perchlorate).<sup>1</sup> Contemporary solid propellant is safe to handle and also useful for prolonged storage. Rocket engines of solid propellant are distinguished by a simplicity of design, high reliability and, which the most important, extreme simplicity of operation. The RDTP are engines of short-term operation, but in two-three minutes they are able to develop enormous pulses.

Liquid propellant used in a ZhRD are extraordinarily diverse. The most widespread and effective of them (according to data given in the foreign press) are the following:

*oxidizer* - nitric acid, liquid oxygen, tetroxide of nitrogen, hydrogen peroxide and others;

---

<sup>1</sup>See Siplach, Effect of rapid pressure drop on the combustion of solid propellant, "Rocket Technology" (ARS Journal in Russian translation), 1961, Vol. 31, No. 11).

*combustibles* - kerosene, alcohol, hydrazine, pentaborane, liquid hydrogen and others.

The enumerated propellants and oxidizer form various kinds of so-called *bipropellant*.

In several ZhRD a single-component fuel, for example, hydrogen peroxide is used. The latter under the action of a catalyst decomposes, forming a working medium - a highly heated mixture of water vapor and oxygen.

Fuels used in ZhRD are characterized by relative cheapness and high calorific power. However, in most cases they are toxic, unstable in storage and are dangerously explosive.

The ZhRD are engines of lasting operation; they allow controlling the thrust over wide limits. Their design is incomparably complicated, and their specific weight is more than that of the RDTT. Operation of the ZhRD requires special measures of precaution.

In recent years "hybrids" of RDTT and ZhRD - *rocket engines of mixed fuel* (RDST) have appeared and rapidly found widespread use. The development of these engines is connected with the trend of combining in them the merits of the RDTT and ZhRD and get rid of deficiencies of engines of these types. In RDST solid combustible and liquid oxidizer are used. Used as a solid propellant is a polymer with powder-like aluminium, and as an oxidizer - nitric acid or hydrogen peroxide. If for the RDTT the fuel (in the form of charges or of unit-casting) fills the volume of the combustion chamber of the engine, for the ZhRD the fuel is stored in separate tanks of the combustible and oxidizer, then for the RDST the solid propellant is contained in the combustion chamber and the liquid oxidizer in a special tank (see work [24]).

Since fuel for rocket engine is stored on-board the vehicle (either directly in the volume of the design of the engine itself or in tanks), then the feed of the rocket engines with the combustible

and oxidizer depends on the condition of the surrounding medium and flight regime. Therefore, rocket engines can be used for flights at very great heights and in space and also over a wide range of supersonic, hypersonic and orbital flight speeds. It is necessary to note that the thrust generated by the rocket engines and their fuel consumption practically do not depend on the altitude and speed of flight.<sup>1</sup>

We have already noted that used as an oxidizer in reaction engines is the oxygen of the surrounding atmosphere, and as the propellant for jet engines common kerosene is used.

It is known that with an increase in altitude air density is diminished, and on very great altitudes the content of oxygen in the air is decreased also. Thus the mass flow of the oxidizer and, consequently, propellant<sup>2</sup> with an increase in altitude of flight of the flight vehicle is decreased. Consequently, the thrust of the jet engine with an increase in flight altitude unavoidably decreases. Thus, the reaction engine is a low-level engine. The effectiveness of its operation is limited by a flight altitude of 30-50 km.

On the other hand, the thrust of a jet engine to a certain extent depends on the flight speed. The greater the flight speed, the greater the inlet pulse of the engine, and the more difficult it is to increase the discharge pulse of the engine. This leads to the fact at high speeds of flight the thrust<sup>3</sup> generated by any jet engine unavoidably begins to drop down to zero. Thus the jet engine is an engine of limited range of flight speeds. The maximum  $M_0$  number of flight of a flying vehicle with a jet engine is different for different types of engines; it depends on a number of design factors and for

---

<sup>1</sup>More accurately, with an increase in altitude the thrust of the rocket engine somewhat increases.

<sup>2</sup>To ensure complete burning of the fuel, the percent ratio of the propellant and oxidizer in the fuel-air mixture must be maintained constant.

<sup>3</sup>The thrust of a jet engine is determined by the differences in the discharge and inlet pulses, i.e.  $R = (M_{\text{out}} c)_{\text{out}} - (M_{\text{in}} c)_{\text{in}}$ .

jet engines of standard designs and types does not exceed  $M_0 = 4-6$ . But jet engines in the region of their preferential use are much more economical than rocket engines whose expenditures for operation to a certain extent are determined by the consumption of an enormous quantity of a special oxidizer.

Reaction engines are extremely diverse in their design, scheme and principle of operation. Depending on the method of air compression, they are subdivided into *compressorless* and *compressor* jet engines.

In compressorless jet engines air compression is accomplished only due to *impact pressure*, i.e., kinetic energy of incident air flow. Such engines are *ramjet engines* (PVRD) and *pulsejet engines* (PuVRD).

Ramjet engines are intended for high supersonic flight speeds. They are extraordinarily simple in design and have little specific weight and good economy in the rated flight regime; however, they are ineffective at low speeds of flight and, specifically, cannot operate and develop thrust in flight. It was attempted to correct this organic flaw of the ramjet engine by transition to a pulsing process of supplying air and combustion of fuel in the engine, at which an increase in air pressure occurs without the use of impact pressure and a compressor.

The principle of operation of the pulse combustion chamber was first developed by the Russian engineer V. V. Karavodin in 1908. The pulsejet engine was developed at the end of the Second World War and was installed by the Germans on "V-1" missiles. Further development of pulsejet engines was not carried out.

In compressors of jet engines air compression is carried out by *mechanical means* with the help of axial or centrifugal types of compressors. These compressors are driven by gas turbines. Such engines are called *gas-turbine engines* (GTD), since in them the most important design element, the source of mechanical rotational energy, is the gas turbine.

There have been attempts to drive compressors of the jet engine by means of a piston engine. However, such jet engines with a *piston-driven compressor* (MRD) proved to be too heavy, bulky and uneconomical. An example of an MRD engine is an engine which was installed on the aircraft of Campini, who accomplished several flights in 1940-1942, and further development of this type of engine did not continue.

Aircraft gas-turbine engines, in turn, are subdivided into *turbojet* (TRD), *turboprop* (TRP) and *ducted-fan turbojet engine* (DFTRD).

When the power of the gas turbine is equal to the power of the compressor, the aircraft gas turbine is called a turbojet engine. In a TRD all the useful operation of the cycle is expended for increasing the kinetic energy of the working medium, for accelerating the flow inside the engine, and for the creation of thrust.

When the power of gas turbine is used also for rotation of the propeller, of the blower or an additional compressor in the *second duct* of the engine, the aircraft gas turbine is correspondingly called a turboprop, turbofan or ducted-fan TRD. In these engines the reactive thrust is created in two ducts, i.e., they have two propelling agents.

The ducted-fan gas turbines, while being more complex in a design respect, are distinguished by high economy and good operational characteristics. Combination of the turbojet and ramjet engines also forms a variety of a ducted-fan gas turbine - *turbo-ramjet engine* (TRPD).

Aircraft gas-turbine engines have become extraordinarily wide spread in air transport because of their high economy, great service life, which provide them the possibility of reliably operating for long time, and the comparatively low specific gravity.

Aircraft gas turbines are engines of wide range designed for subsonic and supersonic flight speeds. They form the technical basis of contemporary transport aircraft engine construction. The technical and economic achievements of contemporary civil aviation are connected precisely with the successful development aircraft GTD and with the high level of their technical perfection.

The peculiarities described above of rocket and jet engines and their comparative merits and deficiencies have led to attempts of the creation of mixed or combined *rocket-jet engines*, which, on idea, must possess considerable advantages over the "original" engines and could be successfully used in a wide range of altitudes and  $M_0$  numbers of flight. Such engines are the *rocket-ramjet engines* (RPD) and *rocket-turbine engines* (RTD).

### 1.3. Layouts, Design and Principle of Operation of Jet Engines

#### 1.3.1. Ramjet Engine [PVRD)

The ramjet engine (Fig. 1.4) is the simplest jet engine. It consists of an inlet supersonic diffuser 1, ramjet combustion chamber 2, equipped with a frontal, device 3 for fuel injection, the formation of a fuel-air mixture and flame stabilization, and also a supersonic discharge nozzle of the type of Laval nozzle 4.

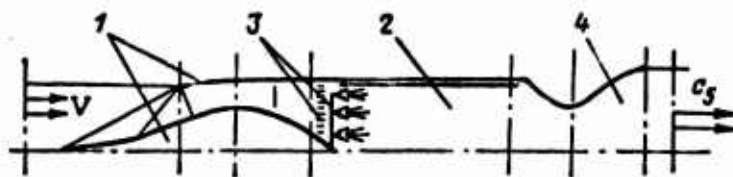


Fig. 1.4. Diagram of a ramjet engine (PVRD):  
1 - inlet supersonic diffuser; 2 - ramjet combustion chamber; 3 - device for fuel injection and of flames stabilization; 4 - discharge nozzle.

In the diffuser of the ramjet engine at supersonic flight speeds deceleration of the flow is carried out by a system of oblique shocks, as a result of which there is an intensive increase in air pressure with little losses.

In the combustion chamber, as a result of the combustion of the fuel-air mixture, combustion products of high temperatures are generated. Since in the gas and air channel of the PVRD mobile elements are absent, then the temperature of the gases at the outlet from the combustion chamber can be raised up to its limiting value ( $T_3^* = 2000-2800^{\circ}\text{K}$ ), which corresponds to the stoichiometric mixture ratio ( $\alpha = 1.0$ ).

In the discharge nozzle of the PVRD there is expansion of the gases up to the external pressure (counterpressure), as a result of which they flow out into the surrounding medium at high speed, forming a discharge pulse of the engine.

Ramjet engines are intended for use as the basic power plant of flight vehicle at high supersonic flight speeds ( $M_0 > 3.0$ ).

### 1.3.2. Turbojet Engine (TRD)

The TRD (Fig. 1.5a) is the simplest type of aircraft gas turbine. The basic design elements are: inlet device B multi-stage axial compressor (one-or two-shaft) K with a developed mechanism and control system, combustion chamber K.C. mostly of the annular type with individual flame tubes and sprayers for effective fuel combustion, one-or two-stage axial turbine T and a jet nozzle P.C. When a short-term increase (boost) of thrust of the engine is necessary, after the turbine of the TRD a transient diffuser D and afterburners O.K. are installed (see Fig. 1.5b).

The turbojet engine operates on the thermodynamic Brayton cycle in the following manner: in flight the air from the external medium is sucked into the inlet device. The axial velocity in front of the compressor reaches 150-200 m/s, and the rarefaction

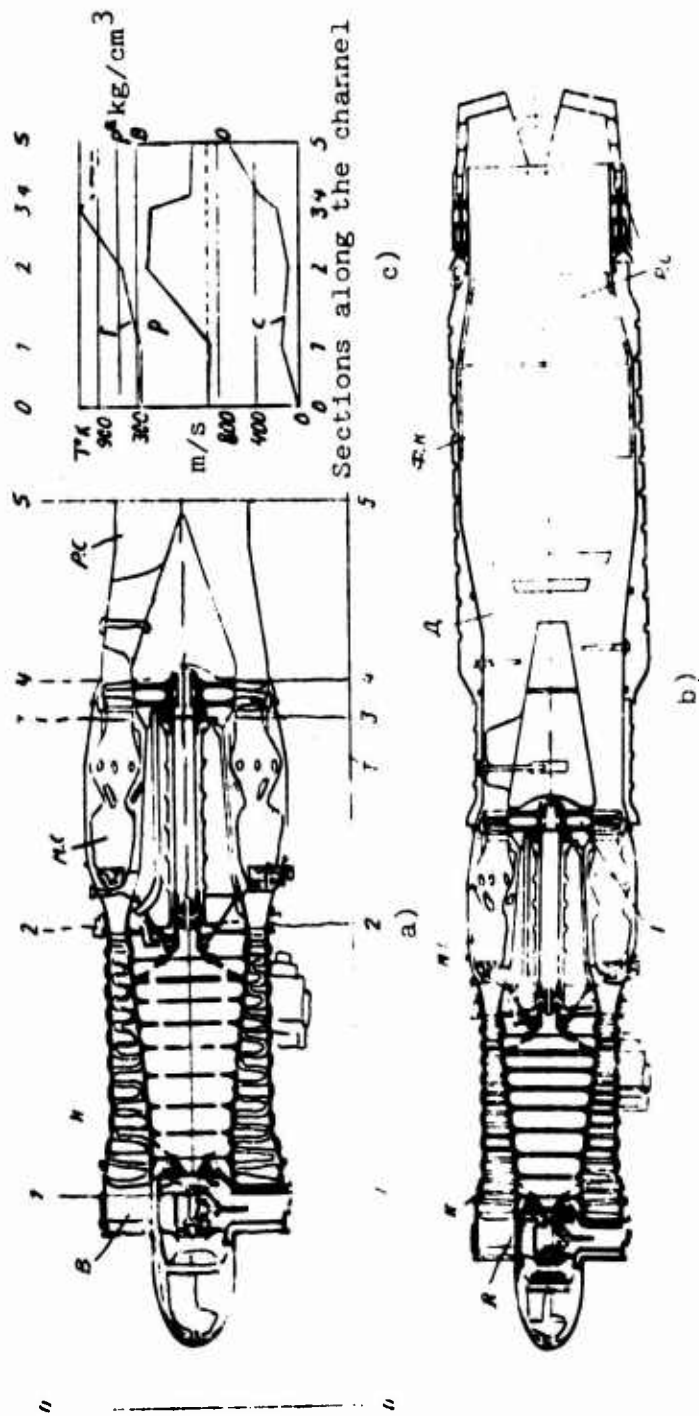


Fig. 1.5. Diagrams of turbojet engines: a) TRD; b) TRDF; c) curves of the change in parameters of gas along the gas-air channel of the engine.

appearing here is respectively equal to  $\Delta p = 0.15-0.20$  at. In flight at high speeds the air undergoes dynamic compression in the free jet and in the supersonic diffuser. The second step of compression is the multi-stage axial compressor. Compressors of TRD have compression ratios  $\pi_{\text{H0}}^* = 6-14$  and consist of 7-17 stages. Preheating of the air in the compressor is  $220^\circ-380^\circ$ . The axial velocity at the outlet from the compressor is equal to 100-120 m/s.

As a result of the combustion of the fuel-air mixture in the combustion chamber, the temperature of working medium reaches  $1100^\circ-1400^\circ\text{K}$ ; in this case the pressure of the gas drops 3-6%.

The obtained combustion products are expanded in the turbine (first stages of expansion) for the creation of power necessary to drive the compressor, and, finally, are expanded in the discharge nozzle (second step of expansions). The axial gas velocity at the inlet into the turbine is equal to 180-200 m/s ( $M_{3a} = 0.15-0.20$ ) and at the exit from the turbine, 300-450 m/s ( $M_{4a} = 0.50-0.75$ ).

The velocity of outflow of gases from the jet nozzle during complete expansion reaches 600-750 m/s. The temperature at the outlet from the nozzle is equal to  $900-1000^\circ\text{K}$ . At high  $T^*$  and  $p^*$  the pressure differential in the discharge nozzle on a test stand reaches critical and supercritical values. If the TRD is intended for flight at speeds corresponding to  $M > 1.0$ , then it must be equipped adjust with a discharge nozzle of the Laval type of nozzle. As a result of the outflow of gas at high speed from the discharge nozzle, reaction thrust appears.

Figure 1.5c shows curves of the change in gas parameters ( $p^*$ ,  $T^*$  and  $e$ ) along the gas-air channel of the TRD.

Turbojet engines have received widespread use in military aircraft and partially in transport aircraft. However, in recent years they have been forced out of the air transport by more economic and less "noisy" turbofan engines.

### 1.3.3. Ducted-Fan Engine (DTRD)

The *ducted-fan engine* (Fig. 1.6a and b) is a turbojet engine whose thrust is created in two ducts: gas turbine (first) and fan (second).

The term "*fan*" is conditional: it notes that the compressor of the second duct has considerably less ratio compression than the compressor of main duct. The higher the bypass ratio of the engine ( $\beta$ ), the less ratio the compression of the fan. At high bypass ratios the DTRD is frequently called a turbofan engine (TVLD). There is a large number of ducted-fan TRD of various schemes and types.

The basic design elements of the TVLD (or ducted-fan TRD) are: common intake 1, compressor of the first duct 2, combustion chamber of the first duct 3, multi-stage turbine 4, compressor (fan) of the second duct 5, afterburner of the second duct 6a or common afterburner 6b, discharge nozzles of the first and second ducts (during separate gas outflows) or common discharge nozzle 7 (in the presence of a mixing chamber).

During afterburners the process of forming draught in the second duct in principle does not differ from the process of its formation in the first duct of the DTRD and also in the TRD.

At present the TVLD (DTRD) becomes the basic type of power plant of transport aircraft of main and local air lines.

The main advantages of the DTRD, which provided its widespread introduction into transport aviation, are: high economy at subsonic flight speeds, the possibility of the use of an engine at high supersonic flight speeds, low level of noise produced and, finally, high level of operational reliability.

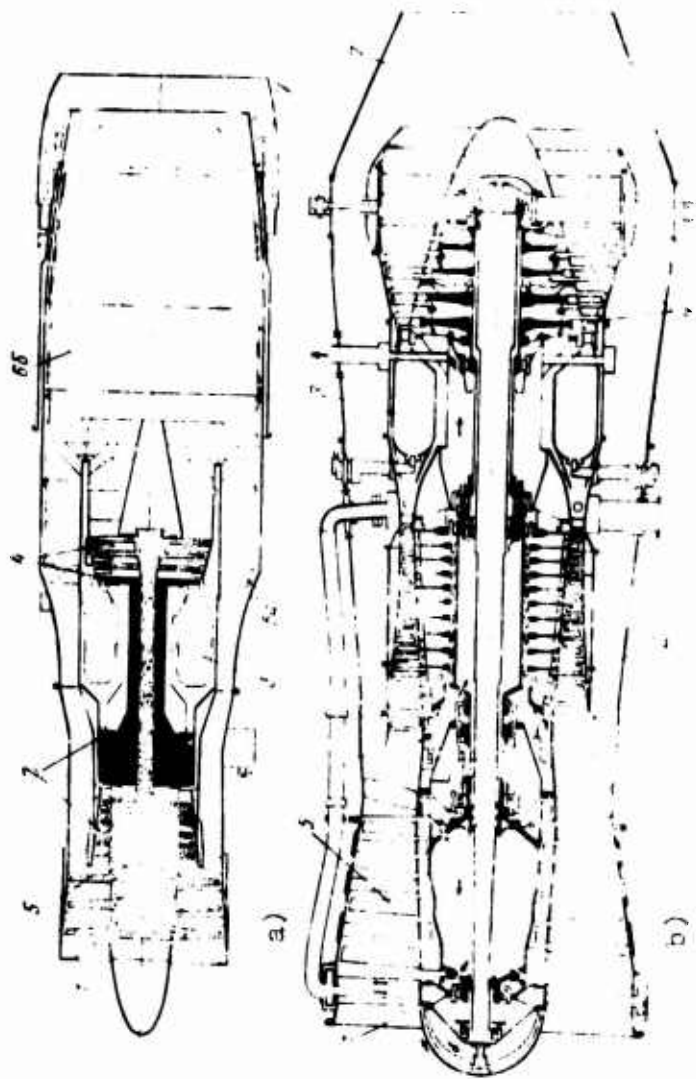


Fig. 1.6. Diagrams of turbofan engines (TVID): 1 - intake; 2 - compressor of the first duct; 3 - combustion chamber of the first duct; 4 - multi-stage turbine; 5 - compressor (fan) of the second duct; 6a - afterburner of the second duct; 6b - afterburner; 7 - discharge nozzle.

### 1.3.3. Ducted-Fan Engine (DTRD)

The ducted-fan engine (Fig. 1.6a and b) is a turbojet engine whose thrust is created in two ducts: gas turbine (first) and fan (second).

The term "fan" is conditional: it notes that the compressor of the second duct has considerably less ratio compression than the compressor of main duct. The higher the bypass ratio of the engine ( $\frac{u_1}{u_2}$ ), the less ratio the compression of the fan. At high bypass ratios the DTRD is frequently called a turbofan engine (TV1D). There is a large number of ducted-fan TRD of various schemes and types.

The basic design elements of the TV1D (or ducted-fan TRD) are: common intake 1, compressor of the first duct 2, combustion chamber the first duct 3, multi-stage turbine 4, compressor (fan) of the second duct 5, afterburner of the second duct 6a or common afterburner 6b, discharge nozzles of the first and second ducts (during separate gas outflows) or common discharge nozzle 7 (in the presence of a mixing chamber).

During afterburners the process of forming draught in the second duct in principle does not differ from the process of its formation in the first duct of the DTRD and also in the TRD.

At present the TV1D (DTRD) becomes the basic type of power plant of transport aircraft of main and local air lines.

The main advantages of the DTRD, which provided its widespread introduction into transport aviation, are: high economy at subsonic flight speeds, the possibility of the use of an engine at high supersonic flight speeds, low level of noise produced and, finally, high level of operational reliability.

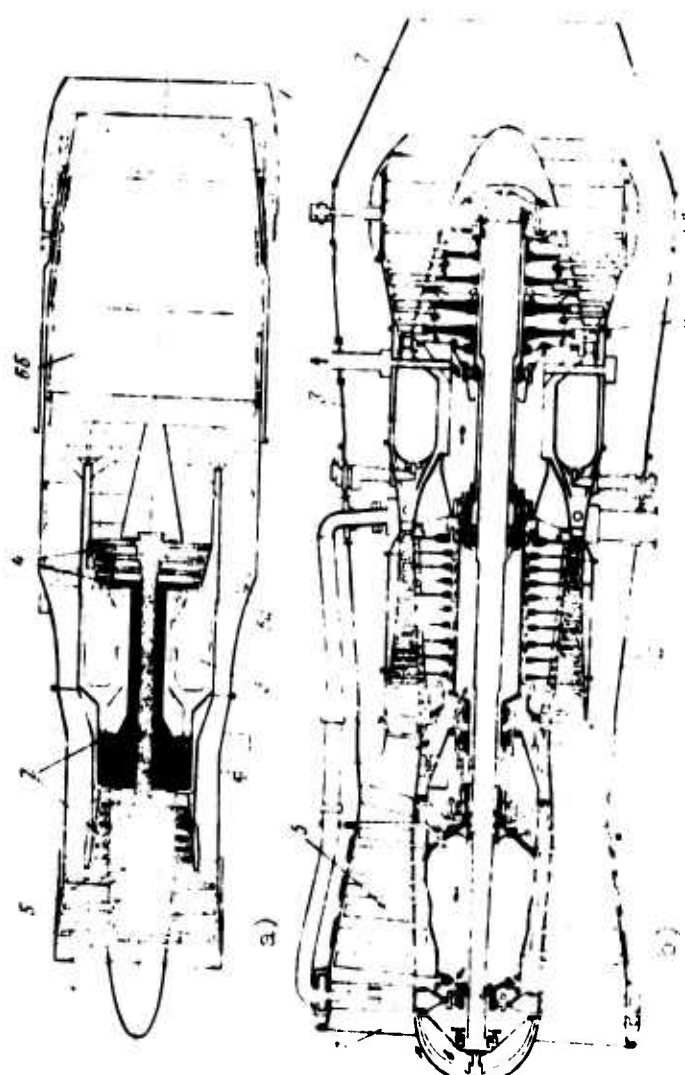


Fig. 1.6. Diagrams of turbofan engines (TVID): 1 - intake; 2 - compressor of the first duct; 3 - combustion chamber of the first duct; 4 - multi-stage turbine; 5 - compressor (fan) of the second duct; 6a - afterburner of the second duct; 6b - afterburner; 7 - discharge nozzle.

#### 1.3.4. Turboprop Engine (TVD)

Since the thrust of a turboprop engine is added from two components, the thrust of the propeller and of reaction thrust appearing in the gas-turbine duct, then the TVD's commonly refers to engines of *indirect reaction* and also *mixed thrust*.

At the same time, the TVD can be conditionally added to the class of *aircraft ducted-fan gas turbine engines*.

The basic design elements of the TVD (Fig. 1.7) are: shaft of propeller 1, reduction gear 2, intake 3, compressor 4, combustion chamber 5, multi-stage turbine 6, exhaust 7.

The working processes in a TVD and TRD in principle are not different from each other; only in the TVD because of the less pressure differential in the discharge nozzle there is considerably less speed of outflow. The reactive component of thrust of the TVD on a test stand does not exceed 10%.

Aircraft with TVD are widely used in air transport at subsonic flight speeds ( $V = 400-700$  km/h). The TVD's provide good takeoff and landing characteristics of aircraft, but in operation they are considerably more complex, than the TRD.

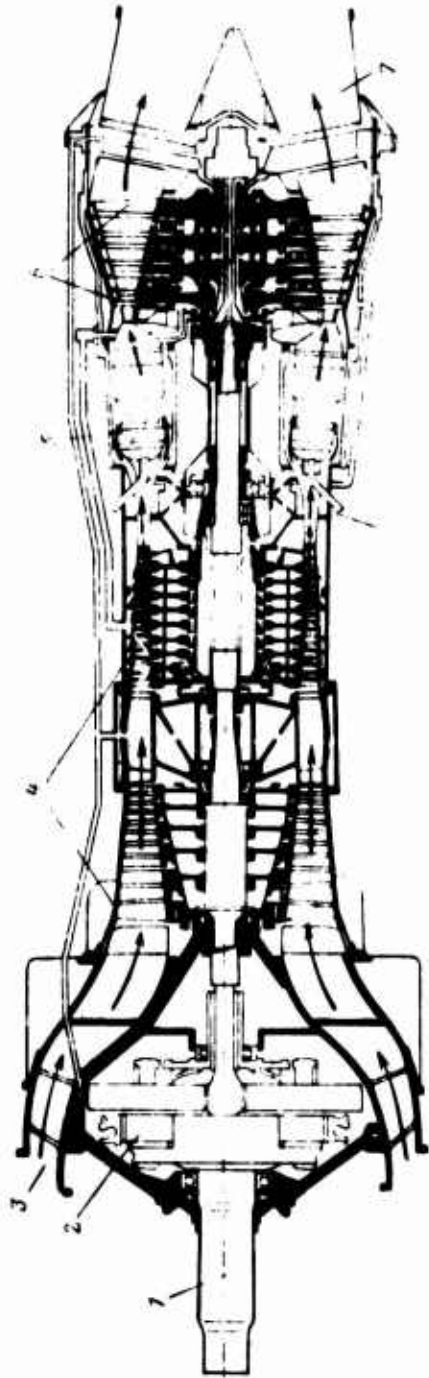


Fig. 1.7. Diagram of a turboprop engine (TVD): 1 - shaft of propeller; 2 - reduction gear; 3 - intake; 4 - compressor; 5 - combustion chamber; 6 - multi-stage turbine; 7 - exhaust.

## CHAPTER 2

### BRIEF DESCRIPTION OF THE HISTORY OF DEVELOPMENT OF REACTION ENGINES

#### 2.1. From Gunpowder Rockets to First Designs of Reaction Engines

The principle of reactive propulsion has long been known to science, and humanity has used it even from ancient times. The initial form of reaction flying vehicles was the gunpowder rocket, which was used for fireworks and also for combat purposes.

First references to rockets are found in ancient Indian and Chinese characters several centuries ago up to our era. In the 12th and 13th centuries Chinese and Arabs widely used reaction arrows equipped with gunpowder charge placed in a small paper cone, which provided them with great distance, accuracy of hit and a penetrative force.

In the 17th and 18th centuries the majority of the European armies showed an interest in the rocket weapon. It is known that Peter the First established in 1710 in Moscow a "Rocket Institution" for the manufacture of rockets and training of specialists on rocket methane. At the end of the 18th century troops of Indian principalities in severe battles with English colonizers used combat rockets on a mass scale. Subsequently, the production of these rockets was studied and adjusted by the enterprising Englishman Congrave. During the Napoleonic Wars the English widely used the combat rockets of Congrave in battles against the French. In 1812, as a

as a result of bombardment by these rockets Copenhagen was burned.

An enthusiast of development of combat rockets in Russia at the beginning of the 19th century was General A. Mazudko. Igniting rockets were used by the Russian and Anglo-French troops during the Crimean War of 1853-1856.

One of the most prominent specialists in field of rocket building in the 19th century was the Russian scientist and artilleryman General K. I. Constantinov. His rockets were successfully used by Russian troops against the Turks in the Russian-Turkish War of 1877-1878. General Constantinov in his work "Combat rockets" was the first who made the important conclusion on the uneconomic use of rockets at low flight speeds.

The gunpowder rocket of the 19th century could not yet be examined as a reaction engine because the time of its operation was very brief, the force of thrust was not regulated, and range of use was too limited.

The Great English Scientist I. Newton is given credit for the invention of the reaction vehicle (1680) being driven by reaction of a jet of steam flowing out of a long nozzle (Fig. 2.1). This vehicle consisted of a burner, a boiler with a nozzle and valve of regulating the velocity of outflow of steam and was a prototype of the reaction power plant with forward motion.

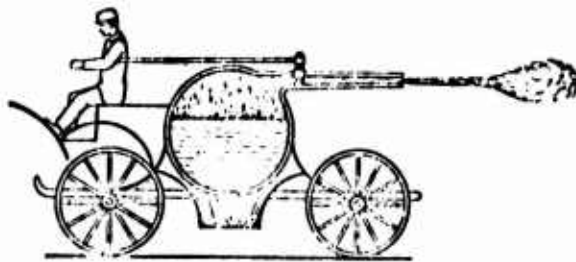


Fig. 2.1. Reaction vehicle of Newton (17th century).

In the 19th century there appeared the first projects of aircraft reaction engines for controlled flying vehicles. Among them an important place is occupied by designs of Russian inventors: I. I. Treteskiy (1849), N. M. Sokovnin (1866), Teleshov (1867), N. I. Kibal'chick (1881), F. Geshvend (1886) and others.

In design of military engineer I. I. Treteskiy and sailor N. M. Sokovnin there were proposals to use for movement of balloons and airships a jet of outflowing compressed air. The design of "thermal blast" of teleshov had basic elements of the contemporary reaction engine: combustion chamber, compressor and reaction nozzle.

The Russian revolutionary and Narodovolets N. I. Kibal'chich, not long before his execution, for the first time substantiated the idea and developed a scheme of an aeronautical apparatus heavier than air with a gunpowder rocket engine. According to the scheme of Kibal'chich the reaction force must be created by gases, flowing from the engine as a result continuous combustion of the charges of pressed powder. The engine (Fig. 2.2) was a cylinder vertically installed on stands above the platform. By changing the position of the cylinder relative to the platform, N. I. Kibal'chich was able to move the apparatus in any direction including the horizontal.

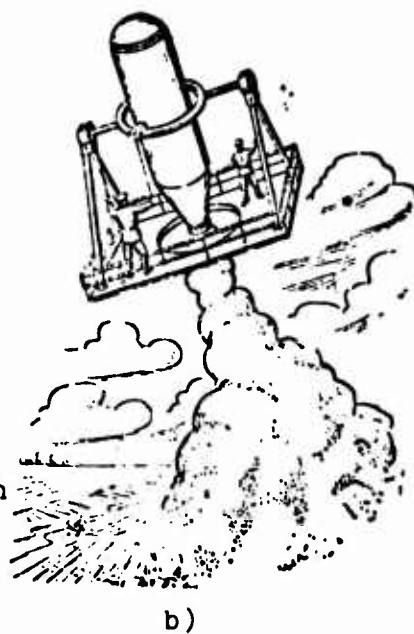
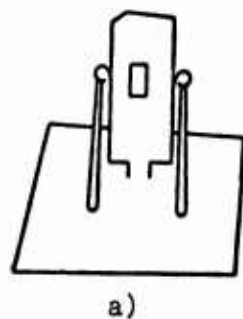


Fig. 2.2. Gunpowder rocket engine of N. I. Kibal'chich (1881): a) sketch of the author; b) sketch of the artist.

Engineer F. Geshvend proposed the original design of a reaction engine developed by him for an aircraft. Used in the engine for the first time was the system of a multi-stage ejector, which served for sucking additional air masses for the purpose of increasing the thrust and efficiency of the power plant. The propulsion system of the aeronautical apparatus of F. Geshvend (Fig. 2.3) consisted of a source of gas, pipeline and an ejector located under the wing. A similar design 34 years later was accomplished by the Frenchman Melot, to whom was attributed preeminence in the creation of such adapters.

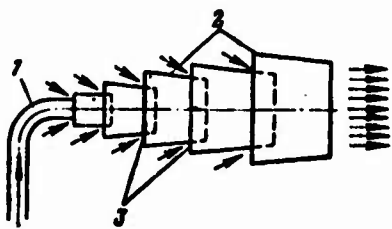


Fig. 2.3. Aeronautical apparatus of F. Geshvend (1886): 1 - working nozzle; 2 - adapters; 3 - slots.

In the beginning of the 20th century there appeared technically validated designs of basic types of jet engines. These include designs of Russian engineers: Antonovich (1909), N. Gerasimov (1909), A. Gorokhov (1911), M. N. Nikol'skiy (1914), V. I. Bazarov (1924) and the design of the ramjet jet engine (1913) of the Frenchman Loren.

The first turbojet engine was invented in Russia by engineer N. Gerasimov.

The first scheme of a pulsing VRD was proposed by engineer Antonovich and was a pipe of variable section open on one end with a distributive mechanism for regulating the air feed. The scheme of Antonovich was used in 1942 by Schmidt during the creation of the winged missile "V-1".

A piston-driven compressor jet engine was developed first by engineer A. Gorokhov. The engine of A. Gorokhov (Fig. 2.4) consisted of two combustion chambers, jet nozzles, and tanks with

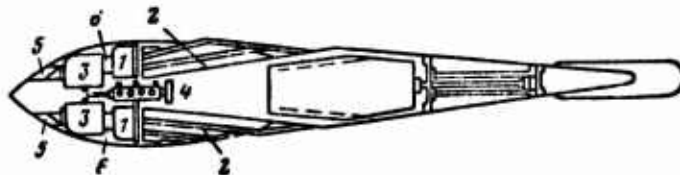


Fig. 2.4. Piston-driven compressor VRD of A. Gorokhov (1911): 1 - combustion chamber; 2 - nozzles; 3 - compressors; 4 - engine for driving of compressor; 5 - inlet channels; 6 - valves for air inlet into combustion chambers.

pipelines. The air entered through the intake into piston compressors of the engine, was compressed in them, and then through valves was guided into combustion chambers where special pumps injected the fuel. Combustion products from the chamber entered into the nozzle, from where they flowed out at high speed into the atmosphere, creating reaction thrust.

The original design of the turboprop aircraft engine was developed by officer M. N. Nikol'skiy. In this engine (Fig. 2.5) the propeller was driven by a three-stage gas turbine operating on combustion products of turpentine and nitric acid. Gases flowing from the turbine were guided into the nozzle and created an additional reaction thrust. In 1914 at a Russian-Baltic plant the building of M. N. Nikol'skiy turboprop engines with a power of 160 hp was started. It was proposed to install four such engines on the aircraft "Il'ya Muromets."

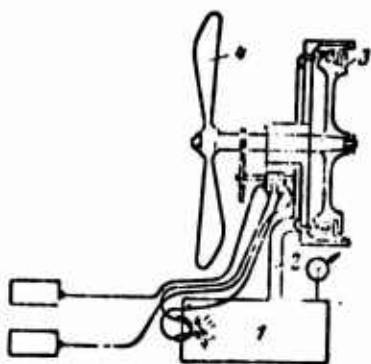


Fig. 2.5. Turboprop engine of M. N. Nikol'skiy (1914): 1 - combustion chamber; 2 - pipeline; 3 - turbine; 4 - propeller.

Further development of the turboprop engine was found in the design of V. I. Bazarov, who offered a new scheme very similar to the contemporary. The basic elements of the TVD of V. I. Bazarov (Fig. 2.6) are: centrifugal compressor, combustion chamber, turbine, discharge nozzle and propeller. In the combustion chamber of the engine of V. I. Bazarov for the first time was applied the principle of the division of air flow into the "primary" and "secondary".

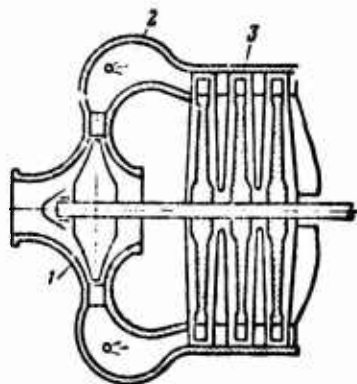


Fig. 2.6. Turboprop engine of V. I. Bazarov (1924): 1 - compressor; 2 - combustion chamber; 3 - turbine.

## 2.2. Development of Principles of the Theory of Reaction Engines

At the end of the 19th century and the beginning of the 20th century works of famous Russian scientists N. Ye. Zhukovskiy, I. V. Meshcherskiy, K. Ye. Tsiolkovskiy developed basic positions of the theory of reaction motion, which unconditionally furthered subsequent scientific and engineering-technical substantiated development of reaction engines.

One of the founders of the theory of reaction motion is rightly considered the famous Russian scientist Nikolay Yegorovich Zhukovskiy. In his words "On the reaction of effluent and inflowing liquid" and "On the theory of vessels driven by the force of reaction effluent water", published, respectively, in 1882-1886 and in 1908, N. Ye. Zhukovskiy was the first to derive the formula for determining the force of reaction and investigated in detail the tractive efficiency of a jet effluent from a moving vessel.

The theoretical principles of the flight of the rocket are given by Prof. I. V. Meshcherskiy, who first determined the dependence of the path passed by the rocket and its flight velocity on the velocity of outflow of gases, resistances of the air, force of attraction and reserve of fuel. I. V. Meshcherskiy created the theory of motion of bodies of variable mass, which include rockets and jet aircraft.

An enormous merit in the theoretical basis of flights of apparatuses heavier than of air with jet engines and in the development of rocket engines belongs to scientist and inventor Constantin Eduardovich Tsiolkovski.

The first classical work of K. E. Tsiolkovski "Investigation of outer space by reaction devices" which brought subsequently to him world reputation, was published in 1903. This work investigates rocket flight in various conditions and derives motion equations of a rocket known as equations of K. E. Tsiolkovski; it gives a scheme of the system of a liquid reaction engine operating on liquid fuels and liquid oxygen, and the advantage of an engine of this type is substantiated.

K. E. Tsiolkovski proposed to accomplish the feed of liquid components of fuel into the combustion chamber by special pumps and produce cooling of the combustion chamber and nozzle with the components of fuel.

Finally, for control of the rocket at high altitudes, Constantin Eduardovich proposed using controls operating in the flow of gases flowing from the jet nozzle.

During 1911-1912 K. E. Tsiolkovski expressed for the first time the idea about the creation of a stage space rocket, which, in his opinion, allows accomplishing taking man beyond the point of the earth's atmosphere.

In his works on rocket dynamics (1927-1929) K. E. Tsiolkovski

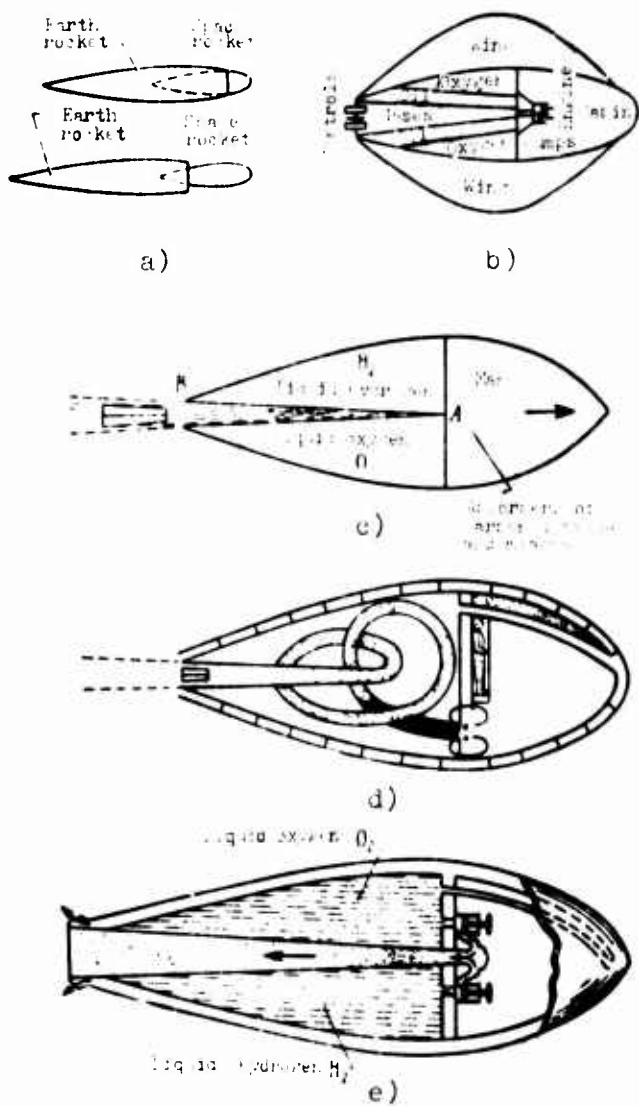


Fig. 2.7. Rockets of K. E. Tsiolkovskiy: a) stage rocket (1929); b) spaceship; c) rocket (1903); d) rocket (1914); e) rocket (1915).

developed the theory of stage rockets, examined advantages and peculiarities of various liquid fuels and oxidizers for the, and also investigated methods of tests of the rockets (1934). He proved the possibility of rocket flight in airless space and calculated the necessary initial velocity of its flight for overcoming the force of the earth's attraction.

K. E. Tsiolkovskiy developed a large number of original schemes of rockets (Fig. 2.7). He also proposed the design of a ducted-fan jet engine (Fig. 2.8).

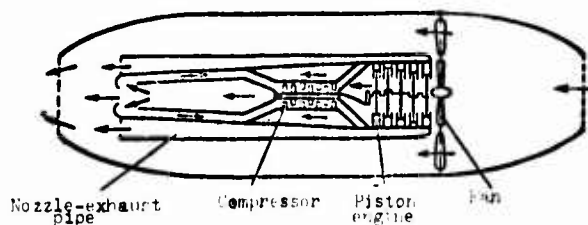


Fig. 2.8. Ducted-fan jet engine of K. E. Tsiolkovskiy (1932).

### 2.3. Development of the First Reaction Engines and Their Subsequent Development

The rapid development of technology in the beginning of the 20th century (of metallurgy, compressor-gas-turbine construction), successes achieved in development of such sciences as aerogasdynamics, the theory of aircraft engines and others created practical prerequisites for the development of technical valid designs and successful construction of reaction engines.

In the 1920's to 1930's in the USSR various types of liquid-propellant rocket engines were created and successfully tested.

The first liquid-propellant rocket engine in the USSR was built in the Gas-Dynamics Laboratory (GDL) in Leningrad in 1930. This engine (Fig. 2.9), called the ORM-1 an experimental reaction motor -- developed a thrust of up to 20 kgf.

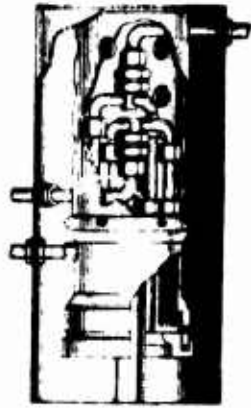


Fig. 2.9. Liquid reaction engine ORM-1 (1930).

Proposed as oxidizers for liquid rocket engine were nitric acid, tetroxide nitrogen (nitric tetroxide), hydrogen peroxide, tetranitromethane, chloric acid and their solution.

The gifted engineer F. A. Tsander in 1932 built and in 1933 tested the jet engine OK-2 (Fig. 2.10) with a thrust of 100 kgf. F. A. Tsander also conducted deep theoretical investigations in the region of reactive motion, developed new thermodynamic cycles of engines (Fig. 2.11) and for the first time proposed a method of thermal calculation the liquid-propellant rocket engine.

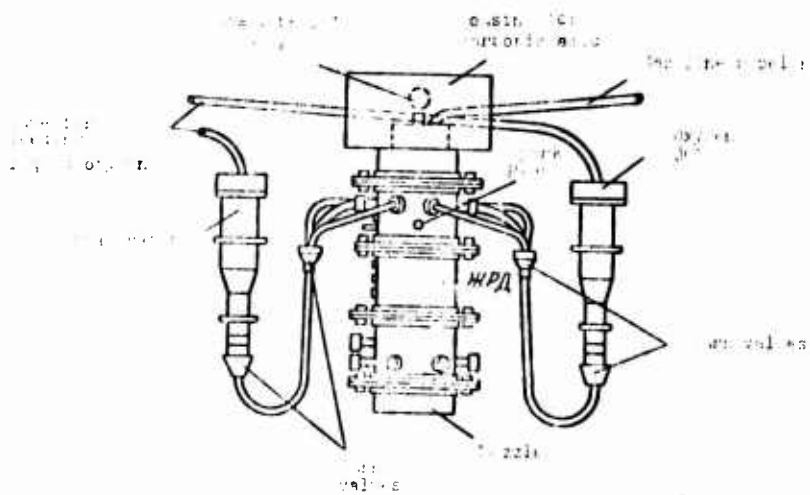


Fig. 2.10. Liquid propellant rocket engine OK-2 of F. A. Tsander (1933).

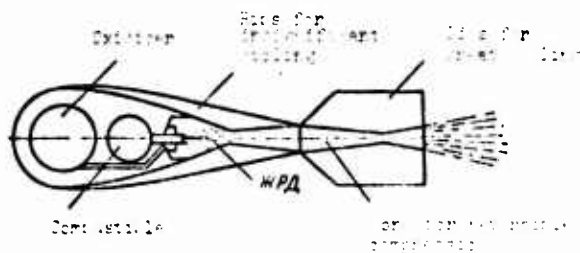


Fig. 2.11. Liquid-propellant rocket engine of F. A. Tsander with isothermal adapter.

F. A. Tsander is also credited with the idea of the use in the rocket of "metallic fuel". By this there is achieved an increase in calorific values of the fuel and, furthermore, an increase in the flight distance of the rocket train as a result of the use of the unneeded body of the spent rocket. For such fuel F. A. Tsander proposed using magnesium, aluminium and other metals.

During the 1920's-1930's abroad a series of rocket engines were built and tested by R. Goddard (USA), G. Oberth and Max Valier (Germany) and others.

The first flight took place in 1940 in the USSR of a reaction glider of the design of S. P. Korolev and the liquid propellant rocket engine RDA-1-150 was installed on it.

In May of 1942 in the USSR there was successfully tested the aircraft developed under the leadership of V. F. Bolkhovitinov, with a liquid propellant rocket engine D-1-A-1100, which was piloted by pilot G. Baxchivandzhi.

Considerable development in rocket building occurred during the Second World War. Fascist Germany, in attempting toward off its inevitable defeat, developed the long-range rocket "V-2" with liquid propellant rocket engine operating on liquid oxygen and alcohol.

#### 2.4. Contemporary Level of Development of Aircraft Reaction Engines

Jet engines were developed in the beginning of the Second World War (1941) and became operational at the end of the war (1944-1945). These include the German turbojet engines with an axial compressor (Yumo-004 and BMV-003) and also the English TRD with a centrifugal compressor of the design of Frank Whittle "Nin-I" and "Derwent-V." These engines were respectively installed on jet bombers Me-262 and fighters Gloster "Meteor", which engaged in limited combat participation on the western front.

In our country development of the first TRD was started prior to the Second World War. The well-known aircraft designer A. M. Lyul'ka as early as in 1937 proposed the plan and design of the first ducted-fan turbojet engine (Fig. 2.12) and in 1947 developed the turbojet engine of original design "TR-1."

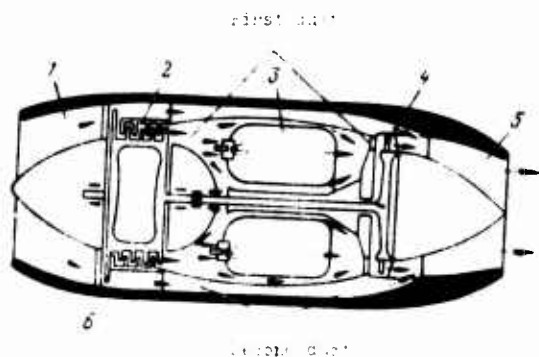


Fig. 2.12. Ducted-fan TRD of A. M. Lyul'ka (1937): 1 - inlet channel; 2 - compressor; 3 - combustion chamber; 4 - turbine; 5 - nozzle; 6 - fan.

The first turbojet engines were far from being technically perfect; the thrust of them did not exceed 800-900 kgf, the specific weight was very great ( $\gamma_{дв.} = 0.40-0.50$  kg/kgf of the thrust); in economy, due to the imperfection of the thermodynamic cycle, they were considerably inferior to piston propeller-driven engines, and their specific fuel consumption on the test stand was much greater

than 1.0 ( $C_{yA} = 1.25-1.35 \text{ kg/kgf}\cdot\text{h}$ ).

Nevertheless, the use of the first jet engines allowed sharply increasing the maximum flight speeds of aircraft (by 200-300 km/h) and achieving the order speeds of 850-900 km/h. It is appropriate to recall that the world record of speed of a special aircraft "Thunder" with a piston engine in 1945 was 805 km/h. The better serial aircraft with a propeller-piston group toward the end of the war developed speeds of not more than 650-700 km/h.

Experience in the construction and outflow of the first turbojet engines was widely used in the USSR and abroad with the subsequent improvement of the jet engine and the creation of new more effective types of aircraft gas-turbine engines. As an illustration, Fig. 2.13-2.17 show cross sections of several gas turbine of the firm Rolls Royce.

During the last 20-25 years the jet engine underwent great development. They became the predominant engine type not only in war but also in civil aviation. Modern jet and gas-turbine engines are installed on flying vehicles of the most diverse types, including helicopters, subsonic and supersonic aircraft, and also "hovercraft" operating on an air cushion. Thus, the field of application of the jet engine covers a broad range of subsonic, supersonic, and also hypersonic flight speeds.

The outflow of jet and gas-turbine aircraft in civil aviation began in 1956. It is connected with the advent of on the air lines of the USSR on first passenger turbojet aircraft in the world, the Tu-104, with two TRD AM-3 of the design of A. A. Mikulin, the thrust of each of which was equal to 8700 kgf.

During 1958-1960 there began the outflow of the aircraft Il-18 with four turboprop engines AI-20, with a power of 4000 hp each of the design of A. G. Ivchenko.

Air lines of the world since 1960 have been successfully flying

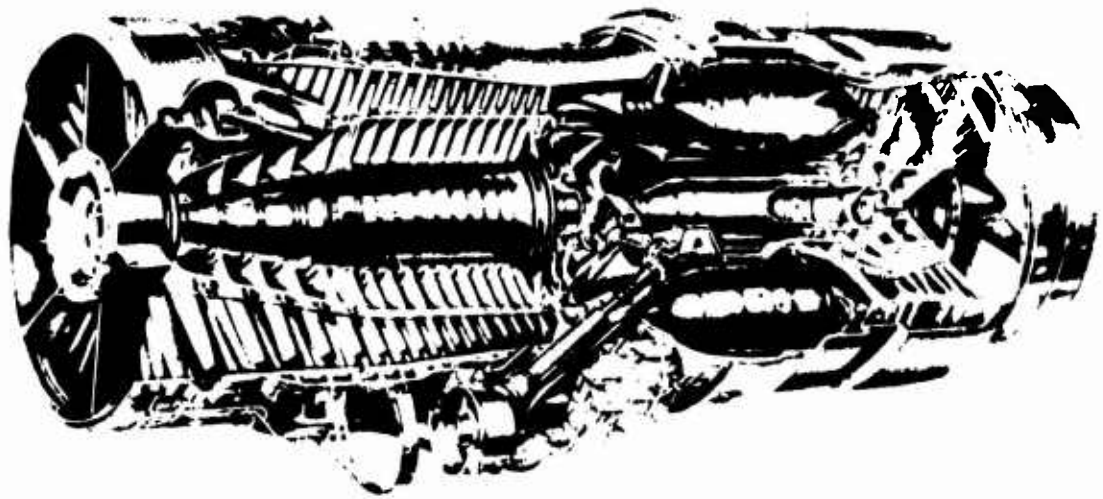


Fig. 2.13. TRD Rolls Royce "Avon" with an axial compressor (cross section).



Fig. 2.14. TVD Rolls Royce "Dart" with a centrifugal compressor (cross section).



Fig. 2.15. Double-shaft disk roller type "dpy" with a short mixer (cross section).

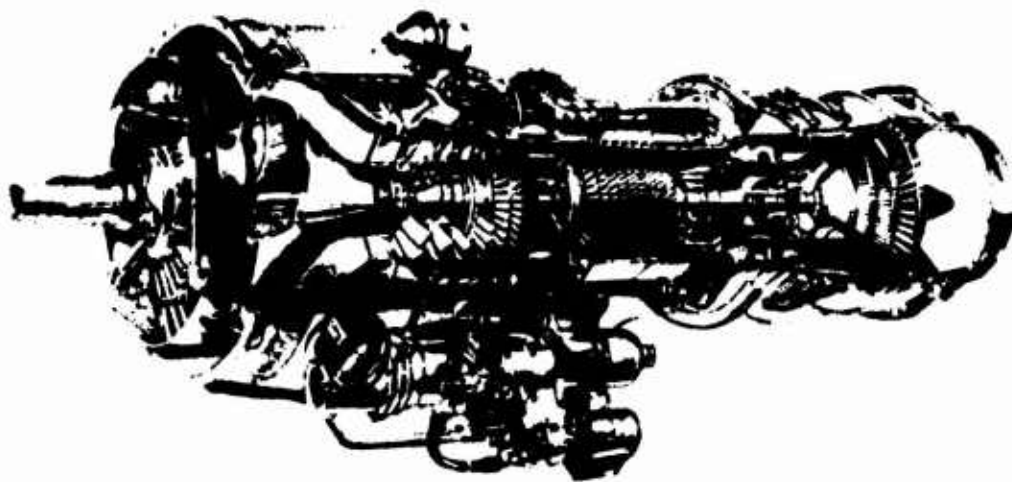


Fig. 2.16. Double-shaft E.V.L. roller type "Tyne" (cross section).

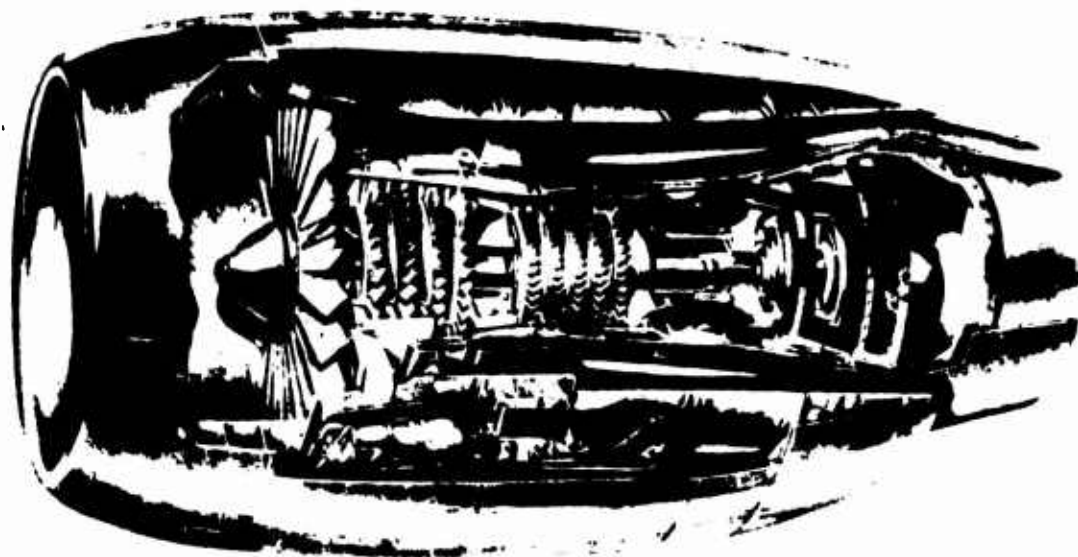


Fig. 2.17. Three-sought DPRD Rolls Royce "Trent" (cut).

the USSR long-range passenger aircraft Tu-114, equipped with turboprop engines NK-12 of the design N. D. Kuznetsov.

Trent successes have been achieved by Soviet military aircraft construction.

The last decade is characterized by the enormous development of world air transport. The air fleet countries foremost in a technical respect was completely renovated and became gas-turbine. At present approximately 3/4 of all passenger travel is accomplished in aircraft equipped with gas-turbine engines, including turbojet, turbofan and turboprop.

Increasing widespread in recent years has been the ducted-fan turbojet engines (see Fig. 2.15 and 2.17). On practically all newly constructed passenger main aircraft and also on the majority aircraft of local lines ducted-fan T40 have been installed.

Ducted-fan turbojet engines conquered universal acknowledgement

because of their *high economy, low level of producible noise* (due to the low velocities of outflow of gas), the possibility of *considerable thrust augmentation* on takeoff and in flight, the possibility of their use over a *wide range of subsonic and supersonic flight speeds* on various aircraft, and the possibility of the concentration of very high thrust in one unit.

Great successes have been achieved in the increase in the service life - period of service of the engines. If the service life of the first TRD was 50-100 hours, then now the better gas-turbine engines of civil aviation have a service life of the order of 4000 hours and more (service life of the DTRD Rolls Royce Conway RCo. 12 is equal to 7800 hours, TVD Rolls Royce "Dart" 6000 hours, and the DTRD Pratt and Whitney JT 3D-1 has a resource of 11,000 hours).

Increased technical perfection of aircraft gas-turbine engines has made it possible to improve considerably the basic technical and economic criteria of passenger aircraft - their speed, altitude and range of flight; to bring down the cost of transportation of each ton-kilometer (or passenger-kilometer) of load.

The 1950's and 1960's are noted for the rapid development of jet and rocket technology.

The largest aircraft engine building firms of the capitalist world Rolls Royce, Bristol Siddley (England), General Electric, Pratt and Whitney (USA), Turbomeca (France), have achieved great successes in the creation of new effective types aircraft GTD, increases in their economy, lowering of specific weight, increase in the service life, and improvement in operational characteristics.

The Soviet school of aircraft engine construction, which is headed by well-known designers A. A. Mikulin, V. Ya. Klimov, A. A. Shvetsov, A. G. Ivchenko, A. M. Lyul'ka, N. D. Kuznetsov, S. K. Tumanskiy and others, for the last 20-25 years achieved great successes.

New types of aircraft gas-turbine engines developed in our country, with respect to their basic technical and economic criteria do not yield to the best models of world aircraft engine design.

At present civil aviation of the USSR is experiencing a responsible stage of renovation and modernization of aircraft technology.

On air lines of the USSR there began operation of long-range main aircraft Il-62 with four DTRD and short-range main aircraft Tu-134 with two ducted-fan jet engines.

During the next two-three years Aeroflot is being replenished by new medium main-line aircraft Tu-154 with three DTRD and also with aircraft of local air lines Yak-40 with three DTRD.

At present in the USSR, England, France and the USA there is being conducted an intensive development of supersonic passenger aircraft, the outflow of which should start in the beginning of the 1970's. These aircraft are designed for cruising  $M$  of flight  $M_{0HP} = 2.2-2.35$  (Tu-144, "Concorde" and  $M_{0HP} = 2.7$  (Boeing 2707), and also altitudes flight of the order of 18-20 km.

Soviet scientists, designers and engineers persistently work over the creation of new, even more technically perfect flying vehicles and engines necessary to the national economy of the country.

#### 2.4.1. Development of Basic Parameters of Aircraft Gas-Turbine Engines (According to Foreign Data)

##### 2.4.1.1. Thrust

During the last 20 years the thrust, generated by some engine has extraordinarily increased. Foreign experimental and designed DTRD for heavy transport aircraft and air buses are calculated for thrust of up to 18-22 tons in one unit.

The minimum magnitude of "equivalent" thrust of the gas-turbine engine designed for auxiliary purposes (units of starting, pressurization, supplies of compressed air) is equal to 100-200 kgf.

#### 2.4.1.2. Rate of Airflow

During the last 20 years the rate of airflow of engines has increased many times. In contemporary large-scale DTRD with a high bypass ratio ( $\gamma = 6-8$ ) the rate of airflow  $G_B$  reaches 400-800 kg/s and more.

#### 2.4.1.3. Specific Thrust of the TRD

The specific thrust of TRD without afterburners in accordance with a certain temperature rise of the gas in front of the turbine during the last 20 years has increased and is the magnitude of 65-75 kgf/(kg/s) on takeoff. The specific thrust of boosted TRD (with afterburning of the fuel behind the turbine) reaches 100-110 kgf/(kg/s).

#### 2.4.1.4. Specific Fuel Consumption of the TRD and DTRD

The specific fuel consumption of a one-duct TRD equipped with a high-pressure axial-flow compressor ( $\pi_H^* = 13-15$ ) on takeoff consists of the magnitude  $C_{yA} = 0.72-0.78$  kg/kgf·h. With a bypass ratio of  $\gamma = 1-2$  the level of specific consumption of fuel is reached by the DTRD of the order of 0.5-0.6 kg/kgf·h. When  $\gamma = 6-8$  the specific consumption of the DTRD on takeoff is  $C_{yA} = 0.30-0.35$  kg/kgf·h.

In the cruising flight regime ( $H = 11$  km and  $M_0 = 0.8$ ) prospective high-temperature DTRD ( $T_3^* = 1300-1400^\circ\text{K}$ ) at high compression ratios of the compressor of the gas generator ( $\pi_H^* = 20-25$ ) and high values of the bypass ratio ( $\gamma = 6-8$ ) are calculated for obtaining a specific fuel consumption of not higher than  $C_{yA} = 0.58-0.64$  kg/kgf·h.

#### 2.4.1.5. Specific Weight

During the last 20 years the specific weight of aircraft turbo-turbine engines has been continually lowered. This trend is explained, on one hand, by the increase in the specific thrust of the TRD (DTRD) and on the other hand, by an increase in the total level of perfection of the design, improvement in technology of finishing and production of aircraft engines, the introduction of new more effective materials (such, as nimonic, titanium, and composite materials: Kevlar and others), and the correct selection of basic regimes of the engine, which increases its service life and reliability.

At present the specific weight of a better subsonic TRD at average values of thrust reach  $\gamma_{\text{дв}} = 0.20-0.22$  kg/kgf. The transition to DTRD with high values of the bypass ratio allow decreasing the magnitude  $\gamma_{\text{дв}}$  down to 0.16-0.17 kg/kgf. Supersonic TRDF are characterized by a specific weight of not more than  $\gamma_{\text{дв}} = 0.16-0.18$  kg/kgf. The TRD of optimum dimension ( $R = 1200-1500$  kgf), such as the General Electric J85, attained a specific weight of the order of  $\gamma_{\text{дв}} = 0.12-0.14$  kg/kgf.

The lowest specific gravity is obtained in special "lift" TRD designed for vertical speed and landing. In these engines (for example, in the engine Rolls Royce RB.162) an extraordinarily low specific weight - about 0.06 kg/kgf has already been reached. In the very near future leading aircraft engine building firms of England (Rolls Royce) and the USA (Allison) propose additionally decreasing the specific weight of "lift" turbojet engines proved to be possible as a result of the following:

- 1) extreme simplification of design (lowering of the number of parts from 10,000-12,000 to 2000-3000; transition to double-bearing design of the engine; decrease in the length of the combustion chamber and others);

- 2) rejecting systems of oil feed, cooling of parts drive of

units; simplification of systems of fuel feed and starting;

3) extensive introduction of fiberglass into the construction of the compressor;

4) rational use of the volume of the construction, specifically, combustion chambers; considerable increase in the thrust falling on  $1 \text{ m}^3$  of volume.

#### 2.4.1. Basic Design Peculiarities of Contemporary TRD

The contemporary turbojet engine installed on passenger aircraft is the synthesis of highest achievements in field of the designer's art applied thermalaerogas dynamics, technology, metallurgy, automation, and the theory of strength and reliability. Its subsequent improvement is possible only on the basis of a thorough calculation of the enormous experience of operation accumulated in military and civil aviation and the critical evaluation of the colossal flow of technical information entering from numerous scientific-research establishments working on separate and complex problems of aircraft engine construction.

Let us mention the basic design peculiarities of contemporary turbojet engines and their most important subassemblies.

##### 2.4.2.1. Intake of the TRD

The intake of the TRD, installed on a supersonic passenger aircraft, is made in the form of a supersonic adjustable diffuser with multishock deceleration of flow. In the rated cruising regime of flight, the coefficient of drop in total pressure of such an air intake is very high, for example, for  $M_0 = 2.2$  it is  $\sigma_{\text{CH}}^* = 0.90-0.92$ .

##### 2.4.2.2. Compressor

The high-pressure axial-flow compressor (Figures 2.18 and 2.19)

Fig. 2.18. Inlet guide vanes of the compressor.

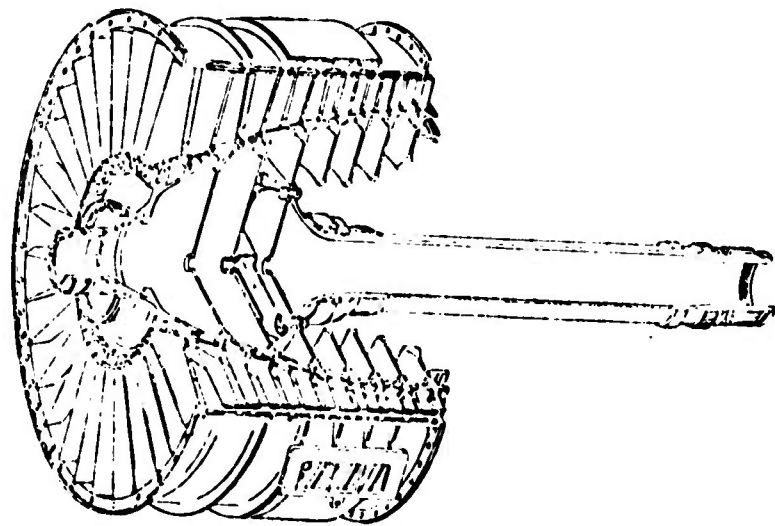
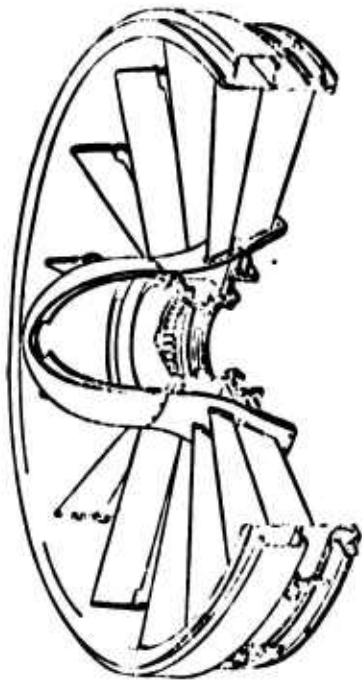


Fig. 2.19. Axial-flow compressor.

is most complex unit of the TRD, which determines to a certain extent the dimensions, weight, economy and reliability of operation of the engine.

At high values of the compression ratio ( $\pi_K^* = 15-25$ ) the compressor is made either with first supersonic stages or completely subsonic. In the latter case it consists of a large number of stages, reaching 12-17. Most frequently the high-pressure compressor is made double-shaft, and furthermore, it is equipped with a system of mechanization, which provides its reliable and steady operation in the whole range of operational regimes.

The mechanization of the compressor includes systems of de-icing, overflow of air from separate stages, and also the control of corner vanes of the stator.

The efficiency of subsonic high-pressure compressors have attained values  $\eta_K^* = 0.86-0.88$ .

#### 2.4.2.3. Combustion Chamber

A tendency of the continuous increase in the turbine inlet gas temperature ( $T_3^*$ ) complicates the problem of the creation of a reliable operating chamber. Nevertheless, engines having the greatest service life (Rolls Royce "Dart" "Conway", "Avon" and "Tyne") are equipped with high-temperature chambers ( $T_3^* \text{ max} = 1270-1350^\circ\text{K}$ ). The combustion chambers of the better subsonic TRD have a coefficient of completeness of combustion, practically equal to 1.0 ( $\xi_{K.C} = 0.98-0.99$ ).

In order to achieve a substantial decrease in the length of combustion chamber (and consequently, weight of the engine) without worsening its effectiveness, in lift TRD zones of the division of air flows, and also processes of carburetion, combustion and mixing of products of combustion with air are combined.

#### 2.4.2.4. Turbine

The TRD (DTRD, TVD) with high-pressure compressor are made multi-stage turbines (Fig. 2.20 and 2.21) with the number of stages from two to five and more. They, just as the compressors, are made one-and-two-shaft.

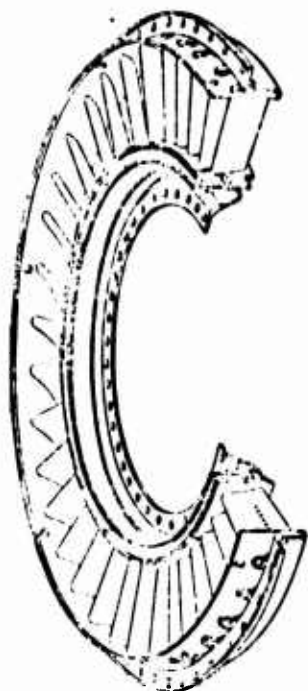


Fig. 2.20. Nozzle box of the turbine.

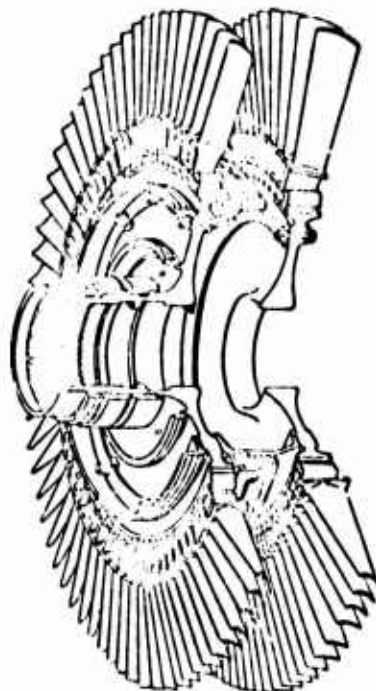


Fig. 2.21. Rotor of the turbine (two-stage).

The rotor blades of contemporary gas turbines, for providing the necessary operational reliability and also for obtaining high efficiency, have a shroud.

Gas turbines of TRD are made reactive ( $Q_{r-r_{cp}} \approx 0,25 \div 0,35$ ); their efficiency is very high and reaches the value  $\eta'_t = 0,92 \div 0,93$ .

For the purpose of providing the necessary reliability of operation of the engine at high temperatures of the gas (TRD and DTRD designed for supersonic passenger aircraft, DTRD with high

values of the bypass ratio, and TVD) air cooling of nozzle and rotor blades of the first or first two stages of the turbine is used.

It is widely acknowledged that the most promising methods of ventilation are methods of porous and film cooling. It is expected that these methods make it possible in the near future to provide reliable cooling of the blades at gas temperatures  $T_3^* = 1600-1800^\circ\text{K}$  with a value of selectism of 5-8% of the air compressed in the compressor.

Figure 2.22 shows a diagram of film air cooling of a rotor blade developed by the firm Rolls Royce. The principle of operation of such a system of cooling consists in the following. Compressed air enters into end of the hollow cast blade and along three radial channels spreads to the periphery of the blade, cooling by means convective heat exchange its interval cavity. Over the entire height of the blade and along its periphery there is drilled a system of microholes through which from within compressed air is extruded. Then the cooling flow flows past the profile of the blade, forming a protective film around it.

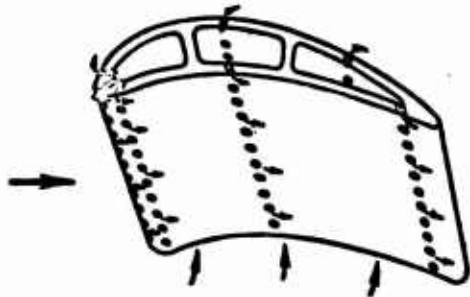


Fig. 2.22. Diagram of film cooling of turbine blades.

#### 2.4.2.5. Exit Section of the TRD

The discharge device of the supersonic TRD has a complex design. It is a nozzle of the Laval type of nozzle, with mechanical or aerodynamic control of the critical and exit sections.

In the case a one-duct TRD or ducted-fan TRD with a low bypass

ratio ( $\gamma < 1.0$ ), the nozzle is equipped with a noise suppressor (Fig. 2.23).

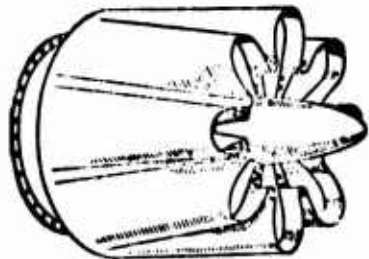


Fig. 2.23. Noise suppressor of the TRD.

A necessary element of the exit system of the TRD (DTRD) of contemporary passenger aircraft is a *reverse* or *thrust deflector*.

#### 2.4.2.6. Control of the Engine in Flight

The control system of contemporary TRD intended for installation on high-speed transport aircraft is designed to ensure minimum fuel consumption in throttle regimes (regimes of partial load) and reliable and steady operation of the engine. Optimization of the regimes is provided with the help of computing devices, which control the elements of control of numbers of revolutions and critical section of the exit nozzle and acting on parameters of gas  $T_3^*$ ,  $\pi_{H1}^*$  and so on.

#### 2.4.2.7. Thrust Augmentation

Turbojet engines of supersonic passenger aircraft, as a rule, are equipped with a system of thrust augmentation, which is used mainly during the transition through the speed of sound at great altitudes. Afterburners of the TRD provide at  $T_{\phi}^* = 2000^\circ\text{K}$  on a test stand an increase in thrust of 35-40% and in the case of a DTRD - an additional thrust of 70-80%.

For compensation of the loss in thrust at high temperatures of the surrounding medium ( $t_H \gg + 15^\circ\text{C}$ ) water injection at entrance

into the axial-flow compressor is used. Such short-term augmentation thrust is especially rational in turboprop engines.

#### 2.4.2.8. Heat Recovery

An effective means of increasing the economy of high-temperature TVD equipped with compressors with moderate compression ratios is the *heat recovery* of exhaust gases. At considerable long flight distance it can reduce the operational consumption 15-20%.

#### 2.4.3. Development of Theory of Jet Engines

The founder of the contemporary theory of jet engines is Academician B. S. Stechkin. Published by him in 1929 in the periodical "Technology of air fleet" the work "Theory of the jet engine" was the basis for further development of the theory of engines of this class. In 1944-1947 B. S. Stechkin and his students developed the theory of processes and of characteristics of basic types of jet engines.

During 1956-1958 the publishing house Oborongiz published a two-volume publication "Theory of reaction engines" (authors - B. S. Stechkin, P. K. Kazandzhan, L. P. Alekseyev, A. N. Govorov, N. Ye. Konovalov, Yu. N. Nechayev, and R. M. Fedorov), which obtained widespread reputation in the USSR and abroad as a student textbook for higher educational schools and a manual for aircraft engineers.

A great contribution to the development of the theory of aircraft gas-turbine engines has been made by Deserved Scientist and Technician of the RSFSR Professor, Doctor of Technical Sciences I. I. Kulagin, who in 1949 published the book "Theory of gas-turbine reaction engines". This book was the first systematized manual in this field. I. I. Kulagin is responsible for the fundamental developments on the theory of ducted-fan VRD and on the theory of control and characteristics of aircraft gas turbines.

An important contribution to the development of the theory of gas-turbine engines was made to the Deserved Scientist and Technician, Professor, Doctor of Technical Science V. V. Uvarov. He is the author of many brilliant engineering ideas, plans and accomplished designs (for example, a compressor with air turbine), and also theoretical developments (stationary cycle  $\nu = \text{const}$  of the gas turbine). His monograph "gas turbine", published in 1935 by the publishing house United Scientific and Technical Presses for many years was the reference book for engineers specializing in the field of gas-turbine construction.

Investigations on the theory of processes and characteristics of jet engines and liquid propellant rocket engines, carried out by Deserved Scientist and Technician Professor, Doctor of Technical Sciences T. M. Mel'kumov, are well-known.

Fundamental investigations on the theory of jet-engines and aircraft gas-turbines belong to professors, Doctors of Technical Sciences N. V. Inozemtsev (processes in VRD) K. V. Kholshchevnikov (theory of two-shaft TRD, development of the theory of axial-flow compressors and gas turbines), P. K. Kazandzhan (characteristics of gas turbines, development of the theory of turboprop engines), G. N. Abramovich (gas dynamics of VRD, theory of turbulent jets) and others.

Of foreign investigations of reaction motion and jet engines works of Moriss Roux\*, Theodor von Karman, J. Griffiths\*, G. Konstant\*, G. Pearson and others received wide recognition. Basic results of these investigations are presented in a 12-volume series of books under general title "Aerodynamic of high velocities and reaction technology", published by the publishing house of Princeton University (USA) edited by T. von Karman H. L. Dryden, M. Summerfield, H. S. Tay\*, K. P. Donaldson\*, J. V. Chirik\* and R. S. Snedecker\*.

[Translator's Note: the initials and spelling of these author's last names are not verified].

## CHAPTER 3

### THRUST OF THE JET ENGINE. BASIC PARAMETERS OF THE JET ENGINES

#### 3.1. Theorem of Thrust of Jet Engine

*Thrust* is called the moving force generated by an engine. Thrust is the main parameter of the jet engine and useful effect of its operation. Therefore, an accurate determination of it is very important.

In its physical sense thrust is the resultant of axial forces applied to all elements of the engine. However, the "term-by-term" finding of its components is very complex and inconvenient.

Thrust of a jet engine is determined with the help of the theorem of Euler on the change in the quantity of motion of a moving mass of gas, examining the engine as a whole.

The theorem of thrust for a jet engine in the whole form was proved by Academician B. S. Stechkin in 1929. Let us prove this theorem in a somewhat changed appearance.

Let us separate the control surface limited by the external surface of the jet passing through the engine and by two sections ( $\mu-\mu$  and 5-5), drawn perpendicular to the line of axial symmetry of the engine (Fig. 3.1).

Section  $\mu-\mu$  is selected in the undisturbed section of the flow; section 5-5 is drawn on the section of the jet nozzle.

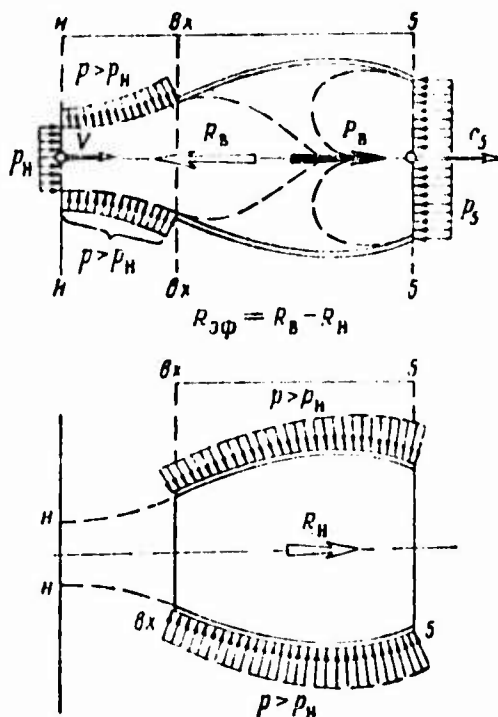


Fig. 3.1. Determination of thrust of a VRL.

Let us stipulate that the engine is motionless and that the air moves relatively to it with flight speed  $V$ .

Let us introduce the concept of *effective thrust* of a VRL, understanding by this term the resultant of axial forces of *internal* and *external* pressures, i.e.,

$$R_{3\phi} = R_B - R_H \quad (3.1)$$

where  $R_B$  - resultant of forces of internal pressure;  
 $R_H$  - resultant of forces of external pressure.

To determine the resultant of forces of the internal pressure, let us apply to the mass of gas limited by the control surface Euler's theorem in the following formulation:

"A change in the quantity of motion of the per second mass of

gas in a given direction is equal to the sum of projections of all external forces applied to the isolated mass in this direction).

By such a direction let us select the direction of the flight. Then let us obtain

$$\frac{G_r}{g} c_s - \frac{G_a}{g} V - P_B + (p_H f_H - p_S f_S) + \int_{f_n}^{f_{n+1}} p df, \quad (3.2)$$

where  $\frac{G_r}{g} c_s$  — per second quantity of motion of the mass of gas flowing out through section  $f_S$ ;

$\frac{G_a}{g} V$  — per second quantity of motion of mass of air flowing out through section  $f_H$ ;

$(p_H f_H - p_S f_S)$  — resultant of forces of gas pressure applied to the frontal planes of the control surface;

$\int_{f_n}^{f_{n+1}} p df$  — resultant of forces of pressure applied to the side surface of the "free" section of the jet;

$df = ds \cos \alpha$  — projection of elementary side surface of the engine  $ds$  on a plane perpendicular to the direction of flight;

$P_B$  — force equivalent to the action of walls of the engine on the gas mass (acts in a direction opposite to the direction of flight).

Let us write by formula (3.2) the expression for  $P_B$ :

$$P_B = \left( \frac{G_r}{g} c_s - \frac{G_a}{g} V \right) + (p_H f_H - p_S f_S) - \int_{f_n}^{f_{n+1}} p df = -R_n. \quad (3.3)$$

Since according to Newton's third law the force of the action of walls of the engine  $P_B$  on the flow will be equal and opposite to the force of action of the flow on walls of the engine, i.e., the resultant of forces of internal pressure  $R_B$ , then the absolute magnitude  $R_B$  will be determined by an expression identical to expression (3.3).

Let us now find  $R_H$ .

We have

$$R_H = X_{1p} + \int_{f_{nx}}^{f_s} p df, \quad (3.4)$$

where  $X_{1p}$  - force of friction of external flow about the surface of the engine;

$\int_{f_{nx}}^{f_s} p df$  - resultant of forces of external pressure applied to the surface of the engine.

Force  $R_H$  acts in a direction opposite to the direction of flight.

Let us substitute expressions  $R_D$  from (3.3) and  $R_H$  from (3.4) into equation (3.1).

Then we obtain

$$R_{s\phi} = \left( \frac{G_r}{g} c_s - \frac{G_n}{g} V \right) + (p_s f_s - p_n f_n) - \int_{f_n}^{f_{nx}} p df - X_{1p} - \int_{f_{nx}}^{f_s} p df. \quad (3.5)$$

Let us note that  $\int_{f_n}^{f_s} p_n df = (f_s - f_n) p_n$ .

Then expression (3.5) can be reduced to the form

$$R_{s\phi} = \left( \frac{G_r}{g} c_s - \frac{G_n}{g} V \right) + (p_s f_s - p_n f_n) - (f_s - f_n) p_n - X_{1p} - \int_{f_n}^{f_s} p df + \int_{f_n}^{f_s} p_n df,$$

or

$$R_{s\phi} = \underbrace{\left( \frac{G_r}{g} c_s - \frac{G_n}{g} V \right)}_1 + \underbrace{f_s(p_s - p_n)}_2 - \underbrace{\left[ X_{1p} + \int_{f_n}^{f_s} (p - p_n) df \right]}_3. \quad (3.6)$$

Here

- (1)  $\frac{G_r}{g} c_s - \frac{G_n}{g} V$  — change in quantity of motion of per second mass of gas flowing through the engine; it is called *dynamic component of thrust*, it is conditioned by a change in the gas velocity;
- (2)  $f_s(p_s - p_n)$  — *static component of thrust*; it is caused by the presence of surplus pressure on the section of the nozzle (case of incomplete gas expansion in the jet nozzle of the engine);
- (3)  $X_{r, \text{д}} + \int_{f_n}^{f_s} (p - p_n) df = X_{r, \text{д}}$  — force of drag of the nacelle of the engine; it acts in a direction opposite to the direction of flight. It is caused by the deviation in pressure on the side surface  $s$  from the atmospheric and also by the presence of friction.

The sum of the dynamic and static components of thrust is called internal thrust of a jet engine  $R$ .

Then 
$$R_{\text{эф}} = R - X_{r, \text{д}} \quad (3.7)$$

Thus, the effective thrust of a jet engine is equal to the internal thrust of the engine less the force of total drag of the nacelle of the engine.

It is possible to write the following equation:

$$\int_{f_n}^{f_s} (p - p_n) df = \int_{f_n}^{f_{\text{нк}}} (p - p_n) df + \int_{f_{\text{нк}}}^{f_s} (p - p_n) df = X_{\text{доп}} + X_p \quad (3.8)$$

where  $X_{\text{доп}}$  — additional resistance conditioned by the deformation of the "free" in flowing jet outside the engine (here this refers to wave resistance of the diffuser at supersonic flight speeds);

$X_p$  - resistance of pressure of the nacelle of the engine.

In general the force of drag of the nacelle of the engine is equal to

$$X_{r,d} = X_{доп} + X_p + X_{тр} + X_{доп}, \quad (3.9)$$

where  $X_{тр}$  - resistance of the surface of friction;

$X_{доп}$  - "ground" (rear) effect conditioned by rarefaction appearing in rear part of the engine.

### 3.1.1. Formula of Internal Thrust

Let us write the working formula of internal thrust of the VRD, having noted that

$$G_r = G_n + G_T = G_n(1 + m_T).$$

Then in general

$$R = \frac{G_n}{g} [(1 + m_T)c_s - V] + f_s(p_s - p_n), \quad (3.10)$$

where  $m_T = \frac{G_T}{G_n}$  - relative fuel consumption, i.e., fuel consumption per 1 kg of air; on the average  $m_T = 0.015-0.020$ .

#### 3.1.1.1. Particular Cases of the Formulas of Internal Thrust (for $m_T \approx 0$ )

a) *Case of complete expansion of gas in a jet nozzle*

We have

$$p_s = p_n.$$

Then

$$R = \frac{G_n}{g} (c_s - V). \quad (3.11)$$

b) *Case of incomplete expansion of gas in a jet nozzle*

We have

$$p_s > p_n \quad \text{and} \quad c_s \geq a_s.$$

Then

$$R = \frac{G_n}{g} (c_s - V) + f_s(p_s - p_n). \quad (3.12)$$

c) Case of operation of the engine on a test stand.

We have  $V = 0$ .

$$\text{Then } R = \frac{G_r}{g} c_s + f_s(p_s - p_H); \quad (3.13)$$

with  $p_5 = p_H$

$$R = \frac{G_r}{g} c_s. \quad (3.14)$$

### 3.2. Reversing and Deviation in Thrust of Turbojet Engines

With the landing of contemporary transport aircraft (its run on an airfield up to stopping) reversing of thrust, i.e., is used widely the reversing of its direction. In this case the thrust becomes "negative" - from a force accelerating movements of the aircraft, it turns into a force braking its movement.

#### 3.2.1. Formula of Reversed Thrust (Fig. 3.2)

Let us designate

- $G_B = G_r = G$  - Gas consumption through the jet nozzle with reverser turned off;
- $R_{p,y}$  - reversed thrust;
- $G_{p,y}$  - gas consumption through the reverser;
- $V$  - flight speed;
- $c_5$  - velocity of the outflow of gas from the jet nozzle;
- $c_{p,y}$  - velocity of the outflow of gas from the reverser;
- $\beta$  - angle of deviation in the flow with thrust reversing  $[(90^\circ < \beta < 180^\circ); 180 - \beta^\circ = \alpha^\circ]$ .

Then

$$\begin{aligned} R_{p,y} &= \frac{(G_r - G_p)}{g} c_s - \frac{G}{g} V + \frac{G_p}{g} c_{p,y} \cos \beta^\circ = \\ &= \frac{G}{g} (c_s - V) - \frac{G_p}{g} (c_s + c_{p,y} \cos \alpha^\circ). \end{aligned} \quad (3.15)$$

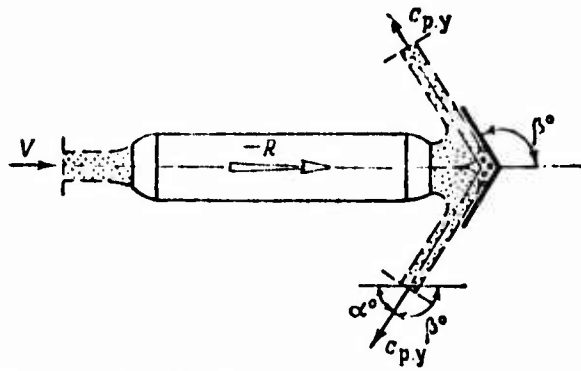


Fig. 3.2. Derivation of the formula of reversed thrust.

Let us call the degree of *draught reversal* the ratio reversed thrust to the original thrust of the TRD (with the reverser turned off), i.e.,

$$\bar{R}_{p,y} = \frac{R_{p,y}}{R} = \frac{\frac{G}{g}(c_s - V) - \frac{G_{p,y}}{g}(c_s + c_{p,y} \cos \alpha)}{\frac{G}{g}(c_s - V)},$$

or

$$\bar{R}_{p,y} = 1 - \frac{G_{p,y}}{G} \frac{(c_s + c_{p,y} \cos \alpha)}{(c_s - V)}. \quad (3.16)$$

Let  $c_{p,y} = \varphi c_s$ , then finally we obtain

$$\bar{R}_{p,y} = 1 - \frac{G_{p,y}}{G} \frac{(1 + \varphi \cos \alpha)}{\left(1 - \frac{V}{c_s}\right)}. \quad (3.17)$$

The condition of the obtaining of negative thrust, i.e., the ensuring condition  $\bar{R}_{p,y} < 0$ ,

$$\frac{G_{p,y}}{G} \cdot \frac{(1 + \varphi \cos \alpha)}{\left(1 - \frac{V}{c_s}\right)} \geq 1. \quad (3.18)$$

Consequently, the greater the degree of thrust reversal then:

- 1) the greater the portion of reversed mass of gas ( $\frac{G_p}{G} \leq 1,0$ );
- 2) the greater the angle of deviation of the jet of gas  $\beta$  (i.e., the less  $\alpha$ );
- 3) the greater the flight speed;
- 4) the less the loss of velocity with reversing of the jet.

The selection of angle  $\alpha$  is determined by need to prevent the entrance of flow of hot outgoing gases into the inlet of the engine. The latter can lead to a surging and spontaneous turning off of the engine. Usually  $\alpha = 30-60^\circ$ .

Let  $\frac{G_{p,y}}{G} = 1,0$ ;  $\varphi = 0,90$ ;  $V = 0$ ;  $\alpha = 60^\circ$ .

Then

$$N_{p,y} = -\varphi \cos \alpha = -0,45.$$

The best reversers have a thrust

$$N_{p,y} = 0,4 \div 0,5.$$

### 3.2.2. Deviation in the Vector of Thrust of Lift Turbojet Engines

Sustainer engines, which are installed on aircraft of vertical takeoff and landing are frequently equipped with special thrust deflectors - for the creation of additional vertical thrust component (Fig. 3.3).

In these cases (i.e., with deviation in the reactive jet of  $90^\circ$ ) at suspension nodes of the engine there will be transferred: negative horizontal thrust equal to

$$R_r = -\frac{G}{k} V,$$

and also vertical thrust equal to

$$R_n = \frac{G}{k} c_{o,y} = \frac{G}{k} \varphi_{o,y} c_{o,y}$$

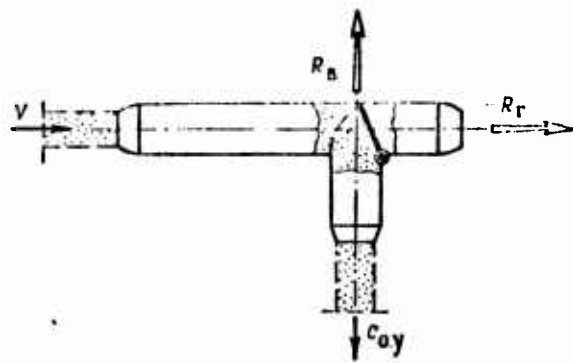


Fig. 3.3. Determination of components of thrust of a TRD equipped with a thrust deflector.

where  $\phi_{0,y}$  - coefficient of velocity in the deflecting device.

In a number of cases lift engines vertically installed on VHL have rotary devices, which by means deflecting the axis of the engine from the vertical (15-30°), makes it possible with takeoff to create an additional horizontal thrust, and with landing - an additional braking force (Fig. 3.4).

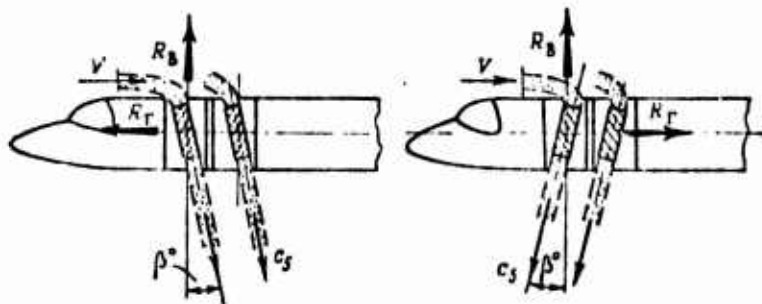


Fig. 3.4. Determination of components of thrust of lift TRD with rotary mechanism.

We have:

a) with takeoff

$$R_r = \frac{G}{g} (c_s \varphi_{0,y} \sin \beta - V);$$

$$R_B = \frac{G}{g} c_s \varphi_{0,y} \cos \beta.$$

b) with landing

$$R_r = -\frac{G}{g} (c_s \varphi_{0,y} \sin \beta - V);$$

$$R_B = \frac{G}{g} c_s \varphi_{0,y} \cos \beta.$$

### 3.3. Basic Parameters of the TRD (VRD)

Definitions and formulas of basic parameters of the VRD are given below and their meanings and dimensions are also given.

#### Rate of Airflow (Gas) Per Second.

The mass flow of air is the quantity (*kilograms*) of air (gas) passing through the engine in one second, i.e.,

$$G_a = m \frac{p_i}{\sqrt{T_i}} f_{i,q}(\lambda_i) \text{ kg/s.} \quad (3.19)$$

#### Thrust of TRD.

With complete expansion of the gas

$$R = \frac{G_a}{g} [c_s(1 + m_f) - V] \text{ kgf.} \quad (3.20)$$

Approximately

$$R \approx \frac{G_a}{g} (c_s - V).$$

#### Specific Thrust.

Specific thrust is the thrust necessary for the rate of airflow at 1 kg per second:

$$R_{y_1} = \frac{R}{G_a} = \frac{c_s(1 + m_f) - V}{g} \frac{\text{kgf}}{\text{kg/s}} \quad (3.21)$$

Approximately

$$R_{y_1} \approx \frac{c_s - V}{g}. \quad (3.22)$$

#### Fuel Consumption Per Second.

The fuel consumption per second is the quantity of fuel

expended by the engine in 1 second:

$$G_r, \text{ kg/s.}$$

Fuel Consumption Per hour.

$$3600G_r, \text{ kg/h.}$$

Specific fuel consumption is the hourly fuel consumption of fuel referred to 1 kgf of thrust in hour, i.e.,

$$C_{y\lambda} = \frac{3600G_r}{R} = \frac{3600m_r}{R_{y\lambda}} \text{ kg/kgf}\cdot\text{h.} \quad (3.23)$$

Relative Fuel Consumption.

The relative fuel consumption is fuel consumption per second referred to the rate of airflow per 1 kg/s, i.e.,

$$m_r = \frac{G_r}{G_a} = \frac{1}{\alpha l_0} = \frac{q_{\text{an}}}{H_u}. \quad (3.24)$$

Coefficient of Air Surplus.

The coefficient of air surplus is the ratio of the actually entered quantity of air to that theoretically necessary for complete combustion of 1 kg of fuel, i.e.,

$$\alpha = \frac{l}{l_0} = \frac{G_a}{G_{a0}}. \quad (3.25)$$

Effective Work.

The effective work is the useful work of a cycle of the VRD equal to the differences of work of expansion and work of compression, i.e.,

$$L_e = l_p - L_c \quad \frac{\text{kgf}\cdot\text{m}}{\text{kg}} \quad (3.26)$$

### Effective Efficiency.

Effective efficiency of the TRD is the ratio of heat equivalent to effective work of the engine to the whole heat introduced with fuel, i.e.,

$$\eta_e = \frac{A L_e}{q_{in}}. \quad (3.27)$$

### Thrust Efficiency.

Thrust efficiency of the TRD is the ratio of work of reactive thrust to effective work of the engine, i.e.,

$$\eta_R = \frac{L_R}{L_e} = \frac{R_{y2} V}{L_e}. \quad (3.28)$$

### Total Efficiency.

The total efficiency of the TRD is the ratio of the heat equivalent to the work of reactive thrust to the whole heat introduced with the fuel, i.e.,

$$\eta_0 = A \frac{R_{y2} V}{q_{in}}. \quad (3.29)$$

### Frontal Thrust.

Frontal thrust of the TRD is the ratio of thrust of the TRD to mid-section<sup>1</sup> of the engine, i.e.,

$$R_{100} = \frac{R}{F_M} \quad (3.30)$$

### Specific Weight.

---

<sup>1</sup>Maximum cross section of the engine.

Specific weight is the ratio of the weight of the engine to the thrust generated by it, i.e.,

$$\gamma_{sp} = \frac{G_{en}}{R} \frac{\text{kg}}{\text{kgf.}} \quad (3.31)$$

Service Life of the Engine.

Service life is the period of service (total duration of operation) of the engine, i.e.,

$\tau$ , h.

---

P A R T T W O

THERMODYNAMIC CYCLES AND WORKING PROCESSES  
OF JET ENGINES

## CHAPTER 4

### THERMODYNAMIC CYCLES AIRBREATHING JET ENGINE

#### 4.1. Ideal Cycles of Jet Engines $p = \text{const}$

Let us examine initially the ideal cycle of a jet engine, i.e., the cycle consisting of ideal reversible processes. Such a cycle is the adiabatic cycle  $p = \text{const}$ .<sup>1</sup> It consists of the following processes (Fig. 4.1):

- 0-2a<sup>2</sup> - adiabatic compression accomplished in a free jet in front of an engine because of the impact pressure (dynamic compression) and in the compressor (mechanical compression);
- 2a-3u - isobaric feed of heat in the combustion chamber;
- 3u-5a - adiabatic expansion in a gas turbine and in a jet nozzle;
- 5a-0 - isobaric rejection of heat from a jet of hot gases flowing from the engine into the external medium.

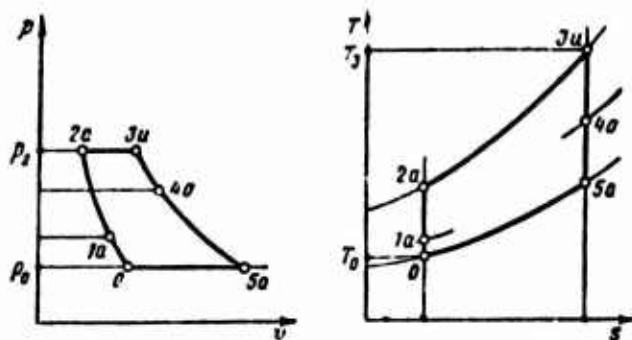


Fig. 4.1. Ideal cycle  $p = \text{const}$ .

<sup>1</sup>Brayton cycle.

<sup>2</sup>Sometimes the section of undisturbed flow is designated by H-H emphasizing by this that it is examined in high-altitude conditions.

The ideal cycle of the jet engine depicted in Fig. 4.1 by circuit 0-2a-3u-5a-0 is a closed air cycle of invariable chemical composition with constant thermal specific heat, which does not depend on temperature. The cycle  $p = \text{const}$  is the basic cycle of the jet engine.

Let us designate by symbols  $\pi = \frac{p_2}{p_0}$  — compression ratio of the working medium;  $\delta = \frac{T_2}{T_0}$  — degree of preheating of the working medium.

The thermal efficiency of the cycle  $p = \text{const}$  is determined by expression

$$\eta_t = 1 - \frac{1}{\pi^{\frac{k-1}{k}}},$$

where  $k = \frac{c_p}{c_v} = 1.4$  — specific heat ratio for air. It depends only on the compression ratio  $\pi$  and continuously increases with its increase.

The area limited by circuit 0-2a-3u-5a-0 depicts in a certain scale the useful work of the ideal cycle  $L_{e(\text{ИД})}$ ; this useful work can be obtained in the form of an increase in kinetic energy of 1 kg of air inside the engine — the case of a turbojet engine or ramjet VRD, — or also partially in the form of mechanical energy tapped through the turbine shaft to that using it. The user of such energy can be a propeller, fan or an additional compressor. In these cases the VRD is respectively called a turboprop, turbofan or ducted-fan turbojet engine.

For proof of this position let us write the equation of the energy of flow for sections 0-0 and 5-5.

We have

$$-AL_m + q_1 = c_p(T_5 - T_0) + A \frac{c_5^2 - v^2}{2g}, \quad (4.1)$$

where  $c_p(T_5 - T_0) = q_{11}$  — heat tapped for the cycle (in the isobaric process 0-5);  $L_{\text{ИД}} = L_s = L_{\text{ИДТ}} = L_{\text{ИД}}$  — external work equal to the mechanical energy tapped for driving the propeller, fan or compressor of the second circuit.

In general

$$L_{\text{net}} = L_1 - L_{\text{fr}} \neq 0.$$

Since the difference between the supplied and tapped heat is equal to the useful work of the cycle, i.e.,

$$q_1 - q_{\text{fr}} = AL_e.$$

then the equation of flow (4.1) is reduced to the form

$$L_e = L_{\text{net}} + \frac{c_s^2 - V^2}{2g}, \quad (4.2)$$

which had to be proven.

The obtained relation (4.2) is valid for any cycle of the VRD - ideal and real.

#### 4.2. Real Cycle of the Jet Engine

The real thermodynamic cycle is considerably distinguished from the ideal cycle  $p = \text{const}$ . It consists of practical, i.e., irreversible processes, which are accompanied by various losses and thermochemical reactions.

Figure 4.2 shows the real cycle, which has identical compression  $\pi$  and preheating  $\delta$  factors with the ideal cycle. It consists of the following:

0-1-2 - polytropic process of compression<sup>1</sup> with the feed of heat from friction (here 0-1 - process of dynamic compression; 1-2 - process of mechanical compression);

2-3 - polytropic feed of heat<sup>1</sup> in the combustion chamber with a drop in pressure because of various losses. As a result of the chemical reaction of combustion of the fuel-air mixture, which occurs at high temperature, the chemical composition of the working

---

<sup>1</sup>Processes of compression, heat feed and expansion are conditionally taken as polytropic.

medium and its quantity change (because of fuel injection), and specific heat of the gas increases;

3-4-5 - polytropic process of expansion<sup>1</sup> (here 3-4 - process of expansion in the turbine; 4-5 - the same in the jet nozzle with heat feed from friction);

5-0 - isobaric process of heat removal.

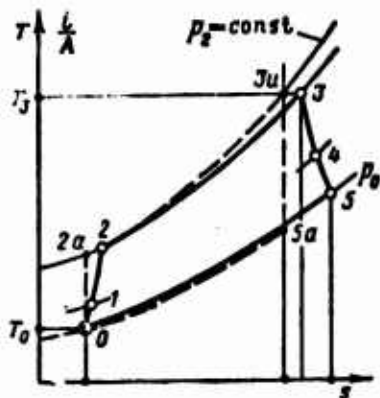


Fig. 4.2. Real cycle of a VRD.

Thus, the real cycle of the VRD, depicted on the circuit 0-1-2-3-4-5-0, is a *polytropic cycle with variable chemical component and variable specific heat of the working medium (air + gas)*.

The real cycle, in contrast to the ideal, is an "open" cycle - gases flowing from the engine no longer take part in the periodically accomplished work and do not enter into the entrance of the VRD.

The presence of friction in all processes occurring in the VRD decreases the useful work of the cycle, which as the final result lowers the thrust of the VRD and worsens its economy. To prove this, it is sufficient to compare both cycles with respect to the quantity of supplied and tapped heat.

Since the interval of preheating in the combustion chamber as a result of preheating from friction in the compressor is decreased

<sup>1</sup>Processes of compression, heat feed and expansion are conditionally taken as polytropic.

$$[(T_3 - T_2) < (T_{3a} - T_{2a})], \text{ then } q_{II(p)} < q_{II(ua)}.$$

The increase in temperature of outgoing gases from the jet nozzle in the case of the real cycle ( $T_5 > T_{5a}$ ) indicates the fact that the quantity of tapped heat grew, i.e.,  $q_{II(p)} > q_{II(ua)}$ . Consequently, the useful work of the real cycle is less than that in the ideal cycle i.e.,

$$L_u < L_{u(ua)},$$

since

$$(q_{I(p)} - q_{II(p)}) < (q_{I(ua)} - q_{II(ua)}).$$

Let us call expression

$$L_r + \frac{c_s^2}{2g} = L_p = \frac{c_p}{A} (T_3^* - T_3)$$

the total work of expansion of the gas.

Similarly, expression

$$L_k + \frac{V^2}{2g} = L_c = \frac{c_p}{A} (T_2^* - T_0)$$

is called, the total work of compression of the air.

If from the total work obtained with expansion ( $L_p$ ), we subtract the total work expended for compression ( $L_c$ ), then we obtain the useful work of the real cycle of the VRD, i.e.,

$$L_p - L_c = l_e = (L_r - L_k) + \frac{c_s^2 - V^2}{2g} = L_{un} + \frac{c_s^2 - V^2}{2g}. \quad (4.3)$$

In the particular case when  $L_r = L_k$ , we find that

$$L_p - L_c = \frac{c_s^2 - V^2}{2g}. \quad (4.3a)$$

Let us apply to processes of compression, of heat feed and of expansion accomplished inside the TRD between sections 0-0 and 5-5, Bernoulli's equation:

$$L_K - L_T = \int_0^5 v dp + \overset{5}{L}_0 + \frac{c_5^2 - V^2}{2g}. \quad (4.4)$$

Assuming for the TRD that  $L_K = L_T$ , we obtain

$$-\int_0^5 v dp - \overset{5}{L}_0 = \frac{c_5^2 - V^2}{2g},$$

where

$$\int_0^5 v dp = \underbrace{\int_0^2 v dp}_{\text{work of compression}} + \underbrace{\int_2^3 v dp}_{\text{work at heat feed}} + \underbrace{\int_3^5 v dp}_{\text{work of expansion}}$$

$-\int_0^5 v dp - L_T$  - work equivalent to the area limited by the circuit of the cycle, or the so-called *indicator* work of the real cycle.

It is convenient to express the indicator work in terms of polytropic works of processes  $L_I = L_{0a,0} + L_{0a,1} - L_{0a,2}$ .

$$\overset{5}{L}_0 = \overset{2}{L}_0 + \overset{3}{L}_2 + \overset{5}{L}_3 - \text{total work of friction.}$$

The work of friction in the process of compression is depicted in  $T-s$ -coordinates (Fig. 4.3) by the area lying under the compression line (area 0-2-b-a-0).

The work of friction in the process of heat feed is depicted in  $T-s$ -coordinates (see Fig. 4.3) by the area 2-3-2'-a-b-2. Actually, the area 2-3-d-b-2 lying under the line of the real process of heat feed is the sum of the external heat and heat of friction; the area lying under isobar 2'-3 is the external heat determined by the same temperature range ( $T_3 - T_2$ ).

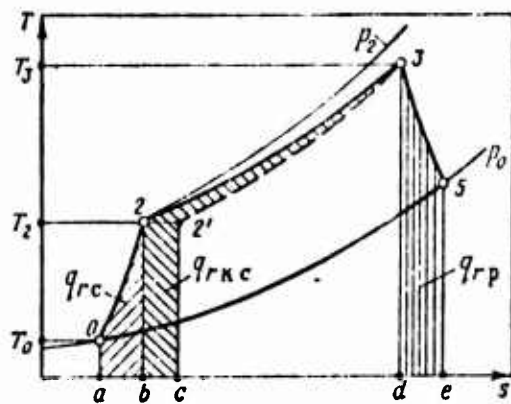


Fig. 4.3. Determination of losses of friction in the real cycle.

Consequently, the difference in areas 2-3-d-1-0 and 2'-3-d-e-1' is equivalent to the heat of friction in the real process of heat feed.

The work of friction in the process of expansion in  $T$ - $s$ -coordinates is depicted as the area which lies under the polytrope of expansion (area 3-5-e-d-3).

Thus, if from the indicator work of the cycle we deduct the sum of works of friction, then we will obtain an increase in the kinetic energy in the real cycle, which is considerably less than the useful work of the ideal cycle, i.e.,

$$L_i - L_r = \frac{c_3^2 - v^2}{2g} \quad (4.4a)$$

#### 4.2.1. Change in Total Energy of Gas Flow in Elements of the TRD

The representation of real gas conditions in parameters of braked flow in  $i$ - $s$ -coordinates makes it possible in simple and graphic form to show the change in total gas energy in separate elements of the TRD (Fig. 4.4).

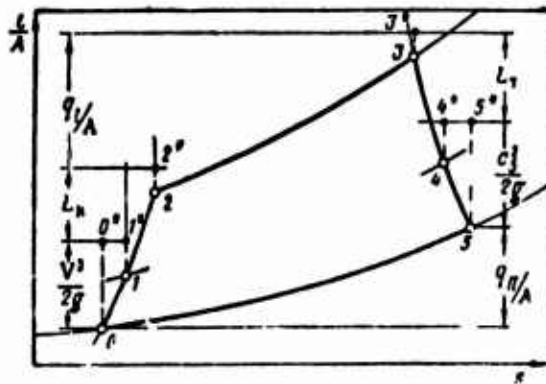


Fig. 4.4. Change in total energy of gas in the real cycle.

Thus, for instance, at the entrance into the engine and the jet nozzle the total energy of the gas remains constant:

$$i_0 = i_1; i_4 = i_5.$$

In the compressor it increases as a result of the feed of mechanical energy:

$$AL_n = i_2 - i_1,$$

and in chamber of combustion - as a result of heat feed:

$$q_1 = i_3 - i_2.$$

In the turbine the total energy of the gas is decreased, which is conditioned by the removal of mechanical energy to the user (compressor):

$$AL_r = i_3 - i_4.$$

#### 4.3. Efficiency of the Process of Compression

Processes of dynamic (outside the engine) and mechanical (in the compressor) of compression of the TRD occur with different hydraulic and gas-dynamic perfection. The criteria of this

perfection are, as is known, for the diffuser -  $\sigma_{\text{д}}^*$ ; for the compressor -  $\eta_{\text{к}}^*$ .

To estimate the effectiveness of the process of compression as a whole, let us introduce the concept of total<sup>1</sup> efficiency of compression.

The efficiency of process of compression is called the ratio of adiabatic work of compression to the expended work of compression, which is equal to the sum of kinetic energy of air in the section corresponding to the undisturbed flow, and the work of compressor (Fig. 4.5), i.e.,

$$\eta_c = \frac{L_{\text{a.v.c}}}{L_c} = \frac{L_{\text{a.v.c}}}{\frac{V^2}{2g} + L_{\text{к}}} \quad (4.5)$$

Let us transform formula (4.5):

$$\begin{aligned} \eta_c &= \frac{\frac{c_p}{A} (T_{2,1}^* - T_u)}{\frac{V^2}{2g} + \frac{c_p}{A} (T_2^* - T_u^*)} = \frac{\frac{c_p}{A} T_u \left[ (\pi_1 \pi_k^*)^{\frac{k-1}{k}} - 1 \right]}{\frac{V^2}{2g} + \frac{c_p}{A} T_u^* \left( \pi_k^{\frac{k-1}{k}} - 1 \right) \frac{1}{\eta_k^*}} \\ &= \frac{(1 + 0,2M_0^2) \sigma_{\text{д}}^{*0,236} \pi_k^{*0,236} - 1}{(1 + 0,2M_0^2) \left[ 1 + \frac{\pi_k^{*0,236} - 1}{\eta_k^*} \right] - 1} \quad (4.6) \end{aligned}$$

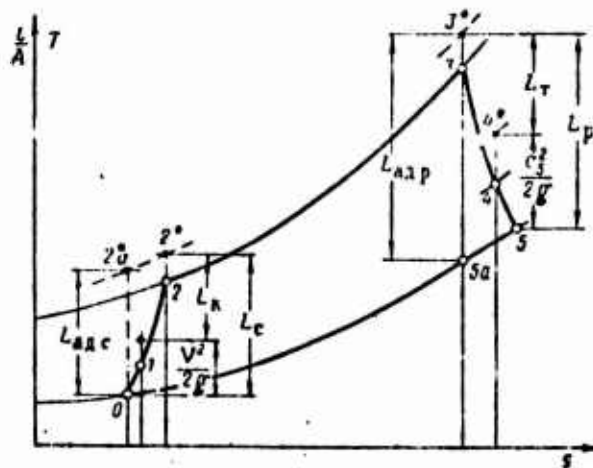


Fig. 4.5. Determination of efficiency of compression and expansion.

<sup>1</sup>Subsequently, for brevity we will omit the work "total".

From formula (4.6) it follows that the efficiency of compression depends on coefficients of losses of partial processes ( $\delta_{\text{д}}^*$ ,  $\eta_{\text{к}}^*$ ), and also on compression factor of the compressor and  $M_0 =$  of flight, i.e., on the part of participation of the partial process in the total process of compression.

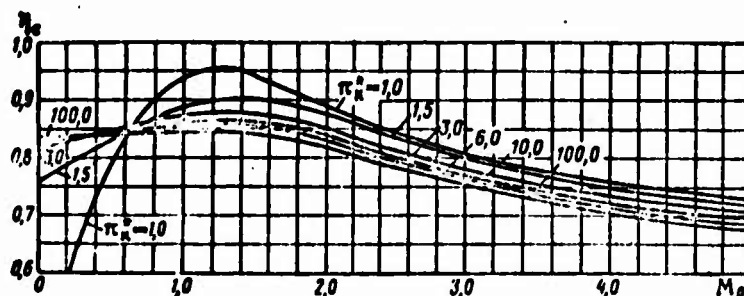


Fig. 4.6. Effect of various factors on efficiency of compression  $\eta_c$ .

Let  $M_0 = 0$ , then

$$\eta_c = \frac{(\sigma_{\text{д}}^{*0.286} \pi_{\text{к}}^{*0.286} - 1)}{(\pi_{\text{к}}^{*0.286} - 1)} \eta_{\text{к}}^* < \eta_{\text{к}}^* \quad (4.7)$$

Let  $\pi_{\text{к}}^* = 1$ , then

$$\eta_c = \frac{(1 + 0.2M_0^2) \sigma_{\text{д}}^{*0.286} - 1}{0.2M_0^2} \quad (4.8)$$

Let  $\sigma_{\text{д}}^* = 1$ , then  $\eta_c > \eta_{\text{к}}^*$ .

Let  $\eta_{\text{к}}^* = 1$ , then

$$\eta_c = \frac{(1 + 0.2M_0^2) \sigma_{\text{д}}^{*0.286} \pi_{\text{к}}^{*0.286} - 1}{(1 + 0.2M_0^2) \pi_{\text{к}}^{*0.286} - 1} \quad (4.9)$$

Figure 4.6 shows the effect of various factors on  $\eta_c$ .

#### 4.4. Efficiency of the Expansion Process

Expansion processes in a turbine and in a jet nozzle are accomplished with different effectiveness and are characterized by

different values of efficiency ( $\eta_r^*$  and  $\eta_{p.c} = \phi_{p.c}^*$ ).

To estimate the effectiveness of the process of expansion as a whole, let us introduce the concept of total efficiency of expansion.

The efficiency of the process of expansion is called, the ratio of the actually obtained work of expansion, equal to the sum of the work of the turbine and kinetic energy at the exit of the jet nozzle, to the adiabatic work of expansion (see Fig. 4.5), i.e.,

$$\eta_p = \frac{L_p}{L_{a.v.p}} = \frac{L_r + \frac{c_3^2}{2g}}{L_{a.v.p}}. \quad (4.10)$$

Let us transform formula (4.10):

$$\eta_p = \frac{L_{a.v.r}^* \eta_r^* + L_{a.v.p.c}^* \varphi_{p.c}^2}{L_{a.v.p}} = \frac{L_{a.v.r}^* \eta_r^* + (L_{a.v.p} - L_{a.v.r}^*) \varphi_{p.c}^2}{L_{a.v.p}}. \quad (4.11)$$

Let us denote

$$\frac{L_{a.v.r}^*}{L_{a.v.p}} = b. \quad (4.12)$$

Then

$$\eta_p = b \eta_r^* + (1-b) \varphi_{p.c}^2.$$

When  $b = 0.5$ , we have

$$\eta_p \approx \frac{\eta_r^* + \varphi_{p.c}^2}{2}. \quad (4.13)$$

#### 4.5. Other Ideal Cycles of Airbreathing Jet Engines

##### 4.5.1. Cycle of the Turboramjet Engine

Figure 4.7 shows in  $p$ - $v$  and  $T$ - $s$ -coordinates the ideal cycle of the TRDF ( $p = \text{const}$ , with stepped heat feed).

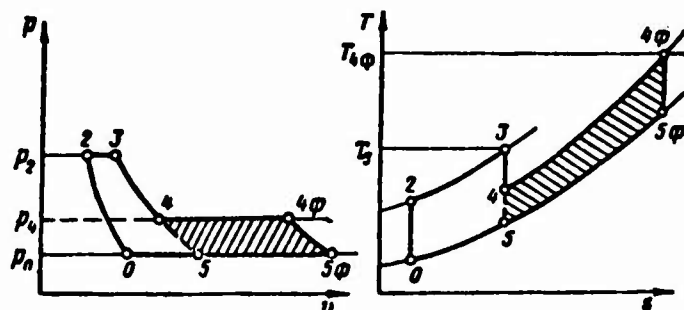


Fig. 4.7. Ideal cycle of the TDRF  
( $p = \text{const}$  with stepped heat feed).

Here

- 0-2 - adiabatic curve of compression;
- 2-3 - isobar of heat feed in the main combustion chamber;
- 3-4 - adiabatic curve of expansion in the turbine;
- 4-4φ - isobar of heat removal in the afterburner;
- 4φ-5φ - adiabatic curve of expansion in the jet nozzle;
- 5φ-0 - isobar of heat removal.

The TRDF cycle is a combination of two cycles  $p = \text{const}$ : main (0-2-3-5) and afterburner (5-4-4φ-5φ); the main cycle has a greater compression ratio than that of the afterburner;

$$\pi = \frac{p_2}{p_0} > \pi_\phi = \frac{p_4}{p_0},$$

and, consequently, a higher thermal efficiency,

$$\eta_i = 1 - \frac{1}{\pi^{\frac{k-1}{k}}} > \eta_{i\phi} = 1 - \frac{1}{\pi_\phi^{\frac{k-1}{k}}}.$$

It is easy to draw the conclusion that the addition of the afterburner cycle to the main cycle  $p = \text{const}$  increases the useful work of the total cycle:

$$L_{i\phi} = L_i + L_{i\phi} = q_i \eta_i + q_{i\phi} \eta_{i\phi},$$

which will be greater, the greater the heat supplied in the afterburner. An increase in useful work of the cycle leads to a growth in specific and also total thrust of the TDRF. At the same

time, the addition of the afterburner cycle with relatively low thermal efficiency lowers the thermal efficiency of the total cycle of the TRDP. Therefore, the switching of the afterburner on the test stand always makes the economy of operation of the engine worse.

#### 4.5.2. Cycle with Isothermal Compression

The tendency to reduce power expenditures in the compression process led to the concept of air cooling in the high-pressure axial-flow compressor (for example, by water injection).

In the particular case of the intensive cooling, the temperature of the compressible air can remain constant. Thus, we arrive logically at the examination of the ideal cycle  $p = \text{const}$  with isothermal compression (Fig. 4.8).

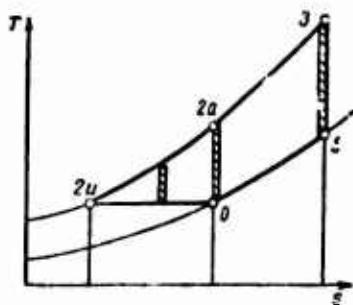


Fig. 4.8. Ideal cycle  $p = \text{const}$  with isothermal compression.

The cycle  $p = \text{const}$  with isothermal compression 0-2u-3-5 is distinguished from usual cycle  $p = \text{const}$  0-2a-3-5 in that the compression of the working medium occurs not along the adiabatic curve but along the isotherm. In this case the work expended for compression is lowered, i.e.,

$$L_{0-2u} < L_{0-2a}$$

Consequently, with the same produced work of expansion the useful work of the cycle increases, i.e.,

$$L_{0-2u-3-5} > L_{0-2a-3-5}$$

As regards the effect of cooling with compression on the thermal efficiency of the cycle, the latter is less with isothermal compression than with the adiabatic process. The latter follows from the comparison of efficiency of elementary Carnot cycles<sup>1</sup>, which form the additional cycle 0-2u-2a (see Fig. 4.8), and also the original Brayton cycle 0-2a-3u-5a (see Fig. 4.1).

Thus, the introduction of isothermal compression increases the useful work of cycle but simultaneously lowers its thermal efficiency and, consequently, makes the economy of thermodynamic cycle worse.

#### 4.5.3. Ideal Cycle $p = \text{const}$ with Heat Recovery

One of the methods of increasing the economy of aviation gas turbine is *heat recovery*.

Heat recovery is understood as the use of heat of gases exhausted in the engine for preliminary preheating of air compressed in the compressor before its feed into the combustion chamber. Heat recovery lowers the quantity of external heat applied to the working medium in the thermodynamic cycle, and, consequently, increases the economy of the engine.

Figure 4.9 shows the ideal cycle  $p = \text{const}$  with recovery heat. It is distinguished from the usual cycle  $p = \text{const}$  in that the preheating of cold air in the process 2-2p accomplished because of the cooling of hot gas in the process 4-4p, i.e., because of the internal heat exchange in the regenerator.

In the ideal case the process of heat exchange in the regenerator occurs isobarically, without losses and the air temperature at the exit from the regenerator is equal to the temperature of the gas

---

<sup>1</sup>The efficiency of elementary Carnot cycle is greater the higher the ratio of temperatures in the adiabatic process of compression, i.e.,

$$\eta = 1 - \frac{T_0}{T_2}$$

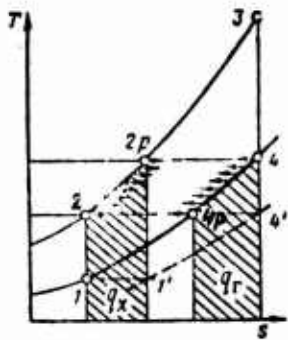


Fig. 4.9. Ideal cycle  $p = \text{const}$  with heat recovery.

entering into the regenerator i.e.,  $T_{2p} = T_4$ . Correspondingly  $T_{4p} = T_2$ .

Let us find the thermal efficiency of the cycle with heat recovery.

We gave

$$\eta_t = \frac{M}{q_1} = \frac{c_p(T_3 - T_4) - c_p(T_2 - T_1)}{c_p(T_3 - T_{2p})}, \quad (4.14)$$

or

$$\eta_t = 1 - \frac{T_2 - T_1}{T_3 - T_4}.$$

Noting that  $\frac{T_2}{T_1} = \frac{T_3}{T_4} = \pi^{\frac{k-1}{k}}$ , we obtain

$$\eta_t = 1 - \frac{T_1}{T_4} = 1 - \frac{1}{\pi^{\frac{k-1}{k}}}, \quad (4.15)$$

where  $\pi = \left(\frac{T_4}{T_1}\right)^{\frac{k}{k-1}}$  — compression ratio of the cycle  $p = \text{const}$  equivalent in efficiency.

Thus the cycle  $p = \text{const}$  with heat recovery (1-2-3-4) with respect to thermal efficiency is equivalent to the usual cycle  $p = \text{const}$  (without heat recovery) but with the raised compression ratio (1'-2p-3-4'):

$$\pi_p = \left(\frac{T_4}{T_1}\right)^{\frac{k}{k-1}} > \pi = \left(\frac{T_2}{T_1}\right)^{\frac{k}{k-1}}.$$

Expression (4.15) can also be represented, in the form

$$\eta_t = 1 - \frac{\pi^{\frac{k-1}{k}}}{\Delta}, \quad (4.16)$$

where  $\Delta = \frac{T_3}{T_1}$  - degree of preheating.

Thus, the efficiency of the cycle  $p = \text{const}$  with heat recovery is more, the higher the degree of preheating of the working medium (i.e., the higher the temperature of the gas  $T_3$ ) and the lower compression ratio. At the same time, in the usual cycle  $p = \text{const}$  the thermal efficiency is higher, the greater the compression ratio (Fig. 4.10).

Let us find the value of the compression ratio of the cycle at which the use of heat recovery appears irrational, i.e.,

$$\eta_t = \eta_t(p).$$

From equalities  $1 - \frac{e}{\Delta} = 1 - \frac{1}{e}$  or  $T_4 = T_2$  we obtain

$$e_{\text{max}} = \pi_{\text{max}}^{\frac{k-1}{k}} = \sqrt{\Delta}. \quad (4.17)$$

For  $\Delta = 4$  ( $T_1 = 288^\circ\text{K}$  and  $T_3 = 1152^\circ\text{K}$ ) we find  $\pi_{\text{max}} = 11.3$ .

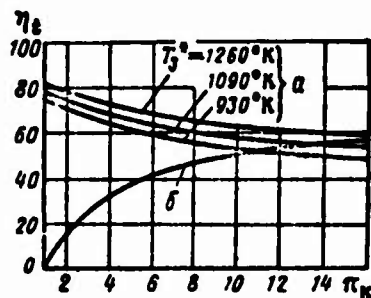


Fig. 4.10. Comparison of thermal efficiency of cycles  $p = \text{const}$ : a-c) heat recovery; b) without heat recovery.

From the aforesaid the conclusion can be made about the fact that the use of heat recovery is expedient in the gas turbine with a high-temperature turbine and low-pressure compressor.

## CHAPTER 5

### INTAKE SYSTEMS OF JET ENGINE

#### 5.1. Purpose of Intake Devices and Their Requirements

Intake systems, or diffusers, of jet engines are intended for effective air compression by means of decelerating the flow entering into the engine. At supersonic flight speeds this function of the diffuser is the main one.

At the same time, intake must at all speeds and processes of flight have high carrying capacity and provide at the inlet into the compressor (or directly into the combustion chamber of ramjet engines) a high level of uniformity of velocity and of pressure fields.

It is necessary also that the energy conversions in diffusers of the test stand and in flight would be accomplished with as less hydraulic and gas-dynamic losses as possible, and they do not lead to the appearance of cutoff and surge conditions, which sharply worsen the operation of the engine.

Since the intake, with their sometimes quite complex configuration, are an integral element of the nacelle of the engine, then it is very important that they do not create considerable external resistance.

With an increase in the speed of flight the role of the diffuser, in providing highly economical operation of the engine, continuously increases.

### 5.1.1. Basic Requirements of Intake

The basic requirements of intake of jet engines are:

- 1) low losses of total pressure in all flight regimes;
- 2) high productivity;
- 3) low external resistance;
- 4) high uniformity of velocity and pressure fields at the inlet into the compressor or into the combustion chamber;
- 5) absence cutoff and surge regimes;
- 6) high weight, simplicity of design and control.

### 5.1.2. Basic Parameters of Effectiveness of the Diffuser

#### 5.1.2.1. Coefficient of Drop in Total Pressure of the Diffuser.

The hydraulic and gas-dynamic perfection of the intake is characterized by the coefficient of the drop in total pressure

$$\sigma_d^* = \frac{P_1^*}{P_0^*}, \quad (5.1)$$

equal to the ratio of total air pressure at the entrance into the compressor or in the combustion chamber to the total air pressure in the section corresponding to the undisturbed flow.

The greater the magnitude  $\sigma_d^*$ , the higher the pressure in gas-air channel of the engine, and, consequently, the greater the total thrust, the lower specific fuel expense of the jet engine.

#### 5.1.2.2. Flow Coefficient of the Diffuser.

The requirement of high productivity of the intake is connected with peculiarities of its operation at supersonic flight speed, when at the assigned area of the inlet into the diffuser the air flow can have different values.

Productivity of the supersonic diffuser is characterized by the flow coefficient, which is the ratio of real rate of air flow through the diffuser to the maximum possible flow when the area of the section of inlet jet in the undisturbed flow is equal to the area of inlet, i.e.,

$$\varphi = \frac{G}{G_{\max}} = \frac{V_n \gamma_n f_n}{V_n \gamma_n f_{n\max}} = \frac{f_n}{f_{n\max}} \leq 1. \quad (5.2)$$

The greater flow coefficient, the higher the thrust.

### 5.1.2.3. Coefficient of Drag of the Diffuser.

It is accepted to estimate the effect of intake systems on the external resistance of engine nacelle by coefficients similar to coefficients of drag of the fuselage in aerodynamics.

The coefficient of resistance of the intake can be referred to its greatest section (mid-section). It is equal to

$$c_{r_{\text{int}}} = \frac{X_{\text{int}}}{\frac{\rho_n V_n^2}{2} \cdot S_M} \quad (5.3)$$

where  $X_{\text{int}}$  - force of drag of the intake;  
 $S_M$  - mid-section of the intake;  
 $\rho_n$ ;  $V_n$  - density and velocity of air in the section corresponding to the undisturbed flow.

### 5.1.3. Concept on External Resistance of the Intake

Earlier, in Section 3.1, we obtained the expression for force of the total drag of the nacelle of the engine in the form

$$X_{r,1} = X_{\text{доп}} + X_p + X_{\text{тп}} + X_{\text{доп}}.$$

In this chapter we will examine the essence of additional resistance of the inlet jet ( $X_{\text{доп}}$ ), and also the resistance of

pressure of the diffuser ( $X_p$ ). Precisely they determine the physical essence of external resistance of the inlet device.

#### 5.1.4. Additional Resistance of the Intake System

The additional resistance of the intake system is the axial component of surplus forces of pressure applied to the border of the surface of the free jet between its section corresponding to the undisturbed flow and the section at the inlet into the engine, i.e.,

$$X_{\text{add}} = \int_0^{\delta x} (p - p_a) df. \quad [\delta x = \text{inlet}]$$

The additional resistance depends on the configuration of the inlet jet and distribution of pressure over its surface. With operation of the engine on a test stand (when  $V = 0$ ) lines of flow "merge" from all sides to the inlet into the diffuser. In this case along each stream there is the velocity increase and a lowering of pressure and temperature (Fig. 5.1a).

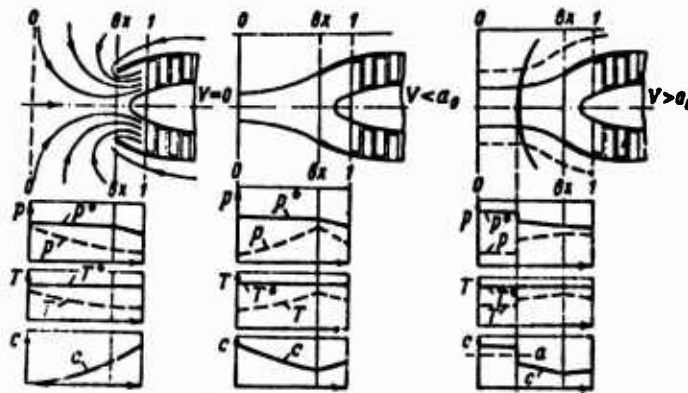


Fig. 5.1. Change in gas parameters at the inlet of the TRD: a)  $V = 0$ ; b)  $V < a_0$ ; c)  $V > a_0$ .

With flight at low speeds (when  $V < a_{Bx}$ ) the boundary flow lines of the inlet jet form a convergent funnel (convergent channel), and in this case along each elementary stream acceleration of flow occurs.

In the particular case when  $V = a_{Bx}$ , flow lines of the entering jet remain parallel; along separate jets of flow energy conversions do not occur.

At great subsonic velocities, when  $a_0 > V > a_{Bx}$  boundary lines of flow of the inlet jet form a divergent funnel (diffuser); in this case along the elementary jets there is deceleration of flow, which is accompanied by an increase in pressure and temperature (see Fig. 5.1b).

At supersonic flight speed in front of diffuser the inlet is established shock wave (see Fig. 5.1c).

In all cases described here (except for  $V = a_{Bx}$ ) in the free jet an additional resistance acting in a direction opposite to the direction of flight appears.

#### 5.1.5. Pressure Drag of the Intake

At subsonic flight speeds and at nonseparated flow of the external surface of the diffuser, pressure drag is absent. What is more, with flow about surfaces of the inlet element of the air inlet as the usual profile, there appear aerodynamic forces, which give an axial component acting in the direction of flight, the so-called *suction* force. The reasons for the appearance of the suction force are easily understood by examining spectra of pressure distribution along the upper and lower surfaces of the inlet element of the diffuser (Fig. 5.2) similar to the aerodynamic profile.

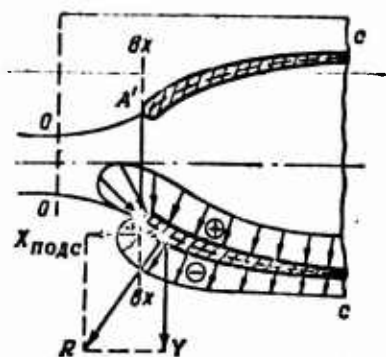


Fig. 5.2. Determination of suction forces of the inlet device at subsonic flight speeds.

In the ideal case of flow when friction, shock waves and separations of flow are absent, the suction force in accuracy is equal to the force of additional resistance of the free jet and is directed opposite to it, and, consequently,

$$X_{вз} = X_{доп} - X_{порс} = 0.$$

In the actual case of flow, the suction force is less than the force of additional resistance, and in the presence of a sharp inlet edges of the diffuser it is practically equal to zero.

At supersonic flight speeds the appearing shock waves increase the pressure at the external surface of the conical casing of the diffuser. As a result of this the resistance of pressure of the diffuser

$$X_p = \int_{\Sigma} (p - p_n) df,$$

which now we will call *wave*, increases sharply.

## 5.2. Thermodynamic Processes in Air Intake (Diffusers)

Let us examine processes of the conversion of energy in the standard (Fig. 5.3) subsonic air intake (diffuser) on a test stand ( $V = 0$ ) and in flight; at subsonic ( $0 < V < a_0$ ) flight speeds. These processes partially occur outside the engine - in the free jet and in the actual air intake. Experience shows that in a free subsonic jet (a test stand and in flight) the process of conversion of energy occurs practically without losses, i.e., isentropically.

The air intake designed for subsonic flight speeds is made usually in the form of a narrowing channel (convergent channel). In such an air intake there is the process of gas expansion, i.e., a certain acceleration of flow. This makes it possible to provide a more even velocity field at entrance into the compressor, prevent the appearance of flow separation and unstable operation and reduce gas-dynamic losses.

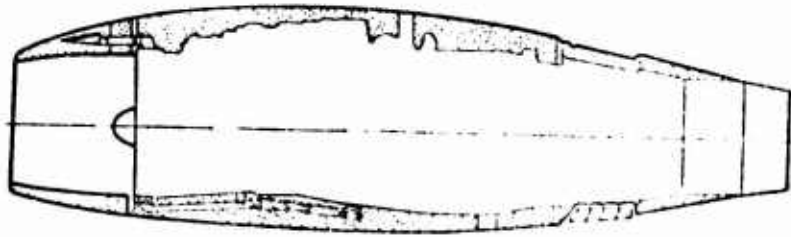


Fig. 5.3. Engine nacelle of subsonic aircraft (cross section).

Figure 5.4 gives at  $T; \frac{l}{A} - s$ -coordinates the process of energy conversion at the entrance into the TRD for cases a) when  $V = 0$  and b) when  $V > c_1$ . The process in a free subsonic jet is shown in the form of the isentrope  $0-1'$ ; the process inside the air intake is depicted in the form of an irreversible adiabatic curve of expansion  $1'-1$  (with an increase in entropy).

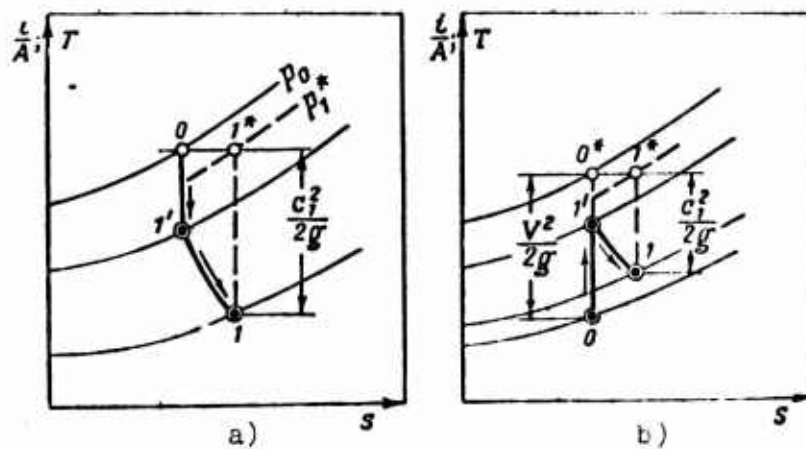


Fig. 5.4. Process of the conversion of energy at inlet of the TRD: a) on a test stand ( $V = 0$ ); b) in flight ( $V > c_1$ ).

Let us formulate the equation of energy for sections 0-0 and 1-1 of the flow at the inlet of the TRD.

We obtain

$$i_0 + A \frac{V^2}{2g} = i_0^* = i_1 + A \frac{c_1^2}{2g} = i_1^* \quad (5.4)$$

Thus, in processes of dynamic deceleration or acceleration of flow, independently of the presence of friction and shock waves, the total energy of 1 kg of air remains constant. The total gas temperature also remains constant:

$$T_0^* = T_1^* \quad (5.5)$$

The total gas pressure, as follows from a comparison of braked flow conditions in sections 0-0 and 1-1, is lowered, i.e.,

$$p_1^* < p_0^*$$

The drop in total pressure appears greater the higher the hydraulic and gas-dynamic losses (in shocks), i.e., the greater the polytropic exponent of the process of compression deviates from the adiabatic curve. The hydraulic and gas-dynamic perfection of the process at the inlet of the jet engine, as is known, is estimated by the coefficient of the drop in total pressure

$$\sigma_A^* = \frac{p_1^*}{p_0^*}$$

It can be represented in the form of the product

$$\sigma_A^* = \frac{p_1^*}{p_1'^*} \frac{p_1'^*}{p_0^*} = \sigma_{BX}^* \sigma_{CH}^* \quad (5.6)$$

where  $p_1' = p_{BX}$ ;  $\sigma_{BX}^*$  - coefficient of losses of total pressure in the intake system; in design conditions  $\sigma_{BX}^* \approx 0,96 \dots 0,985$ ;  $\sigma_{CH}^*$  - the same in the system of shocks at supersonic flight;  $\sigma_D^*$  - coefficient of losses of total pressure in the dynamic process of compression (expansion).

---

<sup>1</sup>Such a recording is conditional, since not always can hydraulic losses (determined by  $\sigma_{BX}^*$ ) and gas-dynamic losses (characterized by  $\sigma_{CH}^*$ ) be separated with respect to elements of the diffuser.

Figure 5.1 gives curves of the change in parameters of gas ( $p$ ,  $T$  and  $c$ ) at the inlet of TRD for characteristic regimes of operation of the air intake; when: a)  $V = 0$ ; b)  $V < a_0$ ; c)  $V > a_0$ .

### 5.3. Operation of a Standard Subsonic Diffuser at Supersonic Flight Speeds

With the flow about the standard subsonic diffuser by supersonic flow, in front of the air inlet a curvilinear shock wave (head wave) appears similar to that which occurs with the flow past a blunt-nosed body or cone with a large aperture angle. In the front part of the diffuser the head curvilinear wave (see Fig. 5.1c) is transformed into a normal shock wave the intensity and position of which are determined by the  $M_0$  of flight and the operating regime of the engine and depend on the configuration of the diffuser.

With an increase in  $M_0$  number of flight, the losses of total pressure in a normal shock increase (Fig. 5.5, curve 1).

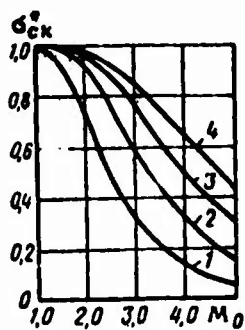


Fig. 5.5. Change in gas-dynamic losses in the system of shocks with respect to  $M_0$  number of flight: 1, 2, 3, 4 - number of shocks.

Table 5.1 gives coefficients of the drop in total pressure in a normal shock ( $\sigma_{np}^*$ ) depending on  $M_0$  number of flight.

Table 5.1.

$N_0$	1,0	1,5	2,0	2,5	3,0	3,5	4,0	4,5	5,0
$\sigma_{np}^*$	1,0	0,93	0,721	0,499	0,328	0,213	0,139	0,10	0,07

With an increase in flight speed the head wave all the more moves away from the inlet of the diffuser. This lowers the coefficient of flow and increases the external resistance of the diffuser.

It is characteristic that when  $M_0 = 1.3-1.4$  losses in the normal shock are relatively few ( $\sigma_{np}^* \approx 0.96-0.98$ ). However, matter not only in the intensity of shocks - the appearing shocks cause separation of vortices from leading edges of the diffuser, which can increase by far the losses of total pressure.

To prevent separations of vortices at supersonic flight speeds the leading edge of the diffuser is made sharp, the angle of opening of the diffuser is made small, turns of the flow are tried to be avoided. One should keep in mind that diffusers with sharp edges (Fig. 5.6) operate poorly in test bench conditions and also with asymmetrical flow (at large angles of attack, etc).

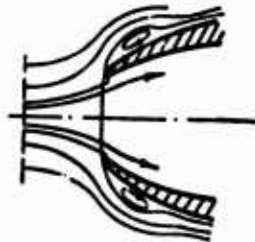


Fig. 5.6. Flow of air intake with sharp inlet edges.

Considering all these circumstances, it is necessary when  $M_0 > 1.4-1.5$  to use special supersonic diffusers.

#### 5.4. Supersonic Diffusers (Design Conditions)

##### 5.4.1. Gas-Dynamic Principles of the Development of Supersonic Diffusers

Gas-dynamic principles in the fulfillment of supersonic diffusers are reduced to effective methods of multishock (theoretically shockfree) conversion of supersonic flow into subsonic.

The replacement of one normal shock by a system of shocks,

including several oblique shocks and a closing normal shock, makes it possible to considerably reduce losses of supersonic deceleration.

Figure 5.6 shows the effect of a reduction in the number of shocks on the total pressure in various multishock systems. With an increase in the number of "provoked" shocks, the intensity of each of them is lowered, and the effectiveness of the supersonic diffuser increases accordingly. Thus, for instance, when  $M_0 = 3.0$  the coefficient of the drop in total pressure is equal to the following:

system of shocks	{	1 normal shock. . . . .	$\sigma_{CR}^* = 0.525$
		1 oblique + 1 normal. . . . .	$\sigma_{CR}^* = 0.600$
		2 oblique + 1 normal. . . . .	$\sigma_{CR}^* = 0.700$
		3 oblique + 1 normal. . . . .	$\sigma_{CR}^* = 0.870$

With a considerable increase in the number of shocks we proceed in the limit to the shockfree deceleration of flow with the coefficient of the drop in total pressure, which approaches unity. With a allowance for friction and the presence of the boundary layer in real isentropic systems of shocks the value  $\sigma_{CR}^*$  is less than unity.

At present it is possible to consider experimentally proven that when  $M_0 = 3.0$ \* values  $\sigma_{CR}^* = 0.90-0.97$  can be obtained (see Fig. 5.7).

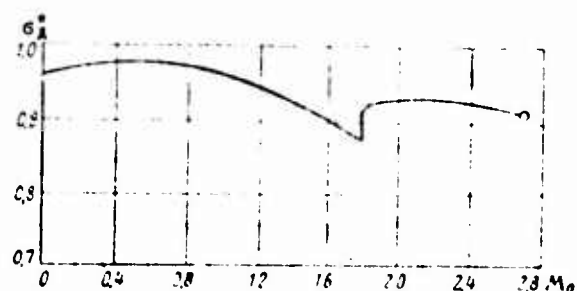


Fig. 5.7. Characteristic of the supersonic diffuser of the aircraft Boeing 2707 ( $M_{0p} = 2.7$ ).

\*The standard high-altitude cruising regime of flight of supersonic passenger aircraft.

#### 5.4.2. Classification of Supersonic Diffusers

Depending on the method of realization of supersonic deceleration, supersonic diffusers (Fig. 5.8) are subdivided into:

a) diffusers with external compression. Such diffusers consist of an external cover and central body with a stepped cone (see Fig. 5.8a);

b) diffusers with internal compression (see Fig. 5.8c);

c) diffusers with mixed compression (see Fig. 5.8b).

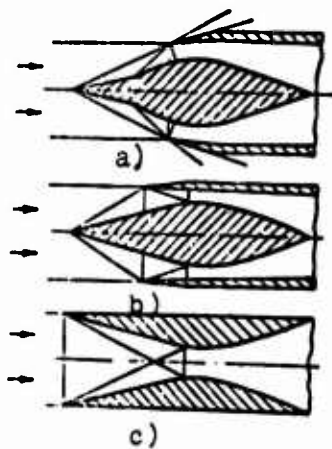


Fig. 5.8. Diagrams of the formation of systems of shock waves: a) with external compression; b) with internal compression.

The types of diffusers given above are made in a round or box section. In them it is possible to accomplish the so-called multishock and theoretically stepless (isentropic) compression (Fig. 5.9a and 5.9b).

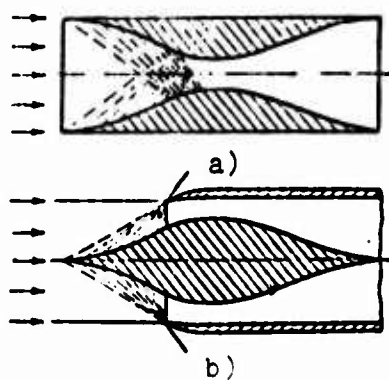


Fig. 5.9. Diagrams of diffusers with isentropic compression: a) internal compression; b) external compression.

If in a diffuser with external compression supersonic deceleration is carried out on a stepped cone outside the diffuser, then in the air intakes with internal compression the whole system of shocks is disposed inside the channel of the diffuser, and it almost is not subjected to the external effect of circumflowing flow.

#### 5.4.2.1. Diffuser with Internal Compression.

Figure 5.10 shows a diagram of the diffuser with internal compression. Such a diffuser is the profiled channel with steady outlines, which is reminiscent of the Laval nozzle.

An ideal diffuser with shockfree deceleration of flow and with the absence of a boundary layer operates in the following manner. In the convergent (supersonic) part of the channel there is deceleration of supersonic flow in compression waves of infinitesimal intensity and in the design regime in the smallest section of the channel  $r-r$  called the "throat" and the velocity of the flow reaches the speed of sound. Further, in the expanding (subsonic) part of the diffuser there is further deceleration of the already subsonic flow.

Thus, an ideal diffuser with internal compression operates as an inverted Laval nozzle; flow parameters along such a diffuser change continuously. Losses of complete pressure are absent.

In a real diffuser the interaction of compression waves with an accumulating boundary layer leads in a certain section the formation of a closing normal or  $\Lambda$ -shaped shock even to the appearance of losses of complete pressure.

The advantage of diffusers with internal compression is their low external resistance.

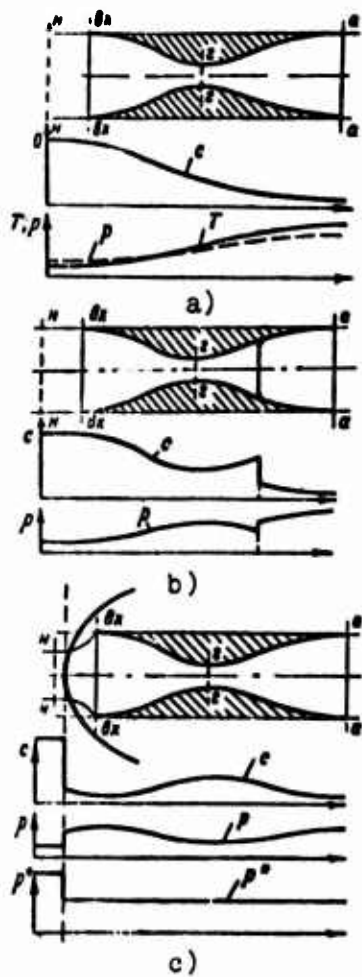


Fig. 5.10. Diagram of a supersonic diffuser with internal compression: a) shockfree deceleration; b) deceleration with a shock formation; c) formation of "ejected" wave.

5.4.2.2. Axisymmetrical Diffuser with a Central Body and External Compression.

One of the widespread schemes of supersonic diffuser is the scheme of the axisymmetrical air intake with the central body and with external compression. The schematic cross section of such a diffuser is shown in Fig. 5.11.

The diffuser consists of an external conical casing and central stepped cone. The inlet edge of the casing is inclined toward the axis of symmetry of the air intake at a certain angle  $\delta$  - the so-called angle of "undercutting".

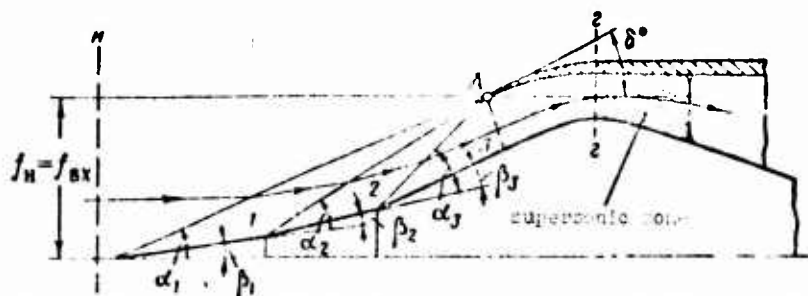


Fig. 5.11. Diagram of a supersonic diffuser with external compression.

The number of the steps of the cone and angles of their setting ( $\beta_1, \beta_2, \beta_3$ ) are determined by the quantity and position of oblique shocks in the design conditions.

The diagram shows a stepped cone with four shocks (three oblique shocks + closing normal shock).

In design conditions shocks are focused on the leading edge of the casing (at point A). The channel behind the closing normal shock is made in the form of a Laval nozzle. Behind the critical section of the nozzle there is the supersonic zone, which is finished by a normal or A-shaped "attendant" shock wave. Behind this shock, up to the entrance into the compressor, the flow of gas is subsonic. With a change in counterpressure at the exit from the diffuser attendant shock is moved in the channel.

#### 5.5. Partial Load Conditions of the Operation of a Supersonic Diffuser

Thus far we have examined the operation of supersonic diffusers in *design conditions of operation*. As is known, in this regime the operation of the diffuser and engine of the TRD is completely consistent: the diffuser operates steady, with few losses and the least external resistances; productivity of the diffuser is maximum -

---

[Translator's Note: This term in Russian literally means "duty" and is used in abstract form].

the coefficient of flow is equal to 1; if in this case the throat of the diffuser is selected at the optimum, then in its critical section the velocity of flow is equal to the speed of sound. However, in operation the supersonic diffuser operates over a wide range of partial load conditions: at various  $M_0$  numbers and flight altitudes, under various atmospheric conditions, and at various revolutions of the engine.

Partial load conditions of operation of the diffuser are characterized by several specific gas-dynamic phenomena, to which belong:

- 1) the change and destruction of the calculated system of shocks;
- 2) ejection of head wave at inlet of the diffuser;
- 3) spreading of inlet jet at supersonic flight speeds;
- 4) unstable operation (surging) of the diffuser;
- 5) appearance of subcritical and supercritical regimes.

#### 5.5.1. Change in the Angle of Slope of Shocks of the Diffuser with External Compression

With deviation of the  $M_0$  number of flight from calculated value the slope of oblique shocks of the diffuser with external compression changes. Now they are no longer focused on the leading edge of the conical casing (Fig. 5.12).

With a decrease in the  $M_0$  number of angles of slope of the shocks increase, the shocks will move away from the leading edge of the diffuser.

With an increase in the  $M_0$  angles number of slope of shocks are decreased, and the shocks now partially enter into the diffusion channel.

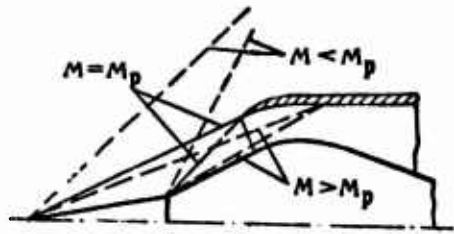


Fig. 5.12. Effect of  $M_0$  number of flight at angles of slope of shocks.

#### 5.5.2. Ejection of the Head Wave

In diffusers of all types in definite regimes of operation, when the carrying capacity of the throat appears insufficient and it cannot pass all the air entering into the inlet channel, in front of the inlet in the diffuser the so-called "ejected" head wave is generated (Fig. 5.13). Such a wave can either partially or completely destroy the rated system of shocks appearing at the diffuser with external compression.

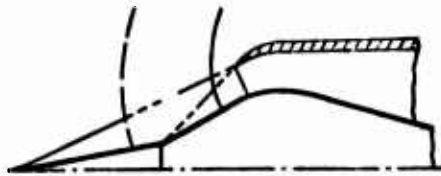


Fig. 5.13. Effect of the ejected head wave on the system of shocks.

The appearance of an ejected wave is an undesirable phenomenon, since it increases losses in total pressure and external resistance of the diffuser, decreases the flow of gas through the diffuser (as a result of the "spreading" of the inlet jet).

In the presence of an ejected head wave, a decrease in the flow of air usually leads to the appearance of surging.

#### 5.5.3. Spreading of the Inlet Jet in Partial Load Conditions

Let us examine the operation of a diffuser with internal compression. In the design supersonic regime the area of the cross

section of the inlet jet in accuracy is equal to the area of the inlet of the diffuser, i.e.,

$$f_H = f_{Bx} \text{ and } \phi = \frac{f_H}{f_{Bx}} = 1.$$

In partial load conditions of the diffuser (see Fig. 5.10c) with the appearance before it of a head (or ejected) wave the inlet jet with section  $f_{Bx}$  no longer can completely enter inside the diffuser. The phenomenon of *spreading* (division) of the jet will begin: its internal part with section  $f_H < f_{Bx}$  will flow into the diffuser; its external part (with section  $f_{Bx} - f_H$ ) will flow around the casing of the intake.

A similar phenomenon takes place in the operation of a multiple-snook diffuser with external compression. In design conditions of flight oblique shocks, which appear with flow around of the stepped cone, are focused on the leading edge of the casing (see Fig. 5.11); in this case  $f_H = f_{Bx}$  and  $\phi = 1$ .

In partial load conditions (with an increase in the angle of slope of oblique shocks on reduced  $M_0$  numbers with the appearance in front of the diffuser of the ejected wave, with the advance from the diffuser of adjustable stepped cone) we have  $f_H < f_{Bx}$ , and, consequently,  $\phi < 1.0$  (see further Fig. 5.15a, b).

Thus, with the spreading of the jet the carrying capacity of the diffuser, and, consequently, and available flow of gas through the diffuser, are decreased; the coefficient of flow becomes less than 1.

The reason of the spreading of the jet is the bend of lines of flow in the supersonic flow behind the oblique shocks and in the subsonic flow behind the head wave. In the case of an uncontrollable diffuser (in the absence of ejected waves) each number  $M > 1.0$  corresponds to the single value  $\phi$ .

At subsonic flight speeds the coefficient of flow of the

subsonic diffuser can also be less than 1. However, in contrast to supersonic flow, each value of the subsonic  $M_0$  number corresponds, depending on the regime of the engine, to various values  $\phi$ ; the greater the number of revolutions of the engine and greater  $q(\lambda_{\text{вх}})$ , the greater  $f_{\text{н}}$  and, consequently,  $\phi$ . Concordance of the necessary flow of the engine and available flow of air intake occurs automatically.

### 5.5.3.1. Effect of Spreading of the Jet on Thrust of the Engine.

The phenomenon of spreading of the jet is an unconditionally harmful phenomenon, since it, first, decreases the thrust of the power unit due to an increase in the flow of air and, secondly, increases the wave resistance of the diffuser (and, consequently, the resistance of the nacelle of the engine). Ultimately the effective thrust of the engine can be considerably reduced.

When the diffuser is not controllable, and the engine operates with a constant number of revolutions, the coefficient of flow depends only on correlation of the rated number of the diffuser  $M_{\text{д(р)}}$  and  $M_0$  numbers of flight. The higher  $M_{\text{д(р)}}$ , the less  $M_0$ , the less  $\phi$ .

Figure 5.14 shows the effect of  $M_{\text{д(р)}}$  on the coefficient of flow and additional wave resistance of the diffuser when  $M_0 = 1.0$ . For  $M_{\text{д(р)}} = 4.5$  we find  $\phi = 0.22$  and  $\chi_{\text{доп}}/R = 0.4$  (i.e., the wave resistance of the diffuser is 40% of the internal thrust).

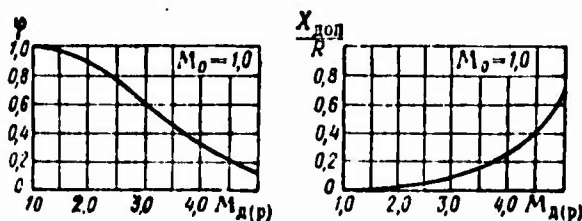


Fig. 5.14. Effect of spreading of inlet jet at supersonic flight speeds on: a) decrease in the flow of air through the engine; b) additional wave resistance of the diffuser.

#### 5.5.4. Concept on the Starting of the Uncontrollable Diffuser

The starting of the diffuser is called the process of putting the diffuser into rated conditions of operation.

To clarify the peculiarities of starting of a supersonic diffuser, let us examine the flow in the diffuser with internal compression in design conditions (see Fig. 5.10a).

Let us formulate the equation of flow for sections in the undisturbed flow (H-H) and the throat of the diffuser (r-r).

We obtain

$$m \frac{p_n^*}{\sqrt{T_n^*}} f_n q(\lambda_n) = m \frac{p_r^*}{\sqrt{T_r^*}} f_r q(\lambda_r), \quad (5.7)$$

whence we find

$$\frac{f_r}{f_n} = \frac{q(\lambda_n)}{q(\lambda_r) c_{n,r}^*} = \frac{f_r}{f_{nx}} \frac{f_{nx}}{f_n} = \frac{\bar{f}_r}{\phi}, \quad (5.8)$$

where  $\bar{f}_r$  - relative area of the throat;  $\bar{f}_r = \frac{f_r}{f_{nx}}$ ;

$\phi$  - coefficient of flow;

$c_{n,r}^* = \frac{p_r^*}{p_n^*}$  - coefficient of drop in total pressure on the section from the undisturbed section to the throat of the diffuser.

Then

$$\bar{f}_r = \frac{q(\lambda_n)}{q(\lambda_r)} \cdot \frac{\phi}{c_{n,r}^*}. \quad (5.9)$$

Let us find  $\bar{f}_r$  for  $\phi = 1$  and  $q(\lambda_r) = 1$  (case of the "optimum" throat).

We have

$$\bar{f}_r = \frac{q(\lambda_n)}{c_{n,r}^*}. \quad (5.10)$$

In the particular case of the isentropic diffuser ( $\sigma_{H,r}^* = 1$ ), we find that

$$f_r = q(\lambda_H). \quad (5.11)$$

Consequently, in the supersonic region of flight with an increase in  $M_H$  number of flight [and, consequently, with a decrease in  $q(\lambda_H)$ ] the necessary relative area of the optimum throat is continuously decreased. The obtained result has a simple physical meaning: the greater the flight speed, and, consequently, the more the dynamic compression ratio, the greater the density of air and the less the passage section of the throat necessary for passing the assigned mass of the working medium.

Let us assume that for the assigned rated  $M_0$  number of flight the geometry of the diffuser with an optimum throat is calculated. With a decrease in the  $M_0$  number ( $> 1.0$ ) the necessary relative area of the throat, according to equation (5.11), continuously increases. Now on reduced numbers  $M_0 < M_{0(p)}$  the throat of the diffuser proves to be already "supercompressed", and it less than the optimum and no longer in a state to pass the whole mass of air inflowing to its inlet section.

The noted contradiction is solved by means of the appearance in front of the intake the "ejected" head wave (see Fig. 5.10c). Since behind the head wave subsonic flow is established, and with the deceleration of which the line of flow is dispersed, then now  $\phi < 1$ , and equality (5.9) is satisfied when  $q(\lambda_H) = 1$  and  $\bar{f}_r = \text{const}$  because with the increase in  $q(\lambda_H)$   $\phi$  decreases when  $q(\lambda_H)\phi/\sigma_{H,r}^* = \text{const}$ .

Physically this means that throat now passes the whole mass of air entering through the inlet section, since the inflow of air to diffuser is decreased, (see Fig. 5.10c).

If now we increase the  $M_0$  number of flight up to its rated value then although the head wave approaches toward the inlet of the diffuser it does not disappear entirely, and, thus the design scheme

of the diffuser will not be restored - the diffuser will not be started. To start the uncontrollable diffuser, the  $M_0$  number of flight over its rated value must be increased. This phenomenon is called "hysteresis". It is natural that such a method of starting of the diffuser is not always possible and convenient.

For the starting of a multishock supersonic diffuser with external compression, it is necessary with the appearance of a head wave, for example, to bring forward the stepped cone, and with its help transform the head wave into a system of oblique shocks, and then move the cone inside the casing (Fig. 5.15).

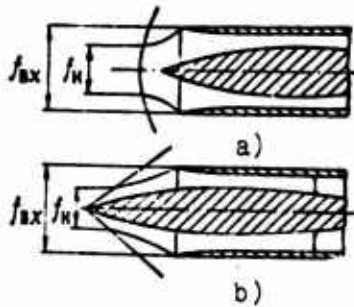


Fig. 5.15. Explanation of methods of starting of the diffuser: a) starting of an uncontrollable diffuser ["ejection" of head wave ( $M_0 < M_p$ )]; b) starting with the help of movement of the cone.

The starting of the diffuser with internal compression can be accomplished by means of adjustment of the area of the throat ("overexpansion" of the throat) with the help of flexible elements and also by means of the use of perforated walls.

#### 5.5.5. Surging of a Supersonic Diffuser

Let us examine the unstable operation (surging) of a multishock supersonic diffuser with a central body. The reason for the appearance of surging of a supersonic diffuser mostly is the separation of the boundary layer from the surface of the stepped cone behind the head wave.

One of the schemes of the appearance of surging is the following (Fig. 5.16). After the head wave there is separation of the boundary layer. The appeared zone (area) of separation with intensive turbulences decreases the effective throat area (see Fig. 5.16a). Rate of air flow is additionally lowered, which, in turn, leads to

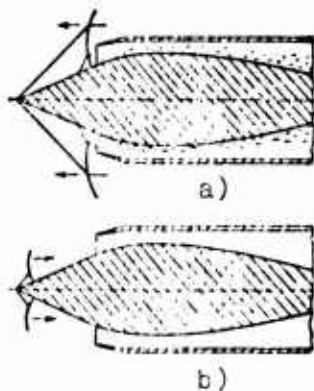


Fig. 5.16. Explanation of the scheme of the appearance of surging of a diffuser.

an even greater shifting of the head wave in the nose part of the cone and to an increase in its intensity.

However, with the approach of the head wave to the vertex of the cone (see Fig. 5.16b) the thickness of the boundary layer, is decreased and the danger of separation of it from the surface of the cone is reduced. Now this circumstance increases the flow of air through the throat and decreases losses of total pressure. As a result the head wave begins to move back toward the throat. Then the cycle is continuously repeated.

The periodic oscillating process of motion of the head wave, which is accompanied by periodic flow separation and pulsation in the air feed, is called *surging of the diffuser*.

## 5.6. Characteristics of Supersonic Diffusers

### 5.6.1. Definition

Characteristics of the supersonic diffuser are dependences of parameters characterizing the effectiveness of diffusers - namely coefficients of flow, of drag and drop in total pressure, - on regime parameters of the diffuser (speed and altitude of flight, external atmospheric conditions, number of revolutions of the engine, position of control elements).

Accordingly, *throttle* and *altitude* and *high-speed* characteristic of the supersonic diffuser, are distinguished.

Subsequently, we will examine only characteristics of uncontrollable diffusers.

### 5.6.2. Throttle Characteristics of the Diffuser

Throttle characteristics of the diffuser are dependences of parameters of effectiveness of the diffuser ( $\sigma_n^*$ ,  $\phi$  and  $\epsilon_x$ ) on the given number of revolutions of the engine or given rate of air flow through the diffuser at a constant  $M_0$  number of flight.

Figure 5.17 shows the throttle characteristic of an uncontrollable diffuser with external compression (Fig. 5.18).

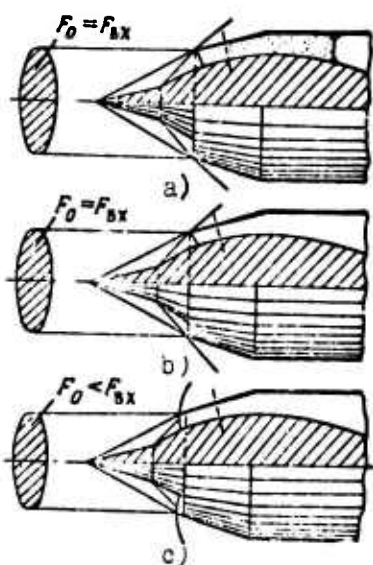


Fig. 5.18. Diagram of flow in the diffuser with respect to the throttle characteristic: a) supercritical regime; b) critical regime; c) subcritical regime.

Let us assume that a certain number of revolutions of the TRD  $n_1$  (see Fig. 5.17) corresponds to the "critical" regime of operation of the diffuser, at which the whole flow in the channel after the normal closing shock (before the throat and after it) appears subsonic (see Fig. 5.18b). In the throat of the diffuser the velocity of flow is equal to the sound speed.

With an increase in the numbers of revolutions over the critical, the counterpressure at the exit from the diffusion channel is lowered. The pressure drop leads to acceleration of flow up to

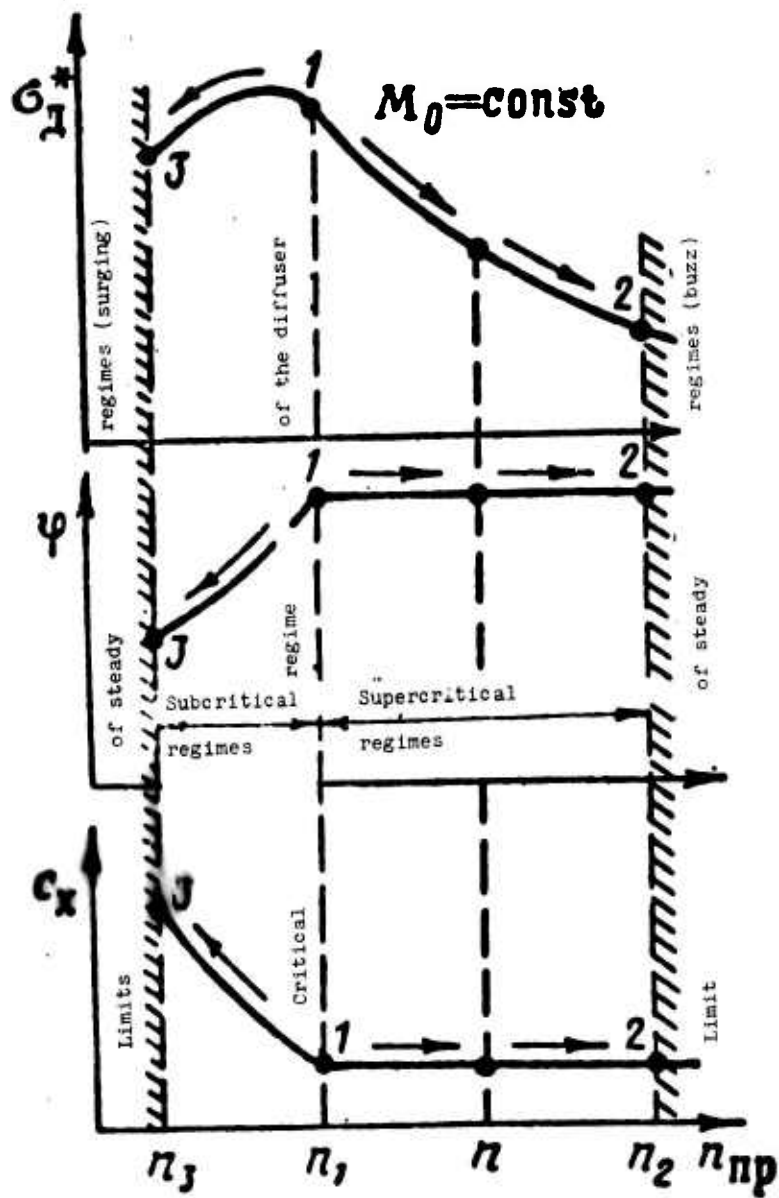


Fig. 5.17. Throttle characteristics of the diffuser.

supersonic values of velocity with the formation of a formal or  $\Lambda$ -shaped shock in the expanding part of the diffuser. A further increase in the number of revolutions of the engine leads to shifting of the barrier (attendant) shock in the channel downward along the flow, and also to an increase in its intensity (see Fig. 5.18a).

At a certain maximum number of revolutions  $n_2$  (see Fig. 5.17) there approaches separation of flow after the barrier shock - a special form of unstable operation of the diffuser, the so-called "buzz" [Translator's Note: only translation found for this term] appears. Auto-oscillations of flow, which appear in this case, are characterized by increased frequency and reduced amplitude.

Regimes of operation of the diffuser, which are characterized by the presence of a barrier shock (i.e., supersonic zone behind the throat) in the diffuser are called "supercritical". Supercritical regimes are distinguished by the constancy of coefficients of flow ( $\phi = 1$ ) and drag  $c_x = c_{x \min} = \text{const.}$  Since with an increase in  $n_{\text{np}}$  losses in the normal shock increase, then  $\sigma_{\text{d}}^*$  is continuously decreased.

Let us lower now the number of revolutions of the engine shown to values less than the critical. An increase in the counterpressure at the exit from the diffuser leads to the fact that in front of the diffuser an ejected head wave is generated. With a lowering of the number of revolutions the head wave will move away from inlet of the diffuser, its intensity will grow, and the spreading of the inlet stream will increase. As a result the coefficient of flow will be continuously lowered ( $\phi < 1.0$ ), and  $c_x$  will grow. Intensive drop in  $\sigma_{\text{d}}^*$  will begin when the head wave outgoing from the casing will destroy the system of shocks (see Fig. 5.18c).

At a certain minimum number of revolutions  $n_3$  (see Fig. 5.17) there will begin surging of the diffuser. Its appearance is connected with the separation of flow, which advances after the ejected head wave, and with the oscillating process of the shifting of the head wave, especially on the stepped cone of the diffuser.

Operating regimes of the diffuser, which are characterized by the formation of the ejected head wave at the inlet of the diffuser (in the absence of a supersonic zone in the channel) are called "subcritical".

### 5.6.3. High-Speed Characteristics of the Diffuser

High-speed characteristics of the diffuser are dependences of parameters of effectiveness of the diffuser ( $\sigma_{\text{д}}^*$ ,  $\phi$  and  $c_x$ ) with the flight  $M_0$  number at a constant number of revolutions of the TRD.

Figure 5.19 gives the high-speed characteristic of a supersonic uncontrollable diffuser with external compression. Point 1 of the characteristic corresponds to the rated  $M_0$  number of the diffuser at which the normal shocks are focused on the leading edge of the casing ( $\phi = 1$ ). Let us assume that the process of operation of the diffuser is supercritical (see Fig. 5.18a).

With an increase in the number  $M_0$  ( $M_0 > M_{\text{п.д.}}$ ) angles of slope of the normal shocks will be continuously decreased, and the latter will enter inside the diffuser (Fig. 5.20a); simultaneously, as a result of the increase in counterpressure at the exit from the diffuser, which will begin with the lowering of the given number of revolutions, the attendant shock will begin to move in the direction of the throat. On the section of characteristic 1-4 (see Fig. 5.19), on which the super-critical regime of operation of the diffuser is preserved, we have  $\phi = 1$  and  $\epsilon_{\text{д}} \approx \text{const.}$  however, coefficient  $\sigma_{\text{д}}^*$  will sharply drop from due to the increase in intensity of oblique shocks.

At point 4 the regime of operation of the diffuser becomes critical (see Fig. 5.20b) (when the attendant shock reaches the throat of the diffuser) and on section 4-5 of the characteristic (see Fig. 5.19) - already subcritical. Now in front of the diffuser the head wave appears ejected (see Fig. 5.20c), which even more lowers  $\sigma_{\text{д}}^*$ , decreases  $\phi (< 1.0)$  and increases  $c_x$ . Finally, at a certain

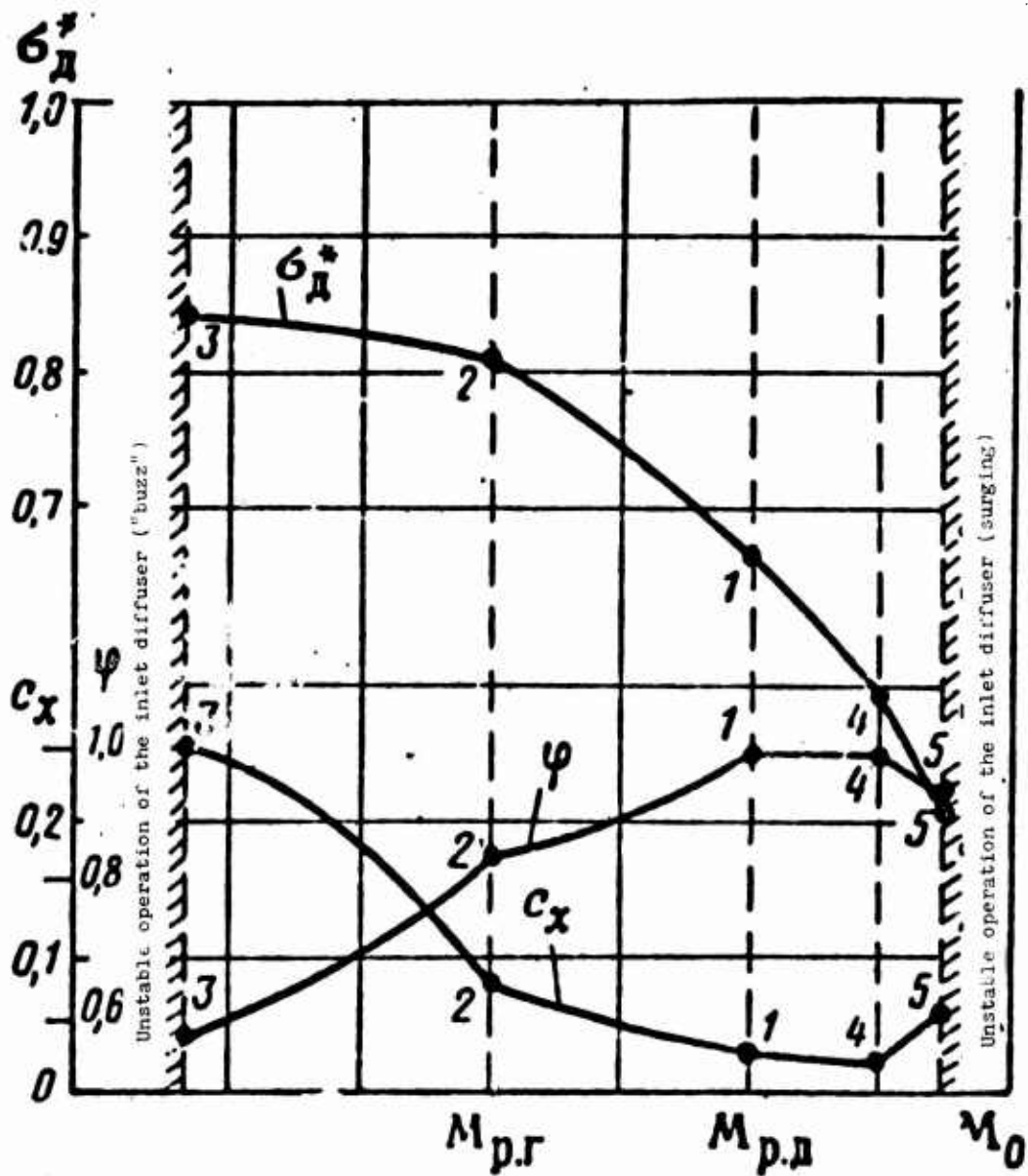


Fig. 5.19. High-speed characteristic of a diffuser.

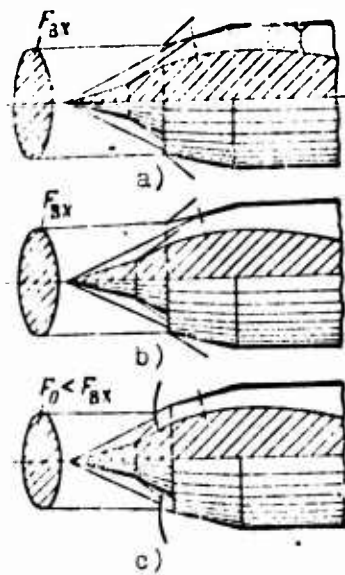


Fig. 5.20. Diagram of flow in a diffuser at  $M_0$  numbers greater than the calculated: a) supercritical regime; b) critical regime; c) subcritical regime.

$M_0$  number of flight surging approaches (point 5 in Fig. 5.19) due to separation of flow after the ejected head wave.

The lowering of  $M_0$  numbers lower than the rated value ( $M_0 < M_{p.d.}$ ) maintains the process of operation of the diffuser supercritical (Fig. 5.21) since with a growth in  $n_{np}$  counterpressure after the diffuser continuously drops. However disruption of the rated diagram of oblique shocks, which move away from the leading edge of the casing (see Fig. 5.21b), sharply decreases  $\phi$  and increases  $c_x$  (section of the characteristic 1-2 on Fig. 5.19). At a certain  $M_0$  number of flight (point 2) throat the overexpanded for the rated regime becomes optimum ( $M_{p.r.} < M_{p.d.}$ ). With a further reduction in  $M_0$  number of flight at the inlet of the diffuser, there is already generated an ejected bow wave, (see Fig. 5.21c), which intensifies the drop  $\phi$  and growth  $c_x$  (section 2-3 in Fig. 5.19). Coefficient  $\sigma_d^*$  with the lowering of  $M_0$  number of flight continuously increases. At point 3 the separation of flow after the intensive attendant shock wave leads to the appearance of "buzz".

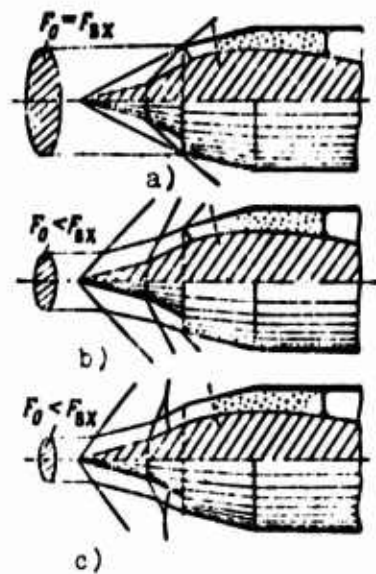


Fig. 5.21. Diagram of flow in a diffuser at  $M_0$  numbers less than the calculated: a) design conditions ( $M_0 = M_{p.d.}$ ); b)  $M_0 < M_{p.d.}$  (throat is more than the calculated); c)  $M_0 \ll M_{p.d.}$  (throat is less than the calculated).

### 5.7. Joint Operation of the Supersonic Diffuser and Compressor

In the "aircraft-engine" system the supersonic diffuser and compressor operate together. This means that the necessary rate of air flow through the compressor must be equal to the available rate of air flow through the diffuser in all regimes of operation of the power system at all values of  $M_H$  and  $n$ .

Concordance of the operation of the supersonic diffuser and compressor is produced either automatically or by forced means with the help of control elements.

Let us examine the joint operation of the uncontrollable diffuser and compressor on  $M_H$  less than the calculated.

When  $n = \text{const}$  with a decrease in the  $M_H$  of flight  $n_{np}$  grows. Consequently, the regime point of the compressor moves along the line of the working regimes from  $A$  and  $B$  (Fig. 5.22b), and the coefficient of flow  $q(\lambda_1)$  grows.

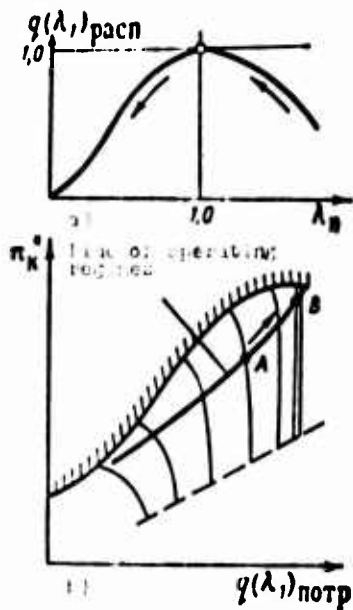


Fig. 5.22. Analysis of joint operation of the compressor and supersonic diffuser.

Let us write the equation of flow for sections H-H and 1-1 of the compressor.

we obtain

$$m \frac{p_n^*}{\sqrt{T_n^*}} f_n q(\lambda_H) = m \frac{p_1^*}{\sqrt{T_1^*}} f_1 q(\lambda_1)$$

Whence by introducing the substitution

$$p_1^* = \sigma_1^* p_n^* \quad \text{and} \quad f_n = f_{n1} \sigma_1^*$$

we obtain

$$q(\lambda_1) = \frac{\sigma_1^*}{\sigma_1^*} \frac{f_{n1}}{f_1} q(\lambda_H) \quad (5.12)$$

From expression (5.12) it follows that with a decrease in the  $M_H$  number [or  $q(\lambda_H)$ ] the available value  $q(\lambda_1)$  of the diffuser must be reduced (see Fig. 5.22a).

Thus, at subsonic flight speeds, with a decrease in  $\lambda_H$  the necessary flow of air through the compressor and available flow of air through the diffuser change in opposite directions. At low

flight speeds and on the test stand, the diffuser is not in a state to pass the entire flow of air required by the engine. To provide the condition

$$G_d = G_n$$

In the diffuser there is reconstruction of the flow: the attendant shock is displaced deep into the diffuser, and its intensity grows (i.e.,  $c_d^*$  drops). As a result of the decrease in the air density, the velocity of the air in front of the compressor increases, and the rates of air flow automatically conform.

The spreading of the jet (i.e., drop in  $\phi$ ), with a decrease in the  $M_d$  number, even more amplifies the intensity of the attendant shock.

Let us now examine the joint operation of the diffuser and compressor with a decrease in the number of revolutions of the engine. With a decrease in  $n$  the necessary flow of compressor is lowered; the available flow of the diffuser when  $\lambda_d = \text{const}$  remains constant. Concordance of regimes of operation of the compressor and diffuser is provided by means of a decrease in the intensity of the attendant shock and moving of it in the direction of the throat of the diffuser, i.e., because of the growth in  $c_d^*$ ; in this case up to the definite limit  $\phi = \text{const}$ .

#### 5.8. Adjustment of the Supersonic Diffuser of the TRD

Assignment control of the supersonic air intake of the TRD (Fig. 5.23) is the concordance of carrying capacities of the diffuser (zone of shocks and throat) and compressor in the system of the engine for the purpose of providing steady surge-free operation of the intake and improvement of its operational characteristics. The latter, as we already saw, can be achieved by means of lowering the internal losses and external resistance.

There is a large number of various methods of controlling supersonic diffusers. The basic ones are the following methods: movement

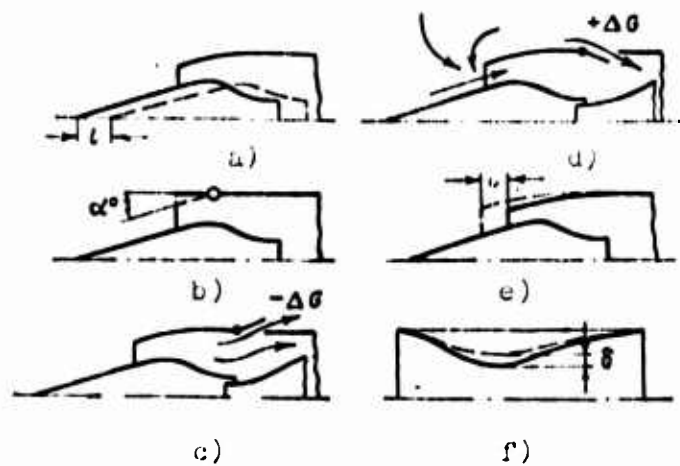


Fig. 5.25. Methods of controlling the supersonic diffuser: a) axial movement of the stepped cone; b) deviation in the inlet edge of the conical casing; c) discharge of air outside; d) intake of air inside the diffuser; e) axial movement of the conical casing; f) adjustment of critical section of diffuser.

of the inner body (conic needle) of the multishock diffuser in an axial direction; change in area of the "throat" of the diffuser, for example, by means of the movement of a special insert or the use of flexible elements; bypass of the air (with the help of valves, shutters or perforations) from the channel of the diffuser into the external medium; additional supply (suction) of air from the external medium into the main cavity of the diffuser; change in angles of slope of the leading edge of the conical casing or generatrix of the central body; suction or blowing away (bleed) of the boundary layer from the central body and wall of the diffuser.

Let us examine the physical principles of separate methods of control, and also let us determine in which partial load conditions and in what manner should one control supersonic diffuser.

#### 5.8.1. Movement of the Central Body of the Diffuser

At the assigned  $M_0$  number flight on the stepped cone of the central body a definite system of shocks is established. With

advancement of the central body from the diffuser, shocks, not changing their angle of slope, will move away from the leading edge of the conical casing, as a result of which spreading of the inlet jet increases, and the coefficient of flow and carrying capacity of the diffuser are lowered; and on the other hand with advancement on the central body inside the diffuser shocks approach to the leading edge of the conical casing - spreading of the jet is lowered, and the coefficient of flow and carrying capacity of the diffuser increase.

Let us note that control of the rate of air flow through the diffuser with the help of axial movement of the central body is effective only when a change in the flow passage section of the throat of the diffuser is carried out simultaneously. The latter is achieved by corresponding shaping of the internal surface of the conical casing.

Let us now examine how the position of the central body in various conditions of operation must be controlled. With an increase in the given number of revolutions  $n_{np}$  (as a result an increase in the physical revolutions, lowering of  $M_0$  number of flight, increase in altitude of flight, lowering of external temperature) productivity of the compressor grows. For a corresponding increase in the productivity of the diffuser, it is necessary to move the conic needle inside the diffuser. Conversely, with a decrease in  $n_{np}$  it is necessary to move the conic needle away from the diffuser.

#### 5.8.2. Control of the Diffuser by Air Bypass

A deficiency in the control of the diffuser with the help of axial movement of the stepped cone is a considerable design complexity of such a diffuser. Therefore, on many military supersonic aircraft of the USA (F-105, F-106) there is used the simpler bypass of air from the air inlet, frequently in combination with the bleed of the boundary layer from the surface of the fuselage.

When the productivity of the diffuser should be increased (takeoff regime, climbing, lowering of  $M_0$  number, reduction of  $T_{H_0}$ ) intake of external air into the basic channel of the diffuser, by passing its throat must be provided. When it is necessary to lower the productivity of the diffuser (increasing  $M_0$  and  $T_{H_0}$ , lowering of  $H$ ) discharge part of the air from the diffuser into the external medium must be provided.

#### 5.8.3. Control of the Supersonic Diffuser on Takeoff

On takeoff the throat area of the supersonic diffuser, as a rule, appears insufficient due to low air density. The position is aggravated by the fact that with the flowing around of sharp edges of the conical casing there appear separations of flow, which causes the additional drop in total pressure, and, consequently, productivity of the diffuser.

For concordance of the operation of the diffuser and engine, removal of the phenomenon of "buzz" and providing the necessary takeoff thrust, it is necessary to remove the stepped cone completely inside the diffuser, and, furthermore, open the inlet ports for the purpose of the additional supply of external air into the engine.

#### 5.8.4. Control of the Supersonic Diffuser of the Turbojet Engine (Olympus) 593 Installed on the Aircraft "Concorde".

Figure 5.24 and 5.25 schematically shows the system of control of the supersonic diffuser of the TRD "Olympus" 593 installed on the aircraft "Concorde".

The diffuser is the channel of rectangular section with variable geometry. Control of the throat of the channel is provided by means changes in the angle between the two inclined planes - flexible elements of the upper surface of the diffuser - with the help of two hinged suspensions (see Fig. 5.24). With rectification of the inclined planes, the area of section of the throat  $f_r$  increases (subsonic flight regime).



Fig. 5.24. Diagram of control of the intake of the TRD Bristol-Siddley "Olympus" 593 installed on the aircraft "Concorde": a) "takeoff" position; b) "supersonic flight" position.

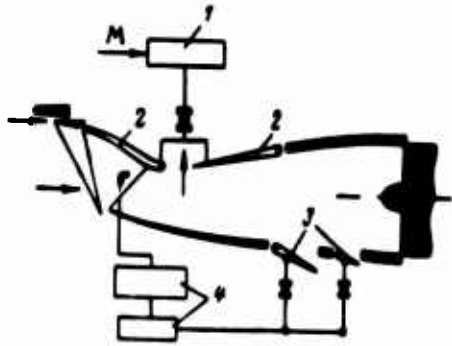


Fig. 5.25. System of control of the diffuser of the TRD Bristol-Siddley "Olympus" 593: 1 - regulator; 2 - flexible panels; 3 - by valve pass; 4 - regulator.

With formation of an obtuse angle between the planes, the area of the critical section of the diffuser is decreased (supersonic flight conditions). In rated supersonic flight conditions ( $M_{kp} = 2.2$ ) a system of two oblique and one closing normal shocks is established.

The air intake of the engine has a channel for the bleed (suction) of the boundary layer with lower surface of the wing, and also two adjusting shutters of air bypass; on takeoff and in a subsonic flight regime an additional air feed *inside the channel* of the diffuser is carried out. In supersonic flight conditions, with the help of these shutters, the surplus quantity of air is discharged *into external medium*.

## CHAPTER 6

### COMBUSTION CHAMBERS OF THE JET ENGINE

#### 6.1. Assignment of Combustion Chambers

Combustion chambers are the most important element of any jet engine. In them the process of heat feed to the working medium, without which it is impossible to realize the thermodynamic cycle of an aircraft engine is accomplished. This process is carried out as a result of the occurrence of reactions of fuel combustion; the thermochemical energy freed in them is expended for the increase in the enthalpy of the working medium (mixture of air and products of combustion) at a high has temperature.

The process of fuel combustion is a very complex physicochemical process, the effectiveness of which affects the *economy* of the engine (determining factor - *completeness of combustion*) and its reliability (determining factor - *stability of combustion* in various regimes, and *high temperature conditions of operation of the chamber*, the danger of warping and burnout of its elements, and also the possibility of carbon formation must be considered).

The chamber of combustion of that element of the engine which is most subjected to the influence of various unfavorable factors in operation and which, to a certain extent, determines the operational reliability of the engine as a whole.

## 6.2. Basic Requirements of Combustion Chambers. Basic Parameters of the Combustion Chamber

Combustion chambers of jet engines have a number of requirements, the most important of which are described below.

### 6.2.1. Highest Possible Completeness of Combustion

Heat imparted to the gas as a result of the incompleteness of combustion and losses to cooling is always less than the theoretically possible quantity, which is distinguished with complete combustion. The completeness of combustion is estimated by the *combustion efficiency* (or liberation of heat), which is determined by the ratio of the actually liberated quantity of heat with the combustion of 1 kg of fuel to lowest calorific value of 1 kg of this fuel, i.e.,

$$\xi_{k.c} = \frac{H}{H_0}. \quad (6.1)$$

In design conditions of operation of the engine the efficiency of combustion is very high and approaches unity. In partial load conditions of the engine, especially at high flight altitudes, the completeness of combustion can sharply worsen. The less the completeness of combustion, the more fuel consumption of the engine, the lower the economy and the less the flight range.

For basic combustion chambers in design regimes

$$\xi_{k.c} = 0,95 \div 0,98.$$

For afterburners

$$\xi_{k.c} = 0,85 \div 0,95.$$

### 6.2.2. High Stability of Combustion in the Whole Range of Operational Regimes of the Operation of the Engine. Absence of Vibratory Combustion

This requirement of combustion chamber is basic. It is necessary that in various regimes of the engine (with a change in altitude and flight speed, at minimum and maximum revolutions of the engine, etc.) combustion is not stopped, separation of the flame does not occur and that special regimes of unstable vibratory combustion, which can lead to the disruption of normal operation of the engine do not appear.

The stability of combustion depends on the correlation of velocities of the distribution of flames and movements of the air (fuel-air mixture), and also on the correlation of rates of air flow and fuels, i.e., on the composition of the fuel-air mixture, or the coefficient of air surplus, which is equal to the ratio of the actually entered quantity of air to that amount theoretically necessary for the complete combustion of 1 kg of fuel, i.e.,

$$\alpha = \frac{l}{l_0} = \frac{G_a}{l_0 G_r} = \frac{1}{m, l_0}. \quad (6.2)$$

To ensure the stability of combustion it is necessary to use special "stabilizers" of flame, the design and principle of operation of which is examined below.

### 6.2.3. Easy and Safe Starting

The combustion chamber must start easily, rapidly and smoothly in any operating conditions, with operation on earth and in flight, including at high altitudes. The easiness and dependability of starting to a certain extent determine the operational reliability of the combustion chambers.

### 6.2.4. Minimum Losses of Total Pressure

The providing of high hydraulic and gas-dynamic perfection of

the combustion chamber is a complex matter. It contradicts requirements of providing good stability of combustion and high completeness of combustion; actually, the use of various devices for the atomization of the fuel and improvement of carburetion and the use of vortex generators of flow and flame stabilizers of flame from the viewpoint of the requirements of hydraulics, aerodynamics and gas dynamics of processes of the flow of gas indicates the introduction of additional and very considerable resistances. These resistances lead to losses of total pressure, which are estimated by the coefficient of the drop in total pressure

$$\sigma_{k,c}^* = \frac{p_3^*}{p_2^*} < 1,0,$$

where  $p_2^*$  - total inlet pressure in the combustion chamber;

$p_3^*$  - total pressure at the exit from the combustion chamber.

For the basic combustion chambers

$$\sigma_{k,c}^* = 0,92 \div 0,97;$$

in afterburners at high temperatures of gas preheating losses of pressure increase:

$$\sigma_{k,c}^* = 0,88 \div 0,95.$$

#### 6.2.5. Small Overall Dimensions and Light Weight

In order to obtain combustion chambers with small overall dimensions and with low weight, or, in other words, with a small working volume, it is necessary to make combustion chambers of high calorific intensity. The latter characteristics the quantity of heat arriving per unit of time on a unit of volume of the chamber referred to the pressure in the chamber, i.e.,

$$Q_{k,c} = \frac{\xi_{k,c} G_{T,k,c} H_u}{V_{k,c} p_2^*} \frac{\text{kcal}}{\text{m}^3 \cdot \text{h} \cdot \text{at}} \quad (6.3)$$

where

$G_{\text{т.чac}}$  - consumption of fuel per hour in kg/h;

$H_u$  - lower calorific value of fuel in kcal/kg;

$V_{\text{к.с}}$  - working volume of the combustion chamber in  $\text{m}^3$ ;

$p_2^*$  - pressure at the inlet of the combustion chamber in at;

$\xi_{\text{к.с}}$  - combustion efficiency.

Calorific intensity of combustion chambers of contemporary gas turbines reaches 40-50 kcal/ $\text{m}^3 \cdot \text{hour} \cdot \text{at}$ ; this is 10-15 times more than for the usual steam-locomotive furnaces.

In order that the length of combustion chamber not be excessive and so that the limit of the flame does not reach the inlet of turbine, as great a completeness of combustion as possible must be provided; however the latter, in turn, depends on the extent of the chamber and presence in it of devices making the combustion process more active. Thus, requirements of obtaining small dimensions and weight of the chamber together with the high completeness of combustion are contradictory. They are solved by the reception of compromise solutions in reasonable limits.

#### 6.2.6. Optimum Law of the Distribution of the Field of Temperatures at the Exit from the Combustion Chamber

The field of temperatures at the exit from the combustion chamber (or which is the same, - at the inlet of turbine) is always characterized by a definite degree of irregularity.

One should distinguish the circumferential and radial irregularity of the gas temperatures. The circumferential temperature irregularity

is harmful, and it should be lowered as far as possible. The radial irregularity must obey the definite most advantageous law, at which the maximum of the temperature must be approximately at a distance, equal to 2/3 of the blade.

The root elements of blades of turbines, subjected to the action of greatest stresses of break, and also outlying elements of the blades, having the least thicknesses and therefore yielding to burning must be washed by the flow of gas of a lower temperature.

The degree of irregularity of temperatures is defined as the ratio of the greatest temperature difference at the exit from the combustion chamber to mean value of temperature, i.e.,

$$\bar{T} = \frac{(T_{\max}^* - T_{\min}^*)}{T_{r,p}} \cdot 100\% < (20 \div 30)\% \quad (6.4)$$

The circumferential irregularity of temperature of the best combustion chamber does not exceed the magnitude  $\Delta T = 50-100^\circ\text{K}$ .

Figure 6.1 shows temperature fields at the exit of combustion chamber, characteristic circumferential and radial irregularities of temperatures of gas, and also the regularity of the temperature variation of the cooled moving blades of the ducted fan jet engine Rolls-Royce "Spey".

### 6.3. Design and Principle of Operation Combustion Chambers. Types of Combustion Chambers

Combustion chambers of jet engines are distinguished from each other by scheme and a number of design peculiarities; however, they all have similar design and similar principle of operation. Figure 6.2a gives an individual combustion chamber installed on a TRD with a centrifugal compressor.

Its main elements are:

- a) diffuser;

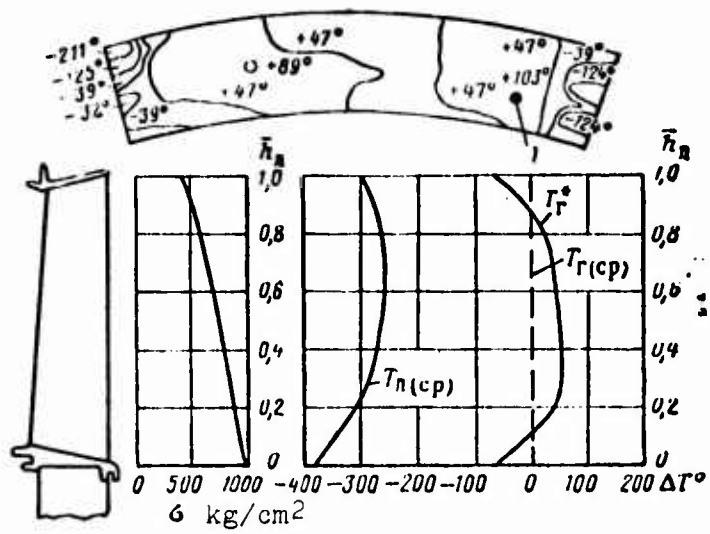


Fig. 6.1. Distribution of the field of temperatures at the exit from the combustion chamber of the ducted fan jet engine Rolls-Royce "Spey".

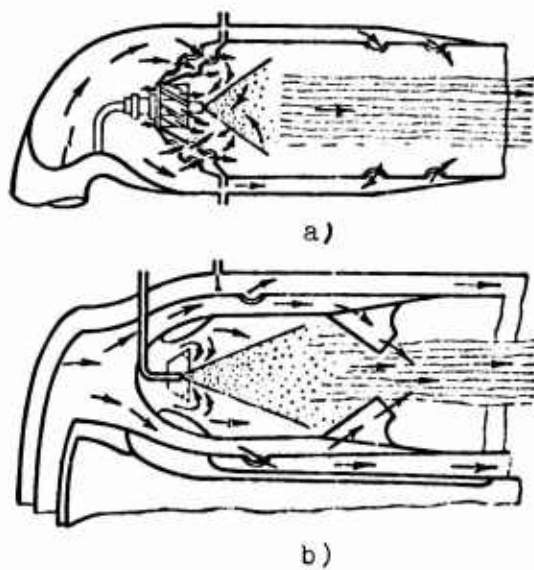


Fig. 6.2. Diagram of combustion chamber of an aircraft GTD: a) individual; b) annular.

b) internal heat pipe;

c) external jacket (body);

d) frontal device consisting of a centrifugal fuel spray nozzle, bladed swirl vane and stabilizer;

e) perforation system (to provide mixing of the air and products of combustion).

Figure 6.2b shows a diagram of an annular combustion chamber.

### 6.3.1. Working Process in the Combustion Chamber

The working process in the combustion chamber (Fig. 6.3) occurs in the following manner. At the exit of the compressor the air has a relatively high velocity (100-120 m/s). At such a velocity the combustion chamber would have a long length with considerable losses of pressure and low completeness of combustion. Therefore, the air flow is initially directed into the diffuser of the chamber in which its velocity is lowered down to 50-70 m/s.

#### 6.3.1.1. Atomization of Fuel and Formation of a Fuel-air Mixture.

Fuel atomization is produced by centrifugal sprayers under high pressure ( $\Delta p_T = 60-80$  at). The angle of the spray cone reaches 110-130°. To ensure the necessary fineness of atomization in all regimes of operation of the engine and at various fuel consumptions two- and even three-channel sprayers are used.

Fuel flows out from the sprayer, forming a continuous thin conic film, which, with removal from the frontal device, is decomposed and split up into smallest drops of various diameter. Investigations show that from 1 cm<sup>3</sup> of fuel up to 10 million drops with a diameter of 10 to 200  $\mu$ m are formed.

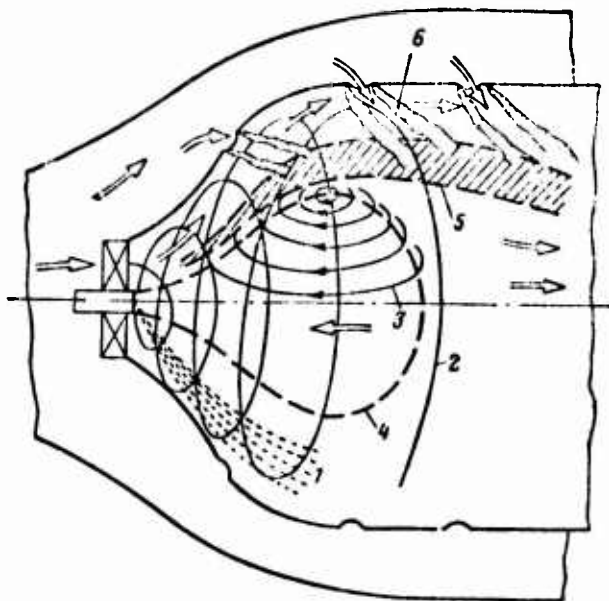


Fig. 6.3. Diagram of processes in the combustion chamber: 1 - spray cone; 2 - swirl air; 3 - reverse flows; 4 - circulating zone; 5 - zone of combustion; 6 - turbulent tracks.

For each sprayer the most advantageous spectrum of atomization is selected. An excessively large or excessively small fuel atomization can lead to a worsening of combustion efficiency and narrowing of the range of steady operation of the chamber (big drops fly through the chamber, not burning; with complete evaporation of the drops there is superenrichment of the mixture, which also make burning worse).

#### 6.3.1.2. Division of Air Flow into Primary and Secondary.

In diffuser the air flow is divided into two parts. Its lesser part (approximately 20-50%) occurs inside the flame tube through the swirl vane of the frontal device and also through the system of openings (perforation) in the front part of the flame tube, is mixed with the atomized fuel being injected by the centrifugal sprayer, and immediately participates in the process of combustion. This part of the air is called *primary air*. It must be noted that the primary air must be fed gradually along the length of the zone of

combustion. This is connected with the fact that in the beginning for the creation of the fuel flame (as a result combustion rapidly evaporating small drops) a small quantity of air is necessary. With preparation of fuel-air mixture, to ensure its complete combustion and prevent dissociation at high temperature, the necessary quantity of air increases (Fig. 6.4). In the zone of combustion the most advantageous concentration of fuel is characterized by the value of the coefficient of air surplus  $\alpha_I = 1.1-20$ .

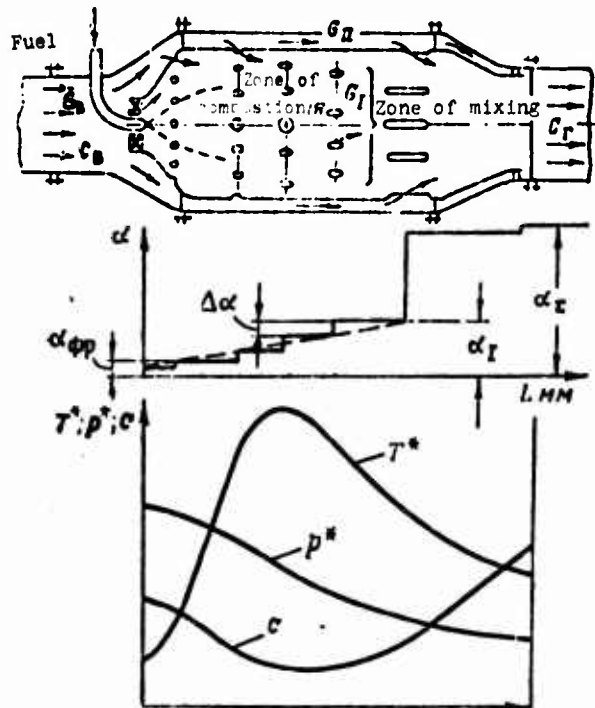


Fig. 6.4. Change in parameters of gas along the length of combustion chamber.

The greater part of air (50-80%) fills the annular cavity contained between the flame tube and external body, and then the air enters also through the system of openings inside the flame tube - into the zone of confusion. This part of the air is called *secondary air*; is mainly for the mixing of hot combustion products with cold air (entering from the compressor) and for lowering the temperature of the obtained mixture down to a safe level, determined by conditions of the providing strength of moving blades of the turbine.

The division of air into primary and secondary is connected with the impossibility of the organization of effective fuel burning at low temperatures (800-1000°C). Therefore, it is necessary in the beginning to organize fuel combustion at high temperature (1600-1900°C) and then accomplish dilution of combustion products by cold air.

#### 6.3.1.3. Stabilization of the Front of the Flames in the Zone of Combustion.

The tendency to boost the combustion chamber, having provided high values of its calorific intensity, conditions the use of high velocities of the flow of air (gas) greater than the normal velocity of the distribution of the flame. From a course in physics of combustion, it is known that in this case (when  $v_f > v_{норм}$ ) for providing stability of combustion and retention of the flame jet in combustion chamber, there must be created a stagnant circulating zone - the zone of reverse flows [ZOT] (ЗОН) of hot gases - capable of continuously and reliably igniting the prepared fuel-air mixture.

To create such a zone, there are employed swirl vanes of flow and various bluff bodies (annular grooves of the corner sections, plates, etc.), behind which an area of low pressure is formed. Such an area is formed along the axis of the flame tube, in its front part, as a result of the ejection of combustion products of the annular (hollow) jet of the mixture of fuel and air.

Figure 6.3 shows the pear-shaped border of the area of the zone of reverse flows.

#### 6.3.1.4. Flow Turbulization in the Combustion Zone.

For the intensification of processes of mass-and heat exchange and likewise for the increase in the velocity of the normal flame propagation, transition from laminar combustion to turbulent is necessary.

Turbulence of flow is achieved with the help of swirl vanes, centrifugal fuel sprayers, bluff bodies, and also by means of the radial admission of jets of cold air through openings in walls in the flame tube.

In chambers without a frontal device a greater part of the fuel burns up in turbulent "tracks" formed with the passage of air through the openings. The correct selection of diameter, disposition and number of openings to a certain extent determines the effectiveness of combustion, limiting dimensions of the zone of reverse flows and having an effect on hydraulic losses in the combustion chamber.

#### 6.3.1.5. Gas-Dynamic Structure of Flows in the Combustion Chamber.

Figure 6.5a, b and c shows respectively, regularities of the distribution of velocity fields  $c$ , fuel concentrations  $K$  and gas temperatures of gas  $T^*$  in sections of chamber 1, 2 and 3.

In an axial direction the total pressure of the gas gradually drops. Gas temperature reaches a maximum in the zone of combustion, and then with the admixture of the secondary air, is gradually reduced down to the required level. The average flow velocity of the gases is lowered in the zone of combustion (midsection of the chamber) - this increases the time of stay of the fuel at high temperatures and assists the complete burning of the mixture. The completeness of combustion sharply increases toward the end of the zone of combustion.

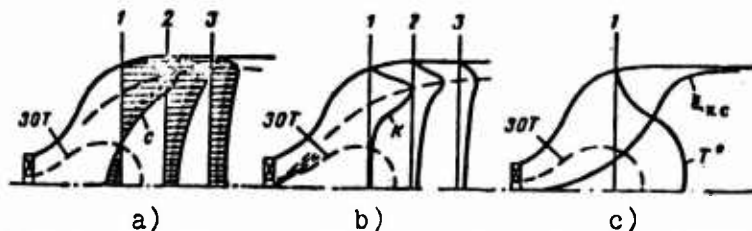


Fig. 6.5. Fields of velocities, temperatures and concentrations of fuel in the combustion chamber.

At the exit from the chamber the total coefficient of air surplus reaches the value  $\alpha_{\Sigma} = 3.5-5.5$ .

In a radial direction the concentration of fuel reaches the maximum in accordance with the trajectory of motion of the fuel particles. The greatest irregularity in the distribution of axial velocities of the air (gas) is observed in sections of the zone of reverse flows. With an approach to the exit of the chamber, the profile of axial velocities is gradually equalized.

Temperature of gas has the greatest and approximately constant value in the zone of the reverse flows and sharply decreases in the direction of the periphery of the flame tube, where admixture of secondary air to the primary occurs.

#### 6.3.2. Types of Combustion Chambers

Combustion chambers of aircraft gas turbines are subdivided into *can (or individual), annular and cannular*.

Tubular chambers are used mainly on engines with a centrifugal compressor. They are convenient in operation, and they allow rapid replacement of chambers without dismantling the whole engine. The use of individual chambers considerably reduces the time of their finishing.

Annular chambers are used on engines with an axial-flow compressor. They are distinguished by great compactness and little weight, since they have less overall dimensions. Annular chambers are characterized by fewer hydraulic losses and have at the exit more uniform fields of temperatures and pressures. Deficiencies of annular chambers they are the complexity of repair and finishing.

At present the most widespread are cannular chambers (with individual flame tubes), which are an intermediate type of chamber. With skillful design fulfillment, they combine the merits of can and annular combustion chambers.

#### 6.4. Change in Pressure in the Combustion Chamber

One should distinguish the change in static and total pressures of gas in the combustion chamber. Static gas pressure, depending on the configuration of the combustion chamber, can decrease, remain constant or, theoretically, even in certain cases, increase; the total gas pressure in the combustion chamber always decreases.

Let us examine these questions in detail.

##### 6.4.1. Change in Static Pressure.

The change in static pressure of the combustion chamber is determined by the presence of hydraulic resistances and acceleration of flow. The greater the hydraulic losses (i.e., the greater the portion of energy of gas necessary to expend for overcoming hydraulic and gas-dynamic resistances) and the greater the acceleration of flow (i.e., the more the increase in kinetic energy of the gas), the greater the drop in static pressure of the gas. The aforesaid follows from an analysis of Bernoulli's equation, written for the process in the combustion chamber:

$$\int_{p_1}^{p_2} v dp = - \left( L_r + \frac{c_3^2 - c_2^2}{2\kappa} \right) \approx 0. \quad (6.5)$$

Hydraulic resistances in the combustion chamber are conditioned by the viscosity of the gas, the presence of various obstacles in the flow - vortex generators of flow and flame stabilizers, - sprayers and deflectors, mixers and separators of flow, and in some chambers - at sharp turns of the flow (up to 180°). Hydraulic resistances can be decreased up to a definite degree, but it is impossible to eliminate them entirely.

Acceleration of flow in the combustion chamber, in turn, depends on a number of factors - shape (profile) of the chamber, intensity of preheating of the gas, and presence of hydraulic resistances.

The combustion chamber, and also the afterburner, from design and technological considerations are usually made of cylindrical form<sup>1</sup>; with configuration of it the preheating of the gas and presence of friction always lead to acceleration of flow and drop in static pressure.

Let us write the equation of momentum for the mass of gas moving in a cylindrical chamber in the presence of preheating without friction. Such a combustion chamber is an ideal thermal nozzle.

We obtain

$$\frac{G}{g} (c_3 - c_2) = f(p_2 - p_3). \quad (6.6)$$

Thus, acceleration of flow ( $c_3 > c_2$ ), conditioned by the preheating of the gas ( $T_3 > T_2$ ), causes a drop in static pressure ( $p_3 < p_2$ ).

Expression (6.6) can be given another form:

$$\frac{G}{g} c_2 + p_2 f = \frac{G}{g} c_3 + p_3 f = \text{const}, \quad (6.7)$$

i.e., the total momentum of flow in the cylindrical chamber remains constant; hence, it follows that the cylindrical pipe does not develop as much reactive thrust as the gas passing through it has warmed up, - its walls are not able to absorb the axial stresses.

Let us find now the quantitative correlations connecting the drop in static pressures with an increase in the preheating of the gas.

Let us transform expression (6.7), having noted that  $G = f c_2 \gamma^2$ .

---

<sup>1</sup>Sometimes it is made slightly expanding.

Then

$$p_2 - p_3 = \frac{c_2 v_2}{g} (c_3 - c_2).$$

Since with  $f = \text{const}$

$$\frac{c_3}{c_2} = \frac{v_3}{v_2}, \quad \text{and} \quad M_2^2 = \frac{c_2^2}{k g R T_2},$$

then

$$\sigma_{\text{н.с.}} = \frac{p_3}{p_2} = 1 - k M_2^2 \left( \frac{c_3}{c_2} - 1 \right) = 1 - k M_2^2 \left( \frac{v_3}{v_2} - 1 \right). \quad (6.8)$$

We see that the process of preheating of the gas in the cylindrical combustion chamber is shown in  $p$ - $v$ -coordinates by the equation of the straight line (Fig. 6.6). The more initial number  $M_2$  of flow, the more intensive the drop in static pressure.

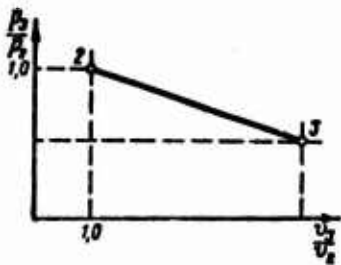


Fig. 6.6. Process of preheating of the gas in the cylindrical combustion chamber.

Let us now derive the simple formula for the calculation of the coefficient of drop in static pressure  $\sigma_{\text{н.с.}} = p_3/p_2$ .

The equation of the momentum of gas (6.7) can be reduced with the help of the gas-dynamic function

$$z(\lambda) = \frac{1}{2} \left( \lambda + \frac{1}{\lambda} \right)$$

to the form

$$z(\lambda) \sqrt{T} = \text{const.} \quad (6.9)$$

or

$$z(\lambda_3) = \frac{z(\lambda_2)}{\sqrt{\Delta}}, \quad (6.10)$$

where  $\Delta = \frac{T_3^*}{T_2^*}$  - degree of preheating of the gas combustion chamber.

On the other hand, the equation of the flow of gas for a cylindrical pipe can be written with the help of the gas-dynamic function  $r(\lambda)$  in the form

$$\frac{p}{r(\lambda)} = \text{const.}$$

where

$$r(\lambda) = \frac{H(\lambda)}{f(\lambda)} = \frac{1 - \frac{k-1}{k+1} \lambda^2}{1 + \lambda^2}.$$

Then

$$\sigma = \frac{p_3}{p_2} = \frac{r(\lambda_3)}{r(\lambda_2)}, \quad (6.11)$$

where the connection between  $\lambda_3$ ,  $\lambda_2$  and  $\Delta$  is found with the help of equation (6.10).

Determination of  $\sigma$  is produced from tables of gas-dynamic functions of Kiselev.

*Example:* Let  $\lambda_2 = 0.20$ ;  $\Delta = 3$ . Then

$$z(\lambda_2) = 2.6; \quad z(\lambda_3) = \frac{2.6}{\sqrt{3}} = 1.5; \quad \lambda_3 = 0.382;$$
$$r(\lambda_2) = 0.956; \quad r(\lambda_3) = 0.855; \quad \sigma = 0.894.$$

#### 6.4.2. Drop in Total Gas Pressure

Preheating of the gas in the combustion chamber of any configuration, independent of the presence of friction, always leads to a drop in total pressure of the gas.

Drop in total pressure, conditioned by the preheating of the gas, is called *thermal resistance*. The physical sense of the concept "thermal resistance" is that at the assigned storage of kinetic energy with preheating of the gas the increase in pressure of the gas, conditioned by deceleration of the flow, continuously drops.

Actually, at the assigned magnitude of adiabatic work of compression equivalent to the kinetic energy of flow,

$$L_{ad} = 102,5T^*(\pi^{0,286} - 1) = \frac{c^2}{2g},$$

where

$$\pi = \frac{p^*}{p},$$

with an increase in  $T^*$  the magnitude  $\pi$  decreases.

Let us examine the combustion chamber of arbitrary configuration in which with the preheating of the gas there is a drop in static pressure. Let us assume that friction is absent. Let us prove graphoanalytically that in this case the total pressure of the gas drops, i.e., that  $p_3^* < p_2^*$  (Fig. 6.7).

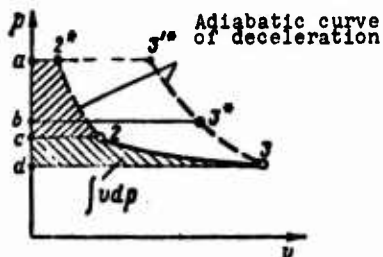


Fig. 6.7. Graphoanalytical illustration of the drop in total pressure of the gas with its preheating in the combustion chamber.

Let us write Bernoulli's equation for process 2-3 in the form

$$\frac{c_3^2}{2g} = \frac{c_2^2}{2g} - \int v dp. \quad (6.12)$$

If the total pressure of the gas in combustion chamber would remain constant, i.e., if  $p_3^* = p_2^*$ , then the area  $3'^*-3-d-a-3'^*$ ,

equivalent to the kinetic energy  $\frac{c^2}{2\kappa}$ , would be more than the area  $2^*-2-3-d-a-2^*$  which depicts the right-hand side of equation (6.12); this would contradict equality (6.12). Consequently,  $p_3^* = p_2^*$ , areas  $3^*3-d-b-3^*$  and  $2^*-2-3-d-a-2^*$  are equal).

The physical sense of the drop in total pressure can be shown still otherwise in the example of the cylindrical combustion chamber.

For subsonic flows we have the approximate equality

$$p^* \approx p + \frac{\rho c^2}{2} = (p + \rho c^2) - \frac{\rho c^2}{2}. \quad (6.13)$$

For cylindrical chambers we write

$$p f + \frac{G}{g} c = \text{const}, \quad \text{and} \quad p + \rho c^2 = \text{const}.$$

Thus, the total pressure of the gas is equal to the constant specific total pulse [less the dynamic addition of pressure (impact pressure)], i.e.,

$$p^* = \text{const} - \frac{\rho c^2}{2}.$$

Since in proportion to feed of heat the dynamic head of the gas  $\left(\frac{\rho c^2}{2} \sim c\right)$  increases, then the total pressure  $p^*$  drops.

#### 6.4.2.1. Determination of the Drop in Total Pressure in the Cylindrical Combustion Chamber.

Let us derive the simple formula for the determination of the coefficient of drop in total pressure

$$\epsilon_i = \frac{p_3^*}{p_2^*}$$

in a cylindrical combustion chamber.

Let us present the equation of the flow of gas with the help of the gas-dynamic function  $f(\lambda)$  in the form (Fig. 6.8)

$$p^* f(\lambda) = \text{const.}$$

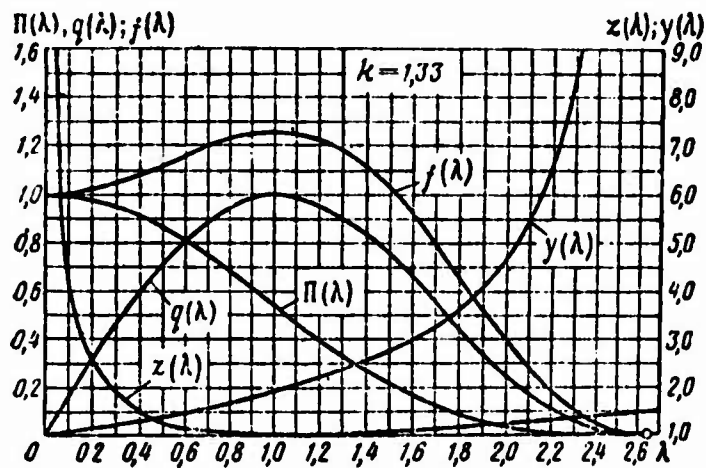


Fig. 6.8. Graphs of gas-dynamic functions

Here

$$f(\lambda) = (1 + \lambda^2) \left( 1 - \frac{k-1}{k+1} \lambda^2 \right)^{\frac{1}{k-1}}.$$

Then

$$\sigma_i^* = \frac{p_3^*}{p_2^*} = \frac{f(\lambda_2)}{f(\lambda_3)}. \quad (6.14)$$

The connection between  $\lambda_3$  and  $\lambda_2$  and  $\Delta$  is found with the help of the momentum equation (6.10).

*Example.*

Let  $\lambda_2 = 0.20$  and  $\Delta = 3$  ( $k = 1.33$ ).

Then  $z(\lambda_2) = 2.6$ ;  $z(\lambda_3) = 1.5$ ;  $\lambda_3 = 0.382$ ;  $f(\lambda_2) = 1.0223$ ;  $f(\lambda_3) = 1.0757$  and  $\sigma_i^* = 0.95$ .

Figure 6.9 gives a graph for the determination of the drop in

total pressure of the gas  $\sigma_T^*$ ;

$$\sigma_T^* = f(\lambda, \lambda_2, \lambda_3).$$

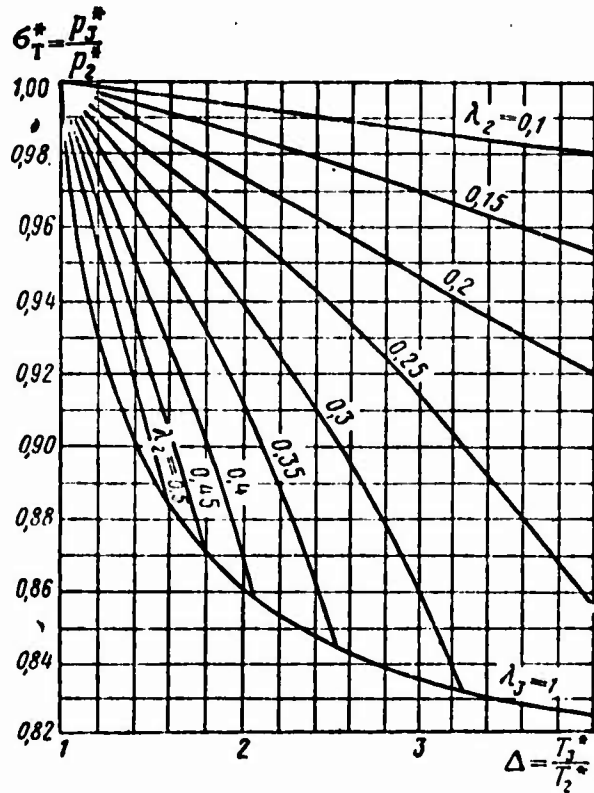


Fig. 6.9. Graph for the determination of the drop of total pressure of the gas in the combustion chamber.

On the graph lines of equal values  $\lambda_2$  and  $\lambda_3$  are plotted. With an increase in  $\Delta$  when  $\lambda_2 = \text{const}$  value  $\lambda_3$  increases. With an increase in  $\Delta$  when  $\lambda_3 = \text{const}$  the value  $\lambda_2$  drops.

Figure 6.9 gives the boundary line  $\lambda_3 = 1$ , which fixes the limiting degree of preheating of the gas at the assigned initial value.

6.4.2.2. Determination of the Limiting Degree of Preheating in the Cylindrical Chamber.

From the momentum equation (6.10) let us find  $\Delta = \frac{z(\lambda_2)}{z(\lambda_3)}$ . When  $\lambda_3 = 1$  and, consequently, when  $z(\lambda_3) = 1$ , magnitude

$$\Delta = \Delta_{max} = z(\lambda_2). \quad (6.15)$$

Several data obtained for this dependence are given in Table

Table 6.1.

$\lambda_2$	0,10	0,20	0,30	0,40	0,50
$\Delta_{max}$	5,05	2,60	1,82	1,45	1,25

Thus, with an increase in the number  $\lambda_2$ , the limiting degree of preheating of the gas in the combustion chamber sharply decreases.

6.4.2.3. Effect of Hydraulic Losses on the Drop of Total Pressure  $p^*$ .

The drop of total pressure, conditioned by the presence of hydraulic losses, is estimated by formula

$$\sigma_r^* = 1 - \xi \frac{\lambda M_2^2}{2}. \quad (6.16)$$

where  $M_2 = 0.07-0.15$  and  $\xi = 8-12$ .

The total losses of total pressure are equal to

$$\sigma_{r,c}^* \approx \sigma_r^* + \sigma_c^*.$$

## 6.5. Factors Affecting the Completeness of Combustion and Stability of Combustion of the Fuel

Earlier we noted the importance of providing high values of the efficiency of combustion for economic operation of the engine. Now we will examine the effect of various regime parameters and also parameters of the process on the magnitude  $\xi_{\text{H.C.}}$ .

The efficiency of combustion considers the *chemical* incompleteness of combustion (being determined by the dissociation of combustion products, the formation aldehydes instead of products of complete combustion  $\text{H}_2\text{O}$  and  $\text{CO}_2$ ) and also the *mechanical* incompleteness of combustion; the latter appears in the form of deposits of carbon deposit on elements of the combustion chamber and the coking of the fuel sprayer; furthermore, part of the fuel is taken away by the flow of gas beyond the engine.

The basic parameters influencing the efficiency of combustion, are: coefficient of air surplus  $\alpha$ , parameters of air at the inlet of the combustion chamber (pressure  $p_2$ , temperature  $T_2$  and velocity  $c_2$ ), altitude of flight  $H$ , number of revolutions of the engine  $n$ , fineness of fuel atomization, determined by the average diameter of the drops of fuel, and others. The enumerated factors have an effect on the very complex physicochemical processes of combustion, intensifying or slowing them down.

### 6.5.1. Effect of Coefficient of Air Surplus $\alpha$

Figure 6.10 shows the effect of the coefficient of air surplus of combustion chamber  $\alpha$  on  $\xi_{\text{H.C.}}$ . The maximum completeness of combustion corresponds to the magnitude of the total coefficient  $\alpha_2 = 3-5$ , i.e., approximately to the stoichiometric composition of fuel-air mixture in the zone of combustion ( $\alpha_1 \approx 1.0$ ); this composition of mixture corresponds to the highest temperature of combustion, smallest volume of combustion, shortest flame.

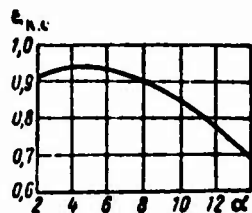


Fig. 6.10. Effect of the coefficient of surplus of air on the completeness of combustion of the fuel.

The impoverishment and enrichment of the mixture lowers the magnitude  $\xi_{N,K}$ , and the greater this is, the greater magnitude  $\alpha_I$  deviates from unity.

At impoverishment of the mixture the flame is decreased in volume, and it becomes shorter - fuel shortage is affected. Hot combustion products, mixing with the primary air, are cooled; as a result the velocity of the occurrence of the chemical reaction is decreased, and the combustion chamber is lowered. All this leads to a lowering of the completeness of combustion. With further decrease of the mixture, the quantity of heat imparted by the zone of reverse flows appears already insufficient for ignition of the fresh fuel-air mixture - flameout of the impoverished mixture approaches.

With enrichment of the mixture the flame is stretched, and it increases in volume. Since the surplus fuel evaporates, this leads to the cooling of the combustible mixture; as a result the induction period of combustion increases, and the completeness of combustion is decreased. With further enrichment the fuel-air mixture can "rush" through the zone of reverse flows not igniting - flameout of the rich mixture approaches.

#### 6.5.2. Effect of Air Pressure $p_2$

A decrease in absolute air pressure at the inlet of the combustion chamber down to  $p_2 \approx 1$  at (Fig. 6.11) has little effect on the completeness of combustion. With further reduction in pressure ( $p_2 < 1$  at) the completeness of combustion is decreased as a result of the lowering of the velocity of combustion and also due

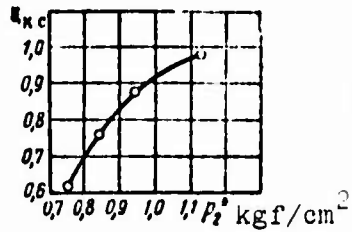


Fig. 6.11. Effect of air pressure in combustion chamber on the completeness of combustion of the fuel.

to the worsening of the atomization (diameter of drops of fuel increases; the fuel drops easily fly through the chamber, without having become ignited).

### 6.5.3. Effect of Air Temperature $T_2$

With a reduction in air temperature at the inlet of the combustion chamber (Fig. 6.12) carburation becomes worse (fuel evaporation is delayed); furthermore, the induction period increases, and the velocity of combustion is lowered. Ultimately the completeness of combustion becomes worse.

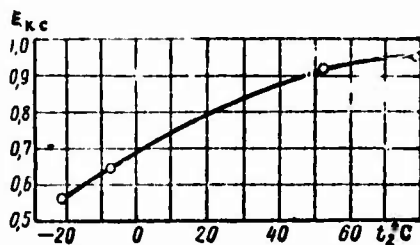


Fig. 6.12. Effect of temperature of air entering into combustion chamber on the completeness of fuel combustion.

### 6.5.4. Effect of the Velocity of Air Flow $c_2$

At the assigned composition of the mixture, the increase in the air velocity at the inlet of the combustion chamber (Fig. 6.13) leads to a decrease in the time of stay of portions of the fresh fuel-air mixture in the zone of reverse flows; this lowers the completeness of combustion and with a further increase in velocity of the flows can lead to flameout.

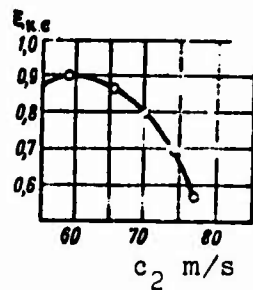


Fig. 6.13. Effect of velocity of air flow at the inlet of the combustion chamber on the completeness of fuel.

#### 6.5.5. Effect of Flight Altitude

With an increase in flight altitude (Fig. 6.14) the pressure and air temperature at the inlet of the combustion chamber decrease. This leads, as we already noted above, to the deceleration of the passage of the chemical reaction and to the worsening of carburetion. Ultimately there is the lowering of the completeness of combustion and especially on reduced regimes of operation. Furthermore, with climbing the range of steady operation with respect to parameter  $\alpha$  is narrowed.

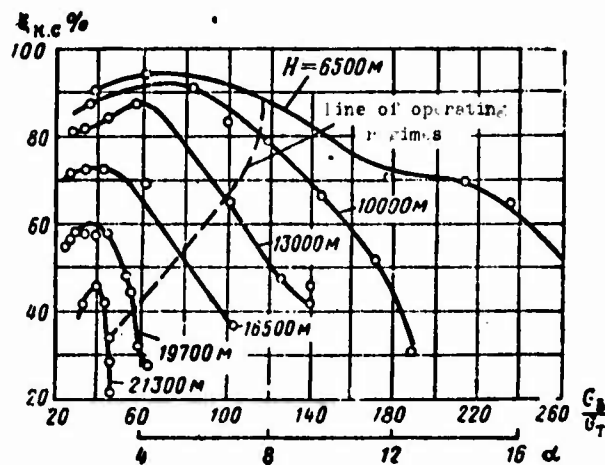


Fig. 6.14. Effect of flight altitude on the completeness of fuel combustion.

#### 6.5.6. Effect of the Number of Revolutions

Extreme throttling of the engine always makes the completeness of combustion worse (Fig. 6.15).

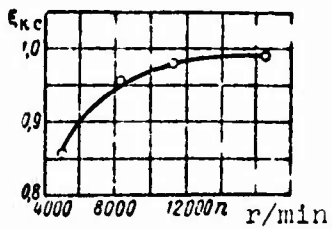
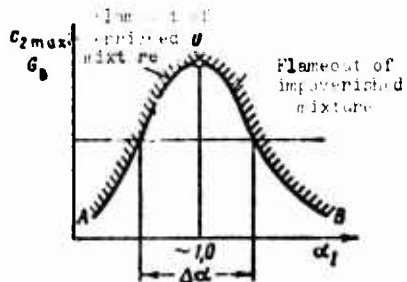


Fig. 6.15. Change in the coefficient of completeness of combustion according to number of revolutions of the engine.

#### 6.5.7. Providing Stabilization of Combustion

Stability of combustion is determined by the range of the change in coefficient of air surplus in which there is not a flameout (on impoverished and enriched mixture).

Figure 6.16 gives the characteristic of the stability of operation of the combustion chamber in the form of dependence  $c_{2max} = f(\alpha)$ . The area under the curve is the area of steady combustion. The left branch of the curve characterizes the limit of separation with respect to the rich mixture and the right branch of the curve - limit of separation with respect to the impoverished mixture.



$\Delta\alpha$  - range of steady combustion

Fig. 6.16. Characteristic of the stability of operation of the combustion chamber.

With an increase in  $c_2$ , with an increase in  $p_2$  and  $T_2$ , with an increase in flight altitude, and with a decrease in number of revolutions of the engine, the stability of combustion of the jet engine is made worse.

### 6.5.8. Evaporative Combustion Chambers

The worsening of fuel atomization and the deceleration of the velocity of occurrence of the chemical reaction of combustion with an increase in altitude, as we have already indicated, lower the completeness of combustion and makes stability of combustion worse.

One of the methods of increasing the effectiveness of combustion on great altitudes is the use of *evaporative* chambers of combustion. Principle of operation of these chambers is simple. It consists in the fact that before its feed into the combustion chamber the fuel preliminarily flows through a system of tubes warmed up on the outside by products of combustion, and it evaporates. Vapors of fuel flowing out of the tubes are mixed in the flame tube with compressed air in various proportion, forming a heterogeneous mixture. The latter, as is known, has wider limits of ignition with respect to  $\alpha$  than does the homogeneous mixture.

In order to eliminate carbon formation on walls of the tubes, air is passed through them, and the fuel is injected in the form of thin axial jets inside the tubes.

Evaporative chambers were used on separate serial gas-turbine engines (TVD Armstrong-Siddley (Mamba), TRD Armstrong-Siddley (Sapphire) AS-65). However, due to their design complexity and large volume, they did not become widespread.

### 6.6. Determination of Relative Fuel Consumption in the Combustion Chamber

With thermal and gas-dynamic calculations of gas-turbine engines and with the calculation of their characteristics, it is necessary to the relative fuel stability

$$m_f = \frac{G_f}{G_a} = \frac{c_{pm}(T_3^* - T_2^*)}{\epsilon_{k,c} H_u} \quad (6.17)$$

Determination of the average (conditional) specific heat  $c_{pm}$  of gas can be produced on special tables or nomograms, compiled, for example, by Ya. T. Il'ichev (see work [30]). In practice it is convenient to determine  $m_T$  by the formula proposed by A. V. Kholshchevnikov and Ya. T. Il'ichev:

$$m_T = \frac{i_2 - i_1}{i_{ka} - f(T_2)} \quad (6.18)$$

with the help of nomograms (see Appendix 1) or tables given in work [21]. These nomograms and tables consider the effect of temperature and  $\alpha$  on the enthalpy of air and of gas.

## CHAPTER 7

### EXHAUST SYSTEMS OF JET ENGINES

Exhaust systems of jet engines and their rational design, effectiveness and method of control acquire an even greater actual importance, especially in connection with the development of engines for high supersonic flight speeds and also for vertical takeoff (landing).

The exhaust systems of the jet engine include: diffuser, extension pipe, jet nozzle with systems of control and cooling noise, suppressor and thrust reverser (deflector). Sometimes the exhaust includes the afterburner, although it is more logical to put it in a special system of the boosting of thrust of an engine.

#### 7.1. Purpose of Exhaust Systems of Jet Engines and Basic Requirements of Them

The purpose of exhaust systems of jet engines is varied - they fulfill a number of responsible functions. Their main purpose is to provide the effective transformation of potential energy of gas pressure behind the turbine into the kinetic energy of outflow of the gas, and to form the output pulse of the jet engine with minimum losses.

At the same time, the exhaust system of the jet engine with the help of special control must provide the necessary change in operating conditions of the engine, control of the direction of the vector (reversing) of thrust and magnitude of thrust from its

maximum positive to its maximum negative values. Furthermore, the exhaust systems of the jet engine must provide the necessary degree of damping of noise produced by the engine. In accordance with the aforementioned, it is possible to formulate the following basic requirements for exhaust systems of jet engines:

- 1) transformation of thermal (potential) energy of gas into kinetic and the creation of the output pulse of engine with minimum losses in all flight regimes;
- 2) providing effective control of processes of operation of the engine in accordance with the profile and flight regime;
- 3) providing control of the magnitude and directions of the vector of thrust over a wide range of values of thrust;
- 4) providing effective damping of noise produced by the engine.

7.2. Process of the Outflow of Gas From the Jet Nozzle

Let us examine the process of the outflow of gas from the jet nozzle (Fig. 7.1) in coordinates  $T, \frac{l}{A} - s$ .

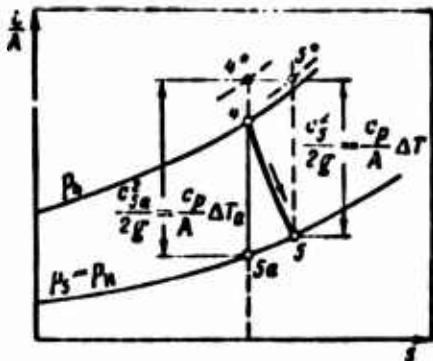


Fig. 7.1. Graphic representation of the process of outflow from the jet nozzle.

Let point 4 characterize the real condition of the gas at the exit from the turbine. Let us draw an isobar of external pressure  $p_u$ . In the absence of losses of friction, the ideal process of

of complete expansion of gas in the jet nozzle (up to external counterpressure  $p_5 = p_H$ ) will be depicted as the isentrope 4-5a. The real process of the outflow occurs along a certain conditional polytrope 4-5. It is accompanied by the growth in entropy due to the presence of friction.

It is not difficult to note that the difference in enthalpies in the adiabatic process 4-5a.

$$\frac{i_4^* - i_{5a}}{A} = \frac{c_{5a}^2}{2g} = \frac{c_p(T_4^* - T_{5a})}{A} \quad (7.1)$$

is the kinetic energy of 1 kg of gas on the section of the nozzle with the ideal process of outflow.

Difference in enthalpies in the real process 4-5

$$\frac{i_4^* - i_5}{A} = \frac{c_5^2}{2g} = \frac{c_p(T_4^* - T_5)}{A} \quad (7.2)$$

is the kinetic energy of 1 kg of gas flowing from the nozzle, with allowance for losses with expansion.

#### 7.2.1. Velocity of Outflow from the Jet Nozzle

Let us find the adiabatic velocity of outflow from the jet nozzle with total expansion of the gas ( $p_5 = p_H$ ) with the help of the energy equation (7.1):

$$c_{5a} = \sqrt{2g \frac{c_{pr}}{A} T_4^* \left[ 1 - \left( \frac{p_H}{p_4^*} \right)^{\frac{k_r-1}{k_r}} \right]}, \quad (7.3)$$

where  $p_4^*$ ,  $T_4^*$  - total pressure and temperature of the gas respectively, at the inlet of the nozzle;  $p_H$  - external counterpressure.

Setting  $k_r = 1.33$  and  $2g \frac{c_{pr}}{A} = 2310$ , it is possible to present in the form formula (7.3)

$$c_{3a} = \sqrt{2310T_4^* \left[ 1 - \left( \frac{p_n}{p_4^*} \right)^{0.25} \right]}. \quad (7.4)$$

If we substitute  $\frac{p_4^*}{p_n} = \pi_{p,c}$  and introduce the gas-dynamic function

$$\varepsilon_{p,c} = 1 - \frac{1}{\pi_{p,c}^{\frac{k-1}{k}}},$$

where  $\pi_{p,c}$  - available degree of expansion of the gas in jet nozzle, then formula (of 7.4) takes the form

$$c_{3a} = \sqrt{2310T_4^* \varepsilon_{p,c}}. \quad (7.5)$$

It is convenient to determine in terms of the given velocity  $\lambda$ ; in this case the velocity of expiration from the nozzle

$$c_{3a} = \lambda_5 a_{kp} = \lambda_5 \sqrt{\frac{2k}{k+1} gRT_4^*}, \quad (7.6)$$

or, substituting  $k = 1.33$ ;  $g = 9.81$  and  $R = 29.5$ , we obtain

$$c_{3a} = 18.3\lambda_5 \sqrt{T_4^*}; \quad (7.7)$$

here

$$\lambda_5 = f\left(\pi = \frac{p_5^*}{p_5}\right),$$

where  $p_5 = p_n$  and  $p_5^* = p_4^*$ .

### 7.3. Methods of Estimating Losses in the Jet Nozzle

The real process of expansion of the gas in the jet nozzle is characterized by hydraulic and gas-dynamic losses, which lower the velocity of outflow and exhaust pulse of the engine. These include losses conditioned by friction in the boundary layer, by the nonuniformity of distribution of axial velocities and by the

velocity (radiality) of flow at the exit of the nozzle, and also losses conditioned by the deviation in the regime from the design regime (losses of "underexpansion" and "overexpansions").

### 7.3.1. Coefficient of Velocity

The ratio of actual (with an allowance for losses) velocity of outflow to the adiabatic (without losses) velocity is called the *coefficient of velocity*

$$\varphi_{p,c} = \frac{c_s}{c_{s0}} < 1, \quad (7.8)$$

which is always less than unity.

The concept of the coefficient of velocity of the jet nozzle is similar to the concept of the coefficient of velocity of the nozzle apparatus of the turbine.

From expression (7.8) it is possible to find the real velocity of outflow

$$c_s = \varphi_{p,c} c_{s0}$$

or

$$c_s = \varphi_{p,c} \sqrt{2310T_1 \left[ 1 - \left( \frac{p_n}{p_1} \right)^{0.25} \right]}. \quad (7.9)$$

usually  $\varphi_{p,c} = 0.97 \div 0.985$ .

Formula (7.9) can be used in all cases of subcritical outflow from the standard converging nozzles and also in cases of supercritical outflow from Laval nozzles, calculated on total expansion of the gas ( $p_n = p_*$ ).

### 7.3.2. Efficiency of the Jet Nozzle

The ratio of the kinetic energy of 1 kg of gas at the exit of

the nozzle in the real process of outflow to the kinetic energy of this gas in the adiabatic process of outflow is the efficiency of the jet nozzle. It is equal to

$$\eta_{p.e} = \frac{c_5^2/2g}{c_{5a}^2/2g} = \left(\frac{c_5}{c_{5a}}\right)^2 = \eta_{p.e}^2 = \frac{\Delta T}{\Delta T_a} \quad (7.10)$$

### 7.3.3. Relative Exhaust Pulse

The effectiveness of the exhaust system of the jet engine is frequently estimated by its relative exhaust pulse. The relative exhaust pulse is understood as the ratio of the real exhaust pulse (with an allowance for hydraulic and gas-dynamic losses and also losses of the overexpansion or underexpansion of gas in the nozzle) to the theoretically highest possible exhaust pulse with complete isentropic expansion of the gas. In this case

$$\bar{I}_s = \frac{I_s}{I_{s(ид)}} = \frac{\frac{G}{g} c_5 + f(p_5 - p_a)}{\frac{G}{g} c_{5(ид)}} = \phi_0 \quad (7.11)$$

where  $I_s = \frac{G}{g} c_5 + f(p_5 - p_a)$  - real discharge pulse;

$I_{s(ид)} = \frac{G}{g} c_{5(ид)}$  - theoretically highest possible (ideal) pulse;

$c_5$  - real velocity of outflow from the nozzle;

$c_{5(ид)}$  - theoretically highest possible velocity of outflow from the nozzle.

Thus, the relative discharge pulse is nothing less than the given coefficient of velocity  $\phi_0$ , which considers all forms of losses in the nozzle, including partial load operating conditions.

Let us express now the relative thrust losses in terms of the discharge pulse  $(1 - \phi_0)$ .

We have:

$$R = I_s - I_0, \text{ and } R_{ид} = I_{s(ид)} - I_0$$

where  $R_{ид}$  and  $R$  - ideal and real thrusts respectively;

$$I_0 = \frac{G}{S} V' - \text{inlet pulse.}$$

Then

$$\Delta \bar{R} = \frac{\Delta R}{R_{(ид)}} = \frac{I_{s(ид)} - I_s}{I_{s(ид)} - I_0}$$

or

$$\Delta \bar{R} = \frac{1 - \varphi_0}{1 - \frac{I_0}{I_{s(ид)}}} = \frac{1 - \varphi_0}{1 - \frac{V'}{c_{(ид)}}}. \quad (7.12)$$

From expression (7.12) it follows that on the test stand (when the inlet pulse is equal to zero) the relative thrust losses is exactly equal to losses of the relative discharge pulse.

At a high flight speed, when magnitudes of the inlet and exhaust pulses are distinguished little from each other, a small change in the parameter  $\phi_0$  can very greatly affect the magnitude of the thrust; at these velocities each percent of the change in the coefficient of velocity of the nozzle can correspond to the change in thrust of 3-5% and more.

Figure 7.2 shows the effect of  $\phi_0$  on  $\Delta \bar{R}$ . From this graph it follows that the 5-percent lowering of the velocity of outflow from the nozzle causes:

- 1) on the test stand ( $M_0 = 0$ ) - drop in thrust of 5%;
- 2) with transition through the speed of sound ( $M_0 = 1.2$ ) - drop in thrust of 8%;

3) in cruising supersonic flight conditions ( $M_0 = 2.2$ ) - drop in thrust of 14%.

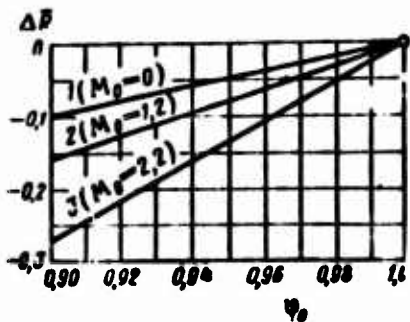


Fig. 7.2. Dependence of losses of relative thrust on losses of relative exhaust pulse for different  $M_0$  numbers.

#### 7.4. Control of Process of Work of Engine

The presence of a regulator of the critical section of the jet nozzle makes it possible to change the regime of operation of the engine (temperature of the gas in front of the turbine, degree of compression of the compressor, number of revolutions), improve the economy of the engine, increase temporarily the thrust of the jet engine and so on. At the same time, by regulating the nozzle throat, it is possible with short-term switching on or switching off of the afterburner to provide invariability to operating conditions of the turbocompressor part of the engine.

##### 7.4.1. Equation of Joint Operation of Turbine and Jet Nozzle of the Turbojet Engine

Let us examine how control of the critical nozzle affect the regime of operation of the engine.

For this purpose let us formulate the equation of flow for critical sections of the nozzle apparatus of the turbine nozzle box assembly [s.a.] (c.a.) and jet nozzle (5-5).

We have:

$$G_{c.a.} = G_5$$

or

$$m_r \frac{p_{c,a}^*}{\sqrt{T_{c,a}^*}} f_{c,a} q(\lambda_{c,a}) = m_r \frac{p_5^*}{\sqrt{T_5^*}} f_5 q(\lambda_5),$$

or

$$\frac{p_{c,a}^*}{\sqrt{T_{c,a}^*}} f_{c,a} q(\lambda_{c,a}) = \frac{p_4^*}{\sqrt{T_4^*}} f_5 q(\lambda_5) \sqrt{\frac{T_4^*}{T_5^*}}. \quad (7.13)$$

Here we assume that the temperature in the critical section of the jet nozzle can be higher than that in the turbine cavity (as a result of the preheating of the gas in the afterburner, i.e.,  $T_5^* = T_\phi^*$ ); it can be lower than  $T_4^*$  (as a result of the heat removal in the extension pipe, i.e.,  $T_5^* = T_x^*$ ).

Then, substituting into expression (7.13)  $\frac{p_3^*}{p_4^*} = \pi_r^*$  and  $\frac{T_3^*}{T_4^*} = \pi_r^{*\frac{n-1}{n}}$  and assuming that in operating regimes  $q(\lambda_{c,a})=1$ , we obtain

$$\pi_r^{*\frac{n+1}{2n}} = \frac{f_5 q(\lambda_5)}{f_{c,a}} \frac{p_{4,5}^*}{p_{c,a}^*} \sqrt{\frac{T_4^*}{T_5^*}}. \quad (7.14)$$

In the absence of an afterburner and with a short gas channel of the exhaust system  $T_5^* = T_4^*$ ; then

$$\pi_r^{*\frac{n+1}{2n}} \sim f_5 q(\lambda_5). \quad (7.14a)$$

From the expression (7.14) it follows that a decrease in the throat area of the nozzle leads to a lowering of the drop in pressure on the turbine. A similar action is produced by an increase in temperature of the gas at the exit of the afterburner.

It is characteristic that the effect of the change in  $f_5$  on  $\pi_r^*$  is valid both in the subcritical and supercritical regions of the outflow of gas from the jet nozzle.

The lowering of the drop in pressures on the turbine leads to a decrease in the operation of the turbine. Consequently, the

the balance of operations of the turbine compressor is disrupted ( $L_T < L_K$ ), and the number of revolutions of the turbocompressor must be decreased. However, the regulator of revolutions of the engine interlinked with the automatic fuel metering increases the supply of fuel and increases it so much that the operation of the turbine at a new, increased value  $T_3^*$  will be equal to the operation of the compressor. It is characteristic that the new equilibrium regime of operation of the TRD will be determined at a higher value of compression ratio of the compressor.<sup>1</sup>

From formula (7.14) there is one more, very important, conclusion, and this is that with an increase in the velocity of outflow in the critical section and with the approach of it to the speed of sound (i.e., with an increase  $\lambda_5 \rightarrow 1$  and  $q(\lambda_5) \rightarrow 1$ ) the drop in pressures in the turbine continuously grows, approaching a certain limiting value.

If the velocity of outflow in the critical section becomes equal to the speed of sound (i.e., the jet nozzle becomes "choked" on the gas flow), then the drop in pressures in the turbine remains constant, independent of the flight conditions (speed and altitude) and the regime of operation of the engine (number of its revolutions), i.e., when  $\lambda_5 = 1$  we have  $\pi_T^* = \text{const}$ . In other words, choking of the jet nozzle and turbine (with respect to the drop in pressures) approaches simultaneously.

#### 7.5. Adjustment of the Jet Nozzle at Supersonic Flight Speeds

With an increase in the flight speeds available drop in pressures in the jet nozzle grows:

$$\pi_{p.c(0)} = \frac{p_4^*}{p_n} = \frac{\pi_{\lambda} \pi_{k.c}^*}{\pi_T^*} = \frac{\pi_{c.c}^*}{\pi_T^*} \sim \pi_c$$

<sup>1</sup>For more detail on this see Section 10.3.

and it grows in proportion to the total compression ratio<sup>1</sup>  $\pi_c$ . Use of the standard converging nozzle at great flight speeds will lead to great losses of thrust due to the underexpansion of flow, and the higher the flight speed, the greater the losses of thrust will be. To ensure complete expansion of the gas at all flight speeds, and mainly at great supersonic velocities, the jet nozzle must be made converging and enlarging (the type of Laval nozzle) with an adjustable ratio of exhaust section of the nozzle to its critical section:

$$\bar{f} = \frac{f_5}{f_{kp}} = \text{var} = \varphi(\pi_{p,c}).$$

The greater the  $M_0$  number of flight, and, consequently, the greater the triggered drop of pressures in the nozzle  $\pi_{p,c} = \frac{P_4}{(P_3 = P_2)}$ , the higher the required ratio of the exhaust section of the nozzle to the critical section  $f_5/f_{kp}$ , and the more it is necessary to "open" the exhaust section  $f_5$ .

Figure 7.3 shows the possible relative increase in the thrust during the transition from the converging nozzle to variable-area nozzle of the Laval type of nozzle depending on the  $M_0$  number of flight (curve 1).

When $M_0 = 1$	the gain in thrust is $\Delta \bar{R} = 4\%$ ;
when $M_0 = 1.5$	" " " " " $\Delta \bar{R} = 10\%$ ;
when $M_0 = 2.0$	" " " " " $\Delta \bar{R} = 18\%$ ;
when $M_0 = 2.5$	" " " " " $\Delta \bar{R} = 30\%$ .

Thus, the jet engine must be equipped with a variable-area jet nozzle of the Laval type of nozzle.

---

<sup>1</sup>When  $q(\lambda_5) = 1$  we have  $\pi_r^* = \text{const.}$

It is possible to select for the engine a simple unregulated jet Laval nozzle so that it would prove to be optimum at a maximum  $M_0$  number of flight (for example,  $M_0 = 2.5$ ); such a nozzle will operate poorly at  $M_0$  numbers less than the maximum, i.e., with drops in pressures less than the rated. The less the  $M_0$  number of flight, the less the required values  $f_5/f_{HP}$ , and the more the so-called degree of overexpansion of the nozzle will be.

The process of outflow of gas from the Laval nozzle in the regime of overexpansion<sup>1</sup> is characterized in a number of cases by the formation inside the nozzle of a normal A-shaped shock wave, behind which subsonic flow is established, just as in the diffuser.

The less the  $M_0$  number of flight, the deeper the shock enters inside the nozzle, the less the velocity of outflow of gas from the nozzle, and the more the relative thrust losses will be.

Figure 7.3 shows the change in thrust of the TRD during the transition from a converging nozzle to a fixed-area Laval nozzle, selected for  $M_{0(\text{расч})} = 2.5$  (curve 2). As we see, when  $M_0 = 0$  the fixed-area of Laval nozzle leads to an 8-percent relative drop in thrust.

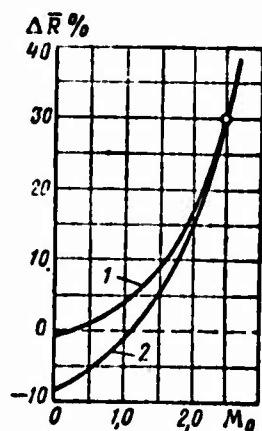


Fig. 7.3. Increase in thrust of a jet engine obtained with substitution of the converging jet nozzle by variable-area and fixed-area Laval nozzles: 1 - variable-area Laval nozzle; 2 - fixed-area Laval nozzle.

<sup>1</sup>In this case separation of flow from the walls are possible.

Thus, from Fig. 7.3 it follows that the fixed-area nozzles (both the converging, and Laval nozzles), intended for operation over a wide range  $M_0$  numbers of flight, are characterized by great losses in thrust: first - at great supersonic  $M_0$  numbers, second - with operation on the test stand and, to a lesser degree, at subsonic and supersonic flight speeds. Jet nozzles of engines of supersonic aircraft must be made *variable-area*; and both the critical section of the nozzle and its exhaust section should be regulated.

The supersonic nozzle with *mechanical adjustment* is complex in control and possesses much weight. The use of nozzles with *aerodynamic adjustment* - the so-called *ejector* nozzles is most rational.

Adjustment of the *critical* section of the nozzle makes it possible to change the regime of operation of the turbo-compressor or maintain it constant. Adjustment of the *exhaust* section of the nozzle provides complete and optimum expansion of the gas in all regimes of flight and operation of the engine.

7.5.1. Determination of Losses of Thrust Which Appear as a Result of the Incomplete Expansion Gas in the Jet Nozzle TRD ( $\phi_{p.c} = 1$ ;  $\phi_0 < 1$ )

Let us assume in general parameters of gas at inlet of the jet nozzle  $p_4^*$  and  $T_4^*$ , and also the external counterpressure  $p_H$ .

Let us express  $I_{5(uA)}$  and  $I_5$  [see equation (7.11)] in terms of gas-dynamic functions  $\lambda_5$ ,  $\kappa(\lambda_5)$  and  $\Gamma(\lambda_5(uA))$ .

We obtain

$$c_5 + \frac{p_5 f_5}{\rho_5 g} = z(\lambda_5) \sqrt{2 \frac{k+1}{k} g R T_5^*}. \quad (7.15)$$

Further let us transform expression

$$\frac{f_5 p_5}{\rho_5 g} = \frac{\kappa(\lambda_5) \sqrt{T_5^*}}{m p_5^* f_{5q}(\lambda_5)} = \frac{\kappa^{11}(\lambda_5(uA)) \sqrt{T_5^*}}{m q(\lambda_5)}. \quad (7.16)$$

Let us present also the ideal velocity  $c_{5(\text{ид})}$  in the form

$$c_{5(\text{ид})} = \sqrt{\frac{2k}{k+1} g RT_5^* \lambda_{5(\text{ид})}}. \quad (7.17)$$

Then, after the appropriate substitutions in formula (7.11) with the help of expressions (7.15), (7.16) and (7.17), we obtain

$$\bar{i}_5 = \frac{1}{\lambda_{5(\text{ид})}} \left[ \frac{k+1}{k} z(\lambda_5) - \frac{\eta(\lambda_{5(\text{ид})})}{g(\lambda_5)} \frac{\left(\frac{k+1}{2}\right)^{\frac{k}{k-1}}}{k} \right]. \quad (7.18)$$

For  $k = 1.33$  we have:

$$\frac{\left(\frac{k+1}{2}\right)^{\frac{k}{k-1}}}{k} = 1.39 \text{ and } \frac{k+1}{k} = 1.75.$$

Then

$$\bar{i}_5 = \frac{1}{\lambda_{5(\text{ид})}} \left[ 1.75 z(\lambda_5) - 1.39 \frac{\eta(\lambda_{5(\text{ид})})}{g(\lambda_5)} \right]. \quad (7.19)$$

From expression (7.19) it follows that the relative loss in the exhaust pulse depends only on the correlation of the available degree of expansion in the jet nozzle  $\left(\pi_{p,c(\text{ид})} = \frac{p_4^*}{p_n}\right)$  and realized expansion ratio  $\left(\pi_{p,c} = \frac{p_4^*}{p_3}\right)$ , or on the correlation of parameters  $\lambda_{5(\text{ид})}$  and  $\lambda_5$ .

If into formula (7.19) we substitute  $\lambda_5 = 1$ , then we will obtain the expression for determining the loss in relative pulse with the use of the standard (converging) nozzle instead of the Laval nozzle.

$$\bar{i}_5 = \frac{1.75 - 1.39 \eta(\lambda_{5(\text{ид})})}{\lambda_{5(\text{ид})}}. \quad (7.20)$$

Figure 7.4 shows the effect of the available drop in pressures  $\pi_{p,c(0)} = p_4^*/p_n$  and  $M_0$  number of flight on losses in thrust  $\Delta \bar{R}$  in the case of the use of simple converging nozzles.

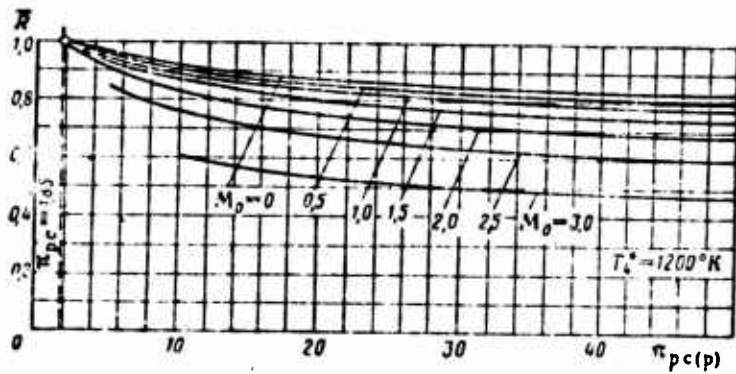


Fig. 7.4. Effect of the available drop in pressures and  $M_0$  number of flight on losses in thrust in the case of the use of converging nozzles.

Figure 7.5 shows the relative thrust losses of fixed-area exhaust Laval nozzles with a different expansion ratio of the supersonic part  $\bar{f}_5 = f_5/f_{kp}$  depending on the available drop in pressures  $\pi_{p.c(0)} = p_4^*/p_0$  in regimes of underexpansion and overexpansions.

In design conditions  $\Delta \bar{R} = 0$ . When  $\bar{f}_5 = 1$  (converging nozzle) with an increase in  $\pi_{p.c(0)}$  losses of underexpansion continuously grow. When  $\bar{f}_5 = 3$  (Laval nozzle with  $\pi_{p.c(p)} = 18$ ) with a decrease in  $\pi_{p.c(0)}$  losses of overexpansion grow.

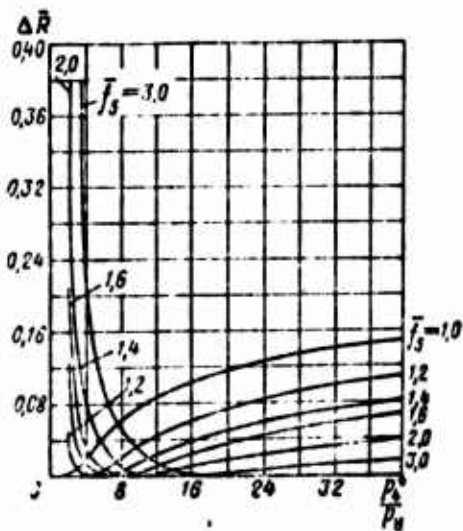


Fig. 7.5. Relative losses of thrust of fixed-area Laval nozzles depending on the available drop in pressures.

7.5.2. Determination of Exhaust Pulse of a Jet with Respect to Total Pressure of the Gas

We have:

$$I_s = \frac{G}{g} c_s, \quad (7.21)$$

where

$$c_s = a_{s(\text{np})} \lambda_s = \lambda_s \sqrt{\frac{2k}{k+1} gRT_s^*}; \quad (7.22)$$

$$G = m \frac{p_s^*}{\sqrt{T_s^*}} f_s q(\lambda_s); \quad (7.23)$$

$$m = \sqrt{\frac{k g}{R}} \sqrt{\left(\frac{2}{k+1}\right)^{\frac{k+1}{k-1}}}.$$

Let us reduce expression (7.23) to the form

$$G = m \frac{p_n f_s}{\sqrt{T_s^*}} \frac{q(\lambda_s)}{\Pi(\lambda_s)}, \quad (7.24)$$

assuming complete expansion of the gas in the jet nozzle and, consequently, the validity of equality  $p_5 = p_H$ .

Let us substitute into (7.21) expressions (7.22) and (7.24). Then, after simple conversions, we find:

$$\frac{I_s}{p_n f_s} = x(\lambda_s) = k \left(\frac{2}{k+1}\right)^{k-1} \frac{\lambda_s q(\lambda_s)}{\Pi(\lambda_s)}. \quad (7.25)$$

It is easy to see that when  $\lambda_5 = 0$  we have  $x(\lambda_5) = 0$  and when  $\lambda_5 = 1.0$  we have  $x(\lambda_5) = k$ .

Figure 7.6 gives dependences  $x = R/p_n f_s = f(\pi_{p,c})$  for  $k = 1.4; 1.33; 1.25$ .

Having these dependences, it is easy according to the measured total pressure on the section of the jet nozzle or in front of the nozzle (with an allowance for losses in the channel) to determine the

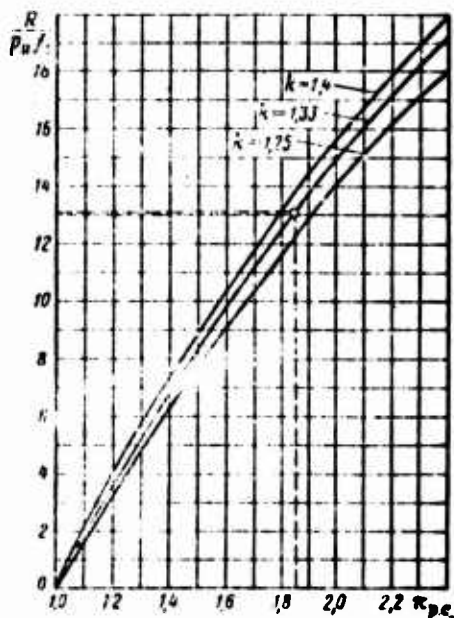


Fig. 7.6. Determination of test stand thrust of a TRD according to the measured total pressure behind the turbine.

given pulse  $I/P_{H1}f_5$ , and then, knowing the area of the exhaust section of the nozzle find the total exhaust pulse.

#### 7.6. Gas-Dynamic and Design Diagrams of Jet Nozzles

Jet nozzles on their gas-dynamic and design peculiarities are subdivided into: converging, fixed-area nozzles of the Laval type of nozzle (including with special shaping the supersonic part), nozzles with a central body, Laval nozzles with mechanical adjustment of the critical and exhaust sections, and ejector nozzles (with aerodynamic adjustment).

Converging nozzles are used when  $M_0 \leq 1.5$ , fixed-area Laval nozzles - when  $M_0 \leq 2.0$ , and ejector nozzles -  $M_0 > 2.0$ .

The subsonic jet nozzle (Fig. 7.7) is in the simplest case (see Fig. 7.7a) an annular converging channel, formed by an interval fixed cone and external housing. For rectification of the flow outgoing from the turbine in a number of cases with considerable twist (up to  $10-15^\circ$ ), and, consequently, for the purpose of using the circumferential component of velocity  $c_{4u}$ , in the jet nozzle aligning streamlined bars are sometimes installed.

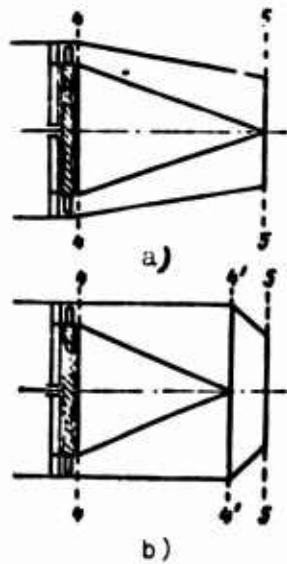


Fig. 7.7. Design diagrams of jet nozzles.

One should, however, keep in mind that the use of the aligning lattice for the swirling flow of gas in the turbine is irrational. Such a lattice can be made only in the diffusion form (Fig. 7.8); the flow in it is characterized by considerable hydraulic losses.

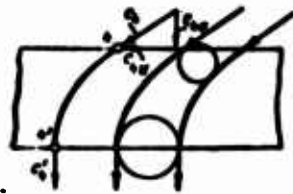


Fig. 7.8. Diagram of aligning turbine lattice.

The less the losses in the jet nozzle, the less its length. However, in a number of cases peculiarities of the arrangement of the TRD on an aircraft require the use of long pipelines (up to 4-7 m and more) for rejection of exhaust gases outside. It is obvious that the gas flow with high velocities (500-600 m/s) over such long connections would lead to great losses in kinetic energy for the overcoming of friction, as a result of which reactive thrust would be decreased considerably.

Therefore, the jet nozzle of the TRD sometimes is made of two elements (see Fig. 7.7b): transitional chamber (diffuser) and inherent jet adapter. In the diffuser there occurs a decrease in

the velocity of outflow (and corresponding increase in the gas pressure), as a result of which with installation of the intermediate extension pipe up to the jet adapter losses of friction proportional to the square of the velocity are decreased by far. Final acceleration of the gas in the short reactive adapter is carried out without losses, in practice along the isentrope.

#### 7.6.1. Jet Nozzle with a Central Body

A jet nozzle with a central body consists of a profiled central body (conical needle) and external casing (crown).

Adjustment of the *critical section* of such nozzles can be carried out either by means of moving the central body in an axial direction or by means of the opening (covering of shutters on the casing).

Adjustment of the *exhaust section* of the nozzle is achieved, for example, by means turning the flow relative to the angular point. Waves of rarefaction outgoing from this point form one family of characteristics. In the nozzle presented in Fig. 7.9 regime of overexpansion practically do not appear. Such a reactive nozzle operates similar to the nozzle box of a turbine with slanting section (line AB - generatrix of the cone of the section).

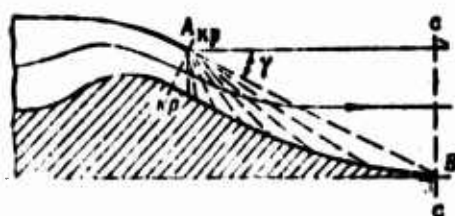


Fig. 7.9. Jet nozzle with a central body.

The maximum expansion ratio of the nozzle, depicted in Fig. 7.9, should be considered as the ratio of the cross section of the jet, which has a diameter equal to the diameter of the exhaust section (c-c) of the casing, to the area of the critical section of the nozzle, i.e.,

$$F = \frac{F_c}{F_{c0}}$$

The basic advantage of nozzles with a central body is their less length ( in comparison with Laval nozzles equipped with rigid walls), and also the automatic adjustment of the expansion ratio. A disadvantage of these nozzles is the difficulty of the realization of their reliable cooling.

### 7.6.2. Ejector Jet Nozzle

An ejector nozzle (Fig. 7.10) consists of the usual converging nozzle and a cylindrical or conic casing (crown) concentrically installed around it. The casing can have a special profile and inlet and exhaust system.

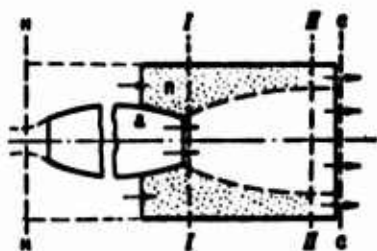


Fig. 7.10. Ejector Jet Nozzle.

From the converging nozzle ejecting (active) gas of high pressure, usually with critical velocity flows out. Entering into the annular cavity, formed by the external surface of the nozzle and internal surface of the casing (crown), with subsonic velocity is the ejected external atmospheric air or high-pressure air jet, bled from the compressor or air intake of the engine (passive gas). The combination of the converging nozzle and external cylindrical casing resembles a shortened ejector (without a long mixing chamber).

The principle of operation of ejector nozzle consists in the following. In a supercritical regime of operation, jet of active gas flowing from the converging nozzle is expanded in accompanying

subsonic flow, acquiring the form of the diverging part of the Laval nozzle with "liquid" walls. Along this jet there is a further acceleration of the flow and also lowering of the temperature and pressure of the gas.

If the casing has a cylindrical form, the increase in flow through cross-section areas of the active jet of gas leads to a narrowing of the passive subsonic jet, along which the velocity gradually increases and the temperature and pressure of the air drop.

At a certain section (of "equal pressures") the static pressures of the active and passive gas are equalized ( $p_{2a} = p_{2n} = p_2$ , see Fig. 7.10).

In other conditions of the operation of the ejector nozzle in the section of equal pressures on the section of the nozzle external pressure ( $p_c = p_n$ ) is established. Such expansion of the gas in the nozzle will be complete.

Let us write the expression of thrust of an engine with an ejector nozzle in the regime of complete expansion of the gas, and let us compare the magnitude of the obtained thrust with the thrust of engine equipped with the standard converging nozzle.

Let us isolate the control surface (see Fig. 7.10) encompassing the external circuit of the total jet flowing into the engine and into ejector circuit and limited by sections of undisturbed flow (a-a) and equal pressures (c-c).

Then the thrust of the TRD with the ejector nozzle will be equal to:

$$R_s = \left( \frac{G_s}{g} c_{s(c)} + \frac{G_n}{g} c_{n(c)} \right) - \frac{(G_s + G_n)}{g} V, \quad (7.26)$$

$$R_s = \frac{G_s}{g} (c_{s(c)} - V) + \frac{G_n}{g} (c_{n(c)} - V). \quad (7.27)$$

It is easy to see that the thrust of the engine with an ejector nozzle is less than the thrust of the engine with a rated mechanical Laval nozzle, i.e.,

$$R_e < R_n,$$

since the thrust of the passive jet  $R_{\Pi}$  with an allowance for losses of friction, is negative and acts in a direction opposite to the direction of flight. Actually, from equality ( $p_c = p_H$ ) it follows that

$$c_{\Pi(c)} < V.$$

At the same time, an analysis of expression (7.27) shows that the thrust of the engine with an ejector nozzle is greater than the thrust of an engine with the standing converging nozzle. Actually, at cylindrical casing the total impulse of flows in sections I and II (see Fig. 7.10) are equal, i.e.,

$$I_{\Pi(a)} + I_{\Pi(n)} = I_{\Pi z} = I_{I(a)} + I_{I(n)} = I_{I z}. \quad (7.28)$$

However, the momentum of passive gas in section I is more than that in section II, in contrast to the momentum of active gas, which is more in section II, i.e.,

$$I_{\Pi(a)} - I_{I(a)} > 0.$$

Consequently,

$$R_e > \left( \frac{G_2}{g} c_{I(a)} - \frac{G_2}{g} V \right) + f_{I z} (p_{I z} - p_H).$$

It is known that the cylindrical casing does not create thrust, since it cannot absorb axial forces (forces of normal pressure are directed in radial directions perpendicular to the casing).

How in this case is it possible to explain physically the

indisputable increase in the exhaust pulse of the engine equipped with a cylindrical ejector casing?

An increase in the exhaust pulse of the converging nozzle in the presence of an ejector crown is explained by the increase in pressure of the passive flow, which is imparted to the external surface of the converging nozzle. As a result of this there appears an additional axial component forces of pressure, which acts in the direction of flight and which increases the thrust of the TRD. Raised static pressure of passive gas appears in flight with acceleration of the flow, which has quite high velocity.

Let us examine now the operation of the ejector nozzle in uncalculated pressure differentials (Fig. 7.11b). With a decrease in the available drop in pressures  $p_4^*/p_{\mu}$  in the nozzle of the active gas (for example, due to a decrease in the flight speed) the section of equal pressures approaches the mouth of the converging nozzle, and exhaust section of the expanding jet is decreased. A change in  $f_{2a}/f_{1a}$  depends on parameters of the passive jet - consumption of pressure and of temperature of the braked flow.

With a further decrease in the pressure differential the section of equal pressures can coincide with the section of the converging nozzle. In this case the jet of the active gas will have a cylindrical shape (see Fig. 7.11a).

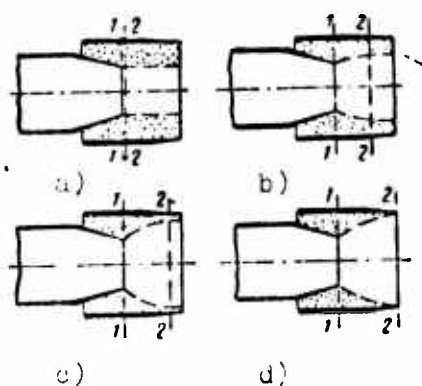


Fig. 7.11. Operation of the ejector nozzle in various regimes: a, b) subcritical regimes; c) critical regimes; d) regime of choking.

With an increase in the drop in pressures (which corresponds to an increase in the flight speeds) the section of equal pressures will move away from the mouth of the nozzle, and the velocity of the active and passive gas in this section will increase. At a definite magnitude of the drop in pressures, the velocity of the passive gas becomes critical. Such a regime of operation of the ejector nozzle is called critical (see Fig. 7.11c). If the drop of pressures increases even more, then the expanding active jet can fill the whole available section of the ejector circuit. In this case (see Fig. 7.11d) the flow of passive gas becomes equal to zero. Such a regime of operation of the nozzle is called *regime of choking*.

Thus, with a change in the regime of operation of the ejector nozzle *automatic control* of its passage sections occurs.

In conclusion one should note the fundamental distinction in the operation of the ejector and ejector nozzle. In the ejector an increase in the thrust occurs because of the addition of additional masses of gas, which as a result of the energy change in the process of mixing between the active and passive gas acceleration is obtained.

In the ejector nozzle the mixing of flows and the exchange of energy between them do not occur. An increase in thrust is accomplished as a result of the additional expansion of gas in the supersonic nozzle with gas-dynamic control of its liquid walls.

### 7.6.3. Comparison of the Effectiveness of Various Reactive Nozzles

Figure 7.12 gives results of the experimental investigation of the effectiveness of various nozzles in the form of dependences of the relative exhaust pulse with the available drop in pressures in the nozzle ( $\pi_{p,c(0)} = p_4^*/p_0$ ).

Curve 1 is the change in relative exhaust pulse of the standard

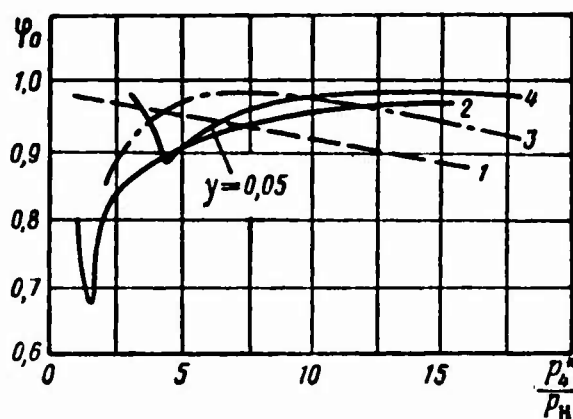


Fig. 7.12. Effectiveness of various jet nozzles on partial load conditions: 1 - converging nozzle; 2 - fixed-area of Laval nozzle; 3 - shortened fixed-area of Laval nozzle; 4 - ejector nozzle.

converging nozzle. With an increase in the drop in pressures in the nozzle the coefficient  $\phi_0$  continuously drops. Being very high ( $\phi_0 = 0.97$ ) when  $\pi_{p.c} = 2$  (regime of expectation of landing of aircraft at subsonic speed), it is lowered to  $\phi_0 = 0.89$  at  $\pi_{p.c} = 15$  ( $M_0 = 2.2$ ).

Curve 2 refers to the fixed-area Laval nozzle with complete expansion selected for  $M_0 = 2.2$ . Such a nozzle with an expansion ratio of the supersonic part of the nozzle  $\bar{f}_5 = f_5/f_{np} = 2.6$  has a very high value  $\phi_0$  ( $\phi_0 = 0.97$ ) in the rated regime ( $\pi_{p.c} = 15$ ) and badly works at subsonic flight speeds. Thus, for instance, for  $\pi_{p.c} = 2$  we find that  $\phi_0 < 0.8$ .

Curve 3 shows a change in coefficient  $\phi_0$  of a shortened fixed-area Laval nozzle with an expansion ratio  $\bar{f}_5 = 1.69$ . Such a nozzle when  $M_0 = 2.2$  has a reduced value of  $\phi_0$  ( $\phi_0 = 0.94$ ).

Finally, the use of an ejector nozzle (curve 4) with an insignificant coefficient of ejection ( $y = 0.05$ ) makes it possible to avoid the dip formed by curve 2 at subsonic speeds and provide a high exhaust pulse at supersonic flight speeds.

Thus, the ejector nozzle has the best thrust characteristics. With an increase in the  $M_0$  numbers of flight characteristics of such a nozzle are improved.

It should be noted once again that losses of thrust at high flight speeds (with an allowance for the input pulse) considerably exceed losses in the exhaust pulse.

Figure 7.13 gives a diagram and principle of operation of a perfected ejector nozzle with three adjustable elements:

- 1) variable-area nozzle of active flow;
- 2) adjustable exhaust shutters of the ejector nozzle;
- 3) adjustable inlet ports for external air.

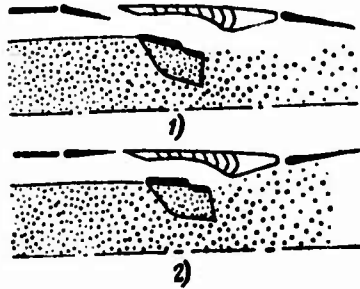


Fig. 7.13. Diagram and principle of operation of the ejector nozzle with three adjustable elements: 1 - altitude; 2 - flight at cruising speed.

#### 7.7. Concept on Base (Stern) Drag of the Exhaust System of the Engine

Base (stern) drag of the exhaust system of the engine is understood as the force of resistance to flight, conditioned by the appearance of stagnant zones of reduced pressure (so-called "base pressure" in the stern part of the nozzle for various end surfaces, and also on the external surface of the casing of the engine nacelle adjacent to the jet nozzle.

The base resistance usually appears on supersonic or low

supersonic flight speeds of reactive nozzles calculated for great supersonic  $M_0$  numbers of flight:

The physical essence of the base resistance is that at reduced uncalculated pressure differentials the jet stream flowing from nozzle is not in a state to fill the whole available exhaust section of the nozzle, and, consequently, in the stern part of the exhaust system zones of reduced pressure are formed.

The base resistance, in accordance with expression (3.9) is determined by formula

$$X_{\text{доп}} = \int_{A_{\text{доп}}} (p - p_w) df, \quad (7.29)$$

where  $p$  - "base" pressure;

$f_{\text{доп}}$  - "base" area.

The more the base area and the lower the base pressure, the more the base (stern) drag.

Let us give several examples of the appearance of base pressure.

#### 7.7.1. Outflow of Gas From the Laval Nozzle with Reduced Drops in Pressures (Regimes of Overexpansion)

Let us assume that the reactive nozzle is calculated for number  $M_{0(p)} = 3.0$  ( $\pi_{p,c} \approx 30$ ) and is made as a variable Laval nozzle ( $f_s/f_{sp} = f = 4.0$ ).

Let us note that the exhaust maximum section of the nozzle determines the outer diameter (mid-section) of the engine nacelle. When  $M_0 = 1.0$  the pressure differential in the nozzle is about 4 and the relative necessary area of the section of the nozzle ( $\bar{f} = 1.25$ ) is by far less than when  $M_0 = 3$ .

If the expanding part of the nozzle is adjusted when  $M_0 = 1.0$  to ensure complete expansion of the gas, then the difference between  $f_{\text{base}}(M_0 = 1.0)$  and  $f_{\text{base}}(M_0 = 1.0)$  "base" area with reduced pressure (Fig. 7.14a) which will cause considerable additional resistance of the engine nacelle.

If the Laval nozzle is fixed-area, nozzle and in the regime of overexpansion of the nozzle ( $\pi_{p.c} = 4.0$ ) there occurs separation of the supersonic flow from walls of the nozzle (see Fig. 7.14b), then in the space of the nozzle unfilled by the jet reduced pressure will be established. This reduced pressure, being imparted on walls and the base area, again will condition the appearance of considerable base drag.

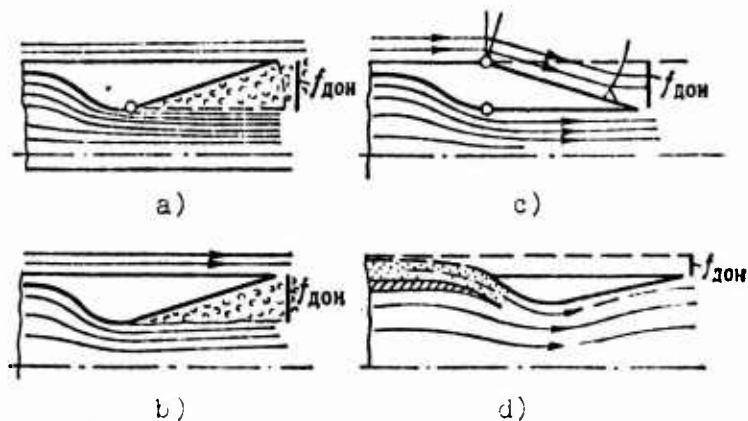


Fig. 7.14. Determination of "base" pressure of a jet nozzle: a) shutters of jet nozzle in subsonic position; b) separation of flow from walls of jet nozzle; c) stern shock on external surface of the nozzle; d) ejecting of air inside jet nozzle.

If we make the external surface of the casing of the engine nacelle when  $M_0 = 1.0$  rotary with shutters of the nozzle, then with flow around of the deflected external curved surface of the casing by supersonic flow a zone of reduced pressure is formed (see Fig. 7.14c), which will condition the formation of base drag.

If, however, in the expanding part of the nozzle in the regime

of overexpansion there will not be any flow separations, but a shock wave will arise, for which the entire flow becomes subsonic, then losses in thrust will be approximately commensurable with losses of base drag.

### 7.7.2. Outflow from the Ejector Nozzle

The use of an ejector nozzle with the injection of external air from the external housing through special ports (slots makes it possible to fill the expanding part of the nozzle and prevent overexpansion of the gas when  $M_0 = 1.0$ . However, in this case in the space between the diameter of the housing and external diameter of the ejector a base area is formed (see Fig. 7.14d).

Figure 7.15 gives the effect of the rated  $M_0$  number of flight on losses of thrust conditioned by base drag of the jet nozzle during flight at the speed of sound ( $M_0 = 1$ ). We see that with an increase in the rated number  $M_{0(p)} > 1.0$  the base drag rapidly increases (due to the increase in base area).

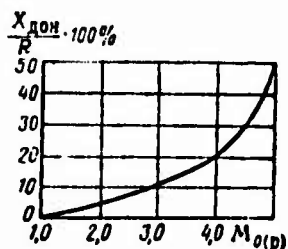


Fig. 7.15. Effect of rated  $M_{0(p)}$  number of flight on losses of thrust conditioned by the base drag.

If when  $M_{0(p)} = 2$  losses in thrust consist of about 4%, and when  $M_{0(p)} = 3$  they are equal to 10%, then when  $M_{0(p)} = 4.5$  losses in thrust already reach 30%.

## CHAPTER 8

### MIXING CHAMBERS OF THE JET ENGINE

#### 8.1. Principles of the Theory of the Mixing of Gas Flows in the Jet Engine

##### 8.1.1. Mixing of Gas Flows in a Ducted-Fan Jet Engine

In connection with the development of a ducted-fan jet engine, designed for wide speed ranges of flight, in recent years the problem of the rational mixing of gas flows has received greater actuality.

The mixing of gas flows in the DVRD is used for various purposes:

- 1) for the suction of an additional mass of gas from without ("ejection") and, consequently, for an increase in momentum of flow coming out of the engine. The appropriate devices are called ejector thrust intensifiers;
- 2) for an exchange of mechanical energy between ducts of the DVRD, as a result of which the total thrust of the engine also increases and specific flow of fuel is lowered;
- 3) for the design simplification of the flowing part of the engine. For example, the unification of flows of gas flowing from ducts of the DVRD makes it possible to simplify the exhaust system of the engine, having replaced it by some variable-area nozzle. In this case systems of noise suppression, cooling and of thrust reversing are simplified;

4) for the lowering of the noise level produced by the flowing jet of gas from the engine;

5) for gas-dynamic control of the supersonic jet nozzle.

### 8.1.2. Actual Regime of Mixing

#### 8.1.2.1. Physical Model of the Mixing of Flows.

Flowing from the nozzle of the active (high-pressure) gas is a jet of gas of mass per second  $M_1 = \frac{G_1}{g}$  with parameters  $c_1$ ,  $p_1$  and  $T_1$  into the space, in which the passive (low pressure) gas of mass per second  $M_2 = G_2/g$  in parallel to the  $x$  axis with parameters  $c_2$ ,  $p_2$  and  $T_2$  flows.

In the case of subsonic flows (Fig. 8.1) the static pressure in the initial jets is equal, i.e.,  $p_1 = p_2 = p$ . Parameters of active gas in section 1-1 and passive gas in section 2-2 are distributed evenly. Flowing out from the nozzle into the surrounding space, the active flow spreads as a free turbulent jet in the wake flow, taking a conic form. On the surface of the cone in the boundary layer of the jet condition  $c_1 = c_2$  is observed.

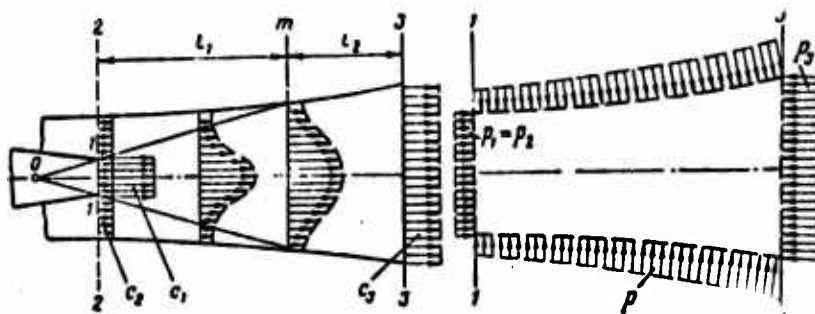


Fig. 8.1. Physical model of mixing of flows (subsonic flow).

Between the initial section of chamber 2-2 and its final section 3-3 there is a mixing of the flows, as a result of which a gradual averaging and levelling off is carried out of fields of static

and complete flow parameters (velocity, pressures and temperatures).

The process of mixing is complete, and the flow appears again, evenly distributed over the cross section.

The interaction in the passive gas by the active flow and mixing of particles of both flows occur because of the presence of transverse turbulent pulsations (mainly in the active jet).

The intensity of the process of mixing depends on correlation of aerodynamic parameters of initial flows and also on the profile geometry of the mixing chamber.

The process in the mixing chamber can be conditionally divided into two areas: area of erosion of the nucleus of active flow by the extending boundary layer of the jet ( $l_1$ ) and area of levelling off of parameters of the mixture, when the boundary layer envelopes the whole mass of the gas ( $l_2$ ).

The physical model of mixing of flows when the outflow of the active gas with supersonic velocity somewhat is distinguished from that described above. In this case at the entrance into the mixing chamber an uneven field of static pressures is established.

If the nozzle of the active gas is made converging then with supercritical drop in pressures, the jet of high-pressure gas flowing into the nozzle is expanded, taking the form of a natural conical nozzle (Fig. 3.2). Along this expanding part of the jet there is further acceleration of flow and a corresponding lowering of the static pressure.

At constant passage sections of confusion chamber the expansion of the supersonic active jet lead to a narrowing of the subsonic jet. Along the latter there is also acceleration of flow and lowering of the static pressure. Finally, in a certain section (1'-2') static pressures of the mixed jets are equalized, i.e.,  $p_1' = p_2' = p'$ .

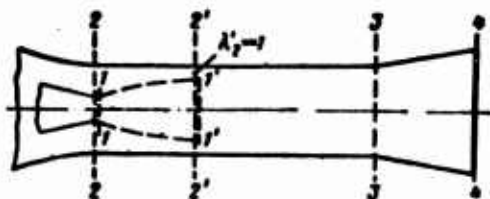


Fig. 8.2. Physical mode of mixing of flows (supersonic flow).

It can be considered that up to this section (of "equal pressures") the gas jets flow in an isolated manner from each other, not mixing.

With removal from the section of equal pressures, as numerous experiments show, there approaches erosion of the border of flows and nuclei of the supersonic jet accompanied by the formation of shock waves; gradually fields of velocities, of total pressures and temperatures of the mixture of gases along mixing chamber are equalized.

#### 8.1.2.2. Basic Assumptions and Concepts.

In the study of the process of mixing we will proceed from the following simplifying suppositions and assumptions:

1) initial flows of gases are homogeneous and identical in their chemical composition, i.e., they have identical gas constants

$$R_1 = R_2 = R_3 = R,$$

and specific heats and specific heat ratios are also identical, i.e.,

$$c_{p1} = c_{p2} = c_{p3} = c_p \quad \text{and} \quad k_1 = k_2 = k_3 = k;$$

2) in sections 1, 2 and 3 parameters of initial flows and mixtures are evenly distributed over the cross section;

3) specific heats of the gas depend on the temperature;

4) hydraulic losses are absent;

Let us introduce the following parameters of mixing and their symbols:

$y = \frac{G_2}{G_1}$  --- coefficient of ejection;

$\pi_0 = \frac{P_1^*}{P_2^*}$  --- available drop in total pressures;

$\pi_3 = \frac{P_3^*}{P_2^*}$  --- compression ratio of low-pressure gas in the mixing chamber;

$\theta^* = \frac{T_2^*}{T_1^*}$  --- available drop in stagnation temperatures;

$x = \frac{c_2}{c_1}$  --- ratio of velocities of initial gas flow.

#### 8.1.2.3. Fundamental Equations of Mixing of Flows.

The basic equations of mixing of gas flows refer to equations of continuity, energy and of momentum. They have the following form:

1. Continuity equation

$$G_1 + G_2 = G_3, \quad (8.1)$$

or

$$G_3 = G_1(1+y). \quad (8.2)$$

2. Equation of energy

$$G_1 i_1^* + G_2 i_2^* = G_3 i_3^*, \quad (8.3)$$

whence

$$c_3^2 = \frac{v_1^2 + v_2^2}{1 + y} \quad (8.4)$$

For  $c_{p1} = c_{p2} = c_p$  we obtain

$$T_3^* = \frac{T_1^* + yT_2^*}{1 + y} \quad (8.5)$$

### 3. Equation of momentum (pulse)

Applying to isolated control surface (see Fig. 8.1) the equation of the change in momentum we obtain

$$\left(\frac{G_1}{g} c_1 + p_1 f_1\right) + \left(\frac{G_2}{g} c_2 + p_2 f_2\right) + \int_{f_1+f_2}^{f_3} p df = \left(\frac{G_3}{g} c_3 + p_3 f_3\right) \quad (8.6)$$

From equations (8.2), (8.4) and (8.6) it follows that the form (profile) of the mixing chamber affects only the momentum equation (8.6).

Let us note that in equation (8.6) the integral of static pressure is a reaction of the action of side walls of the chamber on the flow of gas.

It is characteristic that the momentum equation automatically considers specific losses of kinetic energy, conditional by the difference in gas velocities at the inlet of the mixing chamber ( $c_2 \neq c_1$ ).

#### 8.1.2.4. Losses in the Actual Process of Mixing. Thermodynamics of the Actual Process of Mixing.

The actual process of mixing is accompanied by losses. These include:

- a) losses of diffusion;
- b) losses of kinetic energy with mixing;

c) hydraulic and gas-dynamic losses in all elements of the ejector (including in nozzles of the active and passive gas flow, in the mixing chamber, in the exhaust system of the ejector - diffuser or jet nozzle).

Losses of diffusion and kinetic energy are specific losses of mixing.

In Figure 8.3 in the  $\frac{l}{A}$ - $s$ -coordinates the actual process of the mixing of gas flows in the ejector of the DVRD with a cylindrical mixing chamber is represented.

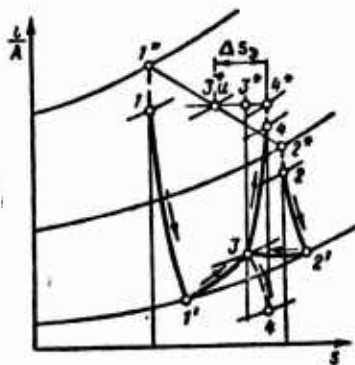


Fig. 8.3. Actual process of mixing of chamber flows of the mixing.

Here: 1-1' - process of expansion of high-pressure gas in the nozzle box assembly;

2-2' -- process of expansion of low-pressure gas in the nozzle box assembly;

1'-3 and 2'-3 - process of the actual mixing of gas with increasing pressure along the chamber;

3-4 - process of deceleration of mixture in the diffuser or acceleration of the mixture in the convergent channel.

Point 3\*<sub>u</sub> characterizes the state of the mixture with ideal mixing;

points 1\*, 2\*, 3\*, 4\* - respectively characterize states of active and passive flows up to mixing, and also the state of the mixture at the exit from the mixing chamber and exhaust system of the ejector;

$\Delta s_3$  - total increase in entropy conditioned by losses in all elements of the ejector.

#### 8.1.2.5. Losses in Kinetic Energy with Mixing.

Losses in kinetic energy with mixing are conditioned by the difference in velocities of outflow of initial flows, i.e.,

$$x = \frac{c_2}{c_1} \neq 1.$$

With the mixing of flows there is collision of particles of gas moving at different velocities, the exchange of momenta of these particles and, thus, averaging and levelling off of the field of velocities of flow. Losses appearing in here are similar to losses of mechanical energy with a shock of inelastic spheres. As is known the kinetic energy of the spheres after their collision is less than the sum of kinetic energies of these spheres prior to collision. Similarly with the mixing of flows the kinetic energy of the mixture is less than the sum of kinetic energies of initial flows up to their mixing, i.e.,

$$G_3 \frac{c_3^2}{2g} < G_1 \frac{c_1^2}{2g} + G_2 \frac{c_2^2}{2g}.$$

Losses in kinetic energy with mixing are conveniently estimated with the help of efficiency of mixing, which for the isobaric chamber ( $p_1 = p_2 = p_3 = p$ ) has the form

$$\eta_{cm} = \frac{G_1 \frac{c_3^2}{2g}}{G_1 \frac{c_1^2}{2g} + G_2 \frac{c_2^2}{2g}}. \quad (8.7)$$

Let us transform expression (8.7), having noted that for the isobaric chamber the pulse of the mixture is equal to the sum of momenta of initial flows, i.e., that [see formula (8.6)]

$$\frac{G_2}{g} c_3 = \frac{G_1}{g} c_1 + \frac{G_2}{g} c_2. \quad (8.8)$$

Introducing the replacement  $c_2/c_1 = x$ ;  $G_2/G_1 = y$  and having substituted value  $c_3$  from (8.8) in (8.7), we obtain after simple conversions

$$\eta_{cm} = \frac{(1 + xy)^2}{(1 + y)(1 + x^2y)}. \quad (8.9)$$

Figure 8.4 gives the effect of the ratio of velocities of initial flows  $x$  and ratio of miscible masses  $y$  on the efficiency of mixing of the isobaric chamber.

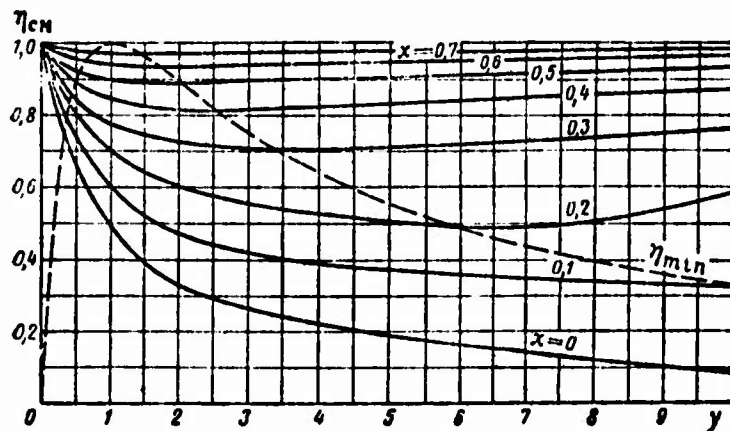


Fig. 8.4. Effect of the ratio of velocities of initial flows  $x$  and ratio of miscible masses  $y$  on the efficiency of mixing  $\eta_{cm}$ .

The greater the relative losses of kinetic energy with mixing of flows, the less the ratio  $x = c_2/c_1$ . They reach the greatest value when  $x = 0$ , i.e., in the case of the outflow of the turbulent jet into the surrounding stationary space; when  $x = 1$  we have  $\eta_{cm} = 1$ .

## 8.2. Process of Mixing in the Cylindrical Chamber

In practice - on different test installations and in wind tunnels - cylindrical mixing chambers ( $f = \text{const}$ ) have become wide spread. The theory of these mixing chambers has been developed in detail.

In this section we will be limited in that we give fundamental equations for the calculation of the process of complete mixing in these chambers, having in mind mainly subsonic flows. Furthermore, let us examine the effect of various factors on the effectiveness of the cylindrical chamber of mixing.

### 8.2.1. Momentum Equation for the Cylindrical Mixing Chamber

For the cylindrical mixing chamber the momentuma equation (8.6) takes the form

$$\left(\frac{G_1}{g} c_1 + p_1 f_1\right) + \left(\frac{G_2}{g} c_2 + p_2 f_2\right) = \left(\frac{G_3}{g} c_3 + p_3 f_3\right). \quad (8.10)$$

Expression (8.10) shows that the total momentum of the mixture is equal to the sum of total momentuma of initial flows.

Expression (8.10) can be transformed, having noted that

$$\frac{G}{g} c + p f = \frac{(k+1)G}{kg} a_{\lambda,p} z(\lambda) = \text{const } G \sqrt{T^*} z(\lambda), \quad (8.11)$$

whence

$$z(\lambda) = \frac{1}{2} \left( \lambda + \frac{1}{\lambda} \right).$$

Then we obtain

$$G_1 \sqrt{T_1^*} z(\lambda_1) + G_2 \sqrt{T_2^*} z(\lambda_2) = G_3 \sqrt{T_3^*} z(\lambda_3), \quad (8.12)$$

whence

$$z(\lambda_3) = \frac{z(\lambda_1) + y \sqrt{\theta^*} z(\lambda_2)}{\sqrt{(1+y)(1+\theta^*y)}}. \quad (8.13)$$

Using tables of gas-dynamic functions, it is easy to determine with respect to the known value  $z(\lambda_3)$  the given velocity  $\lambda_3$ .

### 8.2.2. Determination of the Degree of Increase in Pressure of the Cylindrical Mixing Chamber

Let us replace in equality

$$f_3 = f_1 + f_2$$

values  $f_1$ ,  $f_2$  and  $f_3$  from corresponding equations of flow reduced to the form

$$G = m \frac{p^* f}{\sqrt{T^*}} q(\lambda).$$

Then after simple conversions we obtain

$$\pi_3 = \frac{\sqrt{(1+y)(1+\theta^*y)}}{q(\lambda_3) \left[ \frac{1}{\pi_0 q(\lambda_1)} + \frac{y \sqrt{\theta^*}}{q(\lambda_2)} \right]}. \quad (8.14)$$

Determination of  $q(\lambda_3)$  is produced with respect to the found value  $\lambda_3$  with the help of tables of gas-dynamic functions.

### 8.2.3. Effect of Parameters of Mixing on the Compression Ratio of Low-Pressure Gas in the Cylindrical Chamber

From formula (8.14) it follows that the compression ratio of low-pressure gas in the cylindrical mixing chamber depends on four independent parameters of mixing, i.e.,

$$\pi_3 = f(\pi_0, \theta^*, y \text{ and } \lambda_2).$$

The effect of parameters of initial gas flows on the effectiveness of mixing can be examined as a result of the compression of low-

pressure gas by high-pressure gas with subsequent equalizing of the temperature

### 8.2.3.1. Effect of Available Drop in Pressures $\pi_0$ .

With an increase in the available drop in pressures  $\pi_0$  (for example, as a result of the increase in  $p_1^*$ ) the work of the expanding of active gas, always equal to the work expended for compression of the passive gas, increases. Consequently, the compression ratio  $\pi_3$  and pressure at the exit of the chamber  $p_3^*$  grow. Since with an increase in  $\alpha = c_2/c_1$  is decreased, and losses of kinetic energy with mixing grow, then curve  $\pi_3 = f(\pi_0)$  becomes all the more sloping (Fig. 8.5).

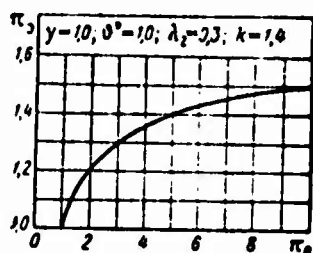


Fig. 8.5. Effect of available drop in pressures  $\pi_0$  on the compression ratio of low-pressure gas  $\pi_3$ .

### 8.2.3.2. Effect of Available Drop in Temperatures $\theta^*$ .

With a decrease in the available drop in temperatures  $\theta^*$  (for example, as a result of an increase in  $T_1^*$ ) the operation of the expansion of active gas increases. Consequently, at the assigned temperature  $T_2^*$  of passive gas its compression ratio  $\pi_3$  grows.

If, however, magnitude  $T_2^*$  is lowered, then at constant expended work of compression the numeral value  $\pi_3$  also increases (Fig. 8.6).

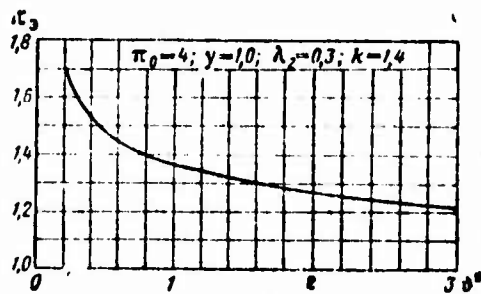


Fig. 8.6. Effect of available drop in temperatures  $\theta^*$  on the compression ratio of low-pressure gas  $\pi_3$ .

### 8.2.3.3. Effect of the Coefficient of Ejection $\gamma$ .

Independently of the magnitude of the coefficient of ejection, the total work of expansion of the active gas as previously is equal to the total work expended on the compression of the passive gas. Consequently, with the increase in  $\gamma$  the expansion ratio of the active gas increases, and the compression ratio of the passive gas  $\pi_3$  is lowered (Fig. 8.7).

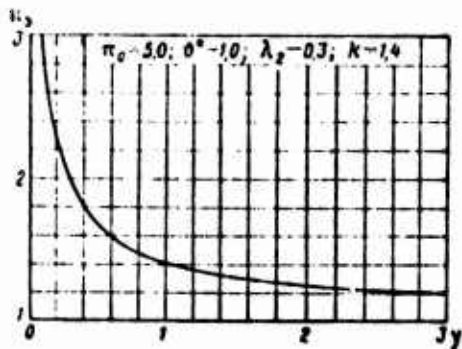


Fig. 8.7. Effect of the coefficient of ejection  $\gamma$  on the compression ratio of low-pressure gas  $\pi_3$ .

### 8.2.3.4. Effect of $\lambda_2(M_2)$ of the Flow of Passive Gas.

At the assigned parameters of mixing  $\pi_0$ ,  $\theta^*$  and  $\gamma$ , losses in total pressure of the mixture are determined by the absolute value of  $\lambda(M)$  numbers of initial flows and also by the ratio of velocities

$x = c_2/c_1$ , which determines the efficiency of the mixing.

The less the absolute value of numbers  $\lambda_1$  and  $\lambda_2$  and the nearer ratio  $c_2/c_1$  to unity, the more complete the pressure of the mixture.

From the expression of the connection of gas-dynamic functions

$$\Pi(\lambda_1) = \frac{\Pi(\lambda_2)}{\pi_0}$$

it follows that any increase in  $\lambda_2$  (when  $\pi_0 = \text{const}$ ) is always accompanied by a growth in  $\lambda_1$ . However, the ratio of velocities

$$\frac{c_2}{c_1} = x = \frac{\lambda_2}{\lambda_1} \sqrt{\theta^*} \quad (8.15)$$

in this case increases, tending to unity. Thus when  $\pi_0 > 1.0$  the growth in number  $\lambda_2$  from zero to 0.6-0.8 usually leads to an increase in pressure of the mixture (i.e., to a growth in  $\pi_3$ ).

When  $\pi_0 = 1$  the ratio of velocities  $c_2/c_1$  with an increase in  $\lambda_2$  remains constant; thus, the absolute growth in numbers  $\lambda_1 = \lambda_2$  leads to an increase in the losses of mixing and to a continuous lowering of a total pressure of the mixture ( $\sigma_{CM}^* < 1$ ).

However, the absolute magnitude of these losses is small and in region  $\lambda_1 = \lambda_2 < 0.5-0.6$  (encompassing possible actual flows in mixing chambers of the ducted fan jet engine) does not exceed 2-2.5% (Fig. 8.8).

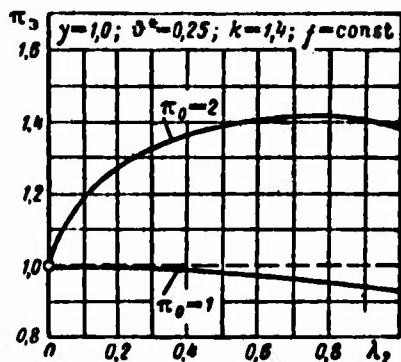


Fig. 8.8. Effect of given velocity of passive gas  $\lambda_2$  on compression of low-pressure gas  $\pi_3$  and coefficient of the drop in total pressure of mixture  $\sigma_{CM}^*$ .

Thus, in depending on the correlation of parameters of initial flows, there always exists the optimum value  $\lambda_2$  at which  $\pi_3$  reaches the maximum.

P A R T T H R E E

TURBOJET ENGINES

## CHAPTER 9

### EFFECT OF PARAMETERS OF THE WORKING PROCESS ON SPECIFIC PARAMETERS AND EFFICIENCY OF THE TURBOJET ENGINE

In this chapter we will examine the effect of parameters of the working process (compression ratio of the working medium; temperature of gas in front of the turbine; temperature of the external medium; efficiency considering losses in processes of compression, heat feed expansion) on specific thermodynamic parameters of the engine (useful work of the cycle; specific thrust and specific fuel consumption), and also on the efficiencies of the engine.

#### 9.1. Work of the Real Cycle of the TRD (Internal Work of the Turbojet Engine)

In Section 4.2 we showed that the work of the real cycle of the TRD is an increase in the kinetic energy of 1 kg of gas inside the engine, i.e., that

$$L_e = \frac{c_2^2 - v^2}{2g} \frac{\text{kgf} \cdot \text{m}}{\text{kg}} .$$

Let us express now the work of the cycle in terms of basic parameters of the working process.

##### 9.1.1. Effect of Parameters of the Working Process of the Work of the Cycle<sup>1</sup> of the Turbojet Engine

The work of the cycle can be expressed as the difference of real (taking into account losses) or works of expanding and compressions:

---

<sup>1</sup>Subsequently, magnitude  $L_e$  will be called *work of the cycle*, the term "*real*."

$$L_e = L_p - L_c \quad (9.2)$$

or as the difference in the adiabatic work of expansion, decreased on losses in the process of expansion, and adiabatic work of compression, increased on losses in the process of compression:

$$L_e = L_{ad,p} \eta_p - L_{ad,c} \frac{1}{\eta_c}, \quad (9.3)$$

where

$$L_{ad,p} = \frac{c_{pr}}{\lambda} T_3 \left[ 1 - \left( \frac{p_4}{p_3} \right)^{\frac{k_p-1}{k_p}} \right];$$

$$L_{ad,c} = \frac{c_{ps}}{\lambda} T_4 \left[ \left( \frac{p_2}{p_1} \right)^{\frac{k_s-1}{k_s}} - 1 \right];$$

$\eta_p, \eta_c$  — total efficiency of processes of expansion and compression.

Then

$$L_e = \frac{c_{pr}}{\lambda} T_3 \left[ 1 - \left( \frac{p_4}{p_3} \right)^{\frac{k_p-1}{k_p}} \right] \eta_p - \frac{c_{ps}}{\lambda} T_4 \left[ \left( \frac{p_2}{p_1} \right)^{\frac{k_s-1}{k_s}} - 1 \right] \frac{1}{\eta_c}. \quad (9.4)$$

Expression (9.4) can be reduced to the form

$$L_e = \frac{c_{ps}}{\lambda} T_3 \left[ 1 - \left( \frac{p_4}{p_3} \right)^{\frac{k_p-1}{k_p}} \right] \eta_p a - \frac{c_{ps}}{\lambda} T_4 \left[ \left( \frac{p_2}{p_1} \right)^{\frac{k_s-1}{k_s}} - 1 \right] \frac{1}{\eta_c}, \quad (9.5)$$

where

$$a = \frac{c_{pr} \left[ 1 - \left( \frac{p_4}{p_3} \right)^{\frac{k_p-1}{k_p}} \right]}{c_{ps} \left[ 1 - \left( \frac{p_4}{p_3} \right)^{\frac{k_p-1}{k_p}} \right]}.$$

Here  $a$  — correction coefficient considering the pressure drop in the combustion chamber and also difference in magnitudes of gas constants and specific heats of the air and products of combustion.

The coefficient  $a$  somewhat exceeds unity (Fig. 9.1). On the average for  $T_3^* = 1000-1400^\circ\text{K}$  and  $\pi = 5-20$  magnitude  $a = 1.02-1.04$ .

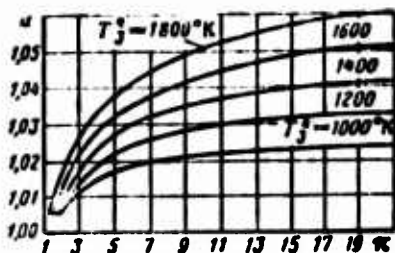


Fig. 9.1. Effect of parameters of the working process on coefficient  $a$ .

With the help of this coefficient we reduce the real cycle of the TRD to the equivalent conditional air cycle  $p = \text{const}^1$  with invariable chemical composition of the working medium and with invariable specific heat capacity.

Let us designate  $p_2^*/p_n = \pi$  — compression ratio of the working medium  $\left(\frac{p_2^*}{p_n}\right)^{\frac{k-1}{k}} = \frac{T_2^*}{T_n} = e$  — ratio of temperatures in the adiabatic process of compression ( $k = 2$ ):

$$c_p = c_p; k_s = k = 1.4; R_s = R = 29.3 \frac{\text{kgf}\cdot\text{m}}{\text{kg}\cdot\text{rad}}.$$

Then formula (9.5) takes the form

$$L_e = \frac{c_p}{\lambda} T_3^* \left(1 - \frac{1}{e}\right) \eta_p a - \frac{c_p}{\lambda} T_n (e-1) \frac{1}{\eta_c}, \quad (9.6)$$

or

$$L_e = \frac{c_p}{\lambda} \left(1 - \frac{1}{e}\right) \left(T_3^* \eta_p a - T_n \frac{e}{\eta_c}\right). \quad (9.7)$$

Thus, the work of the cycle of the TRD

$$L_e = f(T_3^*, T_n, \pi, \eta_p \text{ and } \eta_c)$$

is a function of temperature of the gas in front of the turbine, temperature of the external atmosphere, total compression ratio of the air, and also efficiency of expansion and of compressions.

<sup>1</sup>I.e., to cycle with feed of heat at constant pressure ( $p_1^* = p_0^*$ ).

Let us examine how the enumerated factors effect the work of the cycle.

### 9.1.2. Effect of the Gas Temperature in Front of the Turbine ( $T_3^*$ )

With an increase in gas temperature in front of the turbine  $T_3^*$  (with other factors remaining constant) the work of the gas expansion increases

$$L_2 = \frac{c_p}{\lambda} T_3^* \left(1 - \frac{1}{\epsilon}\right) \eta_p a;$$

with invariable work of the compression this leads to the continuous growth of the work of the cycle (Fig. 9.2) and, consequently, to an increase in the velocity of outflow of gas from the jet nozzle.

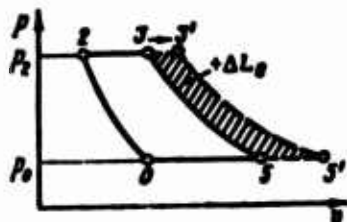


Fig. 9.2. Effect of gas temperature in front of the turbine on the cycle of the TRD.

The increase in the velocity  $a_5$  can be physically explained by the fact that with invariable work of the compressor the growth in gas temperature in front of invariable work of the compressor the growth in gas temperature in front of the turbine leads to a temperature and pressure rise behind the turbine, i.e., at the entrance into the jet nozzle ( $T_4^*$  and  $p_4^*$ ). It is natural that in this case the velocity of outflow of gas continuously increases.<sup>1</sup>

From expression (9.7) it follows that with an increase in  $T_3^*$  the work of the cycle grows according to the linear law (Fig. 9.3).

<sup>1</sup>Here and further we will proceed from the assumption on the complete expansion of the gas.

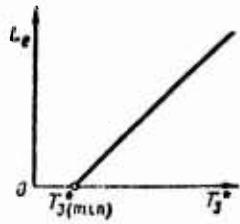


Fig. 9.3. Effect of  $T_3^*$  on  $L_e$ .

Let us find now the minimum value of  $T_{3(\min)}^*$ , at which the work of the cycle becomes zero.

It is obvious that  $L_e = 0$  when  $T_3^* \eta_p a - T_H \frac{e}{\eta_c} = 0$ .  
Then

$$T_{3(\min)}^* = T_H \frac{e}{a \eta_p \eta_c}. \quad (9.8)$$

Table 9.1 gives values  $T_{3(\min)}^*$  for different values of  $\pi_k^*$   
(when  $a \eta_p = 0,94$ ;  $\eta_c = 0,85$ ;  $a \eta_p \eta_c = 0,80$ ;  $T_H = 288^\circ \text{K}$ ):

Table 9.1.

$\pi_k^*$	5	10	15	20	25	30
$T_{3(\min)}^*$	570	696	780	850	900	955

What is the physical meaning of the minimum temperature of the gas in front of the turbine? It consists in the fact that at that the temperature of the work of real processes expended and compressions of the gas are identical, and, consequently, the effective work of the cycle is equal to zero.

### 9.1.3. Effect of External Air Temperature ( $T_H^*$ )

With the reduction of external air temperature  $T_H$  the work expanded for air compression is decreased,

$$L_c = \frac{c_p}{A} T_H (e - 1) \frac{1}{\eta_c}.$$

With constant work of expansion this leads to a growth in the work of the cycle (Fig. 9.4) and to an increase in the velocity of outflow from the jet nozzle. On the other hand, an increase in  $T_H$  the work of the cycle is lowered.

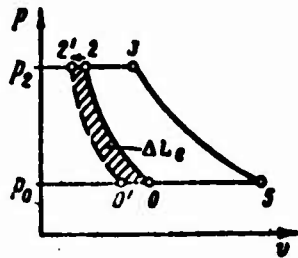


Fig. 9.4. Effect of external air temperature on the cycle of the TRD.

The effect of  $T_H$  and  $L_e$  is depicted as a straight line (Fig. 9.5). The effect of external temperature on the work of the cycle is very considerable. Thus, for instance, the seasonal lowering of  $T_H$  from  $+30^\circ\text{C}$  to  $-30^\circ\text{C}$  increases (with  $T_3 = 1200^\circ\text{K}$ ;  $\pi = 15$ ;  $\sigma_{\eta_p \eta_c} = 0.80$ ) the magnitude  $L_e$  by approximately 43%.

Physically the velocity increase in outflow from the jet nozzle with the reduction of  $T_H$  (and, consequently, with a decrease in the work of compression) is explained by the fact that the total pressure and temperature of the gas at the exit from the turbine increase, i.e., at the entrance into the jet nozzle.

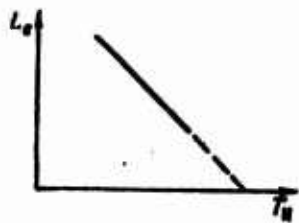


Fig. 9.5. Effect of  $T_H$  on  $L_e$ .

#### 9.1.4. Effect of Compression Ratio of Air ( $\pi$ )

With an increase in the compression ratio of air, the work obtained with the expansion of gas and the work expended for compression of the air increases.

Let us depict the effect  $\pi$  (or  $\sigma$ ) on the work of expansion and work of compression graphically (Fig. 9.6). We see that, in

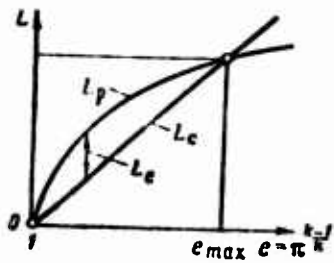


Fig. 9.6. Effect of compression ratio of air on the work of compression and work of expansion.

accordance with expression (9.6), with the increase in  $e$  the work of compression indefinitely grows from zero according to the linear law, and the work of expansion grows according to the hyperbolic law, approaching a certain limiting value when  $e \rightarrow \infty$ .

Thus, the work of the cycle, being equal to zero when  $\pi = 1$ , initially grows, reaches a maximum, and then in the region of high degrees of compression drops, tending to zero.

It is convenient to observe the effect of compression ratio on the work of the ideal cycle in the system of coordinates  $p$ - $v$  and  $T$ - $s$  (Fig. 9.7).

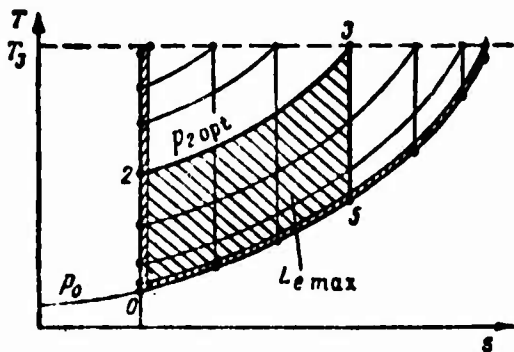


Fig. 9.7. Effect of  $\pi$  on the image of the ideal cycle  $p = \text{const}$  in coordinates  $T$ - $s$ .

Let us draw the isotherm  $T_3 = \text{const}$ , which characterizes the maximum permissible temperature of gas from considerations of strength in front of the turbine. Let us construct a series of cycles  $p = \text{const}$  for various  $\pi$ , beginning from small values and gradually increasing them. We see in Fig. 9.7 that with the increase in  $\pi$  the magnitude of work of the cycle (depicted by the area of the circuit of the cycle) initially grows, reaches a maximum at a certain optimum value  $\pi$  and then drops down to zero. The maximum

of compression ratio at which value  $L_e = 0$  is determined by the point of intersection of the adiabatic curve of compression with isotherm  $T_3 = \text{const}$ , i.e.,  $T_{2a(\text{max})} = T_3$  or  $e = \delta$ .

The physical meaning of this equality is that with a definite, quite large compression ratio of the heat feed to the working medium appears impossible (i.e.,  $q_I = 0$ ), since the final temperature of compression is equal to the maximum permissible temperature of the gas since the turbine. Consequently, the adiabatic curve of expansion coincides with the adiabatic curve of compression, and the useful work of the cycle is equal to zero. In other words, the ideal cycle degenerates into the adiabatic curve.

It is characteristic that in the presence of losses in processes of compression and expanding, the work of the cycle becomes zero with a compression ratio less than that in the case of the ideal cycle. In this case  $T_{2\text{max}} < T_3$ , and consequently, heat feed to the working medium is carried out. However, this heat is sufficient only in order to compensate the appearance of friction losses in the working process. In this case  $q_I = q_{II}$  and  $L_e = L_p - L_c = 0$ .

Let us now find the numerical values of the optimum and maximum compression ratios.

To determine  $\pi_{\text{max}}$  the zero expression (9.7) must be equated, i.e.,

$$T_3^* \eta_p a - T_n \frac{e}{\eta_c} = 0;$$

whence we obtain

$$e_{\text{max}} = \frac{T_3^*}{T_n} \eta_p \eta_c a \quad (9.9)$$

$$\pi_{\text{max}}^{(L_e=0)} = \left( \frac{T_3^*}{T_n} \eta_p \eta_c a \right)^{\frac{k}{k-1}} \quad (9.10)$$

For  $k = 1.4$  we find

$$\pi_{\text{max}} = \left( \frac{T_3^*}{T_n} \eta_p \eta_c a \right)^{3.5} \quad (9.11)$$

Work of the cycle becomes zero also when  $\pi = \pi_{\min} = 1$  (the cycle degenerates into an isobar). However in flight the case  $\pi = 1$  is impossible, since

$$\pi_{\min} = \pi_1 (\pi_2^*)_{\min} = \pi_1 > 1.$$

The value of the optimum compression ratio can be found from the condition

$$\frac{dL_e}{de} = 0.$$

Differentiating equation (9.6), we find

$$\frac{dT_1 \eta_p}{e^2} - \frac{T_w}{\eta_c} = 0,$$

whence

$$e_{\text{opt}} = \sqrt{\frac{T_3^*}{T_w} \eta_p \eta_c \alpha}; \quad (9.12)$$

whence

$$\pi_{\text{opt}} = \sqrt{\left(\frac{T_3^*}{T_w} \eta_p \eta_c \alpha\right)^{1.5}}. \quad (9.13)$$

Comparing expressions (9.11) and (9.13), it is easy to note that

$$\pi_{\max} = \pi_{\text{opt}}^2 \quad (L_e = 0) \quad (L_e = L_{e, \max}) \quad (9.14)$$

$$e_{\max} = e_{\text{opt}}^2 \quad (9.15)$$

i.e., the maximum compression ratio is equal to the square of the optimum compression ratio.

It is characteristic that quantities  $\pi_{\text{opt}}$  and  $\pi_{\max}$  depend on flight speeds. The magnitude of optimum compression ratio of the compressor  $\pi_{x(\text{opt})}^*$  depends on the dynamic compression ratio, i.e., on  $M_0$  of flight. The more  $M_0$ , the less  $\pi_{x(\text{opt})}^*$ .

Thus,

$$\pi_{\pi}^{\circ}(\text{opt}) = \frac{\pi_{\text{opt}}}{\pi_{\pi}}$$

or

$$\pi_{\pi}^{\circ}(\text{opt}) = \frac{\left(\frac{T_3^{\circ}}{T_u}\right)^{1.78} \eta_p \eta_c a}{(1 + 0.2 M_u^2)^{3.5} \sigma_{\pi}^{\circ}} \quad (9.16)$$

Example:

Let  $T_3^{\circ} = 1200^{\circ}\text{K}$ ;  $a\eta_p\eta_c = 0.8$ ;  $H = 11 \text{ km}$  ( $T_u = 216.5^{\circ}\text{K}$ );  $M_0 = 0.9$ . Let us find  $\pi_{\text{opt}}$  and  $\pi_{\text{max}}$ :

$$\pi_{\text{opt}} = \left( \sqrt{\frac{1200}{216.5} \cdot 0.8} \right)^{3.5} = 13.6;$$

$$\pi_{\text{max}} = \pi_{\text{opt}}^2 = 184.$$

Setting  $\sigma_{\pi}^{\circ} = 0.97$ , let us determine

$$\pi_{\pi} = (1 + 0.2 \cdot 0.9^2)^{3.5} \cdot 0.97 = 1.69 \cdot 0.97 = 1.64;$$

$$\text{Then } \pi_{\pi}^{\circ}(\text{opt}) = \frac{13.6}{1.64} = 8.3.$$

Figure 9.8 shows the dependence of the work of the cycle on the compression ratio of the engine.

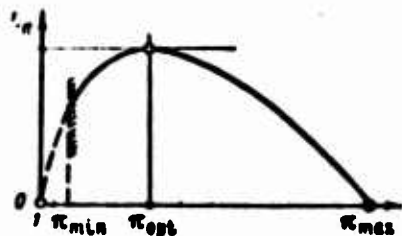


Fig. 9.8. Effect of  $\pi$  on the work of the real cycle.

For test bench conditions on land ( $M_0 = 0$  and  $H = 0$ ) in the temperature range  $T_3^{\circ} = 1100-1300^{\circ}\text{K}$  at achieved values of efficiency of expansion and compression (for example,  $a\eta_p\eta_c = 0.9$ ) we find  $\pi_{\text{opt}} = 7-10$  and  $\pi_{\text{max}} = 49-100$ .

For high-altitude conditions ( $H > 11 \text{ km}$ ) in the same temperature range  $\pi_{\text{opt}} = 12-16$  and  $\pi_{\text{max}} \approx 144-256$ .

### 9.1.5. Effect of Losses With Compression and Expansion

With a decrease in losses in processes of compression and expansion, i.e., with an increase in  $\eta_p$  and  $\eta_c$ , the work of the cycle increases. An increase in the losses, conversely, lowers  $L_p$ . At a certain minimum value of work  $a\eta_p\eta_c$  the work of the cycle becomes zero. This value is equal [see formula (9.8)].

$$(a\eta_p\eta_c)_{\min} = \frac{cT_u}{T_3^*}$$

For  $\pi_k^* = 15$ ;  $T_3^* = 1100$  K;  $T_u = 288$  K we find

$$(a\eta_p\eta_c)_{\min} = \frac{2,17 \cdot 288}{1100} = 0,57.$$

Let  $\sigma = 1,03$  and  $\eta_p = \eta_c = \eta$ .

Then

$$\eta_{p(\min)} = \eta_{c(\min)} \approx 0,75.$$

Thus, the creation of economic gas-turbine engines with a high compression ratio of the working medium is possible only at high values of efficiency of the compressors and turbines. The lower the assimilated value of temperature of gas in front of the turbine, the higher the minimum necessary values of efficiency of expansion and compression for obtaining the effective work of the cycle. Now it is easy to understand that the difficulties were in the creating gas-turbine engines in the 1930's when the efficiency of the first compressors and turbines was very low (did not exceed magnitudes of 0.60-0.65), and the materials used then for the manufacture of blades of turbines did not allow using elevated gas temperatures.

One should note the different (specific weight) of losses of compression and expansion. The point is that the work of expansion is always more than the work of compression, and the more significant this difference the higher  $T_3^*$ , the greater the altitude of the flight (i.e., the lower  $T_u$ ), and the less the compression ratio.

Usually

$$\frac{L_p}{L_c} = \frac{T_3^*}{T_n} \frac{a\eta_p\eta_c}{\epsilon}$$

Therefore, a 1% increase in  $\eta_p$  a numerically greater affect on  $L_e$  than a 1% increase in  $\eta_c$  (two-three times).

## 9.2. Specific Thrust of a Turbojet Engine

Let us express the specific thrust of the TRD in terms of the work of the thermodynamic cycle.

We have

$$R_{ya} = \frac{c_5(1+m_r) - V}{g} \quad (a)$$

$$L_e = \frac{c_5^2 - V^2}{2g} \quad (b)$$

Let us find  $c_5$  from (b) and substitute it into (a); then

$$R_{ya} = \frac{1}{g} [V\sqrt{2gL_e + V^2}(1+m_r) - V]. \quad (9.17)$$

If we can disregard the difference between masses of outflowing gas and inflowing air (i.e., take  $m_r = 0$ ), then

$$R_{ya} = \frac{1}{g} [V\sqrt{2gL_e + V^2} - V], \quad (9.18)$$

and for the case of work of the engine on a test stand ( $V = 0$ )

$$R_{ya} = \sqrt{\frac{2L_e}{g}} \quad (9.19)$$

From formulas (9.17) and (9.18) it follows that the specific thrust depends on the same parameters of the working process as the work of the cycle, and, furthermore, on the flight speeds, i.e.,

$$R_{yA} = f(T_3^*, T_H, \pi, \eta_p, \eta_c \text{ and } V).$$

Let us examine the effect of every factor separately on  $R_{yA}$ .

### 9.2.1. Effect of Gas Temperature in Front of the Turbine

At a certain minimum gas temperature  $T_{3(\min)}^*$  [see formula (9.8)] the specific thrust, just as for the work of the cycle, becomes zero. With an increase in  $T_3^*$  the specific thrust continuously grows, but slower than the work of the cycle (Fig. 9.9).

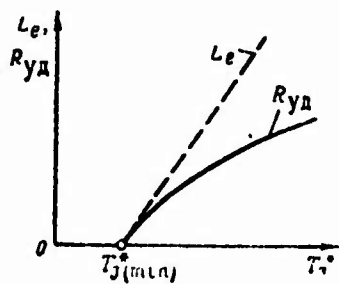


Fig. 9.9. Effect of  $T_3^*$  on specific thrust.

### 9.2.2. Effect of External Air Temperature

With a reduction in external temperature the specific thrust of the TRD increases, and this growth proceeds more slowly than the increase in the work of the cycle (Fig. 9.10).

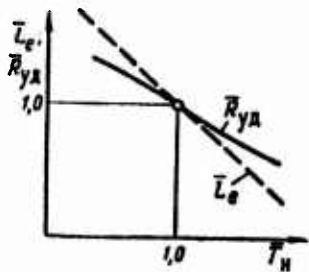


Fig. 9.10. Effect of  $T_H$  on specific thrust.

### 9.2.3. Effect of Compression Ratio

From formula (9.18) it follows that the specific thrust becomes zero and reaches a maximum at the same values of  $\pi$  as does the work of the cycle.

Thus, the character of dependences  $R_{y\pi} = f_1(\pi)$  and  $L_e = f_2(\pi)$  is identical (Fig. 9.11).

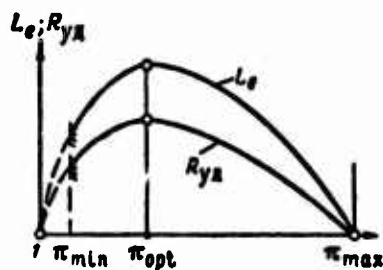


Fig. 9.11. Effect of  $\pi$  on specific thrust and work of the cycle

One ought to note that in flight ( $V > 0$ ) the minimum value

$$\pi_{\min} = \pi_{\min} > 1 \quad (\pi_{\min}^0 = 1).$$

Let us find the magnitude of maximum specific thrust of the TRD with operation on a test stand ( $V = 0$ ). For this let us substitute into expression (9.7) for  $L_e$  the value  $e_{\text{opt}}$  from expression (9.12).

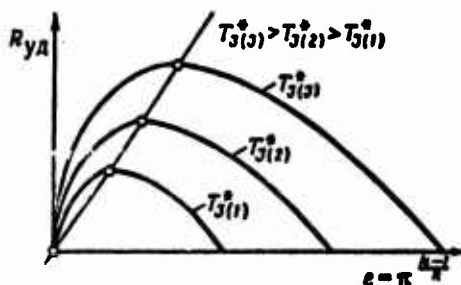


Fig. 9.12. Effect of  $T_3^*$  on specific thrust.

Then after simple conversions let us find:

$$R_{y\pi(\max)} = (e_{\text{opt}} - 1) \sqrt{\frac{2}{\pi} \frac{c_p}{A} \frac{T_3^*}{\eta_c}}. \quad (9.20)$$

When  $T_3^* = 1100 - 1300^\circ \text{K}$ ,  $T_H = 288^\circ \text{K}$ ,  $\eta_p = 0.9$  and  $\eta_c = 0.85$  we gave  $R_{y\pi(\max)} = 55 - 70$  kgf/(kg/s).

Figure 9.12 gives a family of curves  $R_{y\pi} = f(e)$ , plotted for various values of  $T_3^*$ ; through points of maximums of these curves passes a straight line of maximum thrusts corresponding to equation (9.20).

#### 9.2.4. Effect of Flight Speed

Flight speed has an immediate effect on the specific thrust of a designed TRD and generally all forms of the VRD.

At assigned values  $T_3^*$ ,  $\pi$ ,  $\eta_p$  and  $\eta_c$ , being determined by the level of development of technology, and consequently, at the given magnitude of work of the cycle, with an increase in flight speeds the specific thrust of the VRD continuously drops [see formula (9.18)]. The latter is explained in that when  $L_e = \text{const}$  with an increase in  $V$  exhaust velocity from the jet nozzle increases more slowly, so that the difference  $(c_s - V)$ , proportional to the specific thrust, continuously drops.

However, at great flight speeds the inevitable increase in  $\pi$  always leads to a lowering of  $L_e$ . This circumstance accelerates the drop in specific thrust of the TRD in design conditions and limits the range of flight speeds in which utilization of the jet engine is expedient.

### 9.3. Effect of Parameters of the Working Process on Efficiency of the Turbojet Engine

#### 9.3.1. Efficiencies

The economy of the engines is estimated by their efficiencies. For the TRD such coefficients are: *effective (internal)*, *tractive (external)* and *total (complete)* efficiency.

Efficiencies have a clear energy sense, being the ratio of obtained work to that expended; at the same time, they possess that deficiency which cannot be directly measured by devices on the operating engine. For their determination special tests of engines on a test stand and also the known calculating work are necessary. It is convenient to produce all this in laboratory conditions, but it is inconvenient to carry out, for example, in flight. At the same time, knowledge of the efficiency still does not make it possible to

Judge directly the duration, distance of flight, etc.

In the practice of the operation of the engines an estimate of their economy is taken on specific consumptions of fuel referred either to unit of power (work) or unit of thrust.

The use of hour and specific consumption of fuel allows tying economy with the duration of operation of the engine (i.e., with the duration of flight), with necessary fuel reserves on the aircraft, etc.

When the fuel consumption is referred to 1 hp/h, the estimate of economy with respect to efficiency specific consumption is equivalent. In that case when the fuel consumption is referred to 1 kgf of thrust per hour, the estimate of the economy of various engines according to specific fuel consumption is possible only on the condition of identical flight speed.

Since the most important parameter characterizing the effectiveness of the TRD is its draught, then for the determination of its economy we use fuel consumption referred to 1 kg of thrust per hour.

#### 9.3.1.1. Effective (Internal) Efficiency.

The effective (internal) efficiency is called the ratio of heat of equivalent useful work of the cycle to all the heat put into the engine with fuel, i.e.,

$$\eta_e = \frac{A L_e}{q_{in}} = \frac{A \frac{c_p^2 - V^2}{2R}}{q_{in}}. \quad (9.21)$$

Effective efficiency of the TRD estimates the effectiveness (i.e., thermodynamic perfection) of the TRD as a thermal machine (intrinsic engine); it considers all losses connected with the conversion of heat into kinetic energy of gas, i.e., losses of heat with outgoing gases conditioned by the action of the second law of thermodynamics and also by the presence of friction in all elements of the TRD and also losses of heat as a result of the mechanical and chemical incompleteness of combustion.

Factors affecting effective efficiency.

Let us transform the expression

$$\eta_e = \frac{AL_e}{q_{nn}}$$

Let us replace

$$\begin{aligned} AL_e &= c_p \left(1 - \frac{1}{\epsilon}\right) \left(T_3^* a \eta_p - T_n \frac{\epsilon}{\eta_c}\right); \\ q_{nn} &= \frac{c_{pm}}{\xi_{n,c}} \left[T_3^* - T_n \left(1 + \frac{\epsilon - 1}{\eta_c}\right)\right]. \end{aligned} \quad (9.22)$$

Then

$$\eta_e = k_{c_p} \xi_{n,c} \frac{\left(1 - \frac{1}{\epsilon}\right) \left(\delta \eta_p a - \frac{\epsilon}{\eta_c}\right)}{\delta - \left(1 + \frac{\epsilon - 1}{\eta_c}\right)}, \quad (9.23)$$

where  $\xi_{n,c}$  — coefficient of completeness of combustion;  $\delta = \frac{T_3^*}{T_n}$  — degree of preheating of the working medium;  $k_{c_p} = \frac{c_p}{c_{pm}}$  — coefficient considering differences in specific heat of the air and also gas in the combustion chamber;  $k_{c_p} < 1$ ; on the average  $k_{c_p} = 0.90 - 0.92$ ;  $c_{pm}$  — average specific heat in the temperature range  $T_3^* - T_2^*$ .

From formula (9.23) it follows that the effective efficiency of the TRD depends on the ratio of gas temperature in front of turbine to the temperature of the external medium, on compression ratio, efficiency of expansion and compression, and also on the combustion efficiency.

*Effect of the Degree of Preheating  $\delta$  (or  $T_3^*$ )*  
(Fig. 9.13)

When  $\delta = \delta_{min} = \epsilon / \eta_p \eta_c a$  the effective efficiency is equal to zero.

With an increase in the degree of preheating of the working medium effective efficiency of the TRD continuously increases, approaching the limit equal to

$$\eta_{e(\max)} \rightarrow \left(1 - \frac{1}{e}\right) \eta_p a k_{k,c} k_{e,p} \quad (9.24)$$

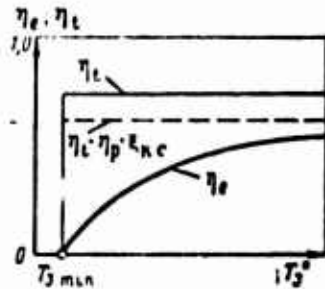


Fig. 9.13. Effect of  $T_3^*$  on effective efficiency.

If in the first approximation we consider that product  $ak_{e,p}$  is distinguished little from unity, then the effective efficiency tends the limit

$$\eta'_{e(\max)} = \left(1 - \frac{1}{e}\right) \eta_p k_{k,c} \quad (9.25)$$

which is always lower than the thermal efficiency of the cycle

$$\eta_t = 1 - \frac{1}{e} \quad (9.26)$$

Physically the continuous increase of effective efficiency, determined by the given value  $\pi(e)$ , with an increase in  $\delta$  (as a result of the growth in  $T_3^*$  or lowerings of  $T_H$ ) is explained by the decrease in a relative portion of the work of compression, taking into account losses of friction in the work of the cycle.

*Effect of Compression Ratio (Fig. 9.14)*

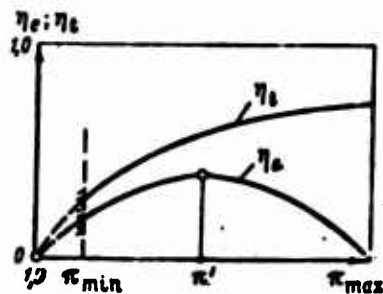


Fig. 9.14. Effect of  $\pi$  on effective efficiency.

From analysis of expression (9.23) it follows that the effective efficiency twice becomes zero - when  $e = 1$  and  $e_{\max} = \frac{T_3^*}{T_H^*} a \eta_p \eta_c$ , i.e., when  $L_e = 0$ ,  $c_3 = V$  and  $R_{yA} = 0$ .

With an increase in  $\pi$  (or  $e$ ) the effective efficiency increases and reaches a maximum at a certain value  $\pi'$ , which is greater than the optimum, i.e.,

$$\pi'_{(c_3=c_e(\max))} > \pi_{\text{opt}}(L_e=L_e(\max)).$$

Actually, with an increase in  $e$  the quantity of heat fed  $q_{\text{in}} \sim (T_3^* - T_2^*)$  continuously decreases according to the linear law. At  $e = e_{\text{opt}}$ , when  $L_e = \text{const}$ , the magnitude  $\eta_e$  continues to increase all the more. The growth in  $\eta_e$  ceases at a certain value  $e' > e_{\text{opt}}$ , when the approaching drop in  $q_{\text{in}}$  compensates continuing lowering of  $q_{\text{in}}$ , i.e., when

$$\frac{dL_e}{de} = \frac{dq_{\text{in}}}{de}.$$

The determination of  $\eta'$  in the general is difficult. Grapho-analytical calculations show that for  $T_3^* = 1100-1300^\circ\text{K}$ ,  $\eta_c = 0,85$ ,  $a\eta_p = 0,94$  and  $T_H^* = 288^\circ\text{K}$  we have  $\pi' = 15-20$ ; in this case the effective efficiency  $\eta_{e(\max)} = 0,22-0,28$ ; for  $T_H^* = 216,5^\circ\text{K}$  ( $H = 11 \text{ km}$ ) and other data given above we find  $\eta_{e(\max)} = 0,32-0,40$ .

Let us note that the effect of  $\pi$  on the thermal and effective efficiency proves to be fundamentally different. Whereas with the increase in  $\pi$  the first efficiency continuously grows, asymptotically tending to unity, the second reaches a maximum (which is considerably below  $\eta_e$ ), and then tends to zero (see Fig. 9.14).

#### 9.3.1.2. Tractive (External) Efficiency.

The tractive (external) efficiency is called the ratio of work of the reactive thrust (tractive work) to the increase in kinetic energy inside the engine, i.e.,

$$\eta_R = \frac{L_R}{L_e} = \frac{R_{y2}V}{\frac{c_s^2 - V^2}{2g}} \quad (9.27)$$

Having substituted  $R_{y2} = \frac{c_s - V}{g}$ , we obtain after reductions

$$\eta_R = \frac{2V}{c_s + V} = \frac{2}{1 + \frac{c_s}{V}} = \frac{2 \frac{V}{c_s}}{1 + \frac{V}{c_s}} \quad (9.28)$$

Thus, the tractive efficiency depends only on the ratio of the flight speed to the velocity of outflow of gas from the engine; with an increase in this ratio from zero to unity the tractive efficiency also increases from zero to unity (Fig. 9.15).

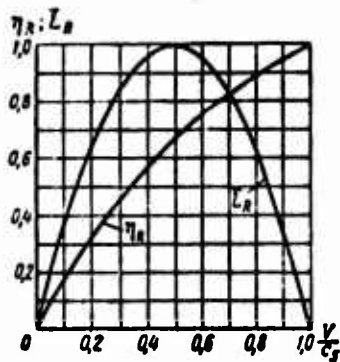


Fig. 9.15. Dependence of thrust efficiency on the ratio of velocities  $V/c_s$ .

Let us examine in more detail the mechanism of formation of reactive thrust of a jet engine. In general the whole increase in the kinetic energy obtained inside the engine is expended for work of reactive thrust and for losses of kinetic energy outside the engine, i.e.,

$$L_e = L_R + L_n$$

or

$$\frac{c_s^2 - V^2}{2g} = \frac{(c_s - V)V}{g} + \frac{(c_s - V)^2}{2g} \quad (9.29)$$

Increase in kinetic energy
Tractive work
Losses in kinetic energy

The physical sense of losses of kinetic energy consists in that it is impossible to transform completely the kinetic energy acquired

inside the TRD into work of reactive thrust. Part of this energy will be uselessly dispersed into surrounding space, outside the engine.

Actually, if the velocity of outflow of gases relative to the engine is equal to  $c_5$  ( $c_5$  - relative velocity, and flight speed of an aircraft  $V$  - transport velocity), then the velocity  $c$  of motion of the jet coming from the engine relative to the ground (absolute velocity) will equal (Fig. 9.16)

$$c = c_5 - V.$$

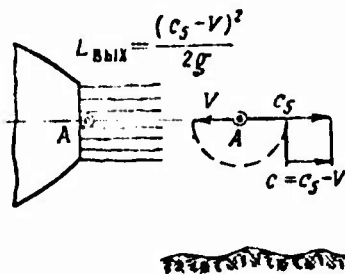


Fig. 9.16. Determination of the concept of losses with exit velocity.

Then the kinetic energy of free jet unused inside engine will equal

$$L_k = \frac{(c_5 - V)^2}{2g}.$$

This energy is also called *loss with exit velocity*.

Thus, the tractive efficiency considers external losses of energy, connected with the transformation of kinetic energy into thrust work: it estimates the perfection of the TRD as a *propelling agent*.

Let us now examine particular cases of operation of the engine.

1. Let  $V = 0$  ( $V/c_5 = 0$ ); in this case  $\eta_R = 0$ . This means that with operation of the engine on the ground (before takeoff) on a test stand the thrust work is equal to zero ( $L_R = 0$ ), since the acting

force does not produce displacement; in this case the whole kinetic energy of jet outgoing from the engine turns into losses.

2. Let  $V=c_5$  ( $V/c_5=1$ ); in this case  $\eta_R = 1.0$ . This means that losses in kinetic energy are absent. However, we think of this case only as being limiting when the increase in kinetic energy of the gas, thrust and tractive work becomes zero.

For the jet engine this case does not represent practical interest.

3. Let us find the ratio of velocities  $V/c_5$ , at which the thrust work reaches a maximum.

From condition  $dL_e/dV=0$  we obtain  $V/c_5=1/2$ . In this case

$$L_e = \frac{3V^2}{2g}; \quad L_R = \frac{2V^2}{2g} \quad \text{and} \quad L_n = \frac{V^2}{2g}.$$

Consequently,  $\eta_R = 2/3$ .

Figure 9.15 gives the curve  $\bar{L}_R = f\left(\frac{V}{c_5}\right)$ .

Effect of parameters of the working process on  $\eta_R$  . .

From expression

$$\eta_R = \frac{2V}{V+c_5} = \frac{2V}{V + \sqrt{2gL_e + V^2}}$$

it follows that at the assigned flight speed any increase in the work of the cycle or velocity of outflow from the nozzle leads to a drop in thrust efficiency as a result of an increase in losses with the exit velocity.

*Effect of Temperature  $T_3^*$  (Fig. 9.17)*

When  $T_3^* = T_{3(\min)}^*$  we have  $L_e = 0$  and  $c_5 = V$ ; consequently,  $\eta_R = 1.0$ . With an increase in  $T_3^*$  magnitude  $c_5$  continuously grows, and is continuously decreased asymptotically approaching zero.

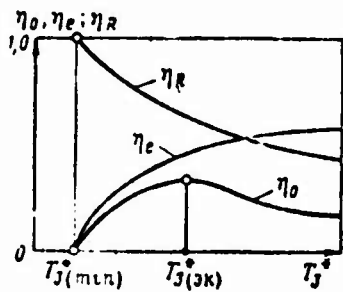


Fig. 9.17. Effect of  $T_3^*$  on the efficiency of the TRD.

*Effect of the Compression Ratio (Fig. 9.18).*

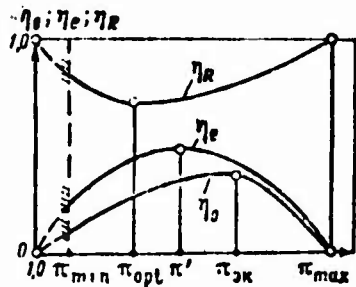


Fig. 9.18. Effect of  $\pi$  on the efficiency of the TRD.

When  $\pi = 1$  and  $\pi = \pi_{\max}$  we have  $c_s = V$ ; consequently,  $\eta_R = 1.0$ .  
 When  $\pi = \pi_{\text{opt}}$  we have  $c_s = c_{s(\max)}$ ; consequently  $\eta_R = \eta_{R(\min)}$ . Thus, the dependence of thrust efficiency on the compression ratio is depicted in the form of a concave curve with a minimum at  $\pi_{\text{opt}}$ .

*Effect of Losses in Processes of Expansion and Compressions*

A decrease in losses in processes of expansion and compression (i.e., growth in  $\eta_p$  and  $\eta_c$ ) leads to a velocity increase in outflow from the nozzle and a result which is paradoxical at first sight - to the lowering of thrust efficiency.

9.3.1.3. General (Complete) Efficiency TRD.

The total (complete) efficiency is called the ratio of heat, equivalent to work of reactive thrust, to the whole heat introduced with the fuel, i.e.,

$$\eta_0 = \frac{AL_R}{q_{\text{in}}} = \frac{AR_{\gamma}V}{q_{\text{in}}}. \quad (9.30)$$

The total efficiency is the product of effective efficiency on thrust efficiency. Actually,

$$\eta_0 = \frac{AL_R}{q_{in}} = \frac{L_R}{L_e} \cdot \frac{AL_e}{q_{in}} = \eta_R \eta_e. \quad (9.31)$$

Thus, the total efficiency estimates *all losses* of heat energy in the TRD, both *internal*, connected with the conversion of heat into kinetic energy, and *external*, connected with the conversion of kinetic energy into thrust work. In other words, the total efficiency estimates the effectiveness of the TRD also as an *engine* and as a *propelling agent*, i.e., as a *power plant* as a whole.

The total efficiency serves as a *criterion of economy* of the TRD.

From a comparison of formula (9.23) and (9.28) it is easy to conclude that the total efficiency depends on the same factors as  $\eta_e$  and  $\eta_R$ , i.e.,

$$\eta_0 = f(T_3^*, T_2, \pi, \eta_p, \eta_e, \xi_{k.c.}, V).$$

*Effect of  $T_3^*$*

Figure 9.17 shows the effect of gas temperature in front of the turbine on  $\eta_e$ ,  $\eta_R$  and  $\eta_0$ .

When  $T_3^* = T_{3(\min)}$  the total efficiency is equal to zero, since the effective efficiency is equal to zero. With an increase in  $T_3^*$  the total efficiency increases, reaching a maximum at a certain economic gas temperature ( $T_{3(\text{em})}^*$ ). With further growth in  $T_3^*$ , with a continuous drop in tractive efficiency, the total efficiency also is continuously lowered.

It is characteristic that the economic value of gas temperature in front of the turbine on a test stand is comparatively low, it increases with an increase in the compression ratio of the working medium.

When  $\pi = 6-10$  and at usual values of  $\eta_p$  and  $\eta_c$ , magnitude  $T_{3(\pi)}^* = 700-850^\circ\text{K}$ . When  $\pi = 15-20$  magnitude  $T_{3(\pi)}^* = 900-950^\circ\text{K}$ .

Thus, assimilated in technology values of  $T_3^*$  considerably exceed its economic values.

#### Effect $\pi$

Figure 9.18 shows the effect of the compression ratio on  $\eta$ ,  $\eta_R$  and  $\eta_0$ .

The total efficiency as an effective efficiency is equal to zero when  $\pi = 1$  and when  $\pi = \pi_{\max}$ . With an increase in  $\pi$  up to a certain economic value ( $\pi_{\text{ec}}$ ) the total efficiency increases, reaching a maximum, and then, with further growth in  $\pi$ , it drops down to zero.

The economic value of the compression ratio does not coincide with that value  $\pi'$  at which the effective efficiency reaches a maximum; it is always more, i.e.,

$$\pi_{\text{ec}} > \pi' > \pi_{\text{opt}}$$

Actually, when  $\pi = \pi'$  the effective efficiency reaches a maximum, and the thrust efficiency increases. Therefore, product  $\eta_e \cdot \eta_R = \eta_0$  also increases. The growth in  $\eta_0$  ceases at the largest compression ratio  $\pi > \pi'$ , when the approaching drop  $\eta_e$  compensates the continuing growth in  $\eta_R$ .

The economic compression ratio of the air of contemporary TRD reaches very high values. At  $T_3^* = 1100-1300^\circ\text{K}$ ,  $T_H = 288^\circ\text{K}$ , at usual values of  $\eta_p$  and  $\eta_c$ , when  $\xi_{\text{ec}} = 0.97$  the magnitude  $\pi_{\text{ec}} = 30-50$ , which is considerably more than the assimilated values  $\pi_{\text{ec}}$  on a test stand.

#### Effect of Flight Speed

With operation of the TRD on the ground ( $V = 0$ ) the total efficiency is equal to zero. With an increase in flight speed the

total efficiency increases. However, at very high flight speeds, when the specific thrust of the TRD is sharply decreased, tending in the limit to zero, the total efficiency also drops down to zero.

#### 9.4. Effect of Parameters of the Working Process on Specific Fuel Consumption

Let us find the connection between specific fuel consumption and total efficiency.

we have

$$C_{ya} = 3600 \frac{m_f}{R_{ya}}. \quad (a)$$

Let us replace  $m_f = \frac{q_m}{H_0}$  and multiply the numerator and denominator of the right side of formula (a) by  $AV$ .

Then we obtain

$$C_{ya} = 3600A \frac{V}{H_0} \frac{q_m}{AR_{ya}V} = 8,43 \frac{V}{H_0 \eta_0}. \quad (9.32)$$

Thus, at the assigned flight speed the specific fuel consumption is inversely proportional to the total efficiency.

Formula (9.32) is unfit for an analysis of operation of the TRD on the test stand, since its right side turns into an indeterminacy (when  $V = 0$  and  $\eta_0 = 0$  we have  $C_{ya} = \frac{0}{0}$ ).

Let us transform formula (9.32).

We have

$$\eta_0 = \eta_c \eta_R = \eta_c \frac{2V}{(V + c_s)}. \quad (9.33)$$

Having substituted value  $\eta_0$  from expression (9.33) into (9.32), we obtain

$$C_{ya} = 4,215 \frac{(V + c_s)}{\eta_c H_u} \quad (9.34)$$

Then for the case  $V = 0$  we find

$$C_{ya} = 4,215 \frac{c_s}{\eta_c H_u} \quad (9.35)$$

From formula (9.32) there can be made conclusion that the specific fuel consumption depends on the same factors as the total efficiency, i.e.,

$$C_{ya} = f(T_3^*, T_2, \pi, \eta_p, \eta_c, i_{a,c}, V).$$

Let us examine the effect of these parameters on the specific fuel consumption.

#### 9.4.1. Effect of Gas Temperature $T_3^*$ (Fig. 9.19)

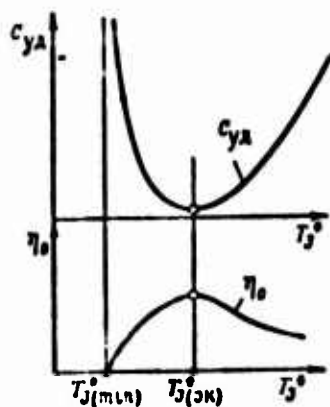


Fig. 9.19. Effect of  $T_3^*$  on the specific fuel consumption.

When  $T_3^* = T_{3(\min)}^*$  the total efficiency is equal to zero. Consequently, the specific fuel consumption is equal to infinity. With an increase in  $T_3^*$  from the minimum to the economic value ( $T_{3(\text{opt})}^*$ ) the specific fuel consumption is continuously decreased, reaching a certain minimum value. A further increase in gas temperature in front of the turbine leads to a continuous increase in  $C_{ya}$ .

Curve  $C_{ya} = f_1(T_3^*)$  graphically is as though it were a mirror image of curve  $\eta_0 = f_2(T_3^*)$  (see Fig. 9.19).

The design point of operation of contemporary TRD on a test stand ( $V=0; \pi=\pi_{расч}$ ) is located on the right branch of curve  $C_{ya}=f_1(T_3^*)$ . In other words, computed value of gas temperature in front of the turbine is much higher than the economic temperature. The latter is explained by the tendency to increase the specific thrust of the engine, reduce its dimensions and specific weight, even to the detriment of the economy of the TRD.

#### 9.4.2. Effect of the Compression Ratio $\pi$ (Fig. 9.20)

At minimum ( $\pi = 1$ ) and maximum ( $\pi=\pi_{max}$ ) values of the compression ratio the total efficiency of the TRD is equal to zero, and the specific fuel consumption of the engine is equal to infinity.

With an increase in  $\pi$  from 1 to the economic value  $\pi_{opt}$  the specific fuel consumption is steadily lowered, reaching a minimum. A further growth in  $\pi$  from  $\pi_{opt}$  to  $\pi_{max}$  already causes a continuous growth of  $C_{ya}$ .

Curve  $C_{ya}=f_1(\pi)$  is graphically as if it were a mirror image of curve  $\eta_0=f_2(\pi)$  (see Fig. 9.20).

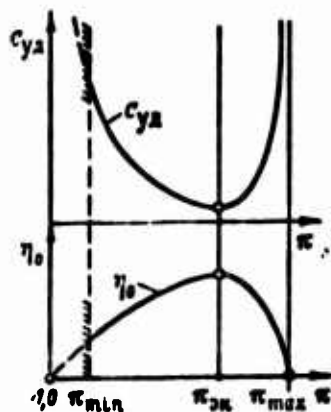


Fig. 9.20. Effect of  $T_3^*$  on the specific fuel consumption.

It is necessary to note that in test stand conditions ( $V=0; T_3=T_{3,расч}$ ) the design point of operation of the engine is located on curve  $C_{ya}=f_1(\pi)$ , between the optimum and economic values of the compression ratio, i.e.,

$$\pi_{opt} < \pi_{prac} < \pi_{th}$$

The last circumstance is explained by the tendency to increase the specific thrust of the TRD, reduce its dimensions, and simplify the design (i.e., reduce the number of stages of the compressor and turbine) and as a result lower the specific weight of the engine with a simultaneous providing of high economy of the engine.

#### 9.4.3. Minimum Possible Specific Fuel Consumption of the TRD

In connection with the tendency to develop highly economical turbojet engines, it is necessary to know at which values of parameters of the working process and also at which parameters of flight does the specific fuel consumption take the minimum possible values.

For this purpose, first of all, let us determine analytically the economic gas temperature  $T_3^*$ .

Let us transform expression

$$C_{ya} = 3000 \frac{m_f}{R_{ya}}$$

having substituted in it

$$m_f = \frac{c_{fm} \left[ T_3^* - T_n \left( 1 + \frac{e-1}{\eta_c} \right) \right]}{\xi_{n,c} H_n}; \quad (9.36)$$

$$R_{ya} = \frac{1}{g} \left\{ \sqrt{2g \frac{c_p}{A} \left[ T_3^* \left( 1 - \frac{1}{e} \right) a \eta_p - T_n \frac{(e-1)}{\eta_c} \right] + V^2} - V \right\}. \quad (9.37)$$

Then after simple conversions we obtain

$$C_{ya} = f \frac{x-b}{\sqrt{x-k-d}}. \quad (9.38)$$

where

$$\begin{aligned}
 x &= T_3^0; \\
 b &= T_3^0 = T_u \left(1 + \frac{e-1}{\eta_c}\right); \\
 k &= T_u \left[ \frac{e}{a\eta_p\eta_c} - 0,2 \frac{M_u^2}{\left(1 - \frac{1}{e}\right)a\eta_p} \right]; \\
 d &= \frac{V}{\sqrt{2g \frac{c_p}{A} \left(1 - \frac{1}{e}\right) a\eta_p}}; \\
 f &= \frac{3600gc_{pm}}{\xi_{u,c} H_u \sqrt{2g \frac{c_p}{A} \left(1 - \frac{1}{e}\right) a\eta_p}}.
 \end{aligned}$$

Let us find the minimum of the function from condition

$$\frac{dC_{ya}}{dx} = 0.$$

Assuming that  $\pi = \text{const}$ ;  $M_u = \text{const}$ ;  $T_u = \text{const}$ ;  $\eta_p = \text{const}$  and  $\eta_c = \text{const}$ , after a series of conversions we obtain

$$\begin{aligned}
 \left(\frac{T_3^0}{T_u}\right)_{\text{opt}} &= 2M_u \sqrt{\frac{\frac{e}{\eta_c} \left(\frac{1}{a\eta_p} - 1\right) + \left(\frac{1}{\eta_c} - 1\right)}{5 \left(1 - \frac{1}{e}\right) a\eta_p}} + \\
 &+ \left[ \frac{e}{\eta_c} \left(\frac{2}{a\eta_p} - 1\right) + \left(\frac{1}{\eta_c} - 1\right) \right]. \quad (9.39)
 \end{aligned}$$

From formula (9.39) it follows that the higher the economic value of the gas temperature in front of the turbine, the greater the  $M_u$  number of flight, the greater the air compression ratio and the lower the efficiency of expanding and efficiency of compression.

Let us examine a particular case.

#### *Operation of a TRD on a Test Stand ( $V = 0$ )*

In this case formula (9.39) takes the following form:

$$\left(\frac{T_3^0}{T_u}\right)_{\text{opt}} = \frac{e}{\eta_c} \left(\frac{2}{a\eta_p} - 1\right) + \left(\frac{1}{\eta_c} - 1\right). \quad (9.40)$$

Having substituted (9.40) into equation for  $C_{ya}$  (9.38), we obtain after simplifications

$$C_{ya(\min)} = \frac{3600c_{pm}}{\xi_{v,c}H_u} \sqrt{\frac{2g}{c_p/A} T_0} \frac{\sqrt{\frac{e}{\eta_c} \left(\frac{1}{a\eta_p} - 1\right) + \left(\frac{1}{\eta_c} - 1\right)}}{\sqrt{\left(1 - \frac{1}{e}\right)a\eta_p}}. \quad (9.41)$$

Let us now find the value of the optimum economic compression ratio at which the minimum specific fuel consumption has the least value - "minimum-minimum" of the specific fuel consumption ( $C_{ya(\min)}$ ).

For this let us investigate the function (9.41) at minimum.

From condition  $\frac{d(C_{ya(\min)})}{d\epsilon_{yk}} = 0$  we find after conversions

$$\epsilon_{yk(\text{opt})} = 1 + \sqrt{\frac{1 - a\eta_p\eta_c}{1 - a\eta_p}}. \quad (9.42)$$

Thus, the economic compression ratio at which the specific fuel consumption reaches an absolute minimum depends only on the efficiency of expansion and compression.

Let us examine the numerical example.

Let us assume that given is:  $T_0 = 288^\circ\text{K}$ ;  $a\eta_p = 0.94$ ;  $\eta_c = 0.85$ ;  $\xi_{v,c} = 0.97$ ;  $H_u = 10250$  kcal/kg.

Further according to equation (9.42) we find  $\epsilon_{yk(\text{opt})} = 2.83$ ;  $\pi_{yk(\text{opt})} = 38$  and  $T_2^* = 910^\circ\text{K}$ . Then according to equation (9.40) we determine  $T_{3(\text{opt})}^* = 1135^\circ\text{K}$ . According to found values of  $T_3^*$  and  $T_2^*$  we find  $c_{pm} = 0.29$  kcal/(kg·deg). Finally, with the help of equation (9.41) let us determine  $C_{ya(\min)} = 0.62$  kg/(kgf·h). In this case  $R_{ya} = 26$  kgf/(kg/s). Calculations show that with further improvement of gas-air channel of the TRD  $C_{ya(\min)} = 0.56-0.58$  kg/(kgf·h) can be obtained.

Figure 9.21 gives dependence  $C_{T,2} = f(T_2^0)$  for different  $\pi = \text{const}$ . There the envelope of these curves are drawn, which fixes: the absolute minimum of specific fuel consumption of the TRD and also optimum values of the economic gas temperature and economic compression ratio.

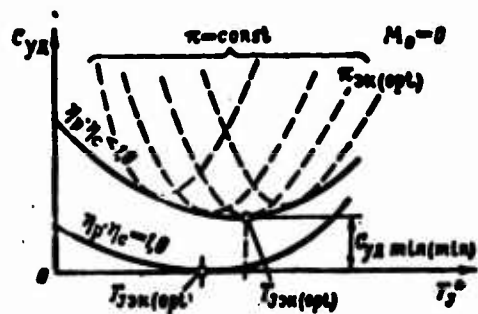


Fig. 9.21. Determination of the concept of minimum possible specific fuel consumption.

## CHAPTER 10

### THERMODYNAMIC PRINCIPLES OF THE CONTROL OF TURBOJET ENGINES

#### 10.1. Concept Operational Characteristics of Aircraft Engines

Operational characteristics of aircraft engines (including gas-turbine) are called dependences which show the effect of conditions of operation on the effectiveness of the engine and its main characteristics - thrust, power, specific and hourly fuel consumption.

These conditions of operation include: state of external atmosphere (pressure, temperature, humidity of the air), flight parameters (altitude and speed of movement of the aircraft), program of control of the engine (determining selected regularity of the change in controllable variables), peculiarity of operation of the engine on the aircraft (system inlet and exit aircraft channels).

Operating conditions determine the *regime of operation* of the engine. The latter is estimated by regime parameters, to which refer such "strictly engine" parameters, as, for instance the number of revolutions of the engine, the position of the regulator of the critical (exhaust) section of the exhaust nozzle and others, and also the above parameters of "*external*" effect on the engine (flight conditions, state of external atmosphere).

The effectiveness of the engine is determined not only by its basic "exhaust" indices (thrust, power, specific fuel consumption), but also by such most important operational properties, as, for

Instance: by the tendency toward unstable operation, the level of noise produced by the engine, level of reliability and service life of the engine.

Thus, the operational characteristics of aircraft gas-turbine engines show the regularities of the change in parameters of effectiveness of the engine from its regime parameters, which considering the variety of operating conditions.

It is necessary to keep in mind that conditions of operation, especially with prolonged operation, have considerable effect on the reliability of the engine, causing mechanical disturbances and deformations of the gas-air channel of the engine and of its elements (warping, dents, corrosion, erosion of blades, carbon formation, ice deposit, growth of radial clearances, wear of labyrinths, misalignment separate subassemblies). This leads to a drop in the efficiency of these subassemblies, conditioning the worsening of basic indices of the engine, disturbs the thermal engine operating regime (overheating of the hot part is possible), and causes unstable operation of the compressor.

#### 10.1.1. Forms of Operational Characteristics

Operational characteristics of aircraft gas-turbine engines are subdivided into *throttle*, *high-speed*, *altitude* and also *special*.

*Throttle characteristics* are dependences of basic indices of operation of the engine (thrust and specific fuel consumption) on its regime parameters (for example, on the number of revolutions) on regimes of "partial" load, with (throttling) of fuel feed into the combustion chambers. The greater the degree of throttling of the fuel feed, the less the thrust of the engine; however, specific regularities of the change in parameters of the engine and also its economy can be different depending on the assigned program of control.

*High-speed and altitude characteristics* of the engine show the change in basic indices of its operation depending on conditions (of velocity and altitude) of flight at the assigned program of control of the engine.

Sometimes the altitude-high-speed characteristics of the engine are depicted in accordance with the specific profile of flight of the aircraft. Such characteristics are very clear since they show in what way in flight the concordance of required thrusts (power) of the aircraft and available thrusts (power) of the engine is produced.

Throttle and high-altitude-high-speed characteristics of the engine must consider the possible physical limitations appearing with the operation of the engine and the specific range of their operation. These include limitations conditioned by the following:

- 1) strength of the parts (subassemblies);
- 2) appearance of maximum permissible gas temperatures;
- 3) appearance of unstable regime of operation;
- 4) appearance of regimes of gas-dynamic choking of the gas-air channel;
- 5) appearance of regime of auto-oscillations and vibrations.

#### 10.1.2. Methods of Obtaining Characteristics of the Engine

Characteristics of the engine can be obtained experimentally by means of tests of the engine on a test stand or in flight on the so-called flying laboratories. They can also be obtained analytically with a high degree of authenticity. To obtain sufficiently accurate characteristics of the engine by calculation, it is necessary to have model or specific characteristics of separate *subassemblies* or semi-empirical dependences, which with acceptable accuracy reproduce such characteristics.

The usual test stands, which are found at aircraft serial or repair plants, allow removing the earthly "test stand" characteristics of the engine and reduce them to the so-called standard atmospheric conditions ( $p_0 = 760$  mm Hg and  $T_0 = 288^\circ\text{K}$  at  $V = 0$  and  $H = 0$ ).

To obtain altitude-high-speed characteristics there must be special test stands, which allow the simulating altitude-high-speed conditions of flight, in other words, to reproduce at the entrance into the engine as well as at the exit from it the necessary values of pressure and of temperatures of the gas. Such special test stands with altitude chambers are very complex, bulky and expensive devices. To operate them, expenditures of enormous energy power are required. The creation of such test stands are of interest only to special scientific-research and designer organizations.

The most reliable method of obtaining flight characteristics of an engine is the use of the flying laboratory. An example of such a laboratory is the English aircraft Avro "Ashton," created on the basis of the bomber Avro "Vulcan" and equipped with four Rolls-Royce "Avon" TRD. As a flying laboratory in the USA it is planned to use the supersonic experimental bomber Boeing [sic] "Valkerie" B-70, designed for flights with an  $M_0 = 3.0$  number.

Disadvantages of flying laboratories are their complexity and high costs and also limitedness of range of high-altitude-high-speed tests (at  $M_0$  and  $H$  numbers), which is determined by flying and technical data of the aircraft laboratory. It is obvious that the new engine cannot be tested at speeds and altitudes of flight which are inaccessible for the aircraft laboratory.

As regards to the analytical method of obtaining characteristics of the engine, at present it has reached a high degree of perfection, especially in connection with the advent of electronic computers. Characteristics of engines obtained in such a way give a small degree of error, as a rule, not exceeding 2-3%.

#### 10.1.3. Control Elements and Controllable Variables of the Gas Turbine

Any gas-turbine engine has regulating elements with the help of which it is possible to assign and change the process of operation of the engine. Control elements of the aircraft gas turbine include,

first of all, a fuel feed regulator, usually interlinked with the automatic regulator of the number of revolutions. The regulator of revolutions is intended for maintaining the constant number of revolutions of the engine at a fixed position of the control lever of the engine [RUD] (PYD). Acting with the help of the RUD on the regulator of the fuel feed, it is possible to change the flow of fuel in the combustion chamber and, consequently, change the regime of operation of the engine determined by its number of revolutions. Thus, the *control element* (regulator of fuel feed) through the *regulating factor* (flow of fuel per second of engine) acts on the *regime parameter* of the engine (number of revolutions).

The basic parameters of the TRD - its thrust and specific fuel flow (at assigned values of efficiency of elements of the engine, and also the speed and altitude of flight) - are functions of two parameters of the working process:  $\pi_n^*$  and  $T_3^*$ . Thus, to control the engine on the test stand and in flight, there must be the two named independent control parameters.

One should keep in mind that immediate control  $\pi_n^*$  is inconvenient, complicates the design of the engine, and requires the introduction of special regulators. It is substituted by the control of numbers of revolutions, which, as is known, furthermore, determine the strength of the elements of the turbocompressor. With an increase in the r/min of the TRD the rate of air flow increases, and  $\pi_n^*$  also increases.

Thus, the control regime parameters of the TRD are  $n$  and  $T_3^*$ .

If the TRD has invariable geometry, the change in fuel feed simultaneously changes the parameters  $n$  and  $T_3^*$  according to the scheme

$$G_f \rightarrow n \rightarrow T_3^*$$

When the engine (TRD) has two control elements independent from each other (for example, a regulator of fuel feed and regulator of exhaust nozzle), and, consequently, two regulating factors (fuel

consumption per second  $G_T$  and critical or exhaust section of the exhaust nozzle  $f_5$ ), the number of regime parameters independently controllable from each other is also equal of two (number of revolutions of the engine  $n$  and temperature of the gas in front of the turbine  $T_3^*$ ). In this case control of the TRD is produced according to the scheme

$$G_T \rightarrow n \text{ and } f_5 \rightarrow T_3^*$$

Generally, the number of independently controllable variables is always equal to the number of controllable factors.

The more complex the aircraft gas turbine, the greater the number of its regulators. Additional regulators of the TRD [TRDF] (ТРДФ) can be these regulators: angles of exit of the nozzle box assembly of the turbine  $\alpha_1$ ; angles of incidence of guide vanes of the compressor  $\varphi_{\text{в.к}}$ ; fuel feed into the afterburner  $G_{\text{т.д}}$  etc. The corresponding regime parameters can be:

$$n^*, G_{\text{т.д}}, T_3^*$$

## 10.2. Control Programs of the Engine

The control program of a gas-turbine engine should be understood as the regularity of the change in processes of operation of the engine and, consequently, parameters of the working process determined by the position of control elements. This regularity of the change in parameters of the engine pursues the goal of providing the most advantageous flow of characteristics of the engine.

Examples of programs of control are programs of control for maximum thrust (power) of the engine, better economy of the engine, conservation of complete similarity of operation of the turbo-compressor minimum sound level of the engine at the assigned thrust, etc.

The simplest programs of control of the engine with respect to speed and altitude of the flight are programs providing the invariability of the flow part of the engine. Such programs are called programs of control with invariable geometry of the engine.

#### 10.2.1. Program of Control of the TFD for Maximum Thrust

One of the most widespread programs is the program of control for maximum thrust. This program automatically provides the obtaining at all speeds and altitudes of flight of maximum thrust. For its fulfillment the observance of the following conditions is necessary:

1) maintaining the maximum and constant number of revolutions of the engine, i.e.,

$$n = n_{\max} = \text{const};$$

2) maintaining the maximum and fixed temperature in front of the turbine, i.e.,

$$T_3^* = T_{3(\max)}^* = \text{const}.$$

Actually, the fulfillment of condition 1 provides the obtaining of the maximum rate of air flow  $G_{\text{a}}$  and maximum compression ratio (see further Fig. 11.6); the observance of condition 2 provides together with the fulfillment of condition  $\pi_k^* = \pi_{k(\max)}^*$  the obtaining of the maximum specific thrust (see Fig. 9.9).

Thus, the product

$$R_{y2(\max)} G_{\max} = R_{\max}$$

appears maximum at any assigned values  $H$  and  $V$ .

Maintaining the maximum number of revolutions is achieved with the help, for example, of a centrifugal regulator of revolutions (of the Watt type of regulator) interlinked with automatic unit of fuel feed.

Maintaining the maximum temperature of the gas  $T_3^*$  is a complex problem. It can be provided by direct and indirect means.

For direct control  $T_3^* = \text{const}$  it is necessary to transmit a pulse obtained from thermocouples installed at the entrance into the nozzle box assembly of the turbine into automatic fuel unit for the limitation or increase in fuel feed supply into the combustion chamber. Such automatic units are installed on a number of Soviet and foreign engines.

In a number of cases the condition of conservation  $T_3^* = \text{const}$  is observed quite accurately automatically. Let us assume that at all flight speeds the pressure difference in the jet nozzle is supercritical, i.e.,  $q(\lambda_5) = 1.0$ . Then, on the basis of expression (7.14), with an increase in the flight speed the drop in pressures in the turbine  $\pi_T^*$  likewise remains constant.

Consequently, from equality

$$L_T = L_u \text{ or } T_3^* = \frac{L_u}{118 \pi_T^*}$$

we find

$$T_3^* \sim L_u$$

If  $L_u = \text{const}$  when  $n = \text{const}$  and  $T_3^* = \text{var}$ , then  $T_3^* = \text{const}$ .

#### 10.2.2. Program of Control of the Turbojet Engine with Invariable Geometry

With invariable geometry ( $f_s = \text{const}$ ;  $\alpha_{c,2} = \text{const}$ ;  $\varphi_{n,2} = \text{const}$ ) the engine has a single automatic unit of fuel feed, interlinked either with the regulator of the number of revolutions or with the regulator of gas temperature in front of the turbine. In this case the possible programs of control with respect to the speed and altitude of flight have the form:

1)  $n = \text{const}$  ( $T_3^* = \text{var}$ ) and 2)  $T_3^* = \text{const}$  ( $n = \text{var}$ ).

When  $q(\lambda_3) = 1.0$  (i.e.,  $\pi_1^* = \text{const}$ ) and  $L_K = \text{const}$  when  $n = \text{const}$ , with a change in speed and altitude of flight we have  $T_3^* = \text{const}$ , and, thus control programs 1 and 2 completely coincide with control program for maximum thrust.

If, however, when  $n = \text{const}$  we have  $T_3^* = \text{var}$ , then, in considering the need of the limitation of temperature  $T_3^*$  by its maximum permissible value, it is easy to draw the conclusions about the fact that at all speeds and altitudes of flight, where  $T_3^* < T_{3(\text{max})}^*$ , the thrust of the TRD will be lower than that in the case of the control program for maximum thrust.

#### 10.2.3. Control Program of the Turbojet Engine for the Greatest Economy

The control program of the TRD for the greatest economy is used for example, in the case of flight range. It consists in the providing of minimum specific fuel consumption at the assigned magnitude of throttled thrust at a cruising regime of flight.

In such a case when the TRD has fixed geometry, the fixed value of thrust with respect to the throttle characteristic corresponds to the single value  $C_{yD}$ . In the presence of the controllable exhaust nozzle, for condition  $R = \text{const}$  it is possible to find the combination of values  $T_3^*$  and  $n$  (or  $T_3^*$  and  $\pi_K^*$ ) at which  $C_{yD} = C_{yD(\text{min})}$ .

#### 10.2.4. Control Program of the Turbojet Engine for Complete Similarity of the Regime of Operation of the Turbocompressor

The above control programs  $n = \text{const}$  have an important general feature - with the change in speed and altitude of flight the regime point of the compressor is moved into the field of the characteristic of the latter. The more the change in  $T_K^*$ , the more change in the given revolutions:

$$n_{sp} = n \sqrt{\frac{288}{T_s^*}}$$

and the greater the danger of the drop in efficiency and productivity of the compressor, appearance of undesirable physical limitations of its operation - separations of flow, surging, local flow chokings; in short, the effectiveness of the compressor can considerably become worse.

The tendency to provide the best and fixed conditions of operation of the compressor and also turbines led to the development of the program of control for complete similarity of the regime of operation of the turbocompressor. Conditions of the realization of such program are:

- 1) constancy of reduced revolutions of the turbocompressor

$$n_{sp} = n \sqrt{\frac{288}{T_s^*}} = \text{const, and } n \sim \sqrt{T_s^*}:$$

- 2) constancy of reduced gas temperature in front of the turbine

$$T_{s,p}^* = T_s^* \frac{288}{T_s^*} = \text{const, or } T_s^* \sim T_s^*.$$

With fixed geometry of the TRD the observance of conditions 1 and 2 automatically provides complete similarity of the regime of operation of the compressor.

Actually, from equality

$$L_1 = L_2$$

or

$$1187 \rho_1^* \eta_1^* = 102,5 T_s^* (\pi_s^{*0,288} - 1) \frac{1}{\eta_2^*},$$

it follows that when  $\frac{T_s^*}{T_s^*} = \text{const}$  we have  $\pi_s^* = \text{const}$ , setting

$$\pi_1^* = \text{const [for } q(\lambda_s) = 1], \eta_1^* = \text{const and } \eta_2^* = \text{const.}$$

The observance of relations  $n_{sp} = \text{const}$  and  $\pi_r^* = \text{const}$  can be examined as the fulfillment of conditions of complete gas-dynamic similarity of the compressor.

The observance of conditions 1 and 2 also automatically provides similarity of the regime of operation of the turbine. Actually, from relation  $L_r = 1187 \pi_r^* \eta_r^*$  when  $\pi_r^* = \text{const}$  (for  $q(\lambda_s) = 1$ ) it follows that

$$\frac{L_r}{T_3^*} = \text{const.} \quad (a)$$

Comparing conditions 1 and 2, we also find that

$$\frac{n}{\sqrt{T_3^*}} = \text{const.} \quad (b)$$

However, equalities (a) and (b) can be examined as conditions of providing the similarity of the process of operation of the turbine.

The control program for complete similarity, guaranteeing the optimum conditions of work and operation for the turbocompressor of the TRD, considerably affects the regularities of the change in thrust and specific fuel consumption of the engine with respect to speed and altitude of flight.

For realization of the considered program of control of the TRD (when  $q(\lambda_s) = 1$ ) it is sufficient to provide fuel feed into the combustion chamber according to the law

$$G_{r,sp} = \text{const, and } G_r \sim p_3^* \sqrt{T_3^*}$$

at which the constancy of reduced temperature  $T_{3,sp}$  is observed, or

$$T_3 \sim T_3^*$$

In this case the constancy of reduced revolutions of the rotor of the TRD will be automatically observed.

### 10.3. Joint Work of Turbine and of Compressor in System TRD

Characteristics of the TRD are to a certain extent determined by the joint operation of basic elements of the engine, in the first place, the compressor and turbine.

With a change in the regime of operation of the engine the compressor and turbine operation *jointly*, their parameters cannot change randomly. The joint operation of the compressor and turbines is determined by the fact that: air outgoing from the compressor enters into the turbine; the power necessary for rotation of the compressor is generated by the turbine; numbers of revolutions of the compressor and turbine are identical (between them there is a rigid kinematic connection).

The basic equations of the joint operation of the compressor and turbine of the TRD pertain to the four equations enumerated below.

#### 1. Equation of flow, or equation of material balance

This equation establishes the dependence between flow rates of air per second at the entrance into the compressor and the gas through the turbine.

It has the form

$$G_r = G_a - G_{er} + G_f, \quad (10.1)$$

where  $G_a$  — flow of air at the entrance into the compressor;  $G_r$  — flow of gas through the turbine;  $G_{er}$  — quantity of air bled from the compressor: for cooling turbines, for aircraft needs (drive of aircraft units, blow away of the boundary layer, etc.), for the antisurge bypass system;  $G_f$  — fuel expense in the combustion chamber.

Expression (10.1) can be written thus:

$$G_r = G_o \left[ 1 + \frac{G_r - G_{or}}{G_o} \right] = \beta G_o \quad (10.2)$$

where

$$\beta = \frac{G_r}{G_o} \cong 1.$$

2. Equation the ballance of power (equation of energy balance)

We have

$$N_r = \frac{N_g}{\eta_m}, \quad (10.3)$$

where  $\eta_m$  -- mechanical efficiency, considering friction in bearings of the turbocompressor, and also expenditures of power for driving the units (fuel pump, counter of revolutions, generator, oil pumps and others). Usually  $\eta_m = 0.99 - 0.995$ .

Let us write down expression (10.3) in terms of work of the compressor and turbine:

$$L_r G_r = \frac{L_g G_o}{\eta_m},$$

or

$$L_r = \frac{L_g}{\beta \eta_m}. \quad (10.4)$$

Equation (10.4) is called the equation of balance of the works.

3. Equation of equality of numbers of revolutions

In turbocompressors of contemporary TRD

$$n_r = n_k = n. \quad 1$$

---

<sup>1</sup>There are schemes of turbofan engines in which  $n_r \neq n_o$ .

4. Correlation between compression ratio of the compressor and expansion ratio of the turbine

$$\pi_T^* = \frac{\pi_{amb} \pi_{c,c}^* \pi_{e,e}^*}{\pi_{p,c(0)}}$$

where

$$\begin{aligned} \pi_{amb} &= \frac{p_1^*}{p_a}; & \pi_{c,c}^* &= \frac{p_2^*}{p_1^*}; \\ \pi_{e,e}^* &= \frac{p_3^*}{p_2^*}; & \pi_{p,c(0)} &= \frac{p_4^*}{p_a}. \end{aligned}$$

10.3.1. Equation of the Line of Working Regime

Using equations (10.1) and (10.4) - joint work of the compressor and turbine, it is possible to derive the generalized equation of the line of working regimes of the TRD in the form of the functional dependence

$$\pi_T^* = f(q(\lambda))$$

and apply it to the characteristic of the compressor of the TRD.

Let us write down the relation between flows of air and gas for the section at the entrance into the compressor (1-1) and critical section of the nozzle assembly box of the turbine (c.a-c.a).

We have

$$pG_1 = G_{c.a.}$$

or

$$m_a \frac{p_1^*}{\sqrt{T_1^*}} f_1(q(\lambda_1)) \beta = m_r \frac{p_{c.a}^*}{\sqrt{T_{c.a}^*}} f_{c.a.}(q(\lambda_{c.a})); \quad (10.5)$$

Noting that  $T_1^* = T_a^*$ ;  $T_{c.a}^* = T_s^*$ ;  $p_{c.a}^* = p_2^* \pi_{c,c}^* \pi_{e,e}^*$ , we reduce equation (10.5) to the form

$$\pi_k^* = \frac{p_2^*}{p_1^*} = Aq(\lambda_1) \sqrt{\frac{T_3^*}{T_u^*}} \beta, \quad (10.6)$$

where

$$A = \frac{f_1 \frac{m_a}{m_r}}{f_{c,a} q(\lambda_{c,a}) \sigma_{c,a}^* \sigma_{k,c}^*} = \text{const.}$$

If we take  $m_a/m_r = 1,0$ ;  $q(\lambda_{c,a}) = 1$ ;  $\sigma_{c,a}^* = 1,0$  and  $\sigma_{k,c}^* = 1,0$ , then  $A = f_1/f_{c,a}$ .

Equation (10.6) is the transformed equation of flow. On the characteristic of the compressor in coordinates  $\pi_k^*$  and  $q(\lambda_1)$  this equation for different values  $\Delta = \frac{T_3^*}{T_H^*} = \text{const}$  is depicted as a pencil of straight lines. The greater  $\Delta$  (i.e., the more  $T_3^*$  and the less  $T_H^*$ ), and the more the slope of the straight line  $\Delta = \text{const}$  (Fig. 10.1).

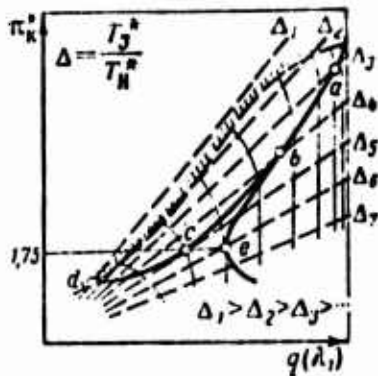


Fig. 10.1. Family of lines  $\Delta = \text{const}$  on the characteristic of the compressor.

Let us now transform the equation of balance of works (10.4).

We have

$$\beta \eta_m 118 T_3^* c_p^* \eta_r^* = 102,5 T_u^* (\sigma_k^* - 1) \frac{1}{\eta_k^*};$$

whence we find

$$\frac{T_3^*}{T_u^*} = \frac{102,5}{118} \frac{(\sigma_k^* - 1)}{\beta \sigma_{c,a}^* \eta_r^* \eta_m^* \eta_k^*}. \quad (10.7)$$

Let us now substitute the obtained value  $T_3/T_2^*$  into the equation (10.6).

Then after simple conversions we obtain

$$\frac{\pi_k^*}{\sqrt{\frac{\pi_k^{*0.286}-1}{\eta_k^*}}} = cq(\lambda_1) \sqrt{\beta}, \quad (10.8)$$

where

$$c = \frac{(m_0/m_1)(f_1/f_{c.a})}{q(\lambda_{c.a}) \sigma_{c.a}^* \sigma_{k.c}^* \sqrt{\frac{118}{102.5} \epsilon_r^* \eta_r^* \eta_m^*}}.$$

Expression (10.8) is called the equation of the line of working regimes.

Let  $\beta = \text{const}$ ;  $\eta_k^* = \text{const}$ ;  $\eta_r^* = \text{const}$  and  $\pi_r^* = \text{const}$  (i.e.,  $\lambda_2 = 1.0$ ).

Then the equation of the line of operating regimes (10.8) will be depicted on the characteristic of the compressor in the form of a parabolical curve *abe* (see Fig. 10.1) with the inflection point at  $\pi_k^* = 1.75^1$ .

---

<sup>1</sup>We have

$$\frac{\pi_k^*}{\sqrt{\frac{\pi_k^{*0.286}-1}{\eta_k^*}}} = Bq(\lambda_1).$$

We find  $\pi_k^* (\text{opt})$  from condition  $\frac{dq(\lambda_1)}{d\pi_k^*} = 0$ ; then

$$\sqrt{\frac{\pi_k^{*0.286}-1}{\eta_k^*}} - \frac{0.286 \pi_k^{*0.286}}{2 \sqrt{\frac{\pi_k^{*0.286}-1}{\eta_k^*}}} = 0,$$

and further

$$2\pi_k^{*0.286} - 2 = 0.286\pi_k^{*0.286},$$

whence

$$\pi_k^* = \left(\frac{2}{1.714}\right)^{3.5} \approx 1.75.$$

Along this curve the gas temperature in front of the turbine  $T_3^*$  continuously drops. This is found in complete correspondence with equation (10.7) at conditions stipulated above ( $\beta=1.0$ ;  $\pi_4^* = \text{const}$ ;  $\eta_4^* = \text{const}$ ;  $\eta_5^* = \text{const}$ ).

If, however, we take into account the practical regularity of the change  $\pi_4^*$  (see further Fig. 11.2), and also the drop in  $\eta_4^*$  and  $\eta_5^*$  (see further Fig. 11.1) in the area of small numbers of revolutions, then the real line of the operating regimes will be depicted by the curve *acd* (see Fig. 10.1). Along this line the gas temperature  $T_3^*$  in the beginning drops, reaches a minimum, and then continuously increases.

#### 10.3.1.1. Effect of Adjustment of the Jet Nozzle on the Position of the Line of Operating Regimes.

The line of operating regimes *acd* (see Fig. 10.1) is conditionally designated as  $f_5 = \text{const}$ , since it is plotted on the assumption that the exhaust (critical) section of the jet nozzle is not regulated.

Each value of  $f_5 = \text{const}$  corresponds to the single line of the operating regimes. With "opening" of the jet nozzle (i.e., with an increase in  $f_5$ ) the line of the operating regimes is displaced into the area of reduced values  $\pi_4^*$  and  $T_3^*$ . With the "closing" of the jet nozzle, conversely, the line of operating regimes shifts into the area of raised values  $\pi_4^*$  and  $T_3^*$ .

Figure 10.2 gives a family of lines of operating regimes  $f_5 = \text{const}$ .

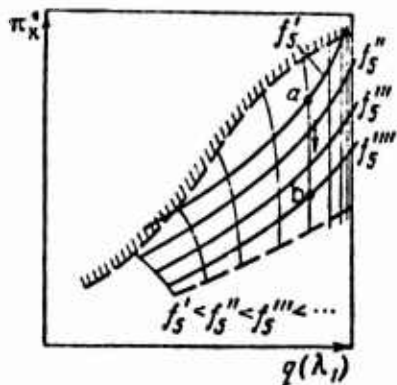


Fig. 10.2. Family of lines of operating regimes  $f_5 = \text{const}$ .

10.3.1.2. Effect of Adjustment of the Jet Nozzle on the Regime of Operation of the Turbocompressor when  $n_{np} = \text{const}$ .

With an increase in the exhaust section of the jet nozzle the regime point of the turbocompressor [TK] (TK) is moved along the pressure characteristic of the compressor ( $n_{np} = \text{const}$ ) into the area of reduced values  $\pi_4^*$  and  $T_3^*$ ; with "closing" of the jet nozzle, conversely, the regime of operation of the TK is displaced in the area of raised values  $\pi_4^*$  and  $T_3^*$ .

Actually, with the "opening" of the jet nozzle, i.e., with an increase in its exhaust (critical) section, instantly the counter-pressure behind the turbine<sup>1</sup> and, consequently, the pressure difference on the turbine increases. Thus, the work of the turbine at the assigned number of revolutions becomes more than the work of the compressor:

$$L_T > L_K$$

and, consequently, the number of revolutions of the turbocompressor tends to grow. However, since the regulator of revolutions maintains  $n = \text{const}$ , then it decreases the fuel feed in the combustion chamber, as a result of which the gas temperature in front of the turbine will decrease. Simultaneously - for concordance of rates of air flow through the compressor and gas flow through the turbine - the compression ratio of the compressor will be lowered. Thus, the regime point of the compressor will be displaced along the line  $n_{np} = \text{const}$  of the compressor from position *a* to a position *b* (see Fig. 10.2).

10.3.1.3. Effect of Adjustment of the Nozzle Box Assembly of the Turbine for the Regime of Operation of the Turbocompressor at  $n_{np} = \text{const}$ .

Let us examine how the adjustment of the critical section of the nozzle box assembly of the turbine affects the regime of operation of the turbocompressor at fixed revolutions of the turbocompressor.

$$\pi_4^* \frac{n+1}{2n} = \text{const} \cdot \frac{f_{sg}(\lambda_g)}{f_{caq}(\lambda_{ca})} \sim f_s \text{ [see equation (7.14)].}$$

Adjustment of the critical section of the nozzle box assembly is carried out by means of synchronous turning of blades of the nozzle box assembly by a special mechanism; the connection between the angle of exit of the nozzle box assembly  $\alpha_1$  and its critical section has the form (Fig. 10.3).

$$f_{c.a(np)} = tb \sin \alpha_1,$$

where  $t$  - blade pitch of the c.a;  $b$  - height of the blades of the c.a.

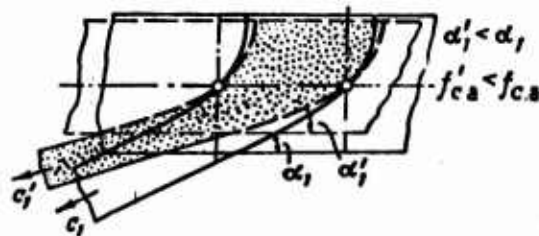


Fig. 10.3. Diagram of an adjustable nozzle box assembly of a turbine.

Thus, with a decrease in  $\alpha_1$  magnitude  $f_{np}$  is decreased; with an increase in  $\alpha_1$  magnitude  $f$  increases.

From the equation of flow (7.14) it follows that an increase in  $f_{c.a}$  decreases the drop in pressures on the turbine  $\pi_t^*$ . Actually, the larger angle  $\alpha_1$ , the less the circumferential component of velocity of outflow from the nozzle box assembly of the turbine  $c_{1u} = c_1 \cos \alpha_1$  and the less the work of the turbine stage

$$L_u = \frac{a}{g} (c_1 \cos \alpha_1 \pm c_2 \cos \alpha_2).$$

Consequently, at the same value  $T_3^*$  the pressure differential  $\pi_t^*$  will be less.

However, with a drop in  $\pi_t^*$  for the conservation of the balanced regime of revolutions the regulator of fuel feed will increase the fuel feed into the combustion chamber. Ultimately  $T_3^*$  increases. This will lead, in turn, to a growth in  $\pi_u^*$  and to the displacement

of the regime point of the TK into the region of raised values  $T_3^*$  and  $\pi_k^*$ .

Thus, the "opening" of the jet nozzle and increase in critical section of the nozzle box assembly of the turbine when  $n_{\text{opt}} = \text{const}$  have an opposite action on the change in  $\pi_k^*$  and  $T_3^*$ .

Figure 10.4 gives a family of lines of operating regimes  $f_{c.a} = \text{const}$ . With an increase in the critical section of the nozzle box assembly of the turbine ( $df_{c.a} > 0$ ), the line of the operating regimes is displaced into the region of raised values  $\pi_k^*$  and  $T_3^*$ .

The method described influences of the change in the critical section of the c.a of the turbine on parameters of the engine are frequently used at aircraft plants in process of finishing of experimental engines.

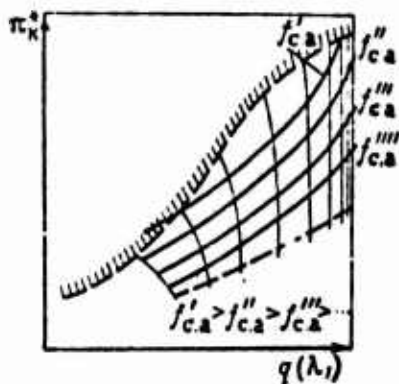


Fig. 10.4. Family of lines of operating regimes  $f_{c.a} = \text{const}$ .

As regards the use in operation of adjustable nozzle box assemblies (r.s.a.), the latter have not become widespread because of organic defects inherent in them: high gas leakage in the radial clearance and difficulties in providing reliable operation of the rotary mechanism at high gas temperatures.

10.3.2. Peculiarities of Passage of Lines of Operating Regimes of High-Pressure and Low-Pressure Compressors of Single-Shaft and Double-Shaft of the TRD (Fig. 10.5)

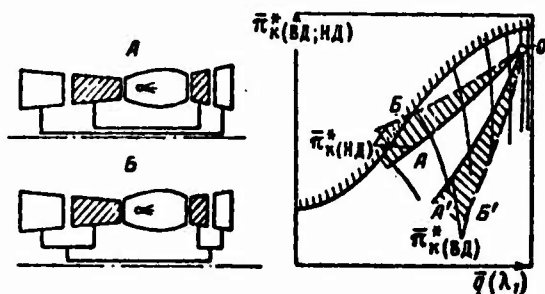


Fig. 10.5. Comparison of lines of operating regimes of single-shaft and double-shaft TRD.

Let us give a comparison of lines of operating regimes of turbo-compressors of high and low pressures in the system of double-shaft TRD (with free cascades) and in the system single-shaft TRD (with these rigidly connected cascades).

Let us assume that in the original, calculated regime, parameters and exhaust indices of single-shaft and double-shaft TRD are identical. Consequently, design conditions of the operation of VD and ND cascades are depicted on characteristics of corresponding compressors, which are plotted in relative parameters of single-shaft and double-shaft TRD, by the same point O (see Fig. 10.5).

With choking of fuel feed in combustion chambers, the line of operating conditions of the ND compressor of the single-shaft TRD (OB) will be *gently sloping*, approaching the border of surging; the latter is explained by the growth in angles of attack on blades of first stages of the ND compressor. In contrast with this, the line of operating regimes of the VD compressor (OB') of the single-shaft TRD will be *steep*, rushing at low revolutions into the region of regimes of "choking."

The line of operating regimes of the ND free cascade of the double-shaft TRD (OA) is considerably steeper than for the connected ND cascade (OB), not intersecting the border of surging. The line of operating regimes of the VD free cascade (OA'), conversely, is

more gently sloping than in the connected VD cascade (OB'), so that regimes of "choking" will be automatically removed.

It is possible to explain this regularity in the following manner. Let us assume that at a certain reduced number of revolutions  $n_1$  of a single-shaft TRD the gas flow is equal to  $G_1$ . Mentally let us disengage at this number of revolutions VD and ND cascades. Then the single-shaft TRD will become a double-shaft TRD.

As a result of the approached unbalance of works of compressors and turbines,

$$\frac{L_{\kappa(\text{ND})}}{L_{\kappa(\text{VD})}} > \frac{L_{\tau(\text{ND})}}{L_{\tau(\text{VD})}},$$

the number of revolutions of free cascade ND will drop, and the number of revolutions of the VD free will increase (in comparison with the number of revolutions of the turbocompressor of the single-shaft TRD). Correspondingly, the ratio of the compression of the ND compressor will drop, and the compression ratio of the VD compressor will increase. The total compression ratio, and also the flow of air through the TRD in this case will change little. The distribution of axial velocities along the compressor will also change little.

It is easy to conclude from an examination of Fig. 10.5 that the drop in  $\pi_{\kappa(\text{ND})}^*$  at  $G = \text{const}$  denotes the deviation in the line of the operating regimes in the direction of the leading of the ND compressor out of surging; an increase in  $\pi_{\kappa(\text{VD})}^*$  when  $G = \text{const}$  leads to a deviation in the line of the operating regimes in the direction of the leading of the VD compressor out of regimes of "choking."

Physically the removal of surging of the ND compressor with choking of the double-shaft TRD according to the number of revolutions is explained in that a decrease in circumferential velocity of the blades at practically the same magnitude of the axial velocity leads to a lowering of angles of attack of the rotor blades; as a result of this the compression ratio of the cascade drops, and the danger of flow separation from the back of blades of the compressor is decreased.

Similarly, the leading of the VD compressor from the zone of "choking" is physically explained by the fact that an increase in circumferential velocity of the blades at practically the same magnitude of axial velocity leads to an increase in angles of attack of the rotor blades; as a result of this compression ratio of the cascade increases, and stages of the VD compressor are led out of the regime of "choking." Nevertheless, the line of operating regimes of the ND compressor (OA) is more gently sloping, i.e., with less a stability margin than for the VD compressor (OA').

## CHAPTER 11

### THROTTLE CHARACTERISTICS OF TURBOJET ENGINES

#### 11.1 Concept of Throttle Characteristics of Turbojet Engines

Under conditions of operation aircraft gas-turbine engines produce a major portion of their service life in reduced, or *throttle*, regimes at which the thrust is considerably less than maximum.

In the simplest case when the engine has fixed geometry (constant flow passage sections), the lowering of the thrust is provided by means of a decrease in the number of revolutions. Dependences of thrust and of specific fuel consumption on the number of revolutions of the engine at the assigned program of adjustment are called *characteristics according to the number of revolutions*. These characteristics are usually supplemented by curves of gas temperature behind the turbine. The latter makes it possible to judge the degree of reliability in the operation of the "hot" part of the engine (combustion chamber, turbine and jet nozzle).

Thus, characteristics according to the number of revolutions is given in the form of curves:

$$R=f(n); C_{y_1}=f(n); T_4^*=f(n).$$

When in a definite interval of thrusts the number of revolutions of the engine is maintained constant, the choking of the thrust is carried out by adjustment of passage flow sections of the TRD (jet nozzle, turbine, compressor). In this case the throttle characteristics are depicted in the form of dependences of thrust

and specific fuel consumption on corresponding parameters of control elements of the engine (for example, areas of critical section of the jet nozzle).

Sometimes throttle characteristics are presented in the form of the dependence of specific fuel consumption on the degree of choking of thrust of the engine, i.e.,  $C_{ya}=f(\bar{R})$ , where  $\bar{R}=R/R_{max}$ .

The change in the number of revolutions of the engine occurs by means of the change in fuel feed into the combustion chamber. The latter is carried out with the help of the shifting of the control lever of the engine (RUD), which the pilot or tester controls.

With an increase in fuel feed into the combustion chamber the turbine inlet gas temperature increases; consequently, the power of the turbine increases and becomes the power of the compressor, the regime of operation of which in the first instant remains constant, i.e.,

$$N_T > N_M.$$

The surplus power of the turbine equal to

$$\Delta N = N_T - N_M,$$

is expended for the accelerated rotation of the turbocompressor of the engine, i.e., for an increase in the number of its revolutions. The increase in the number of revolutions ceases when in a certain regime again there is established the equality of power

$$N_T = N_M.$$

If we decrease the fuel feed into the combustion chamber, then the process will be the reverse: now the changed power of the turbine will be less than the power of the compressor, i.e.,

$$N_T < N_M.$$

The appeared unbalance of power is eliminated by means of the

lowering of the number of revolutions of the engine down to its new balanced value, when again equality of powers will be restored.<sup>1</sup>

## 11.2. Throttle Characteristic of the Turbojet Engine with Fixed Geometry

### 11.2.1. Change in Efficiency and Coefficients of Losses of Basic Elements (Subassemblies) of the Turbojet Engine on the Number of Revolutions

As is known the hydraulic and gas-dynamic perfection of elements of the TRD is estimated with the help of the efficiency  $\eta^*$  (compressor, turbine), coefficients of the drop in total pressure  $\sigma^*$  (inlet device, combustion chamber, afterburner, diffuser) and coefficient of velocity  $\phi$  (jet nozzle).

Of all the enumerated efficiency and coefficients of losses, the most important is the change in efficiency of the compressor according to the number of revolutions. In accordance with the mutual disposition of lines of operating conditions and isolines of efficiency on the characteristic of the compressor (see further Fig. 11.17), with throttling of the engine efficiency of the compressor initially increases (up to magnitude 0.84-0.88 in the zone of maximum efficiency), and with further lowering of the number of revolutions the efficiency of the compressor drops (Fig. 11.1). Thus, the efficiency of the compressor, while being considerably less than 1, moreover, very considerably changes with throttling of the engine

Numerous experimental investigations show that the efficiency of the turbine has a steady value over a wide range of numbers of revolutions and drops only in the region of great choking (see Fig. 11.1).

---

<sup>1</sup>Equation of steady movement (rotation) of the turbocompressor has the form

$$J \frac{d\omega}{dt} = M_T - M_K \text{ or } J \frac{dn}{dt} = \frac{6310}{\pi} (N_T - N_K),$$

whence it is clear that the unbalance of power of the turbine and compressor ( $N_T - N_K \neq 0$ ) leads to a change in the number of revolutions of the turbocompressor.

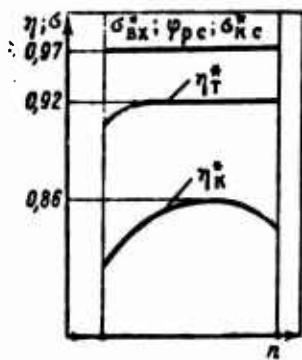


Fig. 11.1. Change in efficiency and coefficients of losses of basic elements of the TRD on the number of revolutions.

As regards coefficients  $\sigma_{ax}^*$ ,  $\sigma_{kc}^*$ ,  $\sigma_{\phi, k}^*$ ,  $\sigma_s^*$ ,  $\varphi_{p.c}$ , with a high degree of accuracy it is possible to assume that in the whole range of operating revolutions they maintain an invariable value, which differs little from unity (see Fig. 11.1).

#### 11.2.2. Change in Gas Pressure in Characteristic Sections of the Gas-Air Channel of the TRD with Throttling of the Engine

With an increase in the number of revolutions of the TRD the work and compression ratio of the compressor continuously increase. This follows from expression

$$L_k = 102,5T_0(\pi_k^{0,286} - 1) \frac{1}{\eta_k^*} \sim n^2.$$

Consequently, the total air pressure behind the compressor  $p_2^*$  continuously increases. The increment in air pressure in the channel of compression is extended on the channel of expansion: the total pressure of the gas in front of the turbine  $p_3^*$ , at the exit from the turbine  $p_4^*$ , and also on the section of jet nozzle  $p_5^*$  increases.

Thus, with an increase in the number of revolutions the total pressure of the gas along the gas-air channel from the compressor to the exit section of the jet nozzle continuously increases (Fig. 11.2).

As regards the total pressure at the entrance into the compressor  $p_1^*$ , with an increase in the number of revolutions it somewhat drops. Here the effect of the increase in hydraulic losses in the inlet device of the engine with an increase in  $\lambda_{1a}$  ( $M_{1a}$ ).

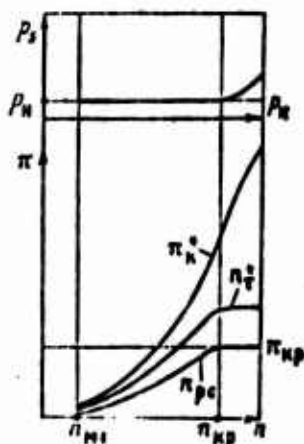


Fig. 11.2. Change in compression (expansion) ratios in elements of the TRD.

Let us now examine expansion ratios of gas in the turbine and the jet nozzle of the TRD change with an increase in the number of revolutions.

An increase in the compression ratio of the compressor leads to an increase in expansion ratios of the turbine and of the jet nozzle, since

$$\pi_{KT}^* \sigma_{KT}^* \sigma_{Kc}^* = \pi_{KP}^* \sigma_{KP}^* \sigma_{Kc}^*(\theta).$$

However, this process is accomplished only in the subsonic region of outflow of the gas from the jet nozzle, up to a certain number of revolutions at which the drop in pressures in the jet nozzle reaches a critical value, i.e.,

$$\frac{P_4^*}{P_5 = P_N} = \pi_{KP}^* = \left( \frac{2}{k+1} \right)^{\frac{k}{k-1}} = 1,85 \text{ (when } k=1,33).$$

With further growth in the number of revolutions and, consequently, the total expansion ratio, the drop in pressures in the jet nozzle remains constant, no matter how much the inlet pressure in the nozzle increases, i.e.,

$$\frac{P_4^*}{P_5} = \text{const.}$$

Thus, the expansion of the gas in the usual (narrowing) nozzle

of the TRD proves to be incomplete; with an increase in the number of revolutions above the "critical" on the section of the nozzle the excess static pressure appears and continuously increases, i.e.

$$p_s > p_n.$$

The described phenomenon leads to one more important circumstance. The appearance of the critical section in the jet nozzle ( $\lambda_5=1$  and  $q(\lambda_5)=1$ ) leads to cutoff of the turbine with respect to the drop in pressures. This denotes that now the expansion ratio of gas in the turbine remains constant, no matter how much the number of revolutions increases, i.e.,

$$\pi_T^* = \frac{p_3^*}{p_4^*} = \text{const.}$$

The latter results from the transformed equation of consumption (7.14) composed for the system "turbine-jet nozzle,"

$$\pi_T^* \frac{n+1}{2^n} = \frac{f_5 q(\lambda_5)}{f_{c.a} q(\lambda_{c.a})}.$$

Actually when  $\lambda_{c.a}=1$  (or const),  $f_5 = \text{const}$  and at the fixed geometry of the engine with an increase in  $\lambda_5$  up to 1 magnitude  $\pi_T^*$  increases; when  $\lambda_5 = 1 = \text{const}$  we find that  $\pi_T^* = \text{const}$ .

### 11.2.3. Redistribution of Total Expansion Ratio Between the Turbine and Jet Nozzle with Throttling of the Turbojet Engine

Let us examine how the total expansion ratio of the TRD will be redistributed between the turbine and jet nozzle at subcritical regimes of expiration from the engine ( $\lambda_5 < 1.0$ ).

Let us introduce the following assumptions:

- 1)  $q(\lambda_{c.a})=1$  or const over a wide range of throttle regimes;

2)  $\eta_i^* = 1$  and, consequently,  $n = k$ ;

3)  $\sigma_{p,c}^* = 1$  (i.e.,  $p_s^* = p_i^*$ ).

Using the system of relative parameters, let us present the equation of flow (7.14) in the form

$$\bar{\pi}_r^* \frac{k+1}{2k} = \bar{q}(\lambda_s). \quad (11.1)$$

Let us replace in equality

$$\bar{\pi}_k^* = \bar{\pi}_r^* \bar{\pi}_{p,c}^*$$

parameter  $\bar{\pi}_r^*$  from equation (11.1). Then we obtain

$$\bar{\pi}_k^* = \frac{\bar{q}(\lambda_s)^{\frac{2k}{k+1}}}{\bar{\Pi}(\lambda_s)}, \quad (11.2)$$

where

$$\begin{aligned} \bar{\pi}_k^* &= \frac{\pi_k^*}{\pi_{k(kp)}^*}; \quad \bar{\Pi}(\lambda_s) = \frac{\Pi(\lambda_s)}{\Pi(\lambda_s)_{kp}}; \\ \bar{q}(\lambda_s) &= \frac{q(\lambda_s)}{q(\lambda_s)_{kp}}; \\ \Pi(\lambda_s) &= \frac{1}{\pi_{p,c}^*} = \frac{p_s}{p_s^*} = \frac{p_n}{p_n^*}. \end{aligned}$$

Subscript "kp" refers to the critical regime of outflow.

Let us introduce the gas-dynamic function of the redistribution of pressure

$$\mu(\lambda) = \frac{q(\lambda)^{\frac{2k}{k+1}}}{\Pi(\lambda)}. \quad (11.3)$$

The dependence of  $\mu(\lambda)$  on  $\lambda$  when  $k = 1.33$  is given on a graph (Fig. 11.3). With an increase in  $\lambda_5$  from zero to unity function  $\mu(\lambda_s)$  likewise increases from zero to

$$\mu(\lambda_s)_{kp} = \frac{1}{\Pi(\lambda_s)_{kp}} = 1,85 \quad (k=1,33).$$

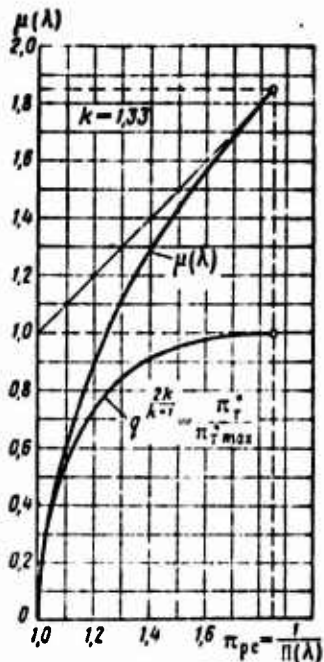


Fig. 11.3. Gas-dynamic function  $\mu(\lambda)$ .

It is easy to see that

$$\bar{\mu}(\lambda_s) = \frac{\mu(\lambda_s)}{\mu(\lambda_s)_{kp}} = \bar{\pi}_k^*.$$

Then the equation of the redistribution of pressure (11.3) takes the form

$$\mu(\lambda_s) = 1,85 \bar{\mu}(\lambda_s) = 1,85 \bar{\pi}_k^* = \frac{q(\lambda_s)^{\frac{2k}{k-1}}}{\Pi(\lambda_s)}. \quad (11.4)$$

The determination of  $\pi_k^*$  and  $\pi_{p,c}$  at any value  $\pi_k^* < \pi_{k^*}^*$  is produced graphically (see Fig. 11.3) or by the tabular method according to the following scheme:

$$\pi_k^* \rightarrow \bar{\pi}_k^* = \bar{\mu}(\lambda_s) \rightarrow \mu(\lambda_s) \rightarrow \Pi(\lambda_s) \rightarrow \pi_{p,c} \rightarrow \pi_r^*.$$

From Fig. 11.3 it follows that in the range of values  $\pi_{p,c} = 1,6 - 1,85$  it is possible approximately to consider  $\pi_r^* = \text{const}$  (when  $\pi_{p,c} = 1,6$  we have  $\bar{\pi}_k^* = 0,97$ ).

#### 11.2.4. Temperature Change in Gas in Characteristic Sections of the Gas-Air Channel of the TRD on the Number of Revolutions

Let us now examine the regularity of the change in total temperature of gas in characteristic sections of the gas-air channel of the TRD with throttling of the engine.

The stagnation temperature of the gas at the entrance into the compressor maintains at all numbers of revolutions the invariable value equal to the external air temperature:

$$T_1^* = T_n^* = T_0 \quad (\text{when } H=0 \quad \text{and } M_0=0).$$

The air temperature behind the compressor with an increase in the number of revolutions continuously increases and approximately according to the quadratic dependence. The latter follows from the equation of energy of flow written for the compressor:

$$T_2^* = T_0 + \frac{L_k}{102.5} = T_0 + Cn^2, \quad \text{where } C \approx \text{const.} \quad (11.5)$$

The most important and complex dependence is the change in gas temperature in front of the turbine  $T_3^*$  according to the number of revolutions. The magnitude of this temperature in the most heated section of gas flow is governed, on the one hand, by the effectiveness of the cycle of engine and its "exhaust" indices and on the other hand, by the calorific intensity of the hot part of the engine.

The regularity of the change in gas temperature in front of the turbine according to the number of revolutions is determined by the equation of balance of works of the turbocompressor

$$L_r = \frac{L_k}{\beta},$$

or

$$118T_3^* \epsilon_r^* \eta_r^* = \frac{Cn^2}{\beta},$$

whence

$$T_3^* = \frac{Cn^2}{1183\epsilon_r^* \eta_r^*}, \quad (11.6)$$

where

$$\epsilon_r^* = 1 - \frac{1}{\pi_r^{*0.95}}.$$

In the range of working numbers of revolutions the value  $C$  changes by 5-10%.

In the supercritical region of outflow of gases from the jet nozzle ( $\lambda_s \gg 1$ ), when  $n > n_{kp}$ , drop in pressures in the turbine  $\pi_r^*$  maintains an invariable value. Consequently, in this region of throttling of the engine, with a decrease in the number of revolutions the gas temperature in front of the turbine is lowered and is approximately proportional to the square of the number of revolutions (Fig. 11.4).

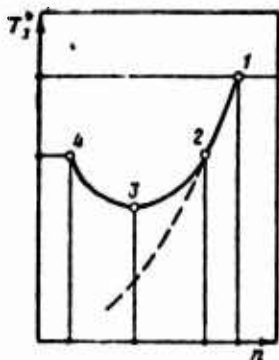


Fig. 11.4. Change in gas temperature in front of the turbine according to the number of revolutions of the TRD.

With a further decrease in the number of revolutions ( $n < n_{kp}$ ) the efficiency of the turbine, determined by its expansion ratio  $\pi_r^*$ , begins to decrease. This circumstance delays the drop in gas temperature  $T_3^*$ , which with a further decrease in the revolutions ceases (see Fig. 11.4).

In regimes of deep throttling of the engine there approaches an

intensive drop in efficiency of the compressor and the turbines<sup>1</sup>; the expansion ratio of the gas in the turbine in this case is so insignificant that realization of the balanced process of work of the engine (i.e.,  $n = \text{const}$ ) appears possible only with increased values of gas temperature in front of the turbine; and, since with a decrease in the revolution number of the engine the drop in  $\pi_3^*$ ,  $\eta_3^*$  and  $\eta_4^*$  is intensified, the increase in  $T_3^*$  also increases.

Thus, the change in  $T_3^*$  according to the number of revolutions is depicted as a concave curve with three characteristic sections (see Fig. 11.4). With a decrease in the number of revolutions of the TRD the gas temperature in front of the turbine initially is sharply decreased (section 1-2), then over a wide range of numbers of revolutions the drop in temperature  $T_3^*$  is slowed down and practically ceases (section 2-3), and, finally, in the region of numbers of revolutions close to "idling" there is an intensive increase in gas temperature in front of the turbine (section 3-4). This increase in temperatures is very considerable and sharp. The illiterate operation of the engine in the regime of "idling" can lead to an inadmissible overheating and even damage of the TRD. Therefore, it is necessary to have means and devices for preventing an undesirable increase in  $T_3^*$  in the zone of maximum and minimum revolutions of the engine.

Figure 11.5 shows the change in  $T_3^*$  according to the number of revolutions of the engine. The stagnation temperature of gas in the whole turbine channel (between sections 4-4 and 5-5) maintains a constant value, i.e.,

$$T_4^* = T_5^*$$

The regularity of the change in this temperature according to the number of revolutions is similar to curve  $T_3^* = f(n)$ . Actually, from the equation of the energy of flow written for the turbine, it follows that

---

<sup>1</sup>Appearance of regimes of separation and "choking" on blades of outer steps in the compressor, and deformation of velocity triangles in revolutions of the TRD.

$$T_4^* = T_3^* - \frac{L_1 + L_2}{118} = T_3^* - Cn^2. \quad (11.7)$$

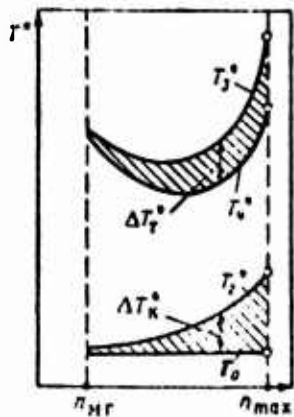


Fig. 11.5. Curves of the change in total gas temperature in characteristic sections of the TRD.

Consequently, in the region of maximum and minimum engine revolution in accordance with a change in  $T_3^*$ , there is an increase in temperature  $T_4^*$ . However, with a reduction in the number of revolutions the temperature range between curves  $T_3^*$  and  $T_4^*$  is decreased gradually. In the zone of revolutions of idling curves  $T_3^*$  and  $T_4^*$  practically coincide. Thus, the temperature  $T_4^*$  is a "satellite" of temperature  $T_3^*$ .

According to the deviation of temperature  $T_4^*$  from the "norm" it is possible to judge quite validly the level of the gas temperature in front of the turbine and the calorific intensity of the engine as a whole.

Figure 11.5 gives a typical curve of the change in total gas temperature in the characteristic sections of the gas-air channel of the TRD.

#### 11.2.5. Change in Air Outflow on the Number of Revolutions

From the theory of turbomachines it is known that the rate of air flow through a compressor increases approximately in proportion to its number of revolutions. However, in the region of maximum revolutions this dependence, as the experiment shows, deviates from

the linear  $G_n = Cn$ , — increase in flow of air is delayed (Fig. 11.6). Such regularity is connected with the phenomenon of "choking" at an entrance into the compressor. With the approach of the axial velocity of inflow  $c_{1a}$  to the speed of sound ( $\lambda_{1a} \rightarrow 1,0$ ) the relative current density  $q(\lambda_1)$  approaches its limiting value and, consequently, the increase in flow of air ceases, i.e.,

$$G_n = m \frac{P_0}{\sqrt{T_0}} f_1 q(\lambda_1) \sim q(\lambda_1).$$

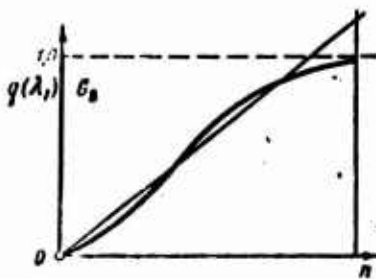


Fig. 11.6. Change in air flow on the number of revolutions of the compressor.

Therefore, the nearer the number  $\lambda_1$  is to 1 in design conditions (which is conditioned by a tendency to decrease the dimensional diameter of the engine), the greater the dependences  $G = f(n)$  deviate from the linear.

#### 11.2.6. Change in Specific Thrust of the TRD According to the Number of Revolutions

With an increase in the number of revolutions the velocity of outflow of gases from the jet nozzle increases and is equal to

$$c_5 = \gamma \sqrt{2g \frac{c_p}{A} T_{1p,c}^*}.$$

where

$$\epsilon_{p,c} = 1 - \frac{1}{\frac{k-1}{k}}; \quad \pi_{p,c}^* = \frac{P_1^*}{P_n}.$$

An increase in  $c_5$  is conditioned by an increase in the drop in pressure in the reactive nozzle and in the region of maximum revolutions by an additional factor — by an increase in stagnation of gas temperature at entrance in reactive nozzle.

Thus, with an increase in the number of revolutions and the specific thrust of the TRD continuously increases (Fig. 11.7) and is equal to

$$R_{yA} = \frac{c_s}{g}$$

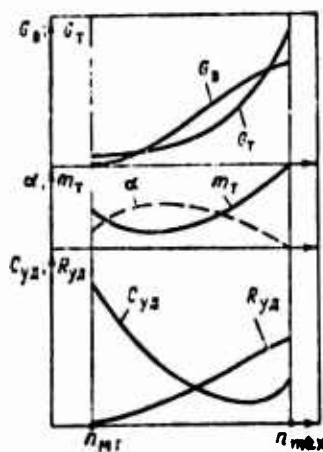


Fig. 11.7. Change in specific thrust, air flow and fuel consumption of the TRD on the number of revolutions.

The underexpansion of the gas, which occurs at supercritical drops in pressures in the usual (convergent) nozzle of the TRD, lowers the specific thrust of the engine. However, calculations show that at any assimilated values of  $T_3^*$  and  $\pi_K^*$  the difference between  $R_{yA}$  with complete and incomplete expansion of the gas in a maximum regime on the test stand ( $V = 0$ ) does not exceed 2-3%.

The increase in specific thrust of the TRD with the increase in revolution number can be given a different explanation connected with a change in work of the cycle of the TRD. It is known that when  $T_3^* = \text{const}$  with an increase in the compression ratio magnitude  $L_e$  increases. The increase in  $L_e$  is intensified at maximum revolutions when these approaches the intensive increase in gas temperature in front of the turbine.

#### 11.2.7. Change in Total Thrust of the Turbojet Engine on the Number of Revolutions

The change in total thrust of the TRD on the number of revolutions (Fig. 11.8) is determined completely by regularities of the change in

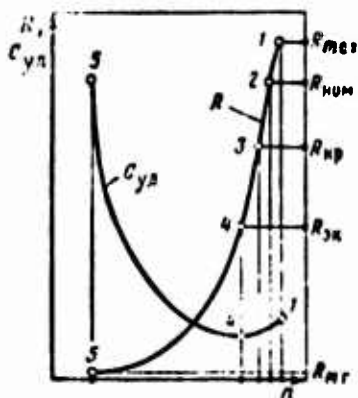


Fig. 11.8. Change in total thrust and specific fuel consumption of the TRD on the number of revolutions.

specific thrust and air flow per second (see Fig. 11.7).

Let us examine the TRD with an average compression ratio of the compressor and moderate value of axial velocity at the entrance into compressor in a maximum regime ( $\lambda_{1a}=0,6$ ). For these conditions we can assume quite accurately that the flow of air is proportional to the number of revolutions in the first degree, and the specific thrust is approximately proportional to the square of the number of revolutions, i.e.,

$$G_s = C_1 n; R_{YK} = C_2 n^2.$$

Then as a first approximation we find

$$R = R_{YK} G_s = C_3 n^3. \quad (11.8)$$

Analysis of numerous experimental data shows that the cubic dependence of thrust on the number of revolutions is valid for the majority of TRD with a program of adjustment  $f_5 = \text{const}$  in the region of numbers of revolutions less than nominal. In the region of nominal and maximum numbers of revolutions, considering peculiarities of the passage of curves  $G_s = f_1(n)$  and  $R_{YK} = f_2(n)$ , the increase in thrust of the TRD is slowed down. In this region the exponent at  $n$  is lowered (at  $\lambda_{1a} \rightarrow 1$ ) from 3-4 to 1.

Thus, the dependence of thrust on the number of revolutions is described by the power dependence

$$R = An^x, \quad (11.9)$$

in which index  $x$  has a variable value  $x = 1-4$ .

#### 11.2.8. Change in Total Coefficient of Air Surplus According to the Number of Revolutions

Let us examine initially how the relative fuel consumption changes

$$m_T = \frac{c_{pm}(T_3^* - T_2^*)}{k_{x,c}H_B} = \frac{G_T}{G_B}$$

according to the number of revolutions of the TRD

From equality  $L_T = L_K$  and on assumption that  $c_{pT} = c_{pB} = c_p$ , there follows the approximate relation

$$T_2^* - T_0^* = T_3^* - T_4^*, \quad \text{or} \quad T_3^* - T_2^* = T_4^* - T_0^*.$$

Thus, parameter  $m_T$  changes in proportion to the stagnation temperature of the gas behind the turbine (see Fig. 11.7).

The total coefficient of air surplus

$$\alpha = \frac{1}{m_T l_0}$$

changes inversely proportion to magnitude  $m_T$ ; Fig. 11.7 gives curves  $\alpha = f(n)$ . With a decrease in the number of revolutions initially there is a depletion in the mixture (down to  $\alpha = 4.5-5.0$ ); with further throttling of the engine the fuel-air mixture is already enriched.

#### 11.2.9. Change in Specific Fuel Consumption According to the Number of Revolutions

The change in specific fuel consumption according to the number of revolutions is determined by peculiarities of the change in parameters of the working process of the engine:  $\pi_n^*$ ,  $T_3^*$ , and also  $\eta_n^*$ .

With a decrease in the number of revolutions of the engine from maximum to minimum, the compression ratio of the compressor is lowered many times, from  $\pi_{\kappa(\text{max})}$  down to a magnitude differing little from unity. This regularity at considerable less oscillations in gas temperature in front of the turbine (ratio  $T_{3(\text{min})}/T_{3(\text{max})} = 0.65-0.80$ ) conditions the basic tendency - an increase in specific fuel consumption with throttling of the engine. However, in the region of maximum revolutions, in which the absolute values are still high, an intensive lowering of the gas temperature in front of the turbine, proportional to the square of the number of revolutions, and also a certain increase in efficiency of the compressor along the line of operating regimes lead to the fact that the specific fuel consumption of the TRD is somewhat initially lowered (by 3-8%).

Thus, the regularity

$$C_{\gamma\kappa} = f(n)$$

has the form of a concave curve with a clearly designated minimum, which determines the so-called "cruising" or "economic" regime of operating the TRD (see Fig. 11.8).

The obtained regularity can be also explained by the joint effect of two factors: specific thrust and relative fuel consumption, since

$$C_{\gamma\kappa} = 3600 \frac{m_T}{R_{\gamma\kappa}}$$

Actually, with throttling the specific thrust of the TRD drops continuously. The relative fuel consumption follows regularity

$$T_4^* = f(n)$$

Thus, the initial depletion of the mixture predetermines the appearance of the minimum on curve  $C_{\gamma\kappa}$ ; the subsequent enrichment of the mixture (increase in  $m_T$ ) intensifies the growth in  $C_{\gamma\kappa}$  in the region of reduced regimes of the TRD (see Fig. 11.7).

Figure 11.9 gives throttle characteristics of the TRD Bristol-Siddley "Viper" 11 and "Viper" 20.

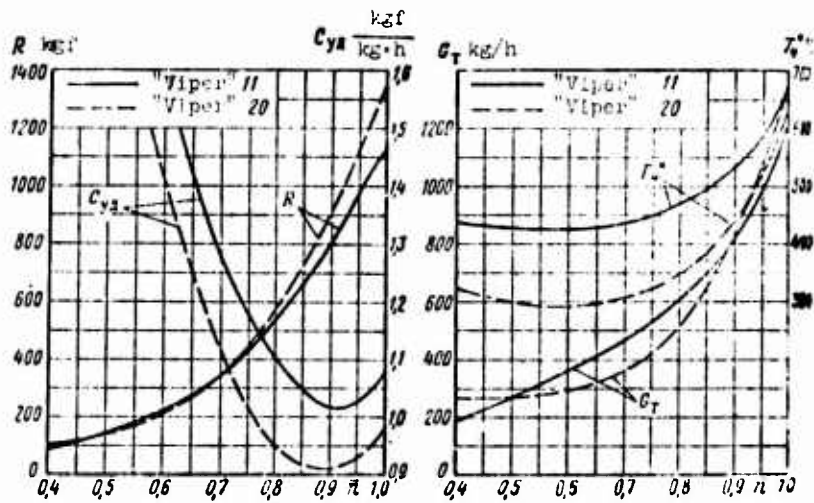


Fig. 11.9. Throttle characteristics of the TRD Bristol-Siddley "Viper" 11 and "Viper" 20.

### 11.3. Throttle Characteristics of the Turbojet Engine with Special Adjustment

#### 11.3.1. Throttle Characteristic of the Turbojet Engine at Constant Revolutions

When the turbojet engine is equipped with an adjustable jet nozzle, the starting of the engine and putting it at maximum revolutions are produced with maximum opening of the critical (exhaust) section of the nozzle. This considerably lowers the time of spinup of the engine and improves its pickup. After exit TRD on maximum revolutions an increase in thrust of the engine is carried out by covering the jet nozzle when  $n = \text{const}$ ; in this case the compression ratio of the compressor and gas temperature in front of the turbine increases. On characteristic of compressor (Fig. 11.10a) has been depicted the line of operating conditions is 1-2-3 for the indicated case. The simultaneous increase in values  $\pi_c^*$  and  $T_3^*$  sharply increases the specific thrust of the TRD. As regards rate of air flow, its change when  $n = \text{const}$  is determined by the peculiarity of the passage of the pressure characteristic of the compressor. Usually the flow of air with covering of the nozzle is either somewhat lowered (inclined characteristic) or even remains constant (case of the vertical characteristic). Thus, thrust of the engine with covering

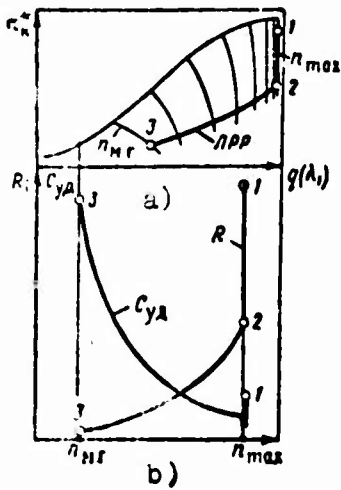


Fig. 11.10. Throttle characteristics of the TRD at  $n = \text{const}$  (b) and line of operating regimes of the compressor (a).

of the jet nozzle of the TRD continuously increases. Specific fuel consumption in this case is initially lowered, and in the region of high values  $T_3^*$  it again increases.

Figure 11.10b shows throttle characteristic of the TRD when  $n = \text{const}$ .

### 11.3.2. Throttle Characteristic of the Turbojet Engines Equipped with an Air Bypass System

Let us assume that a turbojet engine is equipped with an air bypass system (from the intermediate stage of the compressor), which provides steady operation of the compressor in all the whole range of operating numbers of revolutions.

Let us designate the number of revolutions  $n = n_n$ , at which with throttling of the TRD the bypass system operates, and, consequently, part of the compressed air in the compressor is carried off through bypass valves (ports) to the outside. Thus, when  $n < n_n$  we have

$$\frac{a_r}{a_0} = \beta < 1.0.$$

Figure 11.11b gives a throttle characteristic of the TRD equipped with an air bypass system. With throttling of the engine in the region of revolutions  $n_n < n < n_{max}$  (when the bypass valves are closed) curves  $R = f(n)$ ;  $C_{ya} = f(n)$  and  $T_4^* = f(n)$  are in no way distinguished

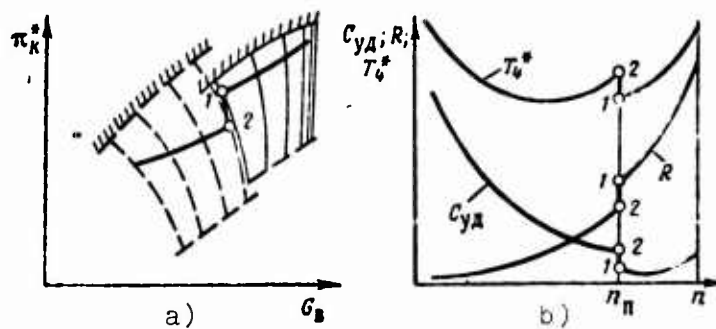


Fig. 11.11. Throttle characteristic of the TRD equipped with an air bypass system.

from the earlier examined dependences (see Fig. 11.9). When  $n = n_{\pi}$  there is expulsion of part of the air into the external medium; disruption of the material balance ( $G_r < G_b$  and  $\beta < 1.0$ ) leads, respectively, to a disruption of the energy balance ( $N_r < N_k$ ); for maintaining the balanced process of operation of the turbocompressor ( $n = \text{const}$ ) the regulator of revolutions increases the fuel feed in the combustion chamber, and the gas temperature in front of the turbine increases in the necessary degree.

Since with the opening of bypass valves the counterpressure at the exit from first steps of the compressor is lowered, then the air flow at the entrance into the compressor usually increases somewhat. Ultimately the compression ratio  $\pi_{\pi}^*$  drops (see Fig. 11.11a). Correspondingly the pressure along the whole gas-air channel is lowered. As a result the velocity of gas consumption, specific thrust, and gas flow through the jet nozzle are decreased. Consequently, the total thrust of the engine drops; the specific fuel consumption increases. The latter is explained by the fact that the interval of preheating of the gas in the combustion chamber ( $T_3^* - T_2^*$ ), whereas the specific thrust is lowered essentially.

Physically the growth in  $C_{y\Delta}$  is explained by the drop in effective efficiency of the cycle due to the poorer use of heat at reduced pressure of the working medium, and likewise uneconomical flow of compressed air.

Figure 11.12 gives the throttle characteristic of the TRD Rolls-Royce "Avon" with two bypass valves.

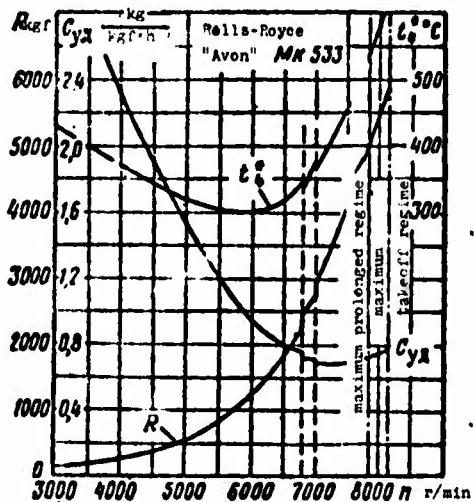


Fig. 11.12. Throttle characteristic of the TRD Rolls-Royce "Avon" with two bypass valves.

### 11.3.3 Throttle Characteristic of the Turbojet Engine Equipped with a Rotary Guide Vane of the Compressor

Figure 11.13 shows by continuous lines the throttle characteristic of the TRD with invariable neutral position of the rotary guide vane ( $\psi_{HA} = 0$ ).

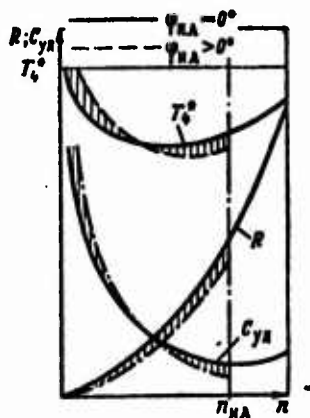


Fig. 11.13. Throttle characteristic of the TRD equipped with a rotary guide vane of the compressor.

Let us assume that with choking of the engine at a certain revolution number  $n < n_{max}$  (when the margin of stability of compressor is small) blades of the rotary guide vane turn at angle  $\Delta\phi$  in the

direction of rotation of the rotor of the compressor, and further throttling is produced at a new and fixed position of the blade (for example,  $\varphi_{n.a} = 10^\circ$ ).

Turning of the guide vane in the direction of rotation of the rotor when  $n = \text{const}$  decreases angles of incidence of flow on rotor blades and, consequently, increases the reserve of the compressor with respect to surging. In this case the work and compression ratio of the compressor drop. Consequently (assuming in the region of high revolutions that  $\pi_3^* = \text{const}$ ), gas temperatures in front of the turbine  $T_3^*$  and behind the turbine  $T_4^*$ . As a result of the turning of the blades of the air flow, specific thrust and total draught drop the guide vane; the specific fuel consumption is also lowered. With great throttling of the TRD, as a result of the sharp lowering of  $\pi_3^*$  and  $\pi_4^*$ , the relative increase in  $C_{yD}$  and  $T_4^*$  is possible (as compared to the case when the guide vane is not adjustable).

Section of characteristic of the TRD with turned blades of the guide vane (at angle  $\varphi_{n.a} = 10^\circ$ ) is depicted in Fig. 11.13 in the form of dot-dashed lines.

#### 11.3.4. Peculiarity of Throttle Characteristics of a Double-Shaft TRD

In comparison with characteristics of the single-shaft TRD, throttle characteristics of a double-shaft TRD possess the following peculiarities. The most important of them is the slip of the rotors; it is expressed in the fact that any change in the regime of operation of the TRD, conditioned by the effect of regulating factors (by the increase or decrease in fuel feed, adjustment of the critical section of the jet nozzle, etc.), leads to a change in the correlation between numbers of revolutions of rotors of high and low pressure, i.e.,

$$\frac{n_{HD}}{n_{BD}} = \text{var.}$$

Let us show this in an example. Let us assume initially, for example, on the maximum regime, drop in pressures in the exhaust

nozzle has the supercritical value, i.e.,

$$\frac{P_4^*}{P_2} > \left(\frac{k+1}{2}\right)^{\frac{k}{k-1}} \approx 1,85 \text{ и } q(\lambda_s) = 1.$$

In this case [see equation (7.14)] with the fixed jet nozzle the pressure differentials in VD and ND turbines remain constant, i.e.,

$$\pi_{r,VD}^* = \text{const} \text{ and } \pi_{r,ND}^* = \text{const}.$$

The ratio of works of the ND and VD turbines equals

$$\frac{L_{r,ND}}{L_{r,VD}} \sim \frac{T_{4VD}^* \epsilon_{r,ND}^* \eta_{r,ND}^*}{T_3^* \epsilon_{r,VD}^* \eta_{r,VD}^*} = \frac{(1 - \epsilon_{r,VD}^* \eta_{r,VD}^*) \epsilon_{r,ND}^* \eta_{r,ND}^*}{\epsilon_{r,VD}^* \eta_{r,VD}^*}, \quad (11.10)$$

where

$$\epsilon_r^* = 1 - \frac{1}{\pi_r^* \frac{k_r - 1}{k_r}},$$

in this case also remains constant.

With choking of the engine (by means of a decrease in fuel feed), in all the balanced regimes the ratio of works of ND and VD compressors equals

$$\frac{L_{k,ND}}{L_{k,VD}} = \frac{L_{r,ND}}{L_{r,VD}}, \quad (11.11)$$

and when  $q(\lambda_s) = 1$  it remains constant.

Since with the decrease in the number of revolutions of the TRD angles of incidence of the flow on blades of the ND cascade increase (the ND compressor is "loaded" and work of compressor relatively increases), and angles of incidence of flow on blades of the VD cascade are decreased (i.e., the VD compressor is "lightened" and work of compressor is relatively lowered), then for observance of condition (11.11) the number of revolutions of the ND compressor

$$^1 T_{4VD}^* = T_3^* - \frac{L_2}{118} = T_3^* (1 - \epsilon_{r,VD}^* \eta_{r,VD}^*).$$

must additionally be lowered<sup>1</sup>, and the number of revolutions of the VD compressor will respectively increase.

Consequently, the ratio  $n_{HD}/n_{RD}$  is decreased, i.e., slip of the rotors will begin (Fig. 11.14). Slip of the rotors is increased in regimes of great throttling when the drop in pressures in the jet nozzle becomes subcritical. In this case the decrease in the total expansion ratio is perceived, first of all, by the ND turbine ( $\pi_{T,HD}^*$  drops - ND turbine is "lightened") and the ratio of works of the turbines  $\left(\frac{L_{T,HD}}{L_{T,RD}}\right)$  drops.

With an increase in fuel feed the ratio  $n_{HD}/n_{RD}$  increases.

Another peculiarity of throttle characteristics of a double-shaft TRD is the higher level of efficiency of the compressor in comparison with the compressor of a single-shaft TRD equipped with the system of air bypass (Fig. 11.15). This circumstance leads to the lowering of the level of gas temperature in front of the turbine in the whole range of operating revolutions even to a corresponding decrease in specific fuel consumption.

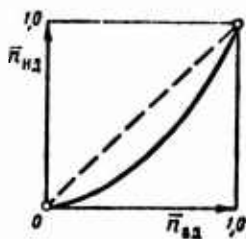


Fig. 11.14.

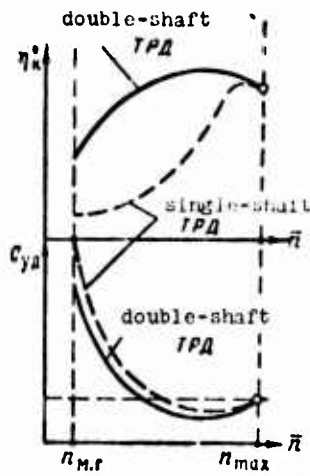


Fig. 11.15.

Fig. 11.14 Slip of rotors of double-shaft TRD.

Fig. 11.15. Comparison of  $\eta_k^*$  and  $C_{\gamma A}$  for single-shaft and double-shaft TRD.

<sup>1</sup>In comparison with balanced revolutions of the TRD for which VD and ND cascades are rigidly connected with each other.

Finally, the third peculiarity of throttle characteristics of the TRD is the regularity of the effect of adjustment of the jet nozzle on the margin of stability of VD and ND compressors.

Earlier (see Section 10.3) we showed that a decrease in the throat area of the exhaust nozzle of the single-shaft TRD when  $n = \text{const}$  decreases the margin of stability of the compressor and increases  $T_3^*$ .

In the case of a double-shaft TRD the covering of the jet nozzle causes the drop in pressures on turbine ND and practically does not affect the drop in pressures on the VD turbine. When  $n_{ND} = \text{const}$  as a result of a decrease in the work of the ND turbine the number of revolutions of the cascade of low pressure falls. The flow of air through the compressor is also decreased but considerably more slowly than the number of ND revolutions (since  $n_{ND} = \text{const}$ ). As a result the ratio  $(c_{10}/u)_{ND}$  increases, i.e., angles of incidence of flow on blades of the ND compressor, and the margin of stability of the ND compressor increases. Consequently, the covering of the jet nozzle moves the line of operating conditions on the characteristic of the ND compressor into the region of raised values  $q(\lambda_1)$  and reduces values  $\pi_4^*$ .

As regards the VD compressor, ratio  $(c_{10}/u)_{VD}$  is decreased, and angles of incidence of flow on blades of the compressor VD increase. As a result the stability margin of the VD compressor is somewhat decreased. The covering of the exhaust nozzle insignificantly moves the LRR into the region of raised values of  $\pi_4^*$  (Fig. 11.16).

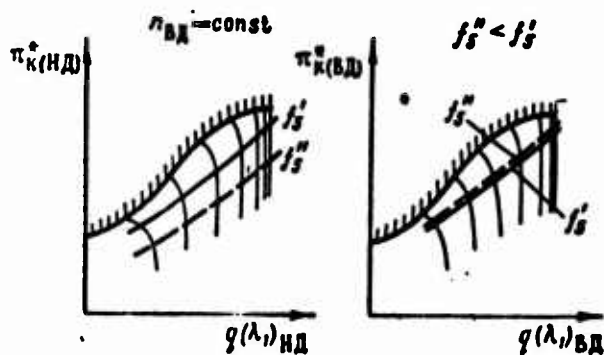


Fig. 11.16. Effect of  $f_5$  on LRR of VD and ND compressors of a double-shaft TRD.

With the program of adjustment  $\pi_{HD} = \text{const}$  cover of the critical section of the exhaust nozzle causes an increase in  $T_3^*$  and also leads to an increase in margin of stability of the ND compressor. Actually, an increase in the number of VD revolutions, conditioned with a growth in  $T_3^*$ , leads to an increase in the total flow of air through the compressor. Consequently, ratio  $(c_{1a}/u)_{HD}$  increases, and angles of incidence of flow on blades of the ND compressor are decreased, and the margin of stability increase. Ratio  $(c_{1a}/u)_{HD}$  is decreased, as a result of which the stability margin of the VD compressor is decreased. Thus, in contrast to the single-shaft TRD, the covering of the jet nozzle of the double-shaft TRD always increases the stability margin in the ND compressor.

#### 11.4. Region of Possible Regimes of Operation of the Turbojet Engine

Above we showed that with adjustment of the exhaust section of the jet nozzle the *line of operating regimes of the TRD*, applied to the characteristic of the compressor, is displaced and thus describes a certain *region of possible regimes of operation*.

However, operation of the TRD appears physically possible and permissible not in the whole field of characteristic of the compressor. In certain regimes of operation of the engine in its separate elements (compressor, combustion chamber, turbine) appear physical disturbances and changes, which limit and narrow the *real* region of possible regimes of the operation. Several process of operation of the TRD can be physically realized.

The noted limitations are connected with the appearance of:

- 1) unstable operation in elements of the engine;
- 2) gas-dynamic "choking" of separate sections of the gas-air channel;
- 3) danger of disruption of strength and reliability of operation of the engine and its separate subassemblies (for example, with an

increase in revolution number of the engine and of gas temperature in front of the turbine above permissible limits).

Figure 11.17 gives a model characteristic of a compressor with lines of limitation of regimes of the turbojet engine applied on it.

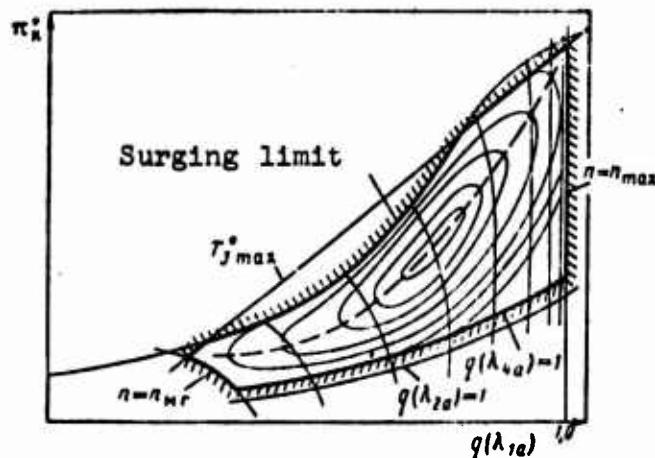


Fig. 11.17. Field of operating conditions of the compressor of the TRD

These refer to:

*The limit of steady operation of the compressor (surging limit); it is locus of regimes of the appearance of surging of the compressor at various numbers of revolutions.*

*The limit of steady operation of the engine at revolutions of idling ( $n = n_{nr}$ ). With lift to an altitude revolutions of idling increases.*

*The limit of gas-dynamic choking at the entrance into the compressor with respect to the axial velocity. Theoretically choking approaches when  $q(\lambda_{1a}) = 1$  (or  $M_{1a} = 1$ ); in practice (with an allowance for narrowings at the entrance channel due to struts) - when  $q(\lambda_{1a}) = 0,80 - 0,85$ . The physical meaning of this choking is that with an increase in the number of revolutions the flow of air through the compressor does not increase.*

*The limit of gas-dynamic choking at the exit from the compressor with respect to the axial velocity.* Theoretically choking approaches when  $q(\lambda_{2a})=1$  (or  $M_{2a}=1$ ). The physical meaning of choking is that with a decrease in counterpressure at the exit from the compressor the compression ratio and work of compressor remain constant.

*The limit of choking at the exit from the turbine with respect to the axial velocity.* Theoretically the choking approaches when  $q(\lambda_{4a})=1$  (or  $M_{4a}=1$ ); in practice (with an allowance for narrowings in the turbine channel) - when  $q(\lambda_{4a})=0,70-0,75$ . The physical meaning of this form of choking is that with an increase in the critical (exhaust) section of the jet nozzle the drop in pressures and work of the turbine no longer increase. The turbine becomes "blunt" and not adjustable.

*The limit of maximum permissible (from conditions of strength) gas temperature in front of the turbine.*

*The limit of maximum permissible (from conditions of strength) of revolutions.*

## 11.5. Unstable Operation of the Compressor (Surging)

### 11.5.1. Physical Essence of Surging

Unstable operation of the compressor appears in the form of periodic and sharp pulsations of air flow - oscillations in pressure, velocity and of flow. Mean pressures generated by the compressor usually drop, and the inlet temperature of compressor considerably increases. At times it is as though the compressor were "flooded," ejecting masses of air in the opposite direction, into the entrance. Surging is accompanied by strong knocks and shocks.

Experimentally it is established that surging is connected with periodic separations of flow appearing mainly on convex surfaces (backs) of profiles of blades with flow about the compressor lattices. At a constant number of revolutions of the compressor (and,

consequently, at a constant circumferential velocity of the blades) a decrease in the flow leads to a decrease in the axial component of velocity of flow at the entrance into the given lattice. Consequently, the relative velocity with flow about the profile in the lattice changes its direction, and the angle of incidence of flow  $i$ , having increased, becomes more than the critical, in consequence of which separation of the flow from the back of the blade appears.

Figure 11.18 shows a diagram of separated flow about the airfoil lattice of the rotor wheel of the axial compressor. Vortices appearing with separation of flow is unstable (see Fig. 11.18a) [sic] and have a tendency toward automatic increase. The forming vortical shroud, extending in an interblade channel under action of centrifugal forces of inertia, decreases the effective section of the flow, as a result of which the flow of air is even more decreased. There comes the moment when the vortices completely fill the interblade channels, and the air supply by the compressor in this case ceases (the air flow is equal to zero). In a subsequent instant there is washing of the vortex sheet; in this case ejection of the air at the entrance into the compressor is possible. Repeated and frequent compression of the same portion of air in the compressor with surging leads to an increase in air temperature at the entrance into the compressor (repeated feed of energy to the same air mass).

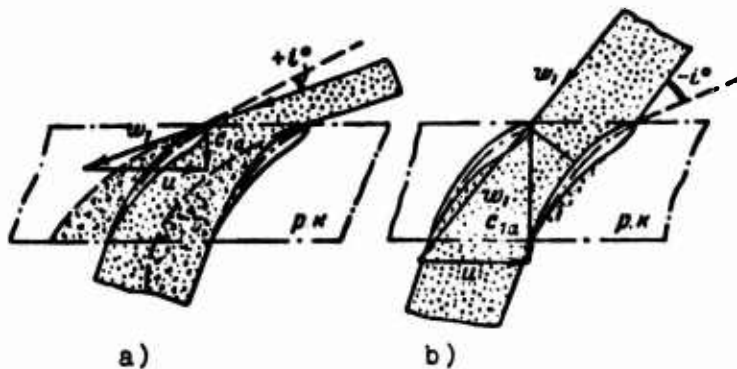


Fig. 11.18. Diagram of choking of flow about an airfoil cascade of a rotor wheel of an axial-flow compressor: a) surging; b) regime of "choking."

With an increase in the air flow (negative angles of attack of the profile) the separation of flow occurs on the concave side of the blade. The vortices generating here are pressed by the main flow to the profile and have a steady character (see Fig. 11.18b).

The given explanation of the physical essence of the phenomena leading to surging is found in accordance with the form of the characteristic; its left branch corresponds to surging and the right branch - steady regimes.

#### 11.5.2. Relative Position of the Limit of Surging and Line of Operating Regimes of the Compressor. The Concept About Margin of Stability with Respect to Surging

The combination of points of the beginning of surging at different numbers of revolutions forms the so-called *limit of surging*. With a decrease in the number of revolutions, the limit of surging is displaced to the side of less flows.

The combination of regime of points in compressors of the TRD forms the operating curve of the compressor. Its form and passage on the characteristic depend on conditions of the joint operation of the compressor and turbine and also on the program of control of the engine.

To provide the normal operation of the TRD in the whole range of numbers of revolutions, velocities and altitudes of flight, the operating curve of the compressor (*a-c-b* in Fig. 11.19a) must pass to the right of the limit of the surging (*a-e-b*).

The calculated regime of operation of the compressor is selected from the condition that at the assigned given numbers of revolutions the surging reserve, being determined by the coefficient of stability,

$$K_s = \left( \frac{\bar{\pi}_{x(n)}}{\bar{\sigma}_{(n)}} - 1 \right) \cdot 100\%, \quad (11.12)$$

where

$$\bar{\pi}_n = \frac{\pi_{n(n)}}{\pi_{n(p)}}; \bar{G}_n = \frac{G_{(n)}}{G_{(p)}}$$

is not less than 12-17% (see Fig. 11.19b).

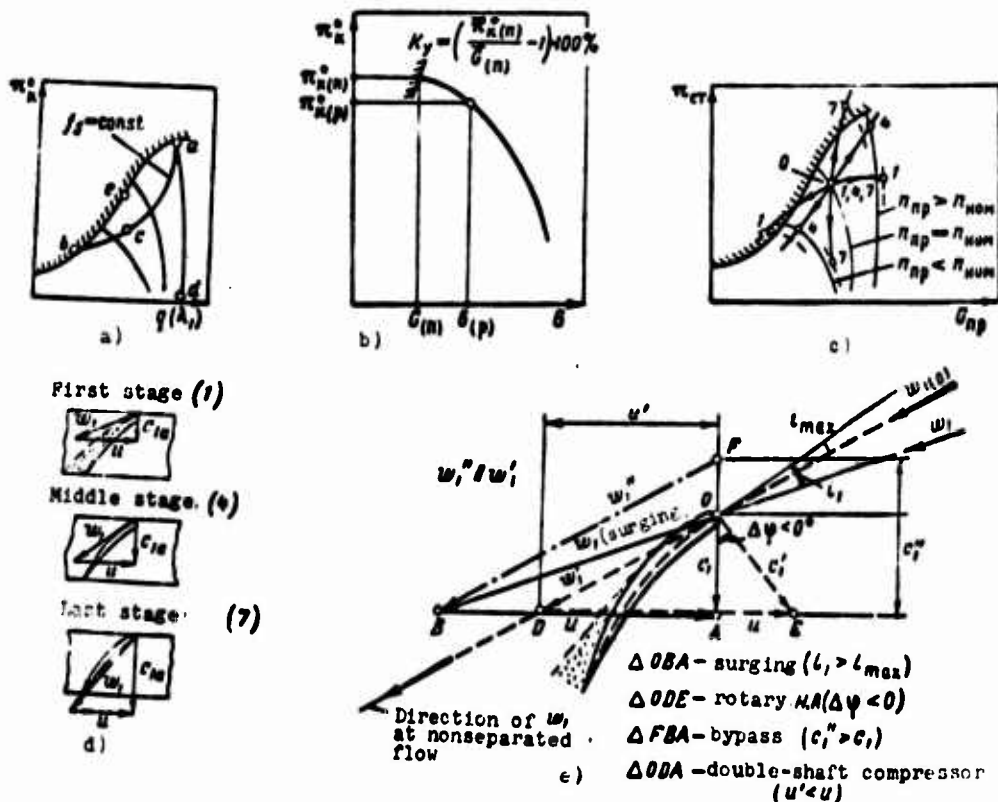


Fig. 11.19. Explanation of surging phenomenon.

In lift engines, which are characterized by increased non-uniformity of the temperature field in the inlet device (due to the possible entrance of hot exhaust gases), the surging reserve increases up to 20-25%.

### 11.5.3. Surging in a High-Pressure Axial-Flow Compressor

The peculiarity of operation of a multi-stage high-pressure axial-flow compressor is a "mismatch" or "divergence" of the operation of extreme (i.e., first and last) stages in uncalculated regimes.

Let us assume that in the calculated regime of operation (for example, at a nominal revolution number) all stages of the compressor operation stably without flow separation, with calculated values of degrees of compression and efficiency. If the compressor does not have special control elements (for example, throttle valves at the inlet and exit), then any change in the regime of its operation, being determined by the revolution number, leads to a change in angles of attack of the blade - in the first place, extreme stages and, to a less extent, middle stages. With a decrease in revolution number angles of attack in the first stages increase, and in the latter stages the decrease. As a result, in first stages of the compressor there appears separation of flow from backs of the blades and, as a consequence of this, surging; in the last stages there appears the so-called turbine process, which is characterized by a sharp drop in compression ratio, and also regime of choking.

The mismatch of the operation of extreme stages is more, the less the number of revolutions and the more the value of compression ratio of the compressor in the initial calculated regime.

With an increase in the number of revolutions above the nominal the mismatch of the operation of extreme stages changes - now surging in the last stages appears; in the first stages with the appearance of sonic and supersonic relative velocities of flow the regime of choking appears.

Figure 11.19c shows diagrams of flow past blades of the first (1), middle (4) and last (7) stages of the axial-flow compressor at a reduced number of revolutions, and Fig. 11.19c gives the combined characteristics of the first, middle and extreme stages of the compressor with lines of operating regimes of these stages applied on the figure.

#### 11.5.4. Measures to Prevent Surging of the Compressor

Measures to prevent surging of the compressor can be subdivided into operational and design.

Operational measures are directed towards not allowing surging and with its appearance - rapidly eliminate it. Preventing the possibility of the appearance of surging is achieved by providing the correct fuel dosage with respect to the number of revolutions both with starting and in transitional regimes of the engine (by the use of automatic units of accelerating capacity) and also by providing the required spinup of the rotor of the engine by the starting starter.

With the appearance of the unstable operation of the engine it is necessary with the help of the RUD to decrease the revolution number of the rotor of the engine up to the disappearance of surging, reduce the flight altitude, or increase the flight speed. Any of these measures lowers the reduced revolution number and transfers the regime point into stable region of the characteristic.

Design measures consist in the fact that:

- 1) at the assigned line of regimes of the joint operation of the compressor and turbine move the limit of surging into the region of less flows. This is achieved by the use of rotary blades of the stator or rotor at the entrance into the axial-flow compressor and at the exit from it, by special selection of angles of setting of the blades of rotor wheel of the axial-flow compressor, etc.;

- 2) at the assigned surge limit of the compressor move the line of regimes of the joint operation of the compressor and turbine into the region of great flows. This is achieved by the use of the adjustable jet nozzle and nozzle box assembly of the turbine;

- 3) provide consistent and surgless operation of all stages of the high-pressure axial-flow compressor. For this purpose air bypass from intermediate stage of the compressor into the atmosphere, rotary blades of the stator, and also double-shaft axial-flow compressors are used.

Figure 11.19e schematically gives methods of eliminating the appeared surging of the stage of the axial-flow compressor with the

help of an adjustable guide vane (i.e., by introduction of preliminary twist of flow at the entrance into the rotor wheel); air bypass (i.e., increase in the axial flow velocity); passage to double-shaft diagram (i.e., lowering of circumferential velocity of rotation of the rotor).

#### 11.6. Nomenclature of Basic Processes of Operation of the Turbojet Engine

At present there is no standard or united nomenclature of basic processes of operation of gas-turbine engines.

Each firm manufacturing aircraft engines and every aircraft company using these engines, in the course of finishing and operation of the gas turbine, refines and changes the enumeration of basic regimes of operation of the engines and the correlation between thrusts, and values of basic parameters of the engine on these processes. In the civil aviation of our country the following nomenclature of basic processes of the TRD has been accepted (see Fig. 11.8)

##### 11.6.1. Maximum (or Takeoff) Regime

In this regime (at maximum revolution number) the engine must develop maximum thrust at continuous operation during a limited time, as a rule, not more than 5-10 minutes. In the maximum regime maximum permissible of the condition of providing the reliability of gas temperature for the turbine is fixed and limited.

The takeoff regime is used in flight, in altitude gain and for the achievement of maximum flight speed in combat conditions (with pursuit of the enemy or withdrawal from him).

##### 11.6.2. Nominal Rating

In this regime (at a nominal revolution number) the engine must develop the greatest thrust at continuous operation for 30 minutes to 1 hour. In the nominal regime maximum permissible gas temperature

behind the turbine is also fixed. The thrust in the nominal regime is usually lower by 10-15% than that in the takeoff process, i.e.,

$$R_{\text{ном}} \approx (0,85 \div 0,90) R_{\text{max}};$$

in this case

$$n_{\text{ном}} \approx (0,96 \div 1,0) n_{\text{max}}.$$

Basic calculations of the engine (for strength, gas-dynamic) and the selection of the flow passage cross-sectional area are produced in the nominal regime.

The nominal rating is the basic process of operation of the engine on a fighter aircraft. On passenger aircraft this regime is used in climbing.

### 11.6.3. Cruising Regime

In this regime the greatest thrust is guaranteed at continuous and reliable operation of the engine during the whole established period of service (service life).

The cruising regime is used in flight over a route, at long range in altitude and high-speed conditions.

Relation between thrust at maximum and cruising processes equals:

$$R_{\text{кр}} = (0,70 \div 0,75) R_{\text{max}} \approx 0,85 R_{\text{ном}};$$

in this case

$$n_{\text{кр}} \approx 0,9 n_{\text{max}}.$$

The indicated regime is frequently called "maximum cruising."

### 11.6.4. Economic Regime (Reduced Cruising Regime)

This regime can be obtained with deeper throttling of the engine; it corresponds approximately to the regime of operation with minimum specific fuel consumption; the relation between thrusts at reduced cruising regime equals:

$$R_{\text{нк}} = (0,5 \div 0,6) R_{\text{max}} \approx (0,60 \div 0,75) R_{\text{ном}}$$

Even more reduced regimes of operation is possible.

#### 11.6.5. Regime of Idling

This regime corresponds to the minimum revolutions at which steady operation is possible of the engine for a limited time (10-15 min) is possible. The thrust in this regime must be 3-5% of the maximum (when  $R_{\text{max}} = 5,000$  kgf we have  $R_{\text{м.г.}} = 150-250$  kgf). This thrust must be sufficient for taxiing an aircraft on an airfield. It must not be excessive to avoid an increase in the run of an aircraft when landing with an operating engine.

Usually,

$$n_{\text{м.г.}} = 0,2 \div 0,4 n_{\text{max}}$$

In the process of idling permissible gas temperature behind the turbine must be regulated.

In a number of cases (special, extreme), in the practice of foreign aircraft engine construction, the so-called *extreme regime* has been introduced. In this (forced) regime the engine, in the case of an emergency situation, must operate for 1-2 minutes without breakdown.

One must distinguish between ground and also altitude and high-speed regimes.

Sometimes the boosting of an engine (i.e., short-term increase in thrust of the gas turbine) on takeoff and in flight is carried out with the help of water injection an the entrance into the compressor (DTRD Rolls-Royce "spey," TRD Rolls-Royce "Tyne") or the afterburning of fuel in the afterburner (TRDF Bristol-Siddley "Olympus" 593), etc.

### 11.7. Effect of External Atmospheric Conditions on the Work of the Turbojet Engine

Above we examined in detail throttle characteristic of the TRD, assuming with its analysis that the external atmospheric conditions remain constant. However, external conditions (temperature  $T_H$  and pressure  $p_H$ ) in itself have a substantial effect on parameters of the working process, regime of operation and basic indices of the turbojet engine.

Let us explain this in detail: let us assume that the number of revolutions of the engine and position of the control elements remain constant (i.e.,  $n = \text{const}$  and  $f_5 = \text{const}$ ).

Let us examine from the beginning the case of the increase in external pressure. An increase in  $p_H$  and, consequently, air density, leads to an increase in the mass flow of air through the engine. Since the change in  $p_H$  causes a proportional change in pressure along the whole channel of the engine, the velocity of outflow of gas from the jet nozzle and, consequently, the specific thrust of the TRD do not change. Ultimately, the total thrust of the TRD increases, and this growth is proportional to the growth in external pressure. With a reduction in  $p_H$ , conversely, thrust of the TRD drops.

Let us now examine the case when external air temperature is decreased. A reduction  $T_H$  leads to an increase in the mass flow of air through the engine (air density  $\rho_H$  increases); furthermore, the specific thrust of the TRD grows up, since with the same expended work for the compression of 1 kg of air

$$L_n = 102,57 \pi_n^{0,238} - 1) \frac{1}{\eta_c} = \text{const}$$

values of the compression ratio of the compressor increase, and, as consequence, temperatures and pressures of the gas at the entrance into the jet nozzle increase. Ultimately the velocity of outflow  $c_5$  from the jet nozzle of the engine increases. Thus, the total thrust of the TRD increases and as a result of the change in its two components ( $G_B$  and  $R_{yA}$ ) and not one ( $G_B$ ), as in the preceding case.

The increase in  $T_H$ , conversely, leads to a drop in thrust of the TRD.

One should keep in mind that the relative oscillations in external pressure are small. Actually, the real change in  $t_H$  from  $-45^\circ\text{C}$  in winter to  $+45^\circ\text{C}$  in summer of the relatively standard temperature ( $t_H = +15^\circ\text{C}$ ) consists of magnitude

$$\overline{\Delta T} = \frac{\Delta T}{T_{cr}} = \frac{90}{288} \approx 31\%.$$

A change in  $p_H$  from 720 mm Hg of the relative standard value  $p_H = 760$  mm Hg gives only

$$\overline{\Delta p} = \frac{\Delta p}{p_{cr}} = \frac{60}{760} = 8\%.$$

Thus, the change in external temperature has a greater total effect on operation of the engine than does change in external pressure. This circumstance is a well proven and established experimental fact.

Thus, for instance, it has been noted that with the exploitation of aircraft with TRD under conditions of the far north engines develop substantially greater thrust (30-40%) than in southern latitudes.

It is known likewise that stationary gas-turbine power units at thermal power stations in Switzerland with operation of them in the winter develop a power 30-40% greater than that with operation in the summer.

From the experience of operation of the TRD in air transport it is known that an increase in  $T_H$  from  $+15^\circ\text{C}$  to  $+30^\circ\text{C}$  (i.e., 5%)<sup>1</sup> leads to a thrust drop in the TRD of 7-11%.

Figure 11.20 shows the effect of  $T_H$  and  $p_H$  on throttle characteristics of the TRD.

---

<sup>1</sup>  $\overline{T}_H = \frac{303}{288} = 1.05.$

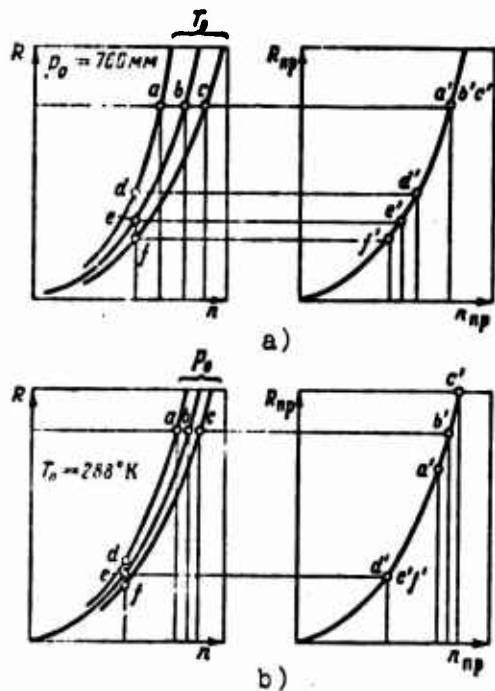


Fig. 11.20. Comparison of normal and universal (reduced) characteristics of the TRD.

Thus, a change in external atmospheric conditions has a considerable effect on the operation of the TRD. The question arises how to take into account the effect of atmospheric conditions on throttle characteristic of the engine. Indeed test bench characteristics of the TRD are taken at various atmospheric conditions. Which indices of the engine should one record in his service record? How does one compare characteristics between each other, for example, of engines of the same series taken at different values of  $p_H$  and  $T_H$ ?

It would be senseless to attempt to take characteristics of the TRD accurately at the same atmospheric conditions. It is obvious that the correct solution to the problem of considering the effect of external atmospheric conditions on characteristics of TRD is in order to: exclude this effect, having taken certain atmospheric conditions as "standard"; reduce results of tests obtained under any conditions to these standard conditions, and, consequently, constant any throttle characteristic of the TRD only for these conditions.

Accepted as standard have been these conditions:  $t_H = +15^\circ\text{C}$  ( $T_H = 288^\circ\text{K}$ );  $p_H = 760$  mm Hg. Conversion of the characteristic of

the TRD, obtained under any external conditions, into standard characteristics is done with the help of the theory of gas-dynamic similarity.

#### 11.8. Application of the Theory of Gas-Dynamic Similarity to the Turbojet Engine

In examining the TRD as an aggregate of separate gas-dynamic elements - inlet device, compressor, combustion chamber, turbines and jet nozzle, - one should draw the conclusion that the gas-dynamic similarity of the TRD as a whole assumes the observance of the similarity of all of its parts. However, it is possible to show that in several elements of the engine gas-dynamic similarity is rarely observed; such elements are the intake and jet nozzle. In other elements of the TRD, as, for instance, in combustion chambers and afterburners, the realization of similar regimes appears generally impossible. The theory of the gas-dynamic similarity is applicable mainly to turbomachines: compressor (fan) and turbine.

Thus, it is more correct to speak not about the *complete similarity* of the regime of operation of the turbojet engine (which does not exist in nature) but about the *partial similarity* of the TRD, understanding by it the similarity of regimes of operation of its turbocompressor part.

Let us look at this question in detail.

##### 11.8.1. Intake System

It is known that a necessary condition of gas-dynamic similarity is kinematic similarity, i.e., the similarity of the configuration of flows and the proportionality of velocities at similar points.

Let us examine the spectrum of flow lines of the standard intake on a test stand ( $V = 0$ ) even in flight ( $V > 0$ ) (Fig. 11.21a and b).

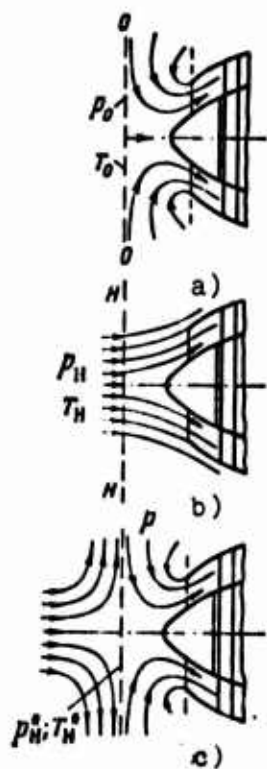


Fig. 11.21. Spectrum of flow lines of inlet device on a test stand and in flight.

On a test stand (see Fig. 11.21a) flow lines at the entrance into the engine converge in the form of a funnel, forming a natural convergent channel. Along each elementary stream the pressure and temperature drop, and the gas velocity increases.

In flight (see Fig. 11.21b), as a result of the deceleration of flow, the flow lines diverge, forming a diffusion channel with "fluid" walls. Now along each elementary stream the pressure and temperature of the gas increase, and the velocity is lowered.

A comparison of spectra of inflow on the two named regimes shows that the geometrical and kinematic similarity of flows entering into the engine is absent; consequently, the gas-dynamic similarity is also absent. At supersonic flight speed there appear shock waves at the entrance into the engine, which continuously (with a growth in velocity) introduce qualitative changes into the physical streamline flow and change the fields of velocities, pressures and temperatures. Thus, the *subsonic and supersonic regimes of the intake system in principle can be similar in a gas-dynamic respect.*

The aforesaid can be generalized in the following manner: since in undisturbed sections of flow on the test stand and in flight  $M$  numbers are not equal, i.e.,

$$M_{(V > 0)} \neq M_{(V=0)},$$

then the gas-dynamic similarity of regimes of operation of the intake of the engine is provided automatically.

Kinematics of the flow entering into the TRD for the case of flight can conditionally be reduced to the case of operation of the intake on the test stand, if we assume that there always exists a certain zone (region) in front of the engine on the border of which the flow is completely braked ( $V=0$ ;  $\rho=\rho_n^*$ ;  $T=T_n^*$ ). With respect to this zone lines of flow have exactly the same form, as those in the case of air inflow on the test stand. Consequently, for case of flight with velocity  $V$  the process at the entrance into the engine can be represented as consisting of adiabatic deceleration (up to parameters  $V=0$ ;  $T_n^*=T_n + \frac{V^2}{2gc_p/A}$ , etc.) and subsequent acceleration of flow in front of the entrance into the compressor (see Fig. 11.21c) [sic].

Such a model of flow, being conditional, in a number of cases considerably simplifies the analysis and calculations of characteristics of the TRD.

#### 11.8.2. Jet Nozzle

Flows in the jet nozzle of the TRD at different flight speeds, generally speaking, are not similar, since on a test stand and in flight expansion ratios of gas in the jet nozzle

$$\pi_{p,e} = \frac{p_e}{p_n} \neq \text{const}$$

are different, and, consequently,  $M_5$  numbers at the exit from the engine are different.

If, however, the jet converging nozzle operates on critical pressure differentials, i.e.,

$$\frac{p_4^*}{p_1} > \pi_{*p} = \left(\frac{k+1}{2}\right)^{\frac{k}{k-1}}$$

then on the section of the nozzle  $M_5 = 1 = \text{const}$ , and such a nozzle operates in a similar regime.

For a jet nozzle of the Laval type of nozzle similar regimes - are regimes of underexpansion when  $p_4 > p_a$ .

### 11.8.3. Combustion Chamber

Flows of gas in combustion chambers (or in afterburners) cannot be similar. Actually, in similar regimes the following conditions must be observed:

$$\frac{T_3^*}{T_2^*} = \text{const} \quad (1)$$

(similarity of temperature fields)

$$\alpha = \text{const.} \quad (2)$$

(constancy of the coefficient of air surplus as a dimensionless parameter)

Having noted that

$$\alpha \sim \frac{1}{T_3^* - T_2^*} = \text{const.} \quad (3)$$

we come to the conclusion that the observance of conditions (1) and (3) is possible only when

$$T_2^* = \text{const and } T_3^* = \text{const.}$$

However, this will denote no longer the similarity but the identity of gas flows.

It is easy to conclude that with a change in regime of the engine (for example, number of its revolutions), and also the

regime of flight (for example, speed and altitude of flight) the regime of operation of combustion chamber changes.

#### 11.8.4. Compressor

Conditions of the observance of similarity of regimes of operation of the compressor are the equality of M numbers with respect to axial and circumferential velocities or magnitudes proportional to them, i.e.,

$$M_{1a} \sim q(\lambda_{1a}) \sim \bar{G}_n = \text{const}; \quad (1)$$

$$M_u \sim \bar{n} \sim \lambda_u = \text{const}. \quad (2)$$

In similar regimes

$$\pi_n^* = \text{const}; \quad \eta_n^* = \text{const}; \quad \bar{L}_{a,n}^* = \text{const}; \quad \bar{N}_n = \text{const}, \text{ etc.}$$

#### 11.8.5. Turbine

The condition of the observance of the similarity of regimes of operation of the turbine is also the constancy of two M numbers with respect to axial and circumferential velocities:

$$M_{1a} \sim q(\lambda_{1a}) \sim \bar{G}_t = \text{const}; \quad (1)$$

$$M_u \sim \bar{n} \sim \lambda_u = \text{const}. \quad (2)$$

In similar regimes

$$\pi_t^* = \text{const}; \quad \eta_t^* = \text{const}; \quad \bar{N}_t = \text{const}; \quad \bar{L}_{a,t}^* = \text{const}.$$

#### 11.8.6. Turbojet Engine

Conditions of the observance of partial similarity of regimes of a geometrically invariable TRD are equalities:

$$1) M_0 = \text{const} \text{ and } 2) M_u = \text{const}.$$

For a test stand ( $M_0 = 0$ ) fulfillment of the single condition  $M_i = \text{const}$  is necessary.

In similar regimes the relative and dimensionless parameters of the TRD maintain the invariable value.

Consequently,

$$\eta_0 = \text{const}; \bar{R} = \text{const}; \bar{C}_{y_1} = \text{const}; \bar{G}_1 = \text{const}, \text{ etc.}$$

#### 11.8.7. Formulas of Similarity

Using the basic positions of the theory of similarity, correlations between parameters of the engine in similar regimes can be found. For this purpose it is necessary to present the investigated parameter of the TRD as a function of three parameters of flow in any  $i$ -th section: pressure  $p_i$ , temperatures  $T_i$  and velocity  $c_i$ ; then, using the property of similar flows - constancy of ratios of pressures and temperatures in any sections and the invariability of  $M_i$  - one should express the parameter of the TRD as a function of magnitudes  $p_H^*$  and  $T_H^*$ .

The connection between gas parameters in sections " $i$ " and " $H$ " has the form

$$p_i \sim p_H^*; \quad T_i \sim T_H^*;$$

$$c_i \sim \sqrt{T_i} \sim \sqrt{T_H^*} \quad (\text{since } M_i = \text{const}).$$

##### 11.8.7.1. Formula of Similarity for Thrust.

We have

$$R = \frac{G}{g} (c_s - V);$$

further we find

$$(c_s - V) \sim \sqrt{T_H^*};$$

$$G \sim \frac{p_i^*}{\sqrt{T_i^*}} \sim \frac{p_H^*}{\sqrt{T_H^*}};$$

Then

$$R \sim p_n^*$$

Consequently, in similar regimes

$$\frac{R}{p_n^*} = \text{const.} \quad (11.13)$$

#### 11.8.7.2. Formula of Similarity for Specific Fuel Consumption.

We have

$$C_{yx} = \frac{8.43V}{H_n \eta_0} \sim \sqrt{T_n^*} \quad (\text{since } \eta_0 = \text{const and } H_n = \text{const});$$

consequently,

$$\frac{C_{yx}}{\sqrt{T_n^*}} = \text{const.} \quad (11.14)$$

#### 11.8.7.3. Formula of Similarity for Fuel Consumption Per Hour (Per Second).

We have

$$G_T = RC_{yx}$$

Using (11.13) and (11.14), let us write

$$G_T \sim p_n^* \sqrt{T_n^*}$$

Consequently,

$$\frac{G_T}{p_n^* \sqrt{T_n^*}} = \text{const.} \quad (11.15)$$

#### 11.8.7.4. Formula of Similarity for Specific Thrust.

We have

$$R_{yx} = \frac{g_s - V}{g} \sim \sqrt{T_n^*}$$

Consequently,

$$\frac{R_{yx}}{\sqrt{T_n^*}} = \text{const.} \quad (11.16)$$

### 11.8.8. Reduction of Parameters of the Turbojet Engine to Standard Atmospheric Conditions

In order that it is possible to use characteristics of the TRD taken on the test stand or in flight independent of external conditions, and in order that these characteristics are *universal*, results of tests and parameters of gas flow and the engine must be reduced to standard atmospheric conditions. Accepted as such conditions are:  $p_{CT} = 760$  mm Hg;  $T_{CT} = 288^\circ\text{K}$ .

Using formulas of similarity for two regimes (measured and standard), the so-called reduction formula can be obtained.

#### 11.8.8.1. Reduction Formula for the Turbojet Engine.

The reduction formula of thrust.

We have

$$\frac{R}{P_n} = \frac{R_{rp}}{P_{CT}}$$

whence

$$R_{rp} = R_{stn} \frac{P_{CT}}{P_n} = R_{stn} \frac{760}{P_n}. \quad (11.17)$$

For test stand conditions ( $V = 0$ )

$$R_{rp} = R_{stn} \frac{760}{P_0}. \quad (11.18)$$

Reduction formula of specific fuel consumption.

We have

$$\frac{C_{ya}}{\sqrt{T_n}} = \frac{C_{ya(rp)}}{\sqrt{T_{CT}}}$$

whence

$$C_{ya(rp)} = C_{ya(stn)} \sqrt{\frac{T_{CT}}{T_n}} = C_{ya(stn)} \sqrt{\frac{288}{T_n}}. \quad (11.19)$$

For test stand condition ( $V = 0$ )

$$C_{YA(nP)} = C_{YA(32M)} \sqrt{\frac{288}{T_0}} \quad (11.20)$$

Reduction formula of the number of revolutions.

We have

$$n_{nP} = n_{32M} \sqrt{\frac{288}{T_0}} \quad (11.21)$$

For test stand conditions

$$n_{nP} = n_{32M} \sqrt{\frac{288}{T_0}} \quad (11.22)$$

#### 11.8.9. Representation of Characteristics of the Turbojet Engine in Parameters of Similarity

In order that the characteristics of the TRD are universal, they are plotted in parameters of similarity in the form of these dependences:

$$R_{nP} = f_1(n_{nP}); \quad C_{YA(nP)} = f_2(n_{nP}); \quad T_{3(nP)} = f_3(n_{nP}).$$

It is easy to see which great convenience is the use of universal characteristics of the TRD. The whole variety of throttle characteristics of thrusts, plotted for various values of  $T_0$  and  $p_0$  (see Fig. 11.20), is turned into a single thrust curve, represented in parameters of similarity.

Let us intersect the family of characteristics  $R = f(n, T_0)$  horizontally (see Fig. 11.20a), and let us note the obtained points of the intersection ( $a$ ,  $b$  and  $c$ ). On the appropriate universal characteristic  $R_{nP} = f(n_{nP})$ , these three points will be depicted in the form of a single point  $a'$  (the same value of reduced revolutions  $n_{nP}$  at various  $T_0$  correspond to different values of physical revolutions  $n$ ).

If, however, we dissect the family of these characteristics by a vertical line, then the obtained points of the intersection ( $d$ ,  $e$

and  $f$ ) will be depicted on the universal characteristic of the TRD in the form of three points:  $d'$ ,  $e'$ , and  $f'$  with different values of reduced revolutions (the same value of  $n$  at different  $T_0$  correspond to different values of  $n_{np}$ ).

Let us now dissect the family of characteristics  $R = f(n, p_0)$  by a horizontal line (see Fig. 11.20b) with points of intersection  $a$ ,  $b$  and  $c$ . On the universal characteristic these points will be depicted also in the form of three points  $a'$ ,  $b'$  and  $c'$  (different values of  $n$  when  $T_0 = \text{const}$  correspond to different values of  $n_{np}$ ). Points  $d$ ,  $e$  and  $f$ , lying on the vertical line, are depicted in the form of a single point  $d'$  on the universal characteristic (since when  $T_0 = \text{const}$  and  $n = \text{const}$  we have also  $n_{np} = \text{const}$ ).

Results of test stand tests of the TRD are reduced to standard atmospheric conditions in the following manner:

1) in accordance with the checked reduced revolution number and external conditions, we determine the physical number of revolutions which the engine must develop, i.e.,

$$n_{\text{act}} = n_{rp} \sqrt{\frac{T_0}{288}}$$

2) on the obtained number of revolutions parameters of engine - thrust, specific fuel consumption, etc., are measured;

3) according to reduction formula (11.17)-(11.22) we determine the reduced values of parameters of the engine and compare them with the reduced characteristic.

The divergence between reduced parameters of different engines of the same series (when  $n = \text{const}$ ) must not exceed 0.5-1.0%. In this case the engines correspond to technical requirements.

With the help of the reduction formula it is possible to solve the inverse problem: determine real parameters of the TRD corresponding to any atmospheric conditions.

## C H A P T E R 12

### HIGH-SPEED CHARACTERISTICS OF TURBOJET ENGINES

Definition. *High-speed characteristics, or characteristics with respect to flight speed,* of turbojet engines are called dependences of thrust and also of specific fuel consumption on flight speed at the assigned program of control of the engine. High-speed characteristics are frequently supplemented by curves of temperature change in the gas in front of the turbine, fuel consumption per hour, and also other magnitudes important in operation.

#### 12.1. High-Speed Characteristics of Single-Shaft Turbojet Engines Without Afterburners

Let us examine high-speed characteristics of single-shaft TRD without afterburners with a program of adjustment for maximum thrust.

Let us analyze the peculiarities of *approximate* characteristics of the TRD obtained by calculation without the use of characteristics of elements of the engine: compressor, combustion chamber, turbine and jet nozzle, considering only the change in gas-dynamic losses in the intake at supersonic flight speeds.

As the basic conditions placed as the basis of the calculation of these characteristics let us take the following:

- 1) constant flight altitude  $H = \text{const}$ ;
  - 2)  $n = n_{\text{max}} = \text{const}$ ;
  - 3)  $T_3^* = T_{3(\text{max})}^* = \text{const}$
- } program of adjustment for maximum thrust.

The basic assumptions usually taken in approximate calculations of high-speed characteristics include:

1) constancy of work of the compressor, i.e.,  $L_k = \text{const}$  when  $n = \text{const}$ ;

2) constancy of efficiency and coefficients of losses of elements of the TRD, i.e.,  $\eta_k^* = \text{const}$ ;  $\eta_r^* = \text{const}$ ;  $\sigma_{k,c}^* = \text{const}$ ;  $\varphi_{p,c} = \text{const}$ ;  $\xi_{k,c} = \text{const}$ .

The roughest assumption is the one about the constancy of efficiency of the compressor. The effect of  $\eta_k^* = \text{var}$  on the high-speed characteristic of the TRD is examined below. As the dependence  $\sigma_{\text{min}}^* = f(V)$  is possible to use the curve given in Fig. 5.7 for the supersonic adjustable diffuser;

3) complete expansion of the gas in the jet nozzle of the TRD, i.e.,  $p_3 = p_{11}$ .

The last assumption assumes the system of the all-regime adjustable jet nozzle of the Laval type of nozzle.

#### 12.1.1. Generalized Characteristics of Compressors and Turbines

An accurate calculation of altitude-high-speed characteristics of aircraft gas turbine engines is very complex and extremely "individualized," since it requires the use of specific characteristics of compressors and turbines.

Analysis of experimental characteristics of a large number of compressors allowed R. M. Fedorov to find and N. D. Tikhonov to refine the semi-empirical dependences of the effect of the computed value  $\pi_{k0}^*$  on the regularity

$$\bar{L}_k = f(n_{np}) \text{ and } \eta_k^* = f(n_{np})$$

with the program of adjustment  $n = \text{const}$  (Figs. 12.1 and 12.2).

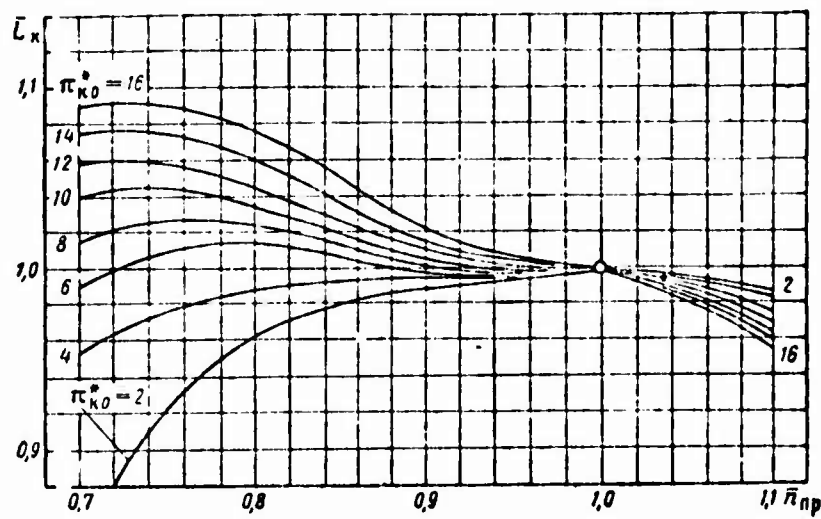


Fig. 12.1. Effect of  $\pi_{k0}$  on the dependence  $L_k = f(\pi_{np})$  when  $n = \text{const}$ .

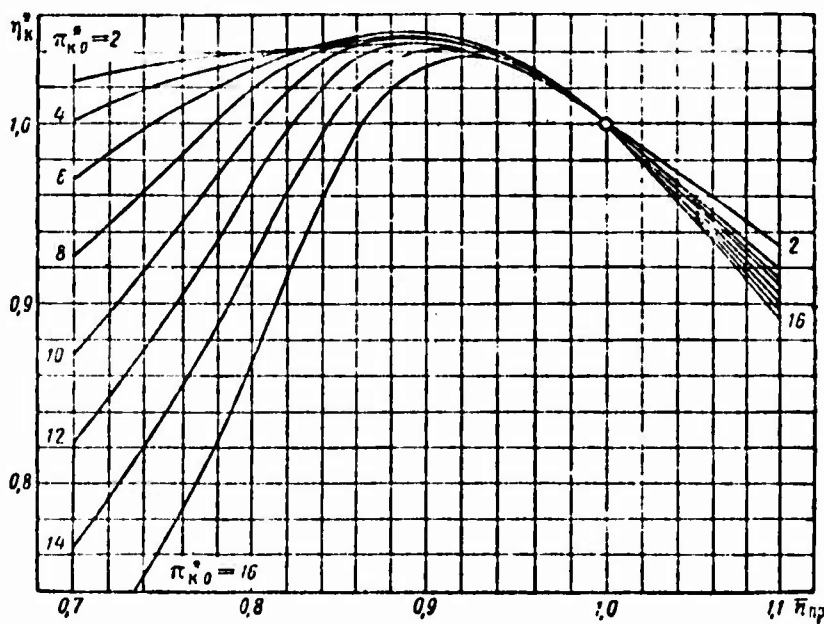


Fig. 12.2. Effect of  $\pi_{k0}$  on dependence  $\eta_k = f(\pi_{np})$  when  $n = \text{const}$ .

The obtained dependences must be examined as certain generalized characteristics of compressors; they can be used for the approximate calculation of altitude-high-speed characteristics of aircraft GTD.

Regularities  $L_k = f(\pi_{np})$  can be explained in the following manner. With an increase in  $T_2^*$  the axial velocity at the exit from the compressor.<sup>1</sup> The axial velocity at the entrance into compressor increases at small values  $\pi_{n0}^*$  and decreases<sup>1</sup> at large values  $\pi_{n0}^*$ . Thus, with the increase in  $T_2^*$  there is redistribution of axial velocities along the compressor; when  $u = \text{const}$  this leads to a change in angles of incidence of flow on rotor blades and, consequently, to a change in the operation of separate stages. As a result at small values  $\pi_{n0}^*$  ( $< 6$ ) with an increase in  $T_2^*$ , due to the decrease in angles of incidence of flow in all stages, the operation of the compressor is decreased; at large values of  $\pi_{n0}^*$  ( $> 6$ ) the work of the compressor increases; when  $\pi_{n0}^* \approx 6$  changes in  $\Delta L_{ct}$  compensate each other, and  $L_k \approx \text{const}$ .

Used in calculated practice frequently are simplified relations when evaluating works of the compressor in the form

$$L_k = \text{const} \text{ and } \eta_k^* = \text{const} \text{ when } n = \text{const}$$

and when evaluating the work of the turbine - in the form

$$L_t = \text{const}, \frac{G_t}{P_3} \sqrt{T_3^*} \sim q(\lambda_{c,t}) = \text{const} \text{ and } \eta_t^* = \text{const}.$$

#### 12.1.2. Effect of Flight Speed on Compression Ratio of Air in the Turbojet Engine

With an increase in the flight speeds the dynamic compression ratio

$$\pi_d = \frac{P_1}{P_n} = (1 + 0.2M_n^2)^{3.5} \sigma_n^*$$

and also the kinetic heating of air in front of the engine.

An increase in stagnation temperature at the entrance into the compressor

---

<sup>1</sup>From the equation of flow for sections 2-2 and c.c-c.c. under the condition that  $T_2^* \approx \text{const}$ , it follows that  $q(\lambda_{c,t}) \sim \sqrt{T_2^*}$ ; on the other hand  $c_{1a} \sim c_{2a} \pi_n^{\frac{1}{n}}$

$$T_2^* = T_1 (1 + 0.2M_0^2)$$

at the same magnitude of expended work

$$L_{\text{tr}} = 102.5 T_1^* (\pi_k^{0.386} - 1) \frac{1}{\eta_k} = \text{const}$$

leads to the fact the compression ratio of the compressor monotonically drops; magnitude  $\pi_k^*$ , with an increase of  $M_0$  number, asymptotically approaches unity.

However, the total compression ratio of the air

$$\pi = \pi_A \pi_k^* = (\epsilon_{\lambda_0}^* + 0.2M_0^2)^{3.5}$$

in this case increases, since the growth in  $\pi_A$ , which proves to be greater the less losses in shock waves appearing in the intake, is the determining one.

Figure 12.3 shows curves of the change in compression ratios  $\pi$ ,  $\pi_k^*$  and  $\pi_A$  with respect to flight speed (according to  $M_0$  number).

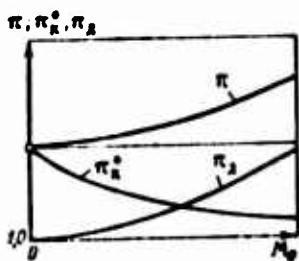


Fig. 12.3. Effect of flight speed on compression ratio of the TRD.

### 12.1.3. Change in Specific Thrust

With an increase in the flight speed the total compression ratio and, consequently, and total expansion ratio continuously increases. Since the pressure differential on the turbine remains constant (when  $\lambda_3 \geq 1$  always  $\pi_t^* = \text{const}$ ), then the expansion ratio of the gas in the jet nozzle continuously grows up also:

$$\pi_{p,c} = \frac{P_4^*}{P_8} = \frac{\pi_p}{\pi_t^*} = \frac{\pi_{p,c}^*}{\pi_t^*} \sim \pi,$$

and it increases in proportion to the compression ratio.

The gas temperature behind the turbine in this case maintains an invariable value:

$$T_4^* = T_3^* - \frac{L_7}{118} = \text{const} \quad (\text{since } T_3^* = \text{const} \text{ and } L_7 = \text{const}).$$

As a result the velocity of expiration of the gas from the jet nozzle, equal to

$$c_8 = \sqrt{2g \frac{c_p}{\lambda} T_4^* \left[ 1 - \left( \frac{p_8}{p_4} \right)^{\frac{k-1}{k}} \right]}.$$

also continuously increases.

The specific thrust

$$R_{ya} = \frac{c_8 - V}{g}$$

with an increase flight velocity is lowered, since a velocity increase in outflow from the nozzle occurs considerably slower than the increase in flight speed (Fig. 12.4).

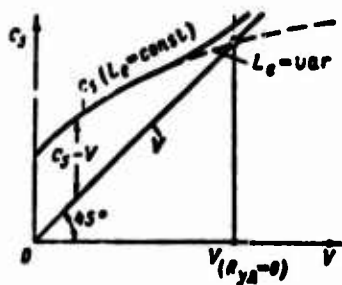


Fig. 12.4. Change in velocity of outflow from the nozzle with respect to flight speed.

The drop in specific thrust of the TRD on flight speed (Fig. 12.5) can be explained still differently.

With an increase in compression ratio when  $T_3^* = \text{const}$  the effective work of the cycle  $L_g$  (being on a test stand close to maximum) drops, approaching zero. Consequently, the specific thrust, as this results from expression

$$R_{ya} = \frac{1}{g} (\sqrt{2gL_g + V^2} - V),$$

also with an increase in  $V$  it approaches zero.

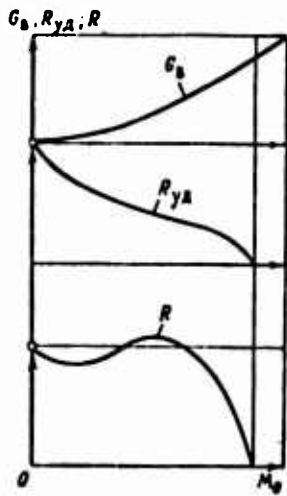


Fig. 12.5. Effect of flight speed on specific thrust, flow of air and total thrust of the TRD.

#### 12.1.4. Change in Air Flow

With an increase in the flight speed the mass flow of air through the engine continuously increases and is proportional to the total compression ratio. It is easy to be convinced of this, having written the expression of the rate of air flow for the critical (throttling) section of the nozzle box of the turbine:

$$G_a \approx G_r = m \frac{p_{c,a}^{\circ}}{\sqrt{T_{c,a}^{\circ}}} f_{c,a}(\lambda_{c,a}),$$

whence we obtain that

$$G_a \sim p_2^{\circ} \sim \pi,$$

since

$$\begin{aligned} T_{c,a}^{\circ} &= T_3^{\circ} = \text{const}; \\ q(\lambda_{c,a}) &= 1 = \text{const}; \\ p_n &= \text{const}. \end{aligned}$$

Figure 12.5 shows the dependence  $G_a = f(M_0)$ .

#### 12.1.5. Change in Total Thrust

The change in total thrust of the TRD with respect to flight speed is determined by regularities of the change in its factors: specific thrust and flow of air, i.e.,

$$R = R_{ya} G_a.$$

Figure 12.5 shows the curve of the change in total thrust  $R$  TRD depending on flight speed ( $M_0$ ). With an increase in  $V(M_0)$  in the region of small values  $M_0$  ( $M_0 < 0.4-0.5$ ) the thrust initially drops, since the lowering of specific thrust is still not compensated by the thrust in mass flow of air; in transonic and supersonic regions of flight the thrust of the TRD increases, and at small compression ratios of the compressor ( $\pi_{\text{co}}^* = 3-5$ ) can considerably exceed the test bench value of thrust  $R_0$ . Such a regularity is explained by the intensive increase in flow of air in combination with the more moderate drop in specific thrust. Finally, at high supersonic flight speeds the thrust of the TRD, having attained a maximum, then drops down to zero in accordance with an inevitable tendency of the drop in specific thrust.

#### 12.1.6. Change in Efficiency of the TRD

Let us examine how with respect to flight speed efficiency of the TRD - effective, tractive and general is changed.

##### 12.1.6.1. Effective Efficiency.

From expression

$$\eta_e = \frac{AL_u}{q_{\text{in}}} = \frac{\frac{c_p^2 - V^2}{2g}}{c_{pm}(T_3^* - T_2^*)} \xi_{\text{K.C}}$$

it follows that the change in effective efficiency is determined by the regularity of the change in useful work of the cycle and introduced (with fuel) heat with respect to the flight speed (Fig. 12.6).

Since the quantity of introduced heat imparted to 1 kg of air with an increase in  $V$  is continuously decreased (due to the increase in air temperature at the entrance into the combustion chamber), and the work of the cycle at subsonic flight speeds changes little, then the magnitude  $\eta_e$  increases initially. At high supersonic

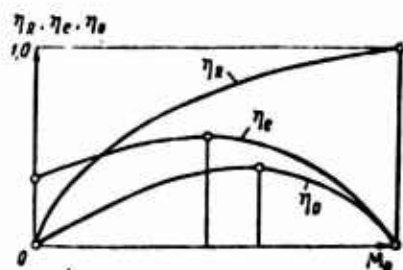


Fig. 12.6. Change in efficiency with respect to flight speed.

flight speeds the increasing drop in work of the cycle leads to a continuous lowering of parameter  $\eta_e$  (down to zero).

#### 12.1.6.2. Thrust Efficiency.

The magnitude of thrust efficiency is determined from the expression

$$\eta_R = \frac{L_R}{L_e} = \frac{2V}{V + c_5}.$$

When  $V = 0$  we have  $\eta_R = 0$ ; when  $V = c_5$  we have  $\eta_R = 1.0$ .

Consequently, with an increase in flight speed the magnitude of thrust efficiency  $\eta_R$  increases from zero to unity (see Fig. 12.6). Thus, with an increase in flight speeds losses of energy with the exhaust velocity are continuously decreased. However at the moment when these losses completely disappear and thrust efficiency reaches the maximum possible theoretical value, thrust of engine disappears.

#### 12.1.6.3. Total Efficiency.

From expression

$$\eta_0 = \frac{AL_R}{q_{00}} = \eta_e \eta_R$$

it follows that a change in total efficiency of the TRD with respect to flight speed is determined by regularities of the change in partial efficiencies: internal and external (see Fig. 12.6).

When  $V = 0$  and when  $V = c_5$  the total efficiency becomes zero. With an increase in  $V$  the total efficiency increases, reaches a maximum at high supersonic velocity, and then drops to zero (see Fig. 12.6).

The change in total efficiency characterizes the economy of the TRD in the whole speed range of flight.

### 12.1.7. Change in Specific Fuel Consumption

The connection between specific fuel consumption and flight speed was determined earlier in terms of total efficiency in the form of expression (9.32):

$$C_{yA} = 8,43 \frac{V}{H_0 \eta_0}.$$

For the case of operation of a TRD on a test stand ( $V = 0$ ) formula (9.32) will become expression (9.35):

$$C_{yA(0)} = 4,215 \frac{c_{3(0)}}{\eta_{v(0)} H_0}.$$

Thus, on a test stand, when  $\eta_0 = 0$ , the specific fuel consumption has a quite definite finite value. For the best TRD

$$C_{yA(0)} = 0,71 + 0,76 \frac{\text{kg}}{\text{kgf} \cdot \text{h}}.$$

With an increase in the flight speed the specific fuel consumption increases, since the increase in total efficiency lags flight speed. At great flight speeds, when  $\eta_0$  reaches a maximum, and then is decreased, the increase in  $C_{yA}$  is intensified. With the approach of  $\eta_0$  to zero the specific fuel consumption approaches infinity.

A continuous increase in the specific fuel consumption with respect to flight speed does not at all indicate the continuous worsening of economy of the TRD, since parameter  $C_{yA}$  is not a criterion of economy. The economy of the TRD is made worse only in that range of flight speeds in which there approaches the drop in total efficiency. In the range of flight speeds from zero to the "economic" speed (at which  $\eta_0 = \eta_{0(\max)}$ ) the economy of the TRD continuously increases (Fig. 12.7).

What is the physical meaning of the continuous increase in  $C_{yA}$ ?

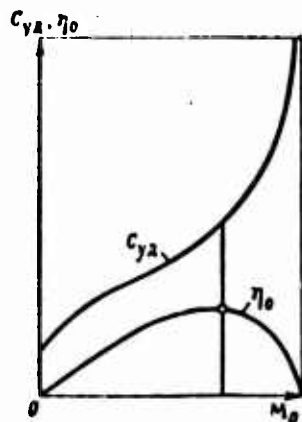


Fig. 12.7. Change in specific fuel consumption with respect to flight speed.

It is that the work of every kilogram of thrust with an increase in flight speed

$$L_{(N=1)} = 1 \cdot V$$

continuously increases. Consequently, the expended heat energy proportional to the expended fuel upon the receiving of this kilogram of thrust must increase; in other words, the specific fuel consumption  $C_{yD}$  increases.

#### 12.1.8. Effect of Parameters of the Working Process (Gas Temperature in Front of the Turbine and Compression Ratio of the Compressor) on Peculiarities of High-Speed Characteristics of the TRD

The given dependences of basic parameters of the TRD on flight speed have a fundamental nature. However, numerical values of specific and dimensionless parameters ( $R_{yD}$ ,  $C_{yD}$ ,  $\eta_e$ ,  $\eta_R$ ,  $\eta_0$ ), which characterize the perfection of the TRD, and magnitudes of flight speeds at which the thrust of the TRD becomes zero depend on the level of parameters of the working process of the TRD ( $T_3^*$  and  $\pi_{*0}$ ).

##### 12.1.8.1. Effect of $\pi_{*0}$ ( $T_3^* = \text{const}$ ).

Each value of complex  $aT_3^*\eta_p\eta_c/T_H$  corresponds to the entirely determined limiting magnitude of the total compression ratio of the TRD equal to

$$\pi_{max} = \left( \frac{aT_3^*\eta_p\eta_c}{T_H} \right)^{1/3} = \text{const} = \pi_{*0}$$

at which  $\sigma_5 = V$  and the useful work of the cycle becomes zero ( $L_e = 0$ ). Consequently, with an increase in the compression ratio of the compressor is a less dynamic compression ratio is necessary, i.e., less flight speed  $V_{\max}$ , for the achievement of  $\pi_{\max}$ .

Thus, with an increase in  $\pi_{\text{co}}$  the specific, and therefore, and total thrust, more sharply drop with respect to flight speed, reaching zero at less values of  $V_{\max}$  (Fig. 12.8). In accordance with the sharper drop in  $R_{yD}$ , there is a faster increase with respect to flight speed in the magnitude of specific fuel consumption, approaching infinity at less values of  $V_{\max}$ . The test bench value of  $C_{yD}$  in this case seems the less, the higher the magnitude  $\pi_{\text{co}}$ .

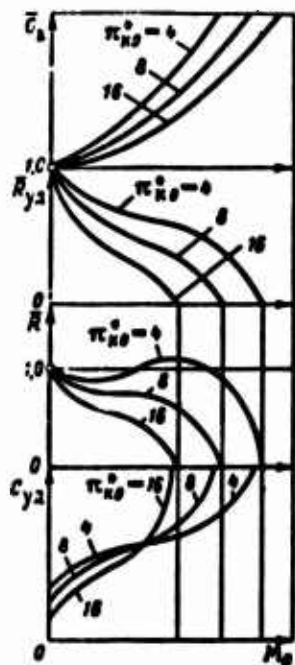


Fig. 12.8. Effect of calculated values  $\pi_{\text{co}}$  on high-speed characteristics of the TRD.

Curves of passages of air flow also depend on the numerical value  $\pi_{\text{co}}$ . The greater  $\pi_{\text{co}}$ , the less the portion of dynamic compression in comparison with the mechanical, the slower the rate of air flow increases with respect to flight speed (see Fig. 12.8).

Thus, larger values of  $\pi_{\text{co}}$  correspond to a sharper drop in  $R_{yD}$  and slower increase in  $C_T$ . This circumstance causes the deformation of curves of thrust of the TRD - with the increase in  $\pi_{\text{co}}$  "hump" on high-speed characteristics gradually disappears. When  $\pi_{\text{co}} > (10-12)$

and at usual values of  $T_3^*$  ( $\leq 1200^\circ\text{K}$ ) the thrust drops continuously in the whole range of speeds of flight (see Fig. 12.8).

An analysis of graphs, given in Fig. 12.8 shows that the use of high values  $\pi_{\lambda 0}^*$  ( $> 12-15$ ) sharply improves the economy of the TRD on the test stand and at subsonic flight speeds. Transition to reduced values  $\pi_{\lambda 0}^*$  (4-8) makes it possible to improve thrust characteristics and raise the economy of engines at supersonic flight speeds.

12.1.8.2. Effect of  $T_3^*$  ( $\pi_{\lambda 0}^* = \text{const}$ ) .

With an increase in gas temperature in front of the turbine, the effective work of the cycle and velocity of gas consumption from the jet nozzle increase. Consequently, the drop in specific thrust with respect to the flight speed is slowed down (Fig. 12.9). Ultimately the specific and total thrusts of the TRD become zero at larger values of  $\pi_{\text{max}}$  and  $V_{\text{max}}$ . Correspondingly, the specific fuel consumption reaches infinity also at larger values of  $V$ . However, with an increase in  $T_3^*$  the test stand value  $C_{yA}$  continuously increases.

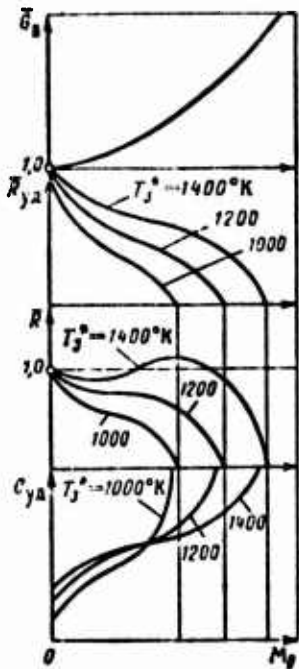


Fig. 12.9. Effect of calculated values  $T_3^*$  on high-speed characteristics of the TRD.

It is characteristic that an increase in  $T_3^*$  does not affect the

regularity of the change in air flow with respect to flight speed. However, passage of the characteristic of total draught becomes more favorable.

Finally, it is possible to note that for the improvement of the economy of work of the TRD on the test stand and at subsonic flight speeds one should use comparatively low values of  $T_3^*$  (1000-1200°K). At supersonic flight speeds an increase in  $T_3^*$  (1250-1300°K) improves the passage of the thrust characteristic and relatively lowers the specific fuel consumption.

Conclusion. To improve the economy of the TRD with its operation on the test stand and at subsonic flight speeds, one should use raised values of  $\pi_{i_0}^*$  and moderate significances of  $T_3^*$ . The use of small values of  $\pi_{i_0}^*$  and high values of  $T_3^*$  makes it possible to improve considerably the economy of the TRD and passage of thrust characteristics of the engine at high supersonic  $M_0$  numbers.

As an example Fig. 12.10 gives a high-speed characteristic of the TRD Rolls-Royce "Avon" with a compression ratio  $\pi_{i_0}^* = 10$ .

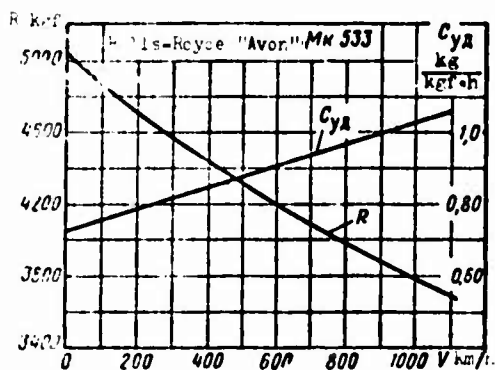


Fig. 12.10. High-speed characteristic of the TRD Rolls-Royce "Avon."

The data are given below on the economy of the TRD intended for the supersonic passenger aircraft "Concord" and Boeing B-2707.

The engine Bristol "Olympus" 593 at  $M_0 = 2.2$  and  $H = 11$  km has  $C_{ya} = 1.23$  kg/(kgf·h) and  $\eta_0 = 0.437$ .

The engine General Electric GE4/J5 at  $M_0 = 2.7$  and  $H = 11$  km has  $C_{yA} = 1.5$  kg/(kgf·h) and  $\eta_0 = 0.438$ .

12.1.9. Plotting of the Line of Operating Regimes of the TRD for the Program of Control  $n = \text{const}$  and  $T_3^* = \text{const}$

The plotting of the line of operating regimes of the TRD (Fig. 12.11) on the characteristic of the compressor for the program of control  $n = \text{const}$  and  $T_3^* = \text{const}$  occurs in such a sequence:

- 1) a series of values  $T_H^*$  is assigned;
- 2) for each value of  $T_H^*$  the reduced number of revolutions

$$n_{np} = n \sqrt{\frac{288}{T_H^*}}$$

and also reduced gas temperature

$$T_{3np}^* = T_3^* \frac{288}{T_H^*}$$

are found;

3) dotted on the characteristic of the compressor are points of the intersection of curves  $n_{np}(i)$  and lines  $T_{3np}^*(i)$ , and they are connected by a smooth curve. This curve is the sought line of operating regimes.

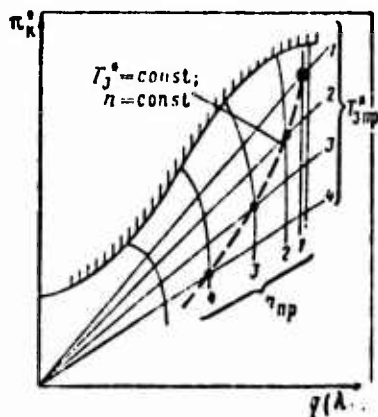


Fig. 12.11. Plotting of the line of operating regimes  $T_3^* = \text{const}$ .

12.1.10. Comparison of Lines of Operating Regimes  
for Two Programs of Control: 1)  $n = \text{const}$ ,  
 $T_3^* = \text{const}$  and 2)  $n = \text{const}$ ,  $f_5 = \text{const}$

Plotted on the characteristic of the compressor (Fig. 12.12),  
constructed in dimensionless coordinates

$$\bar{\pi}_k^* = f[\bar{q}(\lambda_1)],$$

is the line  $T_3^* = \text{const}$  and  $n = \text{const}$ ; its position does not depend  
on the numerical value of the compression ratio of the compressor  $\pi_{k,0}^*$ .  
Lines  $f_5 = \text{const}$  and  $n = \text{const}$  are also plotted there. Their  
position depends on value  $\pi_{k,0}^*$  — the higher  $\pi_{k,0}^*$ , the more sloping is  
the LRR.

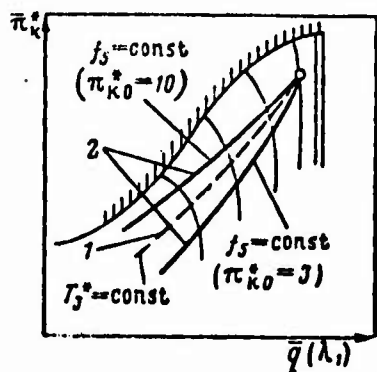


Fig. 12.12. Comparison of lines  
of operating regimes with two  
programs of control:

1— $n=\text{const}$  and  $T_3^*=\text{const}$ ;  
2— $n=\text{const}$  and  $f_5=\text{const}$

Figure 12.12 illustrates the fact that with transition to less  
values of  $n_{up}$  (by means of throttling or an increases in the flight  
speed) various cases of the change in  $T_3^*$  are possible.

12.1.11. High-Speed Characteristics of the Turbojet  
Engine with Program of Control at Complete  
Similarity of the Turbocompressor

The program of control for maximum thrust ( $n=n_{\text{max}}=\text{const}$ );  
 $T_3^*=T_{3(\text{max})}^*=\text{const}$ ) with its use over a wide range of supersonic  $M_0$   
numbers of flight, possesses the following important deficiencies.  
Actually, with a decrease in the reduced numbers of revolutions the  
regime point of the compressor is moved along the LRR (for example,  
from point 1 to point 4 in Fig. 12.13); in this case the efficiency  
of the compressor drops and its productivity, being determined by

magnitude  $q(\lambda_1)$ , is lowered, i.e.,

$$\eta_{k(4)}^* < \eta_{k(1)}^*$$

and

$$q(\lambda_1)_4 < q(\lambda_1)_1.$$

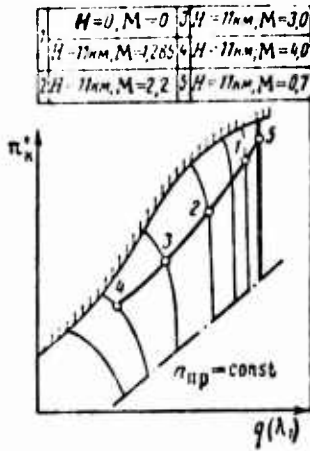


Fig. 12.13. Effect of speed and altitude of flight on the regime of operation of the turbo-compressor.

Thus at the calculated supersonic flight speed ( $M_0 = M_{0(4)}$ ) the flow passage sections and external diameter of the compressor appear oversized in comparison with their values on takeoff. Consequently, at the basic supersonic operating regime (at point 4) the compressor will be overloaded.

Furthermore, at considerable lowering of reduced numbers of revolutions surging can appear. For the prevention of it in flight, the simplest methods of control of the compressor can prove to be irrational. For example, the opening of the bypass valve at supersonic flight speed will lead to a considerable ejection of compressed air into surrounding medium, as a result of which  $\pi_k^*$  and  $\eta_k^*$  will drop and  $T_3^*$  will increase. All this will lead to a drop in thrust of the engine and a sharp worsening of its economy.

With operation of the TRD at great supersonic flight speeds, the program of control for complete similarity of turbocompressor<sup>1</sup> can prove to be expedient:

<sup>1</sup>Program of control "Point."

$$n_{np} = \text{const}; T_{3np} = \text{const}.$$

The essence of this program of control is that in the whole range of the change in velocities and altitudes of flight, the regime of operation of the turbocompressor is maintained constant. As such a regime we select the point (for example, point 1) on the characteristic of the compressor with sufficiently high values  $\eta_c^*$  and  $q(\lambda_1)$  and the necessary surging reserve.

To maintain this regime similar in all velocities and altitudes of flight, it is sufficient when  $f_5 = \text{const}$  and in the presence of a supercritical drop in pressures in the jet nozzle to provide fuel feed according to the law

$$G_{r(np)} = \text{const}, \text{ or } G_r \sim p_n^* \sqrt{T_n^*}.$$

Thus, conditions of operation the compressor and turbine according to the program of control "Point" appear stable and better.

Now let us examine what are the regularities of the change in thrust and specific fuel consumption with respect to the considered program.

With a decrease in the  $M_0$  number of flight and, consequently, magnitude  $T_H^*$ , the physical revolution numbers and also gas temperature in front of the turbine continuously drop (Fig. 12.14) in accordance with the property of similar processes on which

$$\frac{n}{\sqrt{T_n^*}} = \text{const} \text{ and } \frac{T_3^*}{T_n^*} = \text{const}.$$

The compression ratio of the compressor remains constant, whereas with the program of control  $n = \text{const}$  and  $T_H^* = \text{const}$  magnitude  $\pi_c^*$  increases with a decrease in  $T_H^*$ . Finally with a decrease in the flight speed the flow of air, specific thrust, and also total thrust of TRD sharply drop. The specific fuel consumption in this case can increase.

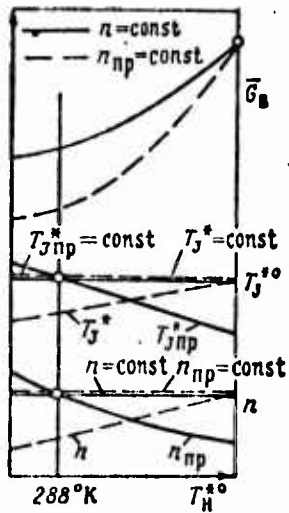


Fig. 12.14. Change in numbers of revolutions, air flow and  $T_3^*$  with two different programs of control.

The drop in total thrust of the TKD (Fig. 12.15) can prove to be so considerable (80-90% and more) that the takeoff thrust will be insufficient for flight of the aircraft. To prevent so sharp a drop in thrust, which appears greater, the more the maximum  $M_0$  number of flight, it is rational to use *combined* program of control, at which at small values of  $T_H^*$  (takeoff, climb, flight at subsonic speed) the program  $n_{np} = \text{const}$  and  $T_{3np}^* = \text{const}$ , and at high values of  $T_H^*$  (flight at great supersonic speed) the program  $n = \text{const}$  and  $T_3^* = \text{const}$  are carried out. Point 2 in Fig. 12.15 determines the  $M_0$  number of flight, which corresponds to the switching of programs of control.

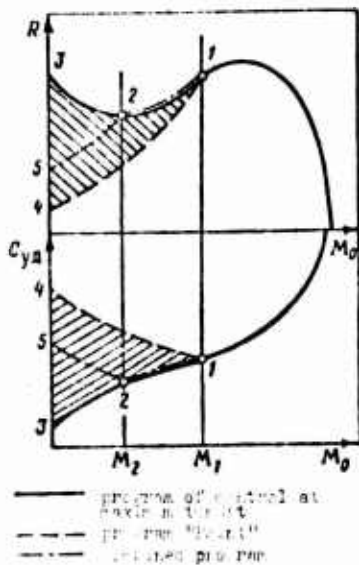


Fig. 12.15. Change in thrust and specific fuel consumption with three different programs of control.

Thus, according to the compromise (which is the combined program) program, the thrust changes according to a certain intermediate law 5-2-1 (see Fig. 12.15) instead of 3-2-1 (program  $n = \text{const}$  and  $T_3^* = \text{const}$ ) and 4-1 (program "Point"). In this case the drop in thrust in the takeoff regime appears permissible and conditions of operation of the compressor entirely satisfactory.

## 12.2. Peculiarities of High-Speed Characteristics of Double-Shaft TRD

Let us examine peculiarities of high-speed characteristics of double-shaft TRD at two different programs of control: 1)  $n_{ВД} = \text{const}$ ;  $f_5 = \text{const}$  and 2)  $n_{ВД} = \text{const}$ ;  $f_5 = \text{const}$ .

First of all, it is necessary to explain how the following magnitudes change with respect to flight speed of: number of revolutions of the free cascade of the compressor and gas temperature in front of the turbine.

Figure 12.16 shows a diagram of a double-shaft TRD with symbols of characteristic sections of the gas-air channel. We will assume that at all speeds and altitudes of flight a jet nozzle operates at a supercritical drop in pressures [ $q(\lambda_5) = 1$ ].

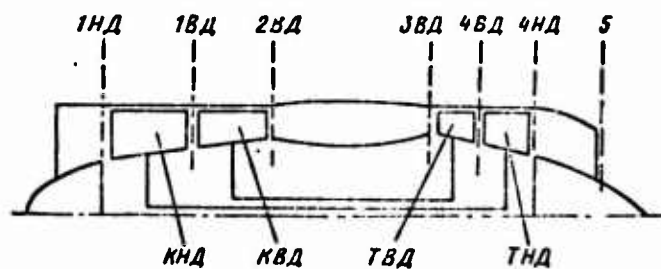


Fig. 12.16. Diagram of double-shaft TRD.

### 12.2.1. Program $n_{ВД} = \text{const}$ and $f_5 = \text{const}$

With an increase in flight speed there approaches a "loading" of the cascade of the low-pressure compressor (angles of attack on

blades and, as consequence increase, in compression ratios and work of the ND compressor increase) and "lightening" of the cascade of the high-pressure compressor (angles of attack on the blades are decreased and, as consequence, significances  $\pi_{\text{KVD}}$  and  $L_{\text{KVD}}$  are lowered). Accordingly, lines of operating conditions of the KND and KVD are deformed, deviating from the direction which they would have if the TRD consisted only of an ND or VD turbocompressor (excluded would be the joint effect of cascades of the compressor).

The lowering of work of the VD compressor when  $n_{\text{VD}} = \text{const}$  leads to a decrease in the fuel feed into the combustion chamber and to a reduction in  $T_3^*$ . Actually, from the balance of works of the KVD

$$L_{\text{KVD}} = L_{\text{TRD}} = 1187 \dot{V}_3^* \pi_{\text{TRD}}^*$$

when  $\pi_{\text{TRD}}^* = \text{const}$  it follows that

$$L_{\text{KVD}} \sim T_3^*$$

A decrease in  $T_3^*$ , in turn, leads to a proportional lowering of the gas temperature in front of the ND turbine  $T_{4\text{VD}}^*$ . Since the ND compressor with an increase in  $V$  is "loaded," then the resulting unbalance of works

$$L_{\text{KND}}/L_{\text{KVD}} > L_{\text{TRD}}/L_{\text{TRD}} = \text{const} \text{ [see equation (11.11)]}$$

is removed only by means of lowering the numbers of revolutions of the ND cascade. Finally, with an increase in flight velocity, the number of revolutions of the ND compressor and gas temperature in front of turbine decrease.

Regime points of KND and KVD are moved along lines of working processes in direction of reduced given numbers of revolutions.

#### 12.2.2. Program $n_{\text{ND}} = \text{const}$ and $f_5 = \text{const}$

With an increase in flight speed, just as in the preceding case, the "loading" of the cascade of the ND compressor and "lightening" of the cascade of the VD compressor approach.

An increase in the work of the ND compressor when  $n_{ND} = \text{const}$  leads to an increase in the fuel feed into the combustion chamber and, consequently, to an increase in  $T_3^*$  and  $T_{ВД}^*$ .

The "lightening" of the VD compressor with a simultaneous increase in  $T_3^*$  leads to an unbalance of works on VD and ND the turbo-compressor, i.e.,

$$L_{КВД}/L_{КНД} < L_{ТВД}/L_{ТНД} = \text{const.}$$

The latter is overcome by means of acceleration of the VD rotor. Finally, with an increase in the flight speed, the revolution number of the VD compressor increases, and the gas temperature in front of the turbine increases.

In conclusion let us note that the change in  $V$  and  $H$  with the program of control  $T_3^* = \text{const}$  and  $f_5 = \text{const}$  leads to spinup one of rotors and to deceleration of the other.

## CHAPTER 13

### ALTITUDE CHARACTERISTICS OF TURBOJET ENGINES

Definition. *Altitude characteristics, or characteristics with respect to altitude of flight* of turbojet engines, are called dependences of thrust and specific fuel consumption on flight altitude with an assigned program of control of the engine. Altitude characteristics, similar to high-speed, are frequently supplemented by curves of the change with respect to altitude of flight of gas temperature in front of the turbine, fuel consumption per hours, and also other parameters important in operation.

Programs of control of the TRD with respect to altitude characteristic.

With an increase in height the same programs of control of the engine as with respect to flight speed are used. We will limit ourselves here to a detailed examination of altitude characteristics of a single-shaft TRD constructed for the program of control at maximum thrust.

#### 13.1. Altitude Characteristics of Single-Shaft Turbojet Engines Without Afterburners

Let us examine altitude characteristics of single-shaft TRD without afterburners plotted as a result of approximate thermal and gas-dynamic calculations of the engine with a program of control for maximum thrust.

Let us take as basic conditions of the construction of altitude characteristics the following:

- 1) constant flight speed

$$V = \text{const};$$

- 2) constant number of revolutions

$$n = n_{\text{max}} = \text{const};$$

- 3) constant gas temperature in front of the turbine

$$T_3^{\circ} = T_{3(\text{max})}^{\circ} = \text{const}.$$

Assumptions usually taken in approximate calculations of altitude-high-speed characteristics, as before, are:

- 1) constancy of work of the compressor at a fixed number of revolutions of it;

- 2) constancy of efficiency and coefficients of losses in elements of the TRD;

- 3) total expansion of gas in the reactive nozzle of the TRD.

The assumption on constancy of the efficiency of the compressor and turbine at high altitudes ( $H > 15$  km) is quite approximate. It is known that at high altitudes fall numbers of Reynolds referred to the chord of the blade - characteristic linear dimension of the compressor and turbine cascades. As a result of this, with a TRD of small dimensions there can be a drop in efficiency of the indicated elements.

The assumption on the invariability of the efficiency of combustion with lifting of the engine in altitude also appears approximate. At very great heights the pressure drop in the fuel system and in combustion chambers leads to a sharp worsening of carburetion and to a drop in mechanical completeness of the fuel

combustion. To maintain the high completeness of combustion, the use of special evaporative combustion chambers, multichannel sprayer of fuel, etc. is necessary.

### 13.1.1. Effect of Flight Altitude on Compression Ratio of the Turbojet Engine

With an increase in altitude up to the isothermal limit ( $H = 11$  km) the external temperature  $T_H$ ; is continuously lowered; consequently there is also a drop in stagnation air temperature at the entrance into the compressor equal to

$$T_1^* = T_n^* = T_n + \frac{V^2}{2gc_p/A}.$$

The indicated circumstance leads, on one hand, to an increase in the  $M_0$ <sup>1</sup> number of flight and to an increase in the dynamic compression ratio

$$\pi_1 = (1 + 0,2M_0^2)^{3,5} \pi_n^*$$

where

$$M_0 = \frac{V}{\sqrt{kgRT_n}},$$

and, on the other hand, to an increase in the compression ratio of the compressor. Actually, from an examination of equality

$$L_n = 102,5T_n^* \left( \pi_n^{*0,286} - 1 \right) \frac{1}{\eta_n} = \text{const}$$

it is easy to conclude that with a reduction in  $T_H^*$  magnitude  $\pi_n^*$  increases.

Thus, the total compression ratio

$$\pi = \pi_1 \pi_n^*$$

also increases (Fig. 13.1).

An increase in the total compression ratio proves to be more considerable, the greater the absolute value of compression ratio of the compressor  $\pi_n^*$ , and the less the flight speed (Fig. 13.2).

<sup>1</sup>Since the speed of sound is decreased.

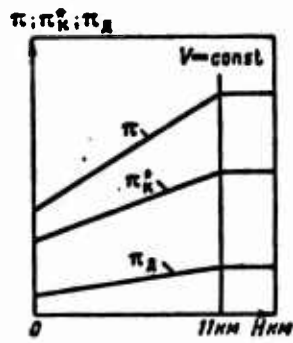


Fig. 13.1.

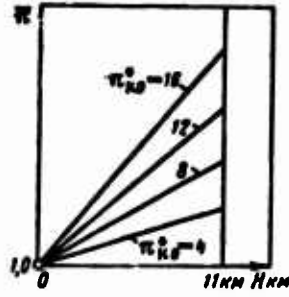


Fig. 13.2.

Fig. 13.1. Effect of flight altitude on the compression ratio of the TRD.

Fig. 13.2. Effect of computed value  $\pi_{K0}$  on the change in total compression ratio with the increase in altitude.

### 13.1.2. Change in Air Flow

Let us now examine how the mass flow rate of air through the TRD changes with an increase in altitude (Fig. 13.3).

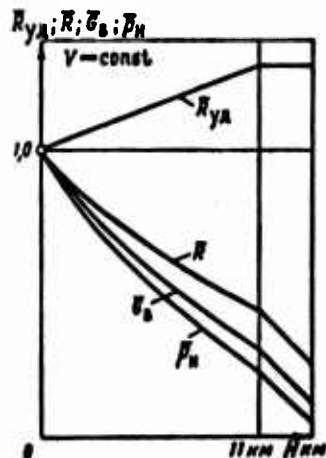


Fig. 13.3. Effect of flight altitude on specific thrust, total thrust and mass flow rate of air through the TRD.

From the expression of the flow of air, recorded for the nozzle box assembly of the turbine,

$$G_a = m \frac{P_3^{1/2} c_{a0}}{\sqrt{T_3}} f_{c.a.}(\lambda_{c.a.})$$

it follows that

$$G_a \sim P_3^{1/2} \sim P_a \pi. \quad (13.1)$$

Thus, rate of airflow through the engine with an increase in altitude is decreased; however it is decreased more slowly than the external pressure drops. The factor delaying the fall in  $G_B$  proves to be the increase in the total compression ratio, which is conditioned by the lowering of the temperature of the external atmosphere up to altitude  $H = 11$  km. At the altitude  $H = 11$  km the relative pressure is

$$\bar{p}_n = \frac{p_n(H=11 \text{ km})}{p_0(H=0)} = 0,223.$$

For  $\pi_{n0}^* = 10$ ;  $M_0 = 0,9$ ;  $H = 11$  km and  $L_n = \text{const}$ , we find the relative compression ratio  $\bar{\pi} = 1,57$ .

Then

$$\bar{G}_n = \bar{p}_n \bar{\pi} = 0,223 \cdot 1,57 \approx 0,35,$$

i.e., with a quintuple drop in external pressure the flow of air is decreased three times.

### 13.1.3. Change in Specific Thrust.

At constant flight speed the change in specific thrust (see Fig. 13.3) depends only on the velocity of outflow of gas from the nozzle.

It is easy to conclude that when  $T_3^* = \text{const}$  and  $L_n = \text{const}$  the velocity of outflow of the gas depends only on the drop in pressures in the jet nozzle, i.e.,

$$c_s \sim \sqrt{\epsilon_{p,c}}$$

where

$$\epsilon_{p,c} = 1 - \frac{1}{(\pi_{p,c})^{\frac{k-1}{k}}};$$

$$\pi_{p,c} = \frac{\pi_{n,c}^*}{\pi_n^*} \sim \pi \text{ (noting that } \pi_n^* = \text{const)}.$$

Since the compression ratio increases with an increase in altitude up to the isothermal limit, then the velocity of outflow from the nozzle of the engine and, consequently, specific thrust increases.

An increase in specific thrust proves to be more intensive, the higher the ground compression ratio of the compressor  $\pi_{\kappa_0}^*$ , the lower the gas temperature in front of the turbine  $T_3^*$  and the greater the flight speed.

Thus, with an increase in altitude up to  $H = 11$  km the specific thrust increases in the considered range of values  $\pi_{\kappa_0}^*$  and  $T_3^*$  by 40-50%.

#### 13.1.4. Change in Total Thrust.

The change in total thrust with an increase in height is determined by a change in its components, i.e.,

$$\bar{R} = \bar{R}_y \bar{G}_y = f(H).$$

The basic factor determining the change in thrust with respect to the altitude of flight is the drop in flow of air, conditioned by the continuous decrease in the external pressure.<sup>1</sup> However, the thrust drop occurs more slowly than the lowering of  $G_B$ . It delays the increase in specific thrust (see Fig. 13.3). With the quintuple drop in external pressure, the air flow is decreased approximately three times, and the thrust of the TRD - no more than two times.

Thrust decay is intensified with an increase in flight speed, with the lowering of  $\pi_{\kappa_0}^*$  and with a decrease in  $T_3^*$ .

#### 13.1.5. Change in Thrust of the Turbojet Engine at Altitudes $H > 11$ km.

On altitudes greater than 11 km, the external temperature maintains a fixed value  $T_H = 216.5^\circ\text{K}$  up to altitude  $H = 25-30$  km. At these altitudes (in the whole isothermal region) we have  $\pi = \text{const.}$  Consequently, the specific thrust is also constant; the drop in air flow and total thrust of the engine is rapid; now it occurs in an accuracy proportional to the atmospheric pressure, i.e.,

$$G_{(H>11\text{ km})} = R = \bar{p}_a.$$

---

<sup>1</sup>Or density of the atmosphere.

### 13.1.6. Change in Efficiency of the Turbojet Engine

#### 13.1.6.1. Effective Efficiency ( $\eta_e$ ).

With an increase in altitude the velocity of outflow from the nozzle and, consequently, kinetic energy of 1 kg of gas at the exit from the engine increases. On the other hand, the quantity of heat fed with the fuel to 1 kg of gas into the combustion chamber increases (since the interval of preheating  $\Delta T_{n,c}^* = T_3^* - T_2^*$ ) increases. Since  $L_e$  increases faster than  $\eta_{th}$ , the effective efficiency of the TRD with an increase in altitude increases (Fig. 13.4).

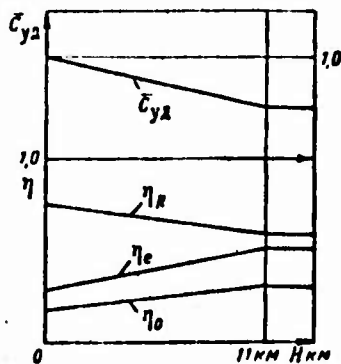


Fig. 13.4. Effect of flight altitude on the efficiency and specific flow of fuel of the TRD.

An increase in  $\eta_e$  with respect to altitude can also be explained by a simultaneous increase in the total compression ratio  $\pi$  and degree of preheating  $\delta = \frac{T_3^*}{T_n}$  of the working medium during the cycle (see Figs. 9.13 and 9.14).

#### 13.1.6.2. Thrust Efficiency ( $\eta_R$ ).

A velocity increase in outflow from the reactive nozzle with fixed flight speed leads to an increase in losses with exhaust velocity and to a drop in thrust efficiency

$$\eta_R = \frac{2V}{V + c_b}$$

with an increase in height. The nearer the magnitude  $\eta_R$  to unity, the less considerable the effect of the increase in  $c_b$ .

### 13.1.6.3. Total Efficiency ( $\eta_0$ ).

The change in total efficiency depends on the change in partial efficiency - its factors:

$$\eta_0 = \eta_c \eta_R.$$

Calculations show that at high values of  $\eta_R$  the determining factor is an increase in effective efficiency. Thus, with an increase in height the total efficiency of the TRD increases. This fact characterizes the improvement of economy of the engine with an increase in flight altitude.

### 13.1.7. Specific Fuel Consumption

Since at a fixed flight speed the specific fuel consumption is inversely proportional to the total efficiency, i.e.,

$$C_{ya} = 8,43 \frac{V}{H \eta_0} \sim \frac{1}{\eta_0},$$

then with an increase in altitude up to  $H = 11$  km, magnitude  $C_{yA}$  is continuously decreased (see Fig. 13.4).

Further ascent in altitude (when  $H > 11$  km) does not have an effect on magnitude  $C_{yA}$ . An exception is those cases when there is worsening of combustion efficiency, as a result of which  $C_{yA}$  will increase, since

$$C_{ya} \sim \frac{1}{\epsilon_{к.с.}}$$

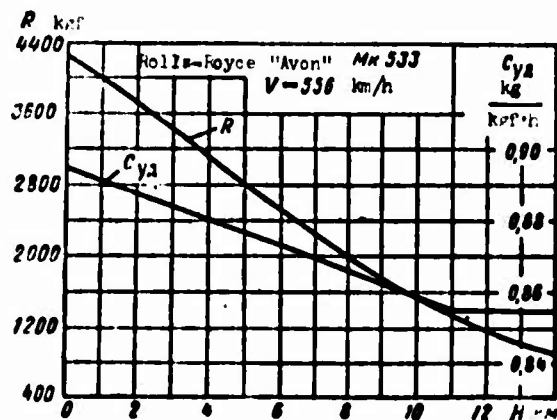


Fig. 13.5. Altitude characteristic of the TRD Rolls-Royce "Avon."

Figure 13.5. gives the altitude characteristic of the TRD Rolls-Royce "Avon."

P A R T F O U R

TURBOJET ENGINES WITH AFTERBURNERS. RAMJET ENGINES

## CHAPTER 14

### METHODS OF THRUST AUGMENTATION

#### 14.1. Concept of Thrust Augmentation

Thrust augmentation is called a short-term increase in the thrust of the engine. Thrust augmentation is used on takeoff - for the reduction of takeoff distance in climbing and during the transition through the speed of sound - for the fastest exit of the aircraft at the calculated regime of flight, at maximum speed in combat conditions - in pursuit of the enemy or withdrawal from him, and in the cruising regime of flight with the failure of one of the engines - for the compensation of thrust losses of the power plant of the aircraft as a whole.

Forcing is also used for the compensation of thrust (power) decay of a gas-turbine engine in unfavorable atmospheric conditions - high temperature and low pressure of the external medium.

#### 14.2 Methods of Thrust Augmentation of Gas-Turbine Engines

There are many different methods of thrust augmentation. These are:

- 1) forcing of the TRD with respect to number of revolutions;
- 2) forcing of the TRD with respect to gas temperature in front of turbine;

- 3) injection of water or special liquids into the compressor;
- 4) injection of water or special liquids into the combustion chamber;
- 5) bleed of air from the compressor into a special boost circuit in combination with water injection into the combustion chamber;
- 6) additional combustion of fuel behind the turbine in the afterburner.

Let us examine the essence and also the comparative merits and deficiencies of these methods.

#### 14.2.1. Forcing of the Turbojet Engine with Respect to the Number of Revolutions

*The forcing of the TRD with respect to the number of revolutions* makes it possible briefly to increase the thrust of the engine by 15-20% and more. For this purpose in a number of engines there is provided the introduction of a special, extreme (emergency), regime, the operation of which is permissible in exceptional cases for 2-3 minutes.

One must keep in mind that the forcing with such method leads to an increase in basic breaking stresses in the turbine blades proportional to the square of the number of revolutions and in the same degree increases the gas temperature in front of the turbine; this substantially lowers the strength of the basic strained element of the hot part of the engine - rotor blade of the turbine.

In a number of cases in instructions on operation there is provided heat removal of the engine, which operated in the extreme regime.

#### 14.2.2. Forcing of the Turbine on Gas Temperature in Front of the Turbine

The possibility of forcing TRD with respect to gas temperature in front of the turbine (when  $n = \text{const}$ ) for the reason mentioned above is also rather limited, and, furthermore, at such a method of forcing the introduction of an adjustable jet nozzle is necessary.

A short-term increase in the temperature  $T_3^*$  of 10%, depending on peculiarities of the characteristic of the compressor, can increase the thrust of the TRD 5-8%.

#### 14.2.3. Injection of Easily Vaporizing Liquids into the Compressor

The simplest method of considerable thrust augmentation of the TRD is water injection at the entrance into the compressor (Fig. 14.1).



Fig. 14.1. TRD diagram with water injection at the entrance into the compressor.

The physical essence of thrust augmentation by this method consists in the following: as a result of intensive heating in compressed hot air the water being injected evaporates; for the transformation of 1 kg of water having a temperature of  $t = 100^\circ\text{C}$  into water vapor with the same temperature heat equal to 539 kcal/kg is expended (so-called latent heat of vaporization). Under the action of intensive heat removal there is either a decrease in temperature of air entering in the compressor (if evaporation of the water is accomplished mainly in front of the entrance into compressor) or the approach of the polytropic process of compression toward the isothermal (if the process of water injection and evaporations is accomplished along the whole air channel of the compressor).

As a result, with invariable work for driving the compressor, being determined by the number of its revolutions, the compression ratio  $\pi_H^*$  of the compressor increases (Fig. 14.2), and, consequently, the gas pressure along the whole gas-air channel of the TRD increases. This leads to a velocity increase in expiration from the nozzle, and consequently, specific thrust of the engine. Since the gas constant of water vapor is much greater than that in usual combustion products ( $R_{H_2O} = \frac{848}{\mu_{H_2O}} = \frac{848}{18} = 47,2 \frac{\text{kgf}\cdot\text{m}}{\text{kg}\cdot\text{deg}}$ ), then this also increases the specific thrust.

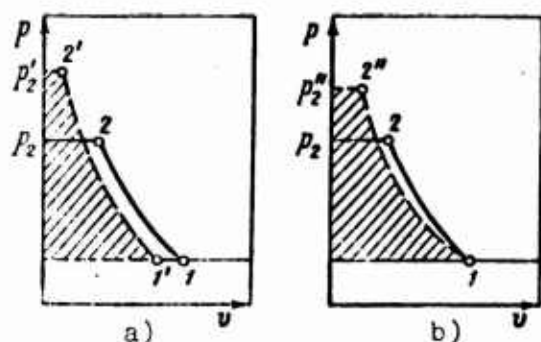


Fig. 14.2. Effect of water injection into the compressor on its compression ratio: a) evaporation occurs at the entrance into the compressor; b) evaporation occurs along the air channel.

One must also take into account the considerable increase in the mass of outflowing gas because of the increase in the air mass and addition of mass of water being injected. All this increases thrust of the TRD.

In practice the method of water injection has the following essential deficiencies.

1. As a result the small time of stay of the water in the gas-turbine channel of the engine (about  $1/100$  s), it does not evaporate. Thus, for instance, in a centrifugal compressor it evaporates under standard atmospheric conditions, at the best, not more than  $1/2$ , and in the axial compressor - not more than  $1/3$  of the water being injected, the relative quantity of which does not exceed 2-3%, i.e.,

$$\bar{G}_{\text{вп}} = \frac{G_{\text{вп}}}{G_{\text{воздуха}}} = 0,02 - 0,03.$$

2. In standard test bench conditions only a very small quantity of water evaporates at the entrance into the compressor ( $\bar{G}_{\text{исп}} \approx 0,25\%$ ). In the exhaust section of the compressor about 5% of the water can be evaporated.

3. The effect of even well atomized particles of water on blades of the compressor leads to erosion of the blade. Steel blades are considerably less subjected to this form of mechanical effect.

4. Finally, in certain cases there appears the danger of jamming of rotor blades of the compressor in housing of the compressor cooled from the peripheral flow of water.

With an increase in the temperature of the surrounding medium (operation of the TRD in tropical conditions), and also with an increase in flight speed, the beneficial effect of water injection on thrust increases. It is equivalent to the result obtained with an increase in the reduced revolutions of the engine.

One should keep in mind that water injection into the compressor leads to a lowering of gas temperature in front of the turbine (flow of gas through the turbine increases faster than the rate of air flow through the compressor), as a result of which the thrust of the TRD (or power of the turboprop engine) can decrease. To maintain  $T_3^* = \text{const}$ , it is necessary with water injection to cover the jet nozzle of the TRD or "load" propeller of the turboprop engine, (i.e., increase the angle of incidence of blades of the propeller  $\phi$ ). In order to avoid the need to install additional regulating and fuel-feed equipment (which complicates the construction and operation of the engine and increases its weight), it is expedient to inject into the compressor not pure water but, for example, water-alcohol (water-metanoic) mixture in a ratio of  $\frac{G_{\text{врал}}}{G_{\text{спирт}}} = \frac{2}{3}$ .

At equal relative quantities of injected liquid, the water-metanoic mixture provides less increase in thrust than does pure water (when  $\bar{G}_{\text{исп}} = 0,03$  and  $t_{\text{н}} = +55^\circ\text{C}$ , respectively, we have  $K_{\text{н-в}} = 1,20$

and  $M_{H_2O}=1,25$ ). However, operational properties of the water-metaneic mixture are more favorable as a result of the low temperature of freezing.

Experimental investigations of water injection in compressors of aircraft gas turbines, conducted abroad and in the USSR, showed that when  $\bar{G}_{H_2O}=0,03$  and  $C_{H_2O}=3,0$  (i.e., with a triple increase in fuel and liquid consumption) the increase in thrust is from 8 to 25%. Less values of the increase in thrust refer to the ducted-fan jet engine, and maximum values - to the turboprop engine. With a quintuple increase in fuel and water consumption the increase in thrust in a TRD and TVD can be 30-35% and more (depending on magnitude  $T_{H_2O}^*$ ).

At present water injection is successfully used in a number of serial engines: TRD Pratt-Whitney JT4A-11, ducted-fan jet engine Rolls-Royce "Spey," turboprop engine Rolls-Royce "Tyne" and the AI-24.

#### 14.2.4. Injection Easily Evaporated Liquids in the Combustion Chamber of the Turbojet Engine

To intensify the evaporation, it is expedient to inject a water or water-metaneic mixture *directly into the combustion chamber* of the turbojet engine (Fig. 14.3).

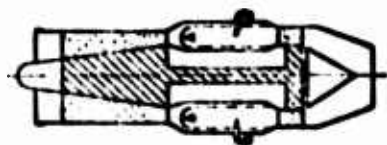


Fig. 14.3. Diagram of a TRD with water injection into the combustion chamber.

The physical essence of the increase in thrust with the injection of easily evaporating liquid into the combustion chamber consists in the increase in the exhaust pulse of gases with a simultaneous decrease in the entrance pulse of the air.

Actually, water injection into the combustion chamber with a "choked" nozzle box assembly of the turbine produces a throttling

action on the operation of the compressor. The regime point of the compressor is displaced in the direction of a decrease in the air flow nearer to the limit of surging. In this case, depending on peculiarities of the characteristic of the compressor, its compression ratio somewhat increases.

The exhaust pulse increases as a result of an increase in the total mass of outflowing gas, and also as a result of an increase in the gas constant. The quantity of liquid injected into the combustion chamber is limited by the allowable reserve of the compressor with respect to surging. The conducted investigations show that for a TRD with an axial-flow compressor with optimum water feed into the combustion chamber equal to  $G_{\text{water}}/G_{\text{air}}=0.16$ , flow of the air through the compressor is lowered 5%, and the gas flow through the turbine increases 10%;  $w_{\text{H}}$  increases from 4.0 to 4.65; the magnitude of thrust of the TRD in this case reaches 35%.

If we take into account the practically total evaporation of the entire water being injected into the combustion chamber, then it turns out that in this case the relative flow of water at an equal increase in thrust is little distinguished from the corresponding flow in the case of water injection at the entrance into the compressor. However, with the usual small reserves with respect to surging of the compressor an increase in thrust of the TRD of more than 15-20% is hardly possible.

#### 14.2.5. Injection of Easily Evaporating Liquids into the Combustion Chamber in Combination with the Overflow of Air from the Compressor

The degree of forcing of the TRD can be considerably increased if the injection of water into the combustion chamber is combined with the overflow of air from the compressor in a special high-temperature afterburner equipped with a jet nozzle (Fig. 14.4). It is obvious that in this case the afterburner of part of the air from the compressor compensates the additional feed of liquid into the

combustion chamber, eliminating the danger of the appearance of surging. Compressed air, being tapped into a special afterburner, is used for the additional fuel combustion, as a result of which with the outflow of gases from the nozzle considerable additional thrust is created. To turn off the boost circuit in usual regimes of operation a special bypass valve is used.

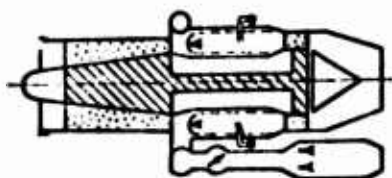


Fig. 14.4. Diagram of the TRD with water injection into the combustion chamber and bleed of air from the compressor into the boost circuit.

One must keep in mind that the boost circuit substantially (15-20%) increases the weight of the power plant and also its external drag.

#### 14.2.6. Additional Fuel Combustion behind the Turbine in the Afterburner

The physical essence of thrust augmentation with additional fuel combustion behind the turbine (Fig. 14.5) consists in the increase in velocity of gas outflow from the jet nozzle, which will be greater, the higher the gas temperature at the exit from the afterburner.

Since in the turbine part of the engine mobile elements<sup>1</sup> are absent, then the gas temperature in this part of the TRD, as a result of afterburning, can be brought up to a very high level; the latter is determined by complete use of an oxidizer, which is contained in combustion products entering from the turbine. The maximum value of this temperature can reach 2000°K and more.

To maintain the constant regime of operation of the turbocompressor with the switching on and off of the afterburner, the engine

---

<sup>1</sup>With the exception of adjustable fold of the nozzle.

must be provided with a jet nozzle with an adjustable critical section.

The high values of the temperature of forcing predetermines the high degree of forcing, which in comparison with other methods of the increase in thrust with equal relative fuel consumption or liquid flow, proves to be the greatest. Actually, the double increase in temperatures of outflowing gases increases the test bench thrust of the TRD by approximately 40% and even more in flight.

The great experience in the creation of afterburners of the TRD shows that with an increase in thrust of the TRD of 40-50% the specific weight of the engine, due to an increase in weight of the construction, is reduced only 10-20%.

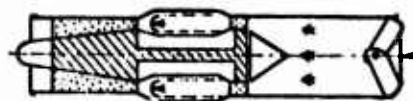


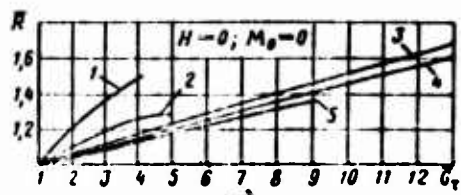
Fig. 14.5. Diagram of a TRD with an afterburner.

#### 14.3. Comparison of Various Methods of Forcing

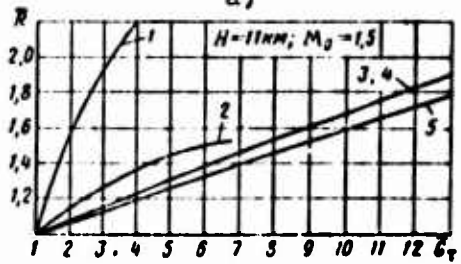
The considerable increase in thrust with a simultaneous decrease in specific weight and specific frontal surface of the engine predetermined the preferential and very wide distribution of the method of forcing of thrust by means of afterburning of fuel behind the turbine.

Water injection at the entrance into the compressor has received considerable development in turboprop engines, whose use of afterburners is not effective.

Figure 14.6a and b gives dependences of the degree of increase in thrust on the relative flow of additional liquid or fuel for various methods of thrust augmentation of the TRD, respectively, on the stand ( $H=0; M_0=0$ ) and in flight ( $H=11$  and  $M_0 = 1.5$ ).



a)



b)

Fig. 14.6. Comparison of effectiveness of various methods of forcing of thrust of the TRD: a) in a test stand ( $H = 0$ ;  $M_0 = 0$ ); b)

in flight ( $H = 11 \text{ km}$ ;  $M_0 = 1.5$ ). 1 - afterburning of fuel behind the turbine; 2 - injection of water at the entrance into the compressor; 3 - rocket boosters; 4 - air overflow; 5 - water injection into the combustion chamber.

## CHAPTER 15

### TURBOJET ENGINES WITH AFTERBURNERS (TRDF)

In the first stage of development of turbojet engines, the forcing of the TRD by means of the additional combustion of fuel behind the turbine was used as a means of a short-term increase in thrust.

At present for many TRD the forcing regime is the basic process of operation of the engine. It is used as a prolonged or even constant means of increasing the specific and total thrust (for the purpose of increasing the maximum flight speed) and lowering the specific weight.

Such a TRDF should be examined as special type of engine possessing important distinctions from the TRD with respect to its thermodynamic properties and operational characteristics.

#### 15.1. Fecularity of the Working Process of the Turbojet Engine with Afterburner

Figure 15.1 shows a schematic diagram of a turbojet engine with an afterburner (TRDF); it is distinguished from the scheme of the standard TRD by a hot turbine part, which consists of a:

- a) diffuser;
- b) afterburner;
- c) adjustable jet nozzle.

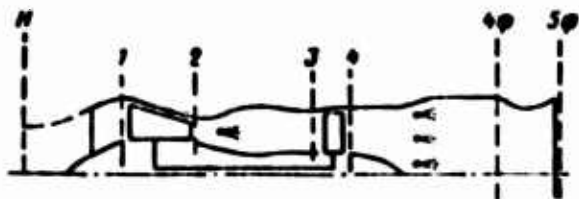


Fig. 15.1. Diagram of a TRDF.

The diffuser is intended for decreasing the  $M$  number of the flow of gas entering into combustion chamber. The less the  $M$  number of flow, the less the hydraulic and thermal losses of total pressure in the afterburner and the higher the maximum possible degree of heating of the gas. Furthermore, the less the  $M$  number of flow, the easier it is to provide a steady and complete combustion of fuel in the chamber of assigned length. However, a lowering of  $M$  number at the entrance into the afterburner lower than values 0.25-0.29 is irrational on account of the fact that this will lead to a considerable increase in the external diameter of the afterburner.

The chamber is a cylindrical tube, inside which determined fuel collectors with sprayers, special igniters and stabilizers are installed; the purpose of the stabilizers is to create a powerful steady source of continuous ignition of fuel-air mixture; they are installed in the immediate proximity of the sprayer (slightly behind them if we look in the direction of flow).

There are various types of flame stabilizers (Fig. 15.2). The simplest and most widespread of them is the corner, curved in the form of a ring or of part (segment) of a ring.

The stabilizers are installed not in one section of the chamber; they are displaced relative to one another along the gas channel of the afterburner, and their number is selected so that the dispersing turbulent tracks, in which combustion of the fuel occurs intensively, cover the whole mass of gas and reach the walls of the afterburner at as less a distance as possible from the frontal device. This makes it possible to reduce in reasonable limits the length and weight of the afterburner and also limit the so-called "blockage" of the chamber and, consequently, decrease the hydraulic resistances of the frontal device (Fig. 15.3).

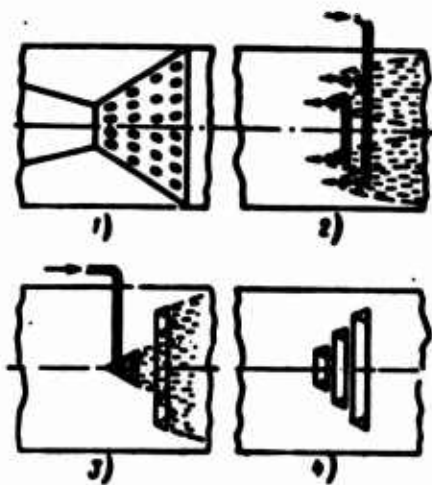


Fig. 15.2.

Fig. 15.2. Different types of flame stabilizers: 1 - "basket"; 2 - aerodynamic stabilizer; 3 - stabilizer with "attendant" source of ignition; 4 - V-shaped stabilizers.

\*[Translator's Note. This term is used in abstract form.]

Fig. 15.3. Dependence of the length of the afterburner on the number of stabilizers.

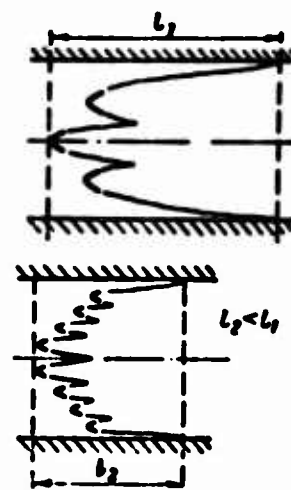


Fig. 15.3.

There are known numerous attempts to use revolving blades of the turbine (blades of the rotor wheel) as stabilizing devices). For this purpose the boost fuel is injected directly in front of the nozzle box assembly of the turbine. Since for the preparation of the chemical reaction of combustion known time (so-called "induction period") is necessary, that again the formed fuel-air mixture before its ignition manages to flow through stages of the turbine, and the front of the flame appears in turbulent tracks behind the revolving operating wheel.

One of the deficiencies of the described method is the reduced stability of combustion at great altitudes, which leads to flameout.

As a result of the high degrees of preheating and relatively great blockage of the cross section of flow, the coefficient of conservation of total pressure of the afterburner is lower than that

in the main combustion chamber; on the average it varies within limits

$$\eta_{\text{ch}}^{\circ} = 0.85 \div 0.95.$$

The efficiency of combustion in the afterburner due to reduced gas pressure is also less than that in the main chamber and varies for altitude conditions within limits

$$\eta_{\text{ch}} = 0.86 \div 0.92; \text{ on the test stand } \eta_{\text{ch}} = 0.94 \div 0.96.$$

The jet nozzle of the TRDF is made with an adjustable critical section.

From the transformed equation (7.14) of the joint operation of turbine and jet nozzle of the TRDF

$$\pi_1^{\frac{1}{\gamma_1} + 1} = \frac{f_{\text{comp}}(h_{\text{cp}})}{f_{\text{comp}}(h_{\text{cr}})} \sqrt{\frac{T_3}{T_{\text{cp}}}}$$

it follows that the drop in pressures on the turbine and, consequently, operating regime of the turbocompressor, is maintained constant when the area of critical section of the jet nozzle changes directly proportional to the square root of gas temperature at the exit from the chamber, i.e.,

$$f_{\text{cr}} \sim \sqrt{T_{\text{cp}}} \quad (15.1)$$

In several designs of the TRDF inclusion of an afterburner with a fixed position of the jet nozzle is provided. The inevitable increase in counterpressure behind the turbine, which in this case begins, displaces the regime point of the compressor along its pressure characteristic nearer to the limit of surging, increasing values of parameters  $\pi_{\text{H}}^{\#}$  and  $T_3^{\#}$ ; ultimately the degree of forcing of the TRD very greatly increases. Such a method of controlling the parameters and thrust of the TRDF is called *thermal control* (in contrast to

mechanical control by an adjustable critical section of the jet nozzle).

### 15.1.1. Real Cycle of the Turbojet Engine with Afterburner

Earlier, in Chapter 4, we noted that the use of the ideal cycle  $p = \text{const}$  with stepped heat feed worsens the thermal efficiency. This is explained by the fact that the heat feed in the additional "boost" cycle is always accomplished at a lower pressure than that in the main cycle (Fig. 15.4a).

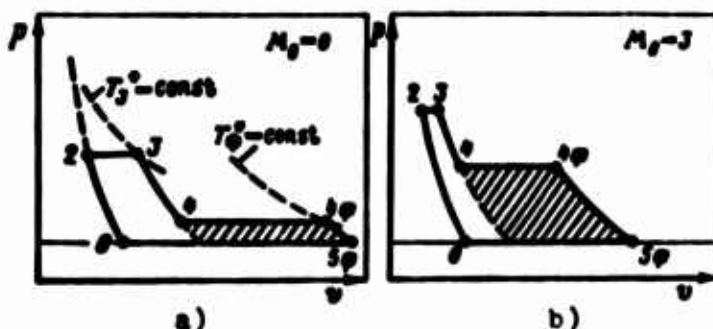


Fig. 15.4. Ideal cycle of the TRDF: a) on a test stand; b) in flight at supersonic speed.

The lowering of thermal efficiency leads to a worsening of effective efficiency of the real cycle and to an increase in specific fuel consumption on the test stand and in flight with moderate speeds.

In flight with great supersonic speed, the inclusion of an afterburner serves as a means of not only thrust augmentation but also improvement of the economy of the engine, i.e., lowering of specific fuel consumption.

Actually, at great supersonic M numbers, the effective efficiency of the cycle of the TRD drops as a result of the excessive increase in the compression ratio and increase in hydraulic losses connected with it in processes of compression and expansion (see Fig. 15.4b).

Effective efficiency of the cycle of the TRDF, because of the high degree of preheating of the working medium at precisely these speeds, reaches very high values (Fig. 15.5a). A sharp increase in effective efficiency leads to an increase in total efficiency and to a relative lowering of specific fuel consumption of the engine with inclusion of the afterburner (see Fig. 15.5b).

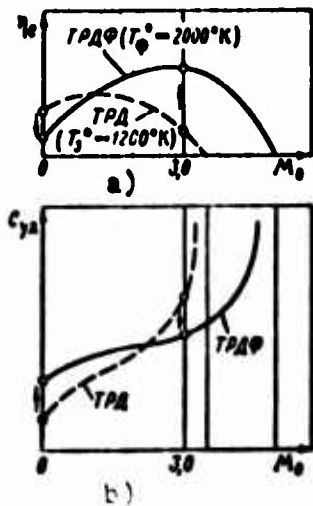


Fig. 15.5. Comparison of effective efficiency (a) and  $c_{ya}$  (b) for the TRD [TRD] and TRDF [TRDF] on a test stand and in flight.

#### 15.1.2. Determination of the Velocity of Outflow from the Jet Nozzle of a Turbojet Engine with Afterburner

The velocity of expiration from the jet nozzle of a TRDF is determined by formula

$$c_{4\phi} = \sqrt{2g \frac{c_{pr}}{\lambda} T_{4\phi}^* \left[ 1 - \left( \frac{p_{4\phi}}{p_{4\phi}^*} \right)^{\frac{\lambda-1}{\lambda}} \right]}. \quad (15.2)$$

If we neglect the relatively small drop in pressure in the afterburner, the velocity of outflow of gas from the jet nozzle of the engine will be proportional to the square root of the temperature of forcing, i.e.

$$\frac{c_{4\phi}}{c_s} = \sqrt{\frac{T_{4\phi}^*}{T_0}}. \quad (15.3)$$

The increase in temperature at the exit from the chamber is two times (from 1000°K to 2000°K) leads to an increase in velocity of outflow and thrust of the TRDF of approximately 40%.

### 15.2. Effect of Parameters of the Working Process on Specific Parameters of the TRDF

Let us examine how parameters of the working process of the TRDF - ratio of compression of the compressor, gas temperature in front of the turbine and gas temperature at the exit from the afterburner - affect the specific parameters of the TRDF ( $R_{yд.φ}$  and  $C_{yд.φ}$ ).

#### 15.2.1. Effect of Ratio of Compression of the Compressor on $R_{yд.φ}$

Let  $M_0 > 1.0$ . At a compression ratio of the compressor equal to unity, the TRDF "degenerates" into a ramjet engine with several values of specific thrust and specific fuel consumption. With an increase in the compression ratio of the compressor and at a constant gas temperature at the exit from the chamber the pressure behind the turbine will increase; consequently, the velocity of outflow of gas from the jet nozzle

$$c_{yд} = \varphi_{p,c} \sqrt{2g \frac{c_{p,r}}{A} T_{4φ}^* \left[ 1 - \left( \frac{p_{t4}}{p_{4φ}^*} \right)^{\frac{k_r-1}{k_r}} \right]}$$

will also grow. It is obvious that the velocity increase in outflow from the nozzle will occur until gas pressure behind the turbine  $p_{t4}^*$  reaches a maximum.

Let us call the value  $\pi_{\kappa}^*$  to which corresponds the maximum of the total pressure behind the turbine and maximum of specific thrust the *optimum* value.

With further growth in  $\pi_{\kappa}^*$  (above the optimum value), in accordance with the drop in  $p_{t4}^*$ , the specific thrust of the TRDF continuously drops. Figure 15.6 gives the change in total pressure

behind the turbine and specific thrust of the TRDF depending on  $w_H^*$  (or on  $e_H^*$ ).

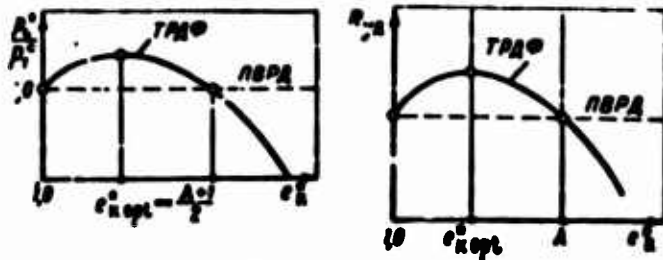


Fig. 15.6. Effect of parameter  $e_H^*$  of the compressor on total pressure behind the turbine and specific thrust of the TRDF [TPДФ].

15.2.1.1. Determination of Optimum Compression Ratio of the Compressor of the Turbojet Engine with Afterburner.

Let us write equation of balance of works of the turbocompressor of the TRDF

$$L_c = L_T$$

or

$$\frac{c_{p0}}{\lambda} r_2 \left[ \left( \frac{P_2}{P_1} \right)^{\frac{\gamma-1}{\gamma}} - 1 \right] \frac{1}{\alpha} = \frac{c_{pT}}{\lambda} r_3 \left[ 1 - \left( \frac{P_2}{P_3} \right)^{\frac{\gamma-1}{\gamma}} \right] \alpha$$

Now let us find

$$\frac{P_2}{P_1} = \frac{P_2 c_{p0}}{P_1} \left\{ 1 - \frac{1}{\lambda} \left[ \left( \frac{P_2}{P_3} \right)^{\frac{\gamma-1}{\gamma}} - 1 \right] \right\}^{\frac{\gamma}{\gamma-1}} \quad (15.4)$$

where

$$\lambda = \frac{c_{pT}}{c_{p0}} \frac{r_3}{r_2} \alpha \quad (15.5)$$

Let us introduce the assumptions:

$$\begin{aligned} k_0 = k_r = k = \text{const}; \quad c_{p_0} = c_{p_r} = c_p = \text{const}; \\ R_0 = R_r = R = \text{const}. \end{aligned}$$

Then we obtain

$$\left(\frac{p_0^*}{p_1^*}\right)^{\frac{k-1}{k}} = e_0^* = e_0^* e_{t_0}^* \left[1 - \frac{(e_0^* - 1)}{\lambda}\right]. \quad (15.6)$$

Let us investigate function (15.6)

$$e_0^* \sim p_0^* \frac{k-1}{k} = f(e_0^*)$$

for a maximum.

We have

$$\frac{de_0^*}{de_0^*} = 0 = e_0^* \left(-\frac{1}{\lambda}\right) + \left[1 - \frac{(e_0^* - 1)}{\lambda}\right];$$

whence after simple conversions we find

$$e_{0^*}^* = \frac{\lambda + 1}{2} = \frac{\frac{T_0^*}{T_1^*} \eta_c \eta_{t_0} + 1}{2}. \quad (15.7)$$

Formula (15.7) was first obtained by A. M. Lyul'ka.

Thus, the optimum ratio of compression of the compressor at which the available drop in pressures of the turbocompressor  $p_0^*/p_1^*$  and, consequently, and specific thrust of TRDF reach a maximum value is greater, the higher the gas temperature in front of the turbine, the greater the altitude of flight  $H$ , the less the  $M_0$  number of flight, and the higher the efficiency of the turbocompressor  $\eta_c \eta_{t_0}$ .

It is easy to show that the optimum compression ratio of the compressor of the TRDF is substantially more than that in the compressor of the TRD. Actually, with an increase in  $\pi_K^*$  when  $T_3^* = \text{const}$  the total pressure behind the turbine of the TRD and TRDF changes according to the same law (see Fig. 15.8). The stagnation gas temperature behind turbine of the TRD ( $T_4^*$ ) continuously drops, whereas for the TRDF magnitude  $T_4^* = \text{const}$ . Consequently, the drop in specific thrust of the TRD comes earlier, i.e., at less values of  $\pi_K^*$  (Fig. 15.7).

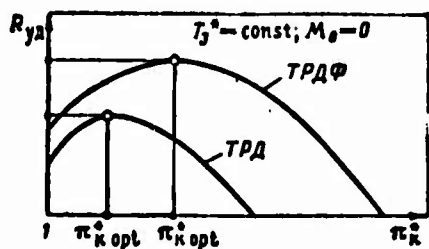


Fig. 15.7. Effect of  $\pi_K^*$  on specific thrust of the TRD [TPD] and TRDF [TPD $\Phi$ ].

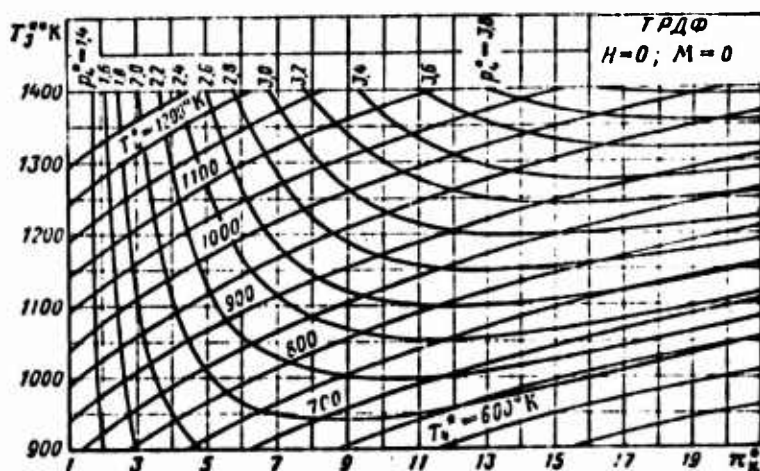


Fig. 15.8. Nomogram for determination of total gas parameters behind the turbine of the TRDF [TPD $\Phi$ ] for test bench conditions.

It is convenient to produce a determination of parameters  $p_4^*$  and  $T_4^*$  for a TRD for bench conditions with the help of a nomogram (Fig. 15.8).

Figure 15.9 gives comparative curves of the change in optimum compression ratio of the TRD (a) and TRDF (b) in flight ( $H = 11$  km).

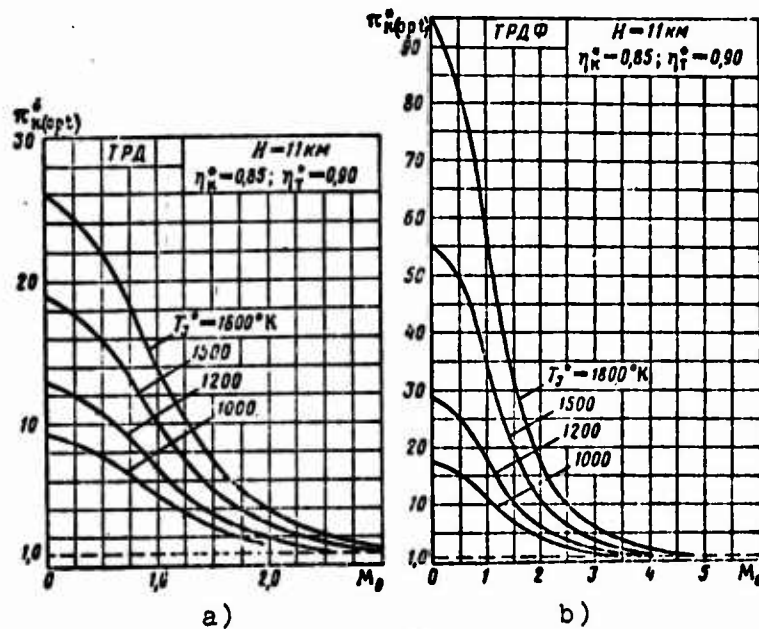


Fig. 15.9. Effect of  $T_3^*$  on  $\pi_k^*$  (opt) for the TRD [TRD] and TRDF [TRDF].

Values  $\pi_k^*$  (opt) when  $T_3^* = 1200^\circ\text{K}$ ,  $\eta_T^* = 0.90$  and  $\eta_k^* = 0.85$  are given in Table 15.1.

Table 15.1.

Type of engine	TRD	TRDF
Conditions of flight		
$M_0 = 0.9; H = 11 \text{ km}$	$\pi_k^*$ (opt) = 7.5	18.0
$M_0 = 2.0; H = 11 \text{ km}$	$\pi_k^*$ (opt) = 2.0	6.0

#### 15.2.1.2. Determination of the Range of Expedient Use of the TRDF on the Compression Ratio of the Compressor.

Let us now find values of  $\pi_k^*$  at which the effectiveness of the TRDF on specific thrust is equalized with the effectiveness of the ramjet engine.

By comparing expressions for velocities of outflow of gas from the jet nozzle of the TRDF

$$c_{3(\text{TRDF})} = \sqrt{2g \frac{c_p}{\lambda} T_{30}^* \left[ 1 - \left( \frac{p_3}{p_{30}^*} \right)^{\frac{k-1}{k}} \right]} \quad (\text{a})$$

and ramjet engine

$$c_{3(\text{ПВРД})} = \sqrt{2g \frac{c_p}{\lambda} T_3^* \left[ 1 - \left( \frac{p_3}{p_3^*} \right)^{\frac{k-1}{k}} \right]} \quad (\text{b})$$

it is easy to conclude that under the condition of the equality of maximum cycle temperatures of the ramjet engine and TRDF, i.e., when  $T_{3(\text{ПВРД})}^* = T_{30(\text{TRDF})}^*$ , the velocity of outflow from the jet nozzles are equalized when  $p_{3(\text{ПВРД})} = p_{30(\text{TRDF})}^*$  or  $p_1^* = p_4^*$  (assuming that  $e_{\text{н.с.}}^* = e_{\text{н.с.}}^*$ ).

Thus, the TRDF is more effective than the ramjet engine with respect to specific thrust in the region, where  $(p_4/p_1) > 1.0$  (see Fig. 15.6).

Let us find the correlation between parameters of gas ( $T_3^*$ ;  $p_3^*$ ) and flight ( $M_0$ ) for which condition  $(p_4/p_1) = 1.0$  is fulfilled.

Having substituted in expression (15.6)  $(p_4/p_1) = 1$ , we obtain (taking for simplicity  $e_{\text{н.с.}}^* = 1$ )

$$e_{\text{н}}^* \left( 1 - \frac{e_{\text{н}}^* - 1}{\lambda} \right) = 1,$$

or

$$(e_{\text{н}}^*)^2 - (\lambda + 1)e_{\text{н}}^* + \lambda = 0 \quad (15.8)$$

Equation (15.8) has two roots:

$$e_{\text{н}}^* (1) = 1 \quad \text{and} \quad e_{\text{н}}^* (2) = \lambda,$$

or

$$\pi_{2(1)}^* = 1 \text{ and } \pi_{2(2)}^* = A^{\frac{\delta}{\delta-1}}. \quad (15.8)$$

When  $\pi_2^* = 1$  the TRDF "degenerates" into a ramjet engine; when  $\pi_2^* = A^{\frac{\delta}{\delta-1}}$  the specific thrust of TRDF and ramjet engine are equalized, and, consequently, the use of TRDF proves to be irrational.

Thus, it is rational to use the TRDF in the range of values

$$1.0 < \pi_2^* < A^{\frac{\delta}{\delta-1}} - \left( \frac{T_3^*}{T_2^*} \eta_2^* \eta_3^* \right)^{\frac{\delta}{\delta-1}}.$$

From expression (15.9) recorded in the form

$$1 + 0.2 M_0^2 = \frac{T_3^*}{T_2^*} \frac{\eta_2^* \eta_3^*}{\pi_2^{\frac{\delta}{\delta-1}}}. \quad (15.10)$$

it is easy to determine the limiting  $M_0$  number of flight for the rational use of the TRDF. With an increase in  $T_3^*$  and with a decrease in  $\pi_2^*$ , magnitude  $M_{0(\max)}$  continuously increases (Fig. 15.10). Finally, having substituted into expression (5.10) value  $\pi_2^* = 1$ , value  $M_{0(\max)}$  can be found, beginning from which the use of the TRDF is generally inexpedient.

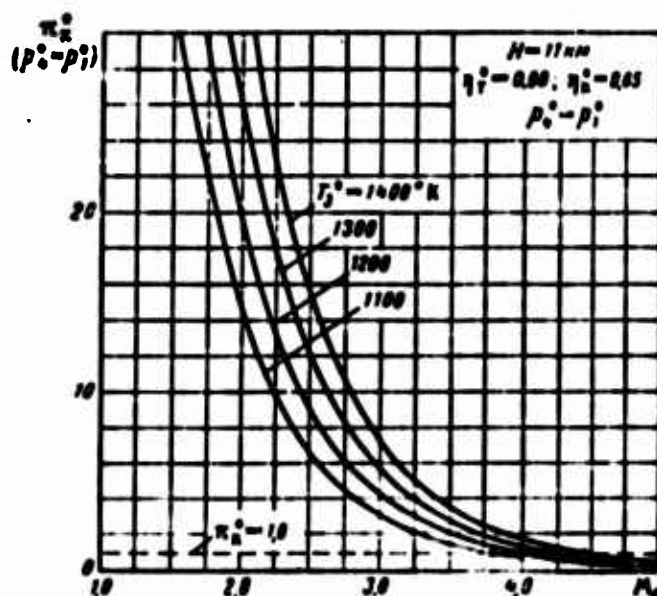


Fig. 15.10. Effect of  $\pi_2^*$  and  $T_3^*$  on limit of rational use of the TRDF with respect to  $M_0$  number.

Figure 15.11 and Table 15.2 give data characterizing the regularity of the change in  $M_{0(max)}$  depending on  $T_3^*$ .

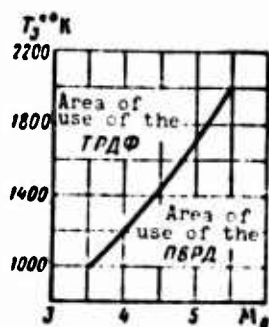


Fig. 15.11. Effect of  $T_3^*$  on the region of rational use of the TRDF [TRDF] and ramjet engine on the  $M_0$  number.

Table 15.2.

$T_3^*$ , °K	1000	1200	1400	1600
$M_{0(max)}$	3.55	4.0	4.40	4.80

15.2.2. Effect of Parameters of the Working Process ( $T_3^*$ ;  $\pi_H^*$ ) on the Total Relative Fuel Consumption ( $m_{r,z}$ ) of the TRDF

Let us examine the effect of parameters of the working process ( $T_3^*$  and  $\pi_H^*$ ) on the total relative fuel consumption ( $m_{r,z}$ ) of the TRDF.

Let us assume that the following are assigned and are fixed:

- 1) gas temperature at the exit from  $T_{\phi}^*$  afterburner;
- 2) temperature of completely stagnant flow of air in front of the engine  $T_H^*$ .

Let us write the equation of energy of flow for sections "H" and "4 $\phi$ " (Fig. 15.1) of the TRDF:

$$i_{4\phi} - i_H = \Delta L_{\phi} - \Delta L_H + q_{r,\phi} + q_{\phi,r}. \quad (15.11)$$

Since

$$L_{\kappa} = L_{\tau}; \quad i_{\phi}^{\circ} = \text{const} \quad \text{and} \quad i_{\kappa}^{\circ} = \text{const},$$

then

$$q_{\Sigma} = q_{\kappa, c} + q_{\phi, \kappa} = \text{const}.$$

Consequently,

$$m_{\Sigma} = m_{\tau(\kappa, c)} + m_{\tau(\phi, \kappa)} = \frac{q_{\Sigma}}{\xi H_{\kappa}} = \text{const}. \quad (19.12)$$

Thus, the total quantity of heat fed to 1 kg of air depends only on parameters  $T_{\kappa}^{\circ}$  (i.e.,  $M_0$  and  $H$ ) and  $T_{\phi}^{\circ}$ , but it does not depend on the compression ratio of the compressor and gas temperature in front of the turbine, i.e.,

$$m_{\Sigma} = f(T_{\phi}^{\circ}; T_{\kappa}^{\circ}).$$

Physically this regularity is thus explained. With an increase in  $T_{\kappa}^{\circ}$  the air temperature at the exit of the compressor increases, the interval of preheating in the main combustion chamber ( $T_3^{\circ} - T_2^{\circ}$ ) is decreased, and, consequently,  $q_{\kappa, c}$  is reduced; however, the increase in work of the compressor and turbine ( $L_{\kappa} = L_{\tau}$ ) leads to a proportional drop in gas temperature behind the turbine and to an increase in the interval of preheating of the gas in the chamber ( $T_{4\phi}^{\circ} - T_4^{\circ}$ ). Thus, magnitude  $q_{\phi, \kappa}$  increases. The total quantity of heat fed into the two chambers of the engine for 1 kg of gas does not change.

Similarly it is possible to show that  $q_{\Sigma}$  depends on  $T_3^{\circ}$ . Actually, with an increase in  $T_3^{\circ}$   $q_{\kappa, c}$  increases, and simultaneously  $T_4^{\circ}$  increases; and this means that  $q_{\phi, \kappa}$  decreases. The total quantity of heat  $q_{\Sigma}$  remains constant.

15.2.2.1. Effect of  $\pi_k^*$  on  $C_{уд.\phi}$

From formula

$$C_{уд.\phi} = 3600 \frac{m_{тг}}{R_{уд.\phi}} \sim \frac{1}{R_{уд.\phi}}$$

it follows that the specific fuel consumption of the TRDF changes back in proportion to the specific thrust, since  $m_{тг} = \text{const}$ . Thus, curve  $C_{уд.\phi} = f(\pi_k^*)$  is as though it were a mirror image of the curve of specific thrust (Fig. 15.12). The optimum compression ratio of the compressor (at which the specific thrust reaches a maximum) coincides with the economic compression ratio (at which the specific fuel consumption takes a minimum value), i.e.,

$$\pi_{k(opt)}^* = \pi_{k(ek)}^*$$

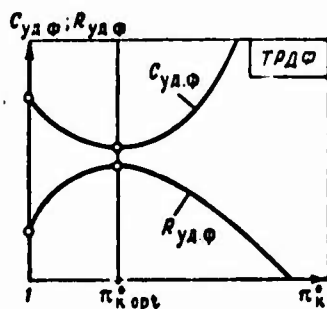


Fig. 15.12. Effect of  $\pi_k^*$  on specific parameters of the TRDF [TRDF].

15.2.2.2. Effect of  $T_3^*$  on  $R_{уд.\phi}$  and  $C_{уд.\phi}$

With an increase in the gas temperature in front of the turbine and at other constants conditions, the total pressure and temperature of the gas behind the turbine increase. At a constant temperature of forcing the increase in  $p_4^*$  leads to a continuous increase in specific thrust of the TRDF. Since the temperature change of the gas  $T_3^*$  when  $M_0 = \text{const}$  and  $T_\phi^* = \text{const}$  does not have an effect on the relative fuel consumption, i.e.,  $m_{тг} = \text{const}$ , then ultimately the specific fuel consumption of the TRDF

$$C_{y\lambda\phi} = 3600 \frac{m_{rs}}{R_{y\lambda\phi}} \sim \frac{1}{R_{y\lambda\phi}}$$

is continuously lowered (Fig. 15.13).

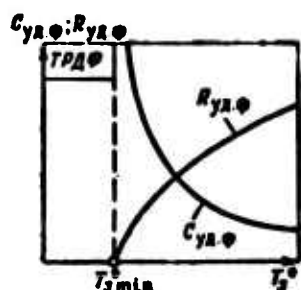


Fig. 15.13. Effect of  $T_3^*$  on specific parameters of the TRDF [TRDF].

### 15.2.2.3. Effect of Forcing Temperature $T_\phi^*$ on $R_{y\lambda\phi}$ and $C_{y\lambda\phi}$ .

With an increase in the forcing temperature of the engine, the specific thrust and also relative fuel consumption  $m_{rs}$  increase. The specific fuel consumption will change differently, depending on region of  $M_0$  numbers of flight in which there is forcing of the TRD.

Thus, for instance, on the test stand and at subsonic flight speeds, the specific fuel consumption increases with an increase in  $T_\phi^*$ ; at moderate supersonic flight speeds  $C_{y\lambda\phi}$  can remain constant; at high supersonic flight speeds ( $M_0 > 3.0$ ) the specific fuel consumption of the TRDF is lowered (Fig. 15.14).

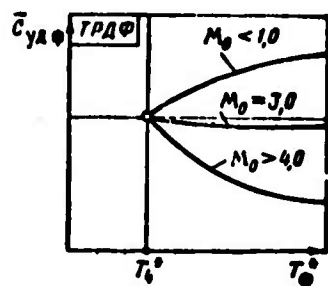


Fig. 15.14. Effect of  $T_\phi^*$  on specific fuel consumption of the TRDF [TRDF].

Actually, at a great inlet pulse, when the specific thrust of the initial TRD is small, an increase in  $T_\phi^*$  leads to an accelerated

increase in specific thrust of the engine in comparison with the relative fuel consumption. On the test stand an increase in  $R_{уд.φ}$  always lags the increase in  $m_{т.т.}$ .

### 15.2.3. Determination of Maximum Possible Gas Temperature in the Afterburner

The highest possible gas temperature in the afterburner is determined by the stoichiometric mixture ratio, i.e., the value of the total coefficient of air surplus equal to unity.

Let us write energy equation of the flow for sections "н" and "4φ" of the TRDF:

$$i_{4φ}^{\circ} - i_n^{\circ} = AL_n - AL_t + q_z = q_z, \quad (15.11a)$$

where  $q_z = \frac{\xi H_n}{\alpha_z l_0}$  — total quantity of heat fed to the main combustion chamber and afterburner.

Thus,

$$i_{4φ}^{\circ} - i_n^{\circ} = \frac{\xi H_n}{\alpha_z l_0}. \quad (15.13)$$

Let us substitute into expression (15.13) value  $\alpha_{\Sigma} = 1$ .

Then we obtain

$$i_{4φ}^{\circ} = \frac{\xi_2 H_n}{l_0} + i_n^{\circ}. \quad (15.14)$$

Assuming for simplicity that  $c_{p_n} = c_{p_{4φ}} = c_p$ , we obtain

$$T_{4φ(max)}^{\circ} = T_n^{\circ} + \frac{\xi H_n}{c_p l_0}. \quad (15.15)$$

From expression (15.15) it follows that the higher the maximum possible gas temperature in the chamber, the greater the flight speed.

It is characteristic that magnitude  $T_{4\phi}^*$  does not at all depend on value  $\alpha$  in the main chamber.

### 15.3. Peculiarities of Altitude-High-Speed Characteristics of the Turbojet Engine with Afterburner

#### Program of control of the TRDF for maximum thrust.

The program of control of single-shaft TRDF for maximum thrust includes the following conditions:

- 1)  $n = n_{max} = \text{const}$ ;
- 2)  $T_3^* = T_{3(max)}^* = \text{const}$ ;
- 3)  $T_{\phi}^* = T_{\phi(max)}^* = \text{const}$ .

#### 15.3.1. Control of Fuel Feed into the Afterburner

In connection with the need to maintain constant gas temperature at the exit from the chamber with respect to speed and altitude of flight, the question arises about the rational basis of principles of control of parameters of the gas-air channel, which provides  $T_{\phi}^* = \text{const}$  at a constant critical section of the jet nozzle. Such a principle is the automatic sustaining of constant drop in pressures on the turbine, i.e.,  $\pi_T^* = \text{const}$ , with the feed of fuel into the afterburner.

Actually, thermal control of the engine, appearing when  $T_{\phi}^* = \text{var}$  and  $f_5 = \text{const}$ , is equivalent in its action to the mechanical control of the critical section of the jet nozzle ( $f_5 = \text{var}$ ) for the TRD. It leads to a change in regimes of operation of the compressor and turbine and also a drop in pressures on the turbine (see equation 7.14a).

It is obvious that the conservation of  $\pi_T^* = \text{const}$  can be the result of only such a law of fuel feed at which  $T_{\phi}^* = \text{const}$ .

### 15.3.2. High-Speed Characteristic of the Turbojet Engine with Afterburner

With an increase in the flight speed the specific thrust of the TRDF

$$R_{y1,\phi} = \frac{c_{\phi} - V}{g}$$

falls; however, as a result of high velocities of gas expiration, its drop occurs substantially more slowly than that of the TRD. The regularity of the change in air flow with respect to flight speed for the TRDF and TRD coincides. As a result the total thrust of the TRD with an increase in  $V$  in the beginning changes little, and then increases very considerably; only in the region of high  $M_0$  numbers does the thrust sharply drop, approaching zero.

Figure 15.15 gives comparative high-speed characteristics of the TRDF with an included and excluded afterburner. We see that in the whole range of  $M_0$  numbers (velocities) of flight the thrust of the TRDF is considerably more than the thrust of the TRD.

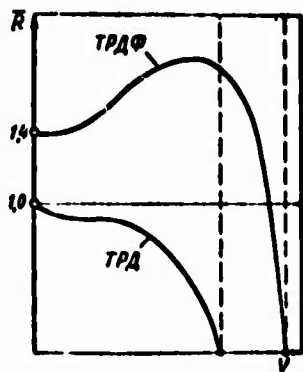


Fig. 15.15. High-speed characteristics of thrust with excluded (TRD) [TRD] and included (TRDF) [TRDF] afterburner.

The specific fuel consumption of the TRDF

$$C_{y1,\phi} = 3600 \frac{m_{y1}}{R_{y1,\phi}} = 8.43 \frac{V}{H_0 \eta_0}$$

with an increase in the flight speed increases; however at supersonic flight speeds a sharp increase of the effective and, consequently, total efficiency can even lead to a certain "local" lowering of  $C_{yД.Ф}$  (Fig. 15.16).

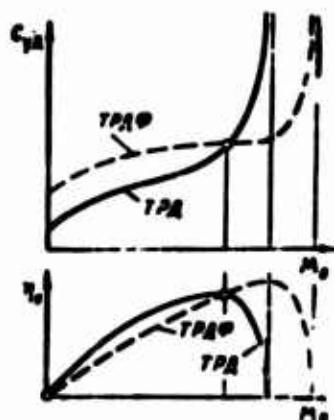


Fig. 15.16. Effect of flight speed on the total efficiency and specific fuel consumption of the TRD [TRД] and TRDF [TRДФ].

Figure 15.16 gives comparative regularities of the changes in total efficiency and specific fuel consumption of the TRDF with the included and excluded afterburner. If on the test stand and at subsonic flight speeds the TRD is more economic than the TRDF, then at greater  $M_0$  numbers of flight ( $M_0 > 3.0$ ) the specific fuel consumption of the TRDF becomes less than that of the TRD.

### 15.3.3. Peculiarities of Altitude Characteristics of the TRDF

Altitude characteristics of the TRDF with a program of control for maximum thrust in practice are no different from characteristics of the TRD. With an increase in altitude the thrust of the TRDF continuously drops; at altitudes greater than 11 km, the drop in thrust is more rapid, and it obeys the regularity

$$R_{(H>11 \text{ km})} \sim P_n$$

As regards the specific fuel consumption, the latter with an increase in altitude is reduced, up to  $H = 11$  km; a further ascent in

altitude leads to a worsening of the economy of the engine only in the case of a decrease in combustion efficiency.

#### 15.3.4. Degree of Forcing of Thrust

The degree of forcing of thrust of the TRDF is called the ratio of forced thrust to the initial nonforced thrust of the engine, i.e.,

$$\bar{R}_\phi = \frac{R_\phi}{R}. \quad (15.16)$$

If with the switching on of the afterburner the regime of operation of the turbocompressor and, consequently, flow of air through the engine, remain constant, then

$$\bar{R}_\phi = \frac{R_{\phi 20}}{R_{\phi 1}} = \frac{c_{20} - V}{c_{10} - V}. \quad (15.17)$$

Let the degree of forcing of the TRDF in test bench conditions be equal to

$$\bar{R}_{\phi(0)} = \frac{c_{20(0)}}{c_{10(0)}} = \sqrt{\frac{T_{20}^*}{T_1^*}}; \quad (15.18)$$

and let at all speeds and altitudes of flight  $T_1^* = \text{const}$  (since  $T_3^* = \text{const}$  and  $\pi = \text{const}$ ) and  $T_{20}^* = \text{const}$ .

Then

$$\frac{c_{20}}{c_{10}} = \frac{c_{20(0)}}{c_{10(0)}} = \bar{R}_{\phi(0)}. \quad (15.19)$$

Having substituted in expression (15.17) the value  $c_{20}$  from equation (15.19), we obtain

$$\bar{R}_\phi = \frac{\bar{R}_{\phi(0)} c_{10} - V}{c_{10} - V}. \quad (15.20)$$

or

$$\bar{R}_\phi = \frac{\bar{R}_{\phi(0)} - \frac{V}{c_5}}{1 - \frac{V}{c_5}}. \quad (15.21)$$

From equation (15.21) it follows that with an increase in flight speed the degree of forcing of the engine continuously increases from  $\bar{R}_{\phi(0)}$  to infinity, since ratio  $V/c_5$  increases from zero to unity (Fig. 15.17).

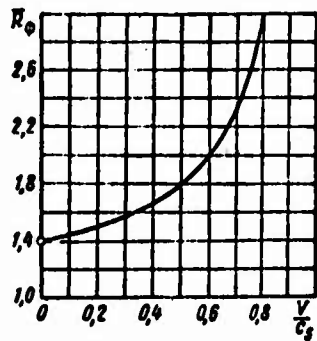


Fig. 15.17. Effect of parameter  $V/c_5$  on the degree of forcing of thrust.

With an increase in altitude of flight when  $V = \text{const}$  the degree of forcing is continuously decreased, since ratio  $V/c_5$  is lowered.

## CHAPTER 16

### RAMJET ENGINES

#### 16.1. Designs and Types of Ramjet Engines

There are the following basic types of ramjet engines: *subsonic*, *supersonic*, and *hypersonic* (Fig. 16.1a, b, c).

The subsonic ramjet engine is a ramjet engine equipped with a subsonic (diverging) diffuser and subsonic (converging) jet nozzle. Such a FVRD is used at subsonic and low supersonic flight speeds; it has low economy.

The supersonic ramjet engine is a ramjet engine equipped with a supersonic diffuser and jet nozzle. Such a ramjet engine is designed for high supersonic flight speeds. If it is used in a wide range of flight speeds (multi-regime ramjet engine), then such an engine, as a rule, is equipped with an adjustable intake and exhaust devices.

If, however, the ramjet engine is designed basically for operation at a definite, maximum,  $M_0$  number (the case of great flight distance of an aircraft), then such single-regime engine (sustainer ramjet engine) is made, for the purpose of simplification of design and of lowering of weight, with fixed geometry.

The hypersonic ramjet engine is a ramjet engine designed at  $M_0$  numbers of flight of more than 5-6. To increase the effectiveness

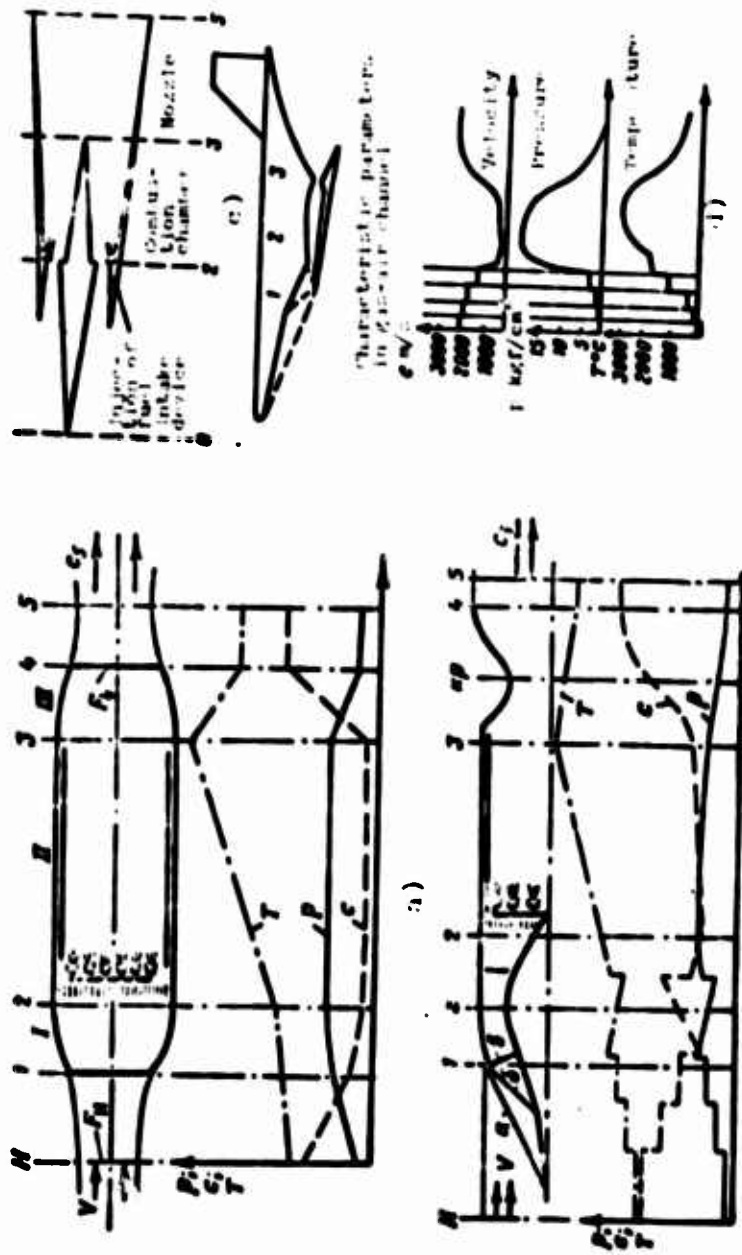


FIG. 10.1. Diagrams of ramjet engines and graphs of the changes in gas parameters along the channel of the engine: a) subsonic; b) supersonic; c) hypersonic; d) hypersonic with supersonic combustion.

and expansion of the range of rational use with respect to  $M_0$  of such a ramjet engine, special kinds of fuel (liquid hydrogen and others) must be used. At  $M_0 \geq 12$  it is expedient to resort to the use of the KTD with supersonic combustion (KTDK), see Fig. 16.1. The use of supersonic combustion (without preliminary deceleration of flow) makes it possible to reduce the temperature and pressure of the gas in combustion chamber, avoid (in full or in part) the dissociation of products of combustion and expansion, provide equilibrium of the occurrence of chemical reactions and processes of outflow. Such ramjet engines can be made more simple in design and with less weight.

In civil aviation, in connection with the creation of supersonic passenger aircraft, one should expect the appearance of supersonic ramjet engines of various types.

Figure 16.1 gives also curves of the change in parameters of gas along gas-air channel of a ramjet engine.

### 16.2. Real Cycle of the Ramjet Engine

Figure 16.2 gives the real (with losses) cycle of a ramjet engine in coordinates  $(i/A)-s$ . It consists of processes of compression 0-2, heat feed 2-3, and expansion 3-5.

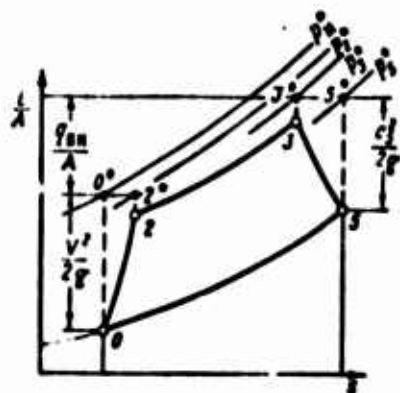


Fig. 16.2. Real cycle of the ramjet engine in coordinates  $(i/A)-s$ .

All processes which are accomplished inside the ramjet engine (compression, heat feed and expansion) are characterized by a drop

in total pressure. The total coefficient of drop in total gas pressure is equal to the product of coefficients of drop in total pressure in partial processes of the ramjet engine, i.e.,

$$\sigma_{\Sigma}^* = \sigma_{\Sigma}^* \sigma_{\text{h.c.}}^* \sigma_{\text{p.c.}}^* = \frac{P_5^*}{P_0^*}. \quad (16.1)$$

The coefficient  $\sigma_{\Sigma}^* = P_5^*/P_0^*$  of the supersonic diffuser in calculated flight conditions depends on  $M_{(0)p}$  and the selected system of shocks. To determine  $\sigma_{\Sigma}^*$  in the range of numbers  $M_0 \leq 5$ , it is possible to use curve (Fig. 16.3).

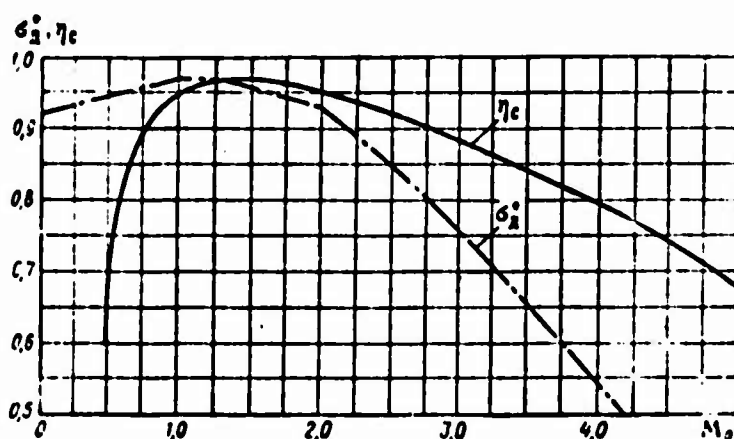


Fig. 16.3. Change in  $\sigma_{\Sigma}^*$  and  $\eta_c$  with respect to  $M_0$  number of flight.

Coefficient  $\sigma_{\text{h.c.}}^*$  depends on  $M_2$  (or  $\lambda_2$ ) number at the entrance into the combustion chamber, on the degree of preheating  $\Delta_{\text{h.c.}} = \frac{T_3^*}{T_2^*}$ , and also on the magnitude of hydraulic losses caused by the frontal system of the chamber. With an increase in  $M_2$  and  $\Delta$ , thermal losses in the chamber increase and magnitude  $\sigma_{\text{h.c.}}^* = P_3^*/P_2^*$  is reduced.

The less the coefficient  $\sigma_{\text{p.c.}}^* = P_5^*/P_3^*$  the  $M_5$  and the lower  $\phi_{\text{p.c.}}$ .

The effectiveness of the process of compression is determined also by the efficiency of compression ( $\eta_c$ ). Let us find the connection between  $\eta_c$  and  $\sigma_{\Sigma}^*$ .

We have

$$\eta_c = \frac{L_{p,c}}{L_c} = \frac{\frac{c_p}{1} T_0 (e-1)}{V^2/2g} = \frac{(e-1)}{0,2M_0^2} \quad (16.1)$$

where

$$e = \pi^{\frac{k-1}{k}} = \left( \frac{\rho_2^*}{\rho_1} \right)^{\frac{k-1}{k}} = (1 + 0,2M_0^2 \sigma_D^*)^{\frac{k-1}{k}}$$

Then after simple conversions we obtain

$$\eta_c = \frac{(1 + 0,2M_0^2) \sigma_D^{*0,256} - 1}{0,2M_0^2} \quad (16.2)$$

From expression (16.3) it follows that when  $\sigma_D^* = 1$  we have  $\eta_c = 1$ .

Dependence  $\eta_c = f(M_0)$  is given in Fig. 16.3 even in Table 16.1.

Table 16.1. Effect of  $M_0$  number of flight on  $\sigma_D^*$  and  $\eta_c$ .

$M_0$	0	1	1,3	2,2	3,0	3,5	4,0	5,0
$\sigma_D^*$	0,92	0,97	0,97	0,80	0,76	0,66	0,55	0,34
$\eta_c$	—	0,95	0,97	0,84	0,88	0,84	0,80	0,68

The effectiveness of the process of expansion in the jet nozzle of the PVRD is evaluated by the efficiency of expansion  $\eta_p$  and coefficient of pressure drop  $\sigma_{p,c}^*$ .

It is possible to show that

$$\sigma_{p,c}^* = \frac{1 - \epsilon_{p,c}}{1 - \epsilon_{p,c} \eta_p} \quad (16.4)$$

where

$$\eta_p = \eta_{p,c}^2$$

### 16.2.1. Velocity of Outflow from the Jet Nozzle of the Ramjet Engine

We have

$$c_s = \sqrt{2g \frac{c_p}{A} T_3^* \left[ 1 - \left( \frac{p_n}{p_s} \right)^{\frac{k-1}{k}} \right]},$$

or

$$c_s = \sqrt{2g \frac{c_p}{A} T_3^* \left[ 1 - \frac{1}{(1 + 0.2M_0^2) \sigma_z^{\frac{k-1}{k}}} \right]}, \quad (16.5)$$

where

$$\left( \frac{p_s}{p_n} \right)^{\frac{k-1}{k}} = (1 + 0.2M_0^2) \sigma_z^{\frac{k-1}{k}}. \quad (16.6)$$

Thus, the greater the velocity of outflow of gas from the jet nozzle of the ramjet engine, the higher the gas temperature in the combustion chamber, the more the  $M_0$  number of flight and the less the hydraulic and gas-dynamic losses in processes of the ramjet engine.

## 16.3. Effect of Parameters of the Working Process and Parameters of Flight ( $T_3^*$ , $\sigma_z^*$ or $\eta_p \eta_c$ , $M_0$ on Specific Parameters of the Ramjet Engine

### 16.3.1. Some Analytical Dependences for the Ramjet Engine

Let us derive several characteristic relations for the determination of parameters of the ramjet engine by parameter  $L_e$ .

16.3.1.1. Effective Work of the Cycle of the Ramjet Engine.

Let us write equation (9.7) in the form

$$L_e = \frac{c_p}{A} \frac{T_0}{\eta_c} \left(1 - \frac{1}{e}\right) (a\delta\eta_p\eta_c - e).$$

Let us find magnitude  $e$  from expression (16.2):

$$e = 1 + 0,2M_0^2\eta_c. \quad (16.7)$$

Then after the substitution of  $e$  in equation (9.7) and simple conversions, we obtain

$$L_e = \frac{V^2}{2g} \left[ \frac{a\delta\eta_p\eta_c}{1 + 0,2M_0^2\eta_c} - 1 \right]. \quad (16.8)$$

16.3.1.2. Velocity of Outflow of Gas from the Nozzle.

$$c_s = \sqrt{2gL_e + V^2} = V \sqrt{\frac{a\delta\eta_p\eta_c}{1 + 0,2M_0^2\eta_c}}. \quad (16.9)$$

16.3.1.3. Specific Thrust.

We have

$$R_{y_A} = \frac{c_s - V}{g} = \frac{a\eta}{g} M_0 \left( \sqrt{\frac{a\delta\eta_p\eta_c}{1 + 0,2M_0^2\eta_c}} - 1 \right). \quad (16.10)$$

Let us find the optimum value of  $M_0$  at which the specific thrust of the ramjet engine reaches a maximum value. From condition

$$\frac{dR_{y_A}}{dM_0} = 0$$

we obtain

$$(1 + 0,2M_0^2\eta_c)^3 = a\delta\eta_p\eta_c$$

whence we find

$$M_{0(opt)} = \sqrt{\frac{5(\sqrt[3]{a\delta\eta_p\eta_c} - 1)}{\eta_c}} \quad (16.11)$$

The specific thrust of the ramjet engine becomes zero at fulfillment of equality

$$a\delta\eta_p\eta_c = 1 + 0,2M_0^2\eta_c$$

whence we find

$$M_{0(max)} = \sqrt{\frac{5}{\eta_c}(a\delta\eta_p\eta_c - 1)} \quad (16.12)$$

The  $M_0$  number at which useful work of the cycle reaches a maximum is determined from condition

$$e(L_e - L_{e max}) = \sqrt{a\delta\eta_p\eta_c}$$

Consequently,

$$M_{0(L_e - L_{e max})} = \sqrt{\frac{5}{\eta_c}(\sqrt{a\delta\eta_p\eta_c} - 1)} \quad (16.13)$$

#### 16.3.1.4. Thrust Efficiency.

We have

$$\eta_R = \frac{2V}{V + c_s} = \frac{2}{1 + (c_s/V)}$$

Having substituted into expression  $\eta_R$  value  $c_D/V$  from (16.9), we obtain

$$\eta_R = \frac{2}{1 + \sqrt{\frac{a^2 \eta_p \eta_c}{1 + 0.2 M_0^2 \eta_c}}} \quad (16.11)$$

Expressions for  $\eta_e$ ,  $\eta_0$ , and  $C_{yD}$  have no peculiarities and are determined according to the appropriate formulas for the TRD.

### 16.3.2. The Effect of Gas Temperature in the Combustion Chamber

The effect of the maximum gas temperature in the thermodynamic cycle on specific parameters of the ramjet engine (Fig. 16.4) is similar to known regularities in the TRD (TRDP).

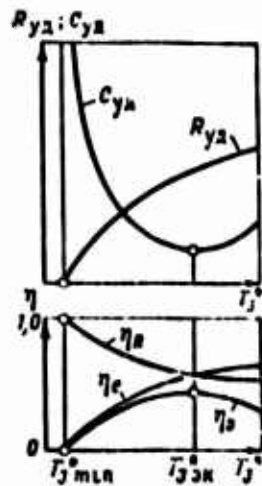


Fig. 16.4. Effect of  $T_3^*$  on specific parameters and efficiency of the ramjet engine.

With an increase in  $T_3^*$  the effective work of the cycle and specific thrust, and also the quantity of heat fed to 1 kg of air (gas) increases. The effective efficiency  $\eta_e$  in this case increases, and the thrust efficiency  $\eta_R$  is continuously lowered. Finally the total efficiency  $\eta_0$  with an increase in  $T_3^*$  initially rises, reaching a maximum, and then drops, asymptotically approaching zero.

The specific fuel consumption changes inversely proportional to the total efficiency, reaching a minimum at a certain value of  $T_{3ЭН}^*$ , which is more, the higher the  $M_0$  number of flight.

### 16.3.3. Effect of Losses of Complete Pressure ( $\sigma_L^*$ )

With a decrease in losses of total pressure the effective work of the cycle and specific thrust of the engine increases and specific fuel consumption is lowered; consequently, the range of expedient use of the ramjet engine with respect to the  $M_0$  number of flight is enlarged.

Since at the assigned values of  $H$ ,  $M_0$  and  $T_3^*$  losses in total pressure do not have an effect on the relative fuel consumption  $m_{ys}$ , then with a change in  $\sigma_L^*$  the specific thrust and specific fuel consumption change inversely proportional to each other, i.e.,

$$R_{ys} = \frac{1}{\sigma_L^*}.$$

Figure 16.5 shows the effect of  $\sigma_L^*$  on the relative specific thrust of the ramjet engine. The drop in total pressure has an especially considerable effect on  $R_{yA}$  at low values of  $\sigma_L^*$ .

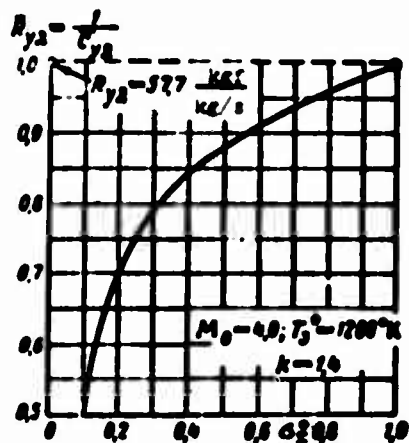


Fig. 16.5. Effect of  $\sigma_L^*$  on the relative specific thrust of the ramjet engine.

#### 16.3.4. Effect of $M_0$ Number of Flight

As is known on takeoff (when  $M_0 = 0$ ) the ramjet engine does not create thrust ( $R_{ya} = 0$ ;  $R = 0$ ;  $C_{ya} = \infty$ ). At low flight speeds (when  $M_0 < 0.3 \div 0.5$ ) the thrust of the ramjet engine is practically absent due to the considerable losses in total pressure, which is inevitable in a supersonic diffuser of an engine in these regimes of operation. Only at increased  $M_0$  ( $> 0.5$ ) numbers, with the increase in surplus pressure in the combustion chamber, the velocity of outflow of gas from the nozzle of the ramjet engine begins to exceed the flight velocity and thrust appears; with a further increase in flight speed the specific and total thrust of the ramjet engine rapidly increase.

When  $T_3^* = \text{const}$  in the range of its values 1000-2000°K the specific thrust reaches a maximum at moderate supersonic numbers  $M_0$  (1.8-2.0). With further growth in the  $M_0$  number the specific thrust of the ramjet engine is reduced down to zero.

Figure 16.6 shows regularities of the change in  $R_{ya}$ ,  $C_{ya}$  and  $L_e$  of the ramjet engine with respect to  $M_0$  number of flight. It is characteristic that optimum values of  $M_0$  numbers, at which the specific thrust and useful work of the cycle reach a maximum, do not coincide with each other, as in other types of jet engines,<sup>1</sup> i.e.,

$$M_{0(L_e = L_{e, \text{max}})} > M_{0(R_{ya} = R_{ya, \text{max}})}$$

The latter is explained by the fact that the useful work of the cycle reaches a maximum at high flight speeds, at which the inlet pulse sharply lowers the specific thrust of the ramjet engine.

Since the external heat fed to 1 kg of air inside the ramjet engine is continuously decreased with an increase in number  $M_0$ ,

<sup>1</sup>  $M_{0(L_e = L_{e, \text{max}})} = M_{0(R_{ya} = R_{ya, \text{max}})}$

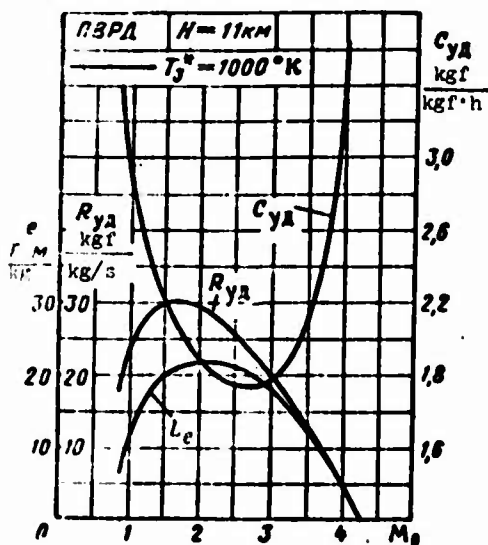


Fig. 16.6. Effect of  $M_0$  of flight on specific parameters of the ramjet engine.

$$q_{\text{sp}} \sim m_{\text{fz}} \sim (T_3^* - T_u^*) \sim (\text{const} - T_u^*),$$

then initially (in accordance with the increase in specific thrust from zero) the magnitude of specific fuel consumption sharply drops (from infinity); at  $M_0 = M_{0(\text{opt})}$ , when  $R_{\text{ya}} = R_{\text{ya max}}$ , the specific fuel consumption decreases even more; it reaches a minimum only when the approaching intensive drop in specific thrust at large  $M_0$  numbers compensates the lowering of  $m_{\text{fz}}$ , i.e., when

$$\frac{dm_{\text{fz}}}{dM_0} = \frac{dR_{\text{ya}}}{dM_0}.$$

The  $M_0$  number at which the specific fuel consumption reaches a minimum, depending on values of  $T_3^*$ , varies within limits of 2.5-3.5; consequently,

$$M_{0(C_{\text{ya}} = C_{\text{ya min}})} > M_{0(R_{\text{ya}} = R_{\text{ya max}})}.$$

With a further increase in  $M_0$  the specific fuel consumption continuously increases, approaching infinity. Calculations show that in the range  $T_3^* = 1000-2000^\circ\text{K}$  magnitude  $C_{\text{ya min}} = 1.8-2.5$   $\text{kg}/(\text{kgf}\cdot\text{h})$ . Similar dependences, plotted with respect to compression ratio, are characteristic for all types of jet engines.

Figure 16.7 shows regularities of the change in efficiency of the ramjet engine – effective, thrust and total – on the  $M_0$  number of flight. Qualitatively they do not differ from corresponding dependences obtained for the TRD.

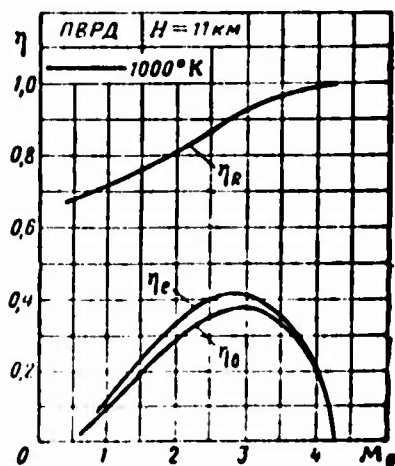


Fig. 16.7. Effect of  $M_0$  of flight on the efficiency of the ramjet engine.

It is easy to determine that the total efficiency  $\eta_0$ , which characterizes the economy of the ramjet engine, reaches a maximum on flight speeds greater than those at which the specific fuel consumption becomes minimum.

Actually, from formula

$$C_{ya} = 8,43 \frac{V}{H \eta_0}$$

It follows that the specific fuel consumption reaches a minimum at such a value of  $M_0$  number at which the first derivative  $d\eta_0/dV = \text{const}$ , and the second derivative  $d^2\eta_0/dV^2$  becomes zero, i.e., at the inflection point of the curve  $\eta_0 = f(M_0)$ , on its left branch.

Consequently, for the ramjet engine, as in all jet engines

$$M_{(C_{ya} = C_{ya \min})} < M_{(\eta_0 = \eta_{0 \max})}$$

The maximum  $M_0$  number of flight at which the specific thrust of the ramjet engine becomes zero proves to be greater, the higher the temperature  $T_3^*$  and the less the coefficient of losses of total pressure  $\sigma_L^*$ . For usual values of  $\sigma_L^*$  and when  $T_3^* = 1000-2000^\circ\text{K}$  the magnitude  $M_{0 \max} = 4-5.5$ . For an ideal ramjet engine ( $\sigma_L^* = 1$ ) and in the same range of values  $T_3^*$ , magnitude  $M_{0 \max} = 4.5-6.5$  (Fig. 16.8). Thus, the range of rational use of the ramjet engines, which operate on kerosene, for  $T_3^* \leq 2000^\circ\text{K}$  is limited by numbers  $M_{0 \max} \leq 5.5-6.5$ .

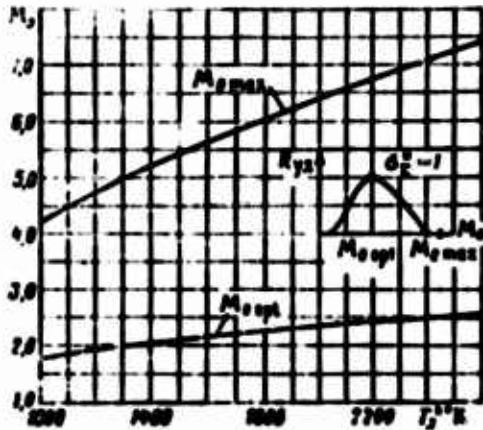


Fig. 16.8. Effect of  $T_3^*$  on  $M_{0 \text{ opt}}$  and  $M_{0 \max}$  ( $\sigma_L^* = 1$ ).

Figure 16.9 gives values of the maximum possible specific thrust of an ideal ramjet engine, obtained at optimum values of  $M_0$  and at different  $T_3^*$ . As we see, when  $T_3^* = 2000^\circ\text{K}$ ,  $M_{0(\text{opt})} = 2.3$  and  $\sigma_L^* = 1$  we obtain

$$N_{\text{max}} \approx 80 \frac{\text{kgf}}{\text{kg/s}},$$

which is considerably lower than the level of maximum possible specific thrusts of the TRD and TRDF.

Such property of the ramjet engine is explained by the fact that the maximum possible specific thrust of the ramjet engine is obtained at considerable supersonic flight speeds, i.e., at much greater values of input pulse than those for the TRD and TRDF.

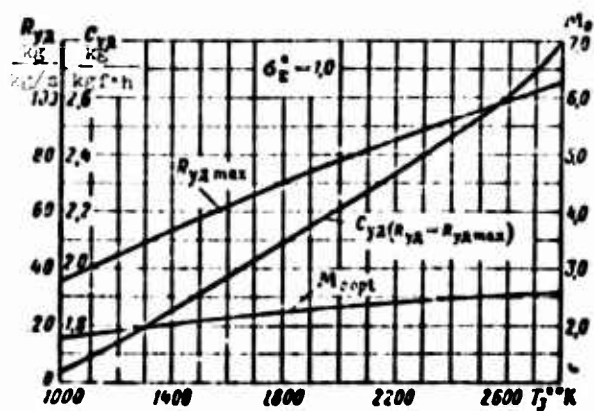


Fig. 16.9. Effect of  $T_3^*$  on  $R_{ya \max}$  and  $C_{ya}(R_{ya} - R_{ya \max})$ .

#### 16.4. Characteristics of Ramjet Engines

Similar characteristics of other types of jet engines, characteristics of the ramjet engines, are subdivided in *throttle, high-speed and altitude*. Characteristics of the ramjet engine to a certain extent are determined by accepted programs of control.

##### 16.4.1. Peculiarities of Programs of Control of the Ramjet Engine

The basic parameters of the working process of the ramjet engine, which determine its thrust and specific fuel consumption, are compression ratio  $\pi_d$  and gas temperature behind the combustion chamber  $T_3^*$ . These parameters of the ramjet engine are the determining ones, and in the first place they are subject to control.

Instead of  $T_3^*$  the coefficient of air surplus  $\alpha$  can be selected by the controllable parameter. At the assigned  $M_0$  number of magnitudes  $T_3^*$  and  $\alpha$  are uniquely connected to each other; the latter follows from expression

$$T_3^* = T_0^* + \frac{M_0^2}{c_{p0} \alpha^2} \quad (16.15)$$

Convenience of the selection of  $\alpha$  as the controllable parameter is that it determines the performance of the combustion chamber and, consequently, the possibility of providing stable and optimum conditions of its operation.

Instead of  $\pi_d$ , as the controllable parameter parameter  $\lambda_2$  can be selected, which determines the performance of the diffuser and, consequently, losses in it.

Other controllable parameters can be gas expansion ratio in the jet nozzle  $p_3^*/p_5$ , coefficient of flow of the diffuser  $\phi$  and others.

The corresponding regulating factors are:

- 1) fuel consumption  $G_T$  per second;
- 2) critical section of the jet nozzle  $f_{p.c(np)}$ ;
- 3) expansion ratio of the supersonic part of the jet nozzle  $f_3/f_{1,p}$ ;
- 4) "throat" section of the diffuser  $f_r$  and so on.

Elements of control of the ramjet engine are the regulator of fuel feed and also regulators of the jet nozzle and diffuser.

Since the regime of operation of the ramjet engine with fixed geometry is determined by one parameter, then it has a unique control element - regulator of fuel feed. The ramjet engine of a multi-regime aircraft has two and more control elements.

The following programs of control of a single-regime ramjet engine are distinguished:

- 1)  $T_3^* = \text{const}$ ; 2)  $\alpha = \text{const}$ ; 3)  $\lambda_2 = \text{const}$ .

The control of one parameter, for example  $T_3^*$ ,

$$G_T \rightarrow T_3^*$$

causes a simple change in other parameters -  $\alpha$  and  $\lambda_2$ , which now will no longer be the independent determining magnitudes.

Programs of control of the multi-regime ramjet engine with partial control are:

- 1)  $T_3^* = \text{const}$  and  $\lambda_2 = \text{const}$ ;
- 2)  $\alpha = \text{const}$  and  $\lambda_2 = \text{const}$ .

#### 16.4.2. Control of a Single-Regime Ramjet Engine

The program of control  $T_3^* = \text{const}$  automatically provides the obtaining of maximum thrust of the ramjet engine at all speeds and altitudes of flight. However, its realization in a wide range of numbers  $M_0 < M_{0\text{opt}}$  is not possible.

Actually, from the equation of flow, written for the exhaust section of the diffuser and critical section of the jet nozzle,

$$m_0 \frac{r_2^2}{\sqrt{T_2}} f_2 q(\lambda_2) = m_c \frac{r_{cp}^2}{\sqrt{T_{cp}}} f_{cp} q(\lambda_{cp}),$$

we find

$$T_3^* \sim \sqrt{T_2} \frac{f_{cp}}{q(\lambda_2) \sigma_{a,c} \sigma_{p,c}} \sim \frac{\sqrt{T_2}}{q(\lambda_2)}. \quad (16.16)$$

From the obtained expression (16.16) it follows that the conservation of  $T_3^* = \text{const}$  with a decrease in the  $M_0 < M_{0\text{opt}}$  numbers (i.e., with a decrease in  $T_2$ ) leads to a considerable lowering of the value of parameter  $q(\lambda_2)$ , which ultimately will lead to unstable operation of the supersonic diffuser.

The program  $\lambda_2 = \text{const}$  ( $G_1 \rightarrow \lambda_2$ ) proves to be more rational. The conservation of  $\lambda_2 = \text{const}$  with operation of the diffuser in supercritical regimes automatically provides its steady operation and also high values of  $\phi$  and  $\pi_d$ . For the realization of this program, the temperature  $T_3^*$  must be lowered with a decrease in the  $M_0$  number of flight. It is natural that this will lead to a relative

thrust decay of the ramjet engine in comparison with the program  
 $T_3^* = \text{const.}$

#### 16.4.3. Control of the Multi-Regime Ramjet Engine

Realization of the program

$$\lambda_2 = \text{const and } T_3^* = \text{const}$$

is carried out with the help of two independent regulators

$$G_1 \rightarrow T_3^* \text{ and } f_{np} \rightarrow \lambda_2.$$

When  $M_0 < M_{0cr}$  the jet nozzle should be opened slightly  
( $f_{np} \sqrt{T_3^*} = \text{const}$ ).

Actually, when  $q(\lambda_2) = \text{const}$  and  $f_{np} = \text{const}$  the gas temperature  $T_3^*$  drops with a lowering of flight speed. In order to pass through the critical section of the nozzle the same mass flow of gas at a higher temperature, the nozzle must be opened slightly.

Realization of the program of control

$$\lambda_2 = \text{const and } a = \text{const}$$

is not difficult and is produced with the help of the same control elements, i.e.,

$$G_1 \rightarrow a \text{ and } f_{np} \rightarrow \lambda_2.$$

From expression (16.16) it follows that with a decrease in flight speeds ( $M_0 < M_{0cr}$ ) the gas temperature also must drop.

#### 16.4.4. Throttle Characteristics

Throttle characteristics of the ramjet engine are dependences of thrust and also specific fuel consumption with gas temperature at

the exit from the combustion chamber at the assigned program of control and constant values of speed and altitude of flight.

Throttle characteristics can also be shown, as the dependence of specific fuel consumption on the degree of throttling of thrust.

Figure 16.10 gives a model throttle characteristic of a ramjet engine equipped with an adjustable jet nozzle.

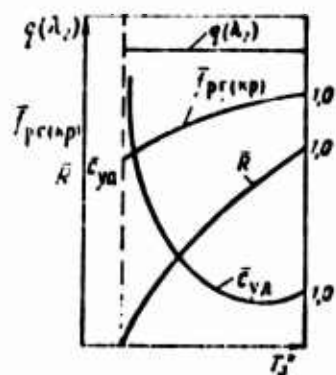


Fig. 16.10. Throttle characteristic of the ramjet engine.

Let us assume that the control of gas temperature occurs at a constant mass flow of gas (program of control  $G_p = \text{const}$ ); for this with a reduction in  $T_3^*$  the critical section of the jet nozzle must decrease. In this case a change in  $T_3^*$  will not have any effect on the operation of the diffuser and on the position of the system of shocks in it, i.e., there will be observed the condition

$$q(\lambda_2) = \text{const.}$$

With a decrease in  $T_3^*$  the specific thrust and total thrust of the ramjet engine sharply drops. The specific fuel consumption initially is somewhat lowered (in accordance with a certain improvement in the total efficiency), and at a considerable decrease in  $T_3^*$  the specific consumption sharply increases. The latter is explained by the fact that considerable worsening of effective efficiency is no longer compensated by the increase in thrust efficiency at reduced values of  $\sigma_5$ .

In the case of the unadjustable jet nozzle (program of control  $f_{T(0.1)} = \text{const}$ ) the lowering of  $T_3^*$  leads to a growth in  $q(\lambda_2)$ .

#### 16.4.5. High-Speed Characteristics

The concept of high-speed characteristics of all jet engines is identical.

The chief characteristic of the high-speed characteristic of the ramjet engine is the extraordinarily intensive increase in thrust with respect to  $M_0$  number of flight (Fig. 16.11). Such regularity

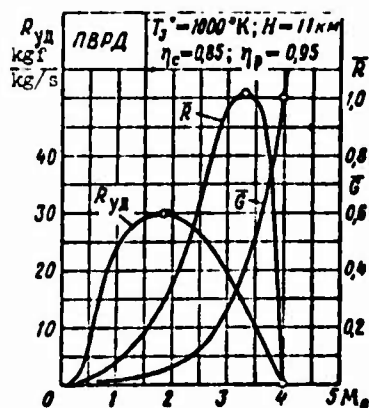


Fig. 16.11. Effect of  $M_0$  number on thrust of the ramjet engine.

is explained first by the increase in specific thrust in the considerable range of flight speeds (in contrast with other types of jet engines in which  $R_{yD}$  is continuously lowered with an increase in the flight speeds), and secondly, by the most rapid (of all types of jet engines) the increase in air flow with respect to  $M_0$  number of flight.

Actually, from formula

$$\bar{G} = \bar{\pi} = \left(1 + \frac{0.2M_0^2}{e_{*0}^*}\right)^{3.5} \quad (16.17)$$

and Fig. 16.12 it follows that with a decrease in  $e_{*0}^*$  (or  $\pi_{*0}^*$ ) down

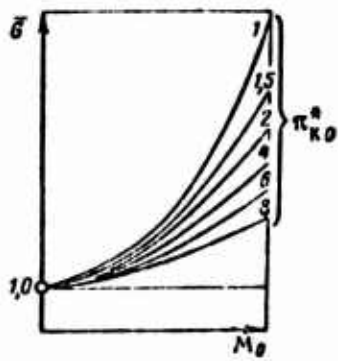


Fig. 16.12. Effect of  $\pi_{k0}^*$  and  $M_0$  numbers on relative air flow.

to unity magnitude  $\bar{G}$  continuously increases. All this leads to the fact that when  $T_3^* = 1000-2000^\circ\text{K} = \text{const}$ , the thrust of the ramjet engine continuously increases, reaching a maximum when  $M_0 = 3.5-5.0$  (see Fig. 16.11).

Let us examine high-speed characteristics of the ramjet engine at two different programs of control (Fig. 16.13 and Fig. 16.14):

- 1)  $T_3^* = \text{const}$  and  $\lambda_2 = \text{const}$ ;
- 2)  $\alpha = \text{const}$  and  $\lambda_2 = \text{const}$ .

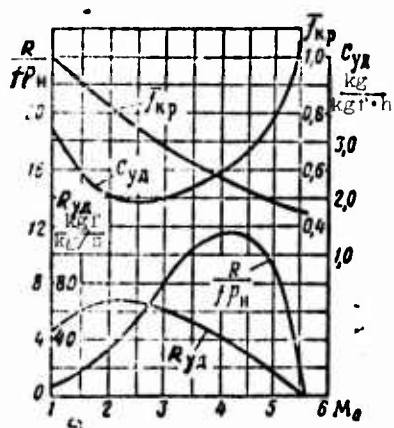


Fig. 16.13

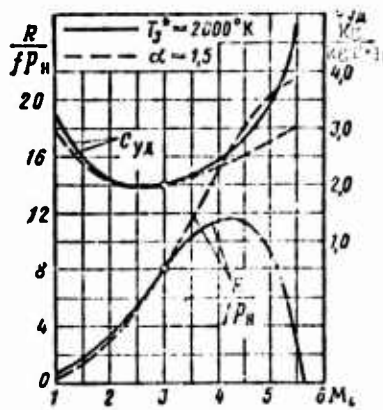


Fig. 16.14.

Fig. 16.13. High-speed characteristic of the ramjet engine ( $T_3^* = \text{const}$ ).

Fig. 16.14. Comparison of high-speed characteristics of the ramjet engine at two different programs of control.

Let us assume that when  $M_0 = 3$  (for  $T_3^* = 2000^\circ\text{K}$  and  $\alpha = 1.5$ ) both programs coincide, and, consequently, the engines develop equal thrusts and have identical specific fuel consumption (see Fig. 16.14).

In the region of numbers  $M_0 < 3$ , where  $T_3^*$  is almost not lowered when  $\alpha = \text{const}$ , curves  $R$  and  $C_{yA}$  with respect to both programs are distinguished little.

In the region of large  $M_0 (>3)$  numbers, where  $T_3^*$  intensively increases when  $\alpha = \text{const}$ , the thrust of the ramjet engine continuously increases. In the case of the program  $T_3^* = \text{const}$  the thrust of the ramjet engine initially increases, and then when  $M_0 = 4-4.5$ , having reached a maximum, begins to drop.

In accordance with different regularities of the change in thrust in terms of the  $M_0$  number curves of specific fuel consumption are deformed: when  $T_3^* = \text{const}$  the magnitude  $C_{yA}$  proves to be substantially greater than when  $\alpha = \text{const}$  (when the thrust is higher).

P A R T F I V E

DUCTED-FAN ENGINES

## C H A P T E R 17

### BASIC PRINCIPLES OF THE OPERATION AND CLASSIFICATION OF AIRCRAFT DUCTED-FAN GAS TURBINES

#### 17.1. Concept on Ducted-Fan Aircraft Gas-Turbine Engines

The *ducted-fan* gas-turbine engine (DGTD) is a gas-turbine engine whose thrust is created in two gas-air circuits (channels). Used as the first circuit of such an engine is the standard (i.e., single-circuit) turbojet engine. The second circuit is either a ramjet engine, or a jet connected to engine (by means of a propeller, fan, compressor or ejector). The jet can be free, i.e., it does not have rigid walls limiting its circuits; it also can flow in a special channel, which has a profiled intake and exhaust jet nozzle.

Between circuits of the engine an exchange of energy is usually accomplished. The most effective method of energy exchange is the transmission of *mechanical energy* from the first circuit to the second with the help of a turbine, which rotates a screw, fan or compressor. Accordingly, the ducted-fan gas turbine is called a *turboprop, turbofan* or *ducted-fan turbojet engine*.

In the presence of a considerable temperature gradient between flows of gas in the circuits energy exchange by means of *heat transfer* in the regenerator or recuperator is possible.

The exchange of mechanical and thermal energy between the circuits can also occur by means of direct contact of gas flows - with the help of the mixing of flows in a special chamber or ejector. Accordingly, turbojet engines with ejector thrust boosters and ejector turbojet engines are distinguished.

#### 17.1.1. Classification of Ducted-Fan Gas Turbines

Figure 17.1 gives the classification of ducted-fan gas turbines with respect to the principle mass transfer, i.e., depending on the correlation of masses of the working medium flowing in the circuits. The ratio of the connected mass of gas in the second circuit to the initial mass of gas of the first circuit, or bypass ratio  $\mu$ , can be changed in wide limits from zero (single-circuit TRD) up to 500-1000 (helicopter turboprop engine).

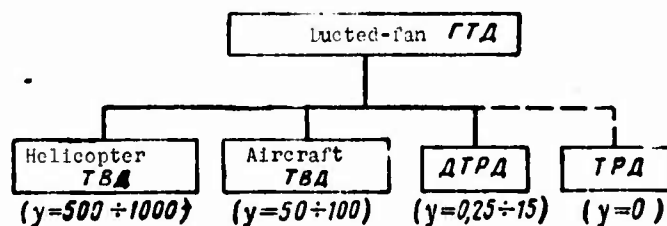


Fig. 17.1. Classification of ducted-fan gas turbines according to the principle of mass transfer.

In contemporary aircraft turboprop engines, through the area, marked by the propeller there passes air of 50-100 times more than that through the main gas-turbine circuit. The bypass ratio of ducted-fan TRD varies over wide limits from 0.25 to 10-12. In special turbofan adapters of lift engines the bypass ratio  $\mu$  reaches 10-15.

Reference of the turboprop engine, turbofan engine and ducted-fan jet engine to one class of *ducted-fan* gas-turbine engine are logically substantiated in that with an increase in the bypass ratio (at the assigned available work of the cycle of the gas generator) compression ratio of the compressor of the second circuit

is continuously lowered. In this case the compressor consecutively turns into a fan, propeller in ring, and in the limit "degenerates" into the aircraft (helicopter) propeller.

Another principle of classification depending on the *method of energy exchange* is assumed as the basis of Fig. 17.2.

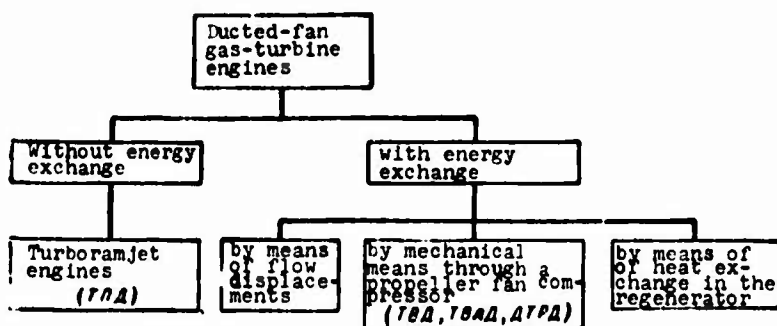


Fig. 17.2. Classification of ducted-fan gas turbines according to the principle of energy exchange.

An example of a ducted-fan gas turbine without energy exchange is a combination of a TRD and ramjet engine-turboramjet engine (TPD).

The ducted-fan gas turbines are distinguished from each other also by the degree of energy exchange between the stages; the latter can change from zero (when the circuits are energy-free) up to unity (when all the available energy of the first circuit is imparted to the second). It is obvious that in the last case the first circuit does not create thrust and also serves only as an energy generator for the second.

Thus, the characteristic indicator of the ducted-fan TRD is the presence of two separate (partially or completely) gas-air channels (gas-turbine and fan) with components of thrust in each of them. Between these channels (circuits) there is energy exchange, and various correlations are possible between masses of flowing gases and various degrees of transmissions of energy from the first circuit to the second.

In many ducted-fan gas turbines the thrust of the second circuit is created as a result of the realization of the thermodynamic cycle which consists of processes of compression, heating, expansion and removal of heat. The work of this cycle as the final result is used for the acceleration of flow and obtaining of thrust.

The physical model of the formation of thrust of the second circuit in the turboprop engine (TVD) is distinguished from that described above. The propeller of the turboprop engine, rotating with its rotation considerable masses of air, directly imparts acceleration to it. Thus, the propeller thrust of the turboprop engine is generated as a result of the action of aerodynamic forces applied to blades of the propeller and not as a result of the action of thermodynamic processes separated along the route of motion of the air. For this very reason the turboprop engine is called *an engine of mixed thrust*.

#### 17.2. Principle of the Addition of Mass (Mass Transfer) in the Ducted-Fan Jet Engine

The addition to the basic engine (or circuit) of additional masses of the working medium with the transmission to them of energy makes it possible to increase the total thrust of the power plant and decrease the specific fuel consumption. This is the basic meaning of the use of the second circuit of the engine.

At the assigned magnitude of the mechanical energy obtained inside the engine as a thermal machine, the thrust of the engine appears greater, the greater this energy is imparted to the mass of the working medium, in other words the more the additional (propelling) propelling agent of the mass. This principle is called the *principle of mass addition (mass transfer)* in a ducted-fan jet engine.

For proof of this important position, let us produce a comparison of two propelling agents with different mass consumption per second of the working medium (Fig. 17.3). Such propelling agents can be: propeller, rocket engine, jet engine, second circuit of a ducted-fan jet engine and so on.

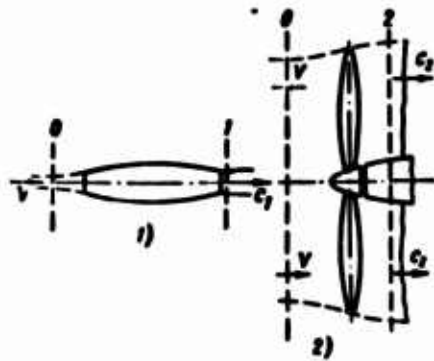


Fig. 17.3. A comparison of two propelling agents: 1 - jet engine; 2 - propeller.

Let us designate by symbols  $V$  - flight speed,  $c_1$  and  $c_2$  - relative velocities of air directly behind the first and second propelling agents, respectively;  $G_1$  and  $G_2$  - consumption of air through the propelling agent per second respectively.

Let us assume now that in both propelling agents, for the creation of work of jet thrust, the same quantity of mechanical (kinetic) energy is expended, i.e.,

$$K_1 = K_2 = K,$$

or

$$G_1 \frac{(c_1^2 - V^2)}{2g} = G_2 \frac{(c_2^2 - V^2)}{2g}. \quad (17.1)$$

Let us assume that  $G_2 > G_1$ ; then  $c_2 < c_1$  and  $\Delta c_2 = c_2 - V < \Delta c_1 = c_1 - V$ , i.e., at equal expenditure of kinetic energy the greater additional mass of gas obtains less acceleration.

Let us now compare thrusts of both propelling agents.

We have

$$R_1 = \frac{G_1}{g}(c_1 - V) \text{ and } R_2 = \frac{G_2}{g}(c_2 - V),$$

whence

$$\frac{R_2}{R_1} = \frac{G_2 (c_2 - V)}{G_1 (c_1 - V)}.$$

Let us find from relation (17.1)

$$\frac{G_2}{G_1} = \frac{(c_1^2 - V^2)}{(c_2^2 - V^2)} \quad (17.2)$$

and let us substitute it into expression (17.2).

Then after simplification, we obtain

$$\frac{R_2}{R_1} = \frac{c_1 + V}{c_2 + V} > 1.$$

Thus, the less the acceleration of the additional mass of the working medium, the more the thrust of the propelling agent, i.e.,

$$R_2 > R_1.$$

Thrust augmentation of the propelling agent with greater additional mass is explained by the fact that the velocity of outflow of gas behind the propelling agent is decreased more slowly than the mass of the working medium connected by it increases.

It is easy to see from relations (17.3) and (17.4) that with a decrease in flight speed the effect of the increase in thrust increases. It appears the greatest with operation of the engine on a test stand ( $V = 0$ ); in this case

$$\frac{G_2}{G_1} = \left(\frac{c_1}{c_2}\right)^2 \quad (17.5)$$

$$\frac{R_2}{R_1} = \frac{c_1}{c_2} = \sqrt{\frac{G_2}{G_1}}. \quad (17.6)$$

Thus, on a test stand ( $V = 0$ ) the thrust of the propelling agent increases directly proportional to the square root of the magnitude of the mass of working medium rejected by it. For example, if the flow of working medium through the propelling agent is increased four times, the velocity of outflow behind the propelling agent will be reduced two times: the thrust of the propelling agent in this case increases two times.

Expression (17.4) in the general case of flight ( $V > 0$ ) can be given a clear physical interpretation.

Noticing that the thrust efficiency of the propelling agent is equal to

$$\eta_R = \frac{2V}{c+V},$$

we obtain

$$\frac{R_2}{R_1} = \frac{c_1 + V}{c_2 + V} = \frac{\eta_{R(2)}}{\eta_{R(1)}}. \quad (17.7)$$

Thus, a deceleration in outflow behind the propelling agent leads to an increase in thrust efficiency. An increase in the latter is caused by a lowering of losses of kinetic energy at the exit from the engine. Actually, from the equation of balance of energy of the propelling agent

$$\underbrace{RV}_{\text{Work of thrust}} = \eta_R \frac{(c^2 - V^2)}{2g} G = \underbrace{G \frac{(c^2 - V^2)}{2g}}_{\text{Expended kinetic energy for the creation of thrust}} - \underbrace{G \frac{(c - V)^2}{2g}}_{\text{Lost kinetic energy}} \quad (17.8)$$

it follows that an increase in thrust efficiency and also total thrust of the propelling agent is explained by the lowering of total losses of kinetic energy with the exit velocity

$$G \frac{(c - V)^2}{2g}.$$

Let us note that a decrease in the increase in velocity of gas inside the engine ( $\Delta c = c - V$ ) with an increase in the additional mass denotes also a continuous drop in specific thrust of the propelling agent.

Since the hourly fuel consumption of a jet engine as a thermal machine when the addition of an additional mass of the working medium remains constant, and the thrust of the engine increases, then the specific fuel consumption is lowered inversely proportional to its increase; in this case

$$\frac{C_{y(2)}}{C_{y(1)}} = \frac{R_1}{R_2} = \frac{c_2 + V}{c_1 + V}. \quad (17.9)$$

Thus, the final result of the addition of additional masses of the working medium of the propelling agent is an increase in economy of the engine, i.e., a lowering of specific fuel consumption. The increase in thrust of the engine is a partial result of the use of a highly productive propelling agent. With the addition of additional air masses it is possible simultaneously to decrease dimensions of the engine so that its thrust remains constant or is even decreased in comparison with its initial value. However, the specific fuel consumption of the engine in this case all the same is reduced, and the more intensive this is, the more added is the mass of the propelling agent. Thus, principle of mass transfer can be formulated thus: *at the assigned magnitude of mechanical energy obtained inside the jet engine as a thermal machine, the specific fuel consumption of the engine will be less, the more the additional mass of the propelling agent, and, consequently, the higher the thrust efficiency.*

Let us specify now how the absolute value of flight speed affects principle of mass transfer formulated above. With an increase in the flight speed and at an invariable magnitude of expended mechanical energy, i.e., when  $L_e = \text{const}$ , the specific thrust of any propelling agent drops. The drop in specific thrust there is faster, the less its absolute value on the test stand (Fig. 17.4), i.e., the less the energy quantity ( $L_e$ ) obtains 1 kg of working medium.

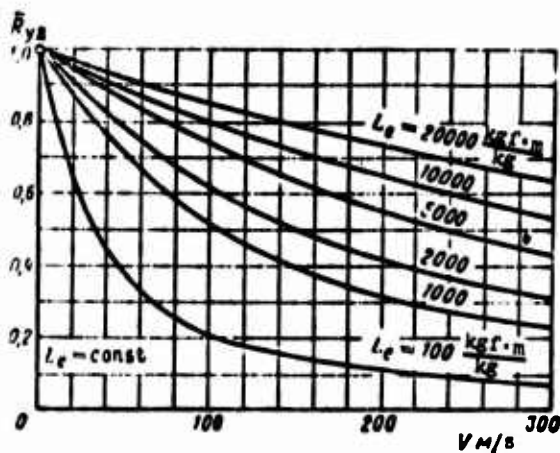


Fig. 17.4. Effect of work of the cycle on the drop in specific thrust of the propelling agent with respect to flight speed.

Thus, at the assigned magnitude of additional mass the thrust of the propelling agent in flight proves to be considerably less than that on the test stand; correspondingly, the effect of the increase in thrust with an increase in productivity of the propelling agent is lowered. The latter also follows from expression (17.7). Actually, with an increase in flight speed thrust efficiency increases. However, when its initial value is great (i.e., is little distinguished from unity), then it is obvious that further deceleration behind the propelling agent by means of the addition of additional air mass can no longer considerably increase  $\eta_R$ .

The presence of inevitable losses with energy exchange and conversion of mechanical energy into work of the jet thrust can lead to the fact that at considerable flight speeds the propelling agent with great additional mass will develop substantially less thrust.

### 17.3. Principle of Energy Exchange in the Ducted-Fan Jet Engine

Thus far we have examined how the quantity of gas mass connected by the propelling agent affects the thrust and specific fuel consumption of the engine; in this case we assumed that a fixed quantity of energy externally are fed to this mass.

Now we will examine the effect of energy exchange between circuits on the thrust of the engine and specific fuel consumption.

We will assume that the correlation of gas flow in the circuits (i.e., bypass ratio of the engine) remains constant.

Let us assume that velocities of the outflow of gas from the initial energy-free circuits are preset. The transmission of energy from the first circuit (with great available effective work) to the second circuit increases the velocity of outflow of gas from the second circuit; simultaneously the velocity of outflow of gas from the first circuit is lowered. Thus, the specific and total thrust of the second circuit (user of energy) increase, and the specific and total thrust of the first circuit (source of energy) are decreased.

When velocities of outflow from the initial circuits are considerably different from each other, the transmission of energy in the second circuit leads to an increase in total specific and total thrust of the engine.

The latter is explained in that with energy exchange velocities of outflow from the first circuit *slowly decrease*, and velocities of outflow from the second circuit *rapidly increase*.

Thus, the total specific and total thrusts of the engine initially increase, reaching a maximum value at a certain optimum magnitude of the transfer energy (optimum degree of energy exchange); further transmission of energy into the second circuit will lead to the lowering of the total thrust of the engine.

Figure 17.5 shows the effect of the degree of energy exchange  $\alpha$  on the velocity of outflow of gas from the first and second circuits of a ducted-fan jet engine and also on the change in total thrust of the engine.

In the absence of losses connected with the transmission of energy from the first circuit to the second, maximum thrust of the ducted-fan jet engine is obtained when the velocities of expiration from the circuits are identical, i.e., when

$$c_5^{II} = c_5^I \quad (17.10a)$$

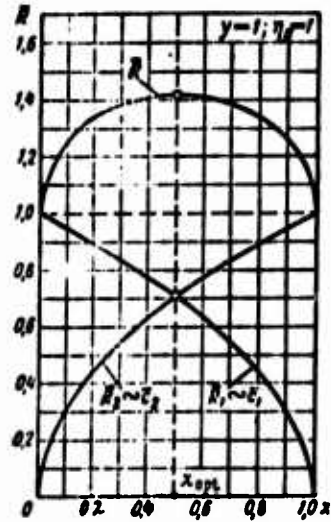


Fig. 17.5. Effect of the degree of energy exchange  $\alpha$  on thrust of a ducted-fan engine and velocity of outflow from the first and second circuits of the engine.

In the real case when part of the energy fed into the second circuit is expended for overcoming the losses ( $\eta_{II} < 1.0$ ), maximum thrust of the ducted-fan jet engine is obtained at less magnitude of the transferred energy; in this case the optimum velocity of outflow from the second circuit proves to be less than the optimum velocity of outflow from the first circuit:

$$c_5^{II} = c_5^I \eta_{II} < c_5^I \quad (17.10b)$$

The energy exchange between circuits is rational only when there exists a considerable difference between initial velocities of gas outflow from both circuits. In that case when velocities of outflow of gas from both circuits are equal, the energy exchange leads only to a drop in total thrust of the ducted-fan jet engine and to an increase in  $C_{yA}$ .

Thus, the principle of energy exchange can be formulated in the following manner: *the minimum specific fuel consumption of the ducted-fan jet engine can be reached at optimum distribution of energy between both circuits when the ratio of velocities of outflow of gas from circuits  $c_5^{II}/c_5^I$  is numerically equal to the efficiency of the energy exchange.*

17.4. Principle of Operation of Ducted-Fan Engine.  
Classification of the Ducted-Fan Engine

The ducted-fan TRD is a turbojet engine whose thrust appears in two circuits.

In Chapter 4 it was shown that jet thrust is generated when a certain mass of gas, in passing through a gas-air channel (circuit) of an engine, accomplishes a thermodynamic cycle, and as a result of this it obtains acceleration. For realization of the thermodynamic cycle in the second circuit there is a compressor, which is rotated from a common or separate turbine arranged inside the basic, first, circuit. Thus, the power of the gas turbine of the ducted-fan engine is equal to the sum of the power of compressors installed in both circuits, i.e.,

$$N_T = N_{KI} + N_{KH}.$$

To provide good economy at subsonic flight speeds, and also to obtain a low specific weight the contemporary serial ducted-fan engines have at the assimilated level of the bypass ratio ( $\gamma = 0.6-2.0$ ) values raised in comparison with the TRD of compression ratio of the compressor of the first circuit ( $\pi_{K1}^* = 14-20$ ) and gas temperatures in front of the turbine:

on takeoff . . . . .	$T_3^* = 1300 \div 1400^\circ \text{K};$
in flight . . . . .	$T_3^* = 1100 \div 1250^\circ \text{K}.$

Such parameters of the working process provide the obtaining of better foreign serial ducted-fan jet engine (Rolls-Royce Spey, Pratt-Whitney JT8D-1) of low values of specific fuel consumption:

on takeoff ( $H=0, M_0=0$ ) . . . . .	$C_{y2} = 0.58 \div 0.60 \text{ kg}/(\text{kgf}\cdot\text{h});$
in flight ( $H=11 \text{ km}; M=0.8$ ) . . . . .	$C_{y2} = 0.76 \div 0.78 \text{ kg}/(\text{kgf}\cdot\text{h}).$

Since on the turbine of the ducted-fan jet engine there occurs an increased pressure differential in comparison with the TRD, and

the greater, the more the bypass ratio of the ducted-fan jet engine, then the pressure and temperature of the gas at the entrance into the jet nozzle of the first circuit of the ducted-fan jet engine proves to be substantially lower than that of the TRD. The gas pressure behind the compressor of the second circuit of the ducted-fan engine usually is little distinguished from its value behind the turbine. Thus, the velocities of the outflow of gas from jet nozzles of the ducted-fan engine prove to be by far lower than those of the TRD, not exceeding when  $\gamma = 1-2$  magnitude of 400-500 m/s. At large values of the bypass ratio ( $\gamma = 6-8$ ) velocities of outflow from circuits of the ducted-fan engine are lowered down to magnitude 200-250 m/s.

The compression ratio  $\pi_{\text{II}}^*$  is usually selected so that the total air pressure behind compressor of the second circuit is equal to the total gas pressure behind the turbine. This provides approximately a minimum specific fuel consumption of the ducted-fan engine at a sufficiently low specific weight of the engine. For values  $T_3^*$  and  $\pi_{\text{II}}^*$ , named above, and also  $\gamma = 1-2$ , this condition limits magnitude  $\pi_{\text{II}}^*$  by values of  $\pi_{\text{II}}^* = 1.8 \div 2.7$ . At high bypass ratios ( $\gamma = 6-8$ ) magnitude  $\pi_{\text{II}}^*$  is lowered down to 1.4-1.5. This means that pressure differentials in jet nozzles of the ducted-fan engine on a test stand ( $V = 0$ ) will be subcritical.

When engine is designed for supersonic flight speeds ( $M_0 = 2.2$  to 3.5) and must develop high thrust for rapid passage through the speed of sound and exit into the cruising regime of flight, the ducted-fan engine is equipped with an afterburner installed in the second circuit or a common afterburner installed behind the confusion chamber of the engine. The common afterburner provides the greatest increase in thrust. The absence of revolving elements behind the chambers of the DTRDF allows when necessary reaching the gas temperature at the exit from the chambers up to maximum high values (2000°K) and more) provide high expiration velocities of gas (1000 to 1300 m/s).

For an increase in the economy of the DTRDF when operation in boost regimes, compression ratio of the compressor of the second circuit must be increased. The forcing of thrust in the second circuit or in two circuits requires the use of adjustable jet nozzles ( $f_{HP} = \text{var}$  and  $f_5/f_{HP} = \text{var}$ ).

At present abroad there are being developed and conducted tests of ducted-fan TRD with forced values of parameters of the working process:  $T_{3(0)}^* = 1400 \div 1530^\circ \text{K}$ ;  $\pi_{k(0)}^* = 20 \div 27$ ;  $\gamma = 6 \div 8$ . Such ducted-fan engines, calculated at subsonic flight speeds, will have very good economy with operation on a test stand [ $C_{yD} = 0.25-0.35 \text{ kg}/(\text{kgf}\cdot\text{h})$ ] and in the cruising regime of flight [ $C_{yD} = 0.58-0.65 \text{ kg}/(\text{kgf}\cdot\text{h})$ ].

Figure 17.6 shows the change in gas parameters in both circuits of a ducted-fan engine in the presence of additional fuel combustion and with its absence.

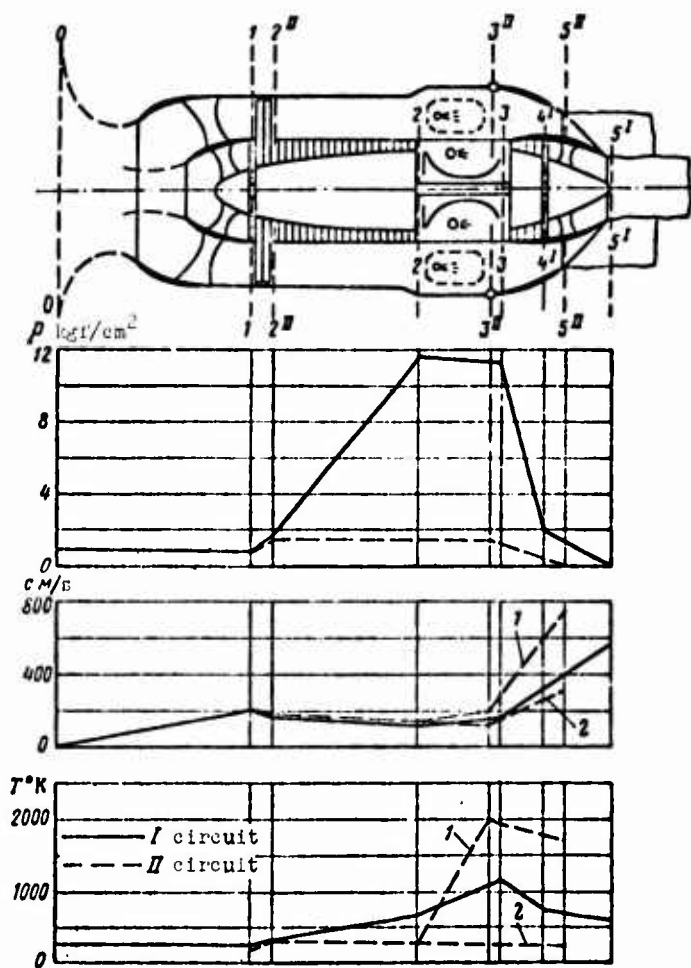


Fig. 17.6. Diagram of a ducted-fan engine and change in gas parameters in both circuits of the engine: 1 - with additional fuel combustion; 2 - in the absence of additional fuel combustion.

### 17.4.1. Designs of the Ducted-Fan Engine

There is a large variety of structural and gas-dynamic designs of the ducted-fan engine (Fig. 17.7), including these: with a front and rear disposition of the fan; with complete and partial division of gas-air channels (circuits); single, double and triple-shaft; with a different number of combustion chambers (forcing) and so on.

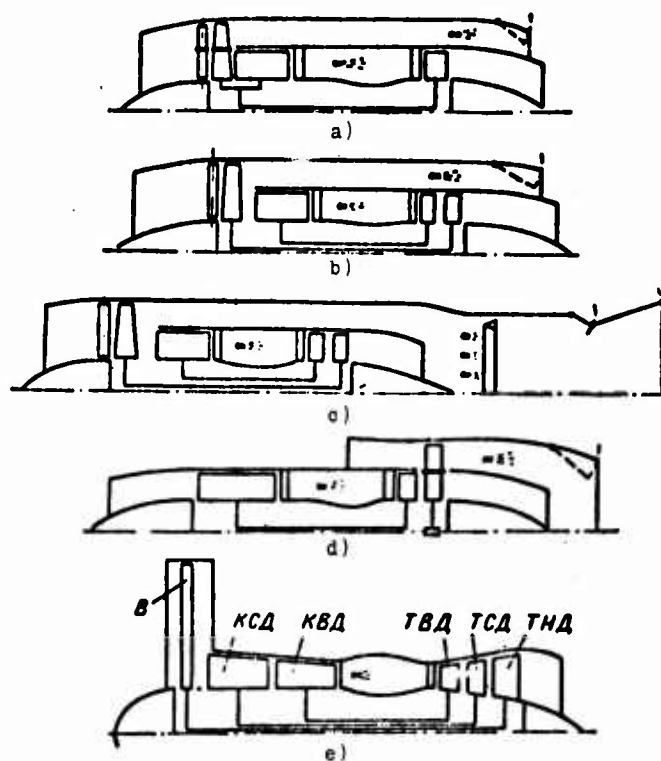


Fig. 17.7. Diagrams of the ducted-fan engine: a) diagram of a single-shaft ducted-fan engine with complete division of flows in the circuits; b) diagram of a two-shaft ducted-fan engine with a common ND compressor and separate exhaust (ducted-fan engine with front turbofan adapter); c) diagram of a two-shaft ducted-fan engine with a common ND compressor, mixing chamber, afterburner and common exhaust; d) diagram of a two-shaft ducted-fan engine with a rear turbofan adapter; e) diagram of a three-shaft ducted-fan engine with a common ND compressor and separate exhaust.

Engines made according to these designs can substantially be distinguished from each other by their operational characteristics, especially in partial load regimes, and also by peculiarities of their arrangement on an aircraft.

The use of a design with rear disposition of the fan makes it possible to create, during a brief time, on the basis of single-circuit TRD well-recommended in operation, ducted-fan engines (General Electric CJ805-23 and CF700). In this design the ventilator and ND turbine are united in one rotor and have combined blades, whose outlying (fan) part is separated by a shroud from the root (turbine) part. Such blades (Fig. 17.8) are greatly loaded and operate in loaded conditions.



Fig. 17.8. Blade of a free turbofan of the engine General Electric CJ805-23.

With the front disposition of the fan the external diameter of the engine is less. New ducted-fan engines are mostly made with front disposition of the fan and with a short air channel of the second circuit.

The ducted-fan TRD can have completely *separate* gas-air channels (separate inlets, compressors, combustion chambers, jet nozzles) or several *common* elements (for example, common inlet, common ND compressor, mixing chamber, common afterburner with a jet nozzle).

The ducted-fan TRD is, as a rule, two-shaft. At very high values of the compression ratio ( $\pi_{\text{к.г.}} = 20 \div 27$ ) and bypass ratio ( $y \geq 3 \div 6$ ) the ducted-fan engine is made in a three-shaft design (engines Rolls-Royce RB.178, RB.207 and RB.211, and also RB.203 "trent" (see Fig. 2.17)). In this case the single-stage fan is single-shaft and the gas generator of the basic circuit - two-shaft.

Such a design substantially improves the operational properties of the engine (facilitates starting, lowers the specific fuel consumption in partial load regimes, increases margins of drag of the compressor) and, specifically, makes it possible by means of adjustment of the number of revolutions of the fan to reduce the level of noise produced by it (upon landing).

#### 17.4.2. Several Design Peculiarities of Elements of the Ducted-Fan Engine

Design peculiarities of elements of the ducted-fan engine are determined by a variety of designs of the engine; they have a considerable effect on the characteristics, specific weight, technological effectiveness of production, peculiarities of operation and other properties of the engine.

##### 17.4.2.1. Fan.

One of the most complex problems in aircraft compressor manufacturing is the creation of high-pressure transonic fan stages with blades of great elongation ( $h/b \geq 6$ ) and with a small hub-tip ratio ( $\bar{d} = d_{\text{н.г.}}/d_{\text{н.г.}} = 0.25-0.3$ ). These stages must be of low weight, have high efficiency and not be subjected to the effect of auto-oscillation (of the "flutter" type). Such fan stages of the ducted-fan engine at present are being developed (for example, the ducted-fan engine Pratt-Whitney JT3D-1 and Rolls-Royce RB.211).

When the designer strives to isolate flows in both circuits from each other, the fan blades are made with a dividing flange. It is as though such blades form two autonomous compressors - external and internal, with various characteristics. Separating flanges complicate the design and technology of production, but then they increase the dynamic strength of the blades.

Common blades of the fan (compressor) possess the valuable property of the flexibility of adjustment, specifically, the ability to redistribute automatically the total flow of air between circuits in partial load regimes, which improves the operational properties of the engine.

Very long blades of the fan possess the deficiency which hampers the obtaining of uniform aerodynamic load along the radius (as a result of a considerable change in circumferential velocities). In this case the peripheral part of them is streamlined by supersonic flow and hub (root) part - subsonic.

All this requires the use of special methods of profiling of the blades and complicates their design and production.

The fans of the ducted-fan engine with a high bypass ratio ( $y = 5-8$ ) and thrust  $R = 18-22 T$  have an external diameter of up to 2.5 m (Fig. 17.9).



Fig. 17.9. Fan of ducted-fan engine Pratt-Whitney JT9D-1 ( $y = 5$ ).

#### 17.4.2.2. Gas Turbine.

At equal thrusts and identical parameters of the working process the gas flow through the turbine of the ducted-fan engine is always less than that of the TRD. This causes less dimensions of the blades of the turbine of the ducted-fan engine. The indicated fact hampers the design fulfillment of a reliably operating system of cooling of the blades of small ducted-fan engines.

Because of the high expansion ratio, the efficiency of the turbine of the ducted-fan engine is always more than that of the TRD; it reaches a value of  $\eta_T^* = 0.93-0.94$ . The quantity of stages of the turbine when  $y = 6-8$  reaches 6-9.

#### 17.4.2.3. Mixing Chamber.

The use of the mixing chamber in nonforced and forced (in both circuits) ducted-fan engines makes it possible to simplify and reduce weight of the exhaust part of the engine and system of its control. As regards the improvement of the economy, then at the best (with effective displacement of flows) it is possible to reduce the specific fuel consumption by 1-1.5%. Usually, they are limited by the use of short *lobe mixers*, with the help of which not so much the *mixing* of the flows is provided as their *unification* (Fig. 17.10).



Fig. 17.10. Lobe mixing chamber of the engine Rolls-Royce RB.141.

#### 17.4.2.4. Afterburner.

In contrast to afterburners of the TRD, the chamber of the ducted-fan engine is characterized by a very considerable fuel consumption and by the need in its control in very wide limits. The indicated circumstance is explained by the great interval of preheating

$$(T_{\phi}^* - T_2^{*II})_{\text{TRD}} > (T_{\phi}^* - T_4^*)_{\text{TRD}}$$

and also the high values of bypass ratio used. This determines the complexity of design of the fuel sprayer of the DTRDF and systems of their control.

The presence of the external (cold) air circuit creates the main possibility of providing effective cooling of walls of the combustion chamber and also unit of the sprayer and frontal device of the chamber.

The degree of forcing of the DTRDF, especially with a common afterburner, at equal values of  $T_{\phi}^*$  is by far more than that of the TRD; this circumstance gives the DTRDF the advantage in all cases when a considerable increase in thrust (takeoff, passage through  $M_0 = 1.0$ , maximum velocity, etc.) must be provided.

Between the afterburner (or mixing chamber) and the jet nozzle it is convenient to install a thrust reverser of the lattice type. At a high bypass ratio a reverser of the bucket type is more expedient (Fig. 17.11).

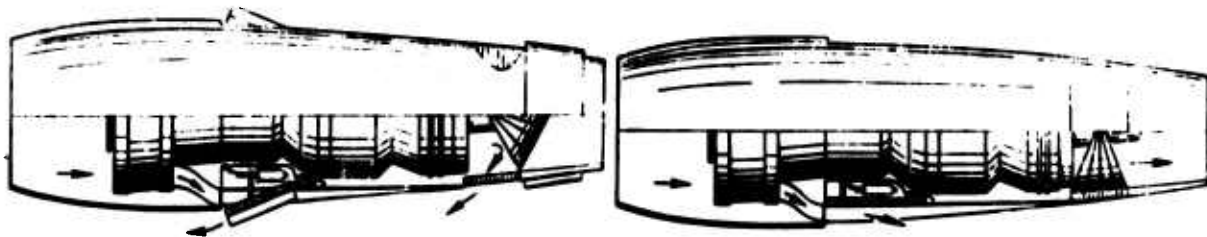


Fig. 17.11. Thrust reversers of the ducted-fan engine Pratt-Whitney JT 3D-1.

#### 17.4.2.5. Jet Nozzles.

In ducted-fan TRD jet nozzles with oblique section are widely used. Since the expansion ratios in the jet nozzles of the ducted-fan engine are less than those of the TRD (at equal values of  $\pi_{k1}^*$ ), then losses of thrust from incomplete expansion will also be less than those in the ducted-fan engine.

Figure 17.7a, b, c, d, and e show basic diagrams of the ducted-fan TRD used abroad.

#### 17.5. Thermodynamic Cycle of the Ducted-Fan Engine

The thermodynamic cycle of the ducted-fan TRD is a combination and aggregate of cycles which are accomplished in both circuits of the engine. It is characterized by the following peculiarities, which include:

- 1) the presence of one, two or three sources of heat (depending on the quantity of combustion chambers in the circuits);
- 2) the existence of energy exchange (in the form of mechanical work) between working media of the circuits;
- 3) in general, various correlations between masses of the working medium in the circuits.

Thermodynamic cycles in the circuits are the successive alternation of processes, as a result of which the working medium, because of the feed of the external energy in the form of heat or mechanical work, continuously accomplishes useful work in the form of a certain increase in kinetic energy of the effluent gas.

To determine velocities of outflow from the circuits and, consequently, specific thrusts, a sequential examination of processes which are accomplished in both circuits is necessary. To estimate the thermodynamic effectiveness of the engine, the cycle of the

ducted-fan engine as a whole must be examined: compare the total tractive work and total increase in kinetic energy of the gas with the total quantity of heat fed during the cycle.

Figure 17.12 shows the actual thermodynamic cycle of the first circuit of the ducted-fan engine ( $0-1-2^I-3-4^I-5^I$ ) in the  $(i/A)-s$  coordinates for the general case of flight ( $V > a_1$ ). It is distinguished from the cycle of the usual TRD by the peculiarity of the expansion process: the total power of the turbine is equal to the sum of the powers of the compressors established in both circuits, i.e.,

$$N_T = N_{K I} + N_{K II} \quad (17.11a)$$

or

$$G_I L_T = G_I L_{K I} + G_{II} L_{K II};$$

whence we obtain, having divided all terms of the equality by  $G_I$ ,

$$L_T = L_{K I} + y L_{K II} = L_{T I} + L_{T II} \quad (17.11b)$$

where  $L_{K I}, L_{K II}$  — the work expended for the compression of 1 kg of gas in the compressor of the first and second circuits respectively;  $L_{T I}, L_{T II}$  — the work of the turbine expended for driving compressors of the first and second circuits respectively.

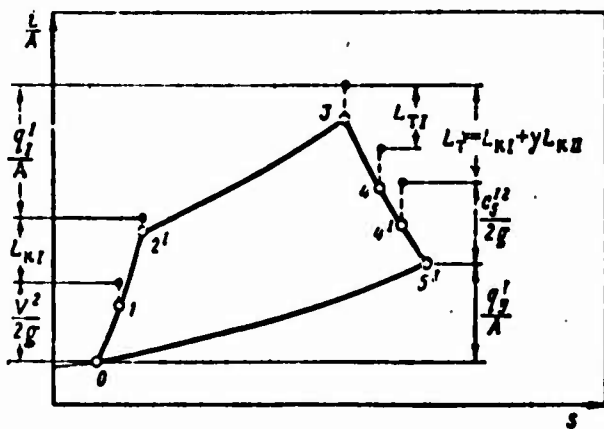


Fig. 17.12. Real thermodynamic cycle of the first circuit of the ducted-fan engine.

Figure 17.12 shows changes in the total energy of 1 kg of gas occurring in basic elements of the first circuit, and kinetic energies of entering and outgoing jets of gas corresponding to these changes, works of the compressor and of turbine, quantity of fed and removed heat.

Let us write the equation of energy for sections 0-5<sup>I</sup> of the flow of gas of the first circuit of the engine.

We have

$$q_1^I + AL_{K1} - AL_T = c_p(T_3^I - T_0) + \frac{A}{2g}(c_3^{I2} - V^2). \quad (17.12)$$

Noticing that  $L_T - L_{K1} = L_{TII}$  and  $q_{II}^I = c_p(T_3^I - T_0)$ , let us write

$$q_1^I - AL_{TII} = q_{II}^I + \frac{A}{2g}(c_3^{I2} - V^2). \quad (17.13)$$

From expression (17.13) it follows that for the assigned thermodynamic cycle of the first circuit and, consequently, for the assigned quantities of the fed ( $q_1^I$ ) and removed ( $q_{II}^I$ ) heat, an increase in kinetic energy in the first circuit is less, the greater the energy  $L_{TII}$  removed for rotation of the compressor secondary circuit.

Let us denote

$$q_1^I - q_{II}^I = AL_e,$$

where  $L_e = \frac{c_3^{I2} - V^2}{2g}$  — available useful work of the cycle of the initial TRD.

Then

$$\frac{c_3^{I2} - V^2}{2g} = L_e - L_{TII} = L_{e(t)}, \quad (17.14)$$

or, having denoted

$$\frac{L_{e1}}{L_e} = x,$$

we obtain

$$L_{e1} = \frac{c_3^{II} - v^2}{2g} = (1-x)L_e, \quad (17.15)$$

where  $x$  - degree of energy exchange between the circuits;  $L_{e(I)}$  - increase in kinetic energy of the first circuit of the ducted-fan engine (useful work of the cycle of the first circuit).

Figure 17.13 shows the real thermodynamic cycle of the second circuit of the ducted-fan engine without fuel combustion in the second circuit ( $0-1-2^{II}-5^{II}$ ) and with fuel combustion ( $0-1-2^{II}-3^{II}-5^{II}_{\phi}$ ). Here

$0-1-2^{II}$  - process of compression in the second circuit;

$2^{II}-3^{II}$  - process of heat feed in the second circuit;

$2^{II}-5^{II}$  and  $3^{II}-5^{II}_{\phi}$  } - processes of expansion in the jet nozzle of the second circuit.

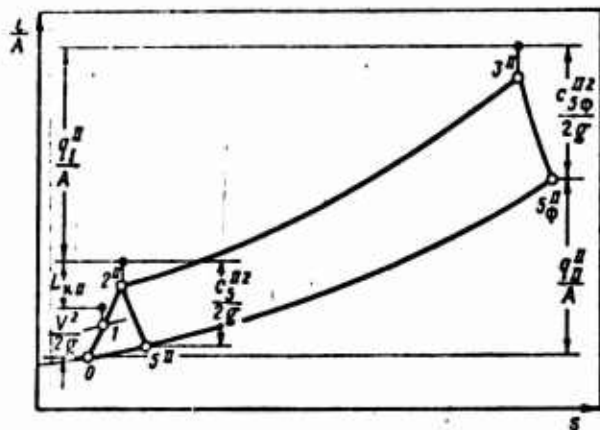


Fig. 17.13. Real thermodynamic cycle of the second circuit of the ducted-fan engine.

Let us now write the equation of energy for sections 0-5<sup>II</sup> of the flow of gas of the second circuit of the ducted-fan engine.

We have in general

$$q_{11}^{II} + AL_{KII} = c_p(T_3^{II} - T_0) + \frac{A}{2g}(c_3^{II2} - V^2). \quad (17.16)$$

Noticing that  $q_{11}^{II} = c_p(T_3^{II} - T_0)$  - heat removed during the cycle, we write

$$(q_1^I - q_{11}^{II}) + AL_{KII} = A \frac{(c_3^{II2} - V^2)}{2g} = AL_{e(II)}, \quad (17.17)$$

where  $L_{e(II)}$  - useful work of the cycle of the second circuit.

From expression (17.17) it follows that for the assigned thermodynamic cycle of the second circuit and, consequently, for assigned values  $q_1^{II}$  and  $q_{11}^{II}$ , the greater the increase in kinetic energy in the second circuit, the more the energy  $L_{KII}$  transferred to compressor (to the fan).

When in the second circuit external heat feed ( $q_{11}^{II}=0$ ) is absent, the increase in kinetic energy of the gas is always less than the energy fed from the first circuit. Part of it is expended for the preheating of the gas (conditioned by hydraulic losses) with passage of it through the circuit.

Thus

$$L_{e(II)} = L_{KII} - \frac{q_{11}^{II}}{A} < L_{KII}. \quad (17.18)$$

In the particular case when in the second circuit the energy is not fed to the gas either in the form of heat or in the form of work, the equation of energy assumes the form

$$A \frac{(V^2 - c_3^{II2})}{2g} = c_p (T_3^{II} - T_0). \quad (17.19)$$

Since in real processes of compression and broadening, because of the presence of friction, the entropy increases and heat content of the gas rises ( $T_3^{II} > T_0$ ), then the kinetic energy of flow of the energy-free circuit can only decrease ( $c_3^{II} < V$ ). In this case the second circuit creates a negative thrust

$$R_{II} = -\frac{G_{II}}{g} (V - c_3^{II}). \quad (17.20)$$

#### 17.5.1. Fundamental Equation of Balance of Work of the Second Circuit of a Ducted-Fan Engine

From the equality of powers of the compressor and turbine of the second circuit

$$N_{K II} = N_{T II},$$

or

$$G_{II} L_{K II} = G_I L_{T II},$$

it follows that

$$L_{K II} = \frac{L_{T II}}{y}. \quad (17.21)$$

Substituting  $L_{T II} = x L_c$ , we obtain

$$L_{K II} = \frac{x}{y} L_c. \quad (17.22)$$

Equations (17.21) and (17.22) are called equations of the balance of works of the turbocompressor of the second circuit. They establish the connection between compression degree of the compressor of the second circuit and parameters  $y$  and  $x$ , which characterize,

respectively, the distribution of mass of the working medium and available energy between the circuits.

### 17.5.2. Bypass Parameters

Parameters  $\pi_{KII}^*$ ,  $x$  and  $y$ , or parameters  $L_{KII}$ ,  $L_{TII}$  and  $y$ , are caused by the presence of the second circuit of the jet engine. Let us call them bypass parameters. They can be changed in a wide range of values:

$$0 < x < 1.0; \quad 0 < y < \infty; \quad 1.0 < \pi_{KII}^* < \pi_{KII}^*(x=1.0)$$

Of three parameters  $\pi_{KII}^*$ ,  $x$  and  $y$  any two are independent parameters and the third - a derivative of these two.

### 17.5.3. Determination of Parameters of the Working Process in Characteristic Sections of the Ducted-Fan Engine

We will consider as assigned parameters of the initial TRD the magnitudes  $\pi_K^*$  and  $T_3^*$ , as assigned parameters of second circuit ducted-fan engine of magnitudes  $\pi_{KII}^*$ ,  $y$  and  $T_3^{*II} = T_\phi^{*II}$  (if additionally fuel burns) and as assigned parameters of flight magnitudes  $M_0$  and  $H$ .

#### 17.5.3.1. First Circuit.

The determination of parameters in sections  $1^I$ ,  $2^I$  and  $3^I$  is produced just as it is in corresponding sections of the TRD.

Parameters of gas at the exit from the turbine of the ducted-fan engine.

Let us reduce the equation of the balance of power of the turbine and compressors of the ducted-fan engine to the form

$$L = L_{K1} + yL_{KII}$$

where

$$L_{\text{rot}} = 102,5 T_3^* (\pi_{\text{rot}}^{0,285} - 1) \frac{1}{v_{\text{rot}}}$$

Then the stagnation temperature behind the turbine can be found with the help of the energy equation

$$T_4^* = T_3^* - \frac{L_T}{118} \quad (17.23)$$

The expansion ratio of gas in the turbine  $\pi_T^*$  is easily found from the work equation of the turbine

$$L_T = 118 T_3^* \epsilon_T \eta_T^* \quad (17.24)$$

where

$$\epsilon_T = 1 - \frac{1}{\pi_T^{0,285}} = f(\pi_T^*)$$

Then the total pressure behind the turbine will be determined from expression

$$\pi_T^* = \frac{p_3^*}{p_4^*}$$

Velocity of outflow from the jet nozzle of the first circuit.

We have

$$c_3^1 = v_{p,cl} \sqrt{23107 \epsilon_{p,cl}} \quad (17.25)$$

where

$$\epsilon_{p,cl} = 1 - \frac{1}{\pi_{p,cl}^{0,285}}$$

$$\pi_{p,cl} = \frac{\pi_{\text{rot}}^{0,285} \epsilon_{h,c}}{\pi_T} = \frac{f_4^0}{f_n}$$

17.5.3.2. Second Circuit.

Determination of parameters in sections 1, 2<sup>II</sup> and 3<sup>II</sup> is produced just as in the corresponding sections of the TRD.

Velocity of outflow from the jet nozzle of the second circuit.

For the case of fuel combustion in the second circuit

$$c_{sp}^{II} = \varphi_{p.cII} \sqrt{23107 \frac{T_2^{II}}{T_2^{II}} \epsilon_{p.cII}} \quad (17.26)$$

where

$$\begin{aligned} \epsilon_{p.cII} &= 1 - \frac{1}{\pi_{p.cII}^{0.285}}; \\ \pi_{p.cII} &= \pi_a \pi_{kII} \sigma_{II}^0; \\ \sigma_{II}^0 &= \rho_3^{II} / \rho_2^{II}. \end{aligned}$$

In the absence of heat feed into the second circuit

$$c_{sp}^{II} = \varphi_{p.cII} \sqrt{20107 \frac{T_2^{II}}{T_2^{II}} \epsilon_{p.cII}} \quad (17.27)$$

where

$$T_2^{II} = T_a + \frac{L_{kII}}{102.5}; \quad \epsilon_{p.cII} = 1 - \frac{1}{\pi_{p.cII}^{0.285}}.$$

The determination of magnitudes

$$\pi_a(\epsilon_a); \quad \pi_{p.cI}(\epsilon_{p.cI}); \quad \pi_{p.cII}(\epsilon_{p.cII})$$

is conveniently produced by tables of gas-dynamic function

$$\epsilon = 1 - \frac{1}{\frac{\pi}{k}} = f(\pi)$$

for  $k_r=1,33$  and  $k_e=1,4$ .

Concept of the efficiency of the second circuit.

From an examination of the thermodynamic cycle of the second circuit (without heat feed) (see Fig. 17.13) it follows that the kinetic energy of 1 kg of the effluent gas jet

$$L_{p11} = \frac{c_3^{112}}{2g}$$

is always less than the energy expended for the compression of 1 kg of gas:

$$L_{c11} = L_{s11} + \frac{V^2}{2g}$$

Let us call the ratio of the obtained useful work of expansion to the expended work of compression of 1 kg of gas in the second circuit the efficiency of the second circuit of the ducted-fan engine, i.e.,

$$\eta_{11} = \frac{L_{p11}}{L_{c11}} = \frac{\frac{c_3^{112}}{2g}}{L_{s11} + \frac{V^2}{2g}} \quad (17.28)$$

It is approximately equal to the work of the efficiency of processes of compression and expansion in the second circuit. Actually,

$$\eta_{11} = \frac{L_{s11} \eta_{p11}}{\frac{L_{s11}}{\eta_{c11}}} = \frac{T_2^{11}}{T_{2s11}} \eta_{p11} \eta_{c11} = \alpha \eta_{p11} \eta_{c11} \quad (17.29)$$

Magnitude  $a^1$  usually does not exceed 1.01-1.04 (Fig. 17.14); with the approach of  $\pi_{KII}^*$  and  $\eta_{KII}^*$  to unity the coefficient  $a$  also approaches unity.

Thus,

$$\eta_{II} \approx \eta_{pII} \eta_{cII}. \quad (17.30)$$

At subsonic flight speeds the efficiency of compression is little distinguished from the efficiency of compressor of the second circuit. With  $M_0 = 0$  we have  $\eta_{cII} < \eta_{KII}^*$ ; with an increase in  $M_0$  magnitude  $\eta_{cII}$  slowly increases (Fig. 17.15).

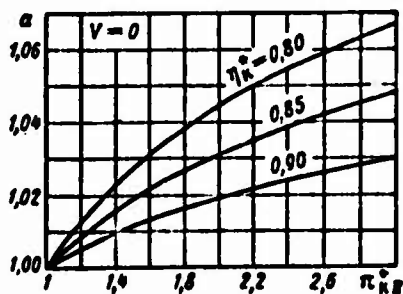


Fig. 17.14. Determination of correction coefficient  $a$ .

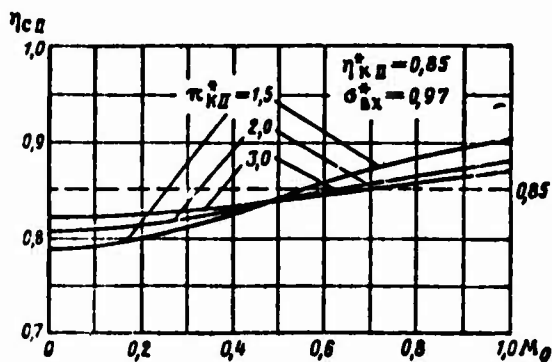


Fig. 17.15. Effect of  $M_0$  number of flight on  $\eta_{cII}$ .

$$a = \frac{T_2^{*II}}{T_{2a}^{*II}} = \frac{1}{\eta_{cII}} \left[ 1 - \frac{(1 - \eta_{cII})}{\sigma_{BK}^*} \right]$$

The efficiency of expansion of the second circuit in the absence of additional hydraulic losses on the section between the compressor and jet nozzle is equal to:

$$\eta_{p,II} = \eta_{p,II}^* \quad (17.31)$$

On the test stand for  $\eta_k^* = 0,82 \div 0,86$ ;  $\eta_{p,c} = 0,97 \div 0,98$  we find  $\eta_{JI} = 0.75$  to 0.80.

### 17.5.3.3. Determination of Velocities of Outflow of gas with the Help of Bypass Parameters.

Solving equation (17.15) with respect to  $c_5^I$  we obtain

$$c_5^I = \sqrt{2g L_e (1-x) + V^2}. \quad (17.32)$$

Similarly, from equation (17.28) we find

$$c_5^{II} = \sqrt{2g \left( L_{k,II} + \frac{V^2}{2g} \right) \eta_{II}}. \quad (17.33)$$

or

$$c_5^{II} = \sqrt{2g \left( \frac{x}{y} L_e + \frac{V^2}{2g} \right) \eta_{II}}. \quad (17.34)$$

Thus, the lower the efficiency of the second circuit, the less the velocity of outflow from it.

## 17.6. Basic Parameters of the Ducted-Fan Engine

Rate of air flow.

$$G = G_I + G_{II} = G_I(1+y). \quad (17.35)$$

Thrust.

Let us call thrust of the ducted-fan engine the sum of jet thrusts of the first and second circuits of the engine, i.e.,

$$R = R_I + R_{II},$$

or

$$R = G_I R_{yI} + G_{II} R_{yII},$$

or

$$R = G_I (R_{yI} + y R_{yII}), \quad (17.36)$$

where

$$R_{yI} = \frac{c_s^I - V}{g}; \quad R_{yII} = \frac{c_s^{II} - V}{g};$$

$R_{yI}$  and  $R_{yII}$  - specific thrusts, respectively, of the first and second circuits.

Then

$$R = \frac{G_I}{g} [(c_s^I - V) + y (c_s^{II} - V)]. \quad (17.37)$$

Specific thrust.

Let us call the specific thrust of the ducted-fan engine the thrust referred to 1 kg of total air flow through the engine, i.e.,

$$R_{yA} = \frac{R}{G} = \frac{R_I + R_{II}}{G_I + G_{II}},$$

or

$$R_{ya} = \frac{R_{yaI} + yR_{yaII}}{1 + y}. \quad (17.38)$$

Fuel consumption per second.

$$G_r = G_{rI} + G_{rII}. \quad (17.39)$$

Fuel consumption per 1 kg of total air flow.

$$m_r = \frac{1}{aI_0} = \frac{G_r}{G_a} = \frac{G_{rI} + G_{rII}}{G_I + G_{II}},$$

or

$$m_r = \frac{m_I + y m_{II}}{1 + y}, \quad (17.40)$$

where

$$m_I = \frac{G_{rI}}{G_I} = \frac{c_{pm}(T_3^{I*} - T_2^{I*})}{\xi_{n,c}^I H_u}; \quad m_{II} = \frac{G_{rII}}{G_{II}} = \frac{c_{pm}(T_3^{II*} - T_2^{II*})}{\xi_{n,c}^{II} H_u}.$$

Specific fuel consumption.

$$C_{ya} = 3600 \frac{m_r}{R_{ya}} = 3600 \frac{m_I + y m_{II}}{R_{yaI} + y R_{yaII}}. \quad (17.41)$$

Increase in the kinetic energy in the ducted-fan engine referred to 1 kg of total air flow.

$$\Delta K = \frac{\Delta K_I + \Delta K_{II}}{1 + y}, \quad (17.42)$$

where

$$\Delta K_I = \frac{c_s^{I2} - V^2}{2g}; \quad \Delta K_{II} = \frac{c_s^{II2} - V^2}{2g}.$$

External heat referred to 1 kg of total air flow.

$$q_{\text{ext}} = \frac{q_{\text{ext}}^I + \nu q_{\text{ext}}^{II}}{1 + \nu}, \quad (17.43)$$

where

$$q_{\text{ext}}^I = \frac{c_{pm}}{\xi_{\text{h.c}}^I} (T_3^{I*} - T_2^{I*}); \quad q_{\text{ext}}^{II} = \frac{c_{pm}}{\xi_{\text{h.c}}^{II}} (T_3^{II*} - T_2^{II*}).$$

Thrust efficiency.

$$\eta_R = \frac{R_{y2} V}{\Delta K} = \frac{(R_{y21} + \nu R_{y211}) V}{\Delta K_I + \nu \Delta K_{II}}. \quad (17.44)$$

Effective efficiency.

$$\eta_e = \frac{A \Delta K}{q_{\text{ext}}} = A \frac{\Delta K_I + \nu \Delta K_{II}}{q_{\text{ext}}^I + \nu q_{\text{ext}}^{II}}. \quad (17.45)$$

Total efficiency.

$$\eta_0 = A \frac{R_{y2} V}{q_{\text{ext}}} = \frac{(R_{y21} + \nu R_{y211}) V}{q_{\text{ext}}^I + \nu q_{\text{ext}}^{II}} A = \eta_R \eta_e. \quad (17.46)$$

Frontal thrust.

The use of the second circuit in the ducted-fan engine is frequently connected with an increase in external diameters of the engine and of nacelle of the engine; therefore, to estimate the effectiveness of the ducted-fan engine frontal thrusts of the ducted-fan engine and TRD must be compared.

Let us call frontal thrust of the ducted-fan engine the thrust referred to 1 m<sup>2</sup> mid-section of the engine,

$$R_{\text{vis}} = \frac{R}{F}.$$

Assuming that the mid-section of the ducted-fan engine is determined by overall dimensions of the compressor, and considering that the axial velocities of flow at the entrance into the compressors of the first and second circuits are equal to each other, let us write

$$f_1 = \frac{G \sqrt{T_1}}{m \rho_1 q(\lambda_1)} = F(1 - d_1^2),$$

where

$$q(\lambda_1) = q(\lambda_1^I) = q(\lambda_1^{II}); \quad f_1 = f_1^I + f_1^{II};$$

then

$$R_{s,1} = \frac{R_{y,2} m \rho_1 q(\lambda_1)}{\sqrt{T_1}} (1 - d_1^2). \quad (17.47)$$

## CHAPTER 18

### THERMODYNAMIC PROPERTIES OF NONBOOSTED AND BOOSTED DUCTED-FAN ENGINES

#### 18.1. Effect of Bypass Parameter on Specific Parameters of Nonboosted Ducted-Fan Engines

Let us examine the thermodynamic properties and peculiarities of a ducted-fan TRD, the effect of bypass parameters and working process, and also flight speed on specific parameters and efficiency of the engines.

##### 18.1.1. Dependence of Total and Specific Thrust of the Ducted-Fan Engine on Bypass Parameters and Cycle

Let us express the specific thrust of the ducted-fan engine

$$R_{y1} = \frac{R_{y11} + yR_{y12}}{1+y}$$

in terms of parameters of the cycle and bypass, having used relations (17.33) and (17.34).

For the general case of flight ( $V > 0$ ) the specific thrust of nonboosted ducted-fan jet engine is equal to:

$$R_{y1} = \frac{1}{g(1+y)} \left\{ (V \sqrt{2g(1-x)L_0 + V^2} - V) + y \left[ \sqrt{(2 \frac{r}{y} L_0 + V^2) \eta_{11}} - V \right] \right\}. \quad (18.1)$$

In the particular case of operation of the ducted-fan engine on a test stand ( $V = 0$ ), we obtain

$$R_{y1} = \frac{1}{g(1+y)} \left( \sqrt{2g(1-x)L_e} + y \sqrt{2g \frac{x}{y} L_e \eta_{II}} \right). \quad (18.2)$$

Let us also write the expression of total thrust of the non-boosted ducted-fan engine

$$R = R_{y1} G_1 (1+y),$$

or

$$R = \frac{G_1}{g} \left\{ \left( \sqrt{2g(1-x)L_e + V^2} - V \right) + y \left[ \sqrt{\left( 2g \frac{x}{y} L_e + V^2 \right) \eta_{II}} - V \right] \right\}. \quad (18.3)$$

Formulas (18.1) and (18.3) make it possible to investigate the effect of bypass parameters on specific and total thrust, and also specific fuel consumption of the nonboosted ducted-fan engine at assigned parameters of the cycle and flight. In other words, they make it possible to compare the basic thermodynamic indices of effectiveness ( $R_{y1}$ ,  $R$ ,  $C_{y1}$ ) of the "original" one-circuit TRD and endless quantity of "derived" ducted-fan TRD, which are distinguished from each other by values of bypass parameters  $y$ ,  $x$  and  $\pi_{HII}^*$ .

Concepts of "derived" ducted-fan engine and "original" TRD are not conditional. There exists, for example, a whole class of ducted-fan engines appearing precisely on the basis of the assigned TRD with the help of the addition of the rear turbofan adapter (for example, General Electric CJ 805-23 and CF700 engines). The derived ducted-fan engine and original TRD formed in this manner have an identical rate of air flow through the basic circuit and also identical parameters of the working process in this circuit.

For any nonboosted ducted-fan engine (independently of its design), it is always possible to find the original TRD if we mentally reject the second circuit with stages of the compressor established in it and decrease the quantity of stages and work of the turbine. Such a comparison of the ducted-fan engine and TRD is the natural and initial method of their comparison with respect to thermodynamic parameters.

#### 18.1.2. Most Advantageous Distribution of Effective Work Between Circuits of the Nonboosted Ducted-Fan Engine

Let us assume that parameters of the working process and consequently, effective work of the "original" TRD is assigned.

Let us assign a certain value of the bypass ratio of "derived" ducted-fan engines ( $y = \text{const}$ ). Let us examine the effect of the degree of energy exchange  $\alpha$  and parameter  $\pi_{KII}^*$  uniquely connected with it on specific parameters  $R_{yA}$  and  $C_{yA}$  of the engine.

With an increase in the portion of work of the cycle transferred to the second circuit, i.e., with an increase in  $\alpha$ , the velocity of outflow of gas from the first circuit  $c_5^I$  is diminished; the velocity of outflow of gas from the second circuit  $c_5^{II}$  (equal to zero when  $V = 0$  and  $\alpha = 0$ ) simultaneously increases. At the assigned air flow through the first and second circuits, the total thrust of the engine with amplification of energy exchange increases, since losses of kinetic energy for the creation of thrust are diminished and thrust and total efficiency of the engine increase.

The specific fuel consumption (for 1 kg of total thrust) in this case is respectively diminished. The latter is explained by the fact that with an increase in total thrust the hourly fuel consumption of the gas generator in the presence of energy exchange between the circuits remains constant.

At a certain optimum value  $x$  (and  $\pi_{\text{HII}}^*$ ) the specific and total thrusts reach a maximum, and then with a further increase in value of  $x$  up to unity, magnitudes  $R_{yA}$  and  $K$  are continuously lowered. According to this, the specific fuel consumption reaches a minimum and then continuously increases.

Let us now find conditions of the most advantageous distribution of the available effective work  $L_e$  between the circuits at which the specific and total thrusts of the ducted-fan engine reach a maximum and the specific fuel consumption - minimum values. For this let us reduce the expanded expression (18.1) for specific thrust of the nonboosted ducted-fan engine

$$R_{yA} = \frac{1}{\kappa(1+\mu)} \left\{ (\sqrt{2g(1-x)L_e + V^2} - V) + \right. \\ \left. + y \left[ \sqrt{\left(2g \frac{x}{y} L_e + V^2\right) \eta_{\text{HII}} - V} \right] \right\}$$

to the form

$$R_{yA} = \frac{V}{\kappa(1+\mu)} \left\{ (\sqrt{B(1-x)+1} - 1) + \right. \\ \left. + y \left[ \sqrt{\left(\frac{x}{y} B + 1\right) \eta_{\text{HII}} - 1} \right] \right\}, \quad (18.4)$$

where

$$B = \frac{L_e}{V^2 2g}.$$

Differentiating  $R_{yA} = f(x)$ , let us find after simple conversions, using condition  $dR_{yA}/dx = 0$ ,

$$x_{\text{opt}} = 1 - \frac{1 + \frac{\mu}{B} (1 - \eta_{\text{HII}})}{1 + y \eta_{\text{HII}}} = \frac{\eta_{\text{HII}} - \frac{1}{B} (1 - \eta_{\text{HII}})}{\frac{1}{y} + \eta_{\text{HII}}}. \quad (18.5)$$

From formula (18.5) it follows that in flight and with operation on the ground with an increase in the bypass ratio and efficiency of energy exchange, the portion of effective work which must be imparted to the second circuit for providing the greatest thrust of the ducted-fan engine continuously increases.

Value  $x_{opt}$  corresponds to optimum values of work of the compressor of the second circuit

$$L_{xII(opt)} = \frac{[(B+1)\eta_{II}-1]}{(1+y\eta_{II})} \frac{V^2}{2g}, \quad (18.6)$$

Velocities of gas outflow from the jet nozzles of the first and second circuits

$$c_s^I = \sqrt{\frac{B+1+y}{1+y\eta_{II}}} \cdot V; \quad (18.7)$$

$$c_s^{II} = \eta_{II} \sqrt{\frac{B+1+y}{1+y\eta_{II}}} \cdot V \quad (18.8)$$

and ratio of velocities of outflow equal to

$$\frac{c_s^{II}}{c_s^I} = \eta_{II} < 1, 0. \quad (18.9)$$

This result is very noteworthy. It expresses the essence of the basic principle of energy exchange in the ducted-fan engine (see Section 17.3)

Having substituted value  $x_{opt}$  from expression (18.5) into (18.4), after several conversions, we obtain expressions for the maximum specific thrust

$$R_{ya(max)} = \frac{V}{g(1+y)} [V\sqrt{(B+y+1)(1+y\eta_{II})} - (1+y)] \quad (18.10)$$

and maximum total thrust of the nonboosted ducted-fan engine

$$R_{max} = \frac{G_1 V}{g} [V(B + y + 1)(1 + y\eta_{II}) - (1 + y)]. \quad (18.11)$$

From expressions (18.7), (18.8) and (18.10) it follows that optimum velocities of outflow from both circuits and also specific thrust of the ducted-fan engine, with an increase in the bypass ratio continuously drop (Fig. 18.1), and, moreover, the faster they do, the more the hydraulic losses in the second circuit. When  $y = 0$  expression (18.10) turns into the usual formula of specific thrust of the TRD.

From expression (18.5) it is evident that in flight with a decrease in  $B$  (i.e., with a drop in  $L_e$  and with an increase in flight speed) the optimum value of the coefficient of distribution of energy  $x_{opt}$  continuously drops, approaching zero. This means that with an increase in the flight speed for obtaining as large a thrust as possible all the lesser part of effective work must be transferred into the second circuit.

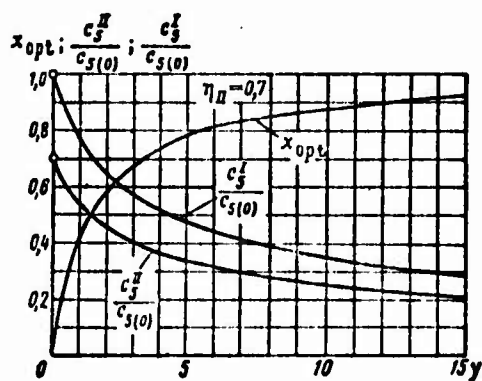


Fig. 18.1. Effect of the bypass ratio on optimum velocities of gas outflow from circuits of the ducted-fan engine.

The velocity at which  $x_{opt} = 0$  determines the theoretical limit of the rational use of the ducted-fan engine.

Having equated  $x_{opt} = 0$ , we obtain

$$B_{min} = \frac{2g l_e}{V^2} = \frac{1}{\eta_{II}} - 1. \quad (18.12)$$

whence it is easy to find the sought velocity  $V_{(x=0)}$ .

The lowering of  $x_{opt}$  with an increase in the flight speed is explained by the relative decrease in effectiveness of mechanical compression at high values of the dynamic compression ratio.

In the ideal case when  $\eta_{II} = 1$ , we find  $B_{min} = 0$ , or  $L_e = 0$ . In other words, in the absence of losses the energy exchange between the first and second circuits is effective in the whole speed flight range.

### 18.1.3. Optimum Values of Bypass Parameters and Parameters of the Engine on a Test Stand

Let us find now  $x_{opt}$  when  $V = 0$ . Having substituted into expression (18.5) the value  $B = \infty$  we obtain

$$x_{opt} = \frac{\mu\eta_{II}}{1 + \mu\eta_{II}} = \frac{1}{1 + \frac{1}{\mu\eta_{II}}}. \quad (18.13)$$

Optimum values of the work of the compressor of the second circuit and also velocities of outflow from jet nozzles of the ducted-fan engine on a test stand ( $V = 0$  and  $B = \infty$ ) are equal to

$$L_{KII(opt)} = \frac{L_e\eta_{II}}{1 + \mu\eta_{II}}; \quad (18.14)$$

$$c_{s(opt)}^1 = \sqrt{\frac{2gL_e}{1 + \mu\eta_{II}}} \quad (18.15)$$

$$c_{s(opt)}^{II} = \eta_{II} \sqrt{\frac{2gL_e}{1 + \mu\eta_{II}}}. \quad (18.16)$$

The expression for maximum specific thrust of the ducted-fan engine has the form

$$R_{yMmax} = \sqrt{\frac{2L_e}{g}} \frac{\sqrt{1 + \mu\eta_{II}}}{(1 + \mu)} = R_{yM(TPD)} \frac{\sqrt{1 + \mu\eta_{II}}}{(1 + \mu)}; \quad (18.17)$$

correspondingly,

$$C_{y_1(\min)} = \frac{C_{y_1(\text{TPD})}}{\sqrt{1+y\eta_{II}}} \quad (18.18)$$

#### 18.1.4. Effect of Parameters of the Cycle and Flight Speed on the Optimum Value of the Bypass Ratio of the Nonboosted Ducted-Fan Engine

On the test stand the increase in the bypass ratio with optimum distribution of energy continuously lowers the specific thrust and specific fuel consumption of the ducted-fan engine (Fig. 18.2). Consequently, when  $y \rightarrow \infty$  we have  $R_{yD} \rightarrow 0$  and  $C_{yD} \rightarrow 0$ .

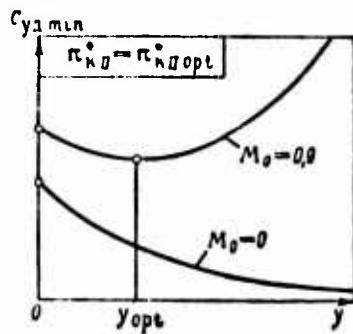


Fig. 18.2. Effect of the bypass ratio on specific fuel consumption of the ducted-fan engine on a test stand ( $M_0 = 0$ ) and in flight ( $M_0 > 0$ ).

In flight the increase in parameter  $y$ , as previously, continuously decreases the specific thrust. The specific fuel consumption is initially lowered, reaching a certain absolute minimum when  $y = y_{opt}$ , and then, with further increase in  $y$ , it increases.

To determine  $y_{opt}$  let us write the expression  $C_{yD(\min)}$  corresponding to the optimum distribution of energy between the circuits,

$$C_{y_1(\min)} = \frac{3600m}{R_{y_1(\max)}} = \frac{\text{const}}{\sqrt{(B+y+1)(1+y\eta_{II})} - (1+y)} \quad (18.19)$$

The optimum value  $y$ , which corresponds to the "minimum minimum" of specific fuel consumption, can be found from condition

$$\frac{dC_{ya}}{dy} = 0.$$

Differentiating the denominator of expression (18.19), we obtain after certain conversions

$$y_{opt} = \frac{b(B+1)-1}{\eta_{II}-b}. \quad (18.20)$$

where

$$b = (1 - \sqrt{1 - \eta_{II}})^2 = f(\eta_{II}).$$

From expression (18.20) it follows that  $y_{opt} = f(V, L_e, \text{ and } \eta_{II})$ . With a decrease in  $L_e$ , with an increase in  $V$  and drop in  $\eta_{II}$  magnitude  $y_{opt}$  is lowered. When  $V = 0$  (independent of  $\eta_{II}$ ), and also when  $\eta_{II} = 1$  (independent of  $V$ ) we have  $y_{opt} = \infty$ .

Let us find the significance  $B$  (and consequently,  $V$ ) at which  $y_{opt} = 0$ , i.e., when the ducted-fan engine degenerates into a TRD.

Having equated  $y_{opt} = 0$  in expression (18.20), we obtain

$$B_{min} = \left( \frac{L_e}{V^2/2g} \right)_{min} = \frac{1}{b} - 1. \quad (18.21)$$

With  $\eta_{p1} = 0.9$ ;  $\eta_{c1} = 0.85$ ;  $T_3^* = 1200^\circ \text{K}$ ;  $\eta_{II} = 0.8$ ;  $\pi_1 = \pi_{opt}$  we find

$$B_{min} = 2.28 \text{ and } M_{0(max)} \approx 1.7.$$

Figure 18.3 shows the change in optimum values of bypass parameters  $x$  and  $y$  on the  $M_0$  number of flight, and also the relative specific fuel consumption corresponding to these changes:

$$\bar{c}_{y_d}(\min) = \frac{C_{y_d}(\text{ДТРД})}{C_{y_d}(\text{ТРД})} = \frac{\sqrt{B+1}-1}{\sqrt{(B+1)+y}(1+y\eta_{11})-(1+y)} \quad (18.22)$$

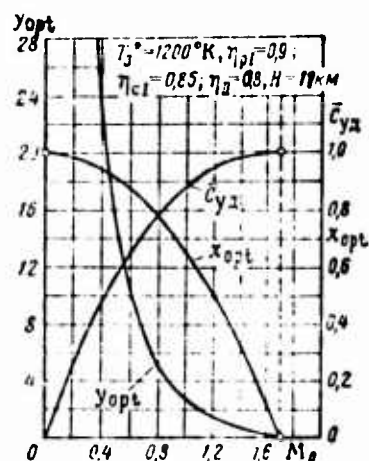


Fig. 18.3. Effect of  $M_0$ , number of flight on the optimum values of the degree of energy exchange  $x$  and bypass ratio  $y$ .

With an increase in  $M_0$  values  $x_{opt}$  and  $y_{opt}$  tend to zero and  $\bar{c}_{y_d}$  - to unity; the "regeneration" of the optimum ducted-fan engine into the TRD at values assigned above of parameters of the thermodynamic cycle approaches when  $M_{0max} = 1.7$ .

#### 18.1.5. Effect of Compression Ratio of the Compressor of the Second Circuit on Specific Parameters of the Ducted-Fan Engine

Earlier [see equation (17.22)] we determined that at a fixed value of the bypass ratio an increase in the degree of energy exchange  $x$  leads to an increase in compression ratio of the compressor of the second circuit  $\pi_{KII}^*$ .

With an increase in  $\pi_{KII}^*$  from unity to the optimum value (at which  $x = x_{opt}$ ) the specific thrust of the ducted-fan engine increases, and the specific fuel consumption is respectively lowered; with a further increase in  $\pi_{KII}^*$  up to a maximum value (at which  $x = 1$ ) the specific thrust of the engine drops, and the specific fuel consumption increases. The optimum value  $\pi_{KII}^*$  (at which the specific thrust reaches a maximum) and the economic value  $\pi_{KII}^*$  (at which the specific fuel consumption reaches a minimum) coincide, i.e., (Fig. 18.4)

$$x_{opt} = x_{ek} \text{ and } \pi_{kII(opt)} = \pi_{kII(ek)}.$$

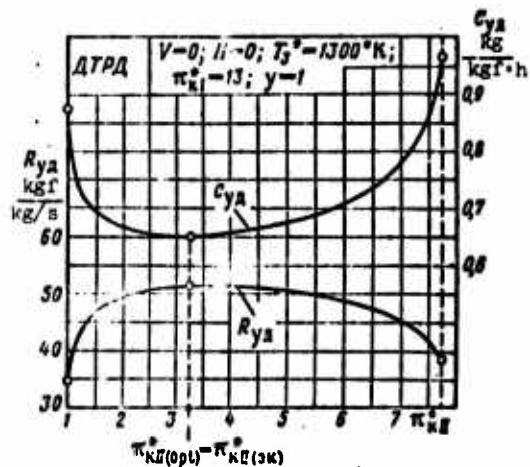


Fig. 18.4. Comparison of optimum and economic compression ratios of the compressor of the second circuit of a nonboosted ducted-fan engine.

Actually, the maximum of specific thrust corresponds to a maximum of total thrust. Since the hourly fuel consumption  $G_{ys} \sim G_{01}(T_3^* - T_2^*)$  depends on  $\pi_{kII}^*$ , then the specific fuel consumption in this case will be a minimum.

Figure 18.5 shows the effect of compression ratio of the compressor of the second circuit on the specific fuel consumption of a ducted-fan engine at various values of the bypass ratio. At small values of  $y$  curve  $C_{yD} = f(\pi_{kII}^*)$  is very sloping and has an unclearly marked minimum. With the increase in  $y$  curve  $C_{yD}$  becomes more steep, and the region of the minimum of fuel consumption is decreased, moving to the side of small values of  $\pi_{kII}^*$ .

An analysis of the effect of compression ratio of the compressor of the second circuit on the change in parameters of the working process of a nonboosted DTRD (Fig. 18.6) shows that at the optimum value  $\pi_{kII}^*$  the pressure differential in the jet nozzle of the second circuit is always more than that in the jet nozzle of the first circuit, i.e., that  $p_2^{*II} > p_2^{*I}$ .

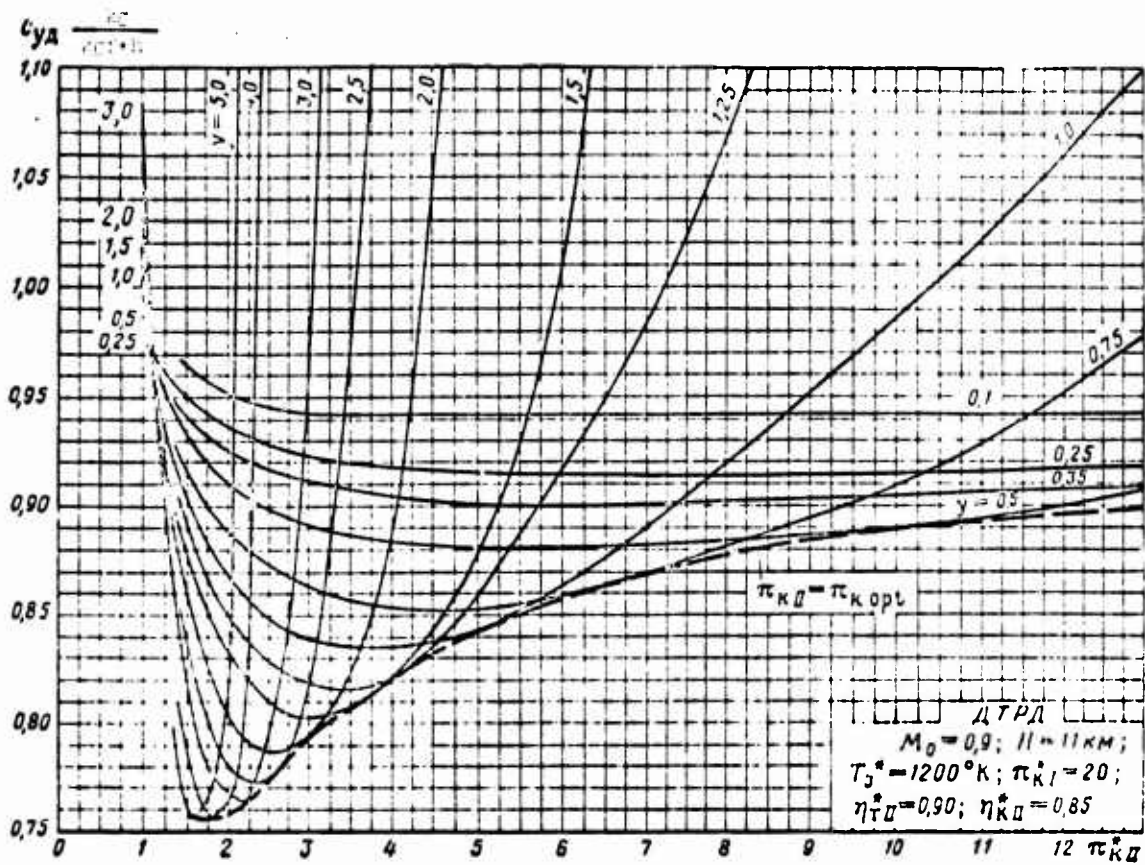


Fig. 18.5. Effect of  $\pi_{kII}^*$  and  $\gamma$  on the specific fuel consumption of a ducted-fan engine.

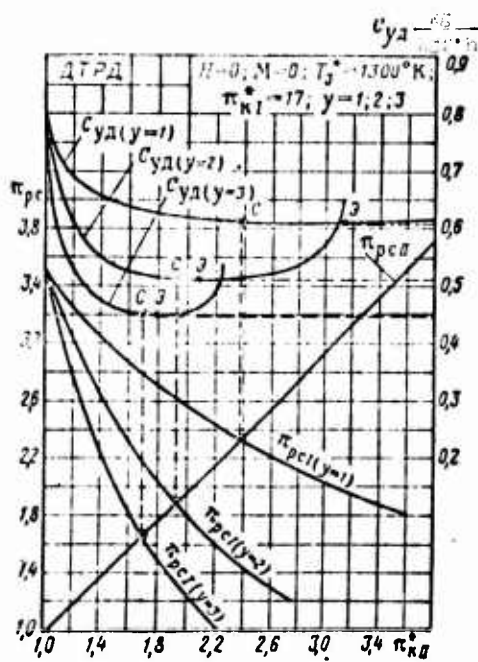


Fig. 18.6. Effect of  $\pi_{kII}^*$  on the expansion ratio of gas in jet nozzles of a ducted-fan engine:  $\alpha$  - greatest economy;  $c$  - equality of pressures in front of the nozzles.

The lowering of  $\pi_{\text{HII}}^*$  down to a magnitude at which the equality of total pressures in the jet nozzles of both circuits is established, i.e.,  $P_2^{*\text{II}} = P_4^{*\text{I}}$ , for small and moderate values of  $y (< 2-3)$  in practice  $C_{y\Delta}$  (to within 0.5-1.0%) increases.

Since in this case magnitudes  $\pi_{\text{HII}}^*$  and  $\pi_{\text{TII}}^*$  are substantially lowered, then this leads to a decrease in the quantity of stages of the turbocompressor of the second circuit and, consequently, and to a decrease in dimensions and weight of the engine. Furthermore, the equality of total gas pressures in channels of expansion of the ducted-fan engine in the presence of the mixing chamber sharply decreases losses in the latter.

Thus when  $y < 2-3$  it is expedient to produce selection of the computed value  $\pi_{\text{HII}}^*$  from the condition of providing the equality of pressures for the compressor and turbine of the second circuit.

At high bypass ratios the relatively small deviation in  $\pi_{\text{HII}}^*$  from its optimum value sharply increases the specific fuel consumption of the ducted-fan engine; the last circumstance is connected with the considerable decrease in the velocity of gas outflow from both circuits at subcritical drops in pressure. In flight this worsening in economy is aggravated by the increase in inlet pulse.

#### 18.2. Effect in Parameters of Working Process on the Specific and Dimensionless Parameters of the Ducted-Fan Engine

The effect of parameters of the working process (compression ratio of the compressor of the first circuit, temperatures of gas in front of the turbine) on the specific and dimensionless parameters in the ducted-fan engine is qualitatively not distinguished from similar dependences for the single-circuit TRD.

For conditions on takeoff ( $M_0 = 0$  and  $H = 0$ ) curves of specific and dimensionless parameters of the ducted-fan engine and TRD are distinguished only by "scale" - at equal  $\pi_{\text{H}\Sigma}^*$  and  $T_3^*$  the specific

thrust and specific fuel consumption of the DTRD in a wide range of parameters of the working process are lower than those of the TRD. The optimum and economic values  $\pi_{\text{HII}}^*$  and  $I_{\text{sp}}^*$  for the TRD and TRD coincide. When  $L_e \rightarrow 0$  the specific thrusts of the DTRD and TRD simultaneously approach zero and specific fuel consumption - infinity.

### 18.2.1. Effect of $\pi_{\text{HII}}^*$ when $M_0 > 0$

Figure 18.7 and Fig. 18.8 show the effect of compression ratio of the compressor of the basic circuit on specific parameters of the ducted-fan engine ( $y = 2$ ) and TRD ( $y = 0$ ) when  $M_0 = 0.9$  and  $H = 11$  km. The distribution of energy between circuits of the ducted-fan engine at all values of the gas parameters is accepted as optimum.

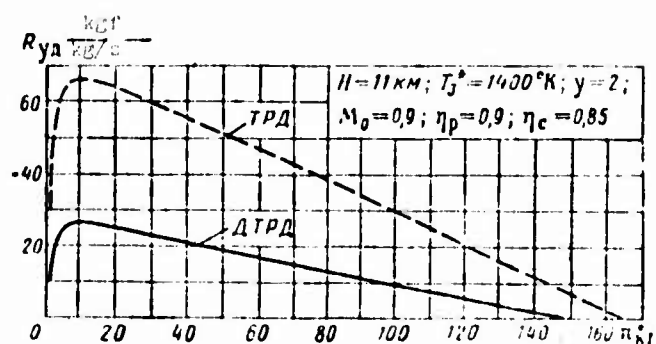


Fig. 18.7. Effect of compression ratio of the compressor of first circuit  $\pi_{\text{HII}}^*$  on the specific thrust of the TRD and ducted-fan engine.

An analysis of expressions for the specific thrust of the ducted-fan engine and TRD allows establishing that in flight the specific thrust of the ducted-fan engine becomes zero when the available effective work of the cycle still has a substantial positive value ( $L_e > 0$ ). The last circumstance is explained by the considerable effect of hydraulic losses in the second circuit at small values of effective work.

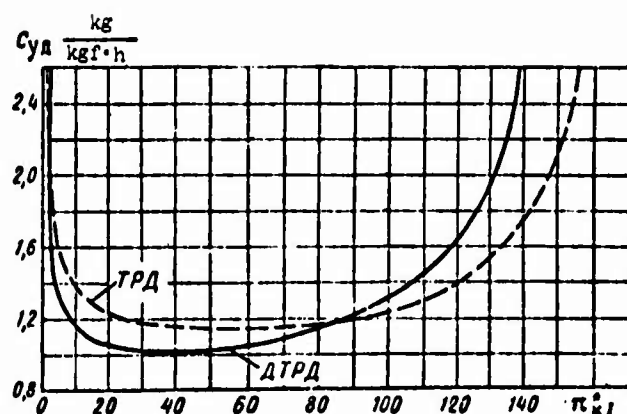


Fig. 18.8. Effect of  $\pi_{kI}^*$  on specific fuel consumption of a TRD [ТРД] and ducted-fan engine.

Thus, specific thrusts of the ducted-fan engine and TRD become zero nonsimultaneous (see Fig. 18.7), i.e., at different values of  $\pi_{kI}^*$ .

The range of positive values of specific thrust of the ducted-fan engine proves to be less than that of the TRD. This circumstance has an effect on the passage of curves of the specific fuel consumption. Curves  $C_{ya} = f(\pi_{kI}^*)$ , plotted for the ducted-fan engine and TRD (see Fig. 18.8), are "stratified," being displaced relative to each other; in this case the economic value of compression ratio of the compressor for the ducted-fan engine moves into the region of values  $\pi_{kI}^*$ . The range of values  $\pi_{kI}^*$  in which the specific fuel consumption of the ducted-fan engine appears lower than that of the TRD in flight is considerably less than it is on takeoff. It is less the greater the  $M_0$  number of flight.

A comparative worsening of the economy of the ducted-fan engine in the region of very small and very large values  $\pi_{kI}^*$  is explained by the sharp worsening of effective efficiency.

#### 18.2.2. Effect of $T_3^*$ when $M_0 > 0$

Figure 18.9 and 18.10 show the effect of gas temperature in front of the turbine  $T_3^*$  on specific parameters of the ducted-fan engine ( $\gamma = 2$ ) and TRD ( $\gamma = 0$ ) when  $M_0 = 0.9$  and  $H = 11$  km.

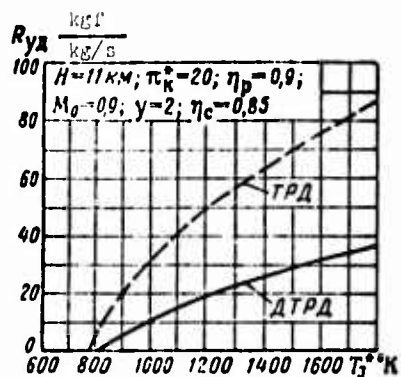


Fig. 18.9. Effect of gas temperature in front of the turbine  $T_3^*$  on specific thrust of the TRD and ducted-fan engine.

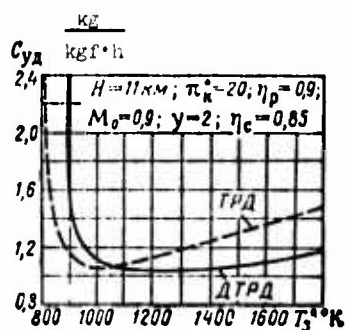


Fig. 18.10. Effect of  $T_3^*$  on specific fuel consumption of the TRD and ducted-fan engine.

It is characteristic that the specific thrust of the ducted-fan engine with a decrease in  $T_3^*$  becomes zero at a higher value of gas temperature in front of the turbine than for the TRD (see Fig. 18.9). This leads to "stratification" of curves of fuel consumption, moving the "economic" temperature of the ducted-fan engine into the region of raised values  $T_3^*$  (150-200°). With an increase in  $T_3^*$  the relative economy of the ducted-fan engine is rapidly improved (see Fig. 18.10). The latter is explained by the fact that the transmission of energy into the second circuit sharply increases the thrust efficiency with insignificant worsening of the effective efficiency. In the region of low temperatures the worsening of the economy of the ducted-fan engine is conditioned by the considerable drop in effective efficiency.

### 18.3. Heat Balance of Nonboosted Ducted-Fan TRD

Let us examine diagrams of heat balance (Fig. 18.11) of a single-circuit (a) and nonboosted ducted-fan (b) TRD constructed for conditions of flight  $H = 11$  km and  $M_0 = 0.7$ . The diagrams are

calculated on the assumption that engines have identical characteristic parameters of the thermodynamic cycle of the original circuit ( $\pi_k^* = 15$ ;  $T_3 = 1400^\circ \text{K}$ ;  $x = 0,55$ ); the bypass ratio of the ducted-fan engine is  $y = 3$ . The efficiency of combustion  $\xi_{k,c} = 0,97$ .

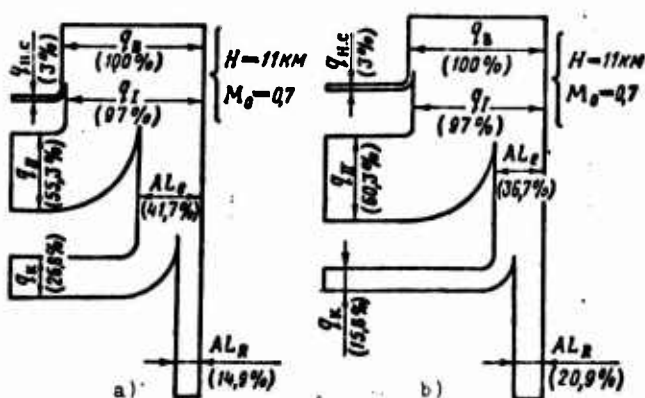


Fig. 18.11. Diagrams of heat balance: a) TRD [ТРД]; b) ducted-fan engine.

Earlier we noted that the transmission of mechanical energy from the first circuit to the second is connected with the appearance of additional hydraulic losses ( $\eta_{II} < 1.0$ ), as a result of which gases effluent from the jet nozzle of the second circuit take away part of the energy in the form of heat.

Consequently, the total increase in kinetic energy of gas flows in both circuits of the ducted-fan engine proves to be less than the increase in the kinetic energy of the original TRD, i.e.,

$$(L_{e1} + yL_{e11}) < L_e$$

Ultimately the effective efficiency of the ducted-fan engine also proves to be lower than the effective efficiency of the TRD:

$$\eta_{e(\text{ДТРД})} = \frac{A(L_{e1} + yL_{e11})}{q_{\text{вн}}} < \eta_{e(\text{ТРД})} = \frac{AL_e}{q_{\text{вн}}}$$

In the given specific example the effective efficiency drops from 41.7% to 36.7%, i.e., 12%.

Further, the imparting of approximately the same magnitude of kinetic energy to a considerably greater (in this case, four times) gas mass leads to a sharp decrease in losses with the exhaust velocity; as a result of this, a very considerable increase in thrust efficiency approaches, i.e.,

$$\left( \eta_{R(A\Gamma P \Delta)} = \frac{L_R}{L_e} = \frac{(R_{y \Delta 1} + y R_{y \Delta 11}) V}{L_{e1} + y L_{e11}} \right) > \left( \eta_{R(\Gamma P \Delta)} = \frac{R_{y \Delta(0)} V}{L_e} \right).$$

In the given specific example the thrust efficiency increases from 35.7% to 56.8%, i.e., almost 60%.

Finally, the total efficiency of the ducted-fan engine also increases, since a decrease in losses with exhaust velocity with a surplus overlaps the presence of hydraulic losses in the second circuit; consequently,

$$\left( \eta_{0(A\Gamma P \Delta)} = \frac{(R_{y \Delta 1} + y R_{y \Delta 11}) V}{q_{\text{DH}}/A} \right) > \left( \eta_{0(\Gamma P \Delta)} = \frac{R_{y \Delta(0)} V}{q_{\text{DH}}/A} \right).$$

In the considered specific case the total efficiency of the power plant increases from 14.9% to 20.9%, i.e., 40%.

#### 18.4. Thermodynamic Properties of Boosted Ducted-Fan Engines

The additional fuel combustion in the second circuit and also in both circuits of the ducted-fan engine is a very efficient means of increasing the specific and total thrust of the engine. It is used for a short time on takeoff for the reduction of the distance of the run, and also for the time of putting the aircraft into calculated cruising flight conditions.

Thrust augmentation is used even as a prolonged means of increasing the maximum velocity of the aircraft.

The additional fuel combustion at great supersonic flight speeds ( $M_0 = 2.2$  and  $3.0$ ) is also a means of improving the engine economy. If relatively low boost temperature ( $T_{\phi}^{*II} = 900-1200^{\circ}\text{K}$ ) is used, then it appears possible to reduce the specific fuel consumption in comparison with the flow of the nonforced ducted-fan engine.

The use of boost makes it possible to decrease somewhat the specific weight of the engine, since the inevitable increase in weight of the ducted-fan engine, as a result of the installation of afterburners, proves to be less considerable than the increase in thrust.

Below the thermodynamic properties and peculiarities of a boosted ducted-fan engine are examined.

#### 18.4.1. Ducted-Fan Engine with Thrust Augmentation in the Second Circuit

##### 18.4.1.1. Effect of Boost Temperature in the Second Circuit on Specific Parameters of the DTRDF when Operating on a Test Stand ( $V = 0$ and $H = 0$ ).

With an increase in the gas temperature at the exit from the afterburner of the second circuit, the velocity of gas outflow from the jet nozzle ( $c_{\phi}^{II} \sim \sqrt{T_{\phi}^{II}}$ ) increases. Consequently, the specific thrusts of the second circuit and also entire engine increase. Simultaneously there is an increase in the relative fuel consumption in this circuit proportional to the interval of preheating

$$m_f^{II} \sim (T_{\phi}^{*II} - T_2^{*II}) \sim q_1^{II}.$$

Since the quantity of external heat introduced with the fuel increases considerably faster than the specific thrust, then the specific fuel consumption (for 1 kg in thrust) increases. In other words, with an increase in  $T_{\phi}^{*II}$  there is a continuous lowering of the effective efficiency of the cycle (Fig. 18.12). The latter is

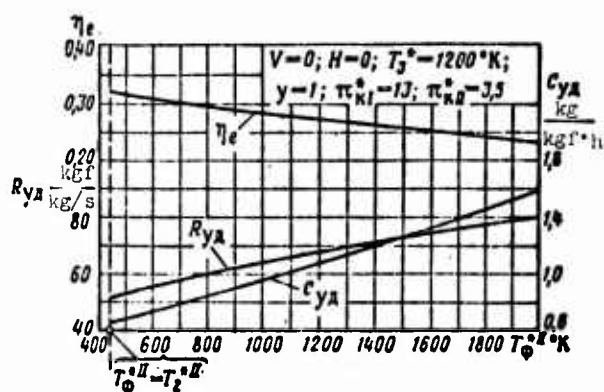


Fig. 18.12. Effect of boost temperature in the second circuit on  $\eta_e$  and specific parameters of the DTRDF II [ДТРДФ II].

explained by the fact that the thermal and effective efficiency of the second circuit on a test stand are considerably lower than those in the original TRD or ducted-fan engine, since the heat feed in this circuit is carried out at a lower pressure than that in the first circuit. The higher the boost temperature, the greater the portion of work of the cycle of the second circuit in the thermal balance of the engine, and the lower the effective efficiency of the DTRDF II. For example, if for the nonboosted ducted-fan engine  $\eta_e=0.32$ , then for the DTRDF II when  $T_{\phi}^*=2000 \text{ K}$  we have  $\eta_e=0.23$  ( $\eta_{eI}=0.16$  and  $\eta_{eII}=0.25$ ).

#### 18.4.1.2. Effect of $\pi_{\kappa II}^*$ on specific

Parameters of the DTRDF II ( $V = 0$ ).

Figure 18.13 shows the effect of  $\pi_{\kappa II}^*$  on specific parameters of the DTRDF II when  $T_{\phi}^{*II} = \text{const}$ . With an increase in  $x$  and  $\pi_{\kappa II}^*$  the specific thrust of the engine increases, reaches a maximum, and then drops. The specific fuel consumption, conversely, in the beginning is lowered, and then, having reached a minimum, it increases. However, with heat feed in the second circuit of the DTRDF the optimum value of the degree of energy exchange  $x_{opt}$  (at which the specific thrust reaches a maximum) and its economic value  $x_{\text{ЭК}}$  (at which the specific fuel consumption becomes minimum) do not coincide. The economic value of the degree of energy exchange is always more than the optimum, i.e.,

$$x_{\text{ЭК}} > x_{opt}.$$

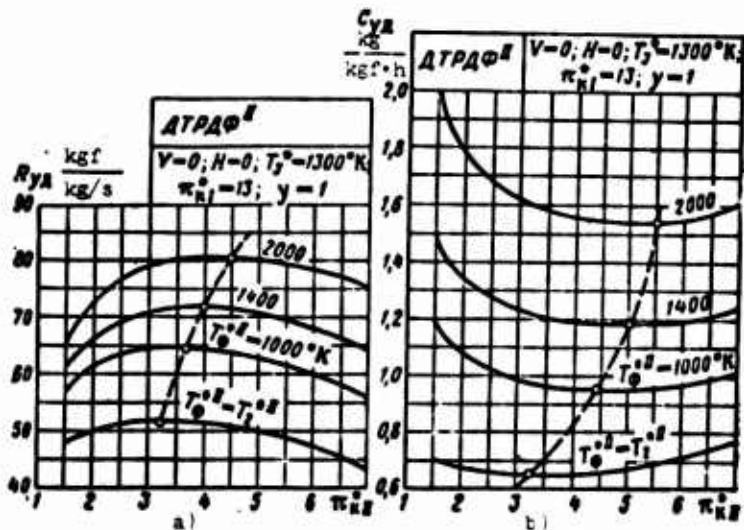


Fig. 18.13. Effect of  $\pi_{кII}^*$  and  $T_{\phi}^{*II}$  on the specific thrust of the DTRDF<sup>II</sup> (a) and specific fuel consumption of the DTRDF<sup>II</sup> (b).

When  $\gamma = \text{const}$  this means that

$$L_{кII(\text{opt})} > L_{кII(\text{opt})} \text{ and } \pi_{кII(\text{opt})}^* > \pi_{кII(\text{opt})}^* \text{ (see Fig. 18.13).}$$

With an increase in  $T_{\phi}^{*II}$  values  $\pi_{кII(\text{opt})}^*$  and  $\pi_{кII(\text{opt})}^*$  increase, and the discontinuity between them increases.

The obtained regularity has a clear thermodynamic explanation: with the increase in  $\pi_{кII}^*$  the specific thrust of the DTRDF initially increases, reaching a maximum when  $\pi_{кII}^* = \pi_{кII(\text{opt})}^*$ , and then, with a further increase in  $\pi_{кII}^*$ , drops. The relative fuel consumption  $m_{r,II}$  in this case continuously drops, since the interval of preheating in the second circuit  $\Delta T^* = T_{\phi}^{*II} - T_2^{*II}$ . Thus, with an increase in  $\pi_{кII}^*$  the specific fuel consumption of the engine also initially drops, and it reaches minimum at such value  $\pi_{кII}^*$  at which rate of drop of parameters  $m_{r,II}$  and  $R_{y,II}$  seems identical, i.e., when  $\pi_{кII(\text{opt})}^* > \pi_{кII(\text{opt})}^*$  (Fig. 18.14).

We see that the noted property of the DTRDF distinguishes it from the nonboosted ducted-fan engine, in which when  $T_{\phi}^{*II} = T_2^{*II}$  always  $\kappa_{opt} = \kappa_{ЭК}$  and  $\pi_{кII(opt)} = \pi_{кII(ЭК)}$  (see Fig. 18.4).

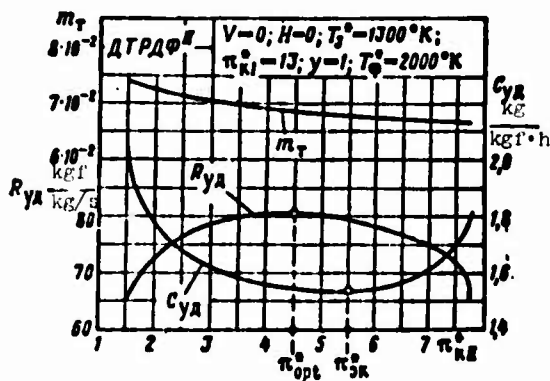


Fig. 18.14. Comparison of optimum and economic compression ratios of the compressor of the second circuit of the DTRDF<sup>II</sup> [DTRDF<sup>II</sup>].

#### 18.4.1.3. Comparison of Specific Parameters of the DTRDF<sup>II</sup> and TRDF on a Test Stand.

Figure 18.15 gives a comparison of specific fuel consumption on a test stand of a TRDF and series of ducted-fan engines with afterburner in the second circuit (DTRDF<sup>II</sup>). The engines being compared are carried out on the basis of the same original TRDF:  $\pi_{кII}^* = 13$  and  $T_3^* = 1300^{\circ}K$ . The bypass ratio of the DTRDF<sup>II</sup> is accepted as  $\gamma = 1$ , and the compression ratio  $\pi_{кII}^*$  changed from 2 to 7. The boost temperature changed in the DTRDF from  $T_{\phi}^* = T_2^{*II}$  up to  $2000^{\circ}K$ , and in the TRDF - from  $T_{\phi}^* = T_4^*$  also up to  $2000^{\circ}K$ .

At equal boost temperatures and identical stagnation pressures at the exit from the afterburner ( $\pi_{p.c II} = \pi_{p.c(I)} = 3.5$ ) in a wide range of values  $T_{\phi}^*$  (1200-2000°K) the specific fuel consumption of the DTRDF<sup>II</sup> proves to be lower than that of the TRDF. For example, when  $T_{\phi}^* = 2000^{\circ}K$  we have for the DTRDF<sup>II</sup>  $C_{yД} = 1.59$ , and for the TRDF  $C_{yД} = 1.85$  kg/(kgf·h) (i.e., 16% more).

Such a result can be explained in the following manner. At equal stagnation temperatures and pressures of the gas at the exit

from the chamber, specific thrusts of the second circuit of the DTRDF<sup>II</sup> and TRDF are equal. The relative fuel consumption of the second circuit of the DTRDF ( $m_{11}$ ), being determined by the interval of preheating ( $T_{\phi}^* - T_{21}^{**}$ ) is always less than that of the TRDF [ $m_{12} \sim (T_{\phi}^* - T_{11}^*)$ ]. Thus, with the considered conditions of comparison, the specific fuel consumption of the separately taken second circuit of the DTRDF is less than that of the TRDF. As regards the specific fuel consumption of the first circuit of the DTRDF, then under optimum conditions of energy exchange for the ducted-fan engine (assuming that  $\alpha_{opt} = \frac{y\eta_{11}}{1+y\eta_{11}}$ ) it is 25-30% higher<sup>1</sup> than in the original TRD;

however, it is considerably lower than that of the TRDF. Since the specific fuel consumption of the DTRDF occupies an intermediate position between  $C_{yA(1)}$  and  $C_{yA(11)}$ , then ultimately  $C_{yA(DTRDF^{II})} < C_{yA(TRDF)}$ .

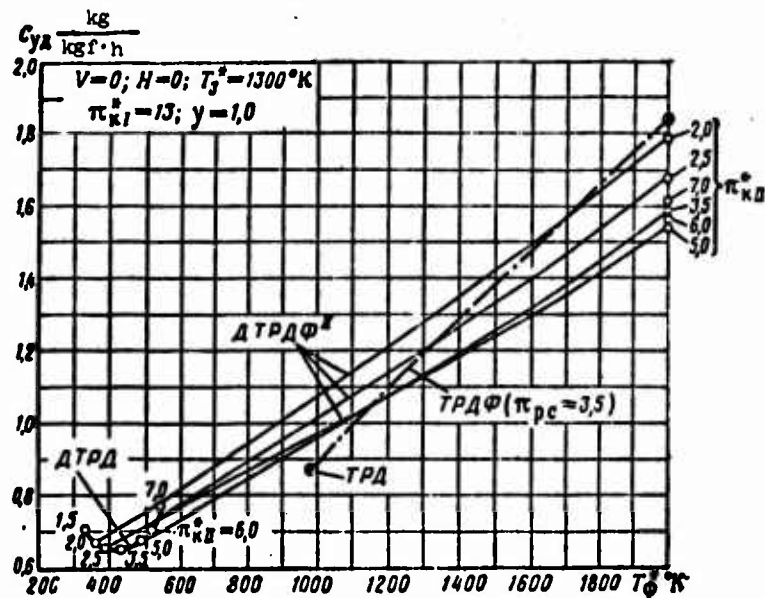


Fig. 18.15. Comparison of specific fuel consumption of the TRDF [TRDF] and DTRDF<sup>II</sup> [DTRDF<sup>II</sup>] on a test stand.

The lower the  $T_{\phi}^*$ , the less the advantage of the DTRDF with respect to economy over the TRDF.

$$^1 \frac{C_{yA(1)}^1}{C_{yA(TRD)}} = \sqrt{1+y\eta_{11}}$$

If now, on the condition that  $\pi_{p.c(II)} = \pi_{p.c(I)}$ , the boost temperature in the second circuit of the DTRDF is reduced to a value of temperature at the exit from the turbine  $T_4^*$  of the original TRD (in our example  $T_4^* = 1000^\circ\text{K}$ ), then the specific fuel consumption of such a DTRDF will be higher than that of the TRD.

This, in turn, is explained thus. With equal specific thrusts of the TRD and second circuit of the DTRDF the interval of preheating in the chamber of the DTRDF, as previously, is less than that in the chamber of the TRD, i.e.,  $(T_4^* - T_2^{**}) < (T_3^* - T_2^*) \approx (T_4^* - T_4^*)$ . Therefore, as previously,

$$C_{y_2(II)} < C_{y_2(TRD)}$$

However, the specific fuel consumption of the first circuit of the DTRDF is considerably more than that in the original TRD, i.e.,

$$C_{y_1(II)} > C_{y_1(TRD)}$$

Ultimately the specific fuel consumption of the DTRDF proves to be higher than that in the original TRD.

The change in  $\pi_{MII}^*$  affects correlation of specific fuel consumptions in both circuits and, depending on the level of the  $T_\phi^*$ , can qualitatively change the result noted earlier. Thus, for instance, at reduced values of  $\pi_{MII}^*$  and  $T_\phi^*$  (for example,  $\pi_{MII}^* = 2$  and  $T_\phi^* = 1400^\circ\text{K}$ ) we have

$$(C_{y_2(\text{ДТРДФ})} = 1,34) > (C_{y_2(\text{ТРДФ})} = 1,29 \text{ kg}/(\text{kgf}\cdot\text{h})).$$

#### 18.4.1.4. Use of the DTRDF<sup>II</sup> at Supersonic Flight Speeds.

With an increase in the boost temperature in the second circuit at subsonic flight speeds, at assigned parameters of the cycle and bypass ratio, and in the whole range of values  $\pi_{MII}^*$  the specific

thrust and specific fuel consumption of the DTRDF continuously increase (Fig. 18.16). However, as A. L. Parkhomov and I. I. Kulagin showed, at great supersonic  $M_0$  numbers (Fig. 18.17) with an increase in  $T_{\Phi}^{*II}$ , the specific fuel consumption of the DTRDF<sup>II</sup> in the beginning is decreased, reaching a minimum, and then again it increases. The "economic" value of the boost temperature increases with an increase in the flight number  $M_0$ .

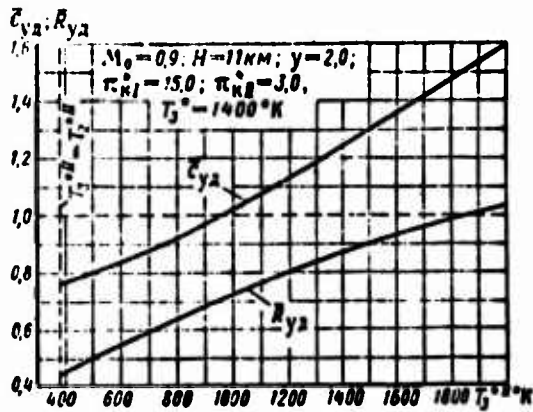


Fig. 18.16. Effect of boost temperature in the second circuit on specific parameters of the DTRDF<sup>II</sup> [ $\Delta T P \Delta \Phi^{II}$ ] ( $M_0 = 0.9$ ).

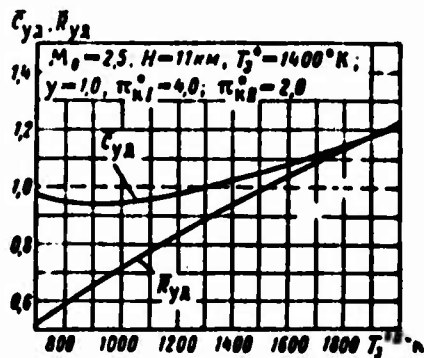


Fig. 18.17. Effect of boost temperature in the second circuit on specific parameters of the DTRDF<sup>II</sup> [ $\Delta T P \Delta \Phi^{II}$ ] ( $M_0 = 2.5$ ).

Figure 18.18 shows the change in  $C_{y\Delta}$  on temperature  $T_{\Phi}^{*}$  for different values of  $\gamma$  (from 0 to  $\infty$ ) when  $M_0 = 1.7$ . As is evident on this graph the optimum value of the bypass ratio is the value  $\gamma = 1$ . Beginning from values of  $T_{\Phi}^{*} \geq 1200^\circ \text{K}$  at identical parameters of the cycle, the DTRDF<sup>II</sup> ( $\gamma = 1$ ) forced in the second circuit has less fuel consumption than the TRDF and ramjet engine. The single-circuit nonboosted TRD under the same conditions is less economical

than the nonboosted ducted-fan engine ( $y = 1$  and  $y = 2$ ); however, the specific thrust of it in this case is substantially higher.

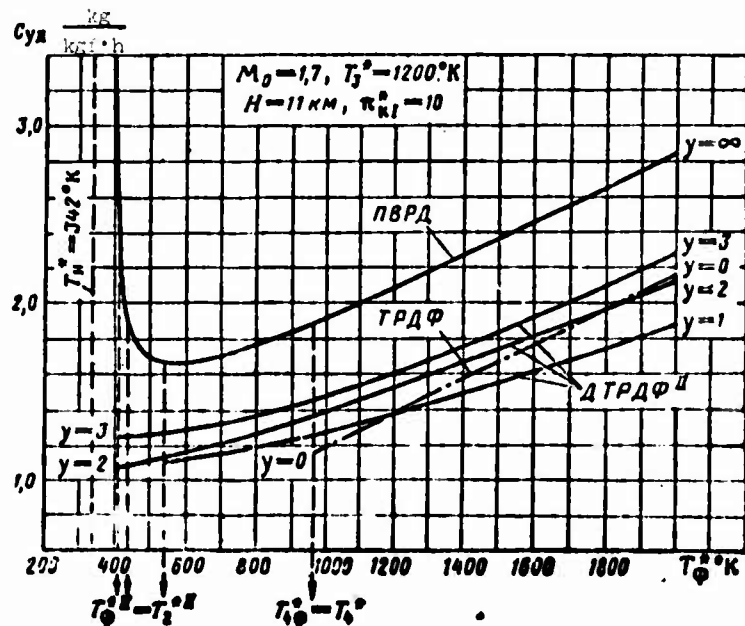


Fig. 18.18. Effect of  $T_{\phi}^*$  and  $y$  on specific fuel consumption of various jet engines ( $M_0 = 1.7$ ).

An increase in  $T_{\phi}^{*II}$  at all flight speeds moves  $\alpha_{opt}$  and  $\alpha_{EK}$  into the region of large values (i.e., the optimum and economic values of  $\pi_{RII}^*$  increase).

Finally, with an increase in the  $M_0$  number (with other conditions fixed) the optimum and economic values of  $\pi_{RII}^*$  are lowered, approaching unity.

The noted tendency is clearly illustrated by graphs (Figs. 18.19 and 18.20) plotted respectively, for  $M_0 = 2.2$  and  $M_0 = 3.0$ . From them it follows that at large numbers of  $M_0$  the expediency of energy exchange between circuits of the engine is decreased, and the optimum  $DTRDF^{II}$  with respect to specific thrust and specific fuel consumption gradually "degenerates" into a simple combination of TRD + ramjet engine.

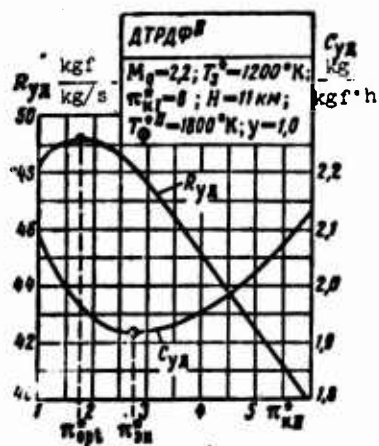


Fig. 18.19.

Fig. 18.19. Effect of  $\pi_{kII}^*$  on specific parameters of the DTRDF<sup>II</sup> ( $M_0 = 2.2$ ).

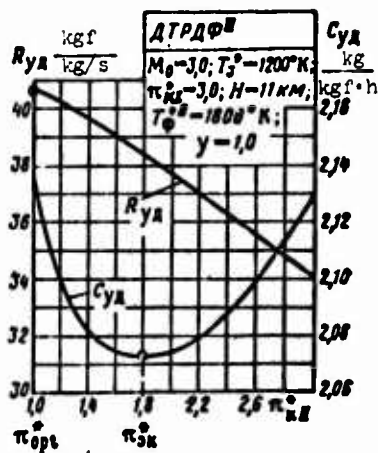


Fig. 18.20.

Fig. 18.20. Effect of  $\pi_{kII}^*$  on specific parameters of the DTRDF<sup>II</sup> ( $M_0 = 3.0$ ).

#### 18.4.2. Ducted-Fan Engine with Thrust Augmentation in Two Circuits

##### 18.4.2.1. Comparison of Relative Fuel Consumption of Various Jet Engines at Identical Maximum Temperatures of the Cycle.

Let us produce a comparison of specific thrusts and specific fuel consumptions of the DTRDF<sup>I+II</sup>, IRDF and ramjet engine at identical temperatures of braked flow at the entrance  $T_H^*$  and equal maximum temperatures of the cycle ( $T_{\diamond}^* = T_{\diamond}^{II} = T_{\diamond}^* = T_{\diamond}^*(\text{ramjet}) = T_{\text{max}}^*$ ). Let us prove that under these conditions the relative fuel consumption (fuel consumption per 1 kg of air) of the indicated three types of engines will be identical.

Actually, having written the equation of energy for 1 kg of air as applied to sections  $n-n$  and  $5-5$  of any of the considered types of engines:

$$i_5^* - i_n^* = q_s = \text{const},$$

we obtain that the total quantity of heat  $q_{\Sigma}$  fed with the fuel to 1 kg of gas is equal in all engines, regardless of whether fuel enters into one combustion chamber (ramjet engine), two (TRDF) or three chambers (DTRDF<sup>I+II</sup>).

It is characteristic that the indicated property of the engine proves to be valid independent of the effect of the specific heat of gas on the temperature.

Thus, the quantity of heat fed to 1 kg of air in the DTRDF<sup>I+II</sup>, TRDF and ramjet engine is equal. Consequently, when  $T_{max}^* = \text{const}$ ,  $T_{II}^* = \text{const}$ ,  $\epsilon_{II} = \text{const}$  and the relative fuel consumption of the engines is identical, i.e.,

$$m_{DTRDF} = m_{TRDF} = m_{DTRDF^{I+II}}$$

independent of values  $\pi_{kI}^*$ ,  $\pi_{kII}^*$ ,  $\gamma$  and gas temperatures  $T_3^*$  in front of the turbine.

On this base the conclusion can be made that when  $T_{max}^* = \text{const}$  the relative thrust of the DTRDF<sup>I+II</sup> (with respect to the thrust of the TRDF or ramjet engine) is always inversely proportional to the relative specific fuel consumption and that, consequently, any advantage of a forced ducted-fan TRD with respect to specific thrust is equivalent to its advantage with respect to economy, i.e.,

$$\bar{R}_{\gamma I} = \frac{1}{\bar{c}_{\gamma I}} \quad (18.23)$$

From expression (18.23) it also follows that the most advantageous degrees of the increase in air pressure in the second circuit of the DTRDF<sup>I+II</sup> with respect to specific thrust and economy always coincide, i.e.,

$$\pi_{kII}^* (\text{opt}) = \pi_{kII}^* (\text{ek})$$

Let us assume that at a certain value of  $M_0$  number the total pressure behind the turbine of the TRD is equal to the complete inlet pressure of compressor ( $p_4^* = p_1^*$ ). In this case the specific thrusts of the ramjet engine, TRDF and combination of the TRDF and ramjet engine are identically equal.

As regards the DTRDF<sup>I+II</sup>, then its specific thrust under these conditions, and when  $x$  is close to zero, has approximately the same value as that in the ramjet engine and TRDF. With an increase in  $x$ , i.e., with an increase in removal of mechanical energy into the second circuit, the specific parameter of the DTRDF will be worse. When  $p_4^* > p_1^*$  the specific thrust of the optimum DTRDF is more than in the ramjet engine but less than in a TRDF; when  $p_4^* < p_1^*$  the specific thrust of the DTRDF is more than in a TRDF but less than in a "pure" ramjet engine.

#### 18.4.2.2. Most Advantageous Distribution of Energy of the Ducted-Fan Engine with Thrust Augmentation in Two Circuits.

Let us examine now conditions of the most advantageous distribution of energy between circuits in the case of the ducted-fan engine with additional fuel combustion in both circuits.

Let us assume that stagnation temperatures of the gas at the exit from the afterburners are identical, i.e.,

$$T_{\phi}^{*I} = T_{\phi}^{*II} = T_{\phi}^*.$$

It is obvious that the condition of the most advantageous distribution of energy between the circuits (at assigned values of parameters  $M_0, y, T_3^*, T_{\phi}^*, \pi_n^*$ , and also efficiency and coefficient of losses of particular processes) is as previously, a guarantee of the maximum specific thrust, i.e.,

$$R_{y_{a,\phi}} = \frac{R_{y_{a,\phi}(I)} + y R_{y_{a,\phi}(II)}}{1 + y} = R_{y_{a,\phi}(max)},$$

or, which is the same thing, a guarantee of the minimum specific fuel consumption, since on account of the fact that  $m_{r,\phi} = \text{const}$ ,

$$C_{y_{r,\phi}} \sim \frac{1}{R_{y_{r,\phi}}}.$$

From the theorem of the most advantageous degree of energy exchange between the circuits, it follows that the maximum of specific and maximum of total thrusts of the DVRD corresponds in the ideal case (when  $\eta_{II} = 1,0$ ) to the equality of velocities of gas outflow from the circuits. With the equality of boost temperatures ( $T_0^{*I} = T_0^{*II} = T_0^*$ ) this condition is observed if pressure differentials in jet nozzles of circuits are identical, i.e., if

$$\pi_{p,cI} = \pi_{p,cII}.$$

In other words, the total pressures of gas behind the turbine of the second circuit and air behind the compressor of second circuit must be identical, i.e.,  $p_4^I = p_2^{*II}$ . As was proved above (see Chapter 8), this condition provides a minimum of losses in the mixing chamber of the DTRDF<sup>I+II</sup>.

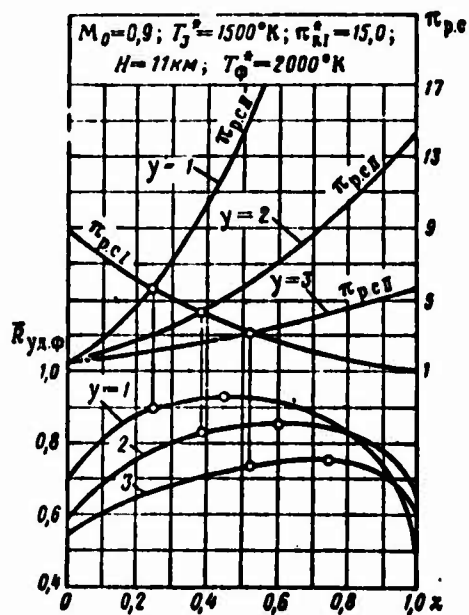


Fig. 18.21. Effect of bypass parameters on expansion ratio of gas in both circuits and specific thrusts of the DTRDF<sup>I+II</sup> [ $\Delta T P \Delta \phi^{I+II}$ ].

Figure 18.21 clearly confirms that the equality of total pressures in circuits in practice provides the maximum of specific thrust of the DTRDF<sup>I+II</sup>.

18.2.2.5. Effect of Bypass Parameters on Specific Thrust and Specific Fuel Consumption of the DTRDF<sup>I+II</sup>.

With an increase in the compression ratio of the compressor of the second circuit  $\pi_{\kappa II}^*$ , the specific thrust of the DTRDF<sup>I+II</sup> initially increases, reaching a maximum at equal drops in pressures in jet nozzles of the circuits ( $\pi_{p.c(I)} = \pi_{p.c(II)}$ ), and then drops. Since the relative fuel consumption  $m_T$  preserves the fixed value, the specific fuel consumption changes inversely proportional to the specific thrust (Fig. 18.22).

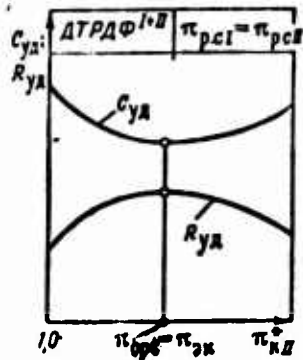


Fig. 18.22. Comparison of optimum and economic compression ratios of the compressor of the second circuit of the DTRDF<sup>I+II</sup>.

An increase in the bypass ratio at optimum distribution of the energy between the circuits decreases drops in pressures in the jet nozzles. Consequently, velocities of outflow from the circuits, and this means specific thrust of the engine, also decrease. The specific fuel consumption of the DTRDF<sup>I+II</sup> in this case continuously increases (Fig. 18.23).

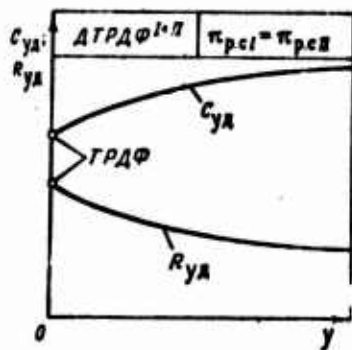


Fig. 18.23. Effect of the bypass ratio on specific parameters of the DTRDF<sup>I+II</sup> ( $\pi_{p.c(I)} = \pi_{p.c(II)}$ ).

Consequently, at equal parameters of the cycle the specific thrust of the DTRDF<sup>I+II</sup> is lower and the specific fuel consumption is higher than those in the TRDF.

### 18.5. Ducted-Fan Engine With the Mixing of Flows

During recent years ducted-fan TRD with the mixing of flows have become widespread. The mixing of flows is applied both in nonboosted and in forced ducted-fan engines (with additional fuel combustion).

The use of mixing chambers makes it possible to simplify structurally the exhaust part of the engine and decrease its weight (systems of forcing, cooling of the exhaust part and adjustment of the common jet nozzle are simplified).

The use of mixing chambers also allows in the case of the boosted ducted-fan engine reducing the specific fuel consumption by 1.5-3%, and this lowering proves to be greater for the high-temperature ducted-fan engine at relatively high values of the bypass ratio ( $y = 1-2$ ). One should point out that the noted thermodynamic effect of the mixing of flows can be realized only when it is possible to obtain an even field of temperatures at the exit from the mixing chamber. However, the equalizing of field of temperatures is a complex matter. The use for this purpose of short "lobe" mixers (of the type of mixer of the engine Rolls-Royce RB.141) gives only a partial result. The use of mixing chambers of great length is irrational due to the increase in weight of the engine.

#### 18.5.1. Effect of the Difference in Temperatures of Initial Flows on the Increase in Thrust of a Ducted-Fan Engine with the Mixing of Flows

Under equal total pressures of initial flows and in the absence of losses in the mixing chamber, velocities of outflow from the jet nozzles are proportional to  $\sqrt{T^*}$ , i.e.,

$$c_3^I \sim \sqrt{T_4^*}; \quad c_3^{II} \sim \sqrt{T_2^*}; \quad c_{3(cu)} \sim \sqrt{T_{cu}^*}.$$

where

$$T_{cm}^* \approx \frac{T_4^{*I} + yT_2^{*II}}{1+y}$$

Then

$$\bar{R}_{cm} = \frac{(G_I + G_{II})V\bar{T}_{cm}^*}{G_I V' \sqrt{T_4^{*I}} + G_{II} V' \sqrt{T_2^{*II}}} = \frac{V(1+y)(1+y\theta^*)}{1+yV'\theta^*}, \quad (18.24)$$

where

$$\theta^* = \frac{T_2^{*II}}{T_4^{*I}} < 1.0.$$

Table 18.1 gives data on thrust augmentation of the ducted-fan engine with the mixing of flows depending on  $\theta^*$  for  $y = 1.0$ , which were obtained from equation (18.24).

Table 18.1.

$\theta^*$	0,20	0,25	0,30	0,35	0,40	0,45	0,50
$\bar{R}_{cm}$	1,070	1,054	1,042	1,032	1,025	1,019	1,015

Thus when  $y = 1$  and  $\theta^* = 0,25 \div 0,40$  an increase in thrust and, consequently, lowering of specific fuel consumption, taking into account the losses, does not exceed 1.5-3%.

## CHAPTER 19

### OPERATIONAL CHARACTERISTICS OF THE DUCTED-FAN ENGINE

#### 19.1. Thermodynamic Bases of Control of the Ducted-Fan Engine

##### 19.1.1. Control Elements and Controllable Parameters of the Ducted-Fan Engine

The presence of the second circuit of the ducted-fan engine allows having in this engine additional, in comparison with the TRD, control elements and controllable parameters.

The maximum number of controllable parameters at fixed values of  $M_0$ ,  $H$  and efficiency of separate elements results from equations for thrust (13.3) and specific fuel consumption (17.41). Since  $R=f(\pi_k^*, T_3^*, x, y)$  and  $R_\phi=f(\pi_k^*, T_3^*, T_\phi^*, x, y)$ , then for the ducted-fan engine the number of controllable parameters reaches four and for the DTRDF<sup>II</sup> - five.

Instead of  $\pi_k^*$  as an adjustable regime parameter it is convenient to select  $n$ , instead of  $x$  - compression ratio  $\pi_{kII}^*$ , instead of  $y$  - the flow of air  $G_I$  or  $G_{II}$ .

The enumerated quantity of regime of parameters corresponds to an equal quantity of control elements and control factors. The additional control factors in the second circuit of the ducted-fan engine, in comparison with the TRD, are:

- 1) fuel consumption in the second circuit  $G_T^{II}$ ;
- 2) area of critical section of the jet nozzle of the second circuit  $f_5^{II}$ ;
- 3) angle of turning of the guide vane of the fan  $\phi_{H,a}^{II}$  and others.

With fixed geometry of the second circuit and in the absence in it of afterburners, the ducted-fan engine as an object of control is no different from the TRD. In this case the ducted-fan engine and TRD will have the same control elements, controllable parameters and identical structural designs of control.

Table 19.1 shows that, depending on the gas-dynamic scheme of the engine, the number of regime parameters of the ducted-fan engine (DTRDF) varies from one to five; for the TRD (TRDF) - from one to three and for the turboprop engine it is usually equal to two.

Table 19.1.

No.	Type of engine	Control factors	Controllable parameters
1	TRD	$G_T$	$n$ or $T_3^*$
2	TRD	$G_T, f_3$	$n, T_3^*$
3	TRDF	$G_T, f_3, G_{T,\phi}$	$n, T_3^*, T_\phi^*$
4	DTRD	$G_T$	$n$ (or $n_{H\Delta}$ )
5	DTRD	$G_T, f_3^I$	$n, T_3^*$
6	DTRD	$G_T, f_3^I, f_5^{II}$	$n, T_3^*, \pi_{KII}^*$
7	DTRDF	$G_T, G_{T,\phi}^{II}, f_3^I, f_5^{II}, \varphi_{H,a}^{II}$	$n, T_3^*, T_\phi^*, \pi_{KII}^*, \varphi$
8	TVD	$G_T, \varphi_0$	$n, T_3^*$

Let us note that passage to single-shaft design of the engine still does not denote the introduction of an additional controllable parameter. At fixed geometry of the single-shaft ducted-fan engine the unique controllable factor  $G_T$  corresponds to the unique controllable parameter  $n$  (or  $T_3^*$ ). Another parameter  $T_3^*$  (or  $n$ ) automatically and uniquely is connected with the first. In the case of the single-shaft ducted-fan engine this control factor  $G_T$  corresponds, as previously, to the unique controllable parameter, for example, the number of revolutions of the VD cascade. Parameters  $T_3^*$  and  $n_{HD}$  are uniquely connected with  $n_{BD}$ .

Figure 19.1a shows a block diagram of the control of a single-shaft DTRDF<sup>II</sup> with two independent regulators: fuel feed in the main chamber and fuel feed in the afterburner.

The connection between the control factors and controllable parameters of the engine has the following form:

$$\begin{aligned} G_T &\rightarrow T_3^* \rightarrow n; \\ G_{T,\phi}^{II} &\rightarrow T_\phi^{II}. \end{aligned}$$

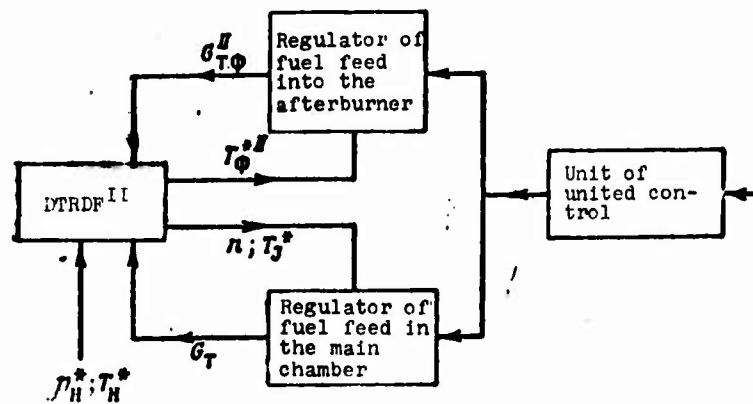
A block diagram of the control of a single-shaft ducted-fan engine with two independent regulators of VD revolutions and a jet nozzle of the second circuit are given on Fig. 19.1b.

The connection between control factors and controllable parameters in such a ducted-fan engine has the following form:

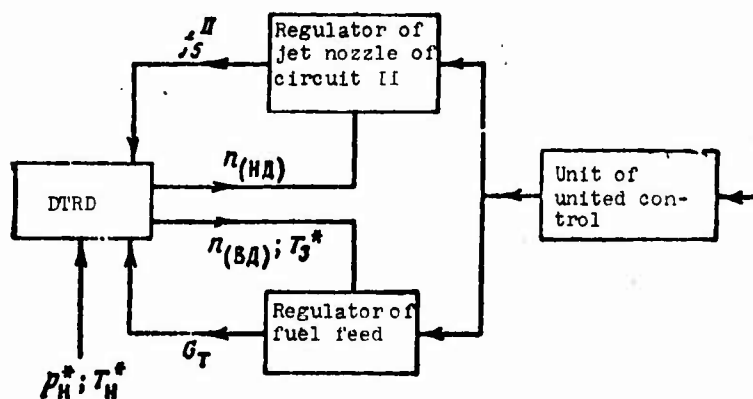
$$\begin{aligned} G_T &\rightarrow n_{(B1)} \rightarrow T_3^*; \\ f_3^{II} &\rightarrow n_{(HD)}. \end{aligned}$$

The connection between control factors and controllable parameters of a geometrically fixed single-shaft ducted-fan engine has the following form:

$$G_T \rightarrow n_{(B1)} \rightarrow T_3^*.$$



a)



b)

Fig. 19.1. Block diagram of control of the ducted-fan engine: a) with two regulators of fuel feed in the main chamber and afterburner; b) with two independent regulators of VD revolutions and jet nozzle of the second circuit.

### 19.1.2. Programs of Control of the Ducted-Fan Engine

Programs of the control of ducted-fan TRD are very diverse. These include programs of control for maximum thrust, the greatest economy in cruising regimes of flight, complete similarity of the regime of the turbocompressor, various combined programs, and others. Due to the presence of additional parameters and control elements (in the second circuit of the engine) the quantity of these programs for the ducted-fan engine is more than that for the usual single-circuit TRD.

Let us examine briefly the peculiarities of control of the ducted-fan engine with respect to certain of these programs.

#### 19.1.2.1. Programs of Control for Maximum Thrust.

To provide control for maximum thrust of the single-shaft ducted-fan engine at all speeds of flight the realization of the same conditions as in the case of the single-shaft TRD is necessary:

- 1)  $n = n_{max} = \text{const}$ ;
- 2)  $T_3^* = T_{3(max)}^* = \text{const}$

and, furthermore, additional conditions -

- 3)  $y = y_{opt}$ ;
- 4)  $x = x_{opt}$  or  $\pi_{k11}^* = \pi_{k11}^*(opt)$ ,

and in the presence of afterburners in the circuits

- 5)  $T_{\phi}^{*I} = \text{const}$ ;
- 6)  $T_{\phi}^{*II} = \text{const}$ .

The observance of these conditions provides the obtaining at all speeds and altitudes of flight of a maximum of airflow and specific thrust and, consequently, a maximum of total thrust.

One should note that the provision of conditions 3) and 4) completely complicates the control of the engine and in practice cannot always be realized. Therefore, parameters  $y$  and  $\pi_{k11}^*$  are usually rejected from special control, allowing them to change in accordance with a change in parameters of the working process with respect to speed and altitude of the flight and also in accordance with conditions 1) and 2).

Maintaining  $T_3^* = \text{const}$  in the case of a single-shaft ducted-fan engine can be accomplished by means of additional control of the critical section of the jet nozzle (first or second circuits, and in the presence of a mixing chamber - common nozzle) and also a guide vane of the compressor of the second circuit.

In connection with this additional conditions of the realization of the considered program of control are distinguished:

- a)  $f_3^{II} = \text{const}; \varphi_{n,a}^{II} = \text{const}; (f_3^I = \text{var});$
- b)  $f_3^I = \text{const}; \varphi_{n,a}^{II} = \text{const}; (f_3^{II} = \text{var});$
- c)  $f_3^I = \text{const}; f_3^{II} = \text{const}; (\varphi_{n,a}^{II} = \text{var}).$

In the case of a double-shaft ducted-fan engine, preservation of  $T_3^* = \text{const}$  is provided automatically with the observance of condition  $n_{(ВД)} = \text{const}$  correct to  $L_{\text{ВД}} = \text{const}$  with respect to the speed and altitude of the flight. The preservation of  $L_{\text{ВД}} = \text{const}$  can be provided by the appropriate selection of the characteristic of VD compressor with a rated compression ratio close to six.

With the observance of conditions  $n_{(HD)} = \text{const}$  and fixed geometry of the engine, the temperature  $T_3^*$  in flight changes. To maintain it, in this case the introduction of earlier examined additional control elements is necessary.

#### 19.1.2.2. Programs of Control of a Geometrically Fixed Ducted-Fan Engine.

Let us examine the program of control of the ducted-fan engine

$$n = \text{const}; f_3^I = \text{const}; f_3^{II} = \text{const}; \varphi_{n,a}^{II} = \text{const}.$$

Let us assume that the ducted-fan engine is single-shaft with separate compressors (see diagram *a* on Fig. 17.7). Let us investigate how in this case the gas temperature in front of the turbine  $T_3^*$  and bypass parameters ( $\gamma$  and  $\varphi_{\text{HII}}^*$ ) change.

With an increase in flight speed the bypass ratio increases

$$y = \frac{G_{11}}{G_1} \approx \frac{\pi_{11}^*}{\pi_{11}^*},$$

since the rate of airflow through the second circuit (with a less value of  $\pi_{11}^*$ ) increases considerably faster than that of the airflow through the first circuit; it is easy to see from the expression of balance of works

$$L_r = (L_{11} + yL_{21}) \sim T_3^*$$

that at a critical pressure differential in the jet nozzle of the first circuit, when  $\pi_T^* = \text{const}$ , the increase in  $y$  leads to a continuous increase in the gas temperature in front of the turbine  $T_3^*$ . It is obvious that system of fuel feed and control of such an engine must have limitations with respect to temperature.

From the approximate equality

$$L_{21} = L_{21(0)},$$

or

$$\frac{x}{y} L_e = \frac{x(0)}{y(0)} L_{e(0)},$$

we find

$$x = x(0) \frac{y}{y(0)} \frac{L_{e(0)}}{L_e},$$

whence it follows that parameter  $x$  with respect to flight speed increases, approaching unity. A sharp increase in values  $y$  and  $x$  at high flight speeds considerably worsens conditions of energy exchange and decreases the thrust of the nonboosted ducted-fan engine. Actually, with the optimum distribution of energy between the circuits with an increase in  $M_0$  of flight, it is necessary that  $y \rightarrow 0$  and  $x \rightarrow 0$  (see Fig. 18.3).

At low flight speeds a shortage of thrust, as a result of reduced values of  $T_3^*$ , also takes place.

Thus, the program of control  $n = \text{const}$  of a geometrically fixed ducted-fan engine can be used only in a comparatively small range of speeds and altitudes of flight.

19.1.3. Joint Work of the Compressor and Turbines in the System of the Ducted-Fan Engine. Effect of Various Control Factors on the Line of the Operating Regimes (LRR) of Compressors of the Ducted-Fan Engine

The passage of throttle and altitude and high-speed characteristics of ducted-fan TRD and the selection of programs of control for their realization are largely determined by peculiarities of the joint operation of the compressor and turbines in the system of the ducted-fan engine, depend on properties, real characteristics of compressors of the first and second circuits and are determined also by peculiarities of the gas-dynamic scheme of the engine.

Below we will examine methods of the construction of the line of operating regimes of compressors of the ducted-fan engine and also the effect of various operational and control factors on their passage.

19.1.3.1. Basic Conditions and Assumptions.

With the construction of lines of operating regimes on characteristics of compressors of the ducted-fan engine of various designs and in the investigation of the effect of various control factors on the regime of operation of the engine, we will proceed from conditions and simplifying assumptions indicated below.

1. Pressure differentials in the first nozzle box assembly of the turbine and also in jet nozzles of both circuits have critical or supercritical values, i.e.,

$$q(\lambda_{c,1}^*)=1; \quad q(\lambda_3^*)=1; \quad q(\lambda_5^*)=1.$$

This means that expansion ratio of the gas in the turbine remains constant, i.e.,  $\pi_T^* = \text{const}$ .

Figure 19.2 gives dependences of the maximum bypass ratio  $y_{\max}$  on parameters of the working process of the basic circuit  $T_3^*$  and  $\pi_{HI}^*$  at which pressure drops in both circuits reach critical values. We see that when  $y \leq 1$ ,  $T_3^* \geq 1200^\circ\text{K}$ ;  $\pi_{HI}^* > 6$  and  $\eta_T^* = 0.9$ ,  $\eta_K^* = 0.85$ , we have

$$\pi_{p,c(I)} = \pi_{p,c(II)} \geq \pi_{k,p} = \left(\frac{k+1}{2}\right)^{\frac{k}{k-1}}$$

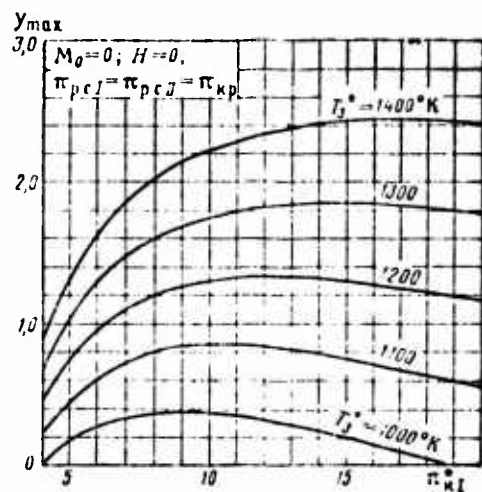


Fig. 19.2. Effect of parameters of the working process of the ducted-fan engine -  $T_3^*$  and  $\pi_{HI}^*$  - on  $y_{\max}$  at the critical outflow of gas from the jet nozzles.

2. Efficiencies of the turbine and also coefficients of partial losses in elements of the engine are invariable, i.e.,

$$\eta_T^* = \text{const}; \sigma_{\pi}^* = \text{const}; \sigma_{k,c}^* = \text{const}; \varphi_{p,c} = \text{const};$$

$$\xi_{k,c} = \text{const}; \sigma_{\phi,k}^* = \text{const}; \xi_{\phi,k} = \text{const}.$$

#### 19.1.4. Double-Shaft Ducted-Fan Engine with Common ND Compressor and Separate Exhaust

##### 19.1.4.1. Equations of Basic Gas-Dynamic Connections.

Equations of basic gas-dynamic connections of the ducted-fan engine made according to diagram *b* (see Fig. 17.7) refer to equations

of flow and balance of works of the ND and VD turbocompressors.

VD Turbocompressors.

*Equation of flow.*

By analogy with the TRD, let us write:

$$\pi_{\kappa(BD)}^{\circ} = c_1 q(\lambda_1)_{(BD)} \sqrt{\frac{T_3^{\circ}}{T_{1(BD)}^{\circ}}}, \quad (19.1)$$

where

$$c_1 = \frac{f_1(BD)}{f_{c, \theta}(\lambda_{c, \theta}) \epsilon_{c, \theta}^{\circ} \epsilon_{\kappa, c}^{\circ}}.$$

*The equation of balance of works*

We have  $L_1(BD) = L_{\kappa}(BD),$  (19.2)

whence we find

$$\frac{T_3^{\circ}}{T_{1(BD)}^{\circ}} = \frac{102,5 (\pi_{\kappa(BD)}^{\circ, 220} - 1) \frac{1}{\eta_{\kappa(BD)}^{\circ}}}{118 \epsilon_{\tau(BD)}^{\circ} \eta_{\tau(BD)}^{\circ}}. \quad (19.3)$$

Having substituted into expression (19.1) the value  $T_3^{\circ}/T_{1(BD)}^{\circ}$  from (19.3), we obtain after transformations

$$\frac{\pi_{\kappa(BD)}^{\circ}}{\sqrt{\frac{\pi_{\kappa(BD)}^{\circ, 220} - 1}{\eta_{\kappa(BD)}^{\circ}}}} = c q(\lambda_1)_{(BD)}, \quad (19.4)$$

where

$$c = \frac{f_1(BD)}{f_{c, \theta}(\lambda_{c, \theta}) \epsilon_{c, \theta}^{\circ} \epsilon_{\kappa, c}^{\circ} \sqrt{\frac{118}{102,5} \epsilon_{\tau(BD)}^{\circ} \eta_{\tau(BD)}^{\circ}}}.$$

Expression (19.4) is the equation of lines of operating regimes of the VD turbocompressor; it has exactly the same form and same

properties as does the corresponding LRR equation for the VD turbo-compressor of a single-circuit TRD [equation (10.8)].

ND Turbocompressor.

*Equation of flow*

Let us write the equation of flow for sections at the entrance into the ND compressor (1-1) and at the exit from the converging jet nozzle ( $5^{II}$ - $5^{II}$ ).

We have

$$G_{1(ND)} = G_5^{II} \left(1 + \frac{1}{y}\right).$$

or

$$m \frac{p_{1(ND)}^{\circ}}{\sqrt{T_{1(ND)}^{\circ}}} f_{1(ND)} q(\lambda_{1(ND)}) = m \frac{p_5^{II}}{\sqrt{T_5^{II}}} f_5^{II} q(\lambda_5^{II}) \left(1 + \frac{1}{y}\right).$$

Introducing the substitution  $T_5^{\#} = T_{2(ND)}^{\#}$  and  $p_5^{II} = p_2^{II} \sigma_{k,c}^{II}$ , we obtain after conversions

$$\frac{\sigma_{k,c}^{II}}{\pi_{k(ND)}^{\circ}} = \frac{\pi_{k(ND)}^{\circ}}{\sqrt{1 + \frac{\pi_{k(ND)}^{\circ} - 1}{\sigma_{k,c}^{II}}}} = \frac{c_2}{\left(1 + \frac{1}{y}\right)} q(\lambda_{1(ND)}), \quad (19.5)$$

where

$$c_2 = \frac{f_{1(ND)}}{f_5^{II} \sigma_{k,c}^{II}}.$$

*Equation of balance of works*

We have

$$G_I L_{T(ND)} = (G_I + G_{II}) L_{k(ND)},$$

whence

$$L_{T(ND)} = (1 + y) L_{k(ND)}. \quad (19.6)$$

Determination of the bypass ratio of the ducted-fan engine.

We have

$$\bar{y} = \frac{\sigma_5^{II}}{\sigma_{1(BD)}} = \frac{\frac{P_5^{II}}{V T_5^{II}} f_5^{II} q(\lambda_5^{II})}{\frac{P_1(BD)}{V T_1(BD)} f_{1(BD)} q(\lambda_1)_{(BD)}}$$

Having noted that

$$P_5^{II} = P_{1(BD)} \sigma_{5,2}^{II} \quad \text{and} \quad T_5^{II} = T_{1(BD)}$$

we obtain after simplifications

$$\bar{y} = \frac{\sigma_{5,2}^{II} f_5^{II} q(\lambda_5^{II})}{f_{1(BD)} q(\lambda_1)_{(BD)}} \quad (19.7)$$

Thus, the bypass ratio of ducted-fan engine, carried out according to scheme *b* (see Fig. 17.7), depends only on the area of the exit section of the jet nozzle of the second circuit and on operating regime of the VD compressor characterized by parameter  $q(\lambda_1)_{(BD)}$ .

When  $f_5^I = \text{const}$  we find (Fig. 19.3) that

$$\bar{y} = \frac{1}{q(\lambda_1)_{(BD)}}$$

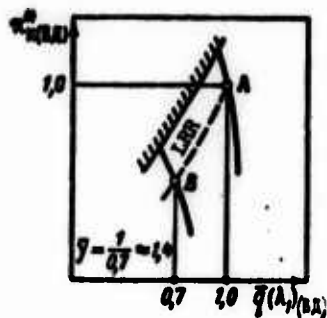


Fig. 19.3. Graphical determination of  $\bar{y}$  according to the characteristics of the VD compressor.

### 19.1.5. Equation of LRR of the ND Turbocompressor:

The equation of the line of operating regimes (LRR) of the ND turbocompressor cannot be expressed in evident form. In implicit form it is represented by equations of gas-dynamic connections of VD and ND turbocompressors and also by the equation of the bypass ratio.

Construction of the LRR of the ND turbocompressor is carried out in the following manner:

- 1) a series of regime points on the LRR of the VD turbocompressor, i.e., a series of joint values  $\pi_{\kappa(ND)}^*$ ,  $\eta_{\kappa(ND)}^*$ ,  $q(\lambda)_{(ND)}$  and  $\gamma$  are assigned;
- 2) from the equation of flow (19.1) for the VD turbocompressor a series of values  $T_3^*/T_{1(ND)}^*$  is found;
- 3) with the help of the equation of energy, written for the VD turbine, a series of values  $T_{4(ND)}^*/T_{1(ND)}^*$  is found;
- 4) from the equation of balance of operation (19.6) of the ND turbocompressor a series of values  $\pi_{\kappa(ND)}^*$  and  $\eta_{\kappa(ND)}^*$  is found;
- 5) from the equation of flow (19.5) for the ND turbocompressor  $q(\lambda)_{(ND)}$  is determined;
- 6) with respect to the combination of values  $\pi_{\kappa(ND)}^*$ ,  $\eta_{\kappa(ND)}^*$  and  $q(\lambda)_{(ND)}$  the line of operating regimes of the ND turbocompressor is constructed.

Using equations (19.1), (19.3), (19.5) and (19.6), it is possible to construct lines of operating regimes on characteristics of VD and ND compressors for the two most frequently encountered programs of control of a geometrical fixed ducted-fan engine:

1.  $n_{\kappa(ND)} = \text{const}$ ;  $f_5^I = \text{const}$ ;  $f_5^{II} = \text{const}$ ;  $\varphi_{n,\lambda} = \text{const}$ ;
2.  $n_{\kappa(ND)} = \text{const}$ ;  $f_5^I = \text{const}$ ;  $f_5^{II} = \text{const}$ ;  $\varphi_{n,\lambda} = \text{const}$ .

19.1.5.1. Comparison of Lines of Operating Regimes on Characteristics of VD and ND Compressors with Two Programs of Control.

By comparing the single-valued correspondence of regime points arranged along lines of operating regimes on characteristics of VD and ND compressors with two programs of control indicated above (Fig. 19.4), one can make the following conclusions:

1. Lines of operating regimes on the characteristic of each of the compressors with the two noted programs of control coincide.

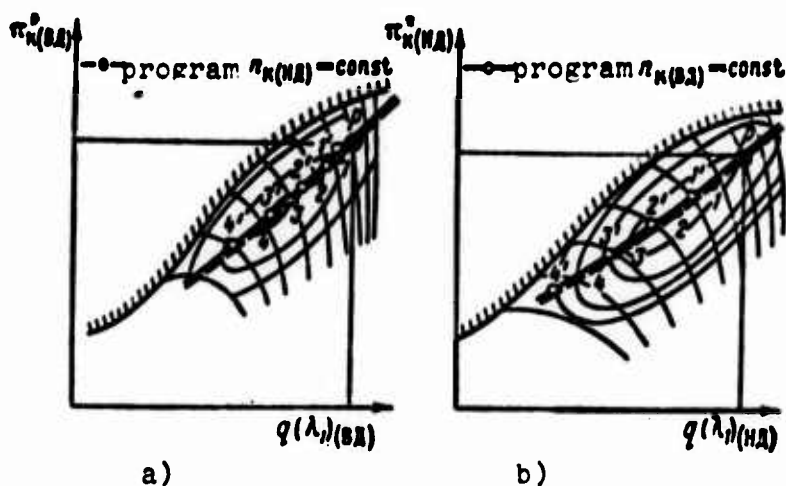


Fig. 19.4. Effect of the program of control on passage of the LRR on characteristics of VD (a) and ND (b) compressors.

2. For both programs of control the relative change in reduced VD revolutions is less than the change in reduced ND revolutions. The latter is explained by the fact that in the assigned interval of the change in  $T_n^* = T_{1(НД)}^*$  the change in parameter  $T_{1(ВД)}^*$  is always less.

3. With an increase in  $T_n^*$  with the program of control  $n_{k(НД)} = \text{const}$  the revolution number of the free ND cascade is lowered  $[(1+\mu)L_{k(НД)} > L_{r(НД)}]$ , and with the program of control  $n_{k(ВД)} = \text{const}$  the revolution number of the free VD cascade increases (to provide

$n_{H2} = \text{const}$  it is necessary to raise  $T_3^*$ , and, consequently,  $L_{(H2)} > L_{(H1)}$ . Thus, the same interval of the change in  $T_3^*$  corresponds with the program of control  $n_{k(H2)} = \text{const}$  to the great change in reduced ND and VD revolutions and their less change with the program of control  $n_{k(H1)} = \text{const}$ . The latter follows from the examination of formulas:

$$n_{H2(\text{opt})} = n_{H1} \sqrt{\frac{288}{T_{1(H2)}}} \quad \text{and} \quad n_{H2(\text{opt})} = n_{H2} \sqrt{\frac{288}{T_3^*}}$$

4. The program of control  $n_{H2} = \text{const}$  corresponds to a great change in  $T_3^*$ .

5. The great change in reduced revolutions causes a great deviation in parameters of the compressor ( $L_k, \eta_k^*, \alpha_k^*$ ) from their initial (calculated) values. In this sense the program of control  $n_{k(H2)} = \text{const}$  is more preferable.

#### 19.1.6. Physical Model of the Change in Bypass Ratio with Respect to Speed and Altitude of Flight

Let us examine the two typical cases of the change in bypass ratio on the speed and altitude of flight:

1) in the presence of delimiting flanges on blades of the ND compressor (scheme of a ducted-fan engine with separation of airflow at the entrance into the compressor);

2) in the presence of common blades of the ND compressor (scheme of a ducted-fan engine without delimiting flanges).

In the first case (Fig. 19.5a) the change in the bypass ratio of the ducted-fan engine on speed and altitude of flight is carried out by means of the *redistribution of the profile of axial velocities* at the entrance into the compressor. For example, with an increase in  $T_H^*$  (and, consequently, parameter  $\gamma$ ) the velocity  $c_1^{\text{II}}$  at the entrance into the compressor of the second circuit increases

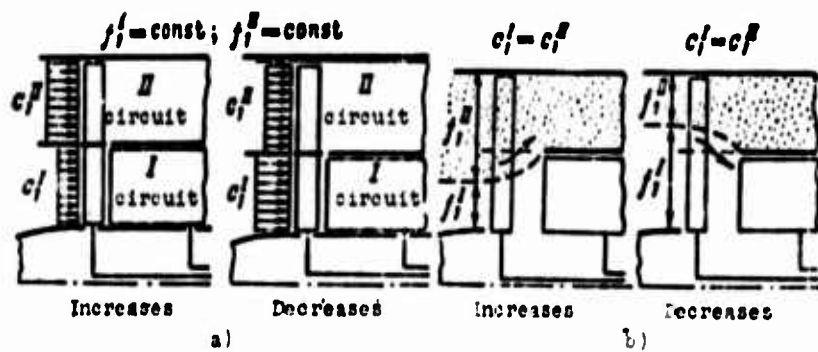


Fig. 19.5. Physical model of the change in the bypass ratio in partial load regimes: a) redistribution of the profile of axial velocities at the entrance into the ND compressor (blade with delimiting flanges); b) deformation of the jet at the entrance into the ND compressor (common blades).

relatively; conversely, with a decrease in  $\gamma$  the velocity at the entrance into the compressor of the first circuit increases relatively.

In the second case (see Fig. 19.5b) the change in the bypass ratio is carried out by means of *deformation of the jet* at the entrance into the compressor. Thus, for instance, with an increase in parameter  $\gamma$  there is an increase in the flow passage cross-sectional area  $f_1^{II}$  of the jet, which flows into the second circuit; correspondingly the jet at the entrance into the compressor of the first circuit is narrowed ( $f_1^I$  is decreased); with a decrease in parameter  $\gamma$ , conversely, the jet at the entrance into the compressor of the second circuit is narrowed and the jet at the entrance into the compressor of the first circuit is expanded.

#### 19.1.7. Effect of Various Factors on the Line of Operating Regimes of the VD Compressor

With "blocking" along the drop in pressures of the VD turbine ( $\pi_{T(n,n)}^* = \text{const}$ ) the position of the line of operating regimes of the VD compressor depends only on parameters and characteristics of the VD turbocompressor ( $\pi_{n(p)}^*$ ,  $T_{3(p)}^*$ , fields  $\eta_n^*$ , peculiarities of

lines  $n_{np} = \text{const}$ ) and does not depend on external factors with respect to the VD turbocompressor. The influence of external atmospheric conditions, parameters and characteristics of the ND turbocompressor, bypass ratio, control factors  $f_5^I$  and  $f_5^{II}$  on the regime of operation of the VD compressor is manifested in terms of the change in complete inlet temperature of the VD compressor ( $T_{i,ND}$ ) in the form of a change in reduced revolutions of the VD compressor.

Thus, for assigned VD compressor, which has no special control elements, the line of the operating regimes remains constant; however, its regime points, in accordance with a change in "outward" factors, can move along the LRR.

#### 19.1.8. Effect of Various Factors on the Line of Operating Regimes of the ND Compressor

The position of the line of operating regimes of the ND compressor is affected by parameters and characteristics of both turbo-compressors (VD and ND), bypass ratio  $\gamma_p$ , various control factors (for example,  $f_5^I$  and  $f_5^{II}$ , etc.). Let us examine this effect in more detail.

##### 19.1.8.1. Effect of Control of the Jet Nozzle of the First Circuit

( $f_5^I = \text{var}$ ) (Fig. 19.6).

Let us assume that the initial regime of operation of the ND compressor (point 1) is characterized by the assigned LRR and the number of revolutions  $n_1$ .

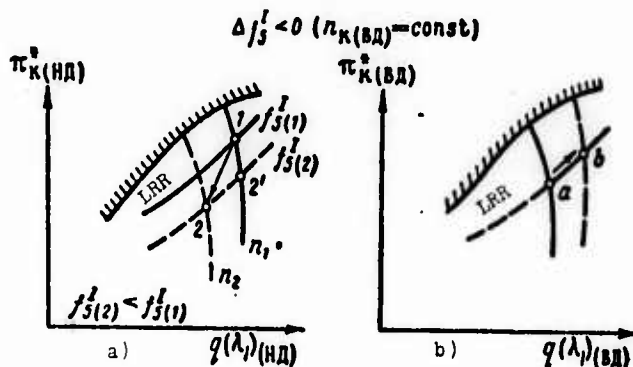


Fig. 19.6. Effect of control of the jet nozzle of the first circuit on the LRR of ND (a) and VD (b) compressors.

With covering of the jet nozzle the first circuit ( $d_5^I < 0$ ) increases the pressure behind the ND turbine. Assuming that a change in pressure  $p_{i(ND)}$  is perceived only by the ND turbine (when  $\pi_{i(ND)} = \text{const}$ ), it is easy to conclude that the work of the ND turbine is decreased.

As a result there is unbalance of works on the ND turbocharger

$$(1 + b)L_{K(ND)} > L_{T(ND)}$$

and the revolution number of the ND compressor is decreased ( $n_2 < n_1$ ).

In this case the temperature at the exit from the ND compressor ( $T_{2(ND)}^* = T_{1(ND)}^*$ ) is decreased, and this means that reduced revolutions of the VD compressor, equal to

$$n_{VD(II)} = n_{VD} \sqrt{\frac{T_{1(ND)}^*}{T_{1(ND)}^*}}, \text{ where } n_{VD} = \text{const},$$

increase.

Consequently, the regime point of the VD compressor moves along the LRR from a to b (see Fig. 19.6b). According to this and equation (19.3), the bypass ratio of the engine decreases. Let us restore now the number of revolutions of the ND compressor (up to  $n = n_1$ ), having increased the fuel feed in the combustion chamber. The bypass ratio in this case decreases even more.

Thus, we restored the original number of revolutions of the ND compressor, but with a considerably less value of the bypass ratio. Consequently, there occurred a *redistribution of airflow between the circuits* - airflow through the first circuit increased, and the rate of airflow through the second circuit was decreased. The decrease in airflow through the second circuit with its fixed geometry ( $f_5^{II} = \text{const}$ ) produces the same effect as the opening of the jet nozzle in the second circuit with fixed flow - pressure behind the ND compressor will drop.

Consequently, the regime point of the ND compressor passes from position 1 to position 2 (see Fig. 19.6a), and the LRR of the ND compressor moves into the region of reduced values  $\pi_{k(ND)}^*$ .

Thus, the "covering" of the jet nozzle of the first circuit displaces the LRR into the region of reduced values  $\pi_{k(ND)}^*$  and, vice versa, the "opening" of the jet nozzle of the first circuit displaces the LRR of ND compressor into the region of raised values  $\pi_{k(ND)}^*$ .

We obtained the result similar to that which is obtained with control of the jet nozzle of the double-shaft TRD.

#### 19.1.8.2. Effect of Control of the Jet Nozzle of the Second Circuit

( $f_s^{II} = \text{var}$ ) (Fig. 19.7).

Let us assume that the initial process of the work of the ND compressor, as previously, is characterized by point 1.

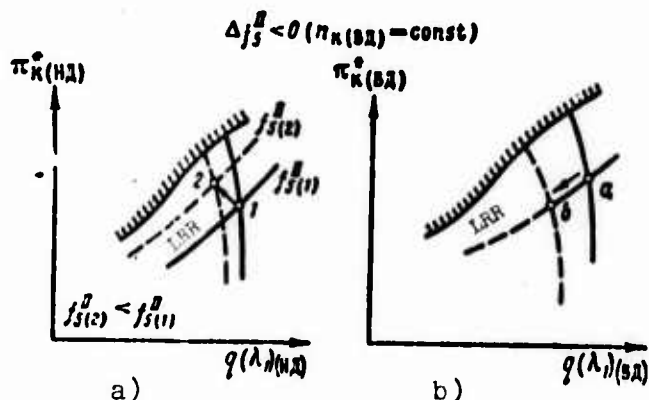


Fig. 19.7. Effect of control of the jet nozzle of the second circuit on the LRR of ND (a) and VD (b) compressors.

With the covering of the jet nozzle of the secondary circuit ( $df_s^{II} < 0$ ) counterpressure behind the ND compressor is increased; consequently, the line of operating conditions of the ND compressor is displaced into the region of increased values  $\pi_{k(ND)}^*$ .

As a result of the approached unbalance of works  $[(1+y)L_{(H2)} > L_{r(H2)}]$  revolutions of the ND compressor drop. An increase in  $T_{i(H2)}$  leads to a shifting of the regime point of the VD compressor from point a to point b.

19.1.8.3. Effect of the Bypass Ratio  $y(p)$  on the Position of the LRR of the ND Compressor (Fig. 19.8).

We will compare the position of lines of the operating regimes of the ND compressors at various values of  $y(p)$  on characteristic of the ND compressor, which is plotted in dimensionless coordinates

$$\pi_{r(H2)}^* = f(q(\lambda, H2)).$$

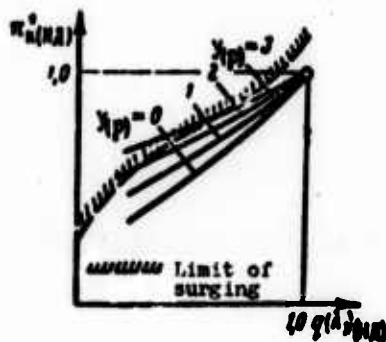


Fig. 19.8. Effect of the bypass ratio on the position of the LRR of the ND compressor.

Let us remind the reader that the more the value of the bypass ratio on the initial "rated" regime, the more it increases with throttling of the engine.

Let us examine the regime of operation of the ND compressor at the same value of the degree of throttling of the revolutions equal to  $\bar{n} = n/n_{(p)} = \text{const}$ . Thus, the more  $y(p)$ , the more the ratio  $y/y(p)$  at the reduced regime. An increase in the bypass ratio in the reduced regime denotes an increase in the airflow through the second circuit, which when  $f_5^{II} = \text{const}$  unavoidably leads to an increase in  $\pi_{r(H2)}^*$  (the effect is equivalent to the covering of the jet nozzle of the second circuit with fixed flow).

Consequently, with an increase in  $y_{(p)}$  the line of the operating regimes on the characteristic of the ND compressor is more sloping, i.e., with the throttling of the revolutions the surging reserve is decreased.

## 19.2. Throttle Characteristics of Ducted-Fan Jet Engines

Throttle characteristics of ducted-fan TRD are called the dependence of total thrust and also specific fuel consumption on the number of revolutions of the turbocompressor (or position of control elements of the engine) at constant speed and altitude of the flight and at the accepted program of control. If the engine is double-shaft, then its characteristics are plotted with respect to the number of revolutions of the turbocompressor of high or low pressure.

Plotted on the throttle characteristic of the ducted-fan engine, as in the case of the TRD, are curves of the temperature change in the gas in the jet nozzle (behind the turbine), hourly fuel consumption, and also other characteristics for the ducted-fan engine of the dependence [for example,  $y = f(n)$ ;  $\pi_{HII}^* = f(n)$ ; and others].

The throttle characteristic of the ducted-fan engine at assigned calculated values of parameters of the working process of the first circuit ( $T_3^*$ ,  $\pi_{\lambda 1}^*$ ) largely depends on the gas-dynamic scheme of the engine (ducted-fan engine with front or rear disposition of the fan; single- or double-shaft engine), the system of its control and characteristic parameters, which determine the distribution of the air and energy between the circuits.

### 19.2.1. Throttle Characteristic of a Single-Shaft Ducted-Fan Engine

#### 19.2.1.1. Change in Drops in Pressures in the Turbine and Jet Nozzle of the First Circuit of the Single-Shaft Ducted-Fan Engine with Throttling.

With a decrease in the number of revolutions of the engine the compression ratio of the compressor of the first circuit is lowered

approximately in the same way as the initial one-circuit TRD. The distinction in dependences

$$\pi_k^* = f(n)$$

in the ducted-fan engine and TRD is determined by peculiarities of the passage of lines of operating regimes on the characteristic of the compressor.

Earlier we explained that the expansion ratio of the turbine of a ducted-fan engine is considerably more than that of the original TRD. Therefore, the drop in pressures in the jet nozzle of the first circuit of the ducted-fan engine is always less than that for the original TRD, i.e.,  $\pi_{p,c(1)} < \pi_{p,c(0)}$ . Let us examine the case when in the maximum operating regime of the engine the drop in pressures in the jet nozzle is subcritical, i.e.,

$$\pi_{p,c(1)} < \pi_{k,p} = \left(\frac{k+1}{2}\right)^{\frac{k}{k-1}} \approx 1,85.$$

This case corresponds at the achieved level of limiting values  $T_3^*$  and  $\pi_k^*$  to values  $\gamma$  exceeding 2-3 (see Figs. 19.2 and 19.9). Then with throttling of the engine with a lowering of the number of revolutions and, consequently, the compression ratio of the compressor, the drop in pressures in the jet nozzle and in the turbine is decreased. Initially the lowering of the total expansion ratio covers mainly the stage of low pressure - the jet nozzle. Then, with the approach of  $\pi_{p,c(0)}$  to unity, the decrease in the drop in pressures in the turbine is intensified (Fig. 19.10).

Thus, the regularity of the change in the drop in pressures in the turbine of the ducted-fan engine is noticeably distinguished from the corresponding regularity for a one-circuit TRD, in which in the considerable range of numbers of revolutions the drop in pressures in the turbine remains constant.

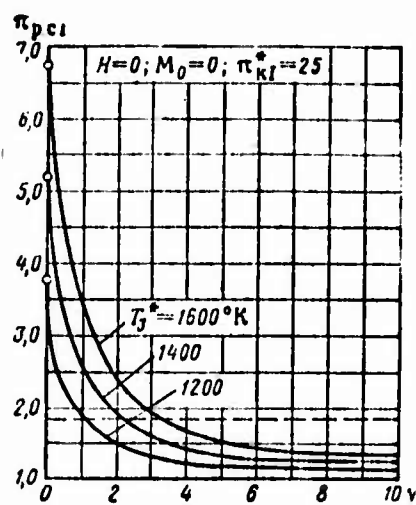


Fig. 19.9.

Fig. 19.9. Effect of the bypass ratio on the drop in pressures in the nozzle of the first circuit ( $\pi_{k1} = \pi_{k1(\gamma)}$ ).

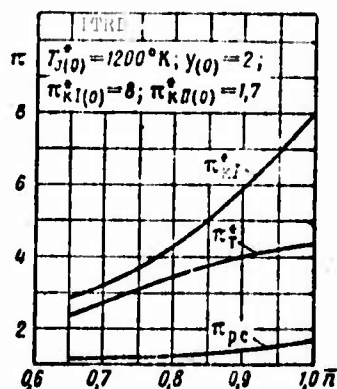


Fig. 19.10.

Fig. 19.10. Redistribution of the drop in pressures between the turbine and the jet nozzle with throttling of a single-shaft ducted-fan engine.

#### 19.2.1.2. Distribution of the Total Expansion Ratio Between the Turbine and Jet Nozzle with Throttling of the Engine.

The distribution of the total expansion ratio between the turbine and jet nozzle in subcritical regimes of the outflow of gas from the jet nozzle can be produced according to methods described in Chapter 11 for the TRD.

Figure 19.10 clearly shows how with throttling of the engine the total expansion ratio of the gas between the turbine and jet nozzle will be redistributed.

Figure 19.10 gives curves of the change in  $\pi_{k1}^*$ ,  $\pi_{k2}^*$  and  $\pi_{pc}$  according to the number of revolutions for a single-shaft ducted-fan engine with initial data in the maximum regime  $T_3^*=1200^\circ\text{K}; \pi_{k1(0)}^*=8.0; \gamma(0)=2.0; \pi_{k2(0)}^*=1.7$ .

19.2.1.3. Change in Bypass Ratio of the Single-Shaft Ducted-Fan Engine with Throttling.

With a decrease in revolution number of a geometrically fixed single-shaft ducted-fan engine, the bypass ratio of it initially increases (Fig. 19.11). Such a regularity is explained by the fact that the mass flow of air through the given circuit depends mainly on the pressure at the exit from the compressor, or, in other words, on the compression ratio of the compressor. With throttling of the engine the compression ratio in the first circuit, which has a higher initial value, is lowered more intensively than the compression ratio in the second circuit. Thus, the flow of air through the first circuit drops much more intensively than the flow of air through the second circuit, as a result of which the bypass ratio

$$y = \frac{a_{11}}{a_1} = \frac{\pi_{k11}^{\circ}}{\pi_{k1}^{\circ}} \sqrt{\frac{T_3^{\circ}}{T_4^{\circ}}} \frac{f_s^{11}}{f_{c.a}^1} \frac{q(\lambda_s^{11})}{q(\lambda_{c.a}^1)} \approx \frac{\pi_{k11}^{\circ}}{\pi_{k1}^{\circ}}$$

increases. Only in the region of deep throttling, when velocities of the outflow of gas from the second circuit are sharply lowered, is there a drop in  $y$ .

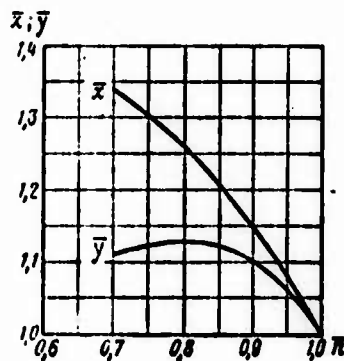


Fig. 19.11. Change in bypass parameters of a single-shaft ducted-fan engine with throttling.

The increase in parameter  $y$  with a decrease in the number of revolutions is an important factor, which, as we will see further, has a serious effect on the operational peculiarities and properties of the ducted-fan engine.

19.2.1.4. Temperature Change in the Gas in Front of the Turbine of a Single-Shaft Ducted-Fan Engine.

The gas temperature in front of the turbine of a single-shaft ducted-fan engine, as in the case of a standard TRD, is determined by the balance of works of the turbine and compressor on balanced numbers of revolutions.

We have

$$L_r = L_{\kappa 1} + yL_{\kappa 11},$$

whence

$$T_3^* = \frac{L_{\kappa 1} + yL_{\kappa 11}}{\frac{c_p r}{A} \varepsilon_r^* \eta_r^*}, \quad (19.8)$$

where

$$\varepsilon_r^* = 1 - \frac{1}{\pi_r^{0.25}}.$$

Let us assume, as previously, that in the original maximum region of the engine  $\pi_{p.c}(0) < \pi_{i.p.}$ . With a decrease in the number of revolutions the work of the compressor will be continuously lowered. If the drop in pressures in the turbine and the bypass ratio remained constant in a certain range of numbers of revolutions, then the gas temperature in front of the turbine of the ducted-fan engine would be initially lowered thus just as for the TRD. However, since parameter  $y$  increases with throttling (the compressor is "loaded," compressing a relatively large quantity of air in the second circuit), and the drop in pressures on the turbine is rapidly lowered (the turbine is "lightened," its efficiency drops), then ultimately the gas temperature in front of the turbine of the ducted-fan engine in comparison with the TRD is decreased insignificantly; then, with further throttling of the engine, the gas temperature, having attained a certain minimum, begins to increase rapidly. In the whole range of operating revolutions,  $T_3^*$  in the derived ducted-fan engine has a considerably larger value than that in the original TRD (Fig. 19.12).

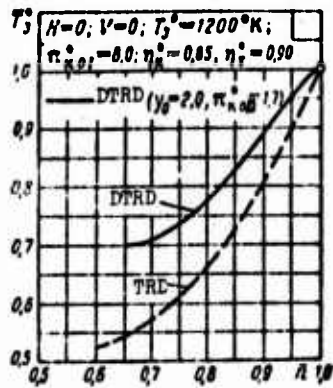


Fig. 19.12. Change in relative temperature of the gas in front of the turbine of a single-shaft ducted-fan engine and TRD with respect to number of revolutions.

Figure 19.12 shows that with the lowering of the revolution number of the engine by 35% the relative value  $\bar{T}_3^*$  for the ducted-fan engine is equal to 0.70 and for the TRD - 0.55; thus, the gas temperature in front of the turbine of the ducted-fan engine proves to be higher by 180°.

Figure 19.13 shows the effect of the bypass ratio on the relative change in temperature of the gas in front of the turbine of the ducted-fan engine. The higher the value  $\gamma$ , and, consequently, the lower  $\pi_{KII}^*$ , the higher the level of temperature  $\bar{T}_3^*$  in the whole range of operating revolutions of the engine.

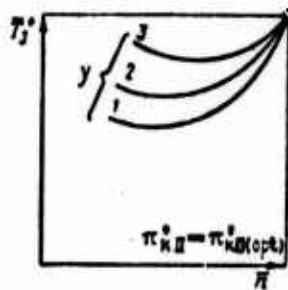


Fig. 19.13. Effect of the bypass ratio on the regularity of the change in  $\bar{T}_3^*$  with throttling of a single-shaft ducted-fan engine.

#### 19.2.1.5. Change in Thrust and Specific Fuel Consumption of a Single-Shaft Ducted-Fan Engine.

Figure 19.14 gives the relative change in thrust and specific fuel consumption of a single-shaft ducted-fan engine on the number of revolutions.

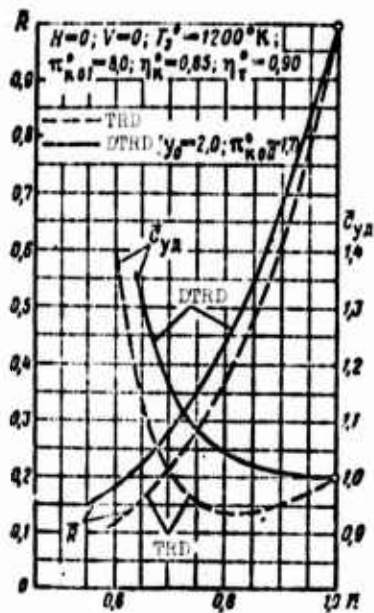


Fig. 19.14. Throttle characteristics of a single-shaft ducted-fan engine and TRD.

In accordance with higher values of gas temperature in front of the turbine and retarded drop in airflow with throttling, the thrust of the ducted-fan engine with respect to the number of revolutions drops relatively slower than that of the TRD, and the specific fuel consumption increases relatively faster. Thus, for instance, when  $\bar{n} = 0.65$  for the ducted-fan engine  $\bar{R} = 0.22$  and  $\bar{C}_{yA} = 1.3$ ; correspondingly for the TRD  $\bar{R} = 0.16$  and  $\bar{C}_{yA} = 1.14$ .

It is characteristic that the curve of specific fuel consumption of a geometrically fixed single-shaft ducted-fan engine has no minimum peculiar for characteristics of the standard one-circuit TRD, owing to which the regime of maximum thrust of the ducted-fan engine coincides with the regime of its greatest economy. In this respect throttle characteristics of the ducted-fan engine are similar to characteristics of turboprop engines.

Physically the continuous increase in specific fuel consumption of a geometrically fixed ducted-fan engine with a lowering of numbers of revolutions is explained by the worsening of effective efficiency of the cycle with a relatively small "specific" weight in the ducted-fan engine of losses with exit velocity. At the same time,

for the TRD the decrease in considerable losses of kinetic energy of flow with the throttling of the engine leads to the appearance of a minimum  $C_{yД}$ . The continuous increase in  $C_{yД}$  with throttling leads to the fact already with a small degree of throttling the advantage of the ducted-fan engine over the TRD with respect to economy disappears. In regimes of deeper throttling the specific fuel consumption of the TRD now proves to be essentially less than that in the ducted-fan engine (Fig. 19.15).

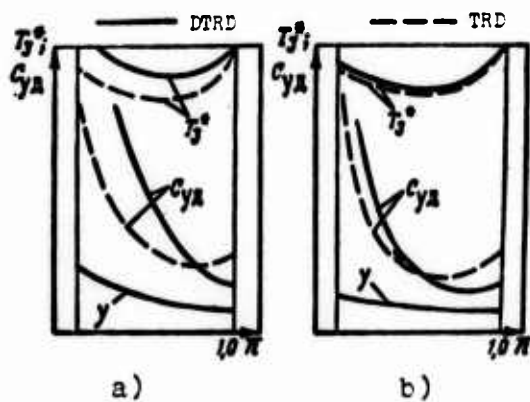


Fig. 19.15. Comparison of throttle characteristics of the ducted-fan engine and TRD: a) single-shaft engines; b) double-shaft engines.

Figure 19.16 shows the throttle characteristic of a single-shaft ducted-fan engine Rato A-65.

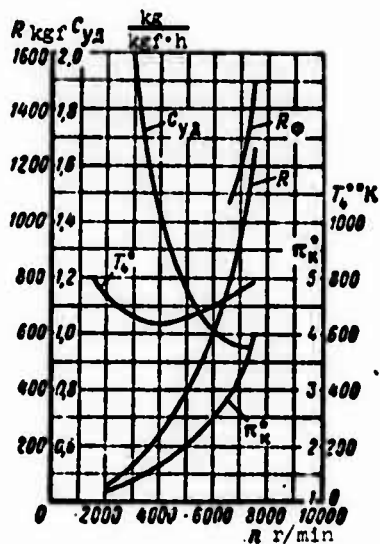


Fig. 19.16. Throttle characteristic of the single-shaft ducted-fan engine Rato A-65.

We see that properties noted above of the throttle characteristic of the single-shaft ducted-fan engine are preserved even at low compression ratios ( $\pi_{k(p)}^* = 4.0$ ). With a decrease in numbers of revolutions the drop in temperature  $T_3^*$  is small and is scarcely  $150^\circ$ ; the specific fuel consumption of the engine in this case continuously increases.

#### 19.2.1.6. Accelerating Capacity of a Single-Shaft Ducted-Fan Engine.

Higher values of gas temperature in front of the turbine of the ducted-fan engine in the whole range of operational regimes indicates the less reserve of surplus power on the shaft of the turbocompressor

$$\Delta N = N_T - N_K,$$

i.e., the difference between the available power of the turbine (determined by the maximum permissible temperature of the gases  $T_{3(max)}^*$ ) and the necessary power of the compressor (which determines the gas temperature in front of the turbine in the given equilibrium regime). This circumstance increases the time of acceleration of the engine (exit into the regime) and, consequently, conditions its poorer accelerating capacity.

The ease of starting (including, the prevention of the inadmissible excess in the gas temperature) and improvement of the accelerating capacity of the single-shaft ducted-fan engine can be achieved by its special control, for example:

- 1) opening of the jet nozzle of the second circuit;
- 2) turning off the operation of the second circuit (by means of covering the blades of rotary guide vane at the entrance into the compressor);
- 3) opening of the jet nozzle of the first circuit;
- 4) passage to a double-shaft scheme of the ducted-fan engine.

At the opening of the jet nozzle of the second circuit the power of the compressor of the second circuit decreases (since the rate of airflow in this case insignificantly increases, and the degree of increase in the pressure is considerably decreased); the same effect is reached with the covering of blades of the rotary guide vane installed at the entrance into the compressor of the second circuit (airflow through the circuit is reduced due to a drop in  $\pi_{MII}^*$  and, furthermore, the effective work of the compressor is decreased).

The complete closing of the blades at the entrance into the compressor transfers the ducted-fan engine into the regime of operation of the TRD, but this method does not prevent a certain expenditure of power to friction and heating of air circulating in the interblade spaces upon the rotation of the rotor. Furthermore, with the turning off of the operation of the compressor, the turbine will cross over to partial load operating regime, which is characterized by additional losses. With the opening of the jet nozzle of the first circuit, the available power of the turbine, as a result of the increase in the drop in pressures triggered in it, increases.

Finally, passage to a double-shaft design of the ducted-fan engine reduces the regularity of the change in  $T_3^*$  with respect to the number of revolutions to the case of the double-shaft TRD.

#### 19.2.2. Throttle Characteristics of a Double-Shaft Ducted-Fan Engine

The tendency to eliminate operational deficiencies inherent in a single-shaft ducted-fan engine and to improve the basic criteria of these engines in the rated regime<sup>1</sup> led to the appearance of a

---

<sup>1</sup>The use of a double-shaft design allows increasing the pressure state of stages of the high-pressure compressor of the first circuit by means of reduction of the circumferential velocity of its blades down to a limiting value. This makes it possible to decrease the overall length and specific weight of the engine.

double-shaft ducted-fan engine in the early stage of their development (engine Rolls-Royce "Conway").

At present the majority of the ducted-fan engines are made in the double-shaft design.

19.2.2.1. Throttle Characteristics of Double-Shaft Ducted-Fan Engines with a Common ND Compressor and Separate Exhaust.

Effect of throttling on the process of expansion of the gas in a double-shaft turbine of a ducted-fan engine. The gas expansion process in the double-shaft turbine of a ducted-fan engine with throttling of the engine occurs just as it does in any multistage turbine with exhaust into the external atmosphere. With a decrease in the numbers of revolutions the drop in pressures in the turbine is lowered, beginning from its last stage (located nearest to the external atmosphere). This lowering of  $\pi_T^*$  gradually covers stages installed upstream.

Let us assume that in the rated operating regime of the engine ( $n = n_1$ ) velocities of the outflow of gas in the jet nozzle of the first circuit and nozzle box assemblies of VD and ND turbines reach critical values, i.e.,

$$q(\lambda_2^!) = q(\lambda_{c.2}^!)_{(VD)} = q(\lambda_{c.2}^!)_{(ND)} = 1.$$

With a decrease in revolution numbers in the supercritical region of outflow from the jet nozzle [ $(\pi_{p,c} > \pi_{np}) = 1,85$ ] the lowering of expansion ratio of the engine initially occurs as a result of a decrease in the pressure on the section of the nozzle. Drops in pressures in VD and ND turbines remain constant (Fig. 19.17).

At a certain value of the revolution numbers  $n_2 < n_1$  in the jet nozzle the subcritical process of outflow is established, i.e.,  $q(\lambda_2^!) < 1,0$ . Beginning from this moment, a drop in pressure at the entrance into the jet nozzle approaches. Simultaneously the expansion ratio in the ND turbine is lowered. Since the regime

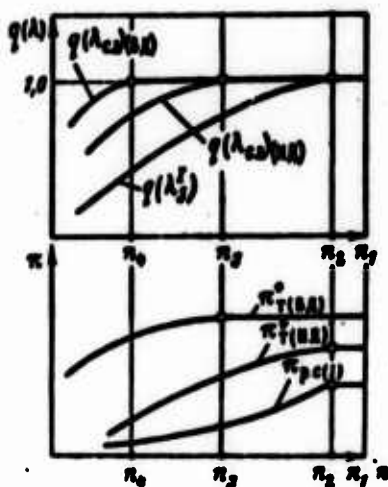


Fig. 19.17. Redistribution of the drop in pressures between VD and ND turbines with throttling of the ducted-fan engine.

of outflow from the first nozzle box assembly of the ND turbine still continues to be preserved critical, the VD turbine remains "blocked" with respect to drop of pressures, i.e.,

$$\pi_{T(ND)}^* = \text{const.}$$

With a further lowering of the number of revolutions down to  $n_3$  the velocity of outflow from the first nozzle apparatus of the ND turbine becomes subcritical. From this moment there already approaches a decrease in the drop in pressures in the VD turbine. Now between VD and ND turbines the diminishing total pressure difference will be redistributed. With the approach of  $\pi_{T(ND)}^*$  to unity the drop  $\pi_{T(ND)}^*$  is accelerated.

Figure 19.18 shows the experimental dependence<sup>1</sup> of the change in  $q(\lambda_{c,0}^1)$  on  $\pi_T^*$ .

Since

$$\pi_{T(ND)}^* \sim \frac{f_{c,0}^1(ND) q(\lambda_{c,0}^1)_{(ND)}}{f_{c,0}^1(ND) q(\lambda_{c,0}^1)_{(ND)}} \sim q(\lambda_{c,0}^1)_{(ND)},$$

<sup>1</sup>After data of Ch. A. Meyer [C. A. Meyer]\* (see the book "Jet Engines," edited by O. Ye. Lancaster [O. E. Lancaster]\*, Voenizdat, 1962, page 77). [\*Translator's note: these names have not been verified].

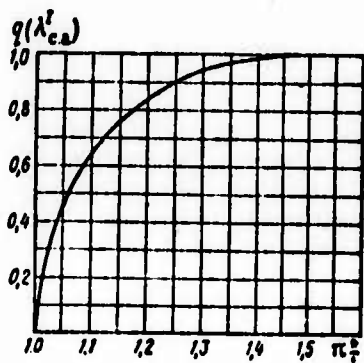


Fig. 19.18. Determination of the regime of operation of the VD turbine.

then this graph shows the qualitative connection of the drop in  $\pi_{T(ND)}^*$  as a function of  $\pi_{T(ND)}^*$ .

Change in temperature of the gas in front of the turbine of a double-shaft ducted-fan engine. The regularity of the change in temperature  $T_3^*$  with respect to the number of revolutions of a double-shaft ducted-fan engine is completely determined by the balance of works of the VD turbocompressor:

$$L_{T(ВД)} = L_{K(ВД)},$$

whence

$$T_3^* = \frac{L_{K(ВД)}}{\frac{c_{pT}}{\lambda} \epsilon_{T(ВД)}^* \eta_{T(ВД)}^*}. \quad (19.9)$$

Since the first nozzle box assembly of the ND turbine in the initial stage of throttling operates at a critical pressure difference, then  $\pi_{T(ВД)}^* = \text{const}$  and  $T_3^* \sim L_{K(ВД)}$ . In this range of numbers of revolutions there appears a lowering of  $T_3^*$ , which is determined by a change in the work of the VD compressor on the number of revolutions. With further throttling of fuel feed the drop in pressures on the VD turbine is lowered (when  $q(\lambda_{ca}^*)_{(ND)} < 1.0$ ), in consequence of which the drop in  $T_3^*$  is slowed down. With a decrease in the number of revolutions, the temperature of the gas in front of the turbine reaches a minimum, and then it begins to increase. The regularity of the change in  $T_3^*$  in a wide range of numbers of

revolutions of the double-shaft ducted-fan engine proves to be similar to the corresponding regularity for the double-shaft TRD.

"Slip" of turbocompressors of high and low pressure. Since with a decrease in the gas temperature  $T_3^*$  in front the VD turbine the gas temperature  $T_4^*$  in front of the ND turbine is lowered, and the bypass ratio  $\gamma$  increases, then the balance of works on the ND turbocompressor is disrupted, i.e.,  $(1+\gamma)L_{\kappa(\text{ND})} > L_{\tau(\text{ND})}$ .

As a result, revolutions of the ND turbocompressor also drop and more intensively than do the revolutions of the VD compressor. The drop in revolutions of the ND turbocompressor is intensified when the drop in pressures in the jet nozzle of the first circuit becomes subcritical, and the drop in pressure difference in the ND approaches (Fig. 19.19). Thus, with throttling of the engine the ratio of numbers of revolutions  $\bar{n} = n_{\text{ND}}/n_{\text{RD}}$  is continuously lowered - a slip of the rotors appears. The slip of rotors in the ducted-fan engine occurs more intensively than it is in the TRD.

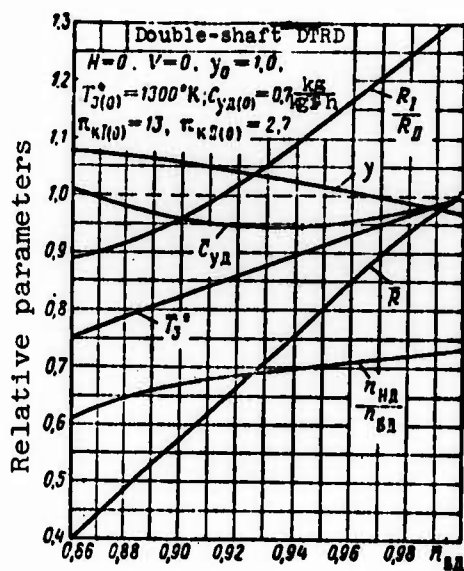


Fig. 19.19. Throttle characteristic of a double-shaft DTRD.

Change in the bypass ratio of the engine with throttling. With a decrease in the numbers of revolutions the bypass ratio of the double-shaft ducted-fan engine increases. The increase in  $\gamma$  is

conditioned, as previously, by the difference in compression ratios of compressors in the circuits ( $\pi_{KII}^* \ll \pi_{KI}^*$ ) and, consequently, by the more rapid drop in airflow through the first circuit as compared to the second. However, the progressing drop in the number of revolutions of the ND compressor accelerates the drop in  $\pi_{KII}^*$  and detains the increase in  $\gamma$ . This considerably improves the throttle characteristics of the double-shaft ducted-fan engine in comparison with the single-shaft (see Fig. 19.19).

Redistribution of thrust of the ducted-fan engine between the circuits with throttling. Figure 19.20 shows the change in velocities of the outflow of gas from the jet nozzles of a double-shaft ducted-fan engine with throttling of the engine.

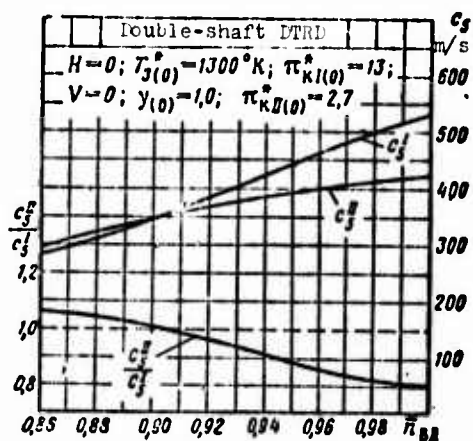


Fig. 19.20. Change in velocities of gas outflow from the jet nozzles of the ducted-fan engine with throttling of the engine.

It is characteristic that with a decrease in the number of revolutions of the engine the ratio of velocities of outflow from circuits  $c_5^{II}/c_5^I$  continuously increases, reaching a value equal to unity when  $\bar{n} \approx 0.9$ . With a further decrease in the number of revolutions  $c_5^{II}/c_5^I$  continues to grow. Thus, the ratio of velocities of outflow deviates from the optimum value ( $c_5^{II}/c_5^I = \eta_{II} \approx 0.8$  in the maximum regime), which indicates the worsening of the distribution of energy between the circuits and leads to a relative increase in the specific fuel consumption of the ducted-fan engine in comparison with the TRD.

At the same time, the relative increase in specific thrust of the second circuit and also the increase in parameter  $\gamma$  leads to a considerable redistribution of thrust between circuits of the ducted-fan engine. Thus, if in the rated regime ( $\bar{n}_{H1} = 1$ )  $R_1/R_{II} = 1.32$ , then when  $\bar{n}_{H1} = 0.86$  we have  $R_1/R_{II} = 0.89$ .

Figure 19.21 shows the throttle characteristic of a double-shaft ducted-fan engine plotted according to the number of revolutions of the ND turbocompressor.

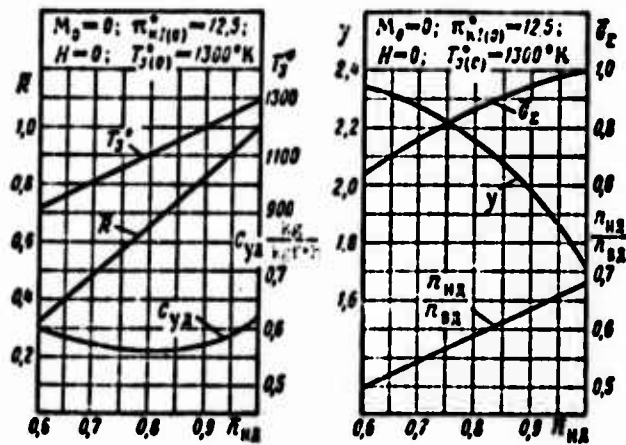


Fig. 19.21. Throttle characteristic of a double-shaft ducted-fan engine.

Comparison of throttle characteristics of double-shaft ducted-fan engine and TRD. Figure 19.22 gives for a comparison throttle characteristics of a double-shaft ducted-fan engine and TRD on the condition that in design conditions

$$T_3 = 1300^\circ\text{K} = \text{const}; \pi_{n1} = 12.5 = \text{const}; \gamma = 1.0; G_1 = \text{const}.$$

We see that transition to the double-shaft design allows considerably expanding the range of operating revolutions, in which the advantage of the ducted-fan TRD over the one-circuit with respect to specific fuel consumption is provided. However, a more intensive drop in the number of revolutions of the ND turbocompressor of the

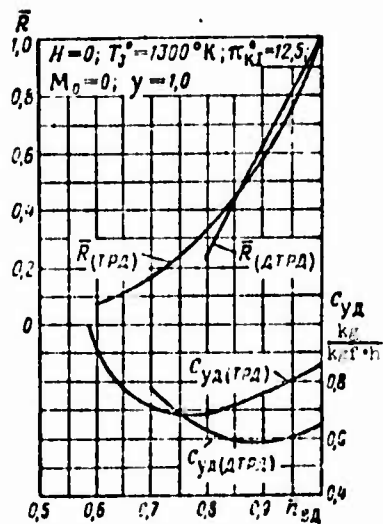


Fig. 19.22. Comparison of throttle characteristics of a double-shaft ducted-fan engine and TRD.

ducted-fan engine and, connected with this, more rapid decrease in the total compression ratio lead to the fact at a certain revolution number ( $\bar{n}_{BD} = 0.75$ ) specific fuel consumptions of the engines are equalized, and then, with further throttling of the engine, the specific fuel consumption of the ducted-fan engine becomes more than that for the TRD. A worsening of economy of the ducted-fan engine in regimes of great throttling is furthered by a sharp drop in the efficiency of the multistage turbine.

In conclusion let us note that the double-shaft ducted-fan engines, with front disposition of the fan, in its operational qualities practically do not yield to the best one-circuit TRD.

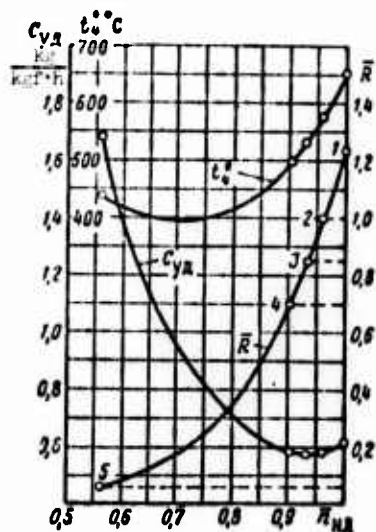


Fig. 19.23. Throttle characteristic and basic operating regimes of a double-shaft ducted-fan engine.

Figure 19.23 gives a throttle characteristic of the model double-shaft ducted-fan engine with designation on it of basic regimes of operation: takeoff (1); nominal (2); 0.85 nominal (3) and 0.70 nominal (4).

### 19.3. High-Speed Characteristics of Ducted-Fan Jet Engines

#### 19.3.1. High-Speed Characteristics of a Single-Shaft Ducted-Fan Engine

##### 19.3.1.1. Nonboosted Ducted-Fan Engine.

Let us examine the high-speed characteristic of a single-shaft nonboosted ducted-fan engine with program of control for maximum thrust:

$$n = \text{const}; T_3^* = \text{const}.$$

Let us assume that in the rated (test stand) regime of operation ( $M_0 = 0$ ;  $H = 0$ ) parameters of the working process of the engine are equal to

$$T_3^* = 1200^\circ \text{K}; \pi_{\kappa 1(0)}^* = 15; \pi_{\kappa 11(0)}^* = 2,15;$$

$$y = 1,0; \eta_T^* = 0,90; \eta_K^* = 0,85; \pi_{p,el} = \pi_{p,cl}.$$

Maintenance of the constant number of revolutions of the turbo-compressor is carried out with the help of a centrifugal regulator of revolutions, interlinked with the automatic fuel feed unit. Conservation of the fixed gas temperature in front of the turbine is provided by the control of the critical section of the jet nozzle of the first circuit ( $f_5^I = \text{var}$ ).

Initially we will examine high-speed characteristics of the ducted-fan engine, obtained as a result of an *approximate calculation*, without the use of characteristics of the compressors, turbines and intakes.

The basic assumptions usually taken in approximate calculations of characteristics refer to: the constancy of operation of the compressors (for both circuits), i.e.,

$$1) L_k = \text{const (with } n = \text{const);}$$

the constancy of particular efficiencies and coefficients of losses, i.e.,

$$2) \eta_k^* = \text{const; } \eta_T^* = \text{const; } \epsilon_{k,c}^* = \text{const; } \epsilon_{p,c} = \text{const; } \epsilon_{k,c} = \text{const}$$

the assumption about the total expansion of the gas in jet nozzles of both circuits, i.e.,

$$3) p_5^I = p_5^{II} = p_a.$$

#### 19.3.1.2. Change in Specific Thrust of the Ducted-Fan Engine.

On the test stand the velocity of gas outflow from the first circuit is more than that from the second. The latter is explained by the fact that at equal pressure differences in jet nozzles the gas temperature behind the turbine is significantly higher than the air temperature at the exit from the compressor of the second circuit. Consequently, specific thrusts of circuits are also different, i.e.,

$$R_{y_2(n)} < R_{y_1(n)}.$$

With an increase in the  $M_0$  number of flight specific thrusts of the circuits continuously drop; however the specific thrust of the first circuit more intensively decreases; since the pressure differentials in the jet nozzle of this circuit increases considerably slower than that in the second. The "opening" of the jet nozzle of the first circuit with an increase in flight speed even more intensifies this tendency (Fig. 19.24).

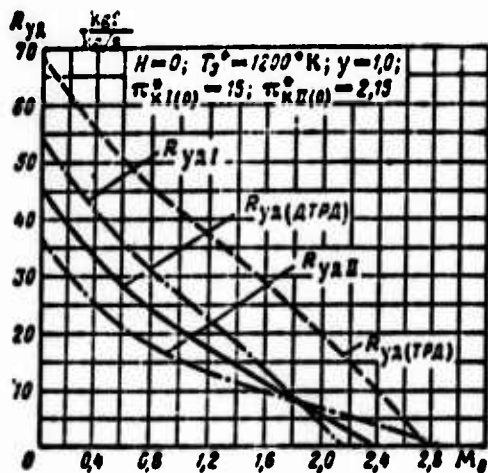


Fig. 19.24. Change in specific thrust of the first and second circuits of the ducted-fan engine with respect to the  $M_0$  number of flight.

The specific thrust of the ducted-fan engine similarly decreases considerably faster than it does in the original TRD. If in TRD the specific thrust becomes zero when  $M_0 \approx 2.8$ , then for the ducted-fan engine we find  $M_{\alpha_{R_{ya}}=0} = 2.4$  (Fig. 19.25).

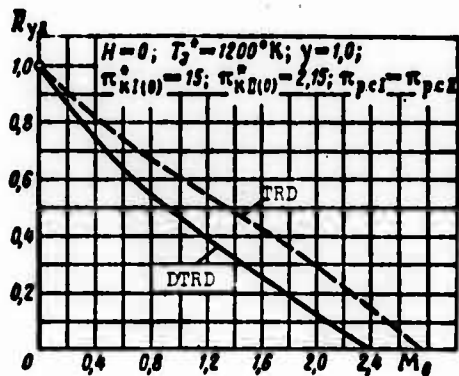


Fig. 19.25. Comparative change in specific thrusts of the ducted-fan engine and TRD according to the  $M_0$  number of flight.

### 19.3.1.3. Change in Bypass Ratio.

With an increase in the flight speed the flow of gas per second through the second circuit increases and much faster than through the first ( $\pi_{kII}^* \ll \pi_{kI}^*$ ). Thus, the bypass ratio of the engine increases

intensively. If when  $M_0 = 0$  we have  $y = 1$ , then when  $M_0 = 3.0$  we find  $y = 1.78$  (Fig. 19.26).

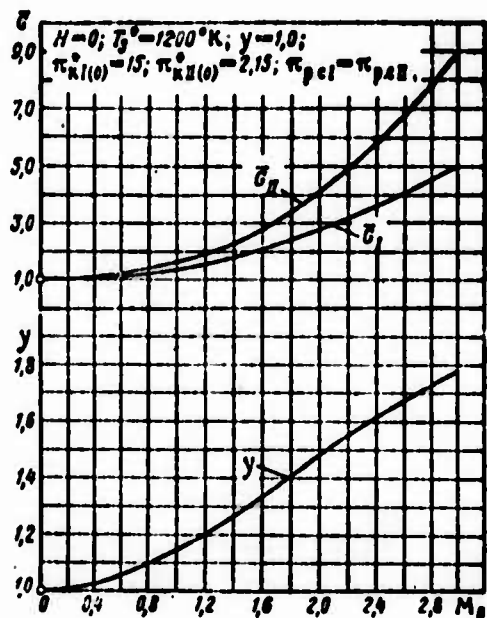


Fig. 19.26. Change in airflow in circuits of the ducted-fan engine and bypass ratio with respect to the  $M_0$  number of flight.

A rapid increase in the bypass ratio of the engine with respect to  $M_0$  number leads to an increase in necessary work of turbine equal to

$$L_T = L_{T1} + yL_{T2}$$

To maintain  $T_3^* = \text{const}$  it is necessary with an increase in  $M_0$  to increase  $\pi_T^*$  and, consequently, "open" the jet nozzle of the first circuit.

#### 19.3.1.4. Change in Total Thrust of the Ducted-Fan Engine.

Peculiarities of the passage of curves of specific thrusts and airflows in the circuits determine regularities of the change in total thrusts  $R_I$ ,  $R_{II}$  and  $R$ . Thus, the thrust in the second circuit drops considerably more slowly than it does in the first. If at subsonic flight speeds  $R_I > R_{II}$ , then at high supersonic flight speeds  $R_{II} > R_I$  (Fig. 19.27).

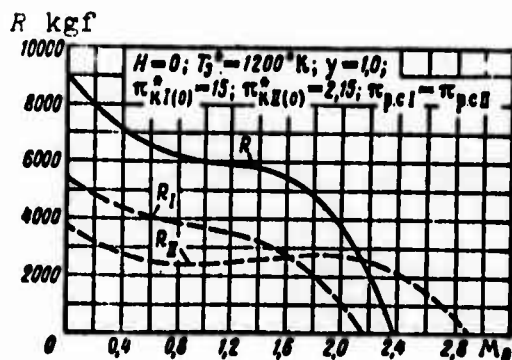


Fig. 19.27. Change in thrust of the first and second circuits of the ducted-fan engine with respect to the  $M_0$  number of flight.

The total thrust of the ducted-fan engine also is continuously lowered with respect to the flight speed, and the rate of its drop is incomparably more rapid than that in the original TRD.

It must be noted that the more bypass ratio of the engine, the steeply the curve of the change in thrust drops with respect to the flight speed, and the less the  $M_0$  number at which the thrust of the engine approaches zero (Fig. 19.28).

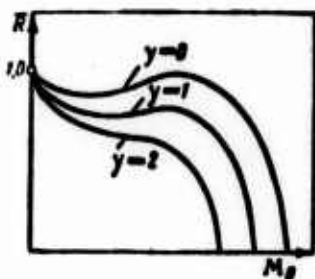


Fig. 19.28. Effect of the bypass ratio on thrust characteristics of the ducted-fan engine with respect to the  $M_0$  number of flight.

#### 19.3.1.5. Change in Efficiency of the Ducted-Fan Engine with Respect to Flight Speed.

Let us compare the change in efficiency (effective, thrust, and total) of a one-circuit and ducted-fan TRD with respect to the speed of flight (Fig. 19.29).

The transmission of mechanical energy (through the turbine and compressor of the second circuit) decreases velocity of outflow

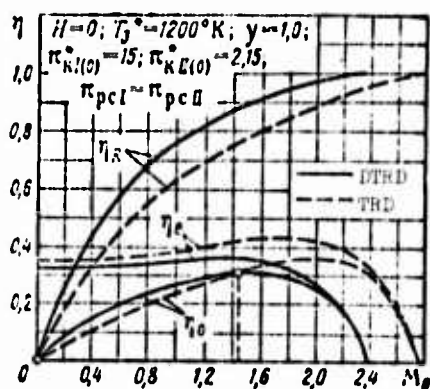


Fig. 19.29. Change in efficiency of a ducted-fan engine and TRD with respect to the  $M_0$  number of flight.

from the first circuit and increases the velocity of outflow from the second circuit; however with the applied methods of the distribution of energy between the circuits the velocity of gas outflow from the second circuit is always less than that from the first (by 30-40%); in any case, numeral values  $a_5^I$  and  $a_5^{II}$  is considerably less than the velocity of outflow from the jet nozzle of the original TRD. Therefore, the thrust efficiency of the ducted-fan TRD at all flight speeds (and specially at the subsonic) is considerably more than that in the one-circuit TRD.

Since the transmission of mechanical energy into the second circuit of the engine occurs with losses, then the effective efficiency of the ducted-fan TRD is less than that in the standard TRD, and this decrease becomes specially noticeable at high supersonic flight speeds. At these flight speeds the transmission of mechanical energy is generally little effective, because it considerably decreases the thrust in the first circuit and insignificantly increases the thrust in the second circuit.

Ultimately, the total efficiency of the ducted-fan engine noticeably exceeds in numeral value the efficiency of the TRD, and in the case of considered parameters of the working process - only in the range of  $M_0$  numbers from zero to 1.4. At high supersonic flight speeds ( $M_0 > 1.4$ ) the total efficiency of the TRD is higher than that in the ducted-fan engine.

19.3.1.6. Change in Specific Fuel Consumption.

On the test stand the specific fuel consumption of the ducted-fan engine with parameters of the working process given above is equal to  $C_{yД} = 0.60$ ; it is considerably less than that in the original TRD for which  $C_{yД} = 0.79$ .

With an increase in the  $M_0$  number of flight the specific fuel consumption of the ducted-fan engine and TRD continuously increases, since the effective work of 1 kgf of thrust increases, and therefore the expended energy in the form of fuel consumption per 1 kgf of thrust per hour increases. However, the rate of increase of the specific fuel consumption of the ducted-fan engine with respect to flight speed is considerably more than that for the TRD. Thus, with an increase in the  $M_0$  number the break between curves  $C_{yД}$  in the ducted-fan engine and TRD is always shortened, and when  $M_0 \approx 1.4$  the economies of the compared engines are equalized. With a further increase in  $M_0$  the specific fuel consumption of the ducted-fan engine already surpasses the  $C_{yД}$  of the TRD (Fig. 19.30).

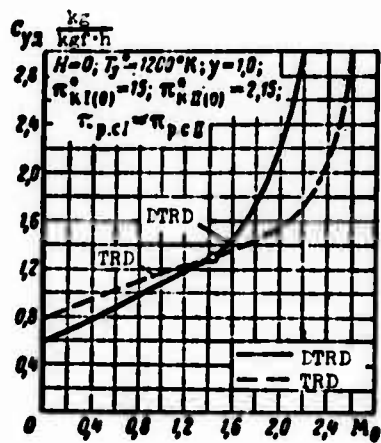


Fig. 19.30. Change in specific fuel consumption of the ducted-fan engine and TRD with respect to  $M_0$  number of flight.

The correlation between specific fuel consumptions of the engines being compared at the same flight speed is equal to

$$\frac{C_{yД(ETRD)}}{C_{yД(TRD)}} = \frac{\eta_0(TRD)}{\eta_0(ETRD)}$$

or

$$\bar{C}_{y_2} \sim \frac{1}{\eta_0}.$$

Figure 19.31 shows the effect of bypass ratio on the change in  $C_{yD}$  of the ducted-fan TRD with respect to flight speed. The more  $y$  is, the less the test stand value  $C_{yD}$ , and the less the number  $M_0$  of flight at which the advantage in the economy of the ducted-fan engine over the original TRD disappears.

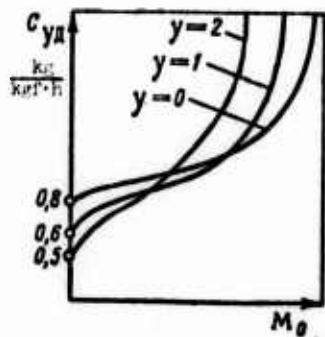


Fig. 19.31. Effect of the bypass ratio on the change in specific fuel consumption of the ducted-fan engine with respect to  $M_0$  number of flight.

It is characteristic that if the efficiency of the second circuit was equal to unity, then in the whole range of  $M_0$  numbers of flight the ducted-fan engine would be more economical than the TRD (Fig. 19.32).

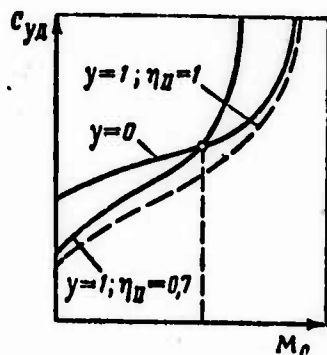


Fig. 19.32. Effect of the efficiency of the second circuit  $\eta_{II}$  on the change in specific fuel consumption of the ducted-fan engine with respect to  $M_0$  number of flight.

### 19.3.2. Peculiarities of High-Speed Characteristics of Double-Shaft Ducted-Fan Engines

Let us examine peculiarities of high-speed characteristics of double-shaft ducted-fan engines with a separate exhaust (see diagram b on Fig. 17.7) with two programs of control:

1)  $n_{H,1} = \text{const}$  and  $f_s = \text{const}$ ;

2)  $n_{H,1} = \text{const}$  and  $f_s = \text{const}$ .

#### 19.3.2.1. Program of Control

$n_{H,1} = \text{const}$

With an increase in the flight speed bypass ratio of the engine increases, since the rate of airflow through the second circuit increases faster than that through the first circuit ( $\pi_{k,II}^* < \pi_{k,I}^*$ ). In this case angles of the advance of flow on blades of the fan increase, and on blades of last steps of the VD compressor they decrease.

If  $\pi_{k,(H,1)}^* \approx 6$ , then the work of the VD compressor, with a decrease in the reduced revolution number  $n_{H,1}(\cdot\varphi)$  approximately maintains a constant value. Then from the equation of balance of works of the VD turbocompressor

$$(L_{k,(H,1)} = L_{t,(H,1)}) \sim T_3^*$$

we find that the gas temperature in front of the turbine also does not change; consequently,  $T_{H,1}^* = \text{const}$ .

Simultaneously, the "loading" of the fan and disruption of the balance of works of the ND turbocompressor approach:

$$(1 + y)L_{k,(H,1)} > L_{t,(H,1)},$$

as a result of which the revolution number of the ND shaft is lowered.

#### 19.3.2.2. Program of Control

$n_{ND} = \text{const}$  .

In this case the "loading" of the fan at a constant number of revolutions of its shaft leads to the fact that the automatic unit of fuel metering increases the fuel feed into the combustion chamber for a corresponding increase in work of the ND turbine. Consequently, gas temperatures  $T_3^*$  and  $T_4^*$  increase.

The unbalance of works on the VD turbocompressor ( $L_T(B.1) > L_K(B.1)$ ) which appeared as a result of the increase in  $T_3^*$ , is eliminated by means of acceleration of the VD turbocompressor.

With an increase in altitude the described regularities change to the opposite.

One should note that with the observance of condition  $T_3^* = \text{const}$  the high-speed characteristics of the single-shaft and double-shaft ducted-fan engine will be distinguished little from each other.

#### 19.3.2.3. Combined Program of Control of the Ducted-Fan Engine: $n_K(B.1) = \text{const}$ and $n_{K(II.1)} = \text{const}$ .

The real limitations appearing during flight operation force in a number of cases the using of a combined program of control, which represents the combination of programs  $n_K(B.1) = \text{const}$  and  $n_{K(II.1)} = \text{const}$ .

Let us examine the operation of the ducted-fan engine according to the program of control

$$n_{K(ND)} = \text{const} \text{ and } f_s = \text{const}.$$

Let  $n_{K(II.1)}$  be the maximum number of revolutions of the ND compressor limited by the *strength* of this cascade (region II on Fig. 19.33).

The range of values  $T_3^*$ , in which there is observed condition  $n_{K(II.1)} = \text{const}$ , is limited on the one hand by a certain minimum value

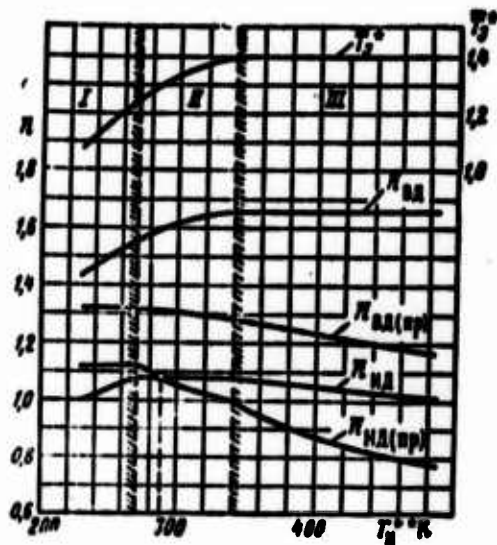


Fig. 19.33. Combined program of control of the DTRDF<sup>II</sup>.

of  $T_H^*$ , at which the reduced revolution number of the ND compressor reaches a maximum, and there approaches "blocking" at the entrance into the compressor along the airflow (i.e., with an increase in  $n_{ND(пр)}$  the increase in  $q(\lambda_1)_{(ND)}$  ceases. Beginning from this number of revolutions, it is necessary to turn to the control of  $n_{ND(пр)} = \text{const}$ . This means that with a further lowering of  $T_H^*$ , physical ND revolutions already must drop.

Thus, in regions of small  $T_H^*$  the limitation with respect to the maximum productivity of the compressor (region I on Fig. 19.33) approaches:

In the region of high values of  $T_H^*$  the limitation of the program  $n_{K(ND)} = \text{const}$  is connected with the maximum permissible value of  $T_3^*$ . Actually, with the increase in  $T_H^*$  the maintaining  $n_{K(ND)} = \text{const}$  is reached by means of an increase in the fuel feed in the combustion chamber, and, as a consequence of this,  $T_3^*$  and the number of VD revolutions increase. It is obvious that at a certain limiting value of  $T_H^*$  magnitude  $T_3^*$  reaches a permissible limit; now to maintain  $T_3^*(\text{max}) = \text{const}$  it is necessary to turn to the control of  $n_{K(ND)} = \text{const}$ ; this means now  $n_{K(ND)}$  will decrease (region III on Fig. 19.33).

Figure 19.33 shows the change in regime parameters of the ducted-fan engine for the considered case of the combined program

of control. We see clearly that section  $n_{H(ND)} = \text{const}$  corresponds to relatively small changes in  $n_{VD(ND)}$  and  $n_{H(ND)}$ , and also a small shift in regime point on characteristics of ND and VD compressors; on section  $n_{H(VD)} = \text{const}$  the drop in reduced numbers of revolutions of ND and VD compressors and also displacement of regime points of the compressor sharply increase.

### 19.3.3. Effect of Forcing on the High-Speed Characteristic of the Ducted-Fan Engine

At large values of  $\pi_{HI}^*$  the nonboosted ducted-fan engine has a continuous drop in thrust and intensive increase in specific fuel consumption on the  $M_0$  number of flight.

The additional fuel combustion in the second circuit at high values of  $T_\phi^*$  sharply increases the specific thrust on the test stand and delays its drop in flight. Thus, the thrust of the DTRDF<sup>II</sup> has no specific dip at low flight speeds and very intensively increases in the supersonic region; only at  $M_0$  numbers of flight, at which in the first circuit negative thrust is formed, a sharp drop in the total thrust of the engine approaches (Fig. 19.34).

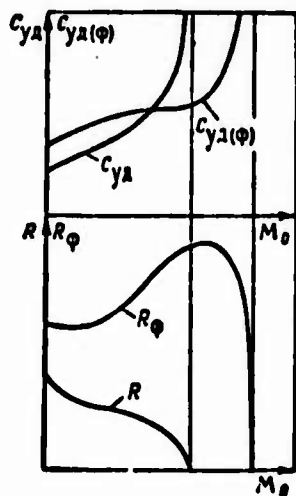


Fig. 19.34. Comparison of high-speed characteristic of the ducted-fan engine and DTRDF.

The introduction of forcing in the second circuit considerably increases the specific fuel consumption on the test stand. With

an increase in  $M_0$  numbers of flight the specific fuel consumption slowly increases<sup>1</sup> so that at supersonic flight speeds it becomes lower than that in the original TRD (see Fig. 19.34).

Figure 19.35 gives high-speed characteristics of a double-shaft DTRDF<sup>II</sup> with combined program control (see Fig. 19.33). Region  $n_{H1} = \text{const}$  corresponds to the increase in parameters  $T_3^*$  and  $T_\phi^*$  at almost a fixed value of the bypass degree. Region  $n_{H1} = \text{const}$  corresponds to the constancy of parameters  $T_3^*$  and  $T_\phi^*$  and increase in  $\gamma$ .

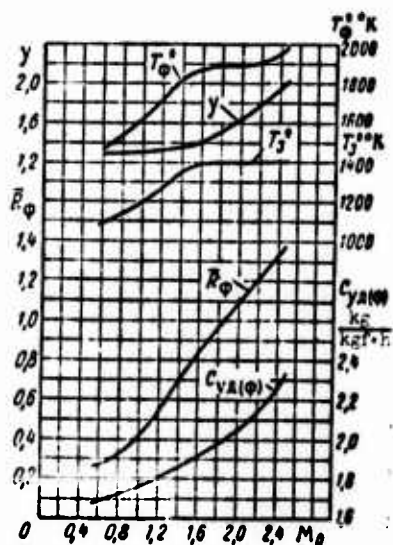


Fig. 19.35. High-speed characteristics of the double-shaft DTRDF<sup>II</sup> with a combined program of control.

The thrust and specific fuel consumption of the DTRDF<sup>II</sup> continuously increase in the interval of numbers

$$M_0 = 0.6 - 2.5.$$

#### 19.4. Altitude Characteristics of Ducted-Fan Engines

Characteristics of ducted-fan TRD with respect to altitude of flight (or altitude characteristics) are dependences of total

<sup>1</sup>At separate sections of the characteristic there can even be a reduction in  $C_{yD}$ .

thrust and also of specific fuel consumption on flight altitude at a constant flight speed (or  $M_0 = \text{const}$ ) and accepted program of control of the engine.

#### 19.4.1. Altitude Characteristic of a Single-Shaft Nonboosted Ducted-Fan Engine

Let us examine the high-speed characteristic of a single-shaft nonboosted ducted-fan engine with a program of control for maximum thrust:

$$n = \text{const} \text{ and } T_3^* = \text{const.}$$

Let us assume that the sustaining of constant gas temperature in front of the turbine is provided by means of adjustment of the critical section of the jet nozzle of the first circuit.

Let us produce the construction and analysis of altitude characteristic initially under the usual assumptions:

- 1)  $L_k = \text{const}$ ;
- 2)  $\eta_k^* = \text{const}$ ;  $\eta_t^* = \text{const}$ ;  $\epsilon_{k,c}^* = \text{const}$ ;  $\varphi_{p,c} = \text{const}$ ;  $\epsilon_{k,c} = \text{const}$ ;
- 3)  $p_3^! = p_3^{!1} = p_n$ .

Let us take as the original "test stand" data the same data as is used in the construction of the high-speed characteristic for a single-shaft ducted-fan engine<sup>I</sup>.

Let us assume that at all altitudes of flight  $M_0 = 0.9 = \text{const}$ .

##### 19.4.1.1. Change in Specific Thrust.

With an increase in altitude when  $n = \text{const}$  ( $L_k = \text{const}$ ) the compression ratio of the compressors in circuits ( $\pi_{k1}^*$  and  $\pi_{k11}^*$ ) increase, and the degree of preheating of the working medium  $\Delta = T_3^*/T_n$  increases; this leads to a velocity increase in the outflow from the jet nozzle

of the first circuit. The velocity of outflow from the second circuit, conversely, slowly decreases, since the temperature  $T_2^{*II}$  at the exit from the compressor is lowered. Ultimately the specific thrust of the first circuit increases very considerably. Magnitude  $R_{yA}$  somewhat increases as a result of a decrease in the flight speed  $V$  when  $M_0 = \text{const}$ . On the whole the specific thrust of the ducted-fan engine increases considerably more intensively than that in the original TRD (Fig. 19.36). Thus, for instance, at the altitude of  $H = 11 \text{ km}$  we have  $R_{yA(\text{DTRD})} = 1.57$ , and  $R_{yA(\text{TRD})} = 1.34$ .

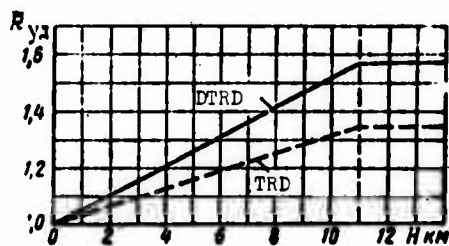


Fig. 19.36. Comparative change in specific thrusts of the ducted-fan engine and TRD with respect to flight altitude.

Thus, the effect of altitude and speed of flight on specific thrusts of the ducted-fan engine and TRD proves to be the opposite.

#### 19.4.1.2. Change in Bypass Ratio of the Engine.

An increase in flight altitude leads to an intensified drop in airflow in the second circuit, i.e., where the compression ratio of the compressor increases more slowly. Ultimately (Fig. 19.37) the bypass ratio of the ducted-fan engine is lowered. True, this lowering does not exceed 20% in the whole range of flight altitudes (up to  $H = 11 \text{ km}$ ).

The decrease in the bypass state has still that sense that the flow of air of the ducted-fan engine drops with an increase in altitude more intensively than in the original TRD ( $\bar{G}_{\text{TRD}} = \bar{G}_1$ ). The latter is clearly shown on Fig. 19.37.

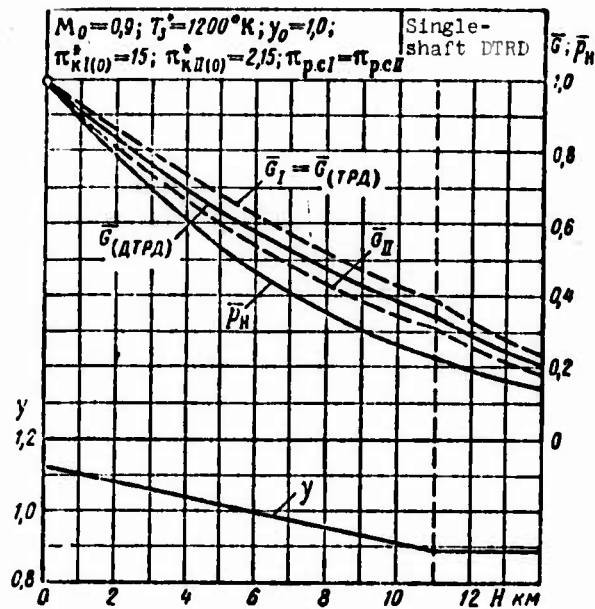


Fig. 19.37. Change in airflow in the first and second circuits and bypass ratio of the ducted-fan engine with an increase in flight altitude.

#### 19.4.1.3. Change in Thrust of the Ducted-Fan Engine.

Thus, the specific thrust of the ducted-fan engine increases with respect to the altitude of flight but more rapidly than that in the original TRD. The airflow of a ducted-fan engine decreases with an increase in flight altitude, and also more intensively than in the TRD. Ultimately the total thrust of the ducted-fan engine with an increase in altitude is lowered somewhat more slowly than that in the TRD (Fig. 19.38).

#### 19.4.1.4. Change in Efficiency of the Engine.

A velocity increase in the outflow from the jet nozzle with the lowering of flight speed always leads to a drop in thrust efficiency. An increase in the compression ratio and degree of preheating of the thermodynamic cycle somewhat improves the effective efficiency.

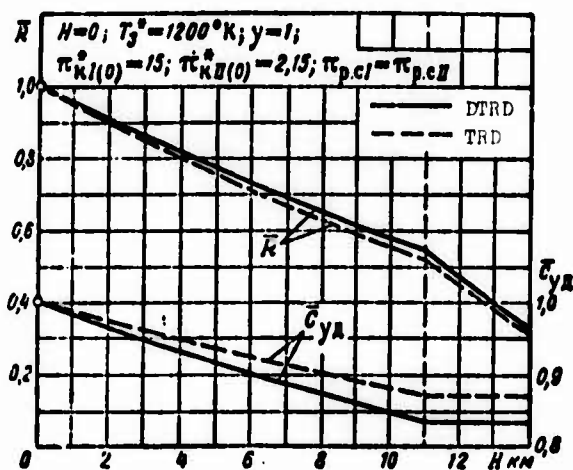


Fig. 19.38. Change in thrust and specific fuel consumption of a ducted-fan engine and TRD with an increase in flight altitude.

Ultimately the total efficiency of the ducted-fan engine with an increase in altitude of flight somewhat increases, whereas at assigned parameters of the working process in the TRD it even slowly drops.

#### 19.4.1.5. Change in Specific Fuel Consumption.

With an increase in flight altitude the specific fuel consumption of the ducted-fan engine is decreased (see Fig. 19.38). The latter is explained by a more effective conversion of heat into thrust work (i.e., increase in  $\eta_0$ ) with a certain decrease in the work of 1 kgf of thrust (as a result of the lowering of  $V$ ).

An increase in the economy of the ducted-fan engine with an increase in flight altitude proves to be somewhat more considerable than that in the TRD (up to 4-5% at the altitude of  $H = 11$  km).

In conclusion let us give the altitude characteristic of a double-shaft ducted-fan engine (Fig. 19.39) plotted taking into account the change in efficiency of VD and ND compressors.

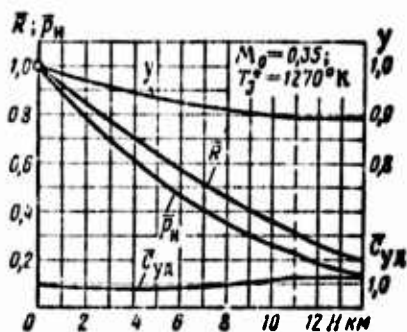


Fig. 19.39. Altitude characteristic of a double-shaft ducted-fan engine ( $\gamma = 1$ ).

### 19.5. Peculiarities of Operational Characteristics of Ducted-Fan TRD at High Bypass Ratios

During recent years the attention of scientists, researchers, and designers, working in the field of aviation has been given to the problem of the creation of large ducted-fan engines with high bypass ratios ( $\gamma = 6-8$ ). Such ducted-fan engines at high values of gas temperature in front of the turbine ( $T_3^* = 1300-1600^\circ K$ ) and total compression ratio ( $\pi_H^* = 25-30$ ) can provide extremely low specific fuel consumptions on the test stand [ $c_{yA} = 0.28-0.35 \text{ kg}/(\text{kgf}\cdot\text{h})$ ] and in flight at subsonic speed [ $c_{yA} = 0.56-0.65 \text{ kg}/(\text{kgf}\cdot\text{h})$  at  $M_0 = 0.7-0.9$  and  $H = 11 \text{ km}$ ]. Consequently, perspective ducted-fan engines being created (for example, the Pratt-Whitney JT 9D-1, Rolls-Royce RB.211, General-Electric TF-39) will be more economical in flight than contemporary turboprop engines (Fig. 19.40), moreover considerably exceeding in their high operational reliability, simplicity of design and low specific weight ( $\gamma_{dB} = 0.15-0.17 \text{ kg/kgf}$  of thrust).

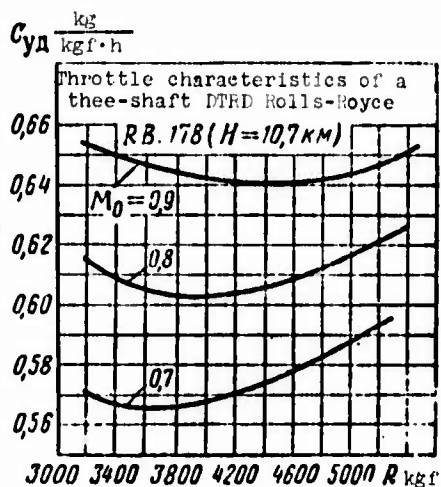


Fig. 19.40. Throttle characteristics of a three-shaft ducted-fan engine Rolls-Royce RB.178 in the cruising flight regime.

Use of the ducted-fan engine with high bypass ratios in civil aviation makes it possible to reduce considerably the operational expenditures (by approximately 1/4) and provide a rapid increase in passenger transportation.

Below certain peculiarities of the operational characteristics of such engines are examined.

19.5.1. Effect of the Bypass Ratio on the Drop  
in Thrust of the Ducted-Fan Engine  
with a Takeoff Run  
of the Aircraft

With the takeoff run of the aircraft on the airfield before the flight the thrust of any TRD (DTRD) always drops. This regularity is caused by the rapid increase in the inlet pulse  $GV/g$  at a practically constant exit pulse for these velocities of motion of the aircraft. For the TRD the drop in thrust is small and does not exceed 5-7%. The thrust decay of the ducted-fan engine is more considerable; the more it is, the less in the absolute value the velocity of gas outflow from the circuits, i.e., the more the bypass ratio of the ducted-fan engine and the less the specific thrust of the engine.

The relative thrust of the ducted-fan engine with a takeoff run of the aircraft can be calculated by the formula

$$\bar{R} = 1 - \frac{V}{\epsilon R_{ya}(0)}, \quad (19.10)$$

where  $R_{ya}(0)$  specific thrust of the ducted-fan engine on takeoff ( $V = 0$ ).

Table 19.2 gives values of  $R$  for the takeoff speed of the aircraft  $V_{отр} = 70$  m/s.

Thrust decay of the DTRD on takeoff must be considered in the calculation of takeoff and landing characteristics of the aircraft.

Table 19.2.

$R_{Y, \Gamma(0)}$ $\frac{\text{kgf}}{\text{kg/s}}$	70	60	55	50	45	40	35	30	25	20
$\bar{R}$	0,90	0,88	0,87	0,86	0,84	0,82	0,80	0,76	0,71	0,64

Figure 19.41 shows the effect of  $R_{Y, \Gamma(0)}$  on the drop in thrust of the ducted-fan engine with takeoff run of the aircraft.

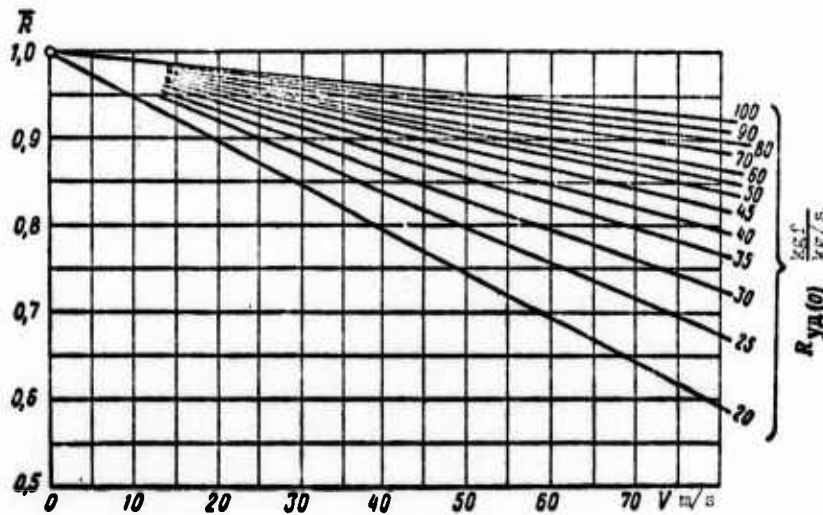


Fig. 19.41. Effect of  $R_{Y, \Gamma(0)}$  on the drop in thrust of the ducted-fan engine with takeoff run of the aircraft.

#### 19.5.2. Effect of the Bypass Ratio on Throttle Characteristics of the Engine in the Cruising Regime of Flight

It is known that the magnitude of thrust of engines of subsonic aircraft is selected from the condition of providing satisfactory takeoff and landing characteristics. In flight at the cruising regime (for example, at  $M_{0(\text{кр})} = 0.8$  and  $H_{(\text{кр})} = 11$  km) the thrust of the powerplant proves to be excessive, and the TRD (ducted-fan engine) must be throttled.

In Chapter 11 it was shown that with the lowering of the revolution number of the TRD (ducted-fan engine) the specific fuel consumption is initially lowered, and only with great throttling of the engine does it begin to increase. However, at high values of  $\gamma$  the throttling of the ducted-fan engine in the cruising flight regime ( $M_0 \approx 0.8$ ;  $H = 11$  km) leads to the fact that lowering of  $C_{yD}$  is slowed down and is even completely ceases. When  $\gamma > 6$  the lowering of the number of revolutions of the double-shaft ducted-fan engine is connected with the continuous increase in specific fuel consumption (Fig. 19.42).

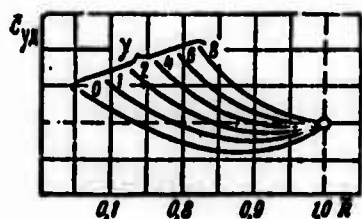


Fig. 19.42. Effect of the bypass ratio on takeoff thrust of the ducted-fan engine with a takeoff run.

### 19.5.3. Effect of the Bypass Ratio on Takeoff Thrust of the Ducted-Fan Engine

Let us assume that the necessary thrust of an aircraft for flight at subsonic velocity at an altitude maintains a fixed value. This means that the engine in the cruising regime must also develop fixed thrust at the given degree of throttling. Then with an increase in the bypass ratio takeoff (maximum) thrust will increase, and the ratio of cruising (flight) thrust to takeoff "bench," i.e.,  $R_{c, n(\gamma)}/R_{0max}$  will continuously drop (Fig. 19.43).

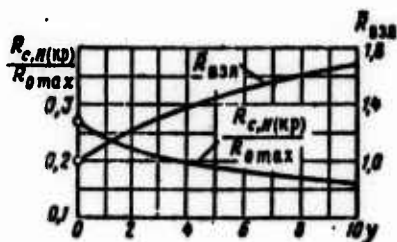


Fig. 19.43. Effect of the bypass ratio on takeoff thrust of the ducted-fan engine with a takeoff run.

When  $y = 8$ , in comparison with  $y = 0$ , the takeoff thrust increases by approximately 60%, and the ratio  $R_{c, H(sp)}/R_{0max}$  will be lowered from 0.27 to 0.17, where  $R_{c, H(sp)}$  - cruising thrust in the altitude-high-speed conditions.

The sharper drop in thrust of the ducted-fan engine with an increase in altitude of flight with an increase in  $y$  is explained by the fact that at subsonic flight speeds (when  $T_H^* < 288^\circ K$ ) the airflow drops more rapidly and the specific thrust of the ducted-fan engine increases more slowly. The latter is conditioned by the fact that with an increase in  $y$ , and, respectively, with less value of  $\pi_{HII}^*$ , thrust of the second circuit drops more rapidly.

An increase in takeoff thrust improves the takeoff and landing characteristics of the aircraft, but it simultaneously leads to a certain loading of the powerplant.

Figure 19.44 shows altitude-high-speed characteristics of the ducted-fan engine Rolls-Royce "Spey" 25 plotted for various regimes of operation of the engine.

#### 19.6. Forcing of Ducted-Fan TRD on Takeoff

One of the important advantages of ducted-fan TRD in comparison with other types of jet engines is the possibility of very considerable forcing of thrust of the engine on takeoff by means of an additional fuel combustion in afterburners.

The greatest increase in thrust of the ducted-fan engine in practice can be obtained with the equality of temperatures of forcing and equal total pressure of gas in both circuits.

With a fixed total rate of airflow ( $G_\Sigma = \text{const}$ ) the degree of forcing of the ducted-fan TRD depends only on the ratio of maximum

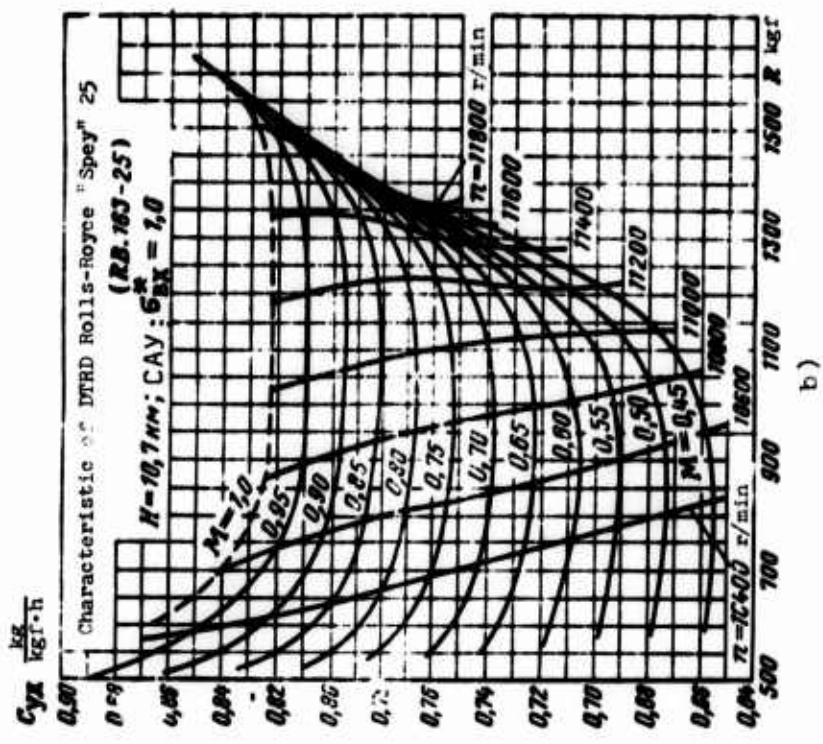
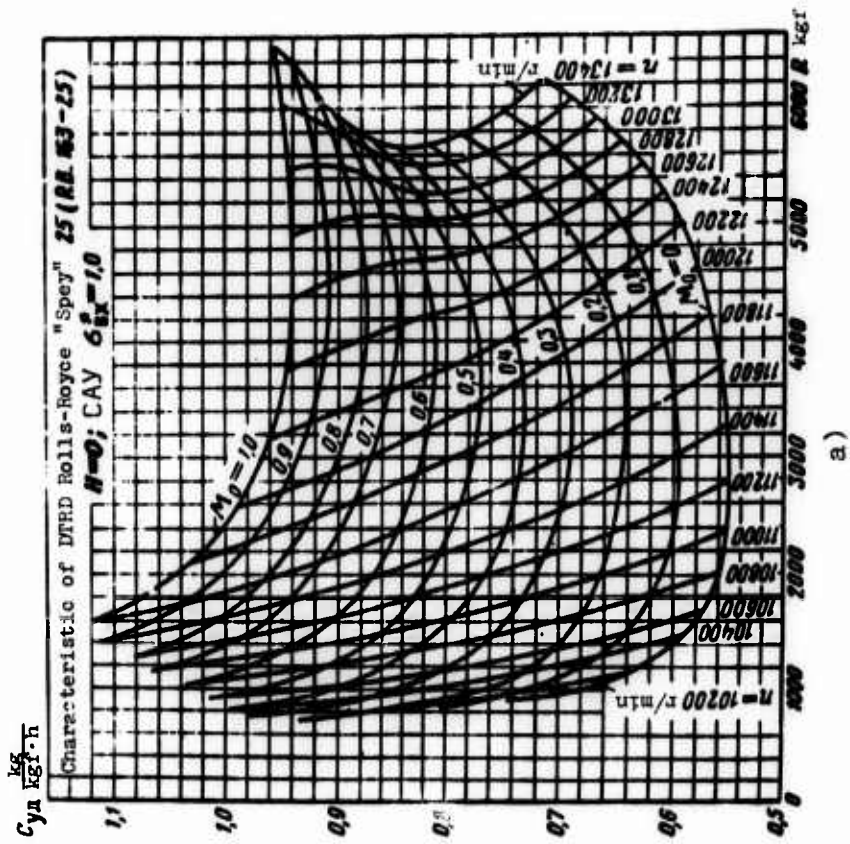


Fig. 19.44. Altitude-high-speed characteristics of the ducted-fan engine Rolls-Royce "Spey" 25 (RB.163-25): a)  $H = 0$ ; b)  $H = 10.7$  km. [CAY - expansion unknown].

temperature of forcing to the averaged mass temperature of the gas in the circuits (before the combustion of the fuel), i.e.,

$$\frac{R_{ДТРД\phi+II}}{R_{ДТРД}} = \sqrt{\frac{T_{\phi}^*}{T_{cp}^*}}$$

where

$$T_{cp}^* = \frac{T_{\phi}^* + \gamma T_0}{1 + \gamma}$$

With an increase in  $\gamma$  the degree of forcing continuously increases (see Table 19.3); when  $\gamma = 2$ ,  $T_{\phi}^* = 2000^{\circ}\text{K}$  and  $T_{\phi}^* = 1000^{\circ}\text{K}$  it is equal to approximately 2 (instead of 1.4 for the TRD).

Table 19.3. Comparison of degrees of forcing and relative thrusts of the ducted-fan engine and TRD ( $T_{\phi}^* = 2000^{\circ}\text{K}$ ;  $T_{\phi}^* = 1000^{\circ}\text{K}$ ;  $G_{\Sigma} = \text{const}$ ) when  $H = 0$ ,  $M_0 = 0$ .

Бypass ratio $\gamma$	0	1	2	3
$\frac{R_{ДТРД\phi+II}}{R_{ДТРД}}$	1.41	1.76	1.95	2.07
$\frac{R_{ДТРД\phi+II}}{R_{ТРД\phi}}$	1.0	0.85	0.75	0.68
$\frac{R_{ДТРД}}{R_{ТРД}}$	1.0	0.68	0.54	0.46

At the same time, an increase in the bypass ratio leads to a decrease in the optimum velocity of outflow of gas from the jet nozzles of the circuits and, consequently, to a decrease in the specific thrust of the ducted-fan engine (DTRDF).

Thus, with an increase in  $\gamma$  when  $G_{\Sigma} = \text{const}$ , the ratio of total (specific) thrust of the DTRDF (DTRD) to the total (specific) thrust

of the TRDF (TRD) continuously drops. Thus, for instance,  $\gamma = 2$ ,  $T_{\phi}^* = 2000^{\circ}\text{K}$  and  $T_{\text{II}}^* = 1000^{\circ}\text{K}$  the following was calculated:

$$\frac{R_{\text{ДТРД}\phi^{\text{I+II}}}}{R_{\text{ГРД}\phi}} = 0,75.$$

Thus, the higher the degree of forcing of the ducted-fan engine, the less its relative thrust in comparison with the TRDF; however, a decrease in the latter is not so great that it is serious to hamper the conditions of takeoff of the aircraft.

Let us note that the ducted-fan engine with a high bypass ratio with the boost system turned off can provide at subsonic flight speeds an exceptionally good economy and with the boost system turned on - a very high degree of increase in thrust.

The advantage of the ducted-fan engine with respect to the degree of forcing increases even more in flight.

P A R T   S I X

TURBOPROP ENGINES

## C H A P T E R 20

### DESIGN OF TURBOPROP ENGINES AND THEIR CLASSIFICATION. BASIC PARAMETERS OF THE TURBOPROP ENGINE

#### 20.1. Design and Principle of Operation of the Turboprop Engine

The turboprop engine is called a gas-turbine engine, the gas turbine of which serves for driving the compressor and the propeller. Consequently, the power of the turbine of the turboprop engine is equal to the sum of the power of the compressor (taking into account expenditures for driving auxiliary units) and propeller.

The turboprop engine refers to engines of mixed thrust, since its thrust is made up of thrust generated by the propeller, and from jet thrust obtained as a result of the increase in the quantity of motion of air in the engine itself.

Basic elements of any turboprop engine (Fig. 20.1) as a power plant are:

- 1) intake;
- 2) compressor (axial-flow, centrifugal or combined);
- 3) combustion chamber;
- 4) turbine;

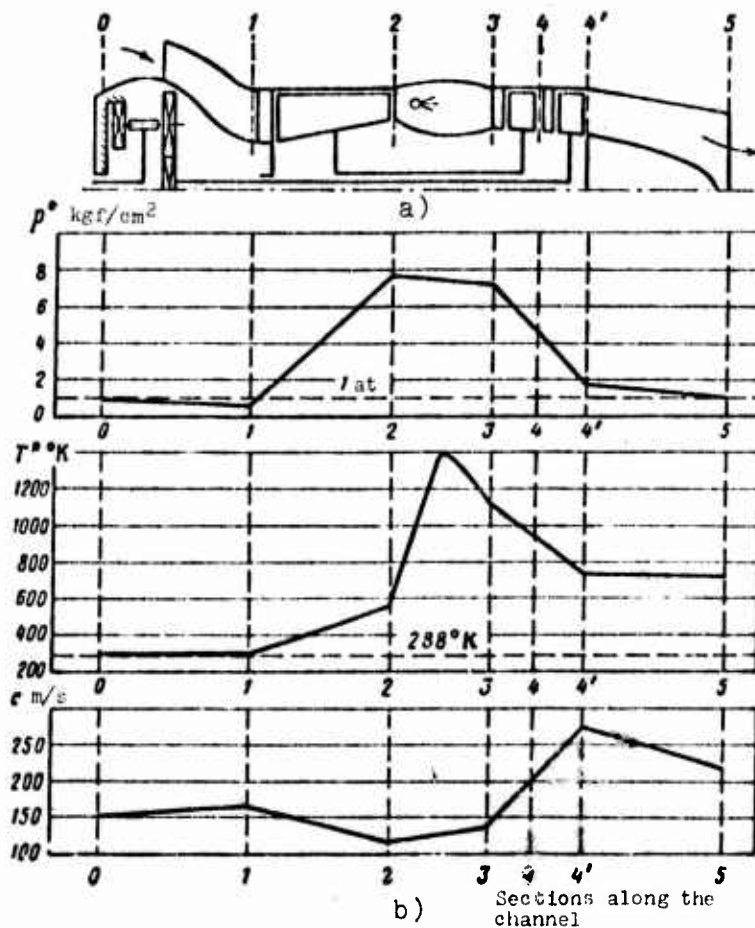


Fig. 20.1. Diagram of a turboprop engine (a) change in parameters of the flow of gas along the channel (b).

- 5) exhaust (jet) nozzle;
- 6) shaft of the propeller;
- 7) reduction gear.

The principle of operation of the turboprop engine consists in the following. Air entering from the external atmosphere is compressed in the compressor, is then heated in the combustion chamber and after this is expanded (usually up to the external counter-pressure) in the gas turbine.

Since as a result of the thermodynamic cycle the power of the turbine proves to be more than the power of the compressor, then its surplus power is transferred through the billow onto the propeller. The propeller with its rotation rejects in a direction opposite the direction of flight considerable masses of air, imparting to it a certain increase in velocity; as a result of this the propeller develops very considerable thrust.

The thrust of the turboprop engine is basically generated because of the thrust of the propeller (on a test stand ~95%) and partially because of the jet thrust (~5%), which additionally appears with the outflow of gases developed in the turbine into external medium.

#### 20.1.1. Design and Gas-Dynamic Peculiarities of the Turboprop Engine. Classification of the Turboprop Engine

In turboprop engines, just as in turbojet engines, axial-flow compressors, which have high efficiency and compression degree and provide, consequently, good economy of the engine, have become widespread. The compression ratio of compressors small turboprop engines, as a rule, is equal to 7-10 and in separate designs of large-scale turboprop engines exceeds this value (turboprop engine Rolls-Royce "Tyne" has  $\pi_H^* = 13.5$ ).

There should be noted as an exception, the wide use in operating by English airlines of the turboprop engine Rolls-Royce "Dart," equipped with a two-stage centrifugal compressor ( $\pi_H^* = 6.3$ ). The use of a centrifugal compressor, which is characterized in its design by simplicity and high reliability in operation, allowed the firm Rolls-Royce to bring the service life of the engine "Dart" up to 6000 hours.

In a number of cases in the turboprop engine (Bristol "Proteus," Lycoming T55-L-11) combined compressors are used, which consist of the several axial stages and radial (centrifugal) stages installed

behind them. Such a combination of axial-flow and centrifugal compressors at high values of the compression ratio and low air flows provides a relatively small overall length of the engine, moderate overall diameter, and also acceptable dimensions of blades of the last stages of the axial-flow compressor. Ultimately, the specific weight of the engine is relatively lowered, and, furthermore, its operational characteristics (reliability, antisurge properties) are improved. Combined compressors are used mainly in turbo-prop engine of moderate and small dimensions (with low rates of air-flow).

The turbine of the turboprop engine is always made multistage (two, three and more numbers of stages). This is conditioned not only by the great drop in pressures triggered in it, but also by the tendency to decrease the overall diameter of the engine,<sup>1</sup> which in the case of the use of the axial-flow compressor is determined by dimensions of the turbine.

Turboprop engines are made according to single-shaft and double-shaft designs (Fig. 20.2).

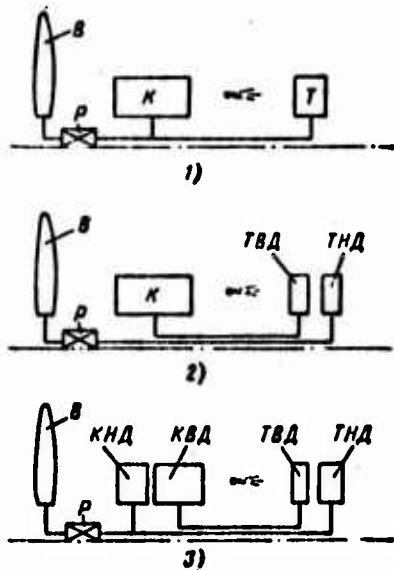


Fig. 20.2. Designs of turboprop engines: 1 - single-shaft turboprop engine; 2 - double-shaft compressor; 3 - double-shaft turboprop engine with two-stage compressor.

<sup>1</sup>At the assigned number of revolutions of the compressor, the less the diameter and, consequently, the less the circumferential velocity of blades of the turbine, the more the necessary number of its stages.

In the single-shaft turboprop engine power of the multistage turbine is expended for rotation of the compressor and propeller, i.e.,

$$N_T = N_K + N_P.$$

Single-shaft turboprop engines are quite simple in the design respect and are distinguished by a low specific weight. Among these are Soviet engines AI-20, AI-24, NK-12, and also foreign turboprop engines Napier "Eland," Rolls-Royce "Dart" and engines of the Allison firm.

In the practice of aircraft engine construction the design of the double-shaft turboprop engine has become widespread in which the free low-pressure turbine rotates the propeller, and the high-pressure turbine rotates the compressor.

Thus,

$$N_{T,P} = N_P \quad \text{and} \quad N_{T,K} = N_K.$$

According to such design turboprop engines Bristol "Proteus," "Orion" and others have been built.

The use of a separate turbine for driving the propeller complicates the design of the engine and in return makes the control of turboprop engine more flexible, since the number of revolutions of the propeller can be changed over wide limits independently of the turn number of the compressor. Furthermore, transition to the double-shaft design facilitates the starting of the turboprop engine and improves its accelerating capacity.

The design of a double-shaft turboprop engine in which the turbine of low pressure (TND) rotates the propeller and compressor of low pressure (KND) is also known; the high-pressure turbine (TVD) rotates the high-pressure compressor (KVD).

Thus,

$$N_{\text{ТВД}} = N_{\text{КВД}} + N_e \text{ and } N_{\text{ТВД}} = N_{\text{КВД}}.$$

The last design has a number of operational advantages; specifically, it provides a steady surge-free operation of the compressor without the use of an uneconomical system of bypass valves. This design is used in the English turboprop engine Rolls-Royce "Tyne."

Turboprop engines are mostly made with total expansion of the gas in the turbine up to the external counterpressure ( $p_4 = p_5 = p_H$ ). In this case the exhaust unit of the engine is not a jet nozzle made in the form of a convergent channel but an exhaust pipe of the diffusion type. Since the velocity of outflow of gases from the turbine exhaust unit exceeds the speed of flight [ $(c_5 \approx c_{4a}) > V$ ], and, consequently, the momentum of the mass of gas inside the engine increases, then in basic circuit of the turboprop engine jet thrust appears.

The turboprop engine is equipped with a reduction gear (usually of the planetary type), which provides rotation of the propeller with the most advantageous number of revolutions at which the efficiency and thrust of the propeller reach the greatest value. The gear ratio of the reduction gear, in accordance with the high number of revolutions of the turbine shaft, is equal to:

$$i_g = \frac{1}{5} + \frac{1}{13}.$$

The reduction gear is very complex, expensive to manufacture and extremely loaded with operation of subassembly. Furthermore, it is distinguished by great weight. Thus, for instance, the weight of the propeller with a reduction gear is almost equal to the weight of the turbocompressor part of the engine. It is known that the introduction into operation of the turboprop engine is usually connected with troubles and defects in the operation of this important subassembly in the highest degree.

During a number of years the aviation industry of many countries have worked on the problem of the creation of special high-speed propellers with a supersonic profile. The introduction of such propellers would make it possible to reject entirely reduction gears and considerably simplify and facilitate the design of the turboprop engine. Unfortunately the effectiveness of supersonic propellers is sharply made worse in variable regimes, which prevents their wide introduction.

Figure 20.1 shows a diagram of a turboprop engine with characteristic sections of a gas-air channel, and a diagram of the change in basic parameters of gas flow is also given.

## 20.2. Basic Parameters of the Turboprop Engine

### 20.2.1. Effective Power ( $N_e$ )

The effective power of the turboprop engine is the power transmitted to the turbine on the shaft of the propeller (through the reduction gear). It is equal to:

$$N_e = \frac{L_{T.B} G}{75} \text{ hp.} \quad (20.1)$$

where  $L_{T.B}$  - work of 1 kg of gas transmitted to the shaft of the propeller;  $G$  - flow of air in kg/s.

### 20.2.2. Propeller Power ( $N_p$ )

The propeller power of the turboprop engine is the power obtained on the nose of the shaft of propeller (i.e., fed to the propeller). The propeller power is less effective, since it considers losses conditioned by friction in the reduction gear; consequently,

$$N_p = N_e \eta_{ред.} \quad (20.2)$$

where  $\eta_{ред.}$  - efficiency of the reduction gear; on the average  $\eta_{ред.} = 0.97-0.98$ .

The propeller power can be determined as

$$N_n = \frac{L_n G}{75} \text{ hp.} \quad (20.3)$$

where  $L_n$  - work of 1 kg of gas fed to the propeller.

The propeller power is the most important parameter characterizing the effectiveness of the turboprop engine. The factory manufacturing the turboprop engine guarantees this power to the user.

#### 20.2.3. Thrust Power of the Propeller ( $N'_n$ )

Not all the power fed to the propeller is used for the creation of thrust. Part of it with rotation of the propeller is irreversibly dispersed in space. These losses of power to friction, rejection and twist of the flow are evaluated with the help of the efficiency of the propeller.

The product of the expended propeller power by the efficiency of the propeller determines the useful thrust propeller power, i.e.,

$$N'_n = N_n \eta_n = \frac{L_n G}{75} \eta_{p.a.} \eta_n \text{ hp.} \quad (20.4)$$

#### 20.2.4. Thrust of the Propeller

The connection between thrust of the propeller and propeller power is determined by expression

$$P_n = \frac{75 N'_n}{V} = \frac{75 N_n \eta_n}{V} \text{ kgf.} \quad (20.5)$$

where  $\eta_n$  - efficiency of the propeller.

#### 20.2.5. Jet Thrust of the Turboprop Engine

By analogy with the TRD, we have for the case of total expansion of the gas in the exhaust instrument of the turboprop engine:

$$R = \frac{G}{g} (c_s - V) \text{ kgf.} \quad (20.6)$$

#### 20.2.6. Thrust of the Turboprop Engine

The thrust of the turboprop engine is composed of thrust of the propeller and jet thrust, i.e.,

$$P = P_p + R. \quad (20.7)$$

Similarly, let us write the expression for specific thrust:

$$P_{ya} = P_{p(ya)} + R_{ya}. \quad (20.8)$$

In expression (20.8) all terms are referred to the flow of gas per 1 kg/s through the basic gas-turbine circuit.

Let us replace in expression (20.7)  $P_p$  and  $R$  by their values from expressions (20.5) and (20.6); then let us obtain

$$P = \frac{75 N_p \eta_p}{V} + \frac{G}{g} (c_s - V). \quad (20.9)$$

Having divided all terms of expression (20.9) by  $G$ , let us obtain the expanded expression for specific thrust of the turboprop engine:

$$P_{ya} = \frac{L_p \eta_p}{V} + \frac{(c_s - V)}{g}. \quad (20.10)$$

With operation on the ground expressions (20.9) and (20.10) turn into uncertainty (when  $V = 0$ , then  $\eta_p = 0$ ). In this case let us use the empirical dependence

$$P_{p(0)} = \beta N_{p(0)}, \quad (20.11)$$

where  $\beta$  - ratio of thrust of the propeller with its operation on the ground to the power fed to the propeller;  $\beta = 1.05-1.15$ ; on the average  $\beta = 1.1$ .

Then for  $V = 0$  we obtain

$$P_{(0)} = \beta N_n + \frac{G}{g} c_s; \quad (20.12)$$

$$P_{y_1(0)} = \beta N_{n(y_1)} + \frac{c_s}{g}. \quad (20.13)$$

Thus, comparing expressions (20.5) and (20.11), we find for  $V = 0$

$$\frac{75\eta_n}{V} = \beta \approx 1.1. \quad (20.14)$$

#### 20.2.7. Equivalent Power of the Turboprop Engine

The equivalent power of the turboprop engine is the conditional power which must be fed to propeller to obtain a draught equal to the total thrust of the turboprop engine. Thus,

$$N_s = \frac{PV}{75\eta_b} = \frac{(P_n + R)V}{75\eta_b}, \quad (20.15)$$

or

$$N_s = N_n + \frac{RV}{75\eta_b}. \quad (20.16)$$

For the case of operation of the turboprop engine on the test stand ( $V = 0$ ), let us transform expression (20.16) with the help of (20.14); then

$$N_{s(0)} = N_{n(0)} + \frac{R_{(0)}}{\beta}. \quad (20.17)$$

Similar to expression (20.16), let us write the expression for the specific equivalent power:

$$N_{s(y_1)} = N_{n(y_1)} + \frac{R_{y_1}V}{75\eta_b}. \quad (20.18)$$

### 20.2.8. Effective Fuel Consumption

Effective fuel consumption is the fuel consumption per hour of the turboprop engine referred to the equivalent power,

$$C_e = 3600 \frac{G_T}{N_e} \frac{\text{kg}}{\text{hp}\cdot\text{h}}. \quad (20.19)$$

The effective fuel consumption is an important parameter characterizing the economy of the turboprop engine as an engine.

### 20.2.9. Equivalent Fuel Consumption

The equivalent fuel consumption is fuel consumption per hour of the turboprop engine referred to equivalent power,

$$C_e = 3600 \frac{G_T}{N_e} \frac{\text{kg}}{\text{hp}\cdot\text{h}}. \quad (20.20)$$

For a comparison of the turboprop engine and TRD the concept of specific fuel consumption (for 1 kg of thrust) is used:

$$C_{y_1} = 3600 \frac{G_T}{P} \frac{\text{kg}}{\text{kgf}\cdot\text{h}}. \quad (20.21)$$

The connection between  $C_{y_1}$  and  $C_e$  can be found, having divided expression (20.21) by (20.20).

Then

$$C_{y_1} = C_e \frac{V}{75n_e}. \quad (20.22)$$

With operation on the ground

$$C_{y_1} = \frac{C_e}{\beta}. \quad (20.23)$$

## 20.2.10. Efficiencies of the Turboprop Engine

### 20.2.10.1. Effective Efficiency.

Effective efficiency of the turboprop engine and TRD are identical:

$$\eta_e = \frac{AL_e}{q_{in}}. \quad (20.24)$$

### 20.2.10.2. Thrust Efficiency.

The thrust efficiency of the turboprop engine is the ratio of the work of total thrust of the engine to its effective work

$$\eta_p = \frac{L_p}{L_e} = \frac{P_{ya}V}{L_e}. \quad (20.25)$$

Since the turboprop engine has two propelling agents - propeller and gas-turbine circuit (jet engine), the thrust efficiency of the turboprop engine numerically occupies an intermediate position between the efficiency of the propeller and thrust efficiency of the jet engine.

### 20.2.10.3. Total Efficiency.

The total efficiency of the turboprop engine is the ratio of the heat equivalent to the work of the total thrust to the heat introduced with fuel into the engine,

$$\eta_0 = \frac{AL_p}{q_{in}} = \frac{AP_{ya}V}{q_{in}}. \quad (20.26)$$

Having multiplied expression (20.24) by (20.25), we obtain

$$\eta_0 = \eta_p \eta_e. \quad (20.27)$$

### 20.3. Peculiarity of Expansion Process of Gas in Turboprop Engine

Figure 20.3 gives in coordinates  $i/A - s$  the expansion process of gas in the turbine of the turboprop engine for three cases:

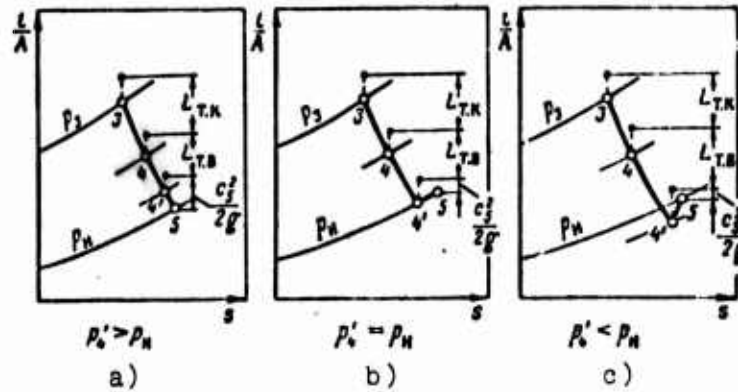


Fig. 20.3. Expansion in the turbine of the turboprop engine: a) turbine with incomplete expansion; b) turbine with complete expansion; c) turbine with over-expansion.

a) when the counterpressure behind the turbine is more external ( $p_4' > p_5 = p_H$ ). In this case the final expansion of the gas behind the turbine is accomplished in the jet nozzle (convergent channel); it is obvious that  $\sigma_5 > \sigma_4$ ;

b) when gas is completely expanded in the turbine up to the external counterpressure ( $p_4' = p_5 = p_H$ ). In this case the exhaust nozzle is almost a cylindrical pipe<sup>1</sup> ( $\sigma_5 \approx \sigma_4$ );

c) when the counterpressure behind the turbine is below the atmospheric ( $p_4 < p_5 = p_H$ ), i.e., a turbine with overexpansion. In this case the exhaust nozzle is a diffusion channel in which the increase in gas pressure up to the external occurs as a result of deceleration of outflow ( $\sigma_5 < \sigma_4$ ).

<sup>1</sup>With an allowance for friction, such a channel has a weak diffusion quality ( $f_5 > f_4$ ).

If from the obtained work of expansion of 1 kg of gas equal to

$$L_p = L_{r.} + L_{r.n} + \frac{c_3^2}{2g},$$

we subtract the work expended for the compression of 1 kg of gas

$$L_c = L_k + \frac{V^2}{2g},$$

then we obtain the effective work of the cycle of the turboprop engine

$$L_e = L_p - L_c = L_{r.n} + \frac{c_3^2 - V^2}{2g}, \quad (20.28)$$

expended for the rotation of the propeller,

$$L_n = L_{r.n} \eta_{\text{ррс}},$$

and for the increase in kinetic energy of gas inside the engine,

$$\frac{c_3^2 - V^2}{2g}.$$

Regulating the exit section of the exhaust unit of the turboprop engine, and thus changing the profile of the exhaust channel from convergent to divergent, it is possible by various means to distribute the effective work of the cycle between the propeller and reaction depending on the speed and altitude of flight.

#### 20.3.1. Determination of Work of the Turbine of the Turboprop Engine with Complete Expansion

Let us find the work of the turbine of the turboprop engine with complete expansion of the gas (Fig. 20.4).

Let us assume that parameters of the gas at the entrance into the turbine  $p_3^*$  and  $T_3^*$ , external counterpressure  $p_4 = p_H$  and velocity of gas at the exit from the turbine  $c_4$  are assigned.



## CHAPTER 21

### EFFECT OF PARAMETERS OF THE WORKING PROCESS ON BASIC PARAMETERS OF THE TURBOPROP ENGINE

#### 21.1. Optimum Distribution of Work of the Cycle of the Turboprop Engine Between the Propeller and Reaction

We already noted in Chapter 20 that in the turboprop engine the work of the cycle is expended for driving the propeller and for the increase in kinetic energy of the gas.

Let us introduce the concept of the degree of energy exchange in the turboprop engine

$$x = \frac{L_p}{L_e}. \quad (21.1)$$

Let us now transform the expression for specific thrust of the turboprop engine:

$$P_{ya} = \frac{L_p \eta_p}{V} + \frac{c_s - V}{g},$$

Having expressed the work of the propeller and velocity of outflow from the nozzle in terms of parameter  $x$ , i.e.,

$$L_p = x \eta_{pca} L_e$$

and

$$c_s = \sqrt{2g(1-x)L_e + V^2}.$$

Then we obtain

$$P_{yA} = \frac{\eta_s \eta_{peA} L_0}{V} x + \frac{1}{g} \left[ V \sqrt{2g(1-x)L_0 + V^2} - V \right]. \quad (21.2)$$

With an increase in the degree of energy exchange the thrust of the propeller increases and the reactive thrust of the turboprop engine is decreased.

The value of the degree of energy exchange  $x$  at which the total specific and also complete thrusts of the turboprop engine reach a maximum value is called the optimum value.

To determine  $x_{opt}$ , let us investigate the function  $P_{yA} = f(x)$  for a maximum.

We have

$$\frac{dP_{yA}}{dx} = \frac{\eta_s \eta_{peA}}{V} - \frac{1}{V \sqrt{2g(1-x)L_0 + V^2}} = 0,$$

whence after simple conversions we find

$$x_{opt} = 1 - \left[ \frac{1}{(\eta_s \eta_{peA})^2} - 1 \right] \frac{V^2}{2gL_0}. \quad (21.3)$$

From expression (21.3) it follows that the more the optimum portion of the work of the cycle transferred to the propeller, the more the work of the cycle, the more the reduced efficiency of the propeller ( $\eta'_s = \eta_s \eta_{peA}$ ), and the less flight speed.

Let us find value  $x_{opt}$  with operation of the turboprop engine on a test stand.

According to expression (20.14) when  $V = 0$ , let us replace in equation (21.3)

$$\frac{V}{\eta_s \eta_{peA}} = \frac{75}{g}.$$

Then let us find

$$x_{opt} = 1 - \left(\frac{75}{\beta}\right)^2 \frac{1}{2\kappa L_c} \quad (21.4)$$

Since for values  $T_3^* = 1100-1300^\circ\text{K}$  and the optimum values of the compression ratio  $L_c(0) = 15,000-25,000 \text{ kgf}\cdot\text{m}/\text{kg}$  (Fig. 21.1), then, respectively,  $x_{opt} = 0.98-0.99$ .

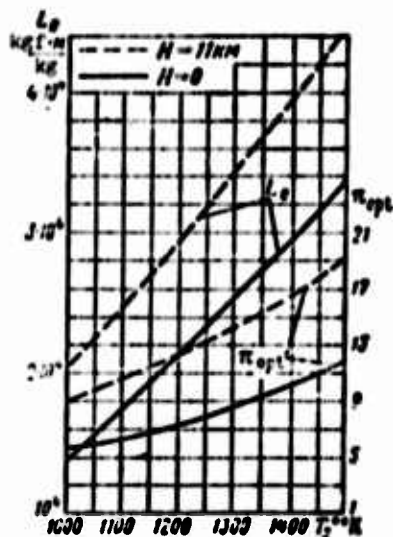


Fig. 21.1. Effect of  $T_3^*$  and  $\eta_{opt}$  on the work of the cycle of the turboprop engine.

Thus, to get the maximum of thrust on the test stand one should use only 1-2% of the work of the cycle for the increase in kinetic energy of the flow, and 98-99% of the work must be transferred to the propeller.

Let us now find the optimum velocity of expiration of the gas from the exhaust unit of the turboprop engine.

Using expression (21.3), let us write down the equality:

$$(1-x) = \left[ \frac{1}{(\eta_b \eta_{opt})^2} - 1 \right] \frac{v_2}{L_c} = \frac{c_3^2 - v_2^2}{L_c}$$

whence we find

$$c_{s(opt)} = \frac{V}{\eta_h \eta_{pe}} \quad (21.5)$$

From expression (21.5) it follows that with an increase in the flight speed and with a lowering of the efficiency of the propeller, the velocity of expiration from the nozzle of turboprop engine must be increased.

Formula (21.5) was derived in 1944 by Academician B. S. Stechkin.

Let us find  $c_{s(opt)}$  for test stand conditions ( $V = 0$ ), having substituted

$$\frac{V}{\eta_h \eta_{pe}} = \frac{75}{\rho}$$

Then we obtain

$$c_{s(opt)} = \frac{75}{\rho} \approx 70 \text{ m/s.} \quad (21.6)$$

It is obvious that to ensure such low velocities of gas outflow from the exhaust nozzle of the turboprop engine, a diffuser with great expansion unit must be installed behind the turbine. If we consider that the minimum velocity of the outflow of gas from the turbine (from considerations of the limitation of its overall dimension) must be not less than  $c_4 = 200 \text{ m/s}$ , then this denotes that when  $\gamma = \text{const}$  the area of the exit section of the diffuser must exceed the inlet section by approximately three times. The latter can considerably increase the dimensions of the turboprop engine and, furthermore, make the distribution of thrust in flight worse (the jet thrust will become negative, because  $c_5 < V$ ). Adjustable exhaust devices of the turboprop engine have not as jet become widespread.

The optimum correlation (21.5) for the velocity of gas expiration from the nozzle of the turboprop engine can be obtained directly, using conditions (18.9) for the optimum distribution of energy in the ducted-fan jet engine:

$$\left(\frac{c_3^{\text{II}}}{c_3^{\text{I}}}\right)_{\text{opt}} = \eta_{11}.$$

In reference to the turboprop engine, the efficiency of the second circuit is the efficiency of the propeller, i.e.,

$$\eta_{11} = \eta_p^{\text{I}} = \eta_p \eta_{\text{prop}}.$$

The velocity of expiration behind the propeller at high bypass ratio is little distinguished from the flight speed, i.e.,

$$c_3^{\text{II}} \approx V.$$

After substitution in expression (18.9) of values  $c_3^{\text{II}}$  and  $\eta_{11}$ , we obtain the sought expression:

$$c_3 = \frac{V}{\eta_p \eta_{\text{prop}}}.$$

#### 21.1.1. Comparison of Thrust of the Turboprop Engine and TRD on a Test Stand

Let us now find the magnitude of specific thrust of the turboprop engine on the test stand. For this into expression (21.2) we substitute

$$\frac{V}{\eta_p \eta_{\text{prop}}} = \frac{75}{\beta}.$$

Then

$$P_{y1(0)} = \frac{\beta}{75} x l_e + \frac{1}{g} \sqrt{2g(1-x)l_e}. \quad (21.7)$$

With work of cycle  $L_e$  identical with the turboprop engine, the specific thrust of the TRD on a test stand is equal to

$$P_{y1(\text{TRD})} = \frac{1}{g} \sqrt{2gL_e}. \quad (21.8)$$

Then the relative specific and total thrusts of the turboprop engine can be determined as

$$\bar{P}_{y_{1,0}} = \beta_0 = \frac{P_{(TRD)}}{P_{(TRP)}} = \frac{9x}{150} \sqrt{2gL_0} + \sqrt{1-x}. \quad (21.9)$$

When  $x = 1$  we find

$$\bar{P}_{y_{1,0}} = \frac{1}{150} \sqrt{2gL_0};$$

when  $x = x_{opt}$  we find

$$P_{y_{1,0}} = \frac{1}{150} \sqrt{2gL_0} + \frac{75}{25} \frac{1}{\sqrt{2gL_0}}.$$

Figure 21.2a gives the dependence of relative thrust of the turboprop engine and also velocities of outflow of gas from the exhaust nozzle on the degree of energy exchange  $x$  when  $V = 0$ .

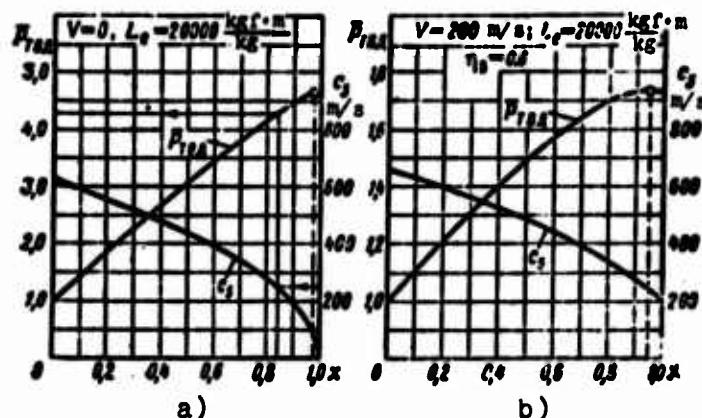


Fig. 21.2. Dependence of relative thrust of the turboprop engine and velocity of gas outflow on the degree of energy exchange: a) on a test stand; b) in flight.

We see that when  $x = x_{opt} \approx 1.0$  the bench thrust of the turboprop engine with the same generator of gas exceeds the draught of

\*) Assuming that the flow of gas through the turbocompressor is identical for the turboprop engine and TRD.

the TRD by more than 4.5 times. An increase in the velocity of outflow from the exhaust unit of the turboprop engine from 70 to 250 m/s lowers the relative thrust of the turboprop engine from 4.5 to 4.3, i.e., 7%.

#### 21.1.2. Comparison of Thrust of the Turboprop Engine and TRD in Flight

Figure 21.2b gives the dependence of relative thrust of the turboprop engine and also velocities of gas outflow from the exhaust nozzle on the degree of energy exchange in flight when  $V = 200$  m/s.

Dependences given in Fig. 21.2a and Fig. 21.2b are identical; however in flight the change in the velocity of gas outflow from the nozzle from 200 to 350 m/s (which corresponds to a change in  $x$  from 1.0 to 0.8) practically has no effect (to within 1%) on the magnitude of relative thrust equal to  $\bar{P}_{\text{ТВД}} = 1.70$ .

Thus, in flight the deviation in magnitude of the degree of energy exchange from its optimum value leads to a less drop in thrust of the turboprop engine than that on a test stand.

#### 21.1.3. Effect of Flight Velocity on $x_{\text{opt}}$

With an increase in the flight velocity magnitude  $x_{\text{opt}}$  is lowered (Fig. 21.3), i.e., the transferring of even less work of the cycle to the propeller becomes expedient.

Let us find the flight speed at which the whole work of the cycle should be used to get jet thrust. It is obvious that at this flight speed the turboprop engine "degenerates" in a TRD.

Let us substitute into the expression for the optimum degree of energy exchange (21.3) value  $x_{\text{opt}} = 0$ ; then we find

$$\eta_{\text{min}} = \frac{1}{\sqrt{\frac{2gL_e}{V^2} + 1}}. \quad (21.10)$$

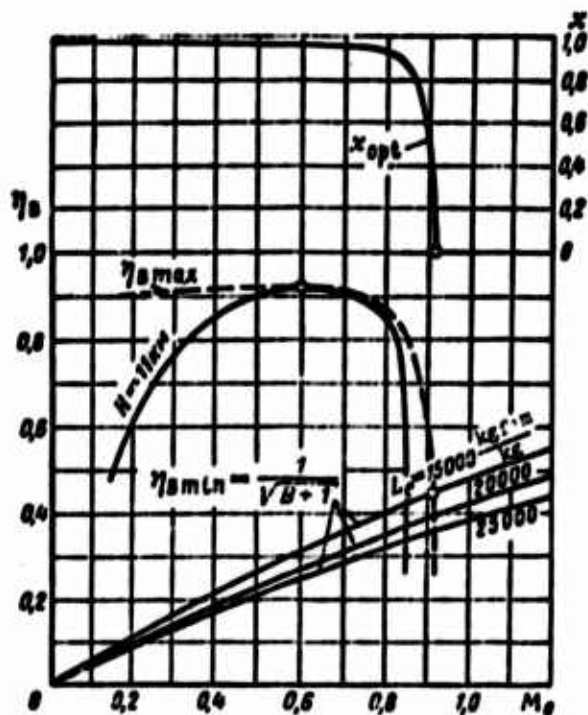


Fig. 21.3. Change in efficiency of the propeller and optimum degree of energy exchange with respect to the  $M_0$  number of flight.

In this formula  $\eta_{\text{emin}}$  is the minimum value of the efficiency of the propeller, which provides the equality of thrusts of the turbo-prop engine and TRD. When  $\eta_{\text{e}} < \eta_{\text{emin}}$ ,  $P_{\text{ТВД}} < P_{\text{ТРД}}$ .

Figure 21.3 shows the change in efficiency of one of the contemporary propellers with respect to flight speed. Lines of minimum permissible  $\eta_{\text{emin}}$  are plotted there. Points of intersection of the real curve  $\eta_{\text{e}}$  with lines of minimum  $\eta_{\text{e}}$ , calculated by formula (21.10), determine the limit of the expedient use of the turboprop engine with respect to thrust and economy. As we see, this limit lies within limits of subsonic flight speeds ( $M_0 \text{ max} \approx 0.9$ ).

21.2. Effect of Basic Parameters of the Working Process on Specific Parameters, Efficiency and Effective Fuel Consumption of the Turboprop Engine

21.2.1. Specific Work Transmitted to the Propeller, Specific Power and Specific Thrust of the Propeller

We will examine how in the case of the TRD how the air cycle  $p = \text{const}$  with the working medium of fixed chemical composition ( $R_{\Gamma} = R_{\text{B}} = R$ ) and fixed specific heat ( $c_{p\Gamma} = c_{p\text{B}} = c_p$ ;  $k_{\Gamma} = k_{\text{B}} = k$ ); the effective work of this cycle is determined by expression

$$L_e = \frac{c_p}{\lambda} \left(1 - \frac{1}{\epsilon}\right) \left(T_3^* \eta_p - T_0 \frac{\epsilon}{\eta_c}\right).$$

The connection of parameters  $L_{\text{B}}$ ,  $P_{\text{B}}(y_{\text{D}})$ ,  $N_{\text{B}}(y_{\text{D}})$  and  $L_e$  has the form

$$L_{\text{B}} = 75 N_{\text{B}}(y_{\text{D}}) = P_{\text{B}}(y_{\text{D}}) \frac{V}{\eta_{\text{B}}} = L_e x \eta_{\text{B, opt}}$$

where for  $V = 0$

$$x_{\text{opt} \eta_{\text{B, opt}}} \approx 1.0.$$

Thus, the specific work transferred to the propeller, specific power of the turboprop engine and specific thrust of the propeller are functions of parameters  $\pi$ ,  $T_3^*$ ,  $T_0$ ,  $\eta_p$  and  $\eta_c$  and change similar to the effective work of the cycle  $L_e$ .

To increase the specific power of the turboprop engine, it is profitable in every way possible to increase the gas temperature in front of the turbine; it is expedient to produce an increase in total compression ratio only up to its optimum value.

On the average for  $H = 0$ ,  $T_3^* = 1100-1300^\circ\text{K}$  and  $\pi = \pi_{\text{opt}}$  we find  $N_{\text{B}}(y_{\text{D}}) = 210-230 \text{ hp (kg/s)}$ .

Figures 21.4 and 21.5 show, respectively, the comparative effect of  $\pi$  and  $T_3^0$  on specific power of the turboprop engine and on specific thrust of the TRD.

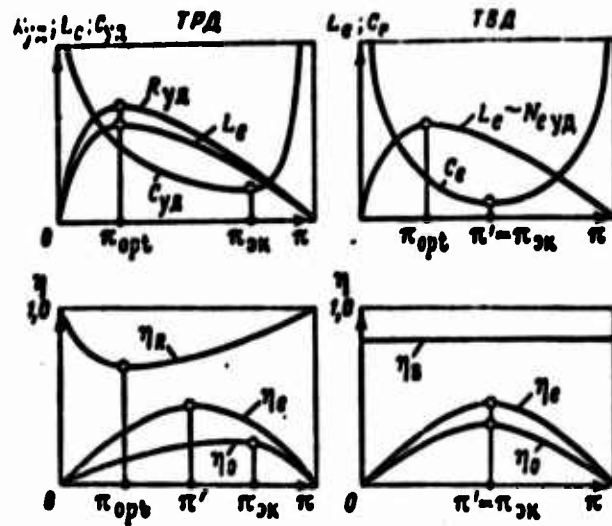


Fig. 21.4. Effect of compression ratio on specific parameters and efficiency of the turboprop engine and TRD.

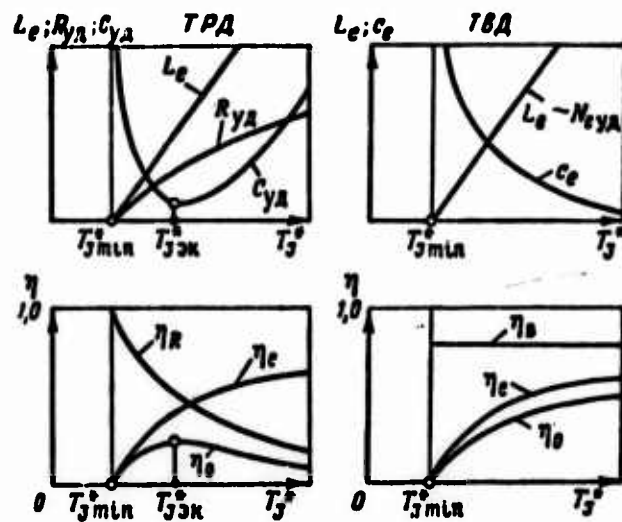


Fig. 21.5. Effect of gas temperature in front of the turbine on specific parameters and efficiency of the turboprop engine and TRD.

Attention is paid to the fact that the specific power of the turboprop engine to a great degree depends on the maximum temperature of the gas  $T_3^*$  than does the specific thrust of the TRD. Whereas the specific power of the turboprop engine is directly proportional to the gas temperature in front of the turbine, the specific thrust of the TRD is proportional to the square root of this temperature. Thus, an increase in  $T_3^*$  from 1150°K to 1250°K (i.e., 9%) increases the specific power of the turboprop engine by 9% and specific thrust of TRD by only 4.5%. Therefore, an increase in  $T_3^*$  is a very effective means of increasing the specific power of the turboprop engine.

Optimum values of  $\pi$ , obtained from the condition of providing maximum specific powers and thrusts for the turboprop engine and TRD, coincide.

#### 21.2.2. Efficiencies of the Turboprop Engine

##### 21.2.2.1. Effective Efficiency.

The effective efficiency of the turboprop engine and TRD is identical. They are determined by the same regularities (20.24).

##### 21.2.2.2. Thrust Efficiency.

For the considered typical case  $\alpha = 1.0$  we have  $\eta_p \approx \eta_B$ .

The efficiency of the propeller does not depend on the thermodynamic cycle, which is accomplished in the basic circuit of the turboprop engine, but only on the number of revolutions, angle of setting of blades of the propeller  $\phi$ , speed and altitude of flight.

Figure 21.3 gives a change in  $\eta_B$  on flight speed ( $M_0$ ). In the range of flight speeds of 300-700 km/h it is possible to assume that  $\eta_B = \text{const}$ . On the average  $\eta_B = 0.8-0.85$ .

### 21.2.2.3. Total Efficiency.

From expression

$$\eta_0 = \eta_e \eta_p \approx \eta_e \eta_g$$

it follows that the total efficiency depends on  $T_3^*$ ,  $T_4$ ,  $\pi$ ,  $\xi_{\text{TRD}}$ ,  $\eta_e$ ,  $\eta_p$ ,  $\eta_g$  and  $V$ .

With an increase in  $T_3^*$  the total efficiency of the turboprop engine continuously increases, in contrast to the total efficiency of TRD, which with values used at present of the degree of increase in pressure  $\pi_{\text{TRD}} = 6-13$  is decreased with an increase in  $T_3^*$ . The latter is explained by the fact that with an increase in  $T_3^*$  the thrust efficiency of the TRD is continuously decreased (losses with exhaust velocity increase), whereas the efficiency of the propeller at the assigned flight speed maintains a fixed value.

The dependence of  $\eta_0$  on flight speed to a certain extent is determined by the characteristic of the propeller. In the case of a standard propeller already at great subsonic flight speeds, a decrease in its efficiency (induced by the appearance of wave losses) and decrease in total efficiency appear.

In the case when the efficiency of the propeller preserves a fixed value ( $\eta_p = \text{const}$ ), the most advantageous values  $\pi$ , at which the effective and total efficiency reach a maximum, coincide, i.e.,  $\pi' = \pi_{\text{ЭМ}}$ .

Figures 21.4 and 21.5 give curves  $\eta_e$ ,  $\eta_g$ , and  $\eta_0$  of the turbo-prop engine in the form of functions of  $\pi$  and  $T_3^*$ . The effect of the same parameters ( $\pi$  and  $T_3^*$ ) on the efficiency of the TRD is shown there.

### 21.2.3. Effective Fuel Consumption

Let us reduce expression (20.19) to the form

$$C_e = 3600 \frac{m}{N_{\text{eff}} A} \frac{\text{kg}}{\text{hp h}} \quad (21.11)$$

Substituting

$$N_{\text{eff}} = \frac{L_p}{75} = \frac{\pi \eta_{pe1}}{75} L_p$$

and

$$m = \frac{q_{\text{in}}}{H_u}$$

we obtain

$$C_e = \frac{q_{\text{in}}}{AL_p} \frac{75 \cdot 3600 A}{H_u \pi \eta_{pe1}} = \frac{632}{H_u \eta_e} \frac{1}{\pi \eta_{pe2}} \quad (21.12)$$

Thus, the effective fuel consumption is inversely proportional to the effective efficiency. With an increase in  $\pi$  to a certain value  $\pi'$ , magnitude  $C_e$  is lowered, reaching a minimum, and with further increase in the compression ratio increases (see Fig. 21.4). With an increase in  $T_3^*$  the effective fuel consumption is continuously decreased (see Fig. 21.5). Thus, for the lowering of  $C_e$  in the turboprop engine it is expedient to use high-temperature turbines with relatively high compression ratios of the compressor.

In contemporary turboprop engines on takeoff the effective fuel consumption changes over wide limits:

$$C_e = 210 \div 300 \text{ g/hp h.}$$

### 21.3. Use of Heat Recovery in the Turboprop Engine

Among various methods of increasing the economy of the turboprop engine, the recovery of heat occupies an important place. Heat regeneration in the turboprop engine was used for the first time in 1946 on the English engine Bristol "Theseus." However, deficiencies of this engine (heavy weight of the regenerator,<sup>1</sup> considerable losses

<sup>1</sup> $G_p = 227 \text{ kg.}$

of pressure in the heat exchanger) led to the fact that it was taken out of production and did not obtain development. Nevertheless, investigations on the use of heat recovery in aircraft engines were continued. In recent years considerable experience has been accumulated in the creation of effective aircraft heat exchangers. A heat regenerator was successfully installed on the turboprop engine Allison T56-A-7. Finally, a special turboprop engine Allison T78 with a regenerator was developed, built and successfully tested. In turn the introduction of the turboprop engine with a regenerator was put into operation.

The basic difficulties, the overcoming of which is necessary for the introduction of heat recovery into the turboprop engine, are:

1) considerable hydraulic losses on cold and hot sides of the heat exchanger, which lower the effective power of the engine;

2) high thermal resistance of the heat exchanger (imperfection of heat exchange in the applied designs of the regenerator), which prevents preheating of the air up to the temperature of hot exhaust gases and lowers the economy of the turboprop engine with the regenerator;

3) considerable relative weight and external diameter of the regenerator;

4) low operational reliability of the heat exchanger (low service life of the heat exchanger, frequent carbon formations and coking of tubes of the matrix of the regenerator).

#### 21.3.1. Design of a Turboprop Engine with a Heat Regenerator

Figure 21.6 gives a fundamental diagram of turboprop engine with a heat regenerator and Fig. 21.7 - cross section of the turboprop engine Allison T56-A-7.

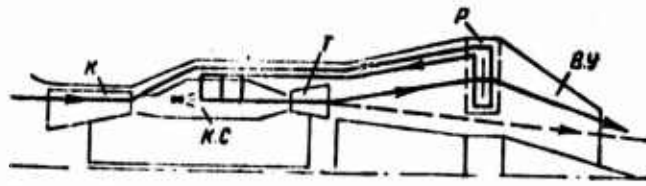


Fig. 21.6. Schematic diagram of a turboprop engine with a heat regenerator.

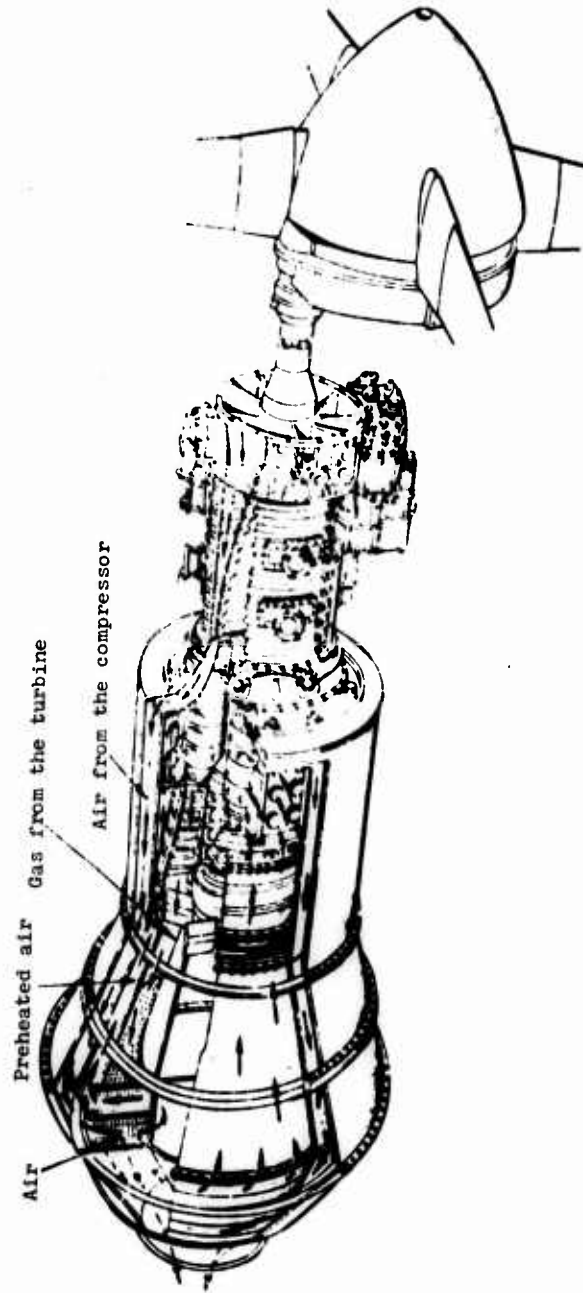


Fig. 21.7. Cross section of the turboprop engine Allison T56-A-7 with a generator.

As a result of the investigation of more than 5000 patents of designs of heat exchangers, the Allison firm has arrived at definite conclusions relative to the optimum design of the installation and type of regenerator used, design of the heat exchanger, and also the method of its control. These considerations lie as a basis of the design of the turboprop engine Allison T56-A-7 and then the turboprop engine Allison T78.

The heat exchanger with cross flow is installed in the turbine space of the engine concentrically relative to the shaft of rotation and provides a direct-flow axial exit for the hot gases from the turbine through the tubular lattice of regenerator into the exhaust nozzle (see Fig. 21.6).

The accepted system of control allows changing the power of the turboprop engine at fixed gas temperature  $T_3^*$  and variable number of revolutions of the engine. This makes it possible to increase the economy of operation of the engine at reduced regimes with the regenerator turned on (cruising flight regime). In those same cases when maximum power from engine is necessary (for example, on takeoff), a special six-segment valve turns off the heat exchanger and provides immediate outflow of the largest gas mass from the turbine to the outside.

To provide reliable operation of the turbine at high gas temperature, the blades of the first two stages of the turbine are made hollow with internal air cooling.

The heat exchanger (Fig. 21.8) consists of 15,000 tubes made from stainless steel. The optimum dimensions of the tubes are a diameter of 7.62 mm, thickness of wall, 0.105 mm, and length, 685 mm. The achieved degree of regeneration  $r = 0.69$  is very high, and an additional total drop in total pressure on the cold and hot sides of the heat exchanger is comparatively little and amounts to 8.96% (as compared to 10.32% of calculated).<sup>1</sup>

---

<sup>1</sup> $\Delta p_x^* = 2.88\%$  and  $\Delta p_r^* = 6.00\%$ .



Fig. 21.8. Regenerator of the turboprop engine Allison T56-A-7.

One should emphasize that the use of the regenerator gives the greatest effect at reduced cruising regimes at small values of  $\pi_H^*$  and maximum possible gas temperature  $T_3^*$ . In the turboprop engine Allison T56-A-7 in these regimes the relative economy in the effective fuel consumption is almost 36% (Fig. 21.9)

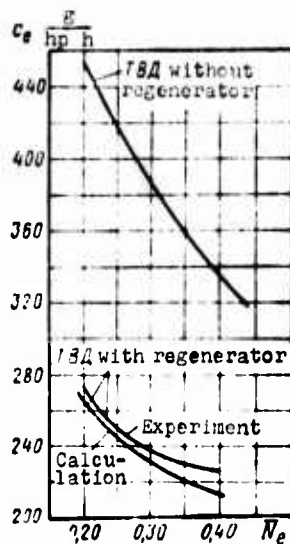


Fig. 21.9. Effect of heat recovery on the effective fuel consumption of the turboprop engine in reduced regimes.

### 21.3.2. Real Cycle of the Turboprop Engine with Heat Recovery

Figure 21.10 gives the real cycle of the turboprop engine with heat recovery. It is distinguished from the ideal cycle in that processes of heat exchange 2-2p and 4-4p are accompanied by a considerable drop in total pressure (due to inevitable hydraulic and thermal losses). Especially considerable is the drop in pressure

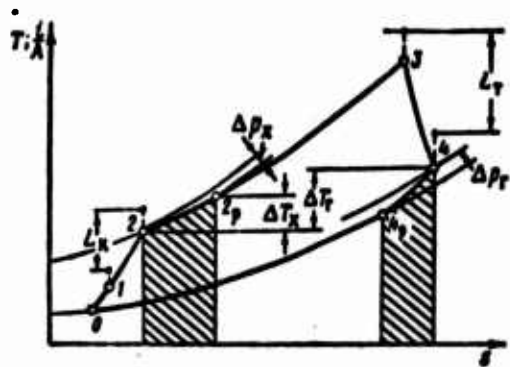


Fig. 21.10. Real cycle of the turboprop engine with heat recovery.

on the hot side of the heat exchanger, where changes in pressures  $\Delta p_1'$  and  $\Delta p_2'$  coincide in sign. In better types of regenerators  $\Delta p_2' = 5-7.5\%$ .

Another distinction of the real cycle from the ideal is the impossibility of preheating of the air in the heat exchanger up to the temperature of the entering gas, i.e.,  $T_{2p} < T_4'$ .

Thus, the degree of regeneration of the heat exchanger, which characterizes the perfection of the heat exchange and is equal to

$$r = \frac{T_{2p} - T_2'}{T_4' - T_2'} = \frac{\Delta T_2}{\Delta T_1}, \quad (21.13)$$

is always considerably less than unity.

In stationary regenerators  $r = 0.7-0.75$ ; in revolving regenerators  $r = 0.9-0.92$ .

Figure 21.11 gives curves showing the effect of the degree of throttling with respect to power  $\bar{N}$  and temperature  $T_3^*$  on the effective efficiency of real cycles of the turboprop engine in the presence of heat recovery and with its absence. Attention is given to the very sloping characteristics of the real cycle in regimes of partial loads (i.e., in cases of throttling of the engine with respect to power when  $T_3^* = \text{const}$ ).

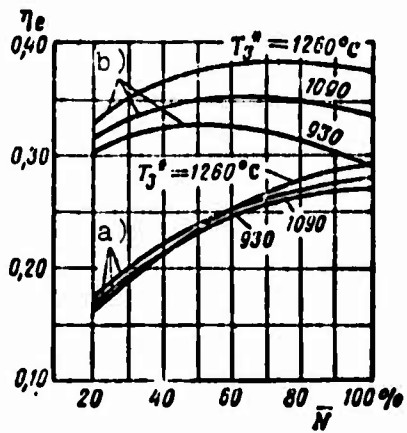


Fig. 21.11. Effect of the degree of throttling with respect to power  $\bar{N}$  and  $T_3^*$  on  $\eta_e$  the turboprop engine in the presence of heat recovery and with its absence: a) without heat recovery; b) with heat recovery.

### 21.3.3. Effect of Heat Recovery on Specific Parameters of the Turboprop Engine

#### 21.3.3.1. Relative Fuel Consumption.

We have

$$m_{\text{r(p)}} = \frac{c_{\text{r(m)}}(T_3^* - T_{2\text{p}}^*)}{\epsilon_{\text{r(c)}} H_u} \quad (21.14)$$

Let us express  $T_{2\text{p}}^*$  in terms of the degree of recovery

$$r = \frac{\Delta T_{\text{r}}}{\Delta T_{\text{p}}} = \frac{T_{2\text{p}}^* - T_2^*}{T_4^* - T_2^*} \quad (21.15)$$

whence we obtain

$$T_{2\text{p}}^* = T_2^* + r(T_4^* - T_2^*) \quad (21.16)$$

where

$$T_4^* = T_3^* - \frac{L_{\text{v}}}{118}$$

Having substituted the expression for  $T_{2\text{p}}^*$  from (21.16) into (21.14), we obtain after simple conversions

$$m_{\tau(p)} = \frac{c_{pm}}{8H_0} \left[ (T_3^* - T_2^*)(1-r) + r \frac{L_r}{118} \right]. \quad (21.17)$$

### 21.3.3.2. Specific Effective Power of the Turboprop Engine.

We have

$$N_{eyd(p)} = \frac{L_{\tau(p)} - L_n}{75} \text{ hp.} \quad (21.18)$$

Let us determine the work of the turbine in the presence of heat recovery taking into account additional losses of total gas pressure on cold and hot sides of the heat exchanger  $\sigma_p^*$ , i.e.,

$$L_{\tau(p)} = 118T_3^* \left[ 1 - \frac{1}{(\sigma_p^*)^{0.25}} \right] \eta_r^*. \quad (21.19)$$

### 21.3.3.3. Effective Fuel Consumption.

We have

$$C_{e(p)} = 3600 \frac{m_{\tau(p)}}{N_{eyd(p)}}. \quad (21.20)$$

Having substituted into expression (21.20) the value  $m_{\tau(p)}$  from (21.17) and  $N_{eyd(p)}$  from (21.18), we obtain

$$C_{e(p)} = \frac{27000c_{pm} \left[ (T_3 - T_2)(1-r) + rT_3^* \left( 1 - \frac{1}{\sigma_p^{*0.25}} \right) \eta_r^* \right]}{8H_0 \left\{ 118T_3^* \left[ 1 - \frac{1}{(\sigma_p^*)^{0.25}} \right] \eta_r^* - L_n \right\}}. \quad (21.21)$$

## C H A P T E R 22

### OPERATIONAL CHARACTERISTICS OF THE TURBOPROP ENGINE

#### 22.1. Throttle Characteristics of the Turboprop Engine

Throttle characteristics of the turboprop engine are called dependences of the propeller (effective) power, effective fuel consumption, and also jet thrust from the change in feed of fuel with throttling of the engine and at the assigned program of its control. Since the change in fuel feed is usually connected with the change in the number of revolutions of the engine, then throttle characteristics are depicted in the form of curves of the dependence of basic parameters of the turboprop engine -  $N_B$ ,  $C_e$  and  $R$  - on the number of revolutions of the shaft of the engine. In the case of a double-shaft turboprop engine the throttle characteristics are depicted as functions of the revolution number of the turbocompressor of the shaft (or cascade of high pressure). In those cases when throttle characteristics and, consequently, and basic regimes of operation of the engine, are obtained with a fixed number of its revolutions, they are depicted in the form of dependences of basic parameters on the fuel consumption per hour:

$$N_B = f_1(\bar{G}_T); C_e = f_2(\bar{G}_T); R = f_3(\bar{G}_T).$$

Plotted on throttle characteristics of the turboprop engine are also the curve of temperature change in gas in front of the turbine or behind it. This curve makes it possible to judge the thermal condition of the hot part of the engine with its operation.

Throttle characteristics of the turboprop engine are obtained usually by experimental means on a test stand. They can be obtained with a high degree of accuracy also by analytical means.

### 22.1.1. Throttle Characteristics Single-Shaft Turboprop Engines

Let us examine the throttle characteristic of a single-shaft turboprop engine Armstrong-Siddeley "Mamba" (Fig. 22.1). Let us assume that in the nominal (or takeoff) regime in the turbine of the turboprop engine complete expansion of the gas takes place, i.e.,

$$p = p_s = p_H.$$

Such a case of the operation of the turbine of a turboprop engine is typical.

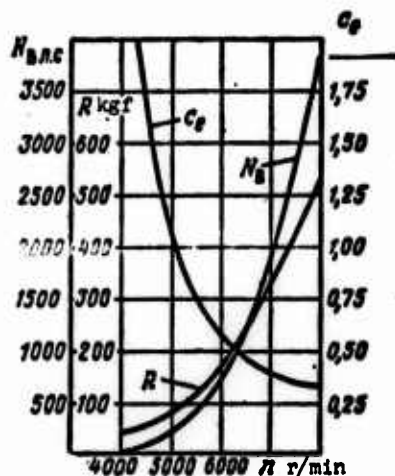


Fig. 22.1. Throttle characteristic of the turboprop engine Armstrong-Siddeley "Mamba."

With a decrease in the fuel feed into the combustion chamber, the temperature of the gas in front of the turbine is lowered. Consequently, the power of the turbine drops, in consequence of which the balance of power is disrupted:

$$N_T < (N_H + N_D);$$

as a result of this the number of revolutions of the engine decreases.

With a decrease in the number of revolutions of the engine at a fixed angle of setting of blades of the propeller, the propeller and equivalent power of the turboprop engine drop, the jet thrust of turboprop engine also decreases, and the effective fuel consumption continuously increases. The gas temperature in front of the turbine (and behind it), having a high initial value in the takeoff regime, with a reduction in the revolution number initially drops, reaching a certain minimum value at average revolutions, but then it continuously increases.

For an explanation of the regularity of passage of basic parameters of the turboprop engine with respect to the number of revolutions, let us examine preliminarily how the temperature and pressure of the gas change in characteristic sections of the engine with its throttling.

22.1.1.1. Change in Temperature and Pressure of the Gas in Characteristic Sections of the Gas-Air Channel of the Turboprop Engine.

Figure 22.2 shows the change in compression ratio of the compressor and of expansion ratio of the turbine of the single-shaft turboprop engine with respect to the number of revolutions. Since the velocity of outflow of gas from the exhaust nozzle of the turboprop engine is low (it is somewhat less than the absolute velocity at the exit from the turbine), then the magnitude  $\pi_T^*$  is little distinguished from  $\pi_H^*$ , and with throttling of the turboprop engine it continuously drops.

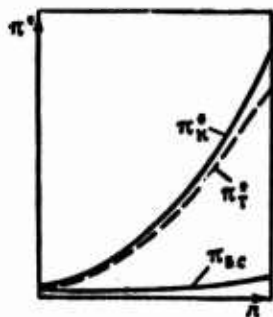


Fig. 22.2. Change in  $\pi_H^*$ ,  $\pi_T^*$  and  $\pi_{B.C.}$  of a single-shaft turboprop engine with respect to the number of revolutions.

The lowering of the drop in pressures in the turbine with throttling of the engine covers initially the last stages of the turbine adjacent to the exhaust and then gradually extends upstream on the stage of high pressure.

The continuous lowering of magnitude  $\pi_T^\#$  with throttling of the engine leads to the fact that the temperature of the gas in front of the turbine of the turboprop engine in the whole range of working numbers of revolutions proves to be significantly higher than that of TRD at equal values of  $\pi_{\kappa(p)}^\#$  and  $T_3^*(p)$  in the initial nominal (or takeoff) regime (Fig. 22.3).

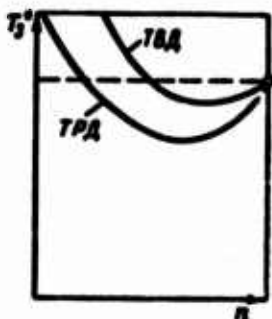


Fig. 22.3. Change in  $T_3^*$  with respect to the number of revolutions for a single-shaft turbo-prop engine and TRD.

Actually, solving the equation of balance of works of the turbo-compressor

$$L_T = 118 T_3^* \left( 1 - \frac{1}{\pi_T^{0.25}} \right) \eta_T = L_K + L_P$$

relative to  $T_3^*$  we obtain

$$T_3^* = \frac{C n^2}{118 \left( 1 - \frac{1}{\pi_T^{0.25}} \right) \eta_T}$$

where  $C = \text{const}$ . Hence it follows that a continuous lowering of  $\pi_T^\#$  with throttling of the engine shifts the dependence  $T_3^* = f(n)$  for the turboprop engine, as compared to the case  $\pi_T^\# = \text{const}$  of the TRD, into the region of raised values of gas temperature. Here we assumed that the specific work of the propeller, just as the work of

the compressor, changes approximately in proportion to the square of the number of revolutions.

22.1.1.2. Change in Propeller Power with Respect to the Number of Revolutions.

Numerous tests of turboprop engines show that the law of the change in propeller power of the turboprop engine with respect to the number of revolutions depends on the angle of setting of blades of the propeller  $\phi^\circ$ .

When  $\phi = \text{const}$  the dependence of the propeller power on the number of revolutions is depicted quite accurately by a cubic parabola

$$N_p = An^3, \quad (22.1)$$

where

$$A = f(\phi).$$

With an increase in the angle of setting of the blades, i.e., with "loading" of the propeller and with a fixed revolution number, the propeller power increases; with a decrease in the angle  $\phi$ , i.e., with a "lightening" of the propeller, the propeller power is lowered. Thus, different values of angle  $\phi$  (5, 10, 15, 20, 25°) correspond to different cubic parabolas  $N_p$ , passing through the origin of the coordinates (Fig. 22.4).

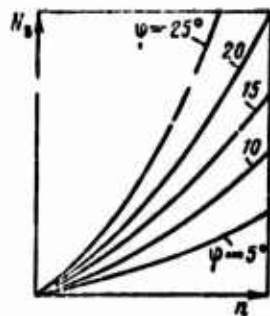


Fig. 22.4. Effect of the angle of setting of the blade of the propeller  $\phi$  on curves  $N_p = f(n)$ .

Let us now explain how with the change in angle  $\phi$  the available power of the turbine of the turboprop engine changes. Let us assume that at a constant number of revolutions of the engine the pilot "loads" the propeller (increasing angle  $\phi$ ). Then the balance of power is disrupted, i.e.,

$$N_T < (N_H + N_P),$$

and the number of revolutions of the turboprop engine must be decreased. However, the regulator of revolutions, striving to preserve  $n = \text{const}$ , will restore the disturbed equilibrium by means of increasing the fuel feed into the combustion chamber (centrifugal small weights of the regulator with a lowering of the angular velocity of rotation will move the throttling needle into the position corresponding to the increase in  $G_T$ ). As a result the gas temperature in front of the turbine increases, and the power of the turbine will increase in accordance with an increase in the power of the propeller.

Thus, the family of curves  $N_B$  (for different values of  $\phi$ ) will correspond to the family of curves  $T_3^*$  and family of curves  $C_e$  (Fig. 22.5). The more  $\phi$ , the higher the temperature of the gas in front of the turbine  $T_3^*$  and the lower the effective fuel consumption  $C_e$ . Actually, when  $n = \text{const}$  the "loading" of the propeller leads to an increase in  $T_3^*$  and  $\pi_H^*$ , which increases the effective efficiency of the engine (see Figs. 21.4 and 21.5) and lowers the effective fuel consumption. The latter follows directly from formula (21.12):

$$C_e = \frac{632}{H_H \eta_e}.$$

Thus, each value  $\phi = \text{const}$  corresponds to definite passage of the line of working processes on the characteristic of the compressor (see further Fig. 22.8). With an increase in  $\phi$  the line of working regimes is displaced nearer to the surging limit.

Since the flow of air changes quite accurately with respect to the linear dependence on the revolution number, i.e.,

$$G_b \sim n,$$

then, in accordance with expression (20.3), it can be concluded that when  $\phi = \text{const}$

$$L_b \sim L_c \sim n^2, \quad (22.2)$$

i.e., the work of the propeller proves to be proportional to the square of the number of revolutions.

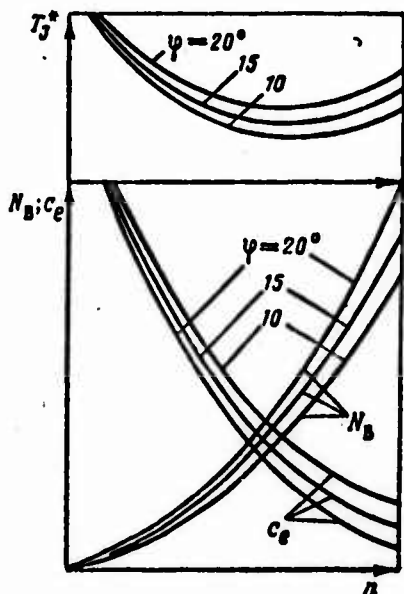


Fig. 22.5. Throttle characteristics of the turboprop engine at various angles of setting of blades of the propeller.

Reasons which lead to an increase in  $L_b \approx L_e$  with an increase in revolution number in the turboprop engine are the same as those for the TRD - the basic reason is the increase in the compression unit of the compressor with a relatively little changing value of  $T_3^*$ .

#### 22.1.1.3. Change in $C_e$ According to the Number of Revolutions.

The continuous lowering of effective fuel consumption with an increase in the revolution number of the single-shaft turboprop engine is explained mainly by the increase in  $\pi_H^*$ . This is furthered in the region of high numbers of revolutions by a considerable increase in the gas temperature  $T_3^*$ . Ultimately  $\eta_e$  increases. Thus,

the regime of maximum propeller power of the turboprop engine coincides with the regime of its greatest economy; any throttling of the turboprop engine is connected with the worsening of the economy of the engine. In this respect properties of the throttle characteristic of the turboprop engine are distinguished from properties of the characteristic of the TRD, with the throttling of which the specific fuel consumption is initially lowered.

22.1.1.4. Effect of the Change in Angle of Setting of Blades of the Propeller on Throttle Characteristics of a Single-Shaft Turboprop Engine.

Let us examine now how the propeller-pitch control affects the throttle characteristics of the single-shaft turboprop engine (Fig. 22.6).

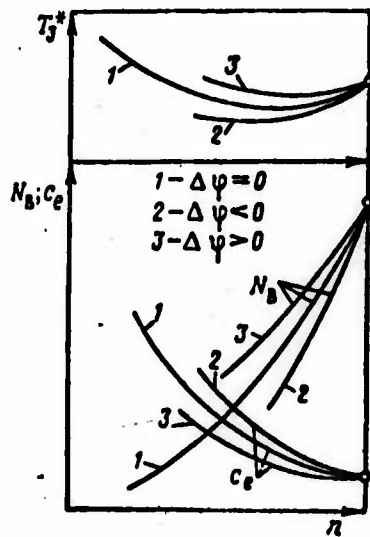


Fig. 22.6. Effect of the change in angle  $\phi$  on throttle characteristics of a single-shaft turboprop engine.

Let us assume that curves 1 correspond to a certain constant angle of setting of the propeller  $\phi = \text{const}$ . With a "lightening" of the propeller with throttling of the engine, power  $N_B$  drops, and the effective fuel consumption increases more sharply (curves 2) than when  $\phi = \text{const}$ . Conversely, with the "loading" of the propeller (curves 3), corresponding throttle characteristics occur

more sloping. Figure 22.6 shows also the effect of control of the propeller on the regularity of the change in  $T_3^*$  on the number of revolutions.

In analyzing the passage of curves in Fig. 22.6, at first sight, it appears expedient with throttling of the turboprop engine always to "load" the propeller. However, this is not exactly correct. For example, with starting of the engine a very important property of any engine is its ability to enter into the regime of maximum power rapidly. For an improvement of accelerating capacity of the turboprop engine in every way, it is necessary that the exceeding of power of the turbine (with  $T_3^*(\max)$ ) over the total power of the compressor and propeller (surplus power of the turbine) would be as much as possible. For this purpose with starting it is necessary for the propeller to "lighten" to a maximum, having set it at an angle close to the angle corresponding to zero power. Then

$$\Delta N_T = (N_{T(\max)} - N_H) = \Delta N_{T(\max)}$$

Figure 22.7b gives the real law of the change in angle  $\phi$  in the number of revolutions of the turboprop engine Armstrong-Siddeley "Mamba"; we see that the acceleration of the engine over the range of revolutions

$$\Delta n = (0,2 \div 0,8) n_{\max}$$

occurs with a minimum angle  $\phi \approx 12^\circ$ . Only in the range

$$\Delta n = (0,8 \div 1,0) n_{\max}$$

there is "loading" of the propeller with an increase in  $\phi$  from  $12^\circ$  to  $23^\circ$ .

In a number of contemporary single-shaft turboprop engines the starting of the engine and reaching of the maximum number of revolutions is accomplished when  $\phi \approx 0^\circ$  (Fig. 22.7a). This denotes that

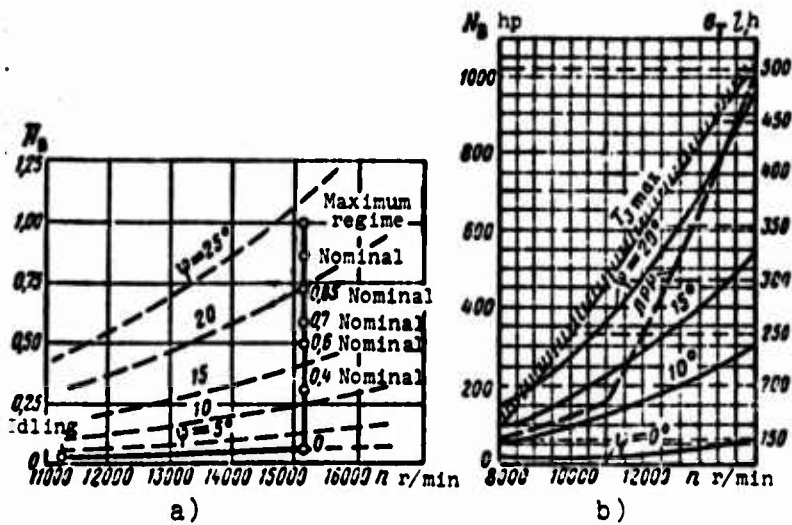


Fig. 22.7. Actual law of the change in  $\phi$  and  $N_B$  with respect to the number of revolutions of the turboprop engine.

control of operating conditions of the turboprop engine in operation occurs when  $n = \text{const}$ . Such a system of control provides good accelerating capacity of the engine.

Figure 22.8 gives a family of lines of working regimes of the compressor of the single-shaft turboprop engine at various  $\phi = \text{const}$ ; with "loading" of the propeller, the line  $\phi = \text{const}$  is displaced into the region of increased values  $T_3^*$  and  $\pi_K^*$ ; in this case the reserve of the compressor with respect to surging is decreased.

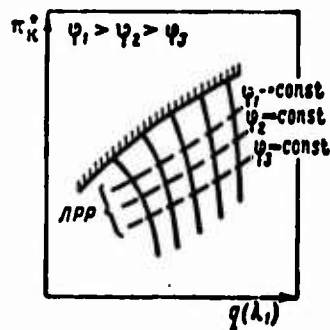


Fig. 22.8. Effect of the change in angle  $\phi$  on the line of operating regimes of the compressor of the single-shaft turboprop engine.

22.1.1.5. Throttle Characteristic of the Turboprop Engine when  $n = n_{\max} = \text{const}$ .

Figure 22.9 gives a standard throttle characteristic of a single-shaft turboprop engine (see diagram 1 in Fig. 20.2) when  $n = n_{\max} = \text{const}$  in the region of operating regimes. The throttle characteristic of the standard single-shaft turboprop engine with respect to fuel consumption per hour, plotted in relative parameters, is given in Fig. 22.10.

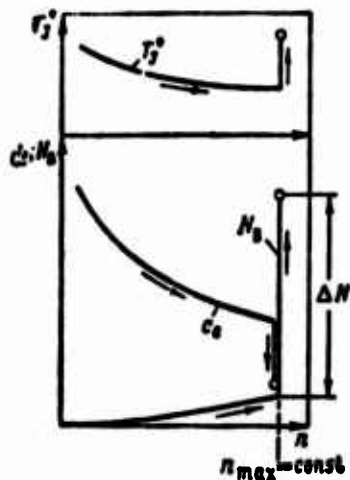


Fig. 22.9.

Fig. 22.9. Throttle characteristic of the turboprop engine when  $n = \text{const}$  (in the region of operating regimes).

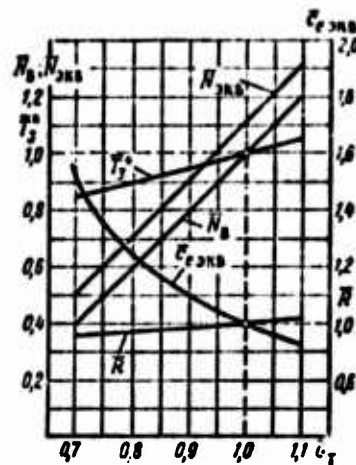


Fig. 22.10.

Fig. 22.10. Throttle characteristic of the single-shaft turboprop engine plotted in relative parameters.

22.1.2. Throttle Characteristics of Double-Shaft Turboprop Engines

Let us examine throttle characteristics of a double-shaft turboprop engine. As previously, we assume that in all regimes of operation of the engine there is observed the condition of total gas expansion in the turbine

$$p_4 = p_3 = p_{11}$$

Figure 22.11 gives the throttle characteristic of double-shaft turboprop engine Rolls-Royce "Tyne" RTu.12 with a two-stage compressor. As we see, with a decrease in revolution numbers of the turbocompressor of high pressure, as previously, propeller power and jet thrust are lowered, and the effective fuel consumption increases. Thus, *qualitative changes* in basic parameters of the turboprop engine ( $N_e$ ,  $R$  and  $\sigma_e$ ) with throttling of single-shaft and double-shaft engines coincide.

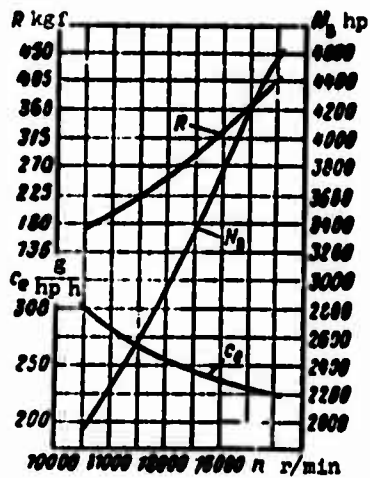


Fig. 22.11. Throttle characteristic of the turboprop engine Rolls-Royce "Tyne" RTu.12.

In order to explain the *quantitative* distinctions in these characteristics, let us examine the regularity of the change in drops in pressures and temperatures of the gas in basic elements of the double-shaft turboprop engine with respect to the number of revolutions.

22.1.2.1. Change in Temperature and Pressures of the Gas in Characteristic Sections of the Double-Shaft Turboprop Engine (Diagram 2 in Fig. 20.2).

Figure 22.12 gives curves of the change in compression unit of the compressor and expansion units of gas in VD and ND turbines of a double-shaft turboprop engine with respect to the number of revolutions. We see that with throttling the VD turbine in a certain

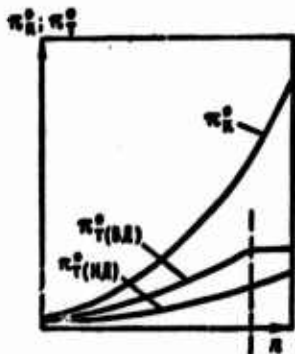


Fig. 22.12. Change in  $\pi_K^*$  and  $\pi_T^*$  of a double-shaft turboprop engine with respect to the number of revolutions.

range of numbers of revolutions appears "blocked" in the drop in pressures until in the first nozzle box assembly of the ND turbine the critical (or constant) regime of outflow is preserved. The law of the change in gas temperature  $T_3^*$  with respect to the number of revolutions is determined by the equation of balance of works of the VD turbocompressor

$$L_{T(BA)} = L_{K(BA)} .$$

whence we find

$$T_3^* = \frac{L_{K(BA)}}{118 \left[ 1 - \frac{1}{\pi_{T(NA)}^{0.25}} \right] \eta_{T(BA)}} .$$

Now it is easy to arrive at the conclusion that at different values  $\pi_{K(BA)}^*$  and  $T_3^*$  in design conditions the regularity of the temperature change in the gas in front of the turbine  $T_3^*$  in a double-shaft TRD, turboprop engine and DTRD is practically the same.

22.1.2.2. Effect of the Change in Angle of Setting of Blades of the Propeller on Throttle Characteristics of a Double-Shaft Turboprop Engine.

In the case of the turboprop engine with total gas expansion in the ND turbine it is possible with a high degree of accuracy to consider that

$$L_s = L_{T(ND)} \approx L_e .$$

Let us examine peculiarities of the process of throttling of the double-shaft TRD. Let us assume that  $\phi = \text{const}$ . With a decrease in the fuel feed into the combustion chamber as a result of the lowering of the gas temperature  $T_3^*$  and appearing unbalance of works of the VD turbocompressor, the number of revolutions of the latter is decreased. However, the power of the ND turbine is decreased more rapidly than the power of the VD turbine, since, except for the decrease in  $T_3^*$  [sic] and  $G_B$ , the drop of pressures ( $\pi_{T(ND)}$ ) still drops. Therefore, the appearing unbalance of works of the ND turbocompressor is removed by means of a more intensive lowering of the angular velocity of rotation of the ND cascade.

How does the propeller-pitch control affect the throttle characteristic of the double-shaft turboprop engine? First of all, let us note that the control of propeller pitch practically does not affect the power and work of the ND turbine, the parameters of the working process of which are determined completely by the VD turbocompressor. Therefore, control of the pitch of the propeller leads only to a change in the number of revolutions of the ND turbocompressor so that, as previously, there is observed the condition

$$N_n = N_{T(ND)}, \text{ or } L_n = L_{T(ND)}.$$

With a change in angle  $\phi$  the number of revolutions of the ND compressor, efficiency of the propeller  $\eta_B$ , efficiency of the ND turbine  $\eta_{T(ND)}^*$  and, in accordance with their change, propeller power  $N_B$  and thrust  $P_B$  change.

Actually,

$$N_n = \frac{G_n L_{T(ND)}^*}{75} \eta_{T(ND)}^* \sim \eta_{T(ND)}^* \quad (22.3)$$

$$P_n = \frac{75 N_n \eta_B}{V} \sim \eta_{T(ND)}^* \eta_B \quad (22.4)$$

Thus, the control of angle  $\phi$  makes it possible, having determined the optimum number of revolutions of the ND cascade, to

provide maximum values  $\eta_{\tau}^{\#}(\text{HD})$  and  $\eta_{\text{B}}$ , and, consequently, maximum values of  $N_{\text{B}}$  and  $P_{\text{B}}$  (Fig. 22.13).

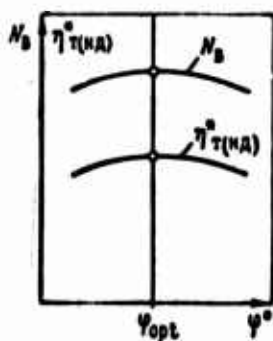


Fig. 22.13. Effect of the change in angle of setting of blades of the propeller  $\phi$  on the propeller power of the double-shaft turboprop engine.

Let us note also that the control of the propeller pitch in the system of the double-shaft turboprop engine does not affect the position of the line of working regimes of the characteristic of the compressor.

Thus, distinctions of throttle characteristics of the double-shaft turboprop engine from corresponding characteristics of the single-shaft turboprop engine include:

1) various regularities of the change in  $T_3^*$  on the number of revolutions, which has a known effect on the course of curves  $N_e$ ,  $R$  and  $C_e$ ;

2) the possibility of providing with the help of the system of two separate turbines of optimum values the efficiency of the propeller and ND turbine (maximum of the product of these efficiencies).

If by a change in  $\phi$  in the system of the single-shaft turboprop engine it is possible to obtain complete identity of the change in  $T_3^*$  with respect to the number of revolutions of the single-shaft and double-shaft turboprop engine, then the advantage of the double-shaft turboprop engine nevertheless remains the possibility of achieving the highest values of  $\eta_{\text{B}}$  and  $\eta_{\tau}^{\#}$ .

### 22.1.3. Reduction of Parameters of the Turboprop Engine to Standard Atmospheric Conditions

The reduction of parameters of the turboprop engine to standard atmospheric conditions is carried out with a fixed propeller pitch ( $\phi = \text{const}$ ).

Formulas of the reduction of thrust, number of revolutions, flow of air and fuel consumption for the TRD and turboprop engine are identical.

#### 22.1.3.1. Formula of the Reduction of Effective (Propeller) Power.

We have

$$N_n \sim L_n G_n$$

where

$$L_n \sim T_n^2, \quad G_n \sim \frac{P_n}{\sqrt{T_n}}$$

Then

$$N_n \sim \rho_n \sqrt{T_n}$$

Hence it is easy to obtain the formula of reduction for the turboprop engine:

$$N_{n(np)} = N_{n(stm)} \frac{760 \sqrt{288}}{\rho_0 \sqrt{T_0}} \quad (22.5)$$

The effective fuel consumption

$$C_e = \frac{632}{H_n \eta_e} \frac{\text{kg}}{\text{hp h}}$$

is not needed in the reduction to standard atmospheric conditions, since in similar regimes it maintains a fixed value ( $\eta_e = \text{const}$ ).

## 22.2. High-Speed Characteristics of the Turboprop Engine

High-speed characteristics of the turboprop engine are called dependences of the propeller or total (equivalent) power and also of effective fuel consumption on flight speed at the assigned program of control.

The high-speed characteristic of the turboprop engine can be obtained by experimental means, for example, in flight tests with the help of the "flying laboratory," and also, approximately, by the analytical method.

### 22.2.1. Programs of Control of the Turboprop Engine in Flight

Programs of control of the turboprop engine refer to programs of control for maximum propeller and maximum total (equivalent) power, for the best economy and others. Each of these programs provides such a change in parameters of the working process at which automatically at all velocities and flight altitudes the assigned regularity of the change in  $N_B$ ,  $N_{ЭKB}$  or  $C_e$  will be realized.

#### 22.2.1.2. Controllable Parameters and Regulating Factors in the Turboprop Engine.

Turboprop engine, which can be examined as a particular case of a double-shaft jet engine, has in general a larger number of regime parameters than the usual TRD, and, respectively, a larger number of control factors and elements. For an example, in the single-shaft turboprop engine an additional, in comparison with the TRD,<sup>1</sup> control factor is the angle of setting of blades of the propeller  $\phi^\circ$ , and, respectively, the additional control element - propeller regulator.

---

<sup>1</sup>We have in mind a single-shaft TRD with fixed geometry.

The change in angle  $\phi$  in the turboprop engine completes the same role as that of control of the critical (exit) section of the reactive nozzle of the TRD, and allows accomplishing independently of each other the change in the number of revolutions of the engine  $n$  and gas temperature in front of the turbine  $T_3^*$ .

Figure 22.14 gives a block diagram of control of a single-shaft turboprop engine with two independent regulators: number of revolutions and fuel feed. The engine has a unit of united control of regulators<sup>1</sup> with a united control lever of the engine. The connection between the control factors and adjustable parameters is carried out according to the scheme:

$$G_T \rightarrow T_3^*; \varphi \rightarrow n.$$

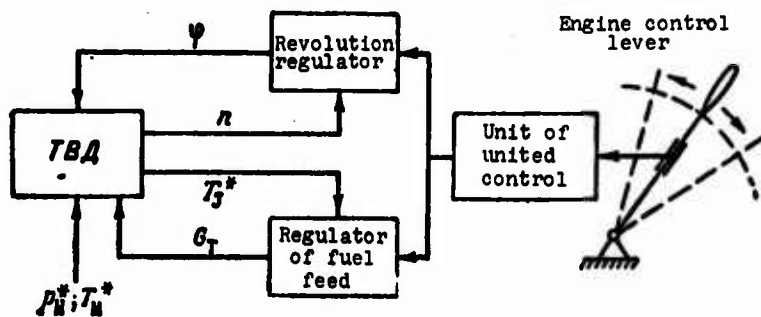


Fig. 22.14. Block diagram of control of a single-shaft turboprop engine.

In the case of a double-shaft turboprop engine the additional control factor proves to be, as previously, the angle  $\phi$ , and the controllable parameter – the number of revolutions of the propeller shaft  $n_B$  or ND cascade –  $n_{HD}$ . In this case the control of the number of revolutions of the VD turbocompressor ( $n_{BD}$ ) and temperature  $T_3^*$  is produced, as in the simple TRD, by the change in fuel feed with the help of automatic unit of fuel feed interlinked with the regulator  $n_{BD}$ ; the control of the number of ND revolutions is carried out by a second, independent of the first, regulator of revolutions.

<sup>1</sup>Command-fuel unit (KTA).

The connection between the control factors and controllable parameters of the double-shaft turboprop engine is carried out according to the scheme:

$$G_T \rightarrow \begin{matrix} n_{TK} \\ T_3^* \end{matrix}; \quad \varphi \rightarrow n_n.$$

Figure 22.15 gives a block diagram of the control of a double-shaft turboprop engine.

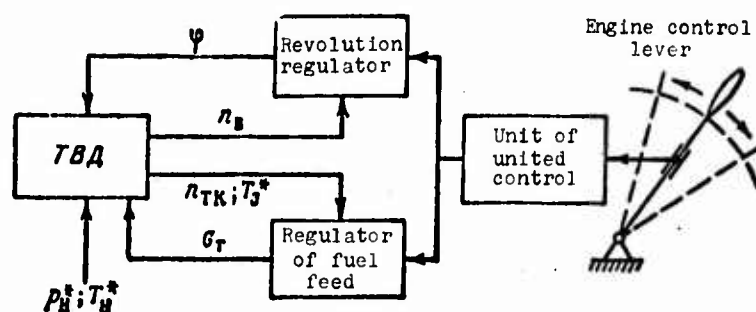


Fig. 22.15. Block diagram of control of a double-shaft turboprop engine.

Control of the engine can be accomplished by one lever, the movement of which makes it possible to maintain automatically at all speeds and altitudes of flight the maximum derivative

$$\eta_n \eta_{T_3}^* = (\eta_n \eta_{T_3}^*)_{max}$$

The introduction of the regulator of the jet nozzle ( $f_5 = \text{var}$ ) in the turboprop engine makes it possible to provide the most advantageous distribution of energy between the propeller and reaction and, consequently, obtain the maximum equivalent (total) power. In accordance with the principle of redistribution of thrust of the turboprop engine, it follows with an increase in the flight speed to cover simultaneously the jet nozzle (for an increase in jet thrust) and "lighten" the propeller (for a decrease in thrust of the propeller), observing conditions

$$n = \text{const and } T_3^* = \text{const.}$$

In this case the "lightening" of the propeller and, consequently, lowering of  $L_B$  will be compensated by a decrease in pressure differential in general turbine so that there will be continuously fulfilled the equality

$$L_T = L_K + L_B.$$

The expediency of the introduction of the regulator of the exhaust nozzle is determined by the effect of the change in velocity of outflow  $c_5$  on the thrust (or equivalent power) of the turboprop engine.

Figure 22.16 shows the dependence of optimum velocity of expiration from the nozzle on the efficiency of the propeller and flight speed. When  $\eta_B = 0.8$  with an increase in flight speed from 0 to 240 m/s, the optimum velocities of expiration must increase from 70 to 300 m/s.

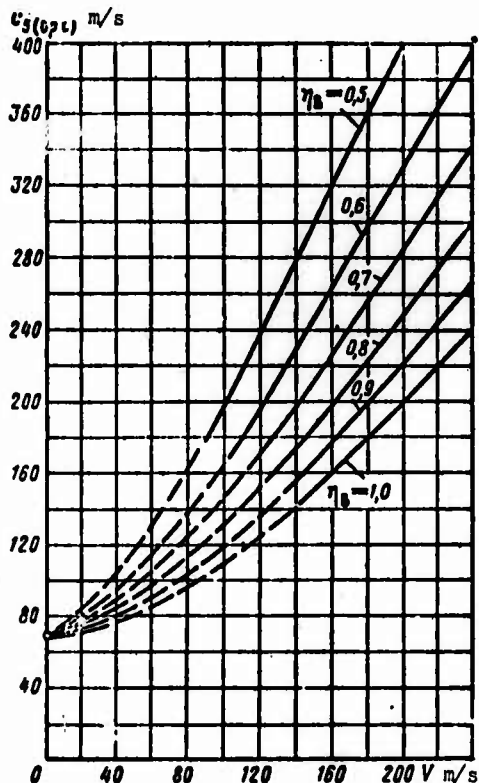


Fig. 22.16. Dependence of optimum velocity of outflow from the nozzle on the efficiency of the propeller and flight speed.

We already noted that on the test stand the deviation of  $c_5 \approx c_{4a}$  from the optimum value leads to a considerable drop in thrust (see Fig. 21.2a). With an increase in the flight speed this effect increasingly weakens more (Fig. 22.17). At high transonic flight speeds the deviation of  $c_5$  from the optimum value has practically little effect on the thrust of the turboprop engine (see Fig. 21.2b). Thus, the control of the exhaust nozzle of the turboprop engine would make sense mainly on the test stand and also at small and moderate flight speeds.

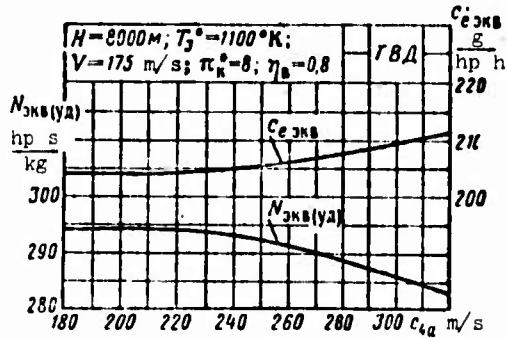


Fig. 22.17. Effect of the velocity of outflow of gas from the turbine on  $N_{ЭНВ}$  and  $C_{ЭНВ}$  in flight.

However, one should take into account that the introduction of a variable-area nozzle will require design complication and an increase in dimensions and weight of the engine, which without the proper compensation in thrust and economy is not justified. Therefore, in practice a turbine with complete expansion of the gas and uncontrollable exhaust system is used. In such a turboprop engine certain losses in thrust take place on the test stand, i.e., under conditions when the relative thrust of the turboprop engine (in comparison with thrust of the TRD) reaches a maximum value.

#### 22.2.2. High-Speed Characteristic of a Single-Shaft Turboprop Engine

Let us examine the high-speed characteristic of the single-shaft turboprop engine calculated for the following conditions:

- 1)  $H = \text{const}$ ;

2) program of control for maximum thrust.

Program of adjustment of the turboprop engine for maximum total thrust or maximum total (equivalent) power consists of the following points:

1)  $n = n_{\max} = \text{const};$

2)  $T_3^* = T_3^*(\max) = \text{const};$

3)  $x = x_{\text{opt}} = f(V)$  or  $C_{5(\text{opt})} = V/\eta_B.$

Fulfillment of points (1) and (2) is provided by means of the use of regulators of the propeller and of fuel feed. The observance of point (3) requires the introduction of a regulator of the jet nozzle. Therefore let us replace point (3) of the program of control by condition (3')

3')  $f_5 = \text{const}$  and  $p_4 = p_5 = p_H.$

At flight speeds of not more than 600-700 km/h the realization of point (3') instead of (3) gives a small difference in results and in practice provides a maximum of thrust of the turboprop engine.

#### 22.2.2.1. Basic Assumptions.

We will assume that:

1) when  $n = \text{const}$  condition  $L_H = \text{const}$  is observed;

2) coefficients of partial losses and the efficiency of the turbine and compressor maintain a constant value, i.e.,

$$\eta_t^* = \text{const}; \eta_k^* = \text{const}; \sigma_{nk}^* = \text{const}; \sigma_{kc}^* = \text{const}; \eta_{n,c} = \text{const}; \xi_{k,c} = \text{const}.$$

Let us examine now peculiarities of the high-speed characteristic of the turboprop engine. With an increase in flight speed

the total compression ratio and, respectively, expansion ratio in turbine increases; the velocities of outflow at the exit from the turbine and from the exhaust pipe of the turboprop engine also increases.

Actually, having written the equation of flow for the critical section of the first nozzle box assembly of the turbine and exhaust section of the exhaust pipe, we obtain

$$\pi_T^{\frac{n+1}{2n}} = \frac{f_{Tq}(\lambda_5)}{f_{c.a}q(\lambda_{c.a})} \sim q(\lambda_5).$$

Thus, with an increase in  $\pi_T^*$   $q(\lambda_5)$  and  $\lambda_5$  increase.

Having written the equation of balance of works of the turbo-compressor in the form

$$L_T = L_K + L_B,$$

let us arrive at the conclusion that for the preservation of  $T_3^* = \text{const}$  with an increase in the  $M_0$  number of flight, and consequently, with an increase in the total work of the turbine  $L_T$ , it is necessary to "load" the propeller. Thus, the surplus work of the turbine is completely used by the propeller.

#### 22.2.2.2. Change in $N_B$ with Respect to Flight Speed.

With an increase in flight speed the rate of airflow  $G_B$  continuously increases, and this increase follows the same regularity as that of the TRD; the specific work of the propeller  $L_B$  also increases as a result of the increase in the drop in pressures on the turbine (Fig. 22.18).

Thus, the propeller power of the turboprop engine with respect to flight speed continuously increases (Fig. 22.19). An increase

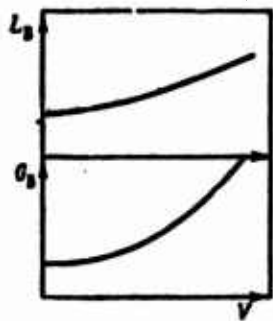


Fig. 22.18.

Fig. 22.18. Change in  $G_B$  and  $L_B$  with respect to flight speed.

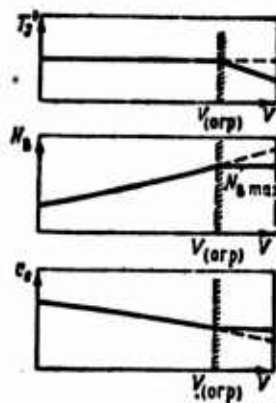


Fig. 22.19.

Fig. 22.19. Change in propeller power of the turboprop engine, temperatures  $T_3^*$  and effective fuel consumption of the turboprop engine with respect to flight speed.

$N_B$  at flight speed  $V = 200-250$  m/s very considerably can be (30-50) % of the original value of the power when  $V = 0$ .

#### 22.2.2.3. Change in $C_e$ with Respect to Flight Speed.

From expression

$$C_e = 3600 \frac{m_f}{N_B(\gamma)} \sim \frac{T_3^* - T_2^*}{L_B}$$

it follows that with an increase in flight speed the effective fuel consumption of the turboprop engine is intensively decreased (see Fig. 22.19). Actually, the relative fuel consumption per 1 kg of air continuously drops, and the specific work of the propeller increases. Thermodynamically the lowering of  $C_e$  with respect to flight speed is explained by the increase in  $\pi \eta_e$  due to an increase in  $\pi$ .

A lowering of  $C_e$  with respect to flight speed  $V = 200-250$  m/s can be 15-25% of the original value of fuel consumption when  $V = 0$ .

#### 22.2.2.4. Change in Jet Thrust.

With an increase in the flight speed the velocity of outflow of the gas at the exit from the turbine increases. However, the specific jet thrust

$$R_{ya} \sim (c_5 - V)$$

in this case drops, and more intensively than for the TRD (because of less initial values of  $c_5(0)$ ). Calculations show that the total jet thrust also drops (Fig. 22.20), especially as in the considered flight speed range the consumption of air increases by a total of (10-15) %.

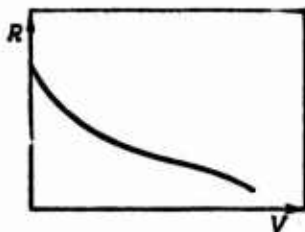


Fig. 22.20. Change in jet thrust of the turboprop engine with respect to flight speed.

The lowering of jet thrust at the flight speed  $V = 200-250$  m/s can be (20-30) % of its takeoff value.

Figure 22.21 gives the high-speed characteristic of the single-shaft turboprop engine.

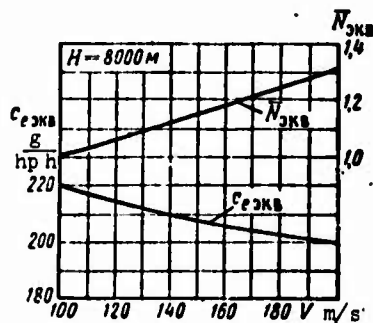


Fig. 22.21. High-speed characteristic of the single-shaft turboprop engine.

#### 22.2.2.5. Limitation of Propeller Power with Respect to Flight Speed.

The continuous increase in propeller power of the turboprop engine leads to an increase in the loads (torsional moment, peripheral stresses) on parts of the planetary reduction gear of the propeller and to an increase in their stresses.

The need to provide reliable operation of this extremely important design subassembly requires either a weight increase in the reduction gear (for strengthening of the parts), or a limitation in the magnitude of the propeller power, beginning with a certain flight speed at which  $N_B$  reaches the assigned limiting value. Limitation of the propeller power (see Fig. 22.19) is carried out according to the torsional moment on the turbine shaft either by means of lowering the number of revolutions of the turboprop engine or decreasing the temperature of the gas in front of the turbine (for example, by "lightening" of the propeller). In turn, the lowering of  $T_3^*$  leads to a worsening of the economy of the engine in regimes of flight with the limitation of power.

#### 22.2.3. Peculiarities of High-Speed Characteristics of Double-Shaft Turboprop Engines

Let us examine peculiarities of high-speed characteristics of double-shaft turboprop engines (diagram 2 in Fig. 20.2).

Let us assume that the program of control of the engine includes the following points:

- 1)  $n_{TH} = n_{max} = \text{const};$
- 2)  $f_5 = \text{const};$
- 3)  $n_B = n_{наиб}$  (from the condition of providing the maximum value of the product  $\eta_{T.B} \dot{n}_B$ ).

In this case when  $n_{TH} = \text{const}$  we have  $L_H(BD) = \text{const}$  and  $\pi_T^*(BD) = \text{const}$ , conditions  $f_5 = \text{const}$  and  $T_3^* = \text{const}$  are equivalent.

Let us assume that, as previously, at all flight speeds

$$p_4^* = p_5 = p_6.$$

With an increase in the flight speed the work of the turbine of the propeller increases

$$L_{r,n} = L_n = 118 T_4^* \left( 1 - \frac{1}{\pi_{r,n}^{*0.25}} \right) \eta_{r,n}^*$$

in accordance with an increase in the pressure differential on it. The temperature of the gas in front of the ND turbine

$$T_4^* = T_3^* - \frac{L_{TK}}{118} = T_3^* \left[ 1 - \left( 1 - \frac{1}{\pi_{r(n)}^{*0.25}} \right) \eta_{r(n)}^* \right]$$

remains constant, since we assume that the drop in pressures in the VD turbine is maintained constant.<sup>1</sup>

Thus, with an increase in the flight speed the consumption of air through the engine increases, and the work of the ND turbine and propeller power of the engine increases. The effective fuel consumption is decreased. In comparison with the characteristic single-shaft turboprop engine, values  $P_B$  and  $N_B$  are somewhat more, and  $C_e$ , respectively, less because of higher values of  $\eta_B$  and  $\eta_{T.B}^*$ .

#### 22.2.3.1. Change in Total Thrust and Specific Fuel Consumption of the Turboprop Engine with Respect to Flight Speed.

An examination of high-speed characteristics of the turboprop engine leads us to the conclusion of the fact that with an increase

<sup>1</sup>This is valid when velocities of outflow from the first nozzle box assembly of the ND turbine reach critical values.

in the flight speed the propeller power  $N_B$  increases, and the effective fuel consumption is lowered *indefinitely* in the whole range of subsonic and supersonic flight speeds.

Does this mean that the use of the turboprop engine is more profitable, the more the  $M_0$  number of flight? No, such a conclusion was completely incorrect.

The basic criteria of effectiveness of the turboprop engine are not the propeller power but the total thrust of the turboprop engine, and not the effective fuel consumption but the specific fuel consumption (referred to 1 kgf of total thrust).

From expressions for total thrust and specific fuel consumption of the turboprop engine

$$P_s = \frac{75N_B \eta_B}{V} + R$$

and

$$C_{ya} = 3600 \frac{G_T}{P_s} = 3600 \frac{m_T}{\frac{75L_B \eta_B}{V} + \frac{c_s - V}{g}}$$

it follows that the total thrust of the turboprop engine with respect to the  $M_0$  number continuously drops, and the specific fuel consumption increases even in that ideal case when  $\eta_B = 1.0$ . However the drop in efficiency of the propeller at high transonic flight speeds noticeably increases the lowering of  $P_s$  and increase in  $C_{ya}$ . If with the same generator of gas (i.e., at assigned values of  $G_B$ ,  $\pi_H^*$  and  $T_3^*$ ) we examine the comparative passage of high-speed characteristics of the turboprop engine ( $x_{(0)} \approx 1.0$ ) and TRD ( $x = 0$ ), then it is found that the very considerable advantage of the turboprop engine over the TRD with respect to the developed thrust and economy on the test stand (4-5 times) with an increase in  $M_0$  number ( $M_0 \approx 0.85-0.90$ ), as a result of a sharp drop in efficiency of the propeller (see Fig. 21.3), the thrusts and specific fuel consumption of the turboprop engine and TRD are equalized (Fig. 22.22).

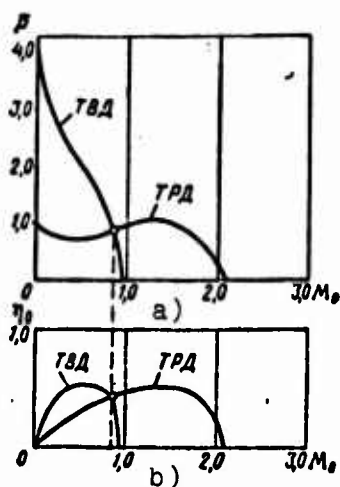


Fig. 22.22. Comparison of high-speed characteristics of turboprop engine and TRD: a) thrust; b) total efficiency.

Thus, the field of the expedient use of the turboprop engine on the economy continually is still as it was 15-20 years ago and is limited by subsonic flight speeds. Attempts of the distribution of this region at supersonic flight speeds did not give expected results mainly as a result of difficulties of the creation of supersonic propellers, which have an insufficiently high efficiency on the test stand even at subsonic flight speeds.

### 22.3. Altitude Characteristics of the Turboprop Engine

Altitude characteristics of the turboprop engine are called dependences of the propeller or total (equivalent) power and effective fuel consumption on the altitude of flight at the assigned program of control. Similar to high-speed characteristic, the altitude characteristic can be obtained either in a flight experiment or by analytical means.

#### 22.3.1. Altitude Characteristics of Single-Shaft Turboprop Engines

Let us examine the altitude characteristic of the single-shaft turboprop engine with complete expansion of the gas in the turbine on the condition that  $V = \text{const}$  with the program of control, which includes the following points:

- 1)  $n = \text{const}$ ;
- 2)  $T_3^* = \text{const}$ ;
- 3)  $f_5 = \text{const}$  and  $p_4' = p_5 = p_H$ .

Fulfillment of points (1) and (2) is provided, just as in the case of the high-speed characteristic, by means of the use of two regulators (propeller and of fuel feed) united in the command-fuel unit (KTA).

With an increase in flight altitude, as a result the increase in total compression ratio, increases the drop of pressures on the turbine, and the KTA automatically "loads" the propeller, maintaining the revolution number of the engine and gas temperature in front of the turbine constant.

#### 22.3.1.1. Change in $N_B$ in Flight Altitude.

With an increase in altitude the mass flow of air through the turboprop engine is continuously decreased and according to the same regularity as that of the TRD; the specific work of the propeller increases as a result an increase in  $\pi_T^*$ . Since the drop in air consumption, in comparison with a change in  $\pi_T^*$ , is decisive, which the propeller power of the turboprop engine with an increase in altitude also drops, but more slowly than  $G_B$ ; the fall in  $N_B$  at altitudes more than 11 km is intensified, because at these "isothermal" altitudes the specific work of the propeller already maintains a constant significance. The latter is explained by the fact that on account of the fact that  $T_H = \text{const}$ , the increase in  $\pi_{CW}$  and  $\pi_T^*$  ceases (Fig. 22.23).

At altitudes of  $H > 11$  km we have

$$N_B \sim p_H. \quad (22.6)$$

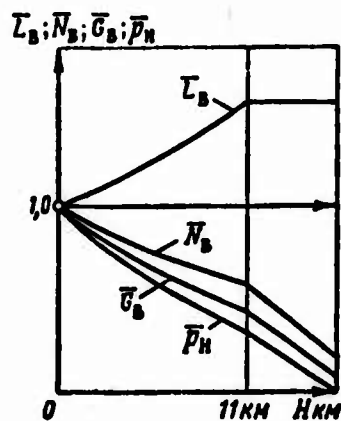


Fig. 22.23. Change in propeller power of the turboprop engine with an increase in altitude of flight.

22.3.1.2. Change in  $C_e$  with Respect to Flight Altitude.

With an increase in altitude the effective efficiency of the cycle  $\eta_e$  increases, which is conditioned by the increase in total compression ratio  $\pi = p_2^*/p_H$  and degree of preheating  $\delta = T_3^*/T_H$ . An increase in effective efficiency leads to the proportional lowering of the magnitude

$$C_e = \frac{632}{H_e \eta_e},$$

which is continued up to the altitude  $H = 11$  km. With a further increase in altitude, on account of the fact that  $T_H = \text{const}$ , parameters  $\eta_e$  and  $C_e$  remain constant (Fig. 22.24).

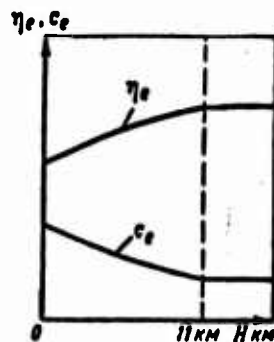


Fig. 22.24. Change in effective fuel consumption and efficiency turboprop engine with an increase in altitude of flight.

An analysis of expression  $C_e$  according to formula (21.11) leads us to the same results, since an increase in  $L_e$  proves to be the factor predominant over increase  $m_T \sim (T_3^* - T_2^*)$ .

### 22.3.2. High-Altitude Turboprop Engines

With an increase in altitude the propeller power of the turboprop engine continuously drops. Thus, the turboprop engine, similar to the turbojet or piston, is a low-level engine.

The last years have been marked by the intensive development of so-called "high-altitude" turboprop engines, the power of which with a raising up to a definite altitude - "altitude of limitations" - remains constant. A peculiarity of these engines is that they are designed for strength not on the ground, but at the mentioned "altitude of limitation," i.e., under conditions of reduced density of the medium and, consequently, at reduced values of aerodynamic forces acting on blades of the compressor and turbine and also the power and peripheral stresses acting on elements of the planetary reduction gear.

Consequently, such a turboprop engine, having in altitude-high-speed conditions the necessary reserve of strength, proves to be lightened in comparison with the standard turboprop engine designed for strength at maximum flight speed near the ground.

With a decrease in altitude of flight of an aircraft with a turboprop engine, loads which are imparted to the basic subassemblies of the engine increase, and, consequently, there appears the need in the limitation of the magnitude of parameter  $N_B$ . For this purpose either the revolution number of the engine or the gas temperature in front of the turbine (simultaneously "lightening" the propeller) must be lowered. For such turboprop engines the altitude characteristic has the form shown in Fig. 22.25. The lowering of  $T_3^*$  at altitudes less than the "altitude of limitation" leads to an increase in  $C_e$ .

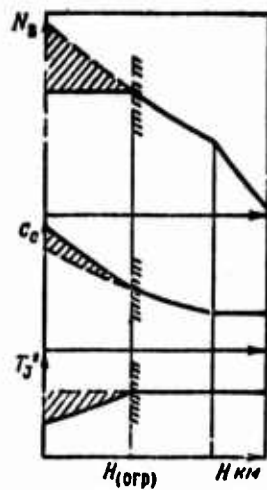


Fig. 22.25. Altitude characteristic of "high-altitude" turboprop engines.

With an increase in the flight speed a decrease in  $T_3^*$  becomes more intensive, and the "altitude of limitation" increases respectively.

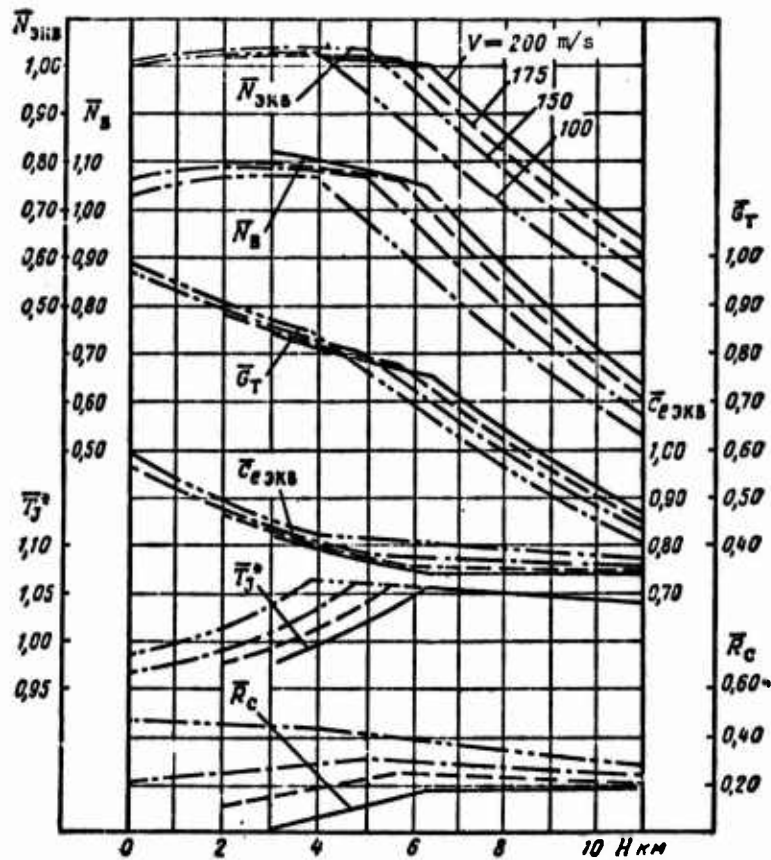


Fig. 22.26. Altitude-high-speed characteristics of a "high-altitude" single-shaft TVD.

Figure 22.26 gives the altitude-high-speed characteristics of a "high-altitude" single-shaft turboprop engine.

P A R T   S E V E N

SPECIAL OPERATIONAL CHARACTERISTICS  
OF AIRCRAFT GAS TURBINES

## CHAPTER 23

### STARTING AND TRANSITIONAL REGIMES OF GAS TURBINES

#### 23.1. Starting of the Gas Turbine

Peculiarities of the starting of gas-turbine engines, including aircraft, is that it proves to be possible only with the help of outside source of energy, which is quite powerful and acts for a relatively long time interval.

In this respect the starting of the gas turbine is considerably distinguished from the starting of piston engines, for the realization of which the turning of the crankshaft of the engine by hand or mechanical means for 2-3 revolutions is sufficient. In gas-turbine engines, only beginning with a definite quite large, number of revolutions (let us call it the "number of revolutions of idling") at which there is created increased pressure at the exit from the compressor, steady operation of the combustion chamber proves to be possible, and the turbine can develop a surplus power necessary for rotation of the compressor. If, however, revolutions of the gas turbine are lower than the *minimum balanced* (at which the power of the turbine at the maximum permissible gas temperature is equal to the work of the compressor), then the autonomous work of the gas-turbine engine is impossible.

Systems which generate power necessary for starting and turning the rotor of the gas turbine up to revolutions of idling are called starters.

### 23.1.1. Types of Starters

The basic requirements of starters are: light weight and small dimensions, high degree of reliability, and the ability to develop short-term high power necessary for rapid starting and putting the gas turbine into the regime of idling.

There is a great number of various means of starting a gas turbine. At present the most widespread are electrical engines (electric starters and starter generators) and turbine starters (gas-turbine engines and turbines operating on various working media: compressed air, gun-powder gases, combustion products of kerosene).<sup>1</sup> The free power of these engines changes from the several tens to several hundreds of horsepower.

### 23.1.2. Dynamics of Starting of the Gas Turbine

#### 23.1.2.1. Fundamental Equation of Starting of a Gas Turbine.

The starting of a gas turbine is a steady process, since the number of revolutions of the rotor changes with time; it can be described by the following equation of dynamics:

$$J \frac{d\omega}{dt} = \Delta M = M_{cr} + M_T - M_K - M_{TP} \quad (23.1)$$

where  $M_{cr}$  - moment of rotation of the starter;  $M_T$ ,  $M_K$  - moments of rotation of the turbine and of compressor, respectively;  $M_{TP}$  - moment expended for overcoming mechanical losses (in bearings) and on the drive of the units;  $\Delta M$  - surplus moment necessary for acceleration of the rotor of the engine;  $J$  - polar moment of inertia of the rotor;  $\epsilon = \frac{d\omega}{dt}$  - angular acceleration of the rotor.

---

<sup>1</sup>Piston starters used in the early stage of the creation of the TRD, as a result of heavy weight and difficulties in starting in winter, did not become widespread.

Having substituted moments of rotation in terms of power with the help of known correlations

$$\omega = \frac{\pi n}{30} \quad \text{and} \quad N = \frac{M\omega}{75},$$

we obtain the fundamental equations of starting in the form:

$$Jn \frac{dn}{dt} = \frac{75 \cdot 000}{\pi^2} (N_{cr} + N_T - N_K - N_{TP}) \quad (23.2)$$

### 23.1.2.2. Stages of Starting.

The process of starting of the gas turbine can be subdivided into three stages (Fig. 23.1).

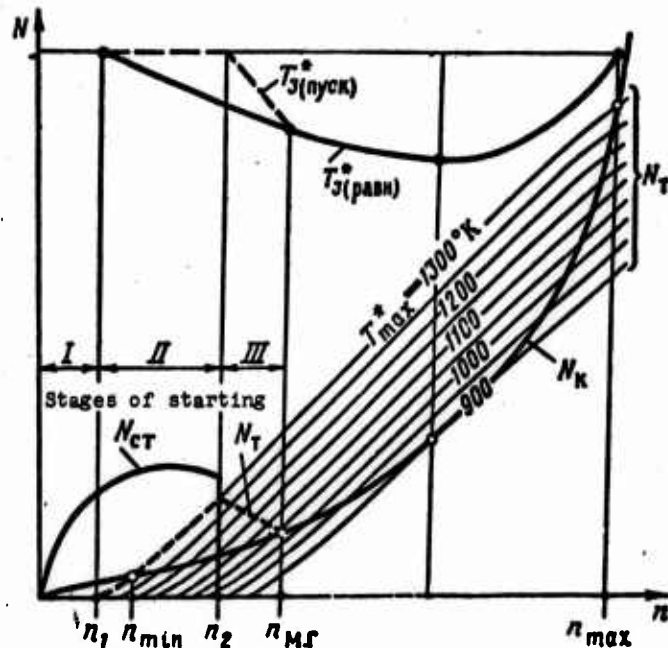


Fig. 23.1. Stages of starting of the gas turbine.

<sup>1</sup>Subsequently, we will refer the power of friction to the power of the compressor.

The *first stage*, when the combustion chambers of the GTD do not operate and the turbine does not develop power. Acceleration of the rotor of the engine occurs as a result of the fact that the power of the starter exceeds the power of the compressor (surplus power of the starter).

The first stage of starting is described by equation

$$Jn \frac{dn}{dt} = 6840(N_{cr} - N_r). \quad (23.3)$$

In this case  $N_T = 0$ .

At the end of the stage ( $n = n_1$ ) a special starting system, consisting of torch igniters and fuse devices (electrical spark plug), feeds into the combustion chamber of the gas turbine a priming fuel (kerosene or gasoline) and ignites it. The initial starting torch serves as subsequent ignition of the basic fuel entering through the main operating sprayers.

The *second stage*, when acceleration of the rotor of the gas turbine occurs as a result of the fact that the total power of the starter and turbines exceeds the power of the compressor. Magnitude  $\bar{T}_3^*$  is maintained at a maximum. The second stage of starting is described by equation

$$Jn \frac{dn}{dt} = 6840[(N_{cr} + N_t) - N_r]. \quad (23.4)$$

At the end of the stage, when the power of the turbine considerably exceeds the power of the compressor, the starter is disconnected; in this case the number of revolutions  $n_2$  is usually 1.5-2.0 times more than the minimum balanced revolutions.

The *third stage*, when acceleration of the rotor occurs only as a result of the fact that the power of the turbine exceeds the power of the compressor.

Equation of the third stage of starting has the form

$$Jn \frac{dn}{dt} = 6840(N_T - N_U). \quad (23.5)$$

In this case  $N_{CT} = 0$ . The gas temperature  $T_3^*$  is gradually lowered.

At the end of the third stage the engine goes into the idling regime ( $N_T = N_H$ ). The revolution number  $n_{M,r}$  does not depend on the starting device but is determined for the given turbocompressor only by a permissible balanced gas temperature  $T_{3(равн)}$ .

The process of starting (including all three stages) is accomplished automatically.

### 23.1.3. Starting of Double Shaft Gas Turbines

The use of double of three-shaft gas turbines simplifies starting, since it considerably decreases the power necessary for acceleration of the rotor. In this case the starter accelerates only the VD rotor having the lesser moment of inertia and revolving under conditions of reduced air density at the entrance.

### 23.1.4. Starting of the TRD in flight

A peculiarity of starting of the TRD in flight is that the need in acceleration of the engine rotor with the help of the starter disappears. The counterflow of air leads the rotor into rapid rotation (process of autorotation), at which for the realization of starting it is sufficient only to ignite the fuel in the combustion chambers.

It is necessary to keep in mind that in the regime of autorotation the compressor develops almost no surplus pressure; therefore conditions of operation of the combustion chamber of the autorotating engine are less favorable than in the case of normal starting on the ground.

With an increase in altitude separation of the already appearing flame is possible. To ensure reliable starting at an altitude

in regimes of autorotation, it is necessary to provide the formation in the combustion chamber a powerful source of flame.

#### 23.1.5. Effect of External Atmospheric Conditions on the Starting of the TRD

With a reduction in external temperature the power of friction increases. As a result of this the surplus power of the starter is lowered, the starting is "prolonged," revolutions of idling are lowered, and conditions of acceleration of the rotor up to the operating regimes are made worse.

To improve the starting of the gas turbine at low temperatures of atmosphere [ $t_H < (-15^\circ\text{C to } -25^\circ\text{C})$ ] it is necessary preliminarily to warm thoroughly the turbine starter, and in order to avoid its thickening, to dilute the oil with gasoline.

#### 23.2. Transient Conditions of the Gas Turbine

After the process of starting has been completed and the turbojet engine has been put into the regime of idling, further acceleration of the TRD up to maximum revolutions is carried out only by means of an increase in fuel feed in the combustion chamber; in practice this is achieved by means of steady movement of the control lever of the engine, interlinked with automatic unit of fuel feed, until it stops. Since with an increase in fuel feed the gas temperature in front of the turbine instantly increases, then the power of the turbine proves to be more than the power of the compressor, i.e.,  $N_T > N_H$ , and the number of revolutions of the turbocompressor continuously increases.

With a decrease in fuel feed, conversely, the gas temperature in front of the turbine drops, the power of the turbine proves to be lower than the power of the compressor

$$N_T < N_H$$

and the number of revolutions of the compressor is respectively lowered from the maximum to minimum (in the regime of idling).

Processes of the acceleration and deceleration of the turbo-compressor are unsteady transitional regimes of operation of the engine. They are described by the motion equation,<sup>1</sup>

$$Jn \frac{dn}{dt} = \frac{900.75}{n^2} (N_t - N_c). \quad (23.6)$$

Figure 23.2 gives lines of joint modes of the compressor and of turbine for the dynamic transient conditions of acceleration of the TRD turbocompressor. As it appears, this line (AA'mB) is considerably distinguished from the line of operating regimes of the steady (and it is better to say, quasi-static) process (ACB), for which we substitute the infinitely large combination of equilibrium conditions of the turbo-supercharger in different numbers of revolutions. Plotted on Fig. 23.2 is also the line of the dynamic process of deceleration of the TRD turbocompressor (BB'nA).

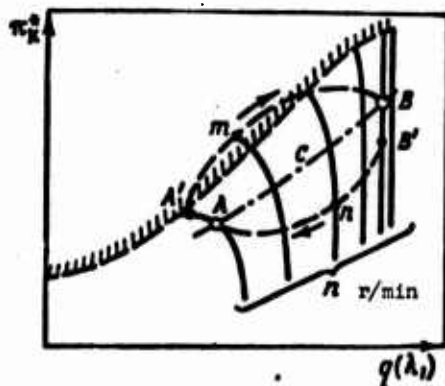


Fig. 23.2. Comparison of dynamic lines of operating regimes of the turbocompressor with an increase and decrease in fuel feed in transitional regimes.

Since with an increase in fuel feed at the first instant the revolution number of the rotor little increases (Fig. 23.3) (and the more slowly it increases, the more moment of inertia of the rotor), the increase in rate of airflow lags the increase in fuel consumption. As a result the gas temperature  $T_3^*$  sharply increases, and the regime point of the compressor is moved in the direction of the limit of surging (see line AA' on Fig. 23.2). Simultaneously,

<sup>1</sup>Dividing the integral transitional regime (from idling to maximum) into elementary sections, it is possible for each of them with the help of equation (23.6) and also dynamic characteristics of the turbine and compressor, according to the number of revolutions, to determine the time of passage of the elementary process and then find the total time of passage of the integral process.

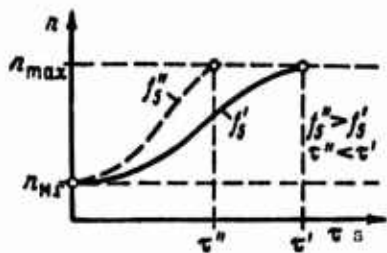


Fig. 23.3. Effect of opening of the exhaust nozzle on accelerating capacity of the TRD.

the coefficient of the surplus of air increases, as a result of which there can occur flameout in the combustion chamber due to the superenrichment of the mixture (Fig. 23.4, curve 4).

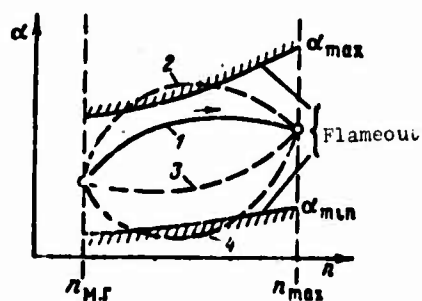


Fig. 23.4. Change in  $\alpha$  on transitional regimes of the TRD.

With an increase in the number of revolutions of the rotor, the dynamic LRR is deformed as is shown in Fig. 23.2, gradually approaching the static LRR.

With a decrease in fuel feed at the first instant there is a lowering of  $T_3^*$  and depletion of the fuel-air mixture (sharp increase in  $\alpha$ ). Now the regime point of the compressor is moved so that the stability margin of the compressor increases; however, there appears the danger of flameout in the combustion chamber due to superenrichment of the mixture (curve 2 on Fig. 23.4).

Subsequently, the dynamic line of working regimes is also intersected with the static LRR.

Thus, the feed of an excessively large quantity of fuel with the acceleration of the gas turbine can lead to disruptions in the

operation of the engine; they are connected with the appearance of unstable operation of the compressor, with the overheating of blades of the gas turbine, and also with flameout in the combustion chamber due to superenrichment of the mixture.

With a drop in revolutions a decrease in the fuel feed can lead to a superenrichment of the mixture (due to a sharp lowering of  $T_3$ ), and, consequently, to a damping of the flame in the combustion chamber.

To prevent these undesirable phenomena in the operation of the TRD and for the purpose of the approach of dynamic lines of operating regimes to the static LRR, special *automatic units of accelerating capacity*, which regulate the fuel feed into the combustion chamber in accordance with the increase in air pressure behind the compressor, are used.

In this case the dynamic lines of operating regimes deviate less from the static line *ACB* (see Fig. 23.2).

### 23.3. Accelerating Capacity of the Gas Turbine

*Accelerating capacity* is understood as the ability of the engine to increase thrust rapidly with the feed of fuel from the minimum of its value up to the maximum. Correspondingly, the time necessary for the transition from the regime of idling to the maximum regime is called the *time of accelerating capacity*. For the majority of gas turbines (with an unvariable exhaust nozzle) it is equal to:

$$\tau_{ap} = 10 \div 15 \text{ s.}$$

When thrust augmentation in the TRD is connected with the acceleration of the rotor ( $f_5 = \text{const}$ ), the time of the accelerating capacity can be determined with the help of the equation of dynamics of acceleration of the TRD in the form

$$Jn \frac{dn}{dt} = \frac{900 \cdot 75}{\pi^2} (N_{1, \max} - N_1) = \frac{900 G_2}{\pi^2} (L_{1, \max} - L_1)$$

whence

$$\tau_{np} = \frac{\pi^2}{100} \int_{n_{id}}^{n_{max}} \frac{Jn \cdot dn}{(L_{Tmax} - L_k) G_0} \quad (23.7)$$

From the obtained integral equation (23.7) it follows that the less the time of accelerating capacity, the less the moment of inertia of the rotor of the turbocompressor of the gas turbine, the more the surplus power of the turbine (i.e., the higher the gas temperature in front of the turbine, the more the drop in pressures on it, and the more the flow of air through the engine) and the more the number of revolutions of idling.

To improve the accelerating capacity of the gas turbine it is necessary: to decrease the moment of inertia of the accelerated masses (by means of the transition from a single-shaft to double-shaft design of the engine, by means of the use of plastics in the construction of the turbocompressor, etc.); to increase the maximum permissible gas temperature in front of the turbine (by means of the use of materials of increased strength and the introduction of cooling of the blades); to increase the drop in pressures on the turbine (by means of complete "opening" of the jet nozzle in the regime of starting; the greater the exit section of the nozzle with starting, the less the time of the gain  $n_{max}$ , see Fig. 23.3). With an increase in  $T_3^*$  in the maximum regime the gas temperature in throttle regimes is sharply lowered (Fig. 23.5), which is explained by the preservation of the drop in pressures on the turbine in the large range of operating regimes. An increase in the permissible interval of the increase in gas temperature  $\Delta T_3^*$  with acceleration improves the accelerating capacity of the gas turbine. Utilization of these means allows in a number of cases reducing the time of accelerating capacity to 6-8 s, and in lift engines - to 4-5 s.

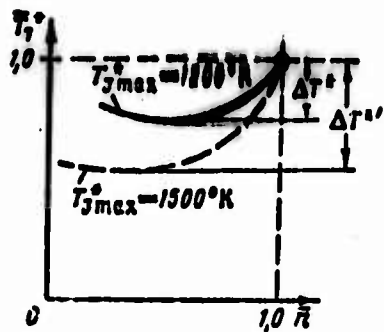


Fig. 23.5. Effect of maximum gas temperature  $T_3^{\max}$  on  $\Delta T$  with throttling of the engine.

### 23.3.1. Effect of Altitude of Flight on the Time of Accelerating Capacity of the Gas Turbine

Since with the increase in altitude the mass exit of air through the engine is decreased, then the surplus power of the turbine drops (Fig. 23.6):

$$\Delta N \sim G_a$$

and, consequently, the time of accelerating capacity increases. At high altitudes (8-11 km and above) the time of accelerating capacity increases 4-5 times (as compared to the test bench), and therefore on these altitudes it is not recommended to throttle the engine. The revolution number of idling of the gas turbine increases with altitude; maneuverable properties of the gas turbine at an altitude are made worse.

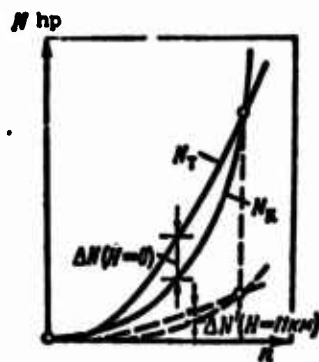


Fig. 23.6. Comparison of accelerating capacity of the TRD on a test stand and in flight.

Figure 23.7 shows curves of the accelerating capacity of a ducted-fan engine Rolls-Royce "Sney" with flight near the ground and at an altitude.

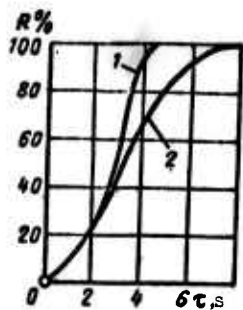


Fig. 23.7. Curves of accelerating capacity of a ducted-fan engine Rolls-Royce "Spey" with flight near the ground (1) and at the altitude of  $H = 7600$  m (2).

## CHAPTER 24

### EFFECT OF CONDITIONS OF OPERATION ON CHARACTERISTICS OF AIRCRAFT GAS TURBINES

#### 24.1. Effect of Various Operational Factors on the Regime of Operation and Parameters of the Turbojet (Turboramjet) Engine

Various operational factors having a considerable effect on the regime of work and parameters of the TRD (TRDF) can be subdivided into the following groups:

1. *External and flight conditions.* These include the state of the external atmosphere (pressure and temperature of the air, humidity of the atmosphere), and also the speed and altitude of flight. The effect of these conditions on the operation of the engine is manifested through a change in complete parameters of the air ( $p_H^*$ ,  $T_H^*$ ).

2. *Factors which lead to additional gas-dynamic and hydraulic losses in the gas-air channel.* Specific conditions of the operating of the engine on an aircraft can cause additional gas-dynamic and hydraulic losses and intensify the nonuniformity of flow in various elements of the engine: in its intake, compressor, combustion chamber, turbine, afterburner, and jet nozzle. These conditions include: the presence of long and curved inlet and exit aircraft channels; the presence of dust and other mechanical particles in the atmospheric air being sucked in, which leads to the working of the surface of working elements of the engine, their warping,

chipping, dents, etc., and to the appearance of ice deposit at the inlet of the engine; operating at very great altitudes at which a sharp lowering of Reynolds numbers approaches, and as a result of this - a drop in efficiency of the compressor and turbine.

An increase in losses in the gas-air channel of the engine, as a rule, disrupts the process of operation of the engine and makes its economy worse.

One should keep in mind that an increase in hydraulic losses in TRD elements is almost always accompanied by the reinforcement of the *nonuniformity* of temperature and high-speed fields, which additionally makes conditions of operation of the engine worse: there is overheating of the engine, cutoff and oscillating regimes appear, and vibrations in subassemblies of the engine appear.

3. *Factors which lead to the worsening of carburetion in combustion chambers and afterburners.* In a number of cases with operation of the engine carburetion in the combustion chambers and afterburners is made worse, as a result of which the completeness of fuel combustion decreases and the specific and consumptions of fuel per hour increase.

Reasons leading to the worsening of carburetion can be: the drop in pressure in the combustion chamber at high altitudes, carbon formation in the fuel sprayers and their obstruction, maladjustment of the fuel pump and so on.

4. *Maladjustment of the engine in the process of operation or repair.* In the process of operation and repair of the engine disruptions in systems of adjustment of its subassemblies, mechanisms, and automatic units are possible. These disruptions, if they in due time are not revealed and not removed, can lead to breakages and damage of the engine. A typical example of "maladjustment" of separate subassemblies of the TRD is the failure of the mechanism of control of the variable-arc jet nozzle at moment of fuel feed into the afterburner of the TRD. As a result of the jet nozzle,

there is an inadmissible excess in temperatures in the main combustion chamber, surging of the compressor and other dangerous consequences.

An incorrect selection of the exhaust section of the standard jet nozzle of the TRD leads to similar results.

Another example of the disruption of adjustment of the engine is the incorrect setting of the inlet guide vane of the compressor, which also can lead to a decrease in surging reserve, an undesirable increase in gas temperature in front of the turbine and to a change in thrust and fuel consumption of the engine. The maladjustment of the fuel system of the engine, which can exclude possibility of normal operation of the engine is especially dangerous.

The effect of separate operational factors on the operation of the TRD when  $\pi = \text{const}$  is illustrated in the table given on Fig. 24.1.

Let us examine in more detail the action of separate factors. The change in external pressure does not have an effect on the regime of operation of the turbocompressor, since it causes a proportional change in pressure along the whole gas-air channel of the TRD without a change in the temperature fields. As a result the velocity of gas outflow from the nozzle of the engine and specific fuel consumption maintain constant values, and the mass flow of air through the engine changes, which proves to be greater the higher the external pressure. In proportion to parameter  $G_g$  the total thrust of the TRD and fuel consumption per hour change.

A change in  $T_H$  leads to a displacement of the regime point of the compressor along LRR (when  $\pi = \text{const}$ ) and considerably changes the flow of air and specific parameters of the engine and especially intensively - total thrust. Temperature  $T_3^*$  with an increase in  $T_H$  can increase or decrease - due to effects  $\pi_{K0}^*$  on  $\bar{L}_H$  (see Fig. 12.1).

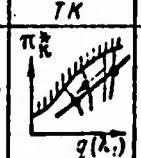

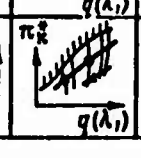

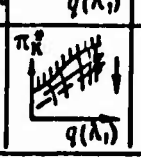
No.	Operational factor	Symbol	Change in regime	Change in parameters of the TRD							Remarks
				$T_J^*$	$R_{y_d}$	$G_B$	$R$	$m_T$	$C_{y_d}$	$G_T$	
1. External atmospheric conditions											
1	External pressure	$P_0$	Similarity is preserved $TK$	const	const	↓	↓	const	const	↓	—
2	External temperature	$T_0$		↑	↓	↓	↓	↓	var	↓	$\pi_k^* > 10$ $L_k \uparrow$
2. Altitude-high speed conditions											
1	Increase in flight altitude	$H \uparrow$		~const	↑	↓	↓	↑	↓	↓	$T_J^* \sim L_k$
2	Increase in flight speed	$V \uparrow$		~const	↓	↑	↓	↓	↑	↑	—
3. Maladjustment of the engine											
1	With forcing the jet nozzle is not opened	$T_\phi^* \uparrow$ $f_s = \text{const}$		↑	↑	const	↑	↑	↑	↑	$T_\phi^* \uparrow$ Surging reserve is decreased
2	After repair the jet nozzle is incorrectly selected	$f_s \uparrow$		↓	↓	const	↓	↓	↓	↓	—

Fig. 24.1. Effect of operational factors on the regime of operation and parameters of the TRD (TRDF) ( $n = \text{const}$ ).


No.	Operational factor	Symbol	Change in regime	Change in parameters of the TRD							Remarks
				$T_3^*$	$K_{YA}$	$G_0$	$R$	$m_T$	$C_{YA}$	$G_T$	
<b>4. Hydraulic and gas-dynamic losses</b>											
1	Losses in the inlet channel	$\zeta_{in}^*$	Similarity is preserved TK	const	↓	↓	↓	const	↑	↓	—
2	Losses in the compressor	$\eta_K^*$	Characteristic of compressor changes	const	↓	↓	↓	const	↑	↓	$L_K=const$
3	Losses in the combustion chamber	$\zeta_{KC}^*$		↑	↑	const	↑	↑	↑	↑	Surging reserve is lowered
4	Losses in the turbine	$\eta_T^*$	"	"	"	"	"	"	"	"	"
5	Losses in the turbine diffuser	$\zeta_A^*$	"	"	"	"	"	"	"	"	"
6	Losses in the afterburner	$\zeta_{AN}^*$	"	"	"	"	"	"	"	"	"
7	Losses in the jet nozzle	$\zeta_{pc}^*$	"	"	"	"	"	"	"	"	"
<b>5. Losses due to incompleteness of combustion</b>											
1	Losses in the combustion chamber	$k_{KC}$	Similarity is preserved TK	const	const	const	const	const	↑	↑	—
2	Losses in the afterburner	$k_{AN}$	Similarity is preserved TK	const	const	const	const	const	↑	↑	—

Fig. 24.1. (Continued).

The effect of losses in the gas-air channel on the operation of the engine has certain peculiarities. Thus, for instance, an increase in losses in various elements of the channel of expansion (in the combustion chamber, turbine, afterburner, jet nozzle) leads qualitatively to the same consequences - to an excess in temperature in front of the turbine, displacement of the line of working regimes to the limit of surging, and worsening of economy of the engine. The thrust of the engine in this case increases.

An increase in losses at the entrance into the TRD does not affect the regime of operation of the turbocompressor, but causes a drop in flow of air and specific and total thrust and a worsening of the economy of the engine.

A decrease in the efficiency of the compressor (when  $L_H = \text{const}$ ) also leads to a lowering of thrust and to an increase in specific fuel consumption. The temperature fields of the TRD, just as in the preceding case, remain constant.

The worsening of carburetion in the combustion chamber always leads to a lowering of combustion efficiency, and, as a consequence, to an increase in specific and hour fuel consumption. The regime of operation of the engine in this case does not change; the thrust of the TRD (to within the magnitude of the change in flow of gas) remains constant.

#### 24.2. Limitation of Thrust of the Turbojet Engine at Low Temperatures of the Surrounding Atmosphere

The question of the effect of temperature of the external atmosphere on the thrust of the aircraft gas turbine has special significance. It is connected with the considerable deviation in air temperature in operation from its standard value according to the International Standard Atmosphere [ISA] (MCA).

Above we noted that the reduction of  $T_H$  (for example, in winter) leads to a considerable increase in the thrust of the TRD

or power of the turboprop engine. In this case moments and forces in elements of construction of the engine and, consequently, stresses increase respectively. Thus, beginning from certain values of  $T_H$ , it is necessary from considerations of strength to introduce the *thrust limitation* of the engine. It is carried out, for example, by means of preserving constant the fuel consumption per second (hour) and corresponding lowering of the number of revolutions and gas temperature in front of the turbine. Thus, beginning with a certain "temperature of limitation"

$$T_H \leq T_{\text{orp}}$$

the thrust (power) of the gas turbine is maintained constant or changes little.

At an air temperature greater than the "temperature of limitation" ( $T_H > T_{\text{orp}}$ ), a drop in thrust appears. However, a considerable drop in thrust, which can arise at high values of  $T_H$ , is very disadvantageous in operation. It hampers takeoff, requires the introduction of special forcing of the gas turbine either with respect to the number of revolutions (which lowers the service life of the engine) or with the help of the injection of a water-methanol mixture at the entrance into the compressor or by means of the afterburning of the fuel behind the turbine. These measures also have definite limitations. It is usually important to maintain constant thrust up to  $t_H = +30^\circ\text{C}$  to  $+40^\circ\text{C}$ , and then it is possible to allow its decrease.

Figure 24.2a gives the dependence of thrust of a ducted-fan engine Rolls-Royce "Spey" on the change in temperature of the external atmosphere without the injection of a water-methanol mixture at the entrance into the compressor (curve 1) and with the injection of this mixture (curve 2).

The injection of a water-methanol mixture allows maintaining the thrust constant up to  $t_H = +35^\circ\text{C}$  ( $\Delta T = +12^\circ\text{C}$ ) and providing at  $t_H > 35^\circ\text{C}$  an increase in thrust by 9%.

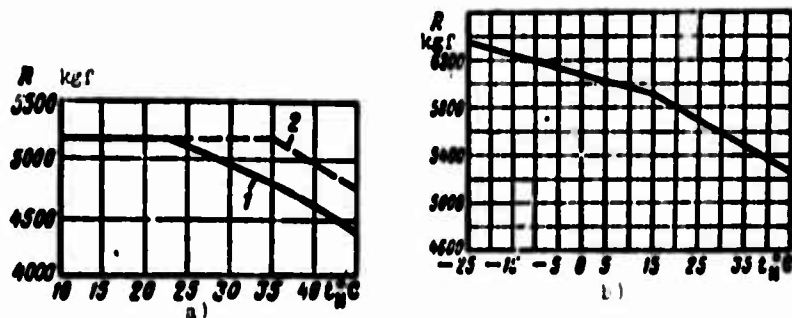


Fig. 24.2. Dependence of thrust of the ducted-fan engine Rolls-Royce "Spey" (a) and TRD Rolls-Royce "Avon" (b) on the temperature of the external medium: 1 - without injection of a water-methanol mixture; 2 - with injection of a water-methanol mixture.

In the turboprop engine "Tyne" a similar injection of the water-methanol mixture provides an increase in effective power up to 28%.

Figure 24.2b shows program of control of thrust of the TRD Rolls-Royce "Avon" depending on external temperature. As we see, in the interval of temperatures from  $t_H = -25^\circ\text{C}$  to  $t_H = +15^\circ\text{C}$  the thrust of the TRD insignificantly drops (from 6350 to 5900 kgf, i.e., 7%). When  $t_H > +15^\circ\text{C}$  the thrust decay is intensified, and it is not compensated.

Regularities of the change in thrusts given on Fig. 24.2a and b are model programs of the control of engines accepted by the firm Rolls-Royce.

### 24.3. Effect of Humidity of the Atmosphere on Parameters of the Aircraft Gas Turbine

*Humidity* of the atmosphere is understood as the content of water vapors and also water in liquid (rain) and solid (snow, ice) forms in the atmosphere. Since the humidity of the atmosphere can change from a minimum (dry air) to a maximum (100% humidity, when the atmosphere contains saturated water vapor), then it is important to know how it affects the operation and basic characteristics of the aircraft engine.

The presence of water vapors in air is conveniently evaluated as *specific* or *relative humidity*  $q$ , understanding by it the quantity of water (of water vapors) in grams which is contained in 1 kg of air. The magnitude of relative humidity is determined basically by air temperature and also pressure of the atmosphere. Numerous tests of engines show that humidity has a noticeable effect on the operation of the gas turbine.

The physical essence of the effect of the humidity of the atmosphere on parameters of the gas turbine is expressed in terms of a change in gas constant of the air, which increases with an increase in  $q$  ( $R_{H_2O} = 47 \text{ kgf}\cdot\text{m}/\text{kg}\cdot\text{deg}$  in comparison with  $R_a = 29.3 \text{ kgf}\cdot\text{m}/\text{kg}\cdot\text{deg}$ ). This circumstance leads to an increase in the thermal heat capacity of the air and, consequently, an increase in the efficiency of the gas and increase in effective operation of the thermodynamic cycle (at assigned values of parameters of the operating regime).

As a result the velocity of outflow of the gas from the engine (proportional to  $\sqrt{R_T}$ ) and also specific thrust of TRD increases.

On the other hand, the presence of water vapors in the air lowers its specific weight. The latter results from the formula

$$\gamma = \frac{p}{RT} \sim \frac{1}{R}.$$

Thus the mass flow of air through the engine drops and more intensively than the specific thrust increases. Consequently, the increase in humidity leads to thrust decay of the TRD.

An increase in the thermal heat capacity of the gas has as its result an intensive increase in hour and especially specific fuel consumptions. The increase of the speed of sound in a moist atmosphere leads to an increase in the balanced numbers of revolutions of the engine (while maintaining the similar regime of the turbocompressor).

Figure 24.3 gives curves of the effect of humidity on basic parameters of the TRD Rolls-Royce "Avon"; on this figure the humidity of the engine changes from the standard ( $q = 0.01$ ) to the maximum ( $q = 0.065$ ).

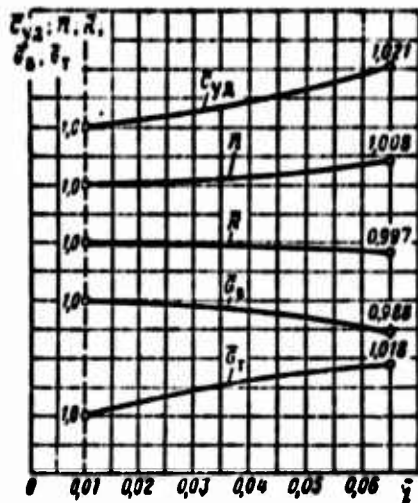


Fig. 24.3. Effect of air humidity on basic parameters of the TRD Rolls-Royce "Avon."

From Fig. 24.3 and also on the basis of the analysis of other data, the conclusion can be made that at the worst, as a result of the increase in the humidity on a hot day ( $t_H = +45^\circ\text{C}$ ) the following occurs:

- a) the thrust of the TRD drops 0.3-0.5%;
- b) specific fuel consumption increases 2.1-2.6%;
- c) fuel consumption per hour increases 1.8-2.1%.

#### 24.4. Effect of Thrust Reversing on the Operation of Turbojet Engines

The continuous increase in maximum flight speeds of transport aircraft leads to an increase to a certain degree of landing speeds. This circumstance requires the realization of design measures with respect to deceleration of movement of the aircraft, which allow

decreasing the distance of the approach of the aircraft to the airfield, and holding before the landing and run with respect to the takeoff-landing strip after the landing. The purpose of these means, as the final result, is to increase the safety of landing of contemporary aircraft.

One of such measures is the use of so-called *thrust reversers*. Newly contemporary created transport aircraft must, as a rule, be equipped with a thrust reverser. The basic purpose of the thrust reverser is for the reduction of the landing run of the aircraft after landing.

Besides the fulfillment of this basic function, the thrust reverser additionally provides:

- 1) fulfillment of landing approach without the lowering of the number of revolutions. This makes it possible when necessary to restore rapidly positive thrust for the approach to the second circle (i.e., provide the safety of departure to the second circle);
- 2) emergency interruption of flight, emergency extinguishing of flight speed;
- 3) increase in the maneuverability of the aircraft when taxiing on the ground and also in flight.

The principle of operation of the thrust reverser is evident from the examination of Fig. 24.4a and b.

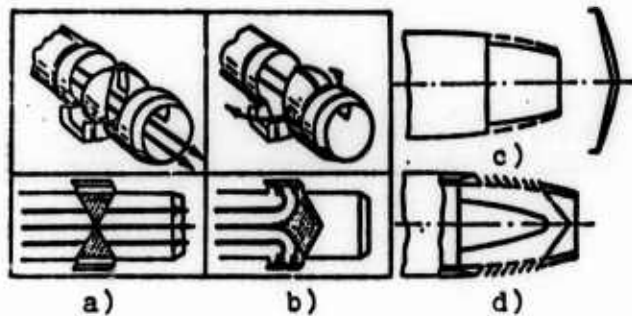


Fig. 24.4. Thrust reverser: a), b) principle of operation; c) hoop type; d) lattice type.

#### 24.4.1. Characteristics of Contemporary Thrust Reversers

Contemporary thrust reversers allow creating negative thrust during landing run of the aircraft equal to 40-50% of the maximum bench thrust. This shortens the landing run by 40-60%.<sup>1</sup> Weight of serial thrust reversers is about 10-12% of the weight of the engine.

The thrust reversers have a number of additional requirements which concern their *speed of response* (change in direction of thrust in 1-5 s), *reliability of operation* of the mechanism, insignificant worsening of the economy of the engine with the reverser turned off (by not more than 1%), and prevention of the entrance of a jet of hot gases with reversing into the *suction intakes* of the engines.

#### 24.4.2. Types of Thrust Reversers

For thrust reversing reversers of predominantly two types are used:

- 1) in the form of a hoop (see Fig. 24.4c);
- 2) in the form of an aerodynamic lattice (see Fig. 24.4d).

In the first case special hoops deflect a jet of gas flowing from the engine at a definite angle. Deviation of the jet in this case practically does not affect the regime of operation of the TRD. In the second case the jet of gas taken from the turbine space of the engine is deflected and led off outside with the help of special aerodynamic lattices. In this case thrust reversing can have an effect on the operation of the engine.

With deflection of the gas jet due to the appearing gas-dynamic and hydraulic losses, the velocity of outflow is lowered.

---

<sup>1</sup>The reduction of landing run with thrust reversing largely depends on the condition of covering of the takeoff and landing strip (runway): with ice on the runway it is very considerable, and with a dry runway it is little.

#### 24.5. Service Life and Reliability of Aircraft Gas-Turbine Engines

Operational characteristics of aircraft gas turbines are determined not only by economic parameters, regularities of the change in thrust and fuel consumption on the speed and altitude of the flight, calorific intensity of the parts characterized by the temperature of the gas in the "hot" part of the engine, but also by the *service life* and *reliability* of the engine.

*Service life* (period of service) is understood as the accrued operating time, i.e., the total time of reliable operation of the engine with a definite correlation between basic modes of engine: takeoff, nominal and cruising. Usually in the takeoff regime it is from 2 to 5% and in the nominal regime from 20 to 30% of the accrued operating time of the engine.

The *assured*, *interrepair* and *general technical service life* are distinguished.

The inter repair service life is the duration of reliable operation of a new or repaired engine installed on the basis of laboratory, flying and other forms of investigations, operational tests and generalization of the experience of mass operation and repair of the engines. After the finishing of the interrepair service life the engine will be subject to repair.

The general technical service life is the total duration of reliable operation of the engine up to such a degree of wear at which further restoration of it by means of repair is economically inexpedient or technically impossible. After the finishing of the general technical service life, the engine will be subject to withdrawal (removal from operation).

In the period of working out the general technical service life of the engine there can be produced up to three capital repairs (overhauls).

The assured service life of the engine is provided and established by the factories (firms)-suppliers. The interrepair service life is established by organizations (airlines) with respect to operation of the aircraft. The latter, depending on the specific operating conditions at the given airline, change the service, increasing or lowering it. Thus, for instance, if the airline passes through tropical countries with difficult operating conditions (for example, Cairo-Accra, Algiers-Johannesburg), then the portion of time of accrued operating time in the takeoff regime, due to great thrust decay at high temperatures of the surrounding air, increases with respect to the corresponding accrued operating time in the takeoff regime on other airlines. As a result the service life of operation of the engine is decreased.

The greater the distance of the line, the less the number of takeoffs in operation of the aircraft, the less the portion of accrued operating of the engine in the takeoff regime. Ultimately, the service life of the gas turbine increases.

The interrepair service life of gas-turbine engines is determined basically by fatigue phenomena in the design (in turbine and compressor blades, etc.) appearing under action of alternating and vibratory loads.

During recent years interrepair service lives of aircraft engines established by the aircraft firms and airlines sharply increased and for various types of gas turbines (turbojet, turboprop and turbofan) consist of several thousands of hours. For example, the service life of ducted-fan engine Rolls-Royce "Conway" consists of 8000 hours, turboprop engine Rolls-Royce "Dart" - 6000 hours, ducted-fan engine Pratt-Whitney JT3D-1 - 11,000 hours.

However, at such service lives of foreign gas turbines the inspection of the hot part of the engine is provided with the substitution of several parts after the finishing of approximately half of the established service life.

In recent years aircraft companies have turned to an estimation of service life according to the actual state of the engine. This requires the introduction of an automatic check on the work of the engine, and this allows the possibility to prevent engine failures in flight and reduce the cost of their technical service.

Figure 24.5a gives curves of the increase in the service life of thrust of engines of the firm Rolls-Royce "Dart," "Avon," "Tyne," "Conway" RCo.12 and RCo.42) with respect to years. From these curves it follows that the establishment of the interrepair service life at 2000 hours for contemporary aircraft gas turbines occurs during two-three years.

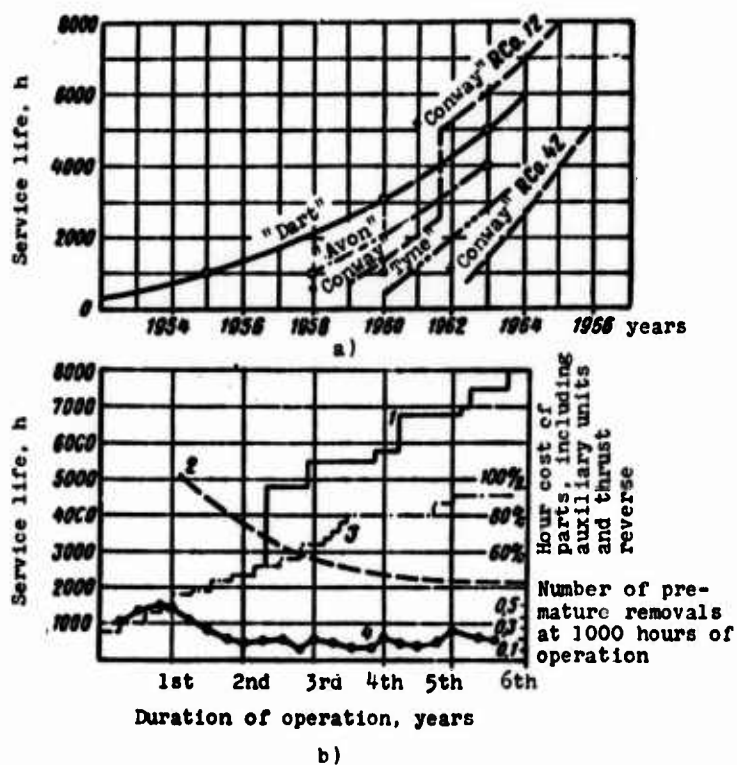


Fig. 24.5. Increase in service life of aircraft gas turbines of the firm Rolls-Royce with respect to years.

The increase in the service life of aircraft engines is an important factor, which has allowed during recent years reducing

sharply the amortization expenditures on aircraft engines and, ultimately, raising the economy of air transportation.

An important operational characteristic of aircraft engines is their *reliability*. The reliability of aircraft gas turbines is determined by the probability of their failure in operation, for example, in flight. It is characterized by the number of produced hours for one premature removal of the engine from the aircraft in operation (or for one failure in flight) or the reciprocal - the quantity of engines taken from the aircraft before the appointed time (or engines which failed in flight), which amounts to 1000 hours of their accrued operating time.

Figure 24.5b shows that the service life of the ducted-fan engine "Conway" RCo.12 in 8000 hours (curve 1) was reached in six years of operation (initial service life was about 800 hours). Curve 3 shows the increase in service life of the engine without an inspection of the hot part (toward the end of the sixty year it reached ~5000 hours). During these years the cost per hour of all parts (including the thrust reverser) was brought down by almost 60% (curve 2).

The number of premature removals of the engine "Conway" RCo.12 was sharply brought down during the first two years of its operation, and then it was stabilized. At present  $K_{1000} = 0.1-0.2$  (curve 4).

The most reliable aircraft gas turbine at present is the engine AI-20K for which  $K_{1000} = 0.05$ .

#### 24.6. Tapping of Compressed Air (Gas) from Aircraft Gas Turbines

The further development of aviation to a certain extent is connected with the creation of aircraft with perfected aerodynamics and also with vertical flight and landing. In the solution of this problem a large role is played by the rational use of energy of gas-turbine engines either in the form of power of the free

turbine or in the form of a pulse of a certain mass of air (gas) of increased pressure tapped from the engine and fed to the user along special communications.

The tapping of compressed air or exhaust gases possessing a surplus pressure, in comparison with the power takeoff of the free turbine, possesses advantages of the greatest flexibility of control, the best transportable state, simplicity of design, and the possibility of a multipurpose use.

The users of compressed air (gas) on the aircraft are:

1) control system of the boundary layer on the wing (blowing, suction) for the increase in  $c_y$  (takeoff, landing) and decrease in  $c_x$  (cruising regime of flight);

2) the system of stabilization and control of the aircraft in regimes of hovering and transition with vertical (shortened) takeoff and landing (jet and gas controls, nose turbofan, etc.);

3) the system of lift turbofan and ejector thrust intensifiers.

Aerodynamic methods of the increase in  $c_y$  and decrease in  $c_x$  and also methods of the creation of vertical thrust can require a considerable tapping of compressed air (gas) - 15-30% and more.

#### 24.6.1. Classification of Methods of the Tapping of Compressed Air (Gas) from Gas-Turbine Engines

There are various methods of tapping the working medium from aircraft gas-turbine engines (Fig. 24.6). These include the tapping of compressed air from the compressor<sup>1</sup> and also the tapping of hot compressed gas from the turbine of the engine.

---

<sup>1</sup>"The tapping from the compressor (of the turbine)" denotes briefly: "Tapping at the exit from the compressor (of the turbine)."

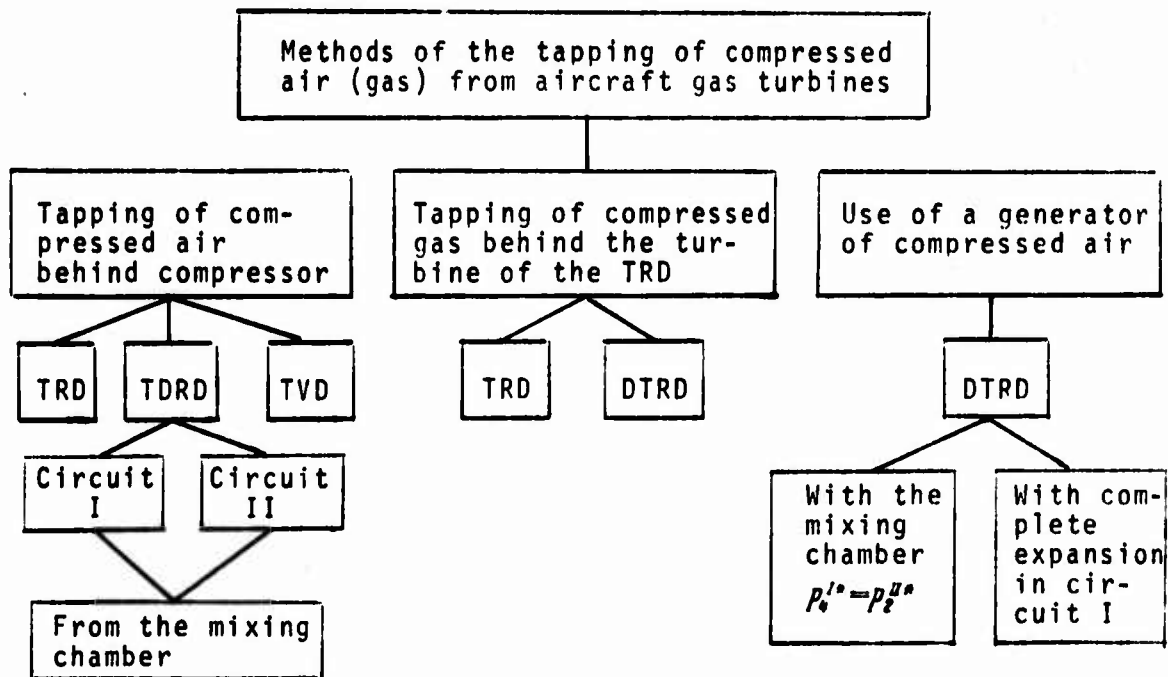


Fig. 24.6. Classification of methods of the tapping of compressed air from gas-turbine engines.

When the tapping of compressed air is produced from the compressor of the basic circuit of the TRD, turboprop engine and ducted-fan engine without the use of special complex control, the regime of operation of the engine changes - with an increase in the tapping of air to the user the compression degree of the compressor drops, and the efficiency of compressor and turbine is lowered. This always intensifies the drop in thrust of the engine and makes its economy worse.

To maintain the regime of the turbocompressor constant, and also to insure a constant value of gas temperature in front of the turbine, special methods of control of the gas turbine must be used. For example, in the TRD it is necessary for this purpose to regulate the jet nozzle and nozzle box assembly of the turbine.

In those cases when the tapping of compressed air is carried out from the compressor of the secondary circuit of the ducted-fan

engine, it proves to be possible comparatively simply to maintain the regime of the operation of the engine constant. In this case the drop in thrust in the second circuit of the ducted-fan engine is determined only by the quantity of tapped air; the specific thrust of the engine with such a tapping remains constant.

One should also keep in mind the circumstance that the tapping of compressed air from the first circuit of the ducted-fan engine is usually connected with an increase in the gas temperature in front of the turbine. The tapping of air from the second circuit most frequently leads to a certain decrease in  $T_3^*$ .

The tapping of hot gas from the turbine space of the TRD has found well-known use on VTOL aircraft because of its design simplicity. With this method it is also possible (with the help of a simple system of control) to maintain the mode of the turbocompressor of the engine constant. At the same time, such a method requires the use of special materials for gas communications of the control system of the boundary layer (UPS) and stabilization and complicates the flying operation of the aircraft.

When the sustainer engine is a ducted-fan engine with a mixing chamber, the tapping of the mixture of gases to the user is of great practical interest. The merit of this method is relatively low value of the mixture, which the lower it is, the higher the bypass ratio.

The tapping of compressed air or hot gas from a sustainer or lift engine for technical purposes (i.e., when the tapped working medium is not used for the creation of additional thrust) always leads to a thrust loss in the power unit, which worsens the energy balance of the aircraft. Therefore, in certain cases the use of special generators of compressed air (GSV), the single purpose of which is to supply the VTOL aircraft with compressed air, is expedient. The generator of compressed air is a ducted-fan engine of the lightened type which creates no thrust, the free turbine of which drives the fan.

Utilization of the GSV, just as the direct tapping of compressed air from the powerplant of the aircraft, increases the takeoff weight of the aircraft and lowers its relative commercial load.

In order that the utilization of GSV would prove to be economically expedient, the generator of compressed air must be made of lightened construction (for example, according to the type accepted in the engine Rolls-Royce RB.162), keeping in mind here the brevity of its operation.

Furthermore, the GSV must be selected at the optimum dimension for providing low specific weight. Number of the GSV must be not less than two for providing reliable takeoff and landing of the aircraft.

#### 24.6.2. Basic Methods of the Tapping of Compressed Air from the Compressor of the TRD and Programs of Control of the Engine

The following methods of the tapping of air from the compressor of the TRD are distinguished:

1) the tapping of compressed air from the compressor with fixed geometry of the engine (fixed position of control elements) and constant number of revolutions

$$(f_s = \text{const and } n_{np} = \text{const});$$

2) tapping of air from the compressor with fixed gas temperature in front of the turbine and constant number of revolutions

$$(n_{np} = \text{const and } T_3^* = \text{const});$$

3) tapping of air from the compressor at a constant gas temperature in front of the turbine and fixed geometry of the engine

$$(T_3^* = \text{const and } f_s = \text{const});$$

4) tapping of air with constant regime of the compressor.

Tapping of air when  $n_{np} = \text{const}$  and  $f_5 = \text{const}$  turns the original TRD (in the calculated regime) into a TRD(0); air bleed is connected with the continuous increase in the gas temperature in front of the turbine necessary for compensation of the relative decrease in flow of gas through the turbine. The compression ratio of the compressor in this case is usually lowered, since an increase in the tapping of the air is equivalent to the opening of the mechanical throttle, as a result of which the counterpressure at the exit from the compressor drops; in other words, the regime point of the compressor is moved along the inclined or vertical pressure characteristic ( $n_{np} = \text{const}$ ). Such a method of control of the engine, while being very simple for realization, is permissible only when in the original regime of operation of the engine (without tapping) the value of  $T_3^*$  is less than the maximum permissible.

With the considered method of tapping the drop in pressures of the gas in the turbine is preserved constant in the supercritical area of outflow from the jet nozzle; when, with an increase in the tapping, the velocity of outflow from the jet nozzle becomes subsonic ( $q(\lambda_5) < 1$ ) the pressure differential in the turbine begins to drop.

The air bleed when  $n_{np} = \text{const}$  and  $T_3^* = \text{const}$  is carried out by means of a continuous opening of the jet nozzle, i.e., an increase in the critical section of the Laval nozzle or of exhaust section of the standard (converging) jet nozzle. Thus, the necessary increase in the operation of the turbine (for ensuring drive of the compressor) is carried out by means of an increase in the pressure differential in it (i.e., increase in  $\pi_T^*$ ). It is obvious that the limiting opening of the jet nozzle is limited, on one hand, by the external diameter of the exhaust section of the diffuser [when  $p_4 < (p_5 = p_H)$ ] and, on the other hand, by the maximum permissible number  $M(\lambda)$  behind the turbine at which its "blocking" with respect to the operation approaches.

Air bleed when  $T_3^* = \text{const}$  and  $f_5 = \text{const}$  is carried out by means of throttling of the engine. It is known that with a lowering of the number of revolutions of the TRD the gas temperature in front of the turbine drops over a wide range of numbers of revolutions. Thus it proves to be possible in reduced regimes of the engine to accomplish tapping of the air with the help of the increase in gas temperature in front of the turbine up to its original value in the calculated regime.

Tapping of the air with a combined program of control when  $n = \text{var}$  and  $f_5 = \text{var}$  is possible also.

The general regularity for all programs of control of the engine with air tapping is the drop in thrust and increase in specific fuel consumption. It is obvious that the optimum program of control is that program which at the assigned magnitude of air tapping provides the least values of the drop in thrust and increase in specific fuel consumption or that which at the assigned thrust decay guarantees a large tapping of air of the assigned pressure.

Methods of air tapping examined above were connected with the change in the regime of operation of the compressor of the tapping circuit. The general deficiency of these methods is the decompression of the air with an increase in the tapped mass, and also the worsening efficiency of the compressor and turbine,<sup>1</sup> drop in specific thrust, and worsening of the economy of the engine accompanying it.

The optimum method of tapping is such a method at which the regime of operation of the turbocompressor of the circuit of air tapping remains constant.

---

<sup>1</sup>The drop in  $\eta_T^*$  takes place with a considerable change in axial velocity along the turbine and also with a sharp deviation in the value of  $u/c_{ad}$  from the calculated value.

In order that the tapping of air would not affect the operation of the turbocompressor and would not be accompanied by a worsening of the operation of the powerplant, it is necessary that the engine have a constant circuit of tapping (without the turbine) used in the calculated regime as a second circuit of thrust. In other words, the original engine should be the TRD(0) ( $\pi_{HTI}^* = \pi_{HI}^*$ ). Then with air tapping for technical purposes the control element of the engine must maintain the counterpressure at the exit of the compressor constant. In other words, with air tapping the total gas flow through the compressor must remain constant, but the "tapped" air now will no longer take part in the creation of thrust of the engine.

In the case of the TRD(0) with a program of control  $\pi_H^* = \text{const}$  and  $n_{np} = \text{const}$ , the tapped air will have the highest and, moreover, constant pressure in the whole range of the flows tapped.

There are still other methods of air bleed while maintaining the constant regime of operation of the compressor of the TRD. These include the control of the jet nozzle (RRS), control of the nozzle box assembly of turbines (RSA) and their combination. These methods are examined below in detail.

#### 24.6.3. Comparison of Effectiveness of Various Methods of the Tapping of Compressed Air in the Turbojet Engine

Let us make a comparison of the effectiveness (with respect to the relative thrust decay  $\Delta \bar{R}$  and relative increase in specific fuel consumption  $\Delta \bar{C}_{yA}$ ) of three basic methods of the tapping of compressed air from the compressor of a TRD:

- 1)  $f_5 = \text{const}$  and  $n_{np} = \text{const}$  ( $T_3^* = \text{var}$ );
- 2)  $n_{np} = \text{const}$  and  $T_3^* = \text{const}$  ( $f_5 = \text{var}$ );
- 3)  $T_3^* = \text{const}$  and  $f_5 = \text{const}$  ( $n_{np} = \text{var}$ )

in reference to the same engine for the following gas parameters in calculated mode:  $T_3^*(p) = 1300^\circ\text{K}$ ;  $\pi_{K(p)}^* = 7$ ;  $M_{4\alpha(p)} = 0.5$  (Fig. 24.7).

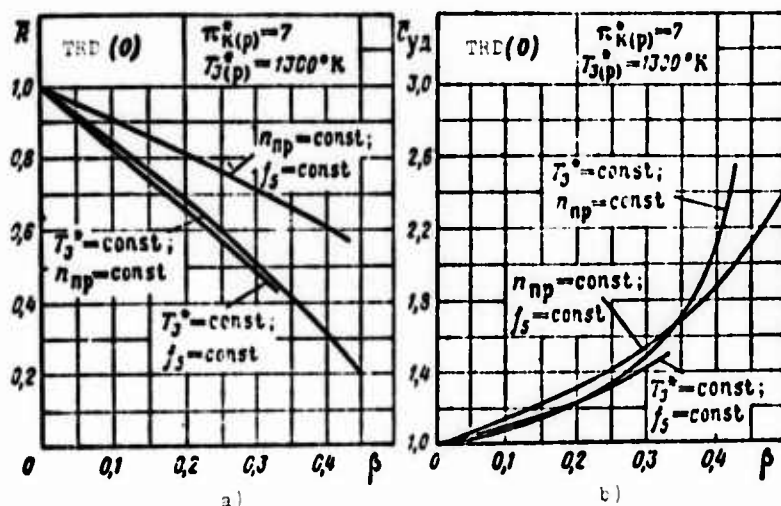


Fig. 24.7. Comparison of the effectiveness of three methods of the tapping of compressed air.

The greatest drop in the thrust of the TRD takes place with air tapping according to the program  $T_3^* = \text{const}$  and  $f_5 = \text{const}$ . A somewhat less thrust decay ( $\Delta \bar{R} = 0.15$  when  $\beta = 0.1$ ) characterizes the program  $n_{np} = \text{const}$  and  $T_3^* = \text{const}$ . A considerably less lowering of the thrust ( $\Delta \bar{R} = 0.09$  when  $\beta = 0.1$ ) is noted in the program  $n_{np} = \text{const}$  and  $f_5 = \text{const}$  when the tapping of air leads to a continuous increase in the gas temperature in front of the turbine (Fig. 24.8). In this case a 10% air bleed leads to an increase in absolute gas temperature of  $84^\circ$  ( $\bar{T}_3^* = 1.065$ ).

As regards the specific fuel consumption, in a wide range of air bleeds ( $\beta \leq 0.3$ ) the least economic, in accordance with the increase in  $T_3^*$ , proves to be the program  $f_5 = \text{const}$  and  $n_{np} = \text{const}$  (when  $\beta = 0.1$  we have  $\Delta \bar{c}_{yd} = 0.13$ ); the remaining programs are approximately equivalent and with 10% air bleed cause an increase in the specific fuel consumption of approximately 10%.

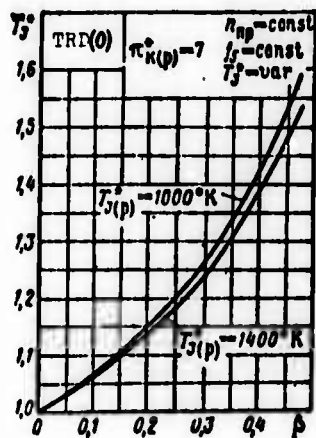


Fig. 24.8. Effect of air tapping on the increase in gas temperature in front of the turbine (method  $n_{np} = \text{const}$  and  $f_5 = \text{const}$ ).

#### 24.6.4. Effect of Bypass Ratio on the Effectiveness of Air Tapping from the First Circuit of the Ducted-Fan Engine

When compressed air of very high pressure is necessary, the tapping of it is produced from the first circuit of the ducted-fan engine.

Let us examine the effect of the bypass ratio on the effectiveness of air tapping from the first circuit of the ducted-fan engine. Let us assume that the increase in  $\gamma$  occurs on the condition that  $T_3^* = \text{const}$  and  $\pi_{KI}^* = \text{const}$  and also with the observance of quality  $\pi_{p.cI} = \pi_{p.cII}$ . It is easy to conclude that the increase in  $\gamma$  leads to a continuous and progressing lowering of the drop in pressures in jet nozzles (and, consequently, specific thrust) and to an increase in the total drop in pressures on the turbine. Thus, air tapping from the first circuit of the ducted-fan engine is accompanied by a considerably sharper drop in thrust and increase in  $C_{yA}$  than for the TRD, and the more intensively it occurs, the more the value of  $\gamma$ . Together with this, in the ducted-fan engine it is considerably earlier, i.e., at less values of the coefficient of tapping  $\beta$ , "blocking" of the turbine with respect to the operation (the more the original value  $\pi_{T(p)}^*$ , the faster the  $M_{4a}$  number increases with air tapping). This, in turn, limits the maximum tapping of air from the ducted-fan engine.

Figure 24.9 gives the effect of  $\beta$  and  $y$  on  $\bar{R}$ ,  $\bar{C}_{yD}$ , and also  $M_{4a}$ , on the condition that:  $T_3^*(p) = 1300^\circ\text{K}$ ;  $\pi_{\kappa I}(p) = 7.0$ ;  $M_{4a}(p) = 0.5$ . If in the ducted-fan engine when  $y = 0.6$ ,  $\beta_\Sigma = 0.04$  we have  $\bar{R} = 0.91$ , then in the ducted-fan engine when  $y = 1$  and  $\beta_\Sigma = 0.04$  we have  $\bar{R} = 0.87$ , and with  $y = 2$  and  $\beta_\Sigma = 0.04$  we have  $\bar{R} = 0.775$ . Correspondingly  $\beta_{\max}$  is equal to 0.21, 0.15 and 0.08.

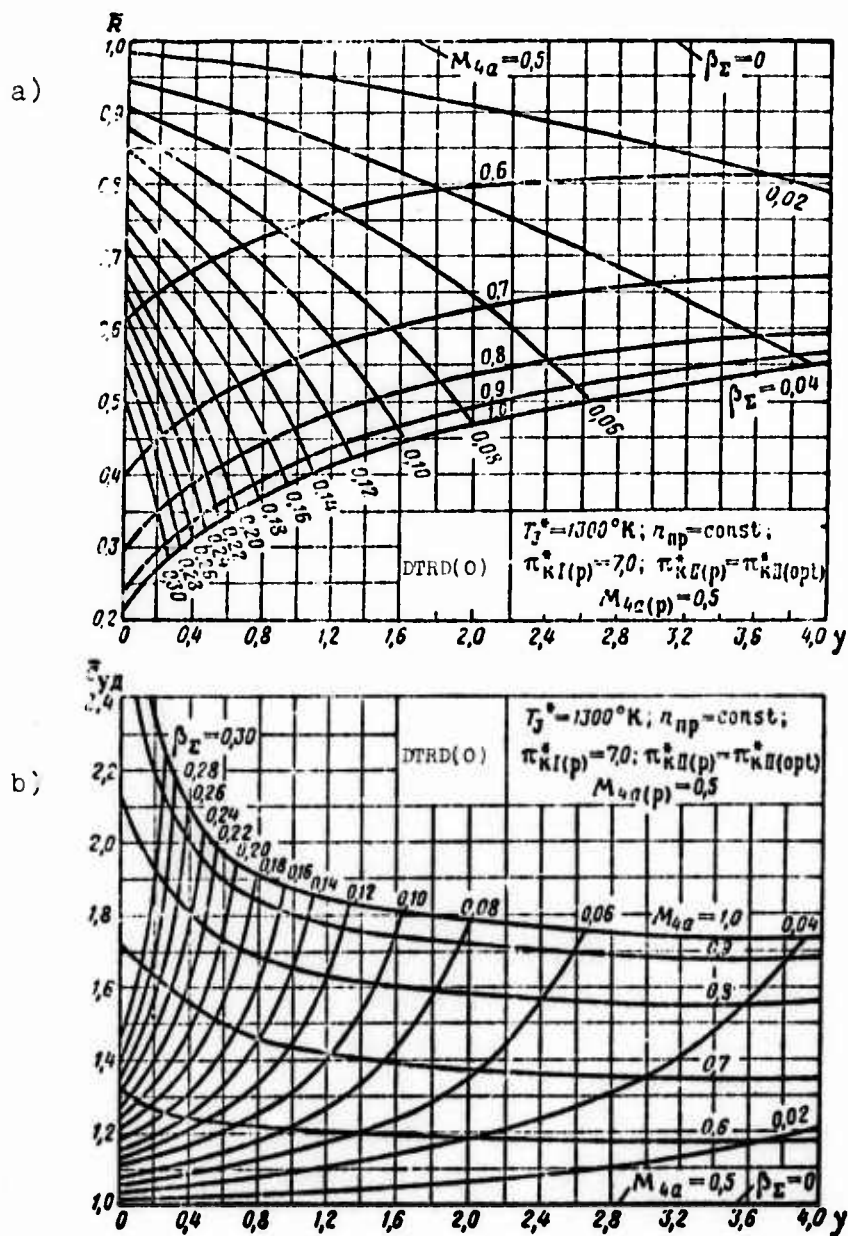


Fig. 24.9. Effect of the tapping of compressed air from the first circuit of the ducted-fan engine on parameters of the engine.

The air bleed from the second circuit in any quantity causes no special difficulties. However, the pulse of it with throttling of the ducted-fan engine sharply drops, and in prelanding flight regimes it becomes insignificantly small.

#### 24.6.5. Comparison of Effectiveness of the Tapping of Compressed Air (Gas) of Various Types of Aircraft Gas Turbines

Figure 24.10 gives a comparison of the regularity of thrust (power) decay in aircraft gas turbines of various types with the tapping of compressed air (gas).

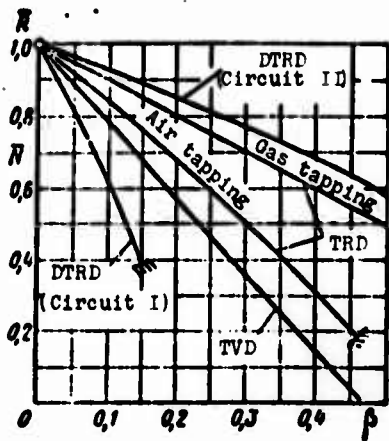


Fig. 24.10. Thrust (power) decay of aircraft gas turbines of various types with the tapping of compressed air (gas).

The most intensive drop in thrust is noted in the ducted-fan engine ( $y = 1.0$ ) with air tapping from the first circuit (for  $\beta = 0.1$  we have  $\bar{R} = 0.64$ ). Then there follows the turboprop engine (when  $\beta = 0.1$  we have  $\bar{R} = 0.78$ ). Further there is the TRD with air tapping (when  $\beta = 0.1$  we have  $\bar{R} = 0.84$ ), and the TRD with gas tapping behind the turbine (when  $\beta = 0.1$  the thrust drops 10%). The least drop in thrust occurs with air tapping from the second circuit of the ducted-fan engine (when  $\beta = 0.1$  we have  $\bar{R} = 0.92$ ).

## CHAPTER 25

### CHARACTERISTICS OF AIRCRAFT GAS TURBINES WITH RESPECT TO THE LEVEL OF NOISE

Decreasing of the noise in contemporary aircraft gas-turbine engines is one of the serious problems of civil aviation.

The mass development of air transport and an increase in power of powerplants of contemporary aircraft lead to the fact that the number of persons which suffer from noise has sharply increased. Not only are the crew and passengers of aircraft on the ground and in the air affected by aircraft noise, but also service personnel in the zone of the airports and the largest group - the population of neighboring regions.

Noise prevents the normal working activity of man, causing premature fatigue and the lowering of work productivity; noise prevents the normal rest of man and causes various nervous illnesses.

The problem of combatting aircraft noise becomes so acute that governments of various countries have been forced to introduce special rigid limitations on the operation of aircraft with respect to time and direction of the flight and permissible noise level and fine airline companies which exceed the permissible noise standards. Table 25.1 gives levels of various noises (in dB).

Table 25.1. Levels of various noises in dB.

Character and source of noises	Level of noise in dB
Threshold of audibility	0-10
Rustle of foliage, noise of slight wind	10-20
Whisper of average loudness at a distance of 1 m	20-30
Quiet habitable room	30
Light radio music in an apartment or habitable room	40
Restaurant of average animation, an establishment	50
Street of average animation, noisy establishment or store	60
Range of the loudness of speech	45-70
Music through a loudspeaker	70-80
Truck	80
Moscow subway (metallic turbines)	90
Loud automobile signal at a distance of 5-7 m	100
Train express, high speed	110
Jet engines with a total thrust of 4500 kgf at a distance of 9 m in noisiest direction:	
turbojet engine	140
turbojet engine with boost	150
solid-propellant rocket engine	155
supersonic propeller	136
Threshold of painful sensation	140
Mechanical damages	160

#### 25.1. Noise Source of the Gas-Turbine Engine

The gas-turbine engine has a number of sources of noise. The main source is the high-speed gas jet flowing from the jet nozzle. This jet, in mixing with the surrounding medium, creates intensive

turbulent pulsations, and at supercritical outflow - a system of shocks,<sup>1</sup> which are powerful noise generators.

At low velocities and altitudes of flight corresponding to regimes of takeoff and climb of aircraft, drops in pressures in the jet nozzle, as a rule, are insufficient for the appearance of powerful shock waves. Consequently, on takeoff the level of noise of the outflowing jet is basically determined by turbulent pulsations. At high-altitude and high-speed cruising flight regime the intensive noise can be produced by fluctuating shock waves and by their interaction with the turbulent pulsations.

Cascade eddy formations in which the kinetic energy of the jet is dispersed, in passing into heat, generate oscillations of pressure, which are sources of sound (noise). The turbulent mixing of the jet with the surrounding medium covers an area the axial length of which is equal to 15-25 diameters of the nozzle. In this area (Fig. 25.1) practically the entire noise of the jet flowing from the engine is generated.

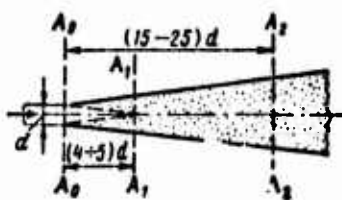


Fig. 25.1. Diagram of a free turbulent jet.

Another powerful noise source is the revolving rotor of the compressor or fan, and also the interaction of the blade of the rotor and stator. Around each blade a field of pressures appears. If the circumferential velocity of the blade is great, then the fields of pressures will be generated through the intake of the compressor in the free space in the form of a wave with increasing intensity.

---

<sup>1</sup>With incomplete expansion of the gas, for example, in the converging nozzle.

The level of noise of the compressor (fan) is usually lower than the level of noise of the jet flowing from the engine, but it is characterized by high-frequency oscillations of pressure - "whistle," which proves to be a most unfavorable physiological effect on man.

The third source of noise in the turboprop engine is the revolving propeller. The aerodynamic noise of tractor and lift propellers consists of *vortical noise*, induced by periodically separating vortices with the flowing around of the blade by a viscous medium, and *noise of rotation*, being generated by pulsations of pressures and velocity near the plane marked by the propeller. These pulsations are connected with the displacement of air by the blades and the formation of pressure differentials on both sides of the blade.

The more the noise level of the propeller, the more the M number on the end of the blade, the less the number of blades of the propeller, and the more the power applied to the propeller.

In normal operation of the gas turbine the appearance of noise is connected also with irregular turbulent combustion. However, this noise is completely disguised by the noise of the outflowing jet.

In certain cases, especially with finishing of afterburners, there appears a special form of pulsating of combustion - the so-called "resonant" combustion. The latter is accompanied by a sharp sound - "shriek" - similar to the sound of an organ pipe.

#### 25.2. Estimation of the Level of Noise of an Outflowing Jet

In accordance with the experimentally proven theory of Lighthill, the acoustic power of the noise of an outflowing subsonic free turbulent jet is determined by formula

$$N = K \frac{\rho_5^2 d_5^5 c_5^8}{\rho_H^2 a_H^2} \frac{\text{kgf} \cdot \text{m}}{\text{s}}, \quad (25.1)$$

where  $d_5$  - diameter of exhaust section of the jet nozzle;  $\rho_5, c_5$  - density and velocity of outflowing gas;  $\rho_H, a_H$  - density of the surrounding medium and speed of sound in it;  $K$  - proportionality factor determined experimentally.

Thus, the power of noise is basically determined by the velocity of outflow of gas and is proportional to its magnitude in the eighth power.

Used in technology as the basic characteristic of noise is the parameter of the level of force of sound (noise)  $L$ :

$$L = 10 \lg \frac{I}{I_0} \text{ dB}, \quad (25.2)$$

where  $I$  - force of sound (noise) on the surface of the hemisphere of radius  $r$ , in the center of which the noise source is found,

$$I = \frac{N}{2\pi r^2};$$

$I_0$  - force of sound on the threshold of audibility.

Thus, the noise level, depending on the velocity of gas outflow, is graphically depicted by a logarithmic curve of the type

$$L = 80 \lg c_5 + 10 \lg A, \quad (25.3)$$

where

$$A = f(d_5, c_5, r \dots).$$

The dependence of the noise level of certain contemporary turbojet engines (with a thrust of  $R \approx 5000$  kgf) on the velocity of gas outflow from the nozzle obtained according to experimental data is given in Fig. 25.2.

Levels of noise of several serial and engines being designed with operation of them in bench conditions in the takeoff regime and at a distance of 250 m from the source of the noise

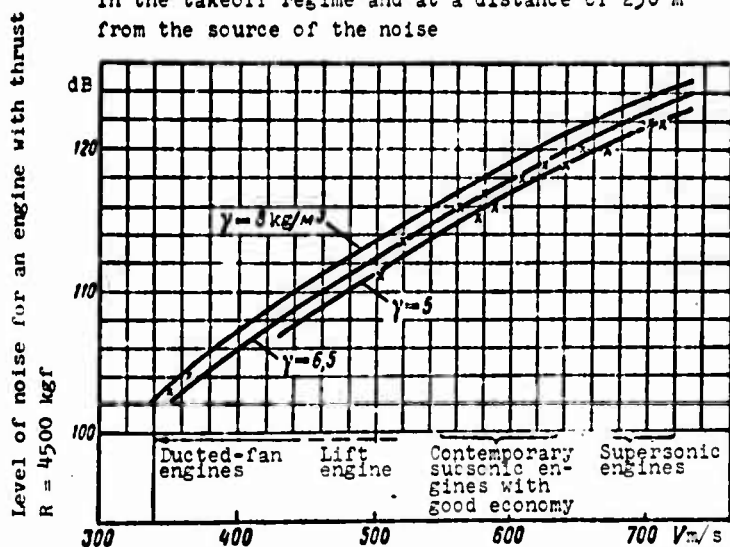


Fig. 25.2. Effect of the velocity of outflow from the jet nozzle of the TRD (DTRD) on the noise level.

The possible distinctions in density and, consequently, in temperature of the outflowing jet, at the assigned velocity of outflow give oscillations of noise intensity of about 2-3 dB. From Fig. 25.2 it follows that if at a distance of 250 m from the aircraft a one-circuit subsonic TRD when  $c_5 = 600$  m/s has a noise level of 118 dB, then the ducted-fan TRD when  $c_5 = 360$  m/s has a noise level of 103 dB, i.e., 15 dB lower. Correspondingly the forced TRD have at the velocity of outflow 720 m/s, a noise level of 124-125 dB.

The reaction of man to noise depends not only on the physical noise level determined by the sound pressure in dB with respect to the method described above, but also on a whole series of factors, including the frequency characteristic (of the spectrum) of the noise, duration, monotony or shock nature of the action, and so on.

As a result of the conducting of special experiments with the participation of a large number of people, at present there is being introduced a new method of the estimation of noisiness with the

help of the *noise* - a unit of perceived noise designated *PN* dB.<sup>1</sup>

One *noise* is equal to the noisiness of an octave range of 600-1200<sup>2</sup> Hz of an arbitrary noise at the level of sound pressure at 40 dB.

A change in frequency of the noise leads to a change in the level of perceived noise. Figure 25.3 gives the dependence of noisiness in *noises* on the level of sound pressure in one *octave*. The higher the frequency of the noise, the more the perceived level of noise in *noises*.

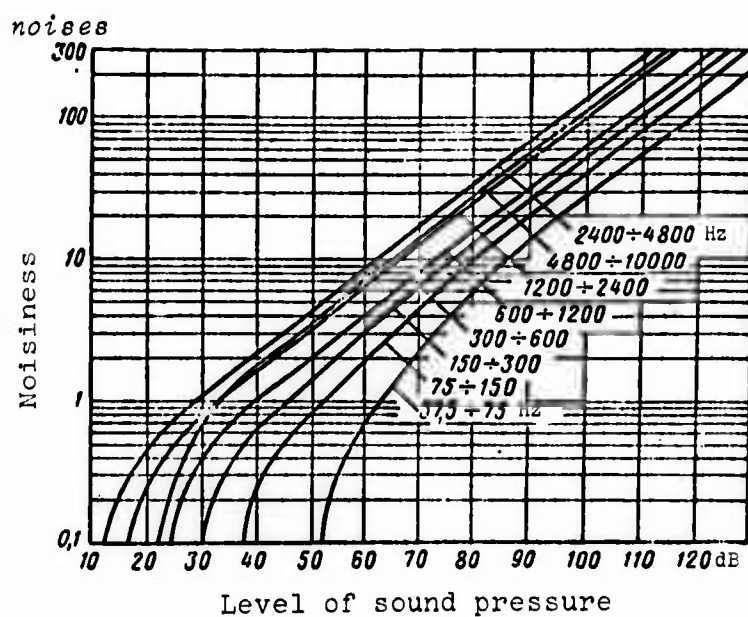


Fig. 25.3. Dependence of noisiness in *noises* on the level of sound pressure in one octave.

Figure 25.4 gives spectrum of noise audible on the ground from a DC-8 aircraft flying at an altitude of 800 m. With the help of

<sup>1</sup>*PN* - perceived noise.

<sup>2</sup>Range of greatest sensitivity of the ear.

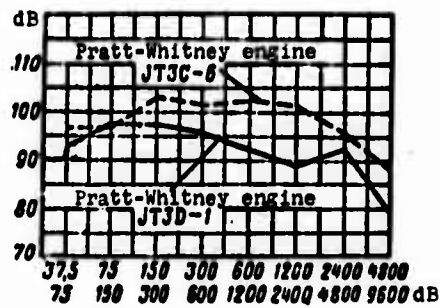


Fig. 25.4. Spectrum of noise of the DC-8 aircraft with one-circuit and ducted-fan engines.

such spectrum it is possible to calculate the integral level of noise in dB and in *PN* dB (totaling acoustic power in the whole frequency range). When the aircraft is equipped with a one-circuit TRD Pratt-Whitney JT 3C-6, the total level of noise produced by it is 110 dB, and the perceived noise is 120 *PN* dB; in the same aircraft with a ducted fan TRD Pratt-Whitney JT 3D-1 noise levels are respectively equal to 104 dB and 114.5 *PN* dB.

The processing of experimental data shows that the level of perceived noise of a jet, as a rule, exceeds by 8-10 dB the level of sound pressure.

### 25.3. Methods of Lowering of Level of Noise

There are various methods for lowering the noise level. These include:

- 1) the use of special noise suppressors of the jet stream, including ejector-type noise suppressors;
- 2) rational mutual disposition of engines on a multiengined aircraft;
- 3) the use of engines with reduced velocity of the outflowing jet (ducted-fan engine);
- 4) the use of acoustic lattices (barriers) in air inlets of the engines or aircraft;

5) rational selection of the profile of takeoff of the aircraft, which decreases noise in the locality.

#### 25.3.1. Use of Noise Suppressors

The principle of the design of noise-reducing nozzles is based on splitting of one powerful jet outgoing from the engine into many small jets. The acoustic interference (interaction) between zones of mixing of divided jets leads to a lowering of the total level of their noise.

Mechanical noise-suppressors (noise-reducing nozzles) have different geometrical configuration and design (tubular, lobe, lobe with a central body, corrugated nozzle, nozzle with ejector, etc.) (Fig. 25.5). Such noise suppressors, as a rule, are equipped on the one-circuit TRD (Rolls-Royce "Avon," Pratt-Whitney JT 3C-6 and others).



Fig. 25.5. Mechanical noise suppressor.

The operating experience of noise suppressors during a number of years has showed that with its help the sound level of the exhaust jet of a TRD can be reduced by approximately 3-5 dB. Only the use of more complex corrugated nozzles with an ejector allows decreasing the sound level 12-15 dB.

The deficiencies caused by the installation of noise-reducing nozzles are: the increase in weight of the powerplant (2-3%),

the lowering of thrust of the engine (2-4%), increase in external drag of the engine nacelle (as a result of the increase of wake drag), and the worsening of the economy of the engine.

In selecting rationally the configuration of the noise-reducing nozzle, it is possible also to obtain the displacement of acoustic energy in the zone of high-frequency oscillations. Such noise, as is known, rapidly attenuates at great distances from the nozzle.

On the whole, one should note that a satisfactory solution to the problem of noise reduction by means of mechanical nozzles has thus far not been found.

### 25.3.2. Rational Location of Engines on the Aircraft

The packet disposition (in one plane) of a series of engines makes it possible to reduce considerably the level of noise generated by the powerplant. The effect of the lowering of the level of noise is explained by the acoustic screening and interaction of zones of mixing of the jets.

The substitution of one powerful engine by a series of engines (of equal total thrust) can reduce by 5-15 dB the total level of noise.

### 25.3.3. Use of Ducted-Fan Turbojet and Turbofan Engines

#### 25.3.3.1. Effect of the Bypass Ratio of the Ducted-Fan Engine on the Level of Noise.

An increase in the bypass ratio with fixed parameters of the working process of the "original" TRD leads to a continuous lowering of velocities of outflow from the circuits and, consequently, to a lowering of the level of noise.

Figure 25.6 shows the effect of the bypass ratio  $y$  on the velocity of outflow of gas from the ducted-fan engine at optimum distribution of energy. Taken as the original TRD is an engine with a velocity of outflow  $c_5 = 600$  m/s. With an increase in  $y$  the average velocity of outflow of the gas is continuously decreased:

- when  $y = 0$ .....  $c_5 = 600$  m/s
- when  $y = 1.0$ .....  $c_5 = 400$  m/s
- when  $y = 2.0$ .....  $c_5 = 320$  m/s
- when  $y = 6.0$ .....  $c_5 = 200$  m/s

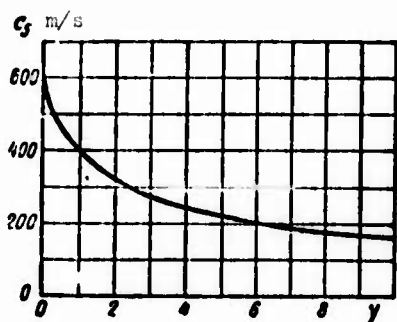


Fig. 25.6. Effect of the bypass ratio  $y$  on average velocity of outflow of gas from the ducted-fan engine.

Figure 25.7 shows the effect of the bypass ratio  $y$  and temperature of the gas in front of the turbine on the relative noise level of the ducted-fan engine. We see that an increase in  $y$  from zero to 1.5 lowers the noise level by 20 dB. At the same time the lowering of  $T_3^*$  from 1350°K to 1200°K (i.e., 150°) decreases the noise level by only 5-7 dB.

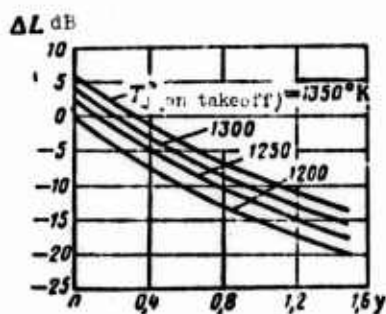


Fig. 25.7. Effect of the bypass ratio  $y$  and gas temperature in front of the turbine on the lowering of the noise level  $\Delta L$  in the ducted-fan engine.

From the viewpoint of providing an allowable noise level of the engine and lowering the operational expenditures, it is expedient over a long range of flight to use low-temperature ducted-fan engines with a high bypass ratio without any additional devices which decrease the noise level. In comparison with the TRD, this provides a considerable economic effect and practically resolves the problem of combatting noise.

The mixing of flows in the nonboosted ducted-fan engine additionally lowers the noise level (by 3-4 dB) as a result of the equalizing of the profile of velocities in the exhaust jet (Fig. 25.8).

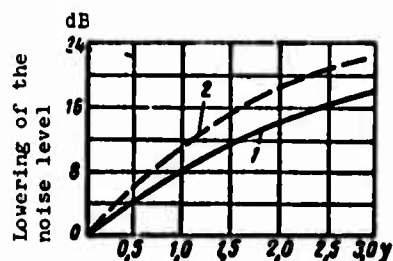


Fig. 25.8. Effect of the mixing of flows in the ducted-fan engine on the noise level: 1 - without mixing of the flows; 2 - with mixing of the flows.

25.5.5.2. Effect of the Bypass Ratio on the Noise Spectrum.

An increase in the bypass ratio leads not only to a lowering of the noise level, but also changes the frequency characteristic of the spectrum of noise, shifting the maximum of its levels into the region of low-frequency oscillations. Thus, the same level of noise will subjectively be perceived by the human ear as a weaker sound (noise).

Figure 25.9 shows curves of the spectra of noise created by the TRD General Electric CJ 805-3 without a noise suppressor and with a noise suppressor and also a TRD with a rear turbofan adapter - General Electric CJ 805-23. As we see, in the region of high-frequency oscillations the engine CJ 805-23 has the lowest sound

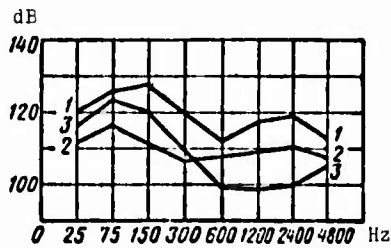


Fig. 25.9. Curves of noise spectra of the TRD and ducted-fan engine: 1 - TRD General Electric CJ 805-3 without a noise suppressor; 2 - TRD General Electric CJ 805-3 with a noise suppressor; 3 - ducted-fan engine General Electric CJ 805-23.

level (10 dB lower than that of the TRD CJ 805-3 with a noise suppressor). This advantages proves to be very considerable if one considers that the use of the turbofan adapter increases the takeoff thrust of the engine by 35-40%.

25.3.3.3. Comparison of Noise Levels of a Lift Turbofan and Compressor.

The use of wing lift turbofans (PTV) with very low velocities of the outflow of gas (air) from the circuits at large values of  $\beta_n$  makes it possible very considerably to lower the sound level. This is clearly shown on Fig. 25.10, from which it follows that when  $c_5 = 180-200$  m/s the noise level of the outflowing jet of gas from the PTV does not exceed 105-107 dB.

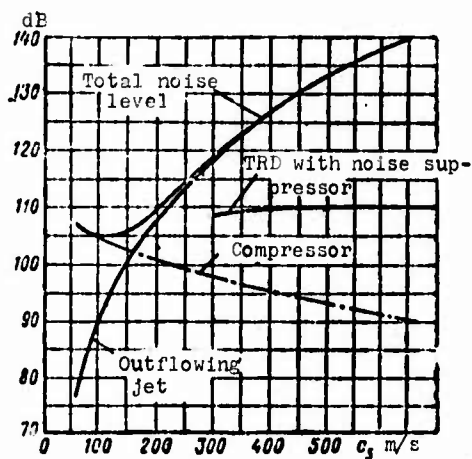


Fig. 25.10. Comparative curves of the level of noise produced by an outflowing jet of gas and by the compressor of a ducted-fan engine.

A further deceleration of the outflow from the PTV, conditioned by the tendency to decrease the noise level even more, is no longer justified as a result of limitations applied by the compressor of

the engine and fan of the PTV. Actually, considerations of the decrease in the dimensions and weight of the engine force designers to use compressor and fan stages with a high axial velocity at the inlet, reaching up to 200 m/s and more. Thus, the noise level at 100-105 dB, determined by the "whistle" of the compressor (fan), apparently, is now the lower limit of noise of the contemporary ducted-fan engine, which in the future should be decreased even more.

25.3.3.4. Effect of Throttling of Ducted-Fan Turbojet Engines on the Noise Level Produced by Them.

Figure 25.11 gives graphs of the measured noise level of four TRD (ducted-fan engine) of equivalent thrust with different values of the bypass ratio (0, 0.9, 1.3 and 6) obtained with throttling of the engine. These graphs characterize the noise levels caused by the three main noise sources in the engine: jet stream (R.S), turbine (T) and fan of the second circuit (V).

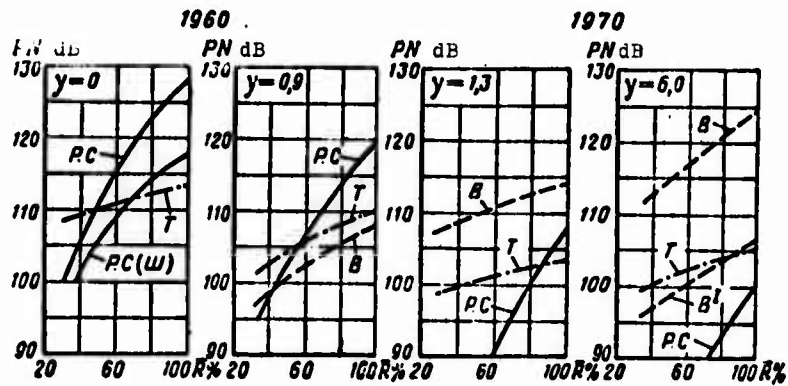


Fig. 25.11. Effect of throttling of the ducted fan engine on elements of the noise level produced by it (according to data of firm Rolls-Royce): [V](B) - fan; [T](T) - turbine; [R.S](P.C) - jet nozzle (jet stream); [Sh](W) - noise suppressor.

When  $y = 0$  and with total load of the engine ( $\bar{R} = 100\%$ ) the noise of the jet stream of the TRD proves to be predominant (128 dB).

It can be reduced down to 118 dB, having used a mechanical noise suppressor, which completely muffles the noise of the turbine, reaching in the TRD a relatively high value (113 dB).

With an increase in the bypass ratio (from zero to 6) in the process of maximum load, noise of the jet stream is sharply lowered (from 128 to 100 dB). The noise of the turbine in this case is also lowered but considerably more slowly. Thus, when  $y = 6$  the noise level of a revolving turbine already exceeds the noise level of the jet stream.

With an increase in the bypass ratio noise of the fan sharply increases, which, beginning from  $y = 1.1-1.2$ , becomes the predominant. When  $y = 6$  the noise of the two-stage fan equipped with a guide vane, reaches a very high level of 124 dB. Having used a single-stage fan (without guide and aligning vanes which create acoustic resonance), it is possible to reduce the noise level down to 106 dB. Approximately such level of noise is measured in three-shaft ducted-fan engine Rolls-Royce RB.211. It is considerably lower than that in any of the ducted-fan TRD known at present.

With throttling of the engine the noise level of the jet stream and, to a lesser extent, the noise of the fan and turbine are sharply lowered. Thus, beginning with  $y \geq 1.0$ , in regimes of moderate throttling of the engine the predominating noise proves to be the noise of the fan. It is characteristic that in a "pure" TRD and in a ducted-fan engine with a high bypass ratio ( $y = 6$ ) with great throttling ( $\bar{R} \leq 40\%$ ) the predominant noise becomes the noise of the turbine ( $\sim 100$  dB).

Figure 25.12 gives directional diagrams of noises being caused by various elements of the TRD (ducted-fan engine) in the takeoff regime of engines with various values of the bypass ratio.

It is characteristic that the fan, depending on the length of inlet or exit channel and place of installation, can radiate noise both in the direction of the front and rear hemisphere.

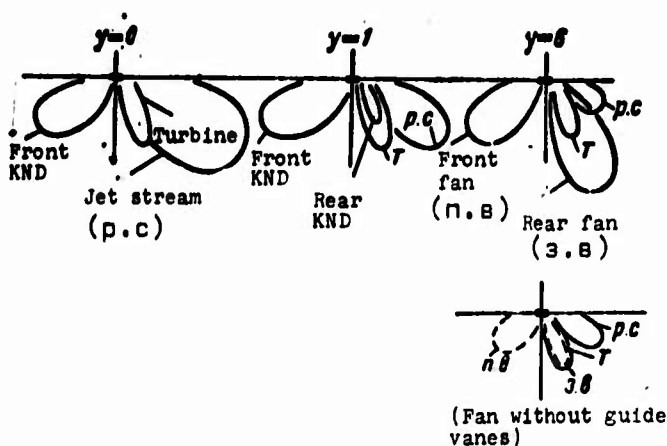


Fig. 25.12. Directional diagrams of noises being caused by various elements of the TRD in the takeoff regime at various values of  $\gamma$ .

#### 25.3.4. Use of Acoustic Lattices

It is possible to prevent the propagation of noise of the compressor (fan) in a surrounding medium, if we in air intake arrange acoustic traps or lattices, which will either dampen the acoustic energy of the revolving rotor or will not let sound oscillations pass upward along the inlet flow. Such devices, according to foreign reports, are used on the ducted-fan engine Pratt-Whitney JT 8D-1.

#### 25.3.5. Rational Selection of Takeoff Profile of an Aircraft Which Decreases the Noise over a Locality

On the basis of the study of noise with the flight of a high-speed passenger aircraft, a rule was made that the maximum level of perceived noise under an aircraft in the region of habitable areas at a distance of 5-6 km from the beginning of the takeoff and landing strip of the airfield (runway) does not exceed a certain permissible limit. The limit in the USA is set for the day standard at 112 dB and night - 104 dB.

By the rational selection of the takeoff profile of the aircraft it is possible to provide observance of these standards

in the limit of the airfield even with an insufficiency of noise-suppression means.

Figure 25.13 shows various trajectories of takeoff of a passenger aircraft of the type Tu-104 with engines RD-3M and the change in noise level under these trajectories.

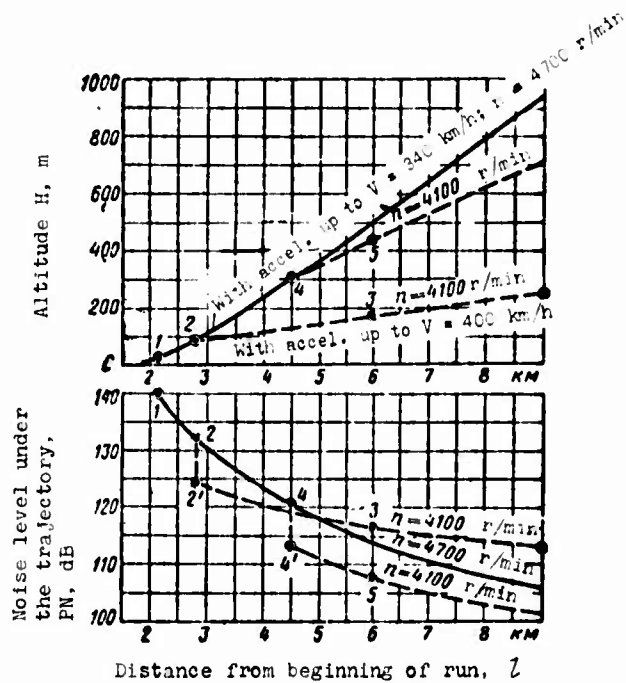


Fig. 25.13. Effect of takeoff trajectory of an aircraft on the noise level at the control point (according to data of B. N. Mel'nikov).

With a sloping takeoff (curve 1-2-3) with acceleration up to a speed of  $V = 400$  km/h at point 2 ( $H = 100$  m;  $L = 2.8$  km;  $n = 4700$  r/min;  $R = 9.5 T$ ) the engines transfer to a cruising regime of operation ( $n = 4100$  r/min;  $R = 6 T$ , line 2-2'); in this case with flight over the control point (point 3,  $H = 180$  m) the noise level is 116 dB (which exceeds the permissible sound level of 112 dB).

If, however, a climb is made at a steep angle on takeoff up to an altitude of 300 m, and then at point 4 ( $H = 300$  m;  $L = 4.5$  km) the engines change to a cruising regime of operation (line 4-4')

and acceleration of the aircraft up to  $V = 340$  km/h is accomplished, then with flight over the control point (point 5,  $H = 340$  m) the noise level will be only 108 dB. The trajectory 1-4-5 has the designation of *low-noise*.

One should note that of the two methods of throttling of the engine (decrease in revolution number when  $f_5 = \text{const}$  and opening of the jet nozzle when  $n = \text{const}$ ) the second is more preferable: with equal lowering of thrust it is characterized by a lower noise level of the outflowing gas jet (Fig. 25.14).

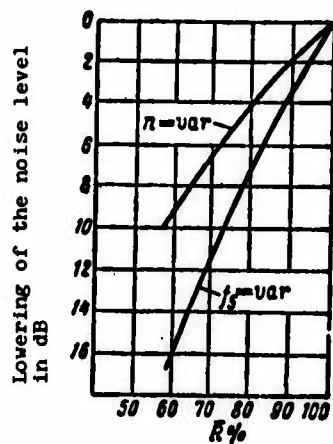


Fig. 25.14. Comparison of two methods of throttling of thrust of the TRD on the noise level.

## CHAPTER 26

### TECHNICAL-ECONOMIC CHARACTERISTICS OF AIRCRAFT GAS TURBINES

#### 26.1. Criteria of the Estimate of Technical-Economic Effectiveness of Aircraft Gas Turbines

Various criteria of the estimate of the technical-economic effectiveness of aircraft gas-turbine engines are known. These include *particular engine* criteria such as, for instance:

- 1) specific fuel consumption  $C_{y_d}$ , kg/(kgf·h);
- 2) specific weight of the engine  $\gamma_{дв}$ , kg/kgf;
- 3) relative frontal drag of the engine nacelle, or the ratio to internal thrust of the gas turbine to its effective thrust,  $K_f$ ;
- 4) service life of the engine  $\tau$ , h.

These include also *total* criteria which determine the effectiveness of the engine installed on the aircraft:

- 5) relative weight of the powerplant and fuel system  $\xi_{c.y+\tau.c}$ ;
- 6) operational expenditures, i.e., the cost of transportation of a ton-kilometer of load  $a'$ , kopecks/(t·km).

The cost of passenger transportation is an important criterion

which determines the economic profitableness of operation of the aircraft with the given engine; it is a function of the particular engine criteria of effectiveness noted above.

Let us examine more specifically certain of the criteria noted above and the effect of various factors on them.

## 26.2. Specific Weight of Aircraft Gas Turbines

The specific weight of an aircraft engine is an important operational factor, which to a certain extent determines the technical-economic effectiveness of its operation.

The specific weight of contemporary aircraft gas turbines depends on many factors, which include, in the first place, the dimensionality of the engine (i.e., magnitude of its thrust), compression ratio of the compressor determining the design complexity of the engine and its dimensional length (number of stages of the compressor and turbine, number of supports, need of adjustment and so on), temperature of gas in front of the turbine conditioning the need of cooling of blades of the turbine, bypass ratio, technological effectiveness and design perfection of the engine.

### 26.2.1. Effect of the Magnitude of Thrust

With a decrease in the linear dimension ( $L$ ) of geometrically similar engines,<sup>1</sup> the thrust of them is lowered proportionally to the square and the weight of the engine - in proportion to the cube of the linear dimension, i.e.,

$$R \sim G_s \sim L^2; \quad (26.1)$$

$$G_{\text{ms}} \sim L^3. \quad (26.2)$$

---

<sup>1</sup>That is, engines having the same thermodynamic cycle, and, consequently, identical specific thrusts.

Consequently, the specific weight of geometrically similar TRD changes in proportion to the linear dimension of the engine, i.e.,

$$\gamma_{1a} = \frac{G_{1a}}{R} \sim L, \quad (26.3)$$

or in proportion to the square root of the thrust, i.e.,

$$\gamma_{1a} \sim R^{0.5}. \quad (26.4)$$

This means that with a decrease in thrust the specific weight of the TRD would be continuously and rapidly decreased. However, practice of designing the TRD shows that, beginning from a certain optimum thrust, a further decrease in the dimensions of the engine no longer leads to a lowering of its weight. This occurs because it proves to be impossible to decrease infinitely dimensions of units of the engine (for example, the fuel pump); also it is impossible to decrease infinitely the thickness of walls of the parts (disks, etc.) due to considerations of the disturbance of rigidity of the design. Thus, a continuous decrease in the thrust will not be accompanied by a progressive lowering of the weight. The weight of the engine in practice can not even be decreased. But this will now lead to an *increase in specific weight* of the engine, i.e., to a fundamental *deviation from the theoretical* law of the change in specific weight (26.4).

For the TRD the optimum value of thrust at which  $\gamma_{da} = \gamma_{min}$  is 1200-1800 kgf.

Figure 26.1 gives the real dependence

$$\gamma_{da} = f(R).$$

constructed according to statistical data for engines with approximately identical parameters of the working process and with similar gas-dynamic and design schemes. We see that in the region of gas turbines of small dimensions the lowering of thrust sharply increases the specific weight.

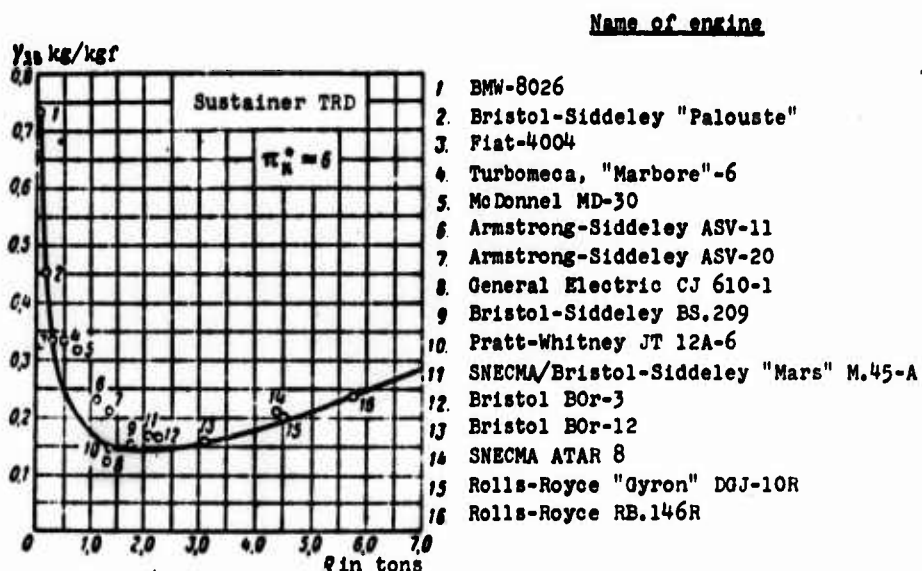


Fig. 26.1. Effect of dimensionality of the engine (thrust) on the specific weight of the TRD.

### 26.2.2. Effect of Compression Ratio of the Compressor

With an increase in the compression ratio of the compressor with constant thrust the length and weight of the engine increase, and, consequently, the specific weight of the gas turbine increases (Fig. 26.2).

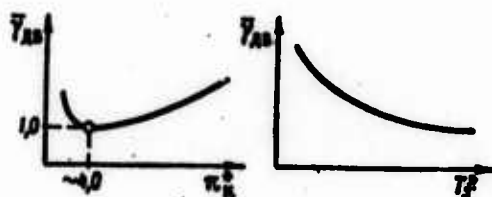


Fig. 26.2. Effect of parameters of the working process on specific weight of the TRD.

In the region of low compression ratios ( $\pi_K^* < 4-5$ ) a further decrease in  $\pi_K^*$  leads to an increase in the specific weight of the engine, since, on the one hand, the specific thrust of the gas turbine rapidly drops, and on the other hand the necessary length of the combustion chamber (determined from the condition of providing complete and stable combustion in the cruising regime of flight)

increases. The latter leads to an increase in the distance between supports of the turbocompressor and, consequently, to the increase in dimensional length and weight of the engine.

The passage from a single-shaft design of the gas turbine to double shaft with an increase in  $\pi_H^*$ , and then to a three-shaft design, must lead to a spasmodic increase in the specific weight of the engine. Meanwhile the analysis of the experience of the development of foreign and Soviet gas turbines shows that the increase in  $\pi_H^*$  in recent years did not lead to an increase in  $\gamma_{AB}$ , but conversely, is accompanied by a lowering of the specific weight. The latter is explained by the general progress of technology of the aircraft engine construction, specifically, the widespread introduction into the design of the engine of light construction materials and alloys (for example, titanium), an increase in pressure state of stages of the compressor, the use in progressive technology, which allowed reducing the vibratory loads of strained subassemblies and parts of the engine and thus decreasing their weight.

#### 26.2.3. Effect of Gas Temperature In Front of Turbine

With an increase in  $T_3^*$  when  $R = \text{const}$  the specific thrust of the gas turbine increases, as a result of which the specific weight of the engine is decreased (see Fig. 26.2). However, this occurs only up to the achievement of a definite level of temperature  $T_3^*$ , beginning from which to provide reliable operation of the engine there must be introduced cooling in the beginning of nozzle and then rotor blades of the gas turbine. The higher the gas temperature  $T_3^*$ , the more it is necessary to use ever more effective methods of cooling of the blades (for example, air, evaporative, liquid, porous); but in connection with this costs for cooling, specifically, in the form of the complication of design and additional weight of the engine will increase. Experience in the development of aircraft gas turbines abroad shows that even the short-term increase in  $T_3^*$  up to values of 1500-1550°K on aircraft requires the introduction of special cooling.

#### 26.2.4. Effect of the Bypass Ratio of the Ducted-Fan Engine

An increase in the bypass ratio in sustainer engines with the assigned gas generator, i.e., with the assigned internal circuit, initially leads to a lowering of specific weight of the engine. This is explained by the fact that with an increase in  $\gamma$  the thrust of the ducted-fan engine increases faster than the addition in weight conditioned by an increase in dimensions of the turbofan (front or rear turbofan adapter). Only at large values of  $\gamma$  does there appear an increase in specific weight of the engine. Thus, curve  $\gamma_{\text{дв}} = f(\gamma)$  (Fig. 26.3a) has a minimum, which is determined by the correlation of weights of the gas generator and adapter.

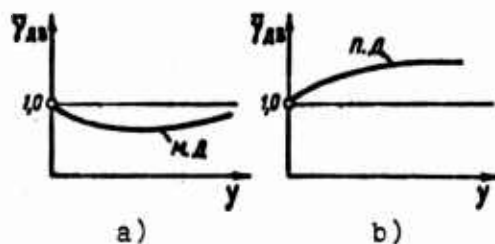


Fig. 26.3. Effect of the bypass ratio on specific weight: a) sustainer TRD; b) lift TRD.

If, however, an increase in the bypass ratio is accomplished with a constant thrust of the ducted-fan engine, then the regularity of the change in  $\gamma_{\text{дв}}$  with respect to  $\gamma$  is determined also by how much the dimensions of the internal circuit deviate from the optimum ( $R_{\text{opt}}(\text{ТРД}) \approx 1200-1800 \text{ kgf}$ ). For example, at this thrust passage to the ducted-fan engine will continuously increase the specific weight of the engine. With a thrust of 18-20 t the introduction of the second circuit to values of  $\gamma = 6-10$  will lower the specific weight of the engine. The specific weight of these ducted-fan engines (Pratt-Whitney JT 9D-1; Rolls-Royce RB.211; General Electric TF 39) will not exceed 0.175-0.180 kg/kgf.

Plotted on Fig. 26.4 is semiempirical curve of the effect of  $\gamma$  on parameter  $A = G_{\text{дв}}/G_{\Sigma}$ , which is the weight of ducted-fan engine per air flow of 1 kg/s. For the majority of contemporary

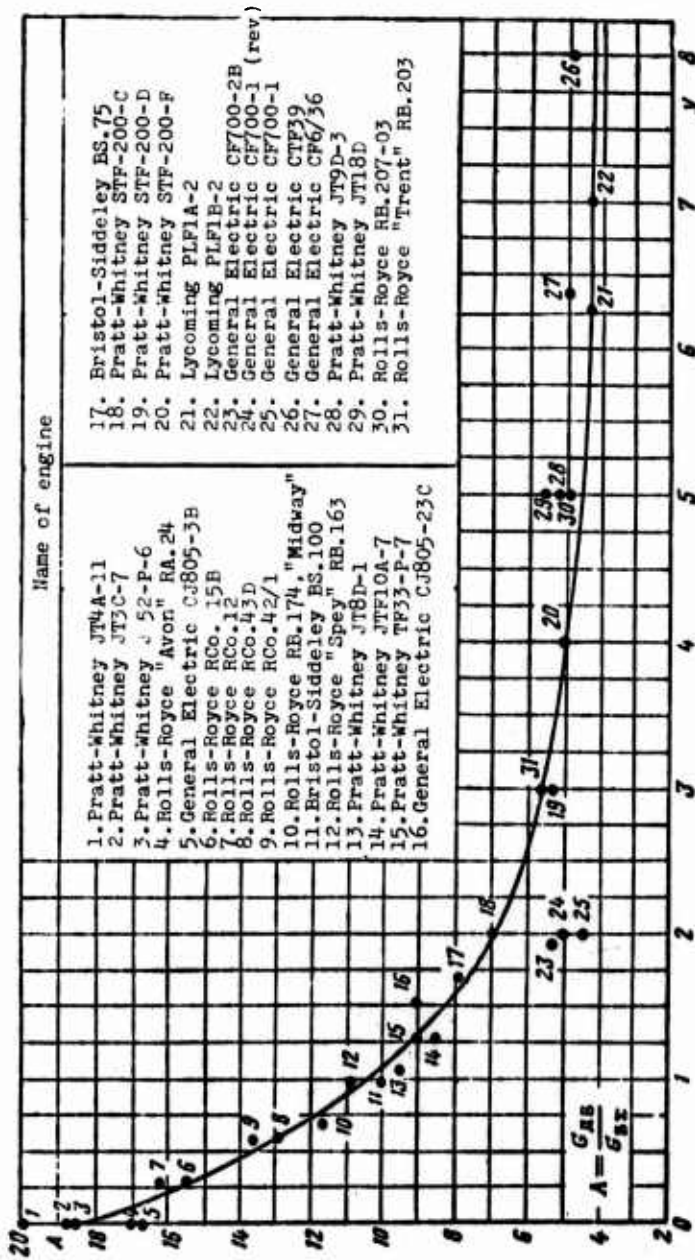


Fig. 26.4. Effect of the bypass ratio on parameter A on the weight of a ducted-fan engine.

double shaft ducted-fan engines of average and high thrusts, with high values of  $\pi_H^* = 12-20$ , statistical values  $A$  are well approximated by the curve given on Fig. 26.4.

The creation of a new class of ducted-fan engines of the "second generation" is connected with the increase in weight perfection of the engines and with a further lowering of the parameter  $A$  at a given magnitude  $y$ .

Figure 26.3b shows the regularity of the change in specific weight of a lift ducted-fan engine from the bypass ratio. Investigations and experience of the creation of lift engines Rolls-Royce RB.162 and Rolls-Royce RB.175 show that with the increase in  $y$  the specific weight of the ducted-fan engine somewhat increases. When  $y = 2$  it exceeds the specific weight of TRD by 5-10%. An increase in  $\gamma_{ДВ}$  of the lift engine with an increase in  $y$  is explained by the fact that with a "super-light" gas generator the addition in weight from the turbofan adapter proves to be more considerable than the increase in thrust of the engine.

### 26.3. Relative Drag of the Engine Nacelle

With an increase in the external diameter and, consequently, midsection of the engine, the frontal drag of the engine nacelle increases, and the ratio of the latter to the total drag of the aircraft in flight:

$$(\overline{c_x S})_{r, \lambda} = \frac{c_{x(r, \lambda)} S_{r, \lambda}}{c_{x \text{ самолета}} S_{\text{КР}}} = \frac{X_{r, \lambda}}{R_{\text{ВН}} = X_{\text{самолета}}}. \quad (26.5)$$

The more the relative drag of the engine nacelle, the greater the ratio of  $K_f$  of internal thrust of the gas turbine to the effective thrust, where

$$K_f = \frac{R_{\text{ВН}}}{R_{\text{ЭФ}}} = \frac{R_{\text{ВТ}}}{R_{\text{ВН}} - X_{r, \lambda}} \approx \frac{R_{\text{ВТ}} + X_{r, \lambda}}{R_{\text{ВН}}} = 1 + \frac{X_{r, \lambda}}{R_{\text{ВТ}}}. \quad (26.6)$$

Here  $R_{BH}$  - internal thrust of a jet engine;  $R_{\text{ЭФ}}$  - effective thrust of a jet engine;  $X_{\text{ПЛ}}$  - drag of a glider.

The coefficient  $K_f$  is inversely proportional to the effective quality of the aircraft:

$$K_f = \frac{K}{K_{\text{ЭФ}}} = \frac{X_{\text{ПЛ}} + X_{r, \text{д}}}{X_{\text{ПЛ}}}. \quad (26.7)$$

With an increase in  $K_f$  there is an increase in effective specific weight of the engine, equal to

$$\gamma_{\text{ЭФ}} = \frac{G_{\text{ЭФ}}}{R_{\text{ЭФ}}} = \gamma_{\text{д}} K_f, \quad (26.8)$$

and effective specific fuel consumption

$$C_{\text{ЭФ}} = 3600 \frac{G_{\text{ЭФ}}}{R_{\text{ЭФ}}} = C_{\text{д}} K_f. \quad (26.9)$$

The relative drag of the engine nacelle at fixed values  $H$ ,  $M_H$ ,  $\lambda_{1(B)}$  and  $\bar{\alpha}_{(B)}$  depends only on  $c_{x(r, \text{д})}$  and on specific thrust of the engine:

$$\bar{X}_{r, \text{д}} = \frac{X_{r, \text{д}}}{R_{\text{ЭФ}}} = A \frac{c_{x(r, \text{д})}}{R_{\text{ЭФ}}},$$

where  $A = \text{const.}$

Consequently, with fixed parameters of the gas generator ( $T_3^*$ ,  $\pi_{\text{К1}}^*$ ) with an increase in the bypass ratio (i.e., with a lowering of specific thrust), the relative drag of the engine nacelle continuously increases; correspondingly  $K_f$  increases.

Figure 26.5 gives the dependence of  $\bar{X}_{r, \text{д}}$  on  $R_{\text{ЭФ}}$  for different  $c_{x(r, \text{д})}$ .

Experimental scavengings of shortened engine nacelles (ducted-fan engine) conducted in wind tunnels at large values of  $\gamma$  ( $\gamma = 5-10$ ) show that by the rational shaping of inlet and exit parts of engine

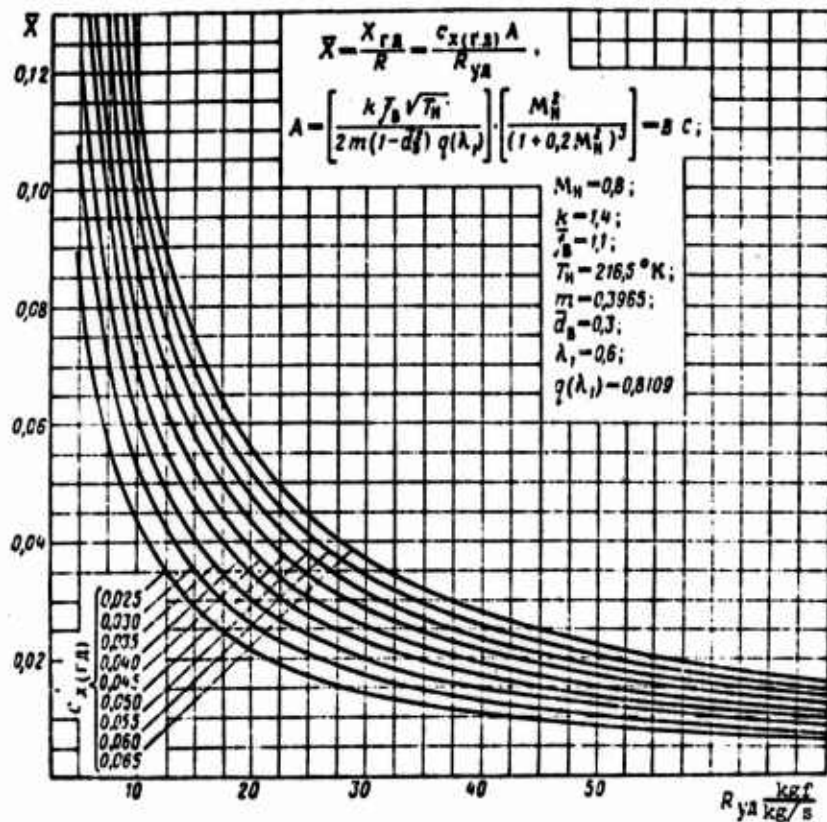


Fig. 26.5. Effect of the bypass ratio on frontal drag of the engine nacelle.

nacelles in combination with the blowing or suction of the boundary layer it is possible to reduce considerably the coefficient  $c_{x(\Gamma.Д)}$ . In this case the product  $c_{x(\Gamma.Д)} S_{\Gamma.Д}$  with an increase in  $y$  can remain practically constant.

At subsonic flight speeds ( $M_0 = 0.8$ ;  $H = 11$  km) the standard engine nacelle ( $c_{x(\Gamma.Д)} = 0.04-0.09$ ) have the magnitude  $K_f = 1.05-1.08$ .

#### 26.4. Specific Weight of the Powerplant and Fuel System

The important total parameter characterizing the economy of the engine and also its weight perfection is the specific weight of the powerplant and fuel system equal to

$$\xi_{c,y} + \xi_{r,c} = \frac{G_{c,y}}{G_{\text{взл}}} + \frac{G_{r,c}}{G_{\text{взл}}}, \quad (26.10)$$

where

$$\xi_{c,y} = K_{\gamma} \frac{G_{\text{дв}}}{R_{\text{дв}}} \frac{R_{\text{дв}}}{G_{\text{дв}}} = K_{\gamma} \mu_{\text{дв}} \gamma_{\text{дв}}(0); \quad (26.11)$$

$$\xi_{\tau,c} = K_{\tau,c} \frac{Q_{\tau(\text{кр})} a R_{\text{кр}}}{R_{\text{кр}} G_{\text{дв}}} = K_{\tau,c} \mu_{\text{кр}} a \left( \frac{L_{\text{кр}}}{3,6 V_{\text{кр}}} + 1 \right) C_{\gamma,1(\text{кр})}. \quad (26.12)$$

Here  $\mu_{\text{дв}}$ ,  $\mu_{\text{кр}}$  - the takeoff and cruising thrust-weight ratio of the aircraft respectively;  $L_{\text{кр}}$ ,  $V_{\text{кр}}$  - range and speed of flight, respectively in the cruising regime;  $\gamma_{\text{дв}}(0)$  - specific weight of the engine;

$G_{\text{дв}}$  - takeoff weight of the aircraft;  $K_{\gamma} = \frac{G_{c,y}}{G_{\text{дв}}}$  - coefficient of weight of the powerplant,  $K_{\gamma} = 1.4-1.5$ ;  $K_{\tau,c} = \frac{G_{\tau,c}}{Q_{\tau}}$  - coefficient of weight of the fuel system,  $K_{\tau,c} = 1.05-1.10$ ;  $a = \frac{Q_{\tau}}{Q_{\tau(\text{кр})}}$  - ratio of reserve of fuel expended during the whole flight to the expended fuel in the cruising section of the flight. Usually  $a = 1.05-1.15$ .

In formula (26.12) the fuel reserve for 1 hour of flight is considered.

The less the specific weight of the engine, the less the takeoff and cruising thrust-weight ratio, and the less the specific fuel consumption, the less the relative weight of the powerplant and fuel system, the greater the relative commercial load of the aircraft and the less operational expenditures.

#### 26.5. Cost of Transportation of a Ton-Kilometer of Load

In civil aviation the basic criterion of the estimate of a technical-economic effectiveness of operation of the aircraft is the cost of transportation of a ton-kilometer of load equal (see work [5]) to

$$a' = (2+2,3) \frac{A}{V_{\text{п}} G_{\text{ком}}} \frac{\text{копейки}}{\text{т} \cdot \text{км}}. \quad (26.13)$$

Magnitude  $a'$  is the ratio of flying expenditures  $A$  per aircraft-hour to the transport productivity of the aircraft  $V_{\text{п}} G_{\text{ком}}$  (taking

into account airport expenditures and of underload of the aircraft).

- In formula (26.13):
- $\alpha$  - expenditure rate of the engine, considering the expenditures for its amortization and repair referred to 1 t of thrust in rubles/(t·h);
  - $P$  - takeoff thrust of the engine in t;
  - $\beta$  - expenditure rate of the aircraft, considering the expenditures for its amortization and repair referred to 1 t of weight of an empty equipped aircraft, in rubles/(t·h);
  - $G_{\text{пуст}}$  - weight of an empty equipped aircraft in t;
  - $\sigma$  - cost of 1 t of kerosene in rubles/t;
  - $Q_{\text{cp}}$  - average hour fuel consumption in t/h;
  - $\gamma$  - wages of flight-lift personnel in rubles/number of passengers·h);
  - $n$  - number of passengers;
  - $V_p$  - trip velocity in km/h;
  - $G_{\text{ком}}$  - commercial load in t.

Factors conditioned by parameters of the engine affecting the cost of transportation are: expenditure rate of the engine depending on the service life (or amortization period) and dimensionality (thrust) of the engine; average hour fuel consumption dependent on the specific fuel consumption; empty weight of the aircraft dependent on specific weight of the engine.

#### 26.5.1. Effect of Service Life of the Engine on the Cost of Transportation

With an increase in the service life of the engine its expenditure rate  $\alpha$  is lowered, and, consequently, the flight expenditures and costs of passenger transportation  $\alpha'$  are decreased also.

Figure 26.6a shows the effect of the increase in service life on the cost of transportation of the average mainline aircraft (SMS), having a takeoff weight of  $G_{\text{B3Л}} = 80 \text{ t}$  and flight range of  $L = 4000 \text{ km}$ .

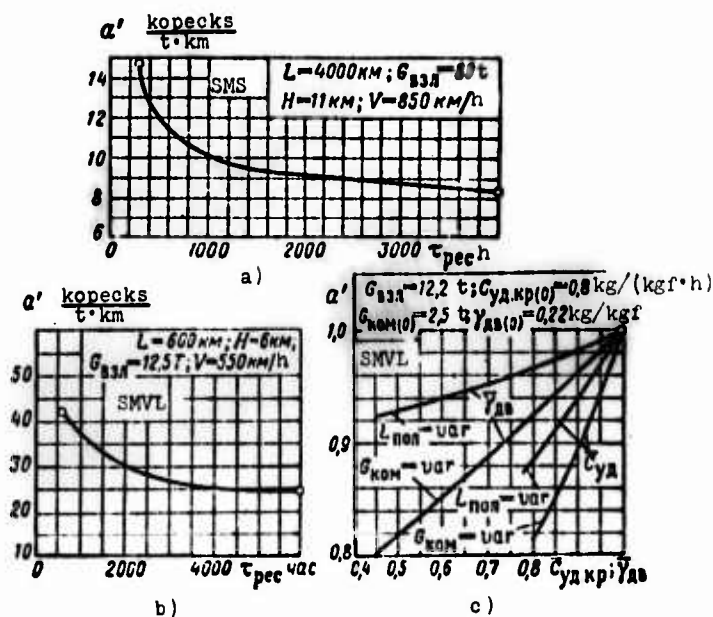


Fig. 26.6. Effect of parameters of the engine on the cost of operation of aircraft of civil aviation: a), b) effect of service life of the engine; c) effect of specific fuel consumption and specific weight of the engine.

If in the initial stage of operation, when the service life of the engine was  $\tau_{\text{pec}} = 300 \text{ h}$ , the cost of transportation was equal to  $a' \approx 14.7 \text{ kopecks/(t·km)}$ , then with a service life at 2000 hours magnitude  $a'$  is lowered down to  $9.2 \text{ kopecks/(t·km)}$ , i.e., almost 40%. Similarly, an increase in the amortization lifetime of the engine on an aircraft of local airlines (SMVL) from 600 to 3000 hours (see Fig. 26.6b) lowers the operational expenditures from 42 to  $27 \text{ kopecks/(t·km)}$ , i.e., 35%.

From the given data it follows that the introduction into operation of engines with great initial service life (about

800-1000 hours) and the increasing of it during a short time to 2000-5000 hours provides a high national economic effect.

#### 26.5.2. Effect of Lowering of Specific Fuel Consumption of the Engine on the Cost of Transportation

With a decrease in the specific fuel consumption of the engine the average fuel consumption per hour of an aircraft is lowered; consequently, at the assigned flight range the fuel reserve necessary for flight is decreased, and moreover it is decreased the more the flight range.

The economy in fuel consumption  $\Delta G_T$ , at a fixed takeoff weight of the aircraft, can be used either for increasing the commercial load or for increasing the flight range. In both cases the cost of the transportation is lowered.

Figure 26.6c shows the effect of the increase in the economy of the engines on the cost of transportation of the aircraft of local airlines (SMVL). When the economy in the fuel consumption is used for increasing the commercial load, a 10% decrease  $C_{yA}$  (for example, from 0.8 to 0.72 kg/(kgf·h) when  $M_0 = 0.8$  and  $H = 11$  km) gives approximately a 10% lowering of operational expenditures. In the same case, when the economy in the fuel consumption is used for increasing the flight range (when  $G_{BЭЛ} = \text{const}$ ), the lowering of operating expenditures is only 6%.

#### 26.5.3. Effect of Lowering of Specific Weight of the Engine on the Cost of Transportation

The lowering of the specific weight of the engine and, consequently, the weight of the powerplant makes it possible at a constant takeoff weight of the aircraft to increase the commercial load or flight range.

Figure 26.6c shows the effect of lowering of the specific weight of engines on operational expenditures. A 10% lowering of  $\gamma_{дв}$

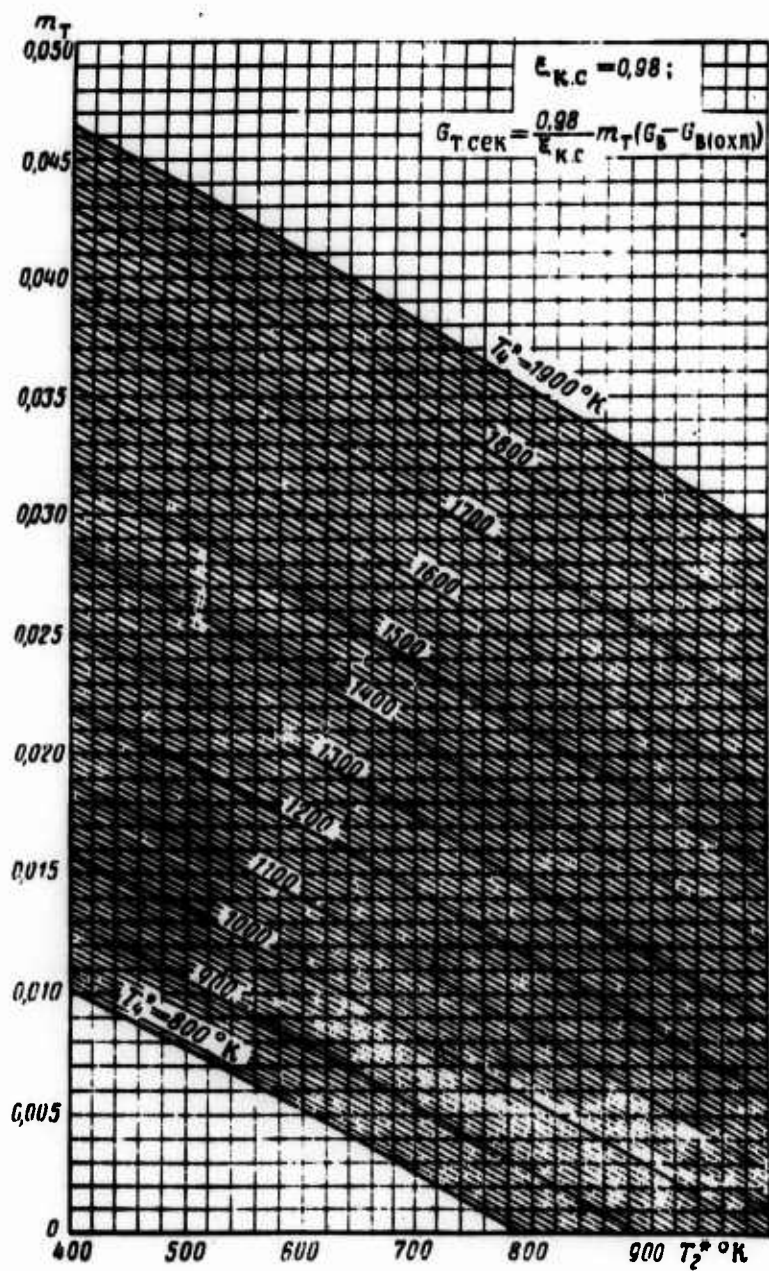
(for example, from 0.22 to 0.20 kg/kgf) gives a 4% economy in the cost of transportation due to the increase in the commercial load and a 2% economy as a result of the increase in the flight range.

26.5.4. Effect of the Improvement of Effectiveness  
of the Engine on the Whole on the Cost  
of Transportation

The ducted-fan engines of the "second generation" being created at present have considerably better criteria (with respect to  $C_{yд}$ ,  $\gamma_{дв}$ ) than do the ducted-fan engines of the "first generation." Calculations show that the lowering of specific fuel consumption in the cruising flight regime (for example, when  $M_0 = 0.8$  and  $H = 11$  km) from 0.78-0.80 to 0.64-0.66 kg/(kgf·h) and a decrease in specific weight of the engine from 0.24 to 0.18 kg/kgf allows bringing down the operating expenditures of long-range and medium-range main-line aircraft by 16-23% (i.e., by 1/4 to 1/6).

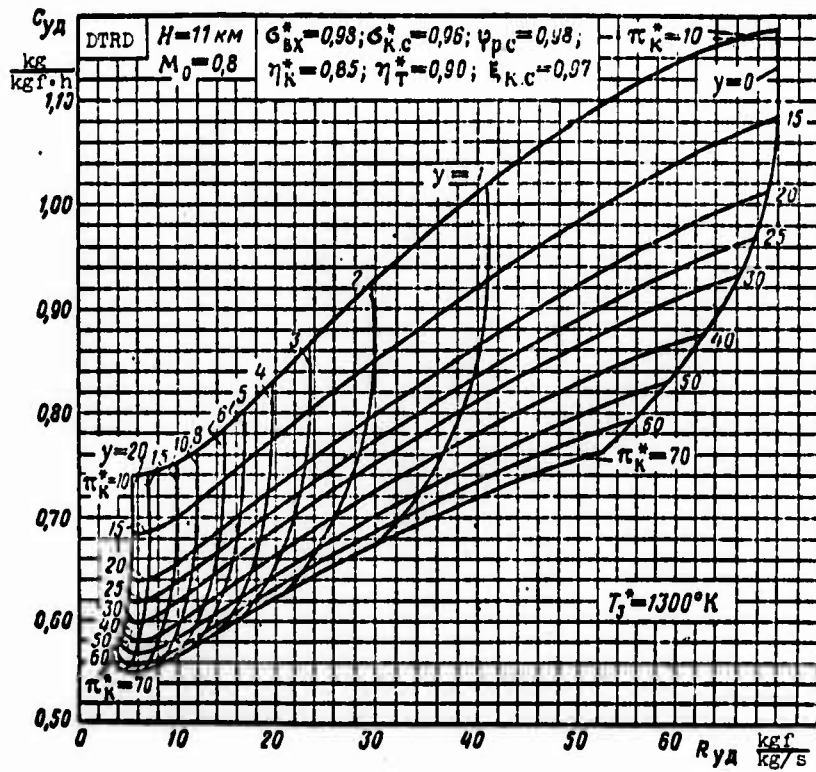
Appendices 1, 2 and 3 give nomograms for the determination of relative fuel consumption of a jet engine and specific parameters of a ducted-fan engine.

APPENDIX 1



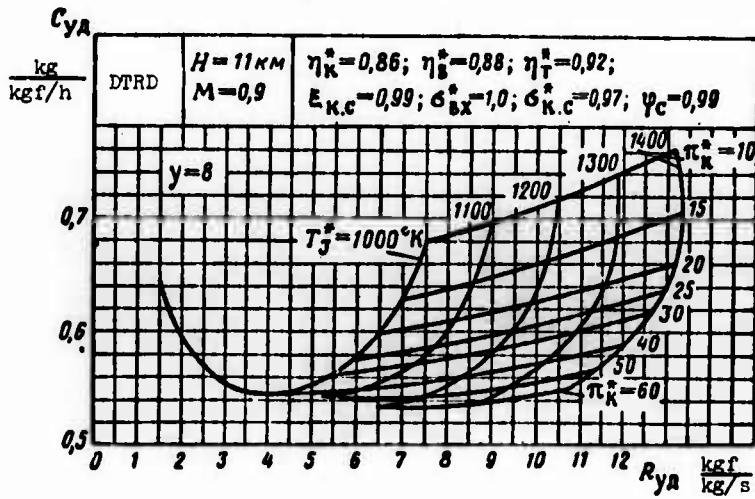
Nomogram for the determination of relative fuel consumption of a jet engine.

APPENDIX 2



Nomogram for the determination of specific parameters of a ducted-fan engine ( $M_0 = 0.8; H = 11 \text{ km}; T_3^* = 1300^\circ\text{K}$ ).

APPENDIX 3



Nomogram for the determination of specific parameters of the ducted-fan engine ( $y = 8$ ).

#### BIBLIOGRAPHY

1. Abiants V. Kh. Teoriya gazovykh turbin reaktivnykh dvigateley (Theory of gas turbines of jet engines), izd-vo "Mashinostroyeniye", 1965.
2. Abramovich G. N. Prikladnaya gazovaya dinamika (Applied gas dynamics), izd-vo "Nauka", 1969.
3. Arzhanikov N. S., Sadekova G. S., Aerodinamika bol'shikh skorostey (Aerodynamics of high velocities), izd-vo "Vysshaya shkola", 1965.
4. Aerodinamika turbin i kompressorov (Aerodynamics of turbines and compressors) (edited by U. R. Hawthorne<sup>1</sup>), Vol. X from the series "Aerodinamika bol'shikh skorostey i reaktivnaya tekhnika" ("Aerodynamics of high velocities and reaction technology"), izd-vo "Mashinostroyeniye", 1968.
5. Gulyagin A. A., Ovrutskiy Ye. A., Proyektirovaniye passazhirskikh samoletov s uchetom ekonomiki ekspluatatsii (Design of passenger aircraft taking into account the economics of operation), izd-vo "Mashinostroyeniye", 1964.
6. Bonni Ye. A., Tsukrov M. D., Besserer K. U., Aerodinamika. Teoriya reaktivnykh dvigateley. Konstruktsiya i praktika proyektirovaniya (Aerodynamics. Theory of jet engines. Construction and practice of designing) (translation from English), Voenizdat, 1959.
7. Borisenko A. I. Gazovaya dinamika dvigateley (Gas dynamics of engines), Oborongiz, 1962.
8. Boshnyakovich F., Tekhnicheskaya termodinamika (Technical thermodynamics), Gosenergoizdat, 1955.

---

<sup>1</sup>[Translator's note: name not verified].

9. Vukalovich M. P., Novikov I. I., Tekhnicheskaya termodynamika (Technical thermodynamics), izd-vo "Energiya", 1968.
10. Vulis L. A., Termodinamika gazovykh potokov (Thermodynamics of gas flows), Gosenergoizdat, 1950.
11. Deych M. Ye., Tekhnicheskaya gazodinamika (Technical gas dynamics), Gosenergoizdat, 1961.
12. Dorofeyev V. M., Levin V. Ya., Ispytaniya vozdušno-reaktivnykh dvigateley (Tests of jet engines), Oborongiz, 1961.
13. Zhiritskiy G. S. et al., Gazovyye turbiny aviatsionnykh dvigateley (Gas turbines of aircraft engines), Oborongiz, 1963.
14. Inozemtsev N. V., Aviatsionnyye gazoturbinnyye dvigateli (Aircraft gas-turbine engines), Oborongiz, 1955.
15. Kazandzhan P. K., Kuznetsov A. V., Turbovintovyye dvigateli (Turboprop engines), Voenizdat, 1961.
16. Kvasnikov A. V., Protsessy i balansy v aviamotornykh ustanovkakh (Processes and balances in aircraft engines), Oborongiz, 1948.
17. Kirillov I. I., Teoriya turbomashin (Theory of turbomachines), izd-vo "Mashinostroyeniye", 1964.
18. Klyachkin A. L., Eksploatatsionnyye kharakteristiki aviatsionnykh gazoturbinnnykh dvigateley (Operational characteristics of aircraft gas-turbine engines), izd-vo "Transport", 1967.
19. Kulagin I. I., Osnovy teorii aviatsionnykh gazoturbinnnykh dvigateley (Principles of the theory of aircraft gas-turbine engines), Voenizdat, 1967.
20. Kyukheman D. and Veber I., Aerodinamika aviatsionnykh dvigateley (Aerodynamics of aircraft engines), IL, 1956.
21. Markov N. I., Bakulev V. I., Raschet vysotno-skorostnykh kharakteristik turboreaktivnykh dvigateley (Calculation of high-altitude and high-speed characteristics of turbojet engines), Oborongiz, 1960.
22. Mel'kumov T. M., Melik-Pashayev N. I. et al., Raketnyye dvigateli (Rocket engines), izd-vo "Mashinostroyeniye", 1968.
23. Nechayev Yu. N., Vkhodnyye ustroystva sverkhzvukovykh samoletov (Intakes of supersonic aircraft), Voenizdat, 1963.
24. Orlov B. V. et al., Osnovy proyektirovaniya raketno-pryamotochnnykh dvigateley (Principles of the design of rocket-ramjet engines), izd-vo "Mashinostroyeniye", 1967.

25. Osnovy gazovoy dinamiki (Principles of gas dynamics) (edited by N. U. Ammons<sup>1</sup>), Vol III from the series "Aerodinamika bol'shikh skorostey i reaktivnaya tekhnika" ("Aerodynamics of high velocities and reaction technology"), IL, 1963.

26. Osnovy proyektirovaniya i kharakteristiki gazoturbinnnykh dvigateley (Design fundamentals and characteristics of gas-turbine engines) (edited by U. R. Hawthorne), Vol XI from the series "Aerodinamika bol'shikh skorostey i reaktivnaya tekhnika" ("Aerodynamics of high velocities and reaction technology"), izd-vo "Mashinostroyeniye", 1964.

27. Reaktivnyye dvigateli (Jet engines) (edited by O. E. Lancaster<sup>1</sup>), Vol. XII from the series "Aerodinamika bol'shikh skorostey i reaktivnaya tekhnika" ("Aerodynamics of high velocities and reaction technology"), Voenizdat, 1962.

28. Skubachevskiy G. S., Aviatsionnyye gazoturbinnnyye dvigateli (Aircraft gas-turbine engines), izd-vo "Mashinostroyeniye", 1965.

29. Stechkin B. S., Kazandzhan P. K., Alekseyev L. P. et al., Teoriya reaktivnykh dvigateley (Lopatochnyye mashiny) (Theory of jet engines (Bladed machines)), Oborongiz, 1956.

30. Stechkin B. S., Kazandzhan P. K., Alekseyev L. P. et al., Teoriya reaktivnykh dvigateley (Rabochiy protsess i kharakteristiki) (Theory of jet engines (Working process and characteristic)), Oborongiz, 1958.

31. Kholshchevnikov K. V., Soglasovaniye parametrov kompressora i turbiny v aviatsionnykh gazoturbinnnykh dvigatelyakh (Concordance of parameters of the compressor and turbine in aircraft gas-turbine engines), izd-vo "Mashinostroyeniye", 1965.

32. Cherkasov B. A., Avtomatika i regulirovaniye vozdushno-reaktivnykh dvigateley (Automation and control of jet engines), izd-vo "Mashinostroyeniye", 1965.

33. Cherkez A. Ya., Inzhenernyye raschety gazoturbinnnykh dvigateley metodom malykh otkloneniy (Engineering designs of gas-turbine engines by the method of small deviations), izd-vo "Mashinostroyeniye", 1965.

34. Ekkert B., Osevyeye i tsentrobezhnyye kompressory (Axial-flow and centrifugal compressors), GNTI, 1959.

---

<sup>1</sup>[Translator's note: name not verified].

UNCLASSIFIED

Security Classification

DOCUMENT CONTROL DATA - R & D		
<i>(Security classification of title, body of abstract and indexing annotation must be entered when the overall report is classified)</i>		
1. ORIGINATING ACTIVITY (Corporate author) Foreign Technology Division Air Force Systems Command U. S. Air Force		2a. REPORT SECURITY CLASSIFICATION UNCLASSIFIED
		2b. GROUP
3. REPORT TITLE  THEORY OF JET ENGINES		
4. DESCRIPTIVE NOTES (Type of report and inclusive dates) Translation		
5. AUTHOR(S) (First name, middle initial, last name)  Klyachkin, A. L.		
6. REPORT DATE 1969	7a. TOTAL NO. OF PAGES 657	7b. NO. OF REFS 34
8a. CONTRACT OR GRANT NO.	8b. ORIGINATOR'S REPORT NUMBER(S) FTD-MT-24-123-70	
b. PROJECT NO. 6040101	8c. OTHER REPORT NO(S) (Any other numbers that may be assigned this report)	
c.		
d. DIA Task Nos T65-04-19A; 18A		
10. DISTRIBUTION STATEMENT Distribution of this document is unlimited. It may be released to the Clearinghouse, Department of Commerce, for sale to the general public.		
11. SUPPLEMENTARY NOTES	12. SPONSORING MILITARY ACTIVITY Foreign Technology Division Wright-Patterson AFB, Ohio	
13. ABSTRACT  The book examines the design operating process, principles of control and operational characteristics of jet engines of various types used in civil aviation (including turbojet, turboprop and turbofan). The classification of the engines is given. Special attention is given to the analysis of peculiarities of throttle and high-altitude and high-speed characteristics of gas-turbine aircraft engines and also the study on the effect of various operating conditions on these characteristics. The book is intended as a text-book for students of mechanical engineering institutes of the Department of Civil Aviation and Civilian Aviation Colleges of the Ministry of Higher and Secondary Special Education. The book can also be used as a manual for engineers specializing in the field of aircraft engine construction.		

DD FORM 1 NOV 65 1473

~~661~~  
658

UNCLASSIFIED

Security Classification

14. KEY WORDS	LINK A		LINK B		LINK C	
	ROLE	WT	ROLE	WT	ROLE	WT
Jet Aircraft Aircraft Engine Jet Thrust Turbojet Engine Jet Engine Combustion Chamber Engine Control System Turbofan Engine Turboprop Engine Gas Turbine Engine						

~~662~~  
659